Vol. 6 No. 3 2021
ISSN:1390-9347

Bionatura

Latin American journal of Biotechnology and Life Sciences

Visual Representation of the Synergistic Immune Response of COVID-19 Convalescent Individuals After Vaccination

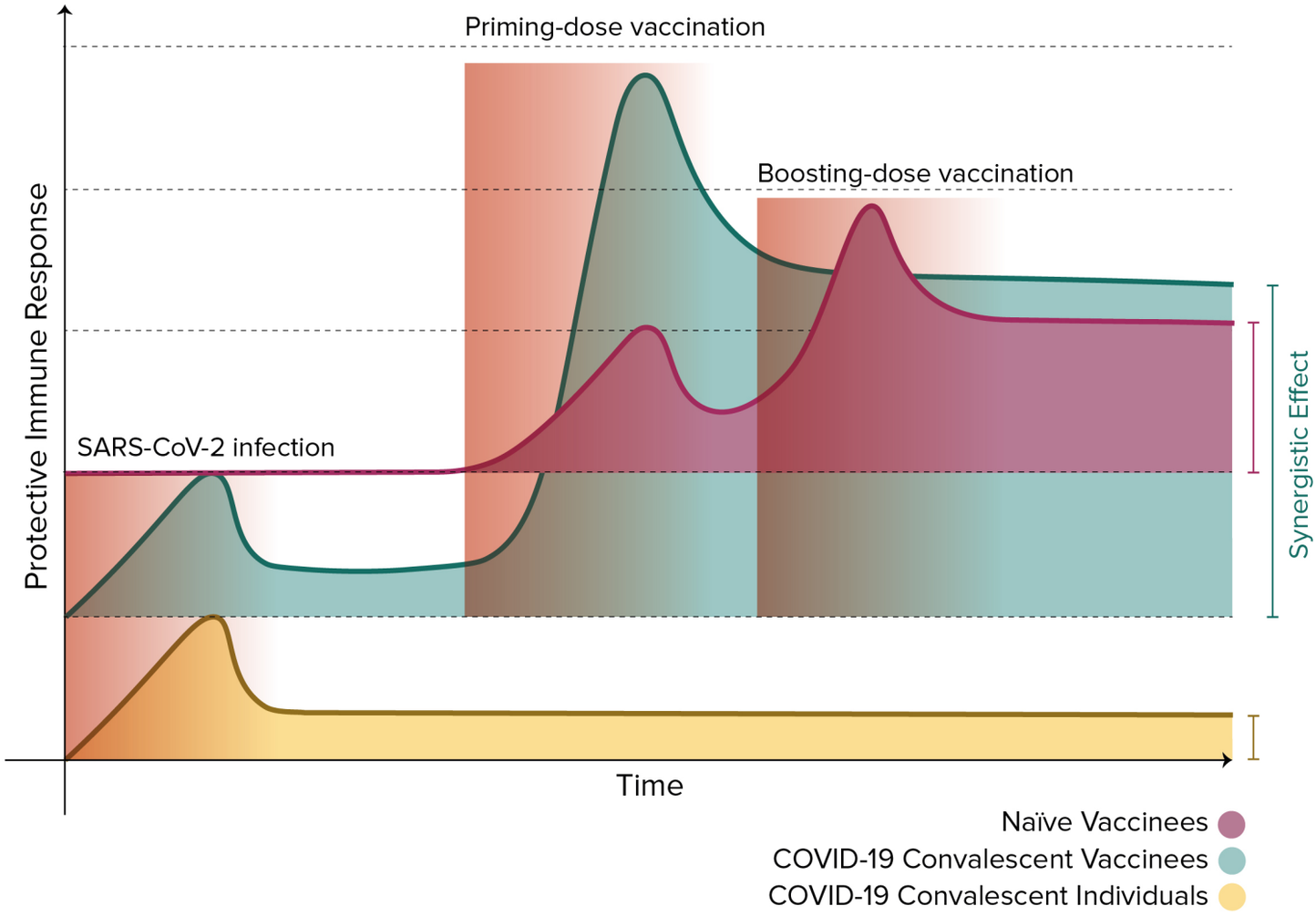

Hybrid immunity: the immune response of COVID-19 survivors to vaccination.

Scopus
UNIVERSIDAD YACHAY TECH
clinicalbiotec.com
UCO Universidad Católica de Oriente
CENTRO DE BIOTECNOLOGÍA Y BIOMEDICINA CBB
http://www.revistabionatura.com/ https://www.facebook.com/bionaturajournal/ https://twitter.com/rbionatura

Es el momento de los que se atreven a soñar y luchan por alcanzar sus metas.

En la UCO te acompañamos

UCO Universidad Católica de Oriente
Acreditación Institucional en ALTA CALIDAD

Vigilada Mineducación

Pregrados

- **Tecnología en Operaciones Financieras**
  SNIES 104841 Registro Calificado - Res. 12903 del 21-08-2015 M.E.N.
  95 créditos - A distancia tradicional - Rionegro Ant.
- **Contaduría Pública**
  SNIES 13018 Registro Calificado - Res. 9256 del 07- 06- 2018
  Acreditación de Alta Calidad 4610 del 21- 03 - 2018 M.E.N.
  165 créditos Presencial - Rionegro
- **Comercio Exterior**
  SNIES 1854 Registro Calificado - Res.14314 del 11-12-2019 M.E.N.
  159 créditos - Presencial - Rionegro Ant.
- **Administración de Empresas**
  SNIES 55096 Registro Calificado - Res. 7658 del 18-04-2017 M.E.N.
  152 créditos - Presencial - Rionegro Ant.
- **Tecnología Agropecuaria**
  SNIES 1850 Registro Calificado - Res. 8684 del 10-07-2013 M.E.N.
  113 créditos - Presencial - Rionegro Ant.
- **Agronomía**
  SNIES 4443 Registro Calificado - Res. 8087 del 17-05-2018
  Acreditación de Alta Calidad N° 29149 del 26-12-2017
  157 créditos - Presencial - Rionegro Ant.
- **Zootecnia**
  SNIES 53037 Registro Calificado - Res. 14466 del 04-09-2014 M.E.N.
  156 créditos - Presencial - Rionegro Ant.
- **Psicología**
  SNIES 8562 Registro Calificado - Res. 9902 del 31-07-2013 M.E.N.
  Acreditación de Alta Calidad N° 17227 del 24 - 10 - 2018
  175 créditos - Presencial - Rionegro Ant.
- **Comunicación Social**
  SNIES 53045 Registro Calificado - Res. 14892 del 11-09-2014 M.E.N.
  146 créditos - Presencial - Rionegro Ant.
- **Trabajo Social**
  SNIES 106586 Registro Calificado - Res. 26741 del 29-11-2017 M.E.N.
  141 créditos - Presencial - Rionegro Ant.
- **Derecho**
  SNIES 53539 Registro Calificado - Res. 10542 del 14-07-2015 M.E.N.
  166 créditos - Presencial - Rionegro Ant.
- **Nutrición y Dietética**
  SNIES 104601 Registro Calificado - Res. 7823 del 01-06-2015 M.E.N
  166 créditos - Presencial - Rionegro Ant.
- **Gerontología**
  SNIES 1853 Registro Calificado - Res. 14839 del 22-10-2013 M.E.N.
  138 créditos - A distancia con apoyo virtual - Rionegro Ant.
- **Enfermería**
  SNIES 91027 Registro Calificado- Res. 12600 del 03-08-2018 M.E.N.
  166 créditos - Presencial - Rionegro Ant.
- **Licenciatura en Filosofía**
  SNIES 106542 Registro Calificado - Res. 22108 del 24 - 10 - 2017 M.E.N.
  164 créditos - Presencial - Rionegro Ant.
- **Licenciatura en Lenguas Extranjeras con énfasis en Inglés**
  SNIES 106647 Registro Calificado - Res. 29529 del 29-12-2017 M.E.N.
  164 créditos - Presencial - Rionegro Ant.
- **Licenciatura en Educación Física, Recreación y Deportes**
  SNIES 106436 Registro Calificado - Res. 17481 del 31-08-2017 M.E.N.
  164 créditos - Presencial - Rionegro Ant.
- **Licenciatura en Educación para la Primera Infancia**
  SNIES 105359 Registro Calificado - Res. 02848 del 16-02-2016 M.E.N.
  164 créditos - Presencial - Rionegro Ant.
- **Licenciatura en Ciencias Naturales**
  SNIES 105898 Registro Calificado - Res.19869 del 18-10-2016 M.E.N.
  164 créditos - Presencial - Rionegro Ant.
- **Licenciatura en Educación Religiosa**
  SNIES 106705 Registro Calificado - Res. 2084 del 13 - 02 - 2018 M.E.N.
  164 créditos - Presencial - Rionegro Ant.
- **Técnico Profesional en Programación Web**
  SNIES 103704 Registro Calificado - Res.14454 del 04-09-2014 M.E.N.
  67 créditos - Presencial - Rionegro Ant.
- **Ingeniería Ambiental**
  SNIES 4361 Registro Calificado - Res. 3654 del 02-03-2018 M.E.N.
  Acreditación de Alta Calidad No. 6543 del 18 - 04 - 2018
  173 créditos - Presencial - Rionegro Ant.
- **Ingeniería de Sistemas**
  SNIES 1855 Registro Calificado - Res. 0178 del 05-01-2019 M.E.N.
  164 créditos - Presencial- Rionegro Ant.
- **Ingeniería Industrial**
  SNIES 1856 Registro Calificado - Res. 1293 del 04-02-2019 M.E.N.
  160 créditos - Presencial- Rionegro Ant.
- **Ingeniería Electrónica**
  SNIES 20271 Registro Calificado - Res. 24646 del 14-11-2017 M.E.N.
  178 créditos - Presencial- Rionegro Ant.
- **Teología**
  SNIES 103450 Registro Calificado - Res. 10638 del 09-07-2014 M.E.N.
  130 créditos - A distancia - Rionegro Ant.

¡HAGAMOS QUE PASE!

www.uco.edu.co @uconiano universidad catolica de oriente 322 569 90 90

Vol. 6 No. 3 2021

Bionatura

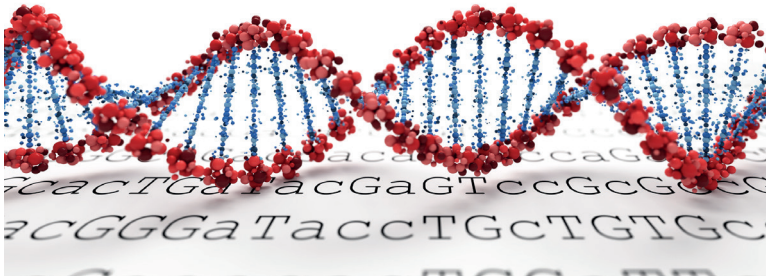

La Revista Bionatura publica trimestral en español o inglés trabajos inéditos de investigaciones básicas y aplicadas en el campo de la Biotecnología, la Inmunología, la Bioquímica, Ensayos Clínicos y otras disciplinas afines a las ciencias biologícas, dirigidas a la obtención de nuevos conocimientos, evaluación y desarrollo de nuevas tecnologías, productos y procedimientos de trabajo con un impacto a nivel mundial.

Equipo editorial

latindex

Index in directory of open access journals

Instrucciones para los Autores

Los Trabajos serán Inéditos: Una vez aprobados, no podrán someterse a la consideración de otra revista, con vistas a una publicación múltiple, sin la debida autorización del Comité Editorial de la Revista. La extensión máxima será 8 cuartillas para los trabajos originales, 12 las revisiones y 4 las comunicaciones breves e informes de casos, incluidas las tablas y figuras. Los artículos se presentarán impresos (dos ejemplares). Todas las páginas se numerarán con arábigos y consecutivamente a partir de la primera. Estos deben acompañarse de una versión digital (correo electrónico o CD) en lenguaje Microsoft Word, sin sangrías, tabuladores o cualquier otro atributo de diseño (títulos centrados, justificaciones, espacios entre párrafos, etc.). Siempre se ha de adjuntar la carta del consejo científico que avala la publicación y una declaración jurada de los autores.

Referencias Bibliográficas. Se numerarán según el orden de mención en el texto y deberán identificarse mediante arábigos en forma exponencial. Los trabajos originales no sobrepasarán las 20 citas; las revisiones, de 25 a 50 y las comunicaciones breves e informes de casos.

En las Referencias en caso de que las publicaciones revisadas esten online se debe proveer un enlace consistente para su localización en Internet. Actualmente, no todos los documentos tienen DOI, pero si lo tienen se debe incluir como parte de la referencias. Si no tuviese DOI, incluir la URL.

Tablas, modelos y anexos: Se presentarán en hojas aparte (no se intercalarán en el artículo) y en forma vertical numeradas consecutivamente y mencionadas en el texto. Las tablas se ajustarán al formato de la publicación se podrán modificar si presentan dificultades técnicas.

Figuras: Las fotografías, gráficos, dibujos, esquemas, mapas, salidas de computadora, otras representaciones gráficas y fórmulas no lineales, se denominarán figuras y tendrán numeración arábiga consecutiva. Se presentarán impresas en el artículo en páginas independientes y en formato digital con una resolución de 300 dpi. Todas se mencionarán en el texto. Los pies de figuras se colocarán en página aparte. El total de las figuras y tablas ascenderá a 5 para los trabajos originales y de revisión y 3 para las comunicaciones breves e informes de casos.

Abreviaturas y siglas: Las precederá su nombre completo la primera vez que aparezcan en el texto. No figurarán en títulos ni resúmenes. Se emplearán las de uso internacional.

Sistema Internacional de Unidades (SI): Todos los resultados de laboratorio clínico se informarán en unidades del SI o permitidas por este. Si se desea añadir las unidades tradicionales, se escribirán entre paréntesis. Ejemplo: glicemia: 5,55 mmol/L (100 mg/100 mL).

Para facilitar la elaboración de los originales, se orienta a los autores consultar los requisitos uniformes antes señalados disponibles en: http://www. fisterra.com/recursos_web/mbelvancouver. htm#ilustraciones%20 (figura)

Los trabajos que no se ajusten a estas instrucciones, se devolverán a los autores. Los aceptados se procesarán según las normas establecidas por el Comité Editorial. El arbitraje se realizará por pares y a doble ciego en un período no mayor de 60 días. Los autores podrán disponer de no más de 45 días para enviar el artículo con correcciones, se aceptan hasta tres reenvíos. El Consejo de Redacción se reserva el derecho de introducir modificaciones de estilo y /o acotar los textos que lo precisen, comprometiéndose a respetar el contenido original.

Bionatura

La **Revista Bionatura** es un medio especializado, interinstitucional e interdisciplinario, para la divulgación de desarrollos científicos y técnicos, innovaciones tecnológicas, y en general, los diversos tópicos relativos a los sectores involucrados en la biotecnología, tanto en Ecuador como en el exterior; así mismo, la revista se constituye en un mecanismo eficaz de comunicación entre los diferentes profesionales de la biotecnología.

Es una publicación sin ánimo de lucro. Los ingresos obtenidos por publicidad o servicios prestados serán destinados para su funcionamiento y desarrollo de su calidad de edición. (http://revistabionatura.com/media-kit.html)

Es una revista trimestral, especializada en temas concernientes al desarrollo teórico, aplicado y de mercado en la biotecnología.

Publica artículos originales de investigación y otros tipos de artículos científicos a consideración de su consejo editorial, previo proceso de evaluación por pares (peer review) sin tener en cuenta el país de origen.

Los idiomas de publicación son el Español e Inglés.

Esta revista utiliza Open Journal Systems, que es un gestor de revistas de acceso abierto y un software desarrollado, financiado y distribuido de forma gratuita por el proyecto Public Knowledge Project sujeto a la Licencia General Pública de GNU.

Nuestros contactos deben ser dirigidos a:
Revista Bionatura: editor@revistabionatura.com

ISSN: 1390-9347 (Versión impresa)
Formato: 21 x 29,7 cm
ISSN: 1390-9355 (Versión electrónica)
Sitio web: **http://www.revistabionatura.com**

Publicación periódica trimestral
Esta revista utiliza el sistema peer review para la evaluación de los manuscritos enviados.

Instrucciones a los autores en:
http://revistabionatura.com/instrucciones.html

Asistente de publicación / Publication assistant
Evelyn Padilla Rodriguez (sales@revistabionatura.com)

ÍNDICE / INDEX

EDITORIAL

LETTER TO EDITOR / CARTA AL EDITOR

RESEARCH / INVESTIGACIÓN

CASE REPORTS / REPORTE DE CASO

REVIEW / ARTÍCULO DE REVISIÓN

EDITORIAL

Hybrid immunity: the immune response of COVID-19 survivors to vaccination

Marlon Gancino[1], Nelson Santiago Vispo[2]

DOI. 10.21931/RB/2021.06.03.1

By the time writing this editorial, around nineteen months (Dec 2019) has passed since the first report of a Severe Acute Respiratory Syndrome Coronavirus 2 (SARS-CoV-2) outbreak in individuals of Wuhan, China[1]. Also, it has been more than sixteen months (Mar 2020) since the declaration of the Coronavirus disease 19 (COVID-19) pandemic by the World Health Organization (WHO)[1]. The evolution and rapid scattering of this novel coronavirus have trapped in an unprecedented global public health crisis, which, so far, has reached 196,553,009 people around the globe, provoking 4,200,412 deaths (31st July 2021)[1].

The global endeavor of defeating contagion has achieved groundbreaking events such as the fastest development and massive application of effective vaccines in history[2]. Currently, +500 SARS-CoV-2 vaccines are being developed over the full spectrum of platforms (i.e., non-viral vector, viral vector, inactivated and live-attenuated virus, and recombinant vaccines); some of which are already pre-clinical and clinical studies[2,3]. Remarkably, ten vaccines are already available on the market[4], from which, by the end of July 2021, +3800 million doses have been administered[1]. Complemented by non-pharmaceutical strategies (e.g., restrictions on international mobility), inducing protective immunity to SARS-CoV-2 massively until attaining herd immunity appears to be the definitive solution to overcome this pandemic[5].

We are reaching milestones daily, so some exciting questions have been raised about immunological memory – the fundamental of protective immunology. This response coordinated by a synchronized orchestra of antibodies, memory B cells, memory CD4+ T cells, and memory CD8+ T cells remains poorly understood[6]. Either infection (natural immunity) or vaccination (vaccine-induced immunity) can trigger immunological memory against SARS-CoV-2, and all nuances in such complexity may provoke different biological outcomes[7]. Diverse investigations have concluded that either path to immunity can confer specific protection to COVID-19[8–11]. Moreover, they have discussed the question: what does it occur when these immunities are overlapped? Acquiring knowledge on the immune response dynamics that convalescent individuals who are subsequently vaccinated develop is essential. The deep understanding of this "hybrid immunity" will allow the design of appropriate vaccination regimes for the vast population of previously infected individuals[12].

Observations on the response kinetics of immune memory from naturally immunized cohorts have found that ~95% of subjects can develop a stable immunity against reinfection, which may last moderately declining over a year after symptoms onset[6,13]. Relevantly, such protective immunity suffers a considerable weakening in the face of current circulating SARS-CoV-2 variants of concern (VOCs) – i.e., B.1.1.7 (Alpha), B.1.351 (Beta), P.1 (Gamma), and B.1.617.2 (Delta) – when compared with the wild-type Wuhan-Hu-1 variant[4,14–16]. As identified by previous works, multiple spike (S) protein mutations in VOCs explain their ability to escape neutralization antibody activity partially, making the acquired natural protective immunology less effective[7,12].

Although to a milder degree, reduction to VOCs neutralization has also been seen in vaccine immunized people[16]. Currently, four main types of vaccines govern the market: mRNA-lipid nanoparticle-based non-viral vectors (BNT162b2 by Pfizer-BioNTech, and mRNA-1273 by Moderna), adenovirus-based viral vectors (ChAdOx1-nCoV-19 by AstraZeneca, Ad26.COV2.S by Johnson & Johnson, Ad5-nCoV by CanSino Biologics, and Sputnik V by Gamaleya), inactivated virus (CoronaVac by Sinovac, BBV152 by Bharat Biotech, WIBP-CorV by Sinopharm (Wuhan), and BBIBP-CorV by Sinopharm (Beijing)), and recombinant protein subunits (NVX-CoV2373 by Novavax)[3,4]. Phase 3 clinical trials showed good overall vaccine efficacies that ranged from ~95% (BNT162b2) to >50% (CoronaVac) at preventing COVID-19 illness, commonly after a two-dose prime-boost regime[17]. In such a sense, it has been observed that vaccination protection effectiveness slightly reduces against VOCs, Delta variant being associated with the highest transmissibility and ability to avoid antibody neutralization[16]. However, although less potent to VOCs, preliminary research suggests that vaccines probably remain efficacious[8,11,16,18]. Now, it is statistically modelized that vaccine-induced neutralization activity would decay in a long non-linearly fashion, causing the vaccines with initial efficacy of 95% to preserve 77% efficacy in a 250-day span[19].

Identifying the differences between natural and vaccine-induced immunities directs us to the proper interrogation: what is there at their interface? As mentioned earlier, numerous research groups have addressed this question, and their results suggest that hybrid immunity has a more robust protective performance than either immunity. In a synergistic character, researchers have seen that previously infected vaccinees mount cross-variant neutralization reactogenicity to the first vaccine dose, which equals or surpasses the observed in naïve individuals after the second vaccine shot[5,7,8,11,16,20,21].

Reports in this regard informed the occurrence of anamnestic reactions in diverse cohorts of previously infected vaccinees after receiving the first vaccine dose of either BNT162b2, mRNA-1273, or ChAdOx1-nCoV-19 with no apparent improvement after the second dose[7–9,11,17,21]. According to Goel *et al.* and Kramer *et al.*, as anticipated, only COVID-19 survivors present detectable levels of immunoglobulin G (IgG) antibodies specialized to recognize the full-length SARS-CoV-2 S protein (anti-S IgG) or the SARS-CoV-2 spike receptor-binding domain (RBD) (anti-RBD IgG) – antibodies associated with SARS-CoV-2 neutralization responses[13]– before vaccination[17,22]. As observed, titers of anti-S IgG and anti-RBD IgG are higher in individuals with a history of SARS-CoV-2 infection pre- and post-vaccination (compared with naïve subjects at the exact sampling times)[17,20,23]. The first vaccine dose induces a variable and inadequate response of neutralizing antibodies generation in SARS-CoV-2–unexposed individuals, which boosts the second vaccination[24]. Contrary, the first vaccine dose triggers

[1] Faculty of Health, NANOMED EMJMD, University of Paris, France.
[2] Professor, School of Biological Sciences and Engineering, Yachay Tech University, Ecuador.

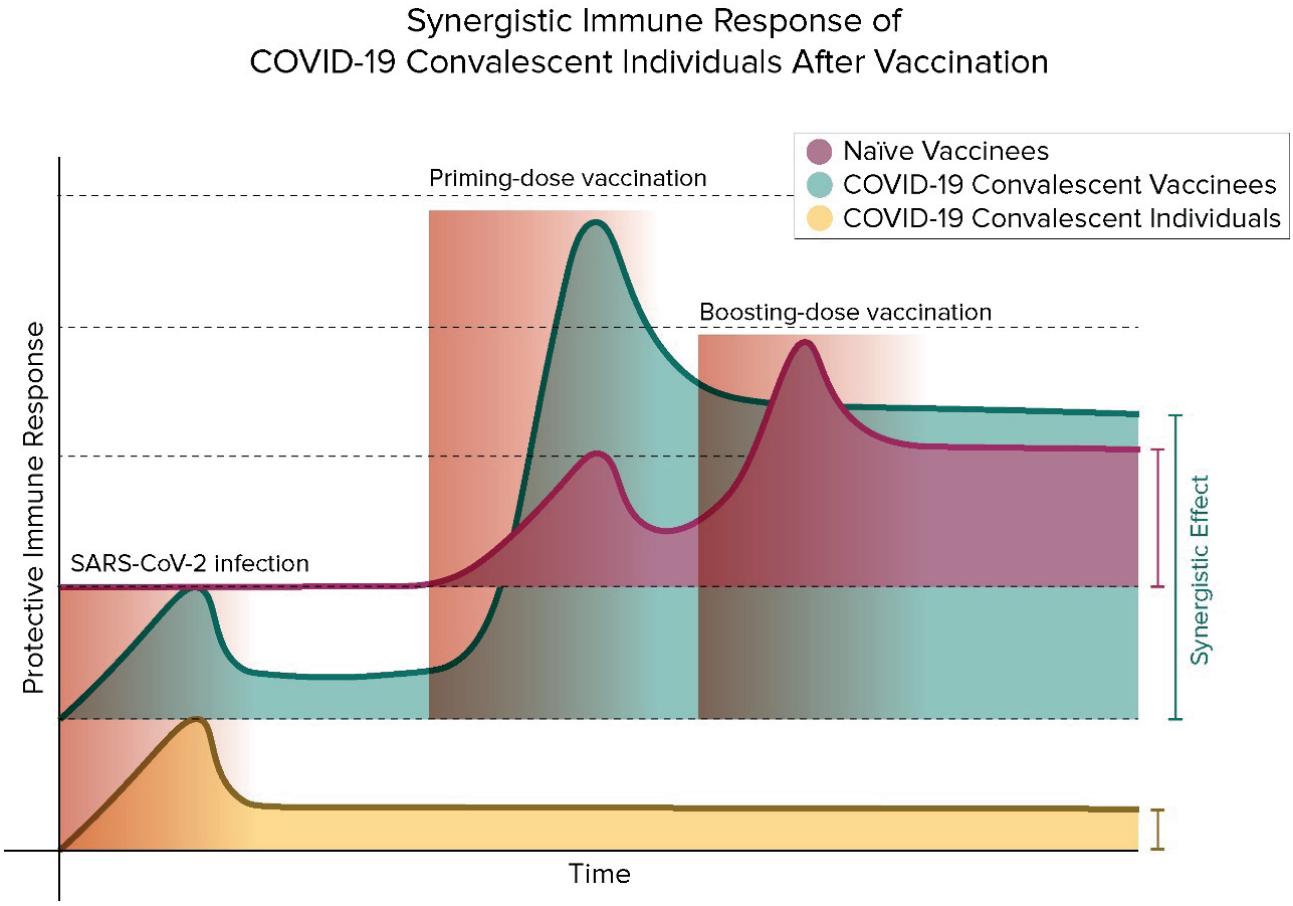

a uniform and rapid amplification of anti-S IgGs and anti-RBD IgGs titers in SARS-CoV-2 experienced individuals[10,11]. While naïve and COVID-19 asymptomatic vaccinees' antibody titers are significantly boosted after the second vaccine dose[21], no significant improvement has been detected in participants with preexisting immunity after the boosting dose, suggesting a possible plateau in the neutralization antibody activity[9,11,20].

Interestingly, as informed by Ebinger *et al.*, neutralizing antibodies levels in naïve individuals who received the first vaccine dose were slightly higher when contrasted with the baseline state of previously infected individuals[23]. In their research, neutralizing antibody levels were statistically similar in both groups, only if compared to the group of previously infected individuals after the first dose with the group of naïve individuals after completing a two-dose vaccination regime[23]. Also, higher frequencies of vaccine-related systemic side effects (e.g., fever, headache, muscle pain, and fatigue) have been associated with COVID-19 convalescent individuals and high IgG responses[9].

As a complement, the humoral immune response of SARS-CoV-2–exposed individuals is boosted above the protective threshold after the first vaccination dose, even against VOCs[8,16]. Planas *et al.* noticed that sera from previously infected one-dose vaccinees displayed a significant increase in neutralizing antibody titers against Alpha, Beta, and Delta SARS-CoV-2 variants, in contrast with non-vaccinated convalescent people[16]. On the contrary, such cross-variant neutralization activity was observed in naïve individuals just days after the second vaccine immunization. Therefore, these emerging data highly advise that SARS-CoV-2 experienced individuals subsequently vaccinated may develop a broad protective immunity against all spreading VOCs[7,16].

Every compartment of the adaptative immune systems is probably involved in prompting this non-anticipated hybrid immunity behaviour[7]. Broadly, as part of the immune response against infection, long-live memory B cells by a previous induction of T cells (specifically, T follicular helper cells) start compiling mutations in immunoglobulin variable gene sequences (somatic hypermutations (SHM)) in favor of a future generation of high-affinity antibodies[13]. Thus, evolved memory B cells can be recruited post-vaccination, which will differentiate into plasma cells producing highly potent neutralizing antibodies[13]. It has been observed that memory B cells continue accumulating somatic mutations over 12 months in germinal centers in individuals who have recovered from COVID-19[13,25]. Those mutations accumulated long after infection are, indeed, though accountable for the high potency in serum neutralization activity of the convalescent vaccinee cohorts against VOCs[12]. Although the study performed by Goel et al. it was not found any change in the levels of SHMs in memory B cell clones from convalescent individuals as a response to vaccination[17], naïve vaccinees also would enter into this memory B cell maturation after antigen exposure (vaccination), if analyzed after long spans[12].

The prime-boost regime strategy chose for most vaccines relies on mounting protective responses through memory recall to antigen reexposure[7]. The natural SARS-CoV-2 infection primes convalescent populations. This primary encounter with the virus promotes the previously infected individuals to develop a T cell memory response to a vast epitope repertoire of the 25 SARS-CoV-2 proteins (S and non-S viral proteins), which according to several studies, are maintained in VOCs[7,15,20]. Most commercial vaccines induce a protective response using only the SARS-CoV-2 S-protein[8,11]. Accordingly, vaccine priming

activates a T cell memory to a restricted number of epitopes in naïve individuals (compared to SARS-CoV-2–exposed individuals)[7]. Therefore, the reactivation of broad infection-primed T cell memory response and the recruitment of long-live mutated memory B cell after first vaccine dose in SARS-CoV-2–exposed individuals probably play a role in the astounding response kinetics of hybrid immunity[20].

The boosting vaccine dose produced in B and T cell kinetics is remarkably similar to the one observed in the serological analysis. That is, boosting effect of the second vaccine dose was only observed in naïve individual[8,11,17,20]. Humoral and cellular immunity of convalescent vaccinees may reach an activity plateau after the first vaccine dose[20]. In this sense, the study of Lozano-Ojalvo et al. reported a reduction in T cell responses in COVID-19 recovered individuals after the second vaccine dose[20]. Taken together, those results reveal that convalescing individuals may request an alternative vaccination regime different that the current prime-boost one developed in naïve individuals.

Global health systems are still battling a colossal challenge aggravated by the shortage in vaccine supply and the occurrence and dissemination of VOCs[5,21]. Vaccine policies are being discussed worldwide, proposing several strategies to address herd immunity to protect their populations[15,24]. A clear example was seen in the United Kingdom when authorities approved extending the time interval between vaccine dosages to apply the first vaccine immunization to the most significant number of citizens[8]. However, as above expose, one dose in naïve individuals may not be enough to protect them from VOCs, such as the Delta variant[16].

Hybrid immunity can become a turning-point opportunity to defeat the infection in context with the current pandemic scenario. Adopting policies aligned with the data mentioned above may be particularly beneficial for regions like Latin America. While this region shares only ~5% of the world population, it accumulates +16% of the ~200 million COVID-19 total cases, so far reported[1]. Acknowledging the reduced diagnostic capabilities of these countries, this entire area is probably one of the most affected globally, leading to one of the more numerous populations of convalescent people. From both an economic and pharmacological perspective, applying a one-dose regime of pertinent vaccines to convalescent individuals is sustainable[5]. As COVID-19 survivors may need just one vaccination to achieve high levels of protective immunity, massive antibody screening for SARS-CoV-2 spike antibodies could help prioritize and free up doses, optimize vaccine supply efficiency, and surpass problems linked to the current vaccine manufacturing bottleneck[5,25,26].

Finally, as all cited reports were performed considering vaccines developed over only mRNA-lipid nanoparticle-based non-viral vectors and adenovirus-based viral vectors, it is vital to extend the research to the rest of marketed vaccines and figure out if the same “hybrid immunity” principles apply to them.

Bibliographic references

1. World Health Organization. Coronavirus (COVID-19) Dashboard. World Health Organization (2021). Available at: https://covid19.who.int/. (Accessed: 31st July 2021)
2. Hrkach, J. & Langer, R. From micro to nano: evolution and impact of drug delivery in treating disease. Drug Deliv. Transl. Res. 10, 567–570 (2020).
3. Li, Q., Wang, J., Tang, Y. & Lu, H. Next-generation COVID-19 vaccines: Opportunities for vaccine development and challenges in tackling COVID-19. Drug Discov. Ther. 15, 2021.01058 (2021).
4. Focosi, D., Tuccori, M., Baj, A. & Maggi, F. SARS-CoV-2 Variants: A Synopsis of In Vitro Efficacy Data of Convalescent Plasma, Currently Marketed Vaccines, and Monoclonal Antibodies. Viruses 13, 1211 (2021).
5. Focosi, D., Baj, A. & Maggi, F. Is a single COVID-19 vaccine dose enough in convalescents ? Hum. Vaccines Immunother. 00, 1–3 (2021).
6. Dan, J. M. et al. Immunological memory to SARS-CoV-2 assessed for up to 8 months after infection. Science 371, eabf4063 (2021).
7. Crotty, S. Hybrid immunity. Science 372, 1392–1393 (2021).
8. Reynolds, C. J. et al. Prior SARS-CoV-2 infection rescues B and T cell responses to variants after first vaccine dose. Science 372, 1418–1423 (2021).
9. Sasikala, M. et al. Immunological memory and neutralizing activity to a single dose of COVID-19 vaccine in previously infected individuals. Int. J. Infect. Dis. 108, 183–186 (2021).
10. Saadat, S. et al. Binding and Neutralization Antibody Titers After a Single Vaccine Dose in Health Care Workers Previously Infected With SARS-CoV-2. JAMA 325, 1467 (2021).
11. Stamatatos, L. et al. mRNA vaccination boosts cross-variant neutralizing antibodies elicited by SARS-CoV-2 infection. Science 372, 1413–1418 (2021).
12. Purushotham, J. N., van Doremalen, N. & Munster, V. J. SARS-CoV-2 vaccines: anamnestic response in previously infected recipients. Cell Res. 2–3 (2021). doi:10.1038/s41422-021-00516-7
13. Wang, Z. et al. Naturally enhanced neutralizing breadth against SARS-CoV-2 one year after infection. Nature (2021). doi:10.1038/s41586-021-03696-9
14. Moyo-Gwete, T. et al. Cross-Reactive Neutralizing Antibody Responses Elicited by SARS-CoV-2 501Y.V2 (B.1.351). N. Engl. J. Med. 384, 2161–2163 (2021).
15. Noh, J. Y., Jeong, H. W. & Shin, E. C. SARS-CoV-2 mutations, vaccines, and immunity: implication of variants of concern. Signal Transduct. Target. Ther. 6, 3–4 (2021).
16. Planas, D. et al. Reduced sensitivity of SARS-CoV-2 variant Delta to antibody neutralization. Nature (2021). doi:10.1038/s41586-021-03777-9
17. Goel, R. R. et al. Distinct antibody and memory B cell responses in SARSCoV-2 naïve and recovered individuals following mRNA vaccination. Sci. Immunol. 6, 1–19 (2021).
18. Jalkanen, P. et al. COVID-19 mRNA vaccine induced antibody responses against three SARS-CoV-2 variants. Nat. Commun. 12, 1–11 (2021).
19. Khoury, D. S. et al. Neutralizing antibody levels are highly predictive of immune protection from symptomatic SARS-CoV-2 infection. Nat. Med. 27, (2021).
20. Lozano-Ojalvo, D. et al. Differential Effects of the Second SARS-CoV-2 mRNA Vaccine Dose on T Cell Immunity in Naïve and COVID-19 Recovered Individuals. SSRN Electron. J. 1–9 (2021). doi:https://doi.org/10.1101/2021.03.22.436441
21. Levi, R. et al. One dose of SARS-CoV-2 vaccine exponentially increases antibodies in individuals who have recovered from symptomatic COVID-19. J. Clin. Invest. 131, (2021).
22. Krammer, F. et al. Antibody Responses in Seropositive Persons after a Single Dose of SARS-CoV-2 mRNA Vaccine. N. Engl. J. Med. 384, 1372–1374 (2021).
23. Ebinger, J. E. et al. Antibody responses to the BNT162b2 mRNA vaccine in individuals previously infected with SARS-CoV-2. Nat. Med. 27, 981–984 (2021).
24. Frieman, M. et al. SARS-CoV-2 vaccines for all but a single dose for COVID-19 survivors. EBioMedicine 68, 103401 (2021).
25. Turner, J. S. et al. SARS-CoV-2 mRNA vaccines induce persistent human germinal centre responses. Nature (2021). doi:10.1038/s41586-021-03738-2
26. Zamora-Ledezma, C.; C., D.F.C.; Medina, E.; Sinche, F.; Santiago Vispo, N.; Dahoumane, S.A.; Alexis, F. Biomedical Science to Tackle the COVID-19 Pandemic: Current Status and Future Perspectives. Molecules 2020, 25, 4620. https://doi.org/10.3390/molecules25204620


UNIVERSIDAD
YACHAY
TECH
DE LA CURIOSIDAD ACADÉMICA
A LA INNOVACIÓN TECNOLÓGICA
ESCUELA DE
CIENCIAS MATEMÁTICAS
Y COMPUTACIONALES
ESCUELA DE
CIENCIAS FÍSICAS
Y NANOTECNOLOGÍA
ESCUELA DE
CIENCIAS QUÍMICAS
E INGENIERÍA
ESCUELA DE
CIENCIAS DE LA TIERRA,
ENERGÍA Y AMBIENTE
ESCUELA DE
CIENCIAS BIOLÓGICAS
E INGENIERÍA

LETTER TO EDITOR / CARTA AL EDITOR

SARS-Cov-2 y tromboembolia pulmonar en pacientes críticamente enfermos, experiencia de una unidad de cuidados criticos

SARS-Cov-2 and pulmonary thromboembolism in critically ill patients, the experience of a critical care unit

Jorge Luis Vélez-Páez[1], Edgar López-Rondón[2], Mario Montalvo-Villagómez[3]

DOI. 10.21931/RB/2021.06.03.2

La pandemia por SARS-Cov-2, que inicialmente se planteó como una afección predominantemente respiratoria, se ha convertido en una noxa con manifestaciones en múltiples órganos, el factor común para la llegada del virus a los mismos son los receptores ACE 2, que es por dónde el virus ingresa a nuestras células.

A nivel vascular, es llamativo la incidencia incrementada de trombosis tanto macroscópica como a nivel de la microcirculación sistémica y pulmonar (microCLOTS) por inmunotrombosis[1], la endotelitis producida por el virus[2,3], parece activar estados protrombóticos por la lesión del glicocálix endotelial, con la consecuente activación de la cascada de coagulación y la adhesión y agregación plaquetaria posterior; sumándose la NETosis, que es un mecanismo de erradicación bacteriana, pero desregulado puede empeorar el estado protrombótico ya narrado. Esto ha planteado si el uso de anticoagulantes debe ser una panacea y si la dosis a recibir debe ser con fines profilácticos o de anticoagulación, parece ser que la anticoagulación con dosis plenas debe indicarse en pacientes con trombosis documentada[4].

La trombosis vascular, en especial tromboembolismo venoso y la tromboembolia pulmonar (TEP) observada a nivel clínico y en autopsias[5], es un hallazgo relativamente frecuente en el COVID-19, pero su comportamiento desconcierta, ya que las escalas habituales para evaluar riesgo y probabilidad clínica de trombosis fallan, así también lo hacen los tratamientos farmacológicos usuales como la trombólisis, la antiagregación y la anticoagulación.

La ecocardiografía al pie de cama del paciente es una herramienta robusta, aun cuando no de primera línea, para el diagnóstico de episodios tromboembólicos pulmonares masivos, y que permite tomar decisiones terapéuticas inmediatas en pacientes con inestabilidad hemodinámica. Datos como el signo de 60/60 y depresión de la contractilidad del ventrículo derecho con evidencia de signo de McConnell son sugestivos de embolia pulmonar[6]. En la COVID 19 se consiguen pacientes sin expresión ecocardiográfica de sobrecarga del ventrículo derecho y si angiotomografía pulmonar positiva para embolismo; tal vez, por la formación de trombosis pulmonares in situ y no provenientes de émbolos de miembros inferiores.

A continuación, presentamos la estadística de los casos de tromboembolia pulmonar, en una serie de 227 pacientes atendidos en nuestra terapia intensiva (tabla 1); 15 pacientes (6%) tuvieron TEP, el 76% fueron hombres y el diagnóstico se realizó con ecocardiografía transesofágica o con angiotomografía pulmonar. La mortalidad fue del 80% y antes del evento todos los pacientes tenían heparina fraccionada a dosis de anticoagulación. A 7 pacientes se les administró terapia trombolítica con estreptoquinasa o con activador del plasminógeno tisular, con resultados no alentadores, ya que sobrevivió solo 1 paciente. Los niveles de dímero D al ingreso y a las 72 horas no parecen guardar relación con la génesis de trombosis en esta serie.

Por lo escrito, el diagnóstico de tromboembolia pulmonar en el paciente con COVID-19 críticamente enfermo tiene una incidencia relativamente elevada, con alta mortalidad, sin una prueba "gold stantard" para el diagnóstico y sin la certeza de la utilidad de la anticoagulación, antiagregación y trombólisis, que eran estrategias farmacológicas tradicionales para el manejo de esta entidad. Esperamos la publicación de trabajos en curso sobre esta temática que aclaren el panorama y nos permitan contar con más herramientas diagnósticas y terapéuticas que mejoren el pronóstico de estos enfermos.

Referencias bibliográficas

1. Ciceri, F.; Beretta, L.; Scandroglio, A.M.; Colombo, S.; Landoni, G.; Ruggeri, A.; Peccatori, J.; D'Angelo, A.; De Cobelli, F.; Rovere-Querini, P.; et al. Microvascular COVID-19 lung vessels obstructive thromboinflammatory syndrome (MicroCLOTS): An atypical acute respiratory distress syndrome working hypothesis. Crit. Care Resusc. 2020. Available online: https://pubmed.ncbi.nlm.nih.gov/32294809/
2. Mosleh W, Chen K, Pfau SE, Vashist A. Endotheliitis and Endothelial Dysfunction in Patients with COVID-19: Its Role in Thrombosis and Adverse Outcomes. Journal of Clinical Medicine. 2020; 9(6):1862. https://doi.org/10.3390/jcm9061862
3. Varga, Z.; Flammer, A.J.; Steiger, P.; Haberecker, M.; Andermatt, R.; Zinkernagel, A.S.; Mehra, M.R.; Schuepbach, R.A.; Ruschitzka, F.; Moch, H. Endothelial cell infection and endotheliitis in COVID-19. Lancet 2020, 95, 1417–1418. [Google Scholar]
4. INSPIRATION Investigators. Effect of intermediate-dose vs standard-dose prophylactic anticoagulation on thrombotic events, extracorporeal membrane oxygenation treatment, or mortality among patients with COVID-19 admitted to the intensive care unit: the INSPIRATION randomized clinical trial. JAMA. Published online March 18, 2021. doi:10.1001/jama.2021.4152
5. Wichmann D, Sperhake JP, Lütgehetmann M,et al. Autopsy findings and venousthromboembolism in patients with COVID-19:a prospective cohort study.Ann Intern Med.2020;173(4):268-277. doi:10.7326/M20-200
6. Stavros V. Konstantinides, , Guy Meyer, et al Cecilia Becattini2019 ESC Guidelines for the diagnosis and management of acute pulmonary embolism developed in collaboration with the European Respiratory Society (ERS) The Task Force for the diagnosis and management of acute pulmonary embolism of the European Society of Cardiology. European Heart Journal 2020 : 41, 543 – 603 doi:10.1093/eurheartj/ehz405.

[1] Hospital Pablo Arturo Suárez, Unidad de Terapia Intensiva, Centro de Investigación Clínica, Quito, Ecuador y Universidad Central del Ecuador, Facultad de Ciencias Médicas, Quito, Ecuador.
[2] Hospital Pablo Arturo Suárez, Servicio de Cardiología Clínica y Ecocardiografía, Quito, Ecuador.
[3] Hospital Pablo Arturo Suárez, Unidad de Terapia Intensiva, Centro de Investigación Clínica, Quito, Ecuador.

Corresponding author: jlvelez@uce.edu.ec

	EDAD	SEXO	DD ingreso	DD 72 h	Test Diagnóstico	Trombolítico	Condición al alta
1	61	M	2625	813	AgioTAC pulmonar	Estreptoquinasa	Muerto
2	65	M	9743	2458	Ecocardiograma	Ateplasa	Muerto
3	49	M	919	1311	Ecocardiograma	Ateplasa	Muerto
4	65	M	996	10000	Ecocardiograma	Estreptoquinasa	Muerto
5	68	M	9839	7261	AgioTAC pulmonar	No	Muerto
6	41	M	5710	4825	Ecocardiograma	Estreptoquinasa	Vivo
7	60	F	4947	1922	Ecocardiografía	Estreptoquinasa	Muerto
8	59	M	10000	1801	Ecocardiografía	No	Muerto
9	55	F	467	-	AngioTAC pulmonar	No	Muerto
10	57	M	1661	526	AngioTAC pulmonar	No	Muerto
11	35	M	545	632	AngioTAC pulmonar	Estreptoquinasa	Muerto
12	55	F	4201	-	AngioTAC pulmonar	No	Vivo
13	65	M	835	5824	AngioTAC pulmonar	No	Muerto
14	48	F	538	885	AngioTAC pulmonar	No	Muerto
15	51	M	10000	1552	AngioTAC pulmonar	No	Vivo
	Media: 55,6	**M74%/F26%**	**Media: 3535**	**Media: 2654**	**ECO:6/AngioTAC:9**		**Mortalidad: 80%**

Tabla 1. Casos de tromboembolia pulmonar, datos clínicos, tratamiento y desenlace.

RESEARCH / INVESTIGACIÓN

Safety and immunogenicity in piglets of two immunization schedules initiated at two or three weeks of age with Porvac®, a classical swine fever subunit marker vaccine

Aymé Oliva-Cárdenas[1], Fé Fernández-Zamora[2], Elaine Santana-Rodríguez[1], Yusmel Sordo-Puga[1], Milagros de la C. Vargas-Hernández[1], María P. Rodríguez-Moltó[1], Danny Pérez-Pérez[1], Talia Sardina-González[1],Carlos A. Duarte[1], Avelina León-Goñi[2], Diurys Blanco -Gámez[2], Francisco Contreras-Pérez[2], Odalys Valdés-Faure[2], Rosmery Hernández-Prado[1], Eric Acosta-Lago[2], Ileana Sosa-Testé[2], Marisela F. Suárez-Pedroso[1]

DOI. 10.21931/RB/2021.06.03.3

Abstract: Classical swine fever is a highly contagious viral disease with a significant impact on food production worldwide. It currently represents one of the main limitations for the development of the pig industry in Cuba. Porvac® is a subunit marker vaccine that confers a very rapid onset of protection. Since there are different production systems in pig breeding, readjustments in the vaccination program are often required. This study compares the safety and efficacy in piglets of two vaccination schedules with Porvac® (0-2 weeks and 0-3 weeks), initiated at two or three weeks of age. Clinical monitoring was conducted, and a neutralization peroxidase-linked assay was used to measure the neutralization titers. All immunization regimens were safe and well-tolerated, without local or systemic adverse reactions in the vaccinated animals. Geometric mean neutralizing antibody titers higher than 1/1500 were detected in all groups during the six months of the trial. One month after the second immunization, piglets primed at two weeks of age, and boostered three weeks later, developed significantly higher neutralization titers (1/15644) compared to those vaccinated at a similar age but with a two-week interval between doses (1/5760). However, no significant differences in the titers were found three and six months after vaccination among the four regimens. In summary, all the variants studied are effective, but it is recommended to start vaccination at two weeks old, with the second dose at either two or three weeks later, depending on the production system and the purpose of the farm.

Key words: Classical swine fever, E2CD154, subunit vaccine, piglets, neutralizing antibodies.

Introduction

Classical swine fever (CSF) is an infectious disease with the most significant economic impact on the swine industry in Cuba and many other countries. The disease is caused by the classical swine fever virus (CSFV), an enveloped, single-stranded RNA Pestivirus. Due to its devastating effects, CSF has been listed as a notifiable disease by the World Organization for Animal Health (OIE)[1]. In endemic areas, prophylactic vaccination is commonly used to limit the effects of the disease or as a first step within a general program to control and eradicate the virus. The modified live vaccines (MLV) are the most widely used in CSF endemic regions and have effectively controlled the disease in several countries such as Brazil, Argentina, and Uruguay.

On the other hand, Cuba is one CSF endemic country where the virus has been emerging for more than 20 years despite the use of an attenuated C strain MLV[2-4]. The lack of discrimination between infected and vaccinated animals, the requirement for a cold chain of distribution, and the interference of maternal-derived neutralizing antibodies (MDNA) are the main drawbacks of MLV, which have limited its use in disease-free regions. Several subunit vaccines have been developed to overcome these drawbacks, but they exhibit a late onset of protection as compared to MLV and provide insufficient protection against vertical transmission[5-8].

Porvac® is a Cuban subunit marker vaccine against CSFV, which is based on a recombinant chimeric antigen comprising the E2 protein of CSFV and the molecular adjuvant CD154. This vaccine has been safe and capable of inducing an unusually rapid onset of protection against a challenge with a highly pathogenic CSFV strain, which is similar to the one described for MLV[9-11]. Porvac® induces both high neutralizing antibodies (NAb) titers and cell-mediated immune response and can interfere with the transmission of the virus from pregnant sows to their offspring[12].

Porvac® has been registered in Cuba and is been currently used in both, large state-owned pig production units and small private farms. Since there are different production systems in swine breeding, readjustments in the immunization schedules must make them compatible with those systems. The present study aimed to compare the safety and efficacy of two different immunization schedules with Porvac® (0-2 weeks and 0-3 weeks), starting at either two or three weeks after birth. These experiments must provide the scientific basis for a more flexible approach in terms of vaccination schedules for the different production systems.

Methods

Porvac® vaccine

The vaccine preparation was obtained from the stable HEK 293 cell line (ATCC CRL1573), which expressed the CSFV E2 antigen fused to the porcine CD154 protein. It was produced under Good Manufacturing Practices in a certified production area of the Center for Genetic Engineering of Camaguey, Cuba, and formulated as a water-in-oil formulation with Montanide ISA50V2 (SEPPIC, France) at a final concentration of 25 µg of E2-CD154 antigen/ mL.

[1] Departamento de Biotecnología Animal, Centro de Ingeniería Genética y Biotecnología (CIGB), Playa, Cuba.
[2] Centro para la Producción de Animales de Laboratorio (CENPALAB), Centro de Toxicología Experimental (CETEX), Boyeros, La Habana, Cuba.

Corresponding author: ayme.oliva@cigb.edu.cu

Experimental animals

The study included the litters from four unvaccinated CSFV-negative sows (Duroc x Yorkshire crossbred swine). The piglets were kept with their mothers until weaning, between 33 and 42 days, each group in a separate experimental room. Trials were carried out under appropriate high containment conditions following the animal welfare regulations and standards according to Good Clinical Practices[13-15]. The study was approved and supervised by the Committee for Care and Use of Laboratory Animals (CICUAL) of the Center for the Production of Laboratory Animals (CENPALAB).

The general clinical conditions of the animals were evaluated during the immunization period, especially the occurrence of adverse reactions at the injection site. The rectal temperature was measured immediately before the first vaccination and 72 hours after each vaccine administration. Blood samples were taken from the ophthalmic venous sinus in the absence of anticoagulant, previous to the first immunization (T0) and at one, three, and six months after the second immunization (T1, T3, and T6, respectively). Hematological and biochemical analyses were conducted at the analytical laboratory of CENPALAB. The levels of total protein, glucose, alkaline phosphatase, alanine aminotransferase, aspartate aminotransferase, albumin, creatinine, uric acid, and urea were measured a Cobas Integra 400 PLUS Analyzer (Roche DiagnosticSystems).

Vaccination

Four experimental groups (G2-2, G2-3, G3-2, and G3-3) were formed with complete litters comprising 9 and 12 piglets per group. Two groups included 2-week old piglets, and the other two were formed with 3-week old piglets on the day of prime vaccination. Each group was further subdivided to receive the vaccine with either two or three-week intervals between the priming and the booster. The intramuscular route inoculated a dose of 2 mL (50 µg of E2-CD154). The first immunization was performed on the right side of the neck and the second on the left side, using 18 x 1'' needles, in agreement with the good veterinary clinical practices.

CSFV-neutralizing antibodies detection

The serum samples were tested by Neutralization Peroxidase Linked Assay (NPLA) to determine the NAb titers against CSFV, following the methods described by OIE Manual[16,17]. National Center provided Margarita CSFV strain for Animal and Plant Health, Mayabeque, Cuba, and the anti E2 Mab CBS-SE2.3 conjugated to horseradish peroxidase by CIGB-Sancti Spiritus, Cuba.

Data analysis

Data analysis was performed using package GraphPad Prism 6 (Prism 6 for Windows, Version 6.01, GraphPad Software, Inc., La Jolla, USA). The Kolmogorov-Smirnov test was used to evaluate normality, and the Levene test assessed the homogeneity of variances in the data. One-way ANOVA, followed by Tukey multiple comparison tests, was applied to compare the temperature values among groups. Kruskal-Wallis non-parametric test, followed by the Dunn test, was used to compare the geometric means (GM) of the antibody titers among the different groups. Statistical significance was considered when $p < 0.05$.

Results

Evaluation of the clinical signs during the 6 months follow-up

The animals exhibited good health conditions at the beginning of the trial. After vaccination, they showed no signs of inflammation, redness, or induration at the inoculation site. No systemic adverse effects or other alterations were observed, regardless of the age of the animals at vaccination and the vaccination schedule applied.

Evaluation of the body temperature during the immunization period

The rectal temperature was monitored before the immunizations as a part of the assessment of the health status of the animals. Subsequent measures of the body temperature were done at 72 h after each immunization (Figure 1). Mean body temperature in all the groups remained within the physiological range, although some hyperthermia values were observed in G2-2 and G2-3 before vaccination and 72 h later. No significant differences were found between the immunization days and 72 h later; therefore, the high values of temperature registered for some individuals were not associated with vaccination. Animals remained healthy until the end of the trial.

Evaluation of hematological and biochemical parameters

The hematological and biochemical parameters of the animals were evaluated before and three months after vaccination (tables 1 and 2). Although some variability was observed at the initial measurements at 15 or 21 days of age, no differences were found among the four groups three months after vaccination (ANOVA $p < 0.05$). At that time all the values were within the normal ranges for the species.

Immunogenicity of Porvac® in piglets

All piglets were CSFV seronegative at the beginning of the study, with NAb titers lower than 1/5. One month after receiving two immunizations, all animals developed NAb titers of 1/3200 or higher, regardless of the schedule applied (Figure 2). Statistical differences were documented among groups (Kruskal-Wallis, $p<0.05$). NAb titers were lower in group G2-2 (GM =1/5552) as compared with groups G2-3 (GM = 1/12800) and G3-3 (GM =1/8300) (Dunn test, $p<0.05$). No significant differences were found between the groups immunized at two and three weeks (G2.2 vs. G3.2 (GM=1/11943) and G2.3 vs. G3.3).

In the evaluation conducted three months after the second immunization, all groups exhibited GM NAb titers above 1/9000, without significant differences among them (Kruskal-Wallis, $p>0.05$).

Six months after vaccination, the NAb titers had decreased as expected, although they remained equal to or higher than 1/400 in all animals. Finally, six randomly selected animals from the different schemes were followed up one year after vaccination. Interestingly, NAb titers of these pigs remained ≥ 1/400 at this time.

Discussion

Vaccination is the most important activity within the CSF prevention program in endemic countries like Cuba since different pig farms use diverse production systems, the evaluation of different vaccination regimes with Porvac® is an important step to adjust vaccination to those production systems.

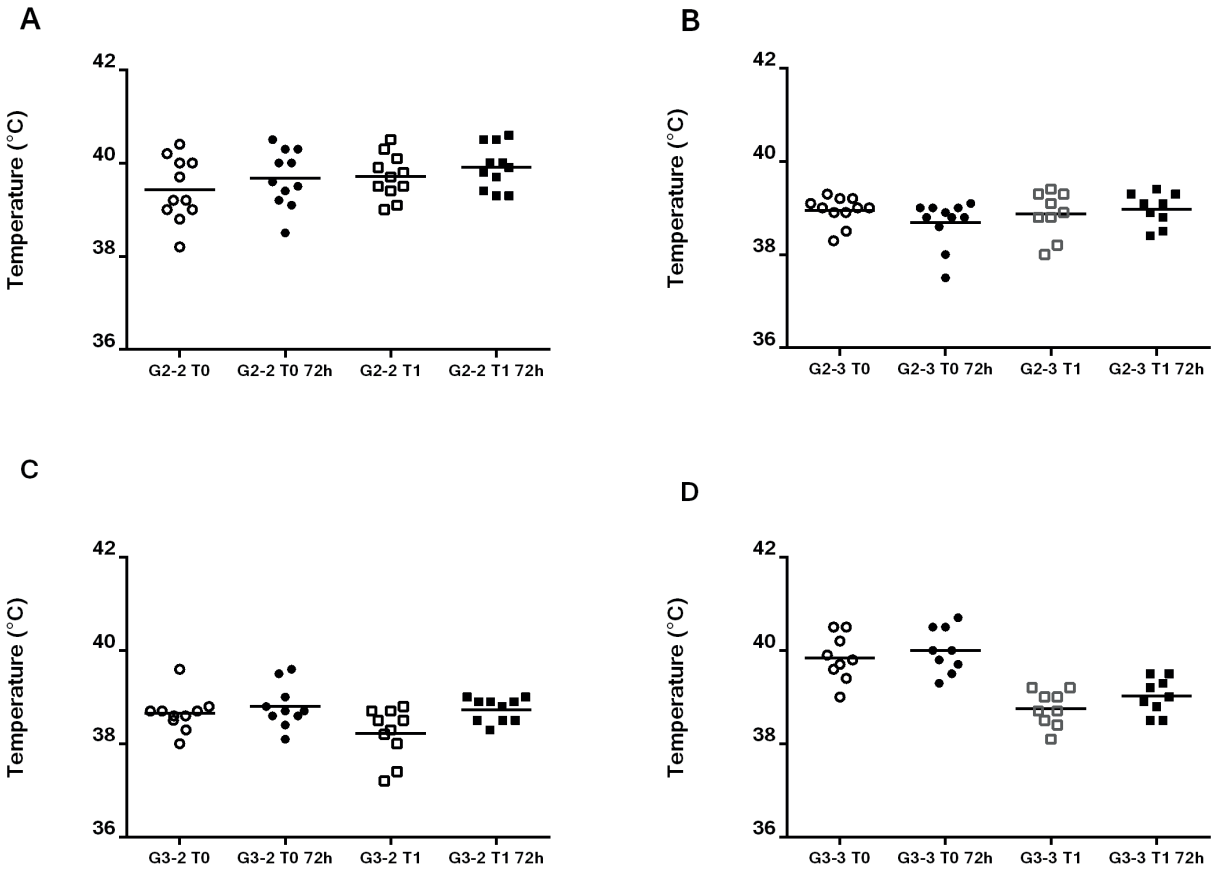

Figure 1. Evaluation of the rectal temperature before and after the vaccination.

In this study, we have evaluated the safety and immunogenicity of four immunization regimens with Porvac®. Two variables were explored: (1) age for the first administration and (2) time interval between the priming and booster doses.

The four regimens were safe and well-tolerated. Neither systemic nor local adverse reactions were observed nor temperature changes associated with vaccination. Those results confirm pre-registration studies in pigs of different ages with this vaccine[10-12,18]. They are also by those obtained in a pre-registration study with a CP7_E2alf marker vaccine and animals of similar age[19].

Concerning some elevated temperature values registered during the immunization period, the physiological temperature in pigs ranges between 38.7 and 39.7 ° C, although this range could reach 40.2 °C in piglets during the first weeks after birth[20]. Our study was conducted between spring and summer with maximum values of ambient temperature above 30° C. This environmental situation can lead to a condition called heat stress, which is characterized by modifying the physiological constants of the animals[21]. Therefore, the experimental manipulations in one of the most sensible pig's categories, and the heat stress could have influenced the temperature ranges observed.

The development of the innate immune system in pigs begins early during gestation. The newborn piglet already has a naive adaptive immune system with low blood levels of natural antibodies, which recognize the most common pathogens[22,23]. Piglets achieve full maturity in their immune system after four weeks of life, which guarantees an adequate immune response to vaccines[24]. Previous studies conducted with other vaccines have found that five-week-old piglets developed a superior NAb response compared to those immunized two weeks earlier[24].

However, in the present study, even two-week-old naïve

	Time (months)	G2-2	G2-3	G3-2	G3-3
Leukocytes (10^9cells/L)	**0**	10.8 ± 1.6	11.3 ± 3.1	13.1 ± 3.1	9.0 ± 2.6
	3	16.0 ± 1.8	16.9 ± 2.7	13.9 ± 2.6	15.7 ± 1.6
Neutrophils (%)	**0**	19.4 ± 5.9	29.5 ± 7.6	38.4 ± 11.1	23.9 ± 5.3
	3	21.1 ± 9.4	30.3 ± 10.5	33.5 ± 8.7	31.1 ± 13.6
Lymphocytes (%)	**0**	80.7 ± 6.0	69.5 ± 7.6	60.9 ± 11.5	75.1 ± 6.2
	3	78.0 ± 9.8	68.9 ± 10.7	64.4 ± 8.1	68.0 ± 13.7
Monocytes (%)	**0**	0.55 ± 0.7	0.64 ± 0.7	0.44 ± 0.73	68.0 ± 13.7
	3	0.50 ± 0.8	0.43 ± 0.5	0.5 ± 0.53	0.3 ± 0.5
Eosinophils (%)	**0**	0.27 ± 0.5	0.36 ± 0.5	0.22 ± 0.44	0.7 ± 0.9
	3	0.38 ± 0.5	0.43 ± 0.5	1.63 ± 1.6	0.9 ± 0.9
Basophils (%)	**0**	0	0	0	0
	3	0	0	0	0

Table 1. Hematological parameters of the animals before and 3 months after vaccination.

Biochemical Parameters	Time (months)	G2-2	G2-3	G3-2	G3-3
Glucose (mmol/L)	0	8.9 ± 1.31	7.1 ± 0.8	7.3 ± 1.8	6.9 ± 1.5
	3	6.0 ± 0.5	5.0 ± 1.0	6.5 ± 1.9	5.2 ± 1.0
Albumin (g/L)	0	38.3 ± 2.6	34.3 ± 3.73	36.5 ± 5.7	32.8 ± 8.7
	3	38.3 ± 2.6	30.7 ± 1.4	38.3 ± 4.7	33.9 ± 4.4
Total protein g/L	0	50.6 ± 3.0	52.1 ± 3.1	50.9 ± 7.8	44.0 ± 10.7
	3	55.6 ± 6.6	55.1 ± 11.0	66.0 ± 5.0	55.9 ± 5.1
Urea (mmol/L)	0	2.4 ± 0.7	3.7 ± 1.44	4.2 ± 1.7	5.2 ± 6.0
	3	7.7 ± 1.4	7.7 ± 1.3	9.5 ± 0.8	6.0 ± 1.5
Creatinine (µmol/L)	0	79.0 ± 6.6	82.2 ± 13.8	91.1 ± 12.5	80.8 ± 30.3
	3	92.1 ± 11.9	103.4 ± 14.0	98.4 ± 20.5	89.9 ± 9.7
Uric acid (µmol/L)	0	4.0 ± 1.6	2.2 ± 1.32	1.7 ± 2.4	3.0 ± 5.6
	3	1.25 ± 1.4	0.63 ± 1.4	0.4 ± 0.5	0.4 ± 0.5
Aspartate aminotransferase (UI/L)	0	59.2 ± 6.7	34.8 ± 10.6	61.1 ± 27.5	50.4 ± 34.2
	3	38.5 ± 5.7	44.1 ± 10.2	66.0 ± 41.2	51.7 ± 17.0
Alkaline phosphatase (UI/L)	0	1013.6 ± 182	617.2 ± 236	290.9 ± 46.1	316.1 ± 139
	3	129.8 ± 26.8	129.6 ± 20.1	125.6 ± 18.4	109.7 ± 20.0
Alanine aminotransferase (UI/L)	0	34.5 ± 4.5	28.2 ± 7.1	41.0 ± 9.9	31.1 ± 12.3
	3	63.3 ± 11.7	55.5 ± 9.0	54.4 ± 4.1	63.8 ± 14.5

Table 2. Biochemical parameters of the animals before and 3 months after vaccination.

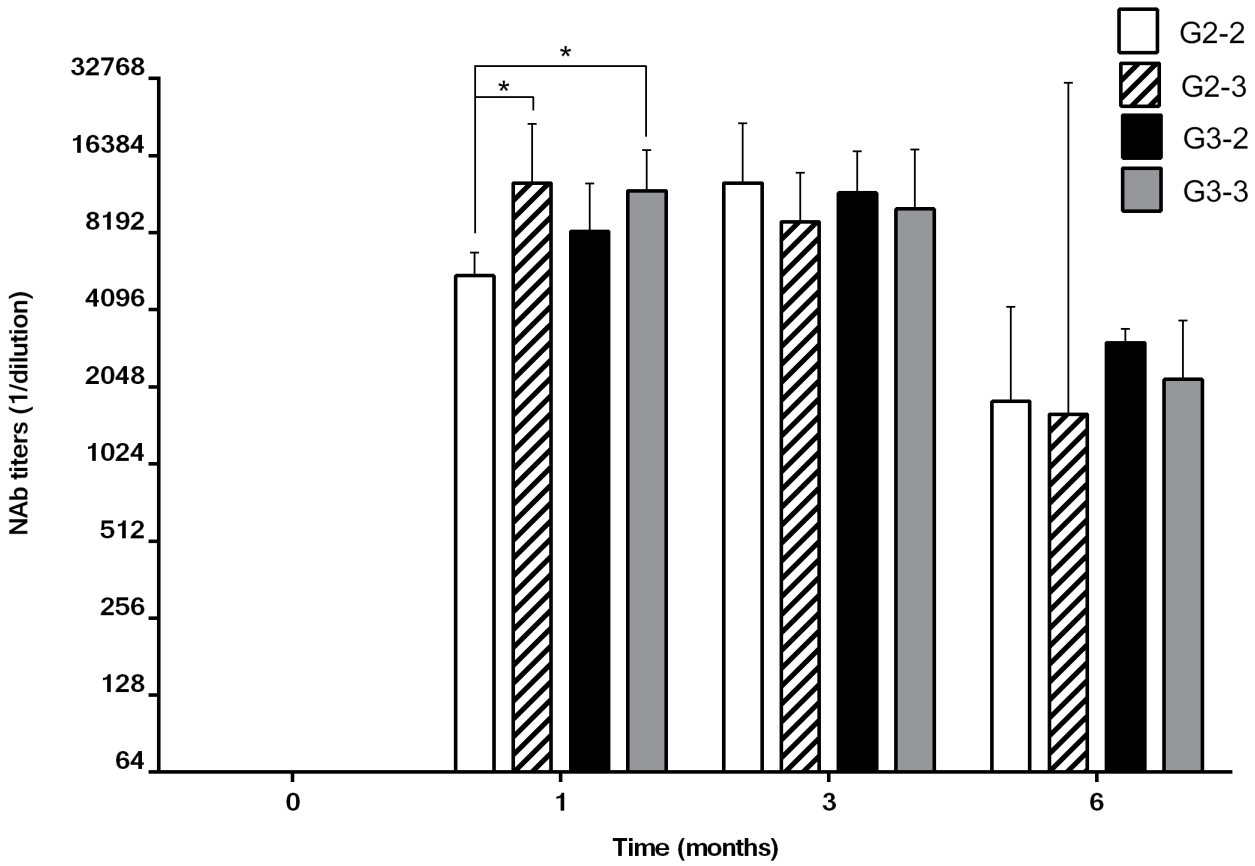

Figure 2. CSFV NAb titers in all experimental groups during the six months follow-up study.

piglets could induce a potent NAb response against CSFV after vaccination with Porvac®. Similar levels of NAb were measured in those animals, at any of the time points evaluated, compared with the group immunized at the age of three weeks.

Additionally, the findings suggest that a three-week interval between immunizations is more effective than two weeks to induce NAb, although these results were found only one month after vaccination. Those differences faded over time and were found neither at 3 nor at 6 months after vaccination.

Even so, it should be noted that, from a practical point of view, the differences above are irrelevant since the NAb titers elicited by the four regimes studied were manifold higher than the protective threshold of 1/50, previously defined by other investigators[25,26].

The high immunogenicity of Porvac®, even at this very early age, is probably due to the action of the CD154 protein (CD40L), which functions as a molecular adjuvant. This molecule is directly involved in the activation and maturation of B lymphocytes, which occupy a central role in the immune response, functioning as precursors of antibody-secreting cells and effective antigen-presenting cells (APC). CD154 also interacts with professional APC such as dendritic cells, promoting their maturation and activation[27,28].

Finally, those results confirm previous findings that PorvacÒ can promote a long-lasting response, which is welcome for breeding gilts and boars, although immune protection for 7–8 months is sufficient for growing and fattening pigs[29]. In the present study, when the vaccinated animals arrived at reproductive age still exhibited protective NAb levels against CSFV, demonstrating that a long-lasting humoral immune response can also be generated by immunizing two-week-old naïve piglets Porvac®. This agrees with the results of pre-registration controlled trials conducted by Suárez *et al.*, 2011[11], where protective NAb titers were still detected at 9 months post-vaccination.

This study was conducted in naïve animals born to unvaccinated sows; therefore, they did not have MDNA at vaccination. It is well known that MDNA can interfere with active immunity, mainly described for MLVs[24,30,31]. However, previous studies have already demonstrated that pre-existing MDNA does not interfere with the immunogenicity of Porvac®[18]. Therefore, it is very likely that the results shown here could be safely extrapolated to those piglets born to Porvac® vaccinated sows.

Conclusions

A three-week interval between doses induced higher NAb titers than a 2-week interval in piglets vaccinated with 2 weeks of age. Those differences were only observed at 1 month, but not at 3 and 6 months after vaccination.

Regarding the time of the prime vaccination, no differences in the NAb response were found between 2 and 3 weeks of age.

The four immunization schedules evaluated in this study induced high titers of NAbs in naïve piglets, well above the protective threshold; therefore any of them could be used in pig production units, harmonized with their respective productive systems. As a general recommendation, all producers could apply the first dose of PorvacÒ at two weeks of age. The animals born in the genetic farms and reproductive centers would receive the second dose two weeks later. The rest of the farms, including medium and small-scale producers, may apply the second dose with either two or three week's interval depending on their production systems.

Acknowledgment

This research was supported by the Center for Genetic Engineering and Biotechnology, Havana, Cuba. The author acknowledges all researchers and technicians from the CENPALAB Center for their unconditional support in handling and care of the animals.

Bibliographic references

1. OIE. Classical Swine Fever (Infection with Classical Swine Fever Virus).
2. Fonseca-Rodríguez O, Centelles Garcia Y, Alfonso Zamora P, et al. Classical Swine Fever in a Cuban Zone Intended for Eradication: Spatiotemporal Clustering and Risk Factors. Frontiers in veterinary science 2020;7:38.
3. Perez LJ, Diaz de Arce H, Perera CL, et al. Positive selection pressure on the B/C domains of the E2-gene of classical swine fever virus in endemic areas under C-strain vaccination. Infection, genetics and evolution : journal of molecular epidemiology and evolutionary genetics in infectious diseases 2012;12:1405-12.
4. Coronado L, Rios L, Frías MT, et al. Positive selection pressure on E2 protein of classical swine fever virus drives variations in virulence, pathogenesis and antigenicity: Implication for epidemiological surveillance in endemic areas. Transboundary and emerging diseases 2019;66:2362-82.
5. Van Oirschot J. Vaccinology of classical swine fever: from lab to field. Veterinary microbiology 2003;96:367-84.
6. Dong XN, Chen YH. Marker vaccine strategies and candidate CSFV marker vaccines. Vaccine 2007;25:205-30.
7. Bouma A, De Smit A, De Jong M, De Kluijver E, Moormann R. Determination of the onset of the herd-immunity induced by the E2 sub-unit vaccine against classical swine fever virus. Vaccine 2000;18:1374-81.
8. Uttenthal A, Le Potier MF, Romero L, De Mia GM, Floegel-Niesmann G. Classical swine fever (CSF) marker vaccine. Trial I. Challenge studies in weaner pigs. Vet Microbiol 2001;83:85-106.
9. Sordo-Puga Y, Suárez-Pedroso M, Naranjo-Valdéz P, et al. Porvac® Subunit Vaccine E2-CD154 Induces Remarkable Rapid Protection against Classical Swine Fever Virus. Vaccines 2021;9:167.
10. Suárez M, Sordo Y, Prieto Y, et al. A single dose of the novel chimeric subunit vaccine E2-CD154 confers early full protection against classical swine fever virus. Vaccine 2017.
11. Suárez-Pedroso M, Sordo-Puga Y, Sosa-Teste I, et al. Novel chimeric E2CD154 subunit vaccine is safe and confers long lasting protection against classical swine fever virus. Veterinary Immunology and Immunopathology 2021;234:110222.
12. Muñoz-González S, Sordo Y, Pérez-Simó M, et al. Efficacy of E2 glycoprotein fused to porcine CD154 as a novel chimeric subunit vaccine to prevent classical swine fever virus vertical transmission in pregnant sows. Veterinary microbiology 2017;205:110-6.
13. VICH. Good clinical practices, GL09. 2000.
14. VICH. Target Animal Safety for Veterinary live and inactivated Vaccines, GL44. 2010.
15. VICH. Harmonization of criteria to waive target animal batch safety testing (TABST) for inactivated vaccines for veterinary use, GL50 2014.
16. OIE. OIE Terrestrial Manual. Chapter 3.8.3. Classical swine fever (hog cholera) infection with classical swine fever virus. In: OIE, ed.: OIE; 2019.
17. Terpstra C, Bloemraad M, Gielkens AL. The neutralizing peroxidase-linked assay for detection of antibody against swine fever virus. Vet Microbiol 1984;9:113-20.
18. Sordo-Puga Y, Pérez-Pérez D, Montero-Espinosa C, et al. Immunogenicity of E2CD154 Subunit Vaccine Candidate against Classical Swine Fever in Piglets with Different Levels of Maternally Derived Antibodies. Vaccines 2021;9:7.

19. Farsang A, Lévai R, Barna T, et al. Pre-registration efficacy study of a novel marker vaccine against classical swine fever on maternally derived antibody positive (MDA+) target animals. Biologicals : journal of the International Association of Biological Standardization 2017;45:85-92.
20. Mount L, Rowell J. Body size, body temperature and age in relation to the metabolic rate of the pig in the first five weeks after birth. The Journal of physiology 1960;154:408.
21. Carroll J, Burdick N, Chase Jr C, Coleman S, Spiers D. Influence of environmental temperature on the physiological, endocrine, and immune responses in livestock exposed to a provocative immune challenge. Domestic Animal Endocrinology 2012;43:146-53.
22. Butler J, Lager K, Splichal I, et al. The piglet as a model for B cell and immune system development. Veterinary immunology and immunopathology 2009;128:147-70.
23. Lim SI, Song JY, Kim J, et al. Safety of classical swine fever virus vaccine strain LOM in pregnant sows and their offspring. Vaccine 2016;34:2021-6.
24. Suradhat S, Damrongwatanapokin S, Thanawongnuwech R. Factors critical for successful vaccination against classical swine fever in endemic areas. Vet Microbiol 2007;119:1-9.
25. Terpstra C, Wensvoort G. The protective value of vaccine-induced neutralising antibody titres in swine fever. Vet Microbiol 1988;16:123-8.
26. Bironт P, Leunen J, Vandeputte J. Inhibition of virus replication in the tonsils of pigs previously vaccinated with a Chinese strain vaccine and challenged oronasally with a virulent strain of classical swine fever virus. Veterinary microbiology 1987;14:105-13.
27. Elgueta R, Benson MJ, de Vries VC, Wasiuk A, Guo Y, Noelle RJ. Molecular mechanism and function of CD40/CD40L engagement in the immune system. Immunol Rev 2009;229:152-72.
28. Xu Y, Song G. The role of CD40-CD154 interaction in cell immunoregulation. Journal of biomedical science 2004;11:426-38.
29. Hua RH, Huo H, Li YN, et al. Generation and efficacy evaluation of recombinant classical swine fever virus E2 glycoprotein expressed in stable transgenic mammalian cell line. PLoS One 2014;9:e106891.
30. Suradhat S, Damrongwatanapokin S. The influence of maternal immunity on the efficacy of a classical swine fever vaccine against classical swine fever virus, genogroup 2.2, infection. Veterinary microbiology 2003;92:187-94.
31. Vandeputte J, Too HL, Ng FK, Chen C, Chai KK, Liao GA. Adsorption of colostral antibodies against classical swine fever, persistence of maternal antibodies, and effect on response to vaccination in baby pigs. American journal of veterinary research 2001;62:1805-11.

Received: 3 April 2021
Accepted: 2 June 2021

RESEARCH / INVESTIGACIÓN

Assessing HeberFast® Line Gavac, a lateral flow immunochromatographic system for the rapid detection of anti-Bm86 antibodies in Gavac vaccinated cattle

Milagros Vargas-Hernández[*1], Yeni Hernández Lorenzo[2], Viviana Pluma Perez[2], Isabel Rosales-Garcia[2], Sunamit Rodríguez-Mendez[2], Enrique Pérez-Cruz[3], Daymi Abreu-Remedios[3], Carlos Montero-Espinosa[1], Ayme Oliva-Cardenas[1], Elaine Santana-Rodriguez[1], Danny Pérez-Pérez[1], Yusmel Sordo-Puga[1], Yohandy Fuentes-Rodríguez[1], Alianne Fundora-Llera[1], Carlos A. Duarte[1], Ernesto Galbán-Rodríguez[4], Carlos Hernandez-Diaz[3], Dayamí Dorta Hernandez[3], Ivis Pasaron Rodriguez[3], Marisela Suarez-Pedroso[1]
DOI. 10.21931/RB/2021.06.03.4

Abstract: *Rhipicephalus Boophilus* microplus cattle tick is a scourge for livestock production. The infestations produced by this pathogen are incompletely contained by chemical treatments, with the associated environmental pollution risks. Vaccination against cattle ticks has emerged as a feasible and environmentally friendly strategy to control tick-borne diseases. In this setting, Gavac® vaccine has proven effective in decreasing cattle tick populations through antibody responses against the tick Bm86 antigen, as part of an Integrated Control Program. However, animal vaccination programs require easy and ready-to-use screening tests to follow up the immune response in vaccinated animals under field conditions. This study reports the evaluation HeberFast® Line Gavac, a lateral flow immunochromatographic system for the rapid detection of anti Bm86 antibodies in vaccinated cattle. The system was tested on 598 serum samples taken from immunized animals, arranged in three groups according to their anti-Bm86 antibody response in ELISA (209 high, 150 medium or 239 low and 100 samples from non-immunized animals. The HeberFast® Line Gavac system was assessed for sensitivity, specificity, and concordance against the ELISA reference test. Consistency was evaluated among production batches and inter-analyst reading-independent consistency at two moments: ten minutes after completing the test and after strip drying. The system showed high sensitivity (81.6%, 82.2%, and 81%), specificity (96.7, 94.6, and 93.3%), and agreement with the ELISA reference test (75%; 74%, and 71%) for high, medium and low anti-Bm86 sera, respectively. The effectiveness of the diagnosis was 87.6; 87.1; 85.9 for high, medium, and low antibody titers, respectively. Consistency among production batches and analysts was documented, and no significant differences between evaluation times were found. These results indicate that HeberFast® Line Gavac is a valuable tool for the serological surveillance of Gavac vaccinated cattle.

Key words: Cattle tick, vaccination, antibody screening strip, lateral flow immunoassay, Bm86, Gavac®.

Introduction

Rhipicephalus (Boophilus) microplus cattle tick is a scourge for livestock production in tropical and subtropical areas. Ticks cause significant losses due to their direct weakening effects in cattle and through tick-borne diseases, ultimately causing animal death[1]. In Cuba, an Integrated Management Program for cattle tick control has been implemented nationwide. This program comprises the combination of Gavac®, a recombinant vaccine against cattle tick, with chemical acaricide treatments, scheduled according to the infestation index, and other measures for the biological, mechanical, immunological, and genetic control of the plague. The application of the vaccine has effectively sparse the number of acaricide treatments required, thereby reducing the environmental pollution risks and diminishing a 98% the deaths rates caused by hemoparasites[2-4].

The active ingredient of Gavac® is the tick gut Bm86 protein. Anti-Bm86 antibodies induced upon vaccination will attach to the gut epithelium of suckling ticks, with deleterious effects on their populations and the size of their progeny[5,6]. Regular immunizations are required to maintain protective anti-Bm86 antibody titers in the blood of the animals[6-8].

Commonly, antibody titers in sera of immunized animals are monitored through antigen-specific Enzyme-Linked Immunosorbent Assays (ELISA) tests, high efficiency, and specificity. However, such assays are troublesome under field conditions, time-consuming, and require specialized laboratory facilities and qualified personnel to perform and evaluate the results objectively. Thus, a fast and easy-to-use screening test is needed to implement and evaluate ongoing, and future cattle tick vaccination campaigns under field conditions.

Therefore, this study aimed to evaluate the performance of HeberFast® Line Gavac, a fast chromatographic screening test for the detection of anti-Bm86 antibodies, and its concordance with the reference ELISA test used in the laboratory. The main parameters to compare were sensitivity, specificity, and consistency.

Materials and methods

Material and Reagents

Ethical statement

Blood was extracted from cattle following an experimental protocol elaborated according to the ethics guidelines for animal care[9] and approved by the Ethics Committee of the Center for Genetic Engineering and Biotechnology (CIGB).

Serum collection and measurement of anti-Bm86 antibody titers by ELISA

Positive and negative anti-Bm86 antibody blood was collected from animals in units either under tick control programs

[1] Departamento de Biotecnología Animal, Dirección de Investigaciones Agropecuarias, Centro de Ingeniería Genética y Biotecnología, La Habana, Cuba.
[2] Unidad de Laboratorios Centrales de Sanidad Agropecuaria (ULCSA), Ministry of Agriculture, Cuba.
[3] Centro de Ingeniería Genética y Biotecnología, Santi Spirítus, Cuba.
[4] Editorial Elfos Scientiae, Dirección de Promoción y Distribución Nacional, CIGB, Cuba.

Corresponding author: milagros.vargas@cigb.edu.cu

with Gavac® vaccination or without vaccination. Blood was taken from healthy cattle, regardless of age, sex, or reproductive categories, and the sera were stored at –20oC until use.

ELISA measured the level of anti-Bm86 antibodies in sera. Briefly, ELISA microplates (Polysorp, Nunc, USA) were coated with Bm86 protein at 2 µg/mL and incubated overnight at 4ºC. Plates were washed with PBS-Tween 20 (0.05%), and blocked with 1% skimmed milk for 1 h at 37ºC. Sera was next diluted 1:500 in PBS-Tween 20 (0.05%) and 100 µL added to each well, and further incubated for 1 h at 37ºC. Next, a rabbit anti-bovine IgG antibody conjugated to horseradish peroxidase was added for 30 min at 37ºC. Finally, the reaction was developed with 0.5 mg/mL ortho-phenylenediamine and 0.015 % H_2O_2, and the reaction stopped 10 min later with H_2SO_4 (1%). The optical density (OD) was measured at 492 nm in an ELISA plate reader (Sunrise, Austria). A standard curve made with five 1:2 serial dilutions of an anti Bm86 positive reference serum reference, starting with 1:640, was used to interpolate the OD values of each serum. The anti Bm86 antibody values were expressed as absorbance units (AU)/mL. Three groups were formed according to the results of this evaluation:

Group 1. High responders: 209 positive samples with anti-Bm86 antibody values higher than 1000 AU/mL.

Group 2. Medium responders (gray zone): 150 samples with anti-Bm86 antibody values between 530 and 1000 AU/mL (minimum protective titers).

Group 3. Low responders: 239 samples with non-protective (negative) antibody values lower than 530 AU/mL.

Another group of negative sera with 100 samples from non-immunized animals was conformed.

HeberFast® Line Gavac

Bm86 protein and its conjugation to colloidal gold

The active pharmaceutical ingredient in GAVAC® vaccine was supplied by its manufacturer, the Center for Genetic Engineering and Biotechnology of Camagüey, Cuba. The conjugation of the Bm86 protein to colloidal gold was carried out according to Bailes *et al.*, 2012[10] using homemade 20 nm colloidal gold particles. The protein was solubilized in 0.005 mol/L of sodium chloride. The colloidal gold was also adjusted to pH 7 with 0.1 M K_2CO_3.

The following flocculation test first determined the amount of protein in relation to a fixed volume of gold: 500 µL of 20 nm colloidal gold at pH 7 were mixed with 100 µL of the protein solution in a range between 4 and 20 µg. The mixture was homogenized and incubated for 10 min at room temperature, and 500 µL of 10% sodium chloride solution was added to each reaction mixture. Finally, the conjugate content in the mixture was quantified by measuring the absorbance at 530 nm in a spectrophotometer (Thermo Scientific GENESYS 10S UV-Vis, Madison, USA).

Once the optimal amount of protein had been selected, the reaction was conducted for 30 min at -20 °C -25 °C, stirring at 300 rpm. The free sites on the colloidal gold particles were blocked with an adequate volume of 10% BSA, for a final concentration of 0.5 %. The final mixture was centrifuged at 16000 x g for 1 hour at 4°C. The conjugate obtained (pellet) was suspended in 0.1 M TBS, BSA 1% pH 7.0, and diluted up to an absorbance of 40 at a wavelength of 530 nm.

Preparation of the immunoreactive strip

The strip components were nitrocellulose (NC) membrane of 15 µm (MDI, type CNPC-SS12-L2-H50, dimensions 7,5 x 26 cm, 1,5 cm of NC), pad for the antigen-gold conjugate (MDI, type PTR-5, dimensions 2,7 x 26 cm), and absorbent pad (MDI, type AP080, dimensions 3,5 x 26 cm) . The conjugate was diluted to an absorbance of 20, at a wavelength of 530 nm and dispensed onto the antigen-gold conjugate pad.

The Bm86 protein, dissolved at 4 mg/mL in phosphate buffer saline (PBS) was absorbed into the membrane in the test line. The mixture of the control line components consisted of a monoclonal antibody against Bm86 protein provided by the Center for Genetic Engineering and Biotechnology of Sancti Spíritus, Cuba at 4 mg/ml, and 0.2 mg/mL of poly L-lysine, dissolved in PBS.

Both the macroporous material and the nitrocellulose membrane were sprayed with the BioDotQuanti 2000, BioJet, England, and then dried in an oven at 37 °C, for 30 min. The NC membrane cards were blocked for 1h at room temperature in blocking solution (0.02% (v/v) Tween 20, 0.02% (w/v) sodium azide, 5% (w/v) sucrose, and 0.5% bovine seroalbumin (BSA), dissolved in PBS. Later they were dried in the oven at 37 °C for 1 h.

Test strip assembly

The NC membrane was coupled in the center of polyvinyl chloride support. The absorbent pad and the conjugate pad were glued by overlapping 1 mm at the top and bottom of the NC Membrane, respectively. The sample pad was then glued by overlapping 2 mm on the bottom of the conjugate pad. The master assembled card was cut into 4 mm wide strips using a CM5000-guillotine-cutter (BioDot, Irvine, USA).

Immunochromatographic assay

The rapid, one-step, and visual reading lateral flow immunoassay (LFIA), branded HeberFast® Line Gavac, consists of a strip of nitrocellulose (NC) membranes to detect antibodies against the Bm86 antigen in bovine serum. The membrane consists of two phases: a fixed phase composed of the Bm86 protein as a capture biomolecule for the specific immunoglobulins present in the serum and a mobile phase containing a protein-colloidal gold marker conjugate, which finally develops the reaction with a specific dye.

Each strip was introduced into 80 µL of bovine serum (previously diluted 1:8 in buffer). The diluted sera migrated by capillarity within the macroporous material, dissolving the Bm86 conjugate labeled with colloidal gold. Two independent reactions could be observed in the virtual window. If the sample was positive, the immune complex reacted with the Bm86 protein attached to the NC membrane, forming a first horizontal redline Positive Line (PL). For all samples, the free conjugate was captured in a second red horizontal line Control Line (CL) where a polyclonal anti-IgG murine antibody is fixed to the solid phase.

Performance evaluation

Strips were used to detect antibody responses in 698 samples of bovine sera, from598 vaccinated and 100 unvaccinated animals. The results of the samples were interpreted at two moments, at the end of the reaction 10 min after the sample was applied and once the strip dried. LFIA tested samples in triplicate. The specificity, sensitivity, positive predictive value (PPV), negative predictive value (NPV), efficacy as well as kappa coefficient (K), were determined.

Kappa coefficient (K)

The Kappa coefficient was calculated to assess the level of significance of the agreement between the ELISA and the LFIA. The following ranges and their respective performance criteria were defined: 0.81-1.00, almost perfect agreement; 0.61-0.80, reasonable agreement, 0.60-0.41, moderate agreement; 0.40-0.21, discrete agreement, 0.20-0.01 insignificant agreement, and lower than 0.01, no agreement[11].

Batch to batch consistency

The samples from all panels were all evaluated by the three batches of strips (Gavac1501, Gavac1502, and Gavac1503). Results were considered valid for samples with coincident results with two different strip batches.

Inter-analyst interpretation

Three analysts read each sample, and results were regarded as valid when two out of the three observers coincided.

Statistical analysis

The LFIA and the ELISA reference system results were statistically compared using the epidemiological analysis of tabulated data (EPIDAT) software, version 3.1[12]. Concordance, sensitivity, specificity, efficacy, positive and negative predictive values, batch to batch consistency, and inter-analyst interpretation were compared. Statistical significance was considered for a 95 % confidence interval.

Results

Evaluation of the panel of samples from unimmunized animals.

All sera from unimmunized animals were negative. Only one signal appeared in the diagnostic control line, which guarantees the validity of the test. This represented a 100% of specificity for the system. Four representative samples from this group are shown in figure 1.

Evaluation of samples from immunized animals

All the strips used were accepted as valid, as the control line indicating their quality and reliability was observed. The intensity of the test capture region line varied depending on the concentration of immunoglobulins in the sample.

The overall false positive rate fluctuated between 3.34% and 6.69%, while a range of 4.78%-5.26% was found for false-negative results for the different lots and times evaluated. As expected, the percentage of false negative and false positive values was highly dependent on anti-Bm86 antibodies in the samples. Samples from group 2 (medium responders) showed the greatest incongruities when compared to the reference ELISA (36% - 38.7% of false negatives) (Table 1). The percentage of false-negative values dropped to 4.8%-5.2% in the group of high responders. On the other hand, the percentage of false positives in the ELISA negative sera was only 3.4-7.1%. Figure 1 shows 4 representative samples from each of the three groups evaluated.

The general agreement of the immunochromatographic strips with respect to ELISA was good for the 3 batches evaluated based on the kappa coefficient (Gav1501, Gav1502, and Gav1503) (Table 2).

The results of sensitivity, specificity, efficacy (test validity index), positive and negative predictive values, and confidence intervals of the 3 batches in studies are shown in Table 3.

Consistency between batches

The agreement among the three batches of strips evaluated (Gav1501, Gav1502, and Gav1503) is shown in Table 4. All batches exhibited high kappa coefficients, which indicate a good, or almost perfect degree of concordance. These results demonstrated the consistency of the manufacturing process.

Independence of the analysts

The concordance among the three analysts that read the assays ranged from good to almost perfect as the concentration of immunoglobulins increased. The results are shown in Table 5. The samples evaluated in the two moments gave no significant differences.

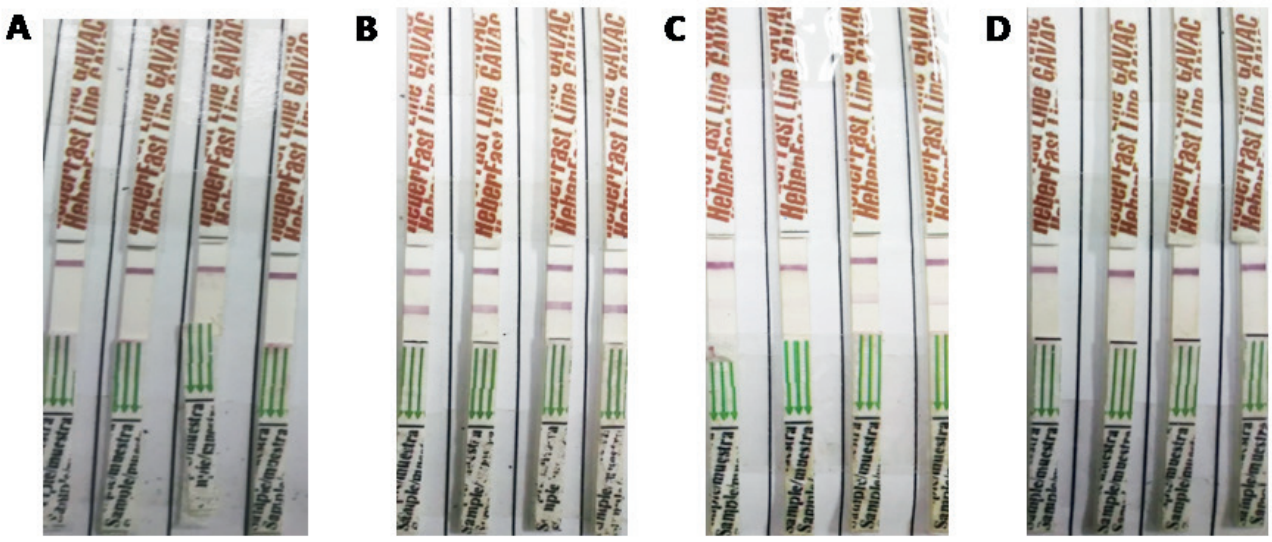

Figure 1. Evaluation of sera from Gavac immunizes animals and unvaccinated controls. Four representative samples per group were included. A: unvaccinated control group; B: high responders, (>1000 AU/mL); C: medium responders (530 - 1000 AU/mL); D: low responders (>530 AU/mL).

anti Bm86 ELISA values (n)	Lot Gav1501				Lot Gav1502				Lot Gav1503			
	reading 1		reading 2		reading 1		reading 2		reading 1		reading 2	
Group 1	P	N	P	N	P	N	P	N	P	N	P	N
> 1000 AU/mL	198	11	198	11	199	10	199	10	199	10	199	10
(209)	94.8 %	5.2%	94.8 %	5.2%	95.2 %	4.8%	95.2 %	4.8%	95.2 %	4.8%	95.2 %	4.8%
Group 2	P	N	P	N	P	N	P	N	P	N	P	N
530-1000 AU/mL	95	55	96	54	96	54	97	53	92	58	92	58
(150)	63.3%	36.7%	64%	36%	64%	36%	64.7%	35.3%	61.3 %	38.7%	61.3 %	38.7%
Group 3	P	N	P	N	P	N	P	N	P	N	P	N
<530 AU/mL	8	231	8	231	13	226	13	226	16	223	17	222
(239)	3.4%	96.6%	3.4%	96.6%	5.4%	94.6%	5.4%	94.6%	6.7%	93.3%	7.1%	92.9%

Reading 1: reading done immediately after the end of the assay (10 min); reading 2: reading done after the strip was dried. The percentages represent the % of agreement of the positive or negative values with respect to the ELISA.

Table 1. Evaluation of the diagnostic strips with a panel of positive anti-Bm86 sera.

Parameters	Reading	Gav1501	Gav1502	Gav1503
Kappa	1	0.75	0.74	0.71
	2	0.74	0.74	0.71
CI	1	0.70-0.80	0.69-0.79	0.66-0.77
	2	0.69-0.80	0.69-0.80	0.66-0.77
Agreement	1	Good	Good	Good
	2	Good	Good	Good

CI, confidence intervals

Table 2. General agreement between the immunochromatographic assay and the reference ELISA.

Parameters	Reading	Gav1501	Gav1502	Gav1503
Sensitivity	1	81.6 (77.5-85.8)	82.2 (78-86,3)	81 (76.9-85.2)
	2	81.9 (77.8-86.3)	82.4 (78.4-86.5)	81 (76.9-85.2)
Specificity	1	96.7 (94.2-99.2)	94.6 (91.5-97.6)	93.3 (89.9-96.7)
	2	95.4 (92.5-98.3)	94.1 (91-97.3)	92.9(89.4-96.4)
Efficacy	1	87.6 (84.9-90.3)	87.1 (84.4-89.9)	85.9 (83- 88.8)
	2	87.3 (84.5-90)	87.1 (84.4-89.9)	85.8 (82.9- 88.7)
PPV	1	97.3 (95.4-99.3)	95.8 (93.4-98.2)	94.8 (92.2-97.4)
	2	96.4 (94.2-98.6)	95.5 (93-98)	94.5 (91.8-97.2)
NPV	1	77.8 (72.9-82.7)	77.9 (73-82.9)	76.6 (71.6-81.7)
	2	77.8 (72.9-82.7)	78.1 (73.2-83)	76.5 (71.5-81.6)

Average (95 % confidence interval). PPV: positive predictive value, NPV: negative predictive value.

Table 3. Performance of the immunochromatographic system.

Discussion

Tick mitigation strategies are part of a long tradition and focus on the local application of acaricides or the search for biological products that reduce the impact of the problem[13]. The use of the Gavac® immunogen within a control program decreases the reproductive parameters of the tick through the specific antibodies developed in the immunized animals[14]. Moreover, the fast development of anti-Bm86 antibody levels guarantees herds immunity and the effective control of tick populations[4].

In this setting, the development of rapid, specific, sensitive, and economically feasible diagnostic methods such as LFIA is of paramount relevance in veterinary medicine. They support the massive screening of samples in a shorter time under field conditions and the early detection of pathogens, further providing specific treatments and monitoring for the control epidemiological units[15].

In this study, the performance of the HeberFast® Line Gavac immune screening test was evaluated for detecting anti-Bm86 antibody titers in sera of immunized cattle. The sensitivity and specificity of the immunochromatographic system for the three batches under study were in the 81-82% and 92-95% ranges, respectively. Similar results have been previously reported for the use of LFIA strips for massive screening. For instance, the direct Sensitive Membrane Antigen Rapid Test

Batches	Positivity criteria	Reading	Parameters			
			Kappa	IC 95 %	P. estad. z	Consistency
Gav1501	Positive	1	0.9252	0.8177-1.0000	23.1678	Almost Perfect
		2	0.9321	0.8350-1.0000	23.3405	
	Gray zone	1	0.8782	0.8135-0.9429	18.6291	Almost Perfect
		2	0.8866	0.8236-0.9495	18.8067	
	Negative	1	0.7459	0.5548-0.9368	19.9723	Good
		2	0.7221	0.5500-0.8941	19.3360	
Gav1502	Positive	1	0.8915	0.7640-1.0000	22.3240	Almost Perfect
		2	0.8915	0.7640-1.0000	22.3240	
	Gray zone	1	0.9226	0.8697-1.0000	19.5719	Almost Perfect
		2	0.9319	0.8818-0.9820	19.7690	
	Negative	1	0.9494	0.8768-1.0000	25.4224	Almost Perfect
		2	0.9526	0.8847-1.0000	25.5071	
Gav1503	Positive	1	0.9661	0.8959-1.0000	24.1902	Almost Perfect
		2	0.9661	0.8959-1.0000	24.1902	
	Gray zone	1	0.9344	0.8862-0.9826	19.8218	Almost Perfect
		2	0.9443	0.9001-0.9886	20.0325	
	Negative	1	0.8925	0.7972-0.9877	23.8984	Almost Perfect
		2	0.8981	0.8079-0.9883	24.0491	

1: reading immediately after the end of the assay (10 min); 2: reading after the strip was dried

Table 4. Consistency in production.

(SMART®; New Horizons Diagnostics Corp., USA) and the direct Pathogen Detection Kit® (PDK; Intelligent Monitoring Systems, USA) were reported to display 100 % sensitivity for cholera diagnosis in diarrheal and semi-formed stool samples, and in intestinal contents of corpses. Furthermore, 100 % specificity was also attained with SMART®, while the same parameter for direct PDK® ranged between 77.4% and 85.7%, depending on sample type[16]. In immunochromatographic studies to detect Giardia spp. and Cryptosporidium spp. in feces, 58-97.2 % sensitivity and 99-100 % specificity were reported[17,18].

In summary, diagnostic tests must perform with high specificity and sensitivity to avoid false positives or false negative results. This is more relevant when diagnosing severe illnesses or other conditions able to compromise herd health and integrity and devoid of any contingency measures other than animal sacrifice. A misdiagnosis can lead to serious economic losses in those situations, as forum treatable pests such as Foot and Mouth Disease, African Swine Fever, Classical Swine Fever, and similar[19,20].

Since the HeberFast® Line Gavac strip will be applied to determine the immune status of animals vaccinated with Gavac®, the specificity of this test is more critical than its sensitivity. Consequently, the essay must exhibit a low fraction of false positives when assessing post-vaccination immunity. The assay's specificity was in the range 92.9-95.4% for the three batches tested, well above its sensitivity values (81-82.4%).

In veterinary medicine, lateral flow immunoassays have been developed for various purposes; detection of diseases in companion and farm animals to achieve better results in the care and development of animals, for example, Parvovirus[21], Newcastle[22], Avian infectious bronchitis virus[23], African swine fever[24] and Babesiosis[25], The rapid detection of these diseases reduces the economic losses. Immunochromatographic methods have also been developed to detect antibiotics and analogs in milk[26], which is greatly important for food safety.

In general, this test offers advantages and benefits, especially in the field, due to its fast and safe use and relatively low production costs. Moreover, it does not require equipment for readouts, and the results are easily interpreted with the naked eye, with high specificity and sensitivity in just 10 min. Finally, this immunoscreening test has been developed to work with serum, a sample that can be easily collected and processed.

HeberFast® Line Gavac is the first rapid kit worldwide for the detection of antibodies against the Bm86 protein. Its introduction in the field could facilitate the follow-up of the immune response against any vaccine based on this antigen and determine the level of immunity achieved in the vaccinated herds.

Analyst	Positivity criteria	Reading	Parameters			
			Kappa	IC 95 %	P. estad. z	Consistency
Analyst 1	Positive	1	0.8643	0.7185-1.0000	21.6410	Almost Perfect
		2	0.8643	0.7185-1.0000	21.6410	
	Gray Zone	1	0.7113	0.6189-0.8037	15.0891	Good
		2	0.7008	0.6068-0.7947	14.8658	
	Negative	1	0.6283	0.4695-0.7871	16.8247	Good
		2	0.6283	0.4695-0.7871	16.8247	
Analyst 2	Positive	1	0.8184	0.6665-0.9703	20.4936	Almost Perfect
		2	0.8184	0.6665-0.9703	20.4936	
	Gray Zone	1	0.7164	0.6238-0.8089	15.1969	Good
		2	0.7157	0.6227-0.8088	15.1828	
	Negative	1	0.6665	0.4843-0.8487	17.8478	Good
		2	0.6558	0.4799-0.8316	17.5602	
Analyst 3	Positive	1	0.8950	0.7657-1.0000	22.4101	Almost Perfect
		2	0.8950	0.7657-1.0000	22.4101	
	Gray Zone	1	0.7150	0.6223-0.8078	15.1684	Good
		2	0.7041	0.6096-0.7985	14.9362	
	Negative	1	0.7221	0.5414-0.9028	19.3360	Good
		2	0.6746	0.5014-0.8478	18.0639	

1: Reading once the technique

Table 5. Analyst Interpretation.

Conclusions

The HeberFast® Line Gavac immunochromatographic system allows the determination of the anti-Bm86 serological status quickly and straightforwardly to a large number of samples in field conditions with minimal effort. The introduction of this test would significantly improve the follow-up of the antibody response to GAVAC in all the country as part of the Integrated Control Program for cattle tick control.

Acknowledgements

This work was carried out thanks to the collaboration with the Unit of Central Laboratories of Agricultural Health (ULC-SA), Ministry of Agriculture, Cuba.

Bibliographic references

1. Rodriguez-Vivas RI, Jonsson NN, Bhushan C. Strategies for the control of Rhipicephalus microplus ticks in a world of conventional acaricide and macrocyclic lactone resistance. Parasitology research 2018; 117:3-29.
2. Valle MR, Mendez L, Valdez M, et al. Integrated control of Boophilus microplus ticks in Cuba based on vaccination with the anti-tick vaccine Gavac. Experimental & applied acarology 2004; 34:375-82.
3. Suarez PM, Méndez, M.L., Valdez, M., Souza, R.M., Camargo, A.J.R., Constanza, N.V., Ascanio, E.E. Control de las infestaciones de la garrapata Boophilus microplus en la ganadería Cubana y en regiones de latinoamérica con la aplicación del inmunógeno Gavac® dentro de un programa de lucha integral. Documento sexta conferencia Electrónica - Redectopar 2007.
4. Suarez M, Rubi J, Pérez D, et al. High impact and effectiveness of Gavac™ vaccine in the national program for control of bovine ticks Rhipicephalus microplus in Venezuela. Livestock Science 2016; 187:48-52.
5. Willadsen P, Kemp D. Vaccination with 'concealed'antigens for tick control. Parasitology Today 1988; 4:196-8.
6. de la Fuente J, Rodriguez M, Redondo M, et al. Field studies and cost-effectiveness analysis of vaccination with Gavac against the cattle tick Boophilus microplus. Vaccine 1998;16:366-73.
7. Lamberti J, Signorini A, Mattos C, et al. Evaluation of the recombinant vaccine against Boophilus microplus in grazing cattle in Argentina. Recombinant Vaccines for the Control of the Cattle Tick (ed De la Fuente, J) 1995:205-27.
8. Vargas M, Montero C, Sanchez D, et al. Two initial vaccinations with the Bm86-based Gavacplus vaccine against Rhipicephalus (Boophilus) microplus induce similar reproductive suppression to three initial vaccinations under production conditions. BMC veterinary research 2010;6:43.

9. Ethical Guidelines for the Use of Animals in Research. 2018. (Accessed 23/10/2021, 2020.
10. Bailes J, Mayoss S, Teale P, Soloviev M. Gold nanoparticle antibody conjugates for use in competitive lateral flow assays. Nanoparticles in Biology and Medicine: Springer; 2012:45-55.
11. Landis J, Koch G. The measurement of observer agreement for categorical data. Biometrics 1977:159-74.
12. EPIDAT 3.1. Una herramienta para el análisis epidemiológico de datos tabulados. Infomed, 2005. (Accessed 14//05/2020, 2020, at http://www.sld.cu/sitios/revsalud/temas.php?idv=1178.)
13. Las garrapatas del bovino y los agentes de enfermedad que transmiten en escenarios epidemiológicos de cambio climático. Guía para el manejo de garrapatas y adaptación al cambio climático. Instituto Interamericano de Cooperación para la Agricultura (IICA), 2016. (Accessed 12/06/2020, 2020, at http://creativecommons.org/licenses/by-sa/.0/igo/.)
14. Vargas-Hernández M, Santana-Rodríguez E, Sordo-Puga Y, et al. Stability, safety and protective immunity of Gavac® vaccine subjected to heat stress. Biotecnología Aplicada 2018; 35:1221-7.
15. Sastre P, Gallardo C, Monedero A, et al. Development of a novel lateral flow assay for detection of African swine fever in blood. BMC veterinary research 2016; 12:1-8.
16. Bolaños HM, Acuña MT, Serrano AM, et al. Desempeño de los sistemas Cholera-SMART® y Pathogen-Detection-Kit® en el diagnóstico rápido del cólera. Revista Panamericana de Salud Pública 2004; 16:233-41.
17. Corripio IF, Cisneros MJG, Ormaechea TG. Diagnóstico de las parasitosis intestinales mediante detección de coproantígenos. Enfermedades Infecciosas y Microbiología Clínica 2010; 28:33-9.
18. Gutiérrez-Cisneros MJ, Martínez-Ruiz R, Subirats M, Merino FJ, Millán R, Fuentes I. Evaluación de dos métodos inmunocromatográficos comerciales para el diagnóstico rápido de Giardia duodenalis y Cryptosporidium spp. en muestras de heces. Enfermedades Infecciosas y Microbiología Clínica 2011; 29:201-3.
19. Knowles N, Samuel A. Molecular epidemiology of foot-and-mouth disease virus. Virus research 2003; 91:65-80.
20. OIE. Chapter 15.2. Infection with classical Swine fever virus. Terrestrial Animal Health code. In: OIE, ed.2019.
21. Sharma C, Singh M, Upmanyu V, et al. development and evaluation of a gold nanoparticle-based immunochromatographic strip test for the detection of canine parvovirus. Archives of virology 2018; 163:2359-68.
22. Li Q, Wang L, Sun Y, et al. Evaluation of an immunochromatographic strip for detection of avian avulavirus 1 (Newcastle disease virus). Journal of Veterinary Diagnostic Investigation 2019; 31:475-80.
23. Liu I-L, Lin Y-C, Lin Y-C, Jian C-Z, Cheng I-C, Chen H-W. A novel immunochromatographic strip for antigen detection of avian infectious bronchitis virus. International journal of molecular sciences 2019; 20:2216.
24. Wang X, Ji P, Fan H, et al. CRISPR/Cas12a technology combined with immunochromatographic strips for portable detection of African swine fever virus. Communications biology 2020; 3:1-8.
25. Stuart Tayebwa D, Magdy Beshbishy A, Batiha GE-S, et al. Assessing the immunochromatographic test strip for serological detection of bovine babesiosis in Uganda. Microorganisms 2020; 8:1110.
26. Peng J, Liu L, Kuang H, Cui G, Xu C. Development of an icELISA and immunochromatographic strip to detect norfloxacin and its analogs in milk. Food and Agricultural Immunology 2017; 28:288-98.

Received: 2 February 2021
Accepted: 2 June 2021

RESEARCH / INVESTIGACIÓN

Formulation and organoleptic evaluation of Poly Herbal Cream of Punica, Neem, Carrot & Jamun as Active Ingredients

Puja Saha[1*], Jayashree Bhowmick[2], Anupam Saha[3]

DOI. 10.21931/RB/2021.06.03.5

Abstract: Assuming that herbal preparation is better with fewer side effects than synthetics, natural treatments are more effective than allopathy in terms of side effects for better human body healing. Herbal products have a growing demand in the world market, and the plants have been reported in the literature as having various pharmacological activities such as anti-microbial, anti-oxidant, anti-inflammatory activity, [UdMO4] anti-cancer, anti-diabetic. The purpose of this study was to develop anti-aging poly-herbal cream by mixing the extract of Punica leaf, Neem Oil, Jamun powder, Carrot powder as the main ingredient, and then creams were developed based on the anti-oxidant ability of herbal extracts and performed their evaluation study. *Punica granatam* leaves were shade dried and extracted using the Soxhlet method with different solvents such as n-hexane, benzene, and alcohol.[UdMO5] Fine extract powder was collected and removed distilled water thoroughly. The cream was formulated into different concentrations, namely F1, F2, F3, and F4. Similar types of research with similar components have been reported, but in this experiment, the formulation is different, and this work is kept cost-efficient and straightforward; it's an attempt to reduce few components and prepare cream and evaluate its potential. According to The International Council for Harmonization of Technical Requirements for Pharmaceuticals for Human Use ICH[UdMO6] guidelines, the cream was stable during stability studies, and F3 turned out to be a better formulation than the other three.

Key words: Anti-aging, Poly-herbs, Herbal Remedy, Herbal Cream, Pharmaceutical Cream, Skin Care.

Introduction

Dermal layer aging results from continual deterioration due to cellular DNA and protein; aging is classed into 2 distinct varieties: sequential skin aging and photo-aging. Each type has distinct clinical and historical options, and sequential skin aging is a universal and specific process characterized by physiological alteration in skin function. Within the aging process, keratinocytes cannot create a helpful stratum corneum, and the rate of formation from neutral lipids slows down, leading to dry pale skin with a wrinkle. In contrast, photo-aging is caused by the disorganization of stratum and dermal parts associated with physiological state and helio dermatitis. Herbs and plants have already proved helpful as a tool in the practice of medicine[1–3].

Cosmetic merchandise is used to shield pores and skin in opposition to exogenous and endogenous dangerous retailers and beautify the splendor and elegance of skin and the usage of cosmetics now not only handiest growing an appealing outside look, but also towards accomplishing sturdiness of suitable fitness via way of means of decreasing skin disorders[3–8]. The artificial or herbal substances found in skincare formulation that helps the health, texture, and integrity of dermis, moisturizing and preserving the pliancy of the skin with the aid of using decreasing the type I collagen, photo-protection, and plenty more, and this belongings of beauty is because of the presence of substances in cosmetics as it allows to lessen the production of loose radicals in the skin and manage the dermal residences which is the obstruction to penetrate the skin for an extended time[3,5,6]. Cosmetic merchandise is the satisfactory desire to lessen dermal problems like hyperpigmentation, skin wrinkling, skin aging, problematic pores, rough skin texture, etc. The need for natural cosmetics is swiftly increasing, and the growth is because of the supply of recent ingredients, the monetary rewards for growing hitting merchandise, customer needs, and higher expertise in dermal biology[3,5,9–11]. The plant parts utilized in cosmetic products should have medicinal properties like anti-inflammatory, anti-oxidant, emollient, anti-seborrheic, antiseptic, anti-bacterial activities, etc. Herbal merchandise declares to have fewer adverse effects, normally visible with merchandise containing artificial agents. The marketplace studies suggest a rise in the trade with the cosmetic industries, a prime function in fueling this international call for herbals[12–14].

Punica leaf, part of the tree pomegranate

P. granatum is one of the most common and potential plants for medicine in managing various ailments[15]. *Punica granatum* L. (belongs to the family *Punicaceae*) has been used to treat many ailments. Various plant parts have been scientifically tested for various pharmacological activities, such as potent antioxidative[15,16], anti-inflammatory, anti-bacterial, anti-microbial, anti-fungal properties, anti-hypertensive, and antiproliferative properties[17,18]. Pomegranate has excellent potential to be developed for use in dermal products[19]. Chlorophyll-a extracted from pomegranate leaf and stem may be a potential source and can supply natural or herbal colorants for the coating enterprises and nail varnish. Pomegranate leaf extracts act on inhibiting the development of obesity and hyperlipidemia in obese mice fed with a high-fat diet[20–22].

Almond oil is the oil isolated from Almonds

The almond *Prunus dulcis* (Mill) D.A. Webb (subfamily Prunoideae of family Rosaceae) contains fixed oil, phenolic compounds abundant in almonds; it also contains and some micronutrients, vitamins, minerals and has different pharmacological activities[23–26]. Almond seeds and oil have cardio-protective, immune-stimulant effects, anti-inflammatory, and reduce irritable bowel syndrome symptoms , and they are also helpful in treating constipation[27,28]. Almond oil has also been used to

[1] Assistant Professor, Department of Pharmaceutics, School of Pharmacy, Seacom Skills University, Bolpur, Birbhum.
[2] Graduated B.Pharm, Bharat Technology, Uluberia, Howrah.
[3] Graduated M.Pharm, Pharmacology, NSHM College Of Pharmaceutical Technology, NSHM Knowledge Campus, B.L. Rd, Kolkata.

Corresponding author: milagros.vargas@cigb.edu.cu

treat dry skin disorders like psoriasis, eczema, and many more disorders in ancient treatment cultures but today it is used in aromatherapy and for producing many skin-hair cosmetics[29].

Jamun powder is made from sun-dried Jamun Seeds

The black Jamun (*Syzygium cumini* L.) is an important indigenous plant of Myrtaceae, commonly known as jamun or Indian blackberry, originally from Indonesia and India, which has anti-oxidant solid antigenotoxic potential[32,33]. The fruit pulp is sweet, and the seeds are acidic and sour. The presence of oxalic, gallic, tannic acids and other alkaloids creates one to feel such an astringency taste. The pulp and seeds are used for traditional medicine against diabetes, diarrhea, and ringworm infection also protect against radiation-induced sickness[32,34–37]. It is very beneficial as it has anti-diabetic, cytoprotective, anticoagulant, analgesic and anti-inflammatory, anti-cancerous, anti-microbial, anti-oxidant, hypo-lipidemic, hepato-protective properties[35,38,39].

Carrots

(*Daucus carota*) are essentially root veggies belonging to the family of *Apeaceae or Umbelliferrous*. These veggies are believed to have originated approximately 5000 years ago. Carrots are to be had in diverse, colorful variations like pink, orange, white, purple, etc; however, the maximum usually observed variants are pink carrots and orange carrots. Carrots have anti-oxidants, which enables in regaining the misplaced glow of the skin. It helps in imparting remedies from scars and blemishes. Carrot is a unique anti-growing old compound due to the presence of Vitamin A.

Additionally, a considerable quantity of Vitamin C. Vitamin A acts as an excellent anti-oxidant, fights with the free radicals of the body, stabilize them, and stops them from unfavorable our pores of skin cells and accordingly prevents the symptoms of growing old like wrinkles, pigmentation, and choppy pores and skin tone. Vitamin C enables the prevention of wrinkles using assisting the manufacturing of collagen in the body, which is a crucial protein required for retaining pores and skin elasticity. Carrot is likewise a wealthy supply of β-carotenoids, which boom or trigger skin immunity in opposition to solar rays and heals sunburns[40–43].

Neem tree

(*Azadirachta indica*) is a local, evergreen, tropical tree to India[44]. Neem is a versatile, multifarious tree with a great capacity to own the most beneficial non-wooden products. Neem has various medicinal properties, including anti-cancer properties. In India, Neem is called the village of pharmacy due to its recovery versatility, and it's been utilized in Ayurvedic medication for extra than 4,000 years because of its medicinal properties[44–47]. Azadirachtin is the principal compound of the neem oil with insecticidal activity[48]. Neem extracts were also reported to possess inhibitory effects on several cancer cell lines such as breast, gynecological, gastrointestinal, hematological, prostate, and skin cancers. Several active chemical compounds were discovered in neems, such as Nimbin, Nimbin, Saladin, azadirachtin (AZA), glycosides, and dihydrochalcone polyphenolics, coumarin, and tannins[49–51]. Pharmacological activities have been reported, including anti-bacterial, anti-inflammatory, anti-fungal, anti-arthritic, anti-pyretic, anti-gastric ulcer, hypoglycemic, and anti-tumor activities[46,49,52–54].

Grapeseed oil

Is obtained from the seeds of grapes, and it was a by-product of winemaking and had many uses ranging from cooking cosmetics in controlling several diseases and wound healing potential[55–57]. *Vitis vinifera* L., which is commonly called grape used as a food and a beverage[58]. It is widely used as cooking oil, in skin care applications, and also as cosmetics. The grape seed oil contains 0.8 to 1.5% of phenols, steroids, and minor amounts of vitamin E. The grape seed oil was reported to possess the highest gallic acid, anti-oxidant, epicatechin, proanthocyanidins, catechin, and procyanidins. It has anti-oxidant, anti-fungal, anti-bacterial, antiviral, and anti-inflammatory activities[59,60].

Peppermint oil

(*Mentha piperita*) extracted from peppermint leaves is an excellent gastric stimulant, carminative, which has also been used in cosmetic formulations as a perfume component and a general skin conditioning agent[61,62]. Peppermint (Mentha × Piperita) is a hybrid mint, which is a cross between Water mint (*Mentha aquatica*) and Spearmint (*Mentha spicata*) that is thought to be grown naturally[62,63].

Similar types of research with similar Active Pharmaceutical Ingredients API have been reported. However, in this experiment, the formulation is different, and in each formulation, peppermint oil is used as the flavoring agent, whereas in the literature review, it is found that each formulation has a different flavoring agent. This work is kept cost-efficient and straightforward, it's an attempt to omit few components and prepare cream and evaluate its potential.

Materials and methods

The plan of work and the procedure followed for this experiment were performed by Matangi and the team in 2014[3]. The experiment was performed in Bharat Technology, Uluberia, in 2018 as an academic project for the partial fulfillment of a Bachelor of Pharmacy degree.

Materials

Glycerin, Propylene Glycol, Zinc oxide, Micro Crystalline Cellulose, Sodium alginate, Methylcellulose, Beeswax, Sodium benzoate/paraben, Almond oil, Punica leaves, Neem oil, Jamun powder, Carrot powder, Vitamin E, Grapeseed oil, Peppermint oil, and Purified water.

Preparation of Punica leaf extract

Punica granatum leaves were bought from the market and dried. The dried leaves were ground to a fine powder in a suitable grinder mixture. Shade dried powder was extracted using a Soxhlet extractor with hexane, alcohol, and distilled water separately to get the semisolid extract. The organic solvents were then recovered by steam distillation. The extracts were then concentrated to remove wetness under reduced pressure and controlled temperature, respectively, and they were preserved in a refrigerator.

Preparation of Jamun Seeds powder

Black Jamun (*Syzygium cumini* L.) were bought from the market, and the seeds are separated from the freshly part of the fruit, washed adequately, and dried. The seeds were dried under the sun for a week. Seeds were pounded along with the outer skin and made into a fine powder.

Ingredients	Category	F1	F2	F3	F4
Jamun Powder	API*	5g	5gm	5gm	5gm
Punica leaf extract	API	2ml	2ml	2ml	2ml
Neem Oil	API	2ml	2ml	2ml	2ml
Carrot Powder	API + Vitamin A Source	3gm	3gm	3gm	3gm
Glycerin	Moisturizer	3ml	3ml	3ml	3ml
Propylene Glycol	Moisturizer + Binder	3ml	3ml	3ml	3ml
ZnO	Skin whitener	3gm	3gm	3gm	3gm
Methyl Cellulose	Polymer	5gm	-	-	-
Sodium Alginate	Polymer	-	2gm	5gm	-
Microcrystalline Cellulose	Polymer	-	3gm	-	5gm
Cetyl Alcohol	Surfactant + emollient	1ml	1ml	1ml	1ml
Beeswax	Base	3gm	-	3gm	-
Grapeseed Oil	Base	-	2ml	-	-
Almond Oil	Base	2ml	2ml	2ml	2ml
Stearic acid	Base	-	-	-	2gm
Lanolin	Base	-	-	-	1gm
Sodium Benzoate	Preservative	2gm	2gm	2gm	2gm
Peppermint Oil	Flavoring agent	2ml	2ml	2ml	3ml
Purified water	Vehicle	QS*	QS	QS	QS

*API – Active Pharmaceutical Ingredient; QS – Quantity as required.

Table 1. Formulation Table.

Cream Formulation

The formula for the cream is given in Table No. 1.

Method For Preparation Of Cream

Shade-dried Punica leaf powder was put separately in a soxhlet extractor, and then ethanol was added successively. The extracts were then concentrated under reduced pressure and controlled temperature for dryness and were stored for stabilization at a specific temperature. Glycerin was applied to the binder and polymer content, the water mixture in a beaker. This forms liquid dispersion and displays the property of slight swelling. The Punica leaf extract, neem oil, and Jamun powder were added to the liquid dispersion. Using a water bath, melted oils together with the base in a separate beaker. Skin whitener and preservative were gradually incorporated along with all other components. Triturated all ingredients above and the requisite consistency was established, which forms poly-herbal anti-aging cream.

Results and discussion

Evaluation of cream

There are various evaluation parameters for cream. For this work, the evaluation parameters chosen are Organoleptic evaluation, Microbial Count test, Stability Studies, pH determination, homogeneity determination, wetness determination, smear determination, emolliency determination, viscosity determination, dilution test, dye solubility test.

Organoleptic evaluation

The cream formulated was evaluated for its organoleptic properties (color, state, and odor). The appearance of the cream was analyzed by its color and roughness visually and by touch. Results are listed in Table No. 2.

Sr. No.	Specification	Limit
1	State	Semi-solid
2	Color	Greyish white
3	Odor	Characteristic
4	Texture	Smooth

Table 2. Organoleptic Properties.

Test for microbial growth in formulated creams

This method was applied from the work of Matangi and Team in the year 2014[3]. Here, Streak Plate Method[64] was used, where the formulated creams were inoculated in a plate with the Muller Hinton agar media. Along with that, a control group was made without the cream for comparison. The plates were kept in the incubator and are incubated for 24 hours at 37°C. After the incubation period, plates were taken out and analyzed for microbial growth by comparing them with the control. Results are listed in Table 3.

Stability studies

Thermal stability testing of cream was done at room temperature with relative humidity (RH) 65%; results are listed in Table 4. To assess the drug and formulation stability for an extended period, accelerated stability studies were done according to ICH guidelines; the results are listed in Table 5.

Sr. No.	Microbial Load	Limits	Result
1	Total Microbial Count	Not More than 100	82
2	Limit Tests: E. coli	No Characteristic Colonies	Complies

Table 3. Microbial Test.

Sr. No		F1	F2	F3	F4
1	Thermal Stability (at RH 65% and 30^{+} °C)	Stable, no oil separation	Stable, no oil separation	Stable, no oil separation	Stable, no oil separation

Table 4. Thermal stability determination.

Stability Studies	F1		F2		F3		F4	
	Initial	After 7 days	Initial	After 7 days	Initial	After 7 days	Initial	After 7 days
Physical Appearance	Semi-solid	Semi-solid	Semi-solid	Semi-solid	Semi-solid	Semi-solid	Semi-solid	Semi-solid
Texture	Ok	Ok	Ok	Ok	Ok	Ok	Ok	Ok
Color	White	White	White	White	White	White	White	White
Thermal Stability	Ok	Ok	Ok	Ok	Ok	Ok	Ok	Ok
Degradation Of The Product	Nil	Nil	Nil	Nil	Nil	Nil	Nil	Nil

Table 5. Accelerated Stability Studies.

Determination of Homogeneity

The formulations were tested for homogeneity by touch for texture and by visual appearance. Result obtained of each formulation is given in Table No. 6,7,8,9.

Determination of the type of smear

It was determined by applying the cream on the surface of the skin of a human volunteer (Self, no ethical permission need as it is non-toxic, natural, and safe components which makes it exceptional[65]. After applying the cream, the type of smear or film formed on the skin was checked. Result obtained of each formulation is given in Table No. 6,7,8,9.

Determination of Viscosity

The viscosity determinations were carried out using a Brookfield viscometer (DV II + Pro model) using spindle number S-64 at 20 rpm at a temperature of 25°C. Result obtained of each formulation is given in Table No. 6,7,8,9.

Determination of pH

Accurately weighed 1gm of the sample was dispersed in 100 ml of water. The pH of the suspension was set at 27°C using a digital pH meter. Result obtained of each formulation is given in Table No. 6,7,8,9.

Spread ability Test

This method was applied from the work of Dhase and Team in the year 2014, Chen and Team in the year 2016[66,67]. Spread ability can be expressed by the extent of the area to which the topical application spreads when applied to the affected parts on the skin and the curative value of the formulation also hang-on upon its spreading value. Hence, it was found obligatory to determine the spread ability of the formulation. For this purpose, a small amount of about 23cm of each formulation was applied in between two glass slides, and they were pressed together to obtain a film of uniform thickness by placing 1000gm weight for 5 minutes. Thereafter a weight of 10gm was added to the pan, and the top plate was subjected to pull with the help of string attached to the hook. The time in which the upper glass slide moves over the lower plate to cover a distance of 10 cm was noted. The Spread ability (S) can be determined using the formula[66,67].

$S = (m \times L)/T$,

Where S–Spread ability;

m - Weight binds to the upper glass slide,

L - Length budged on a glass slide

T - Time is taken.

Results obtained are given in Table No. 10. The cream was found to be easily spreadable.

Dye solubility test

This method was applied from the work of Dhase and Team in the year 2014[66]. In this test, a small sample is mixed with a water-soluble dye and observed under the microscope. If the continuous phase appears red, the cream is O/W (Oil in Water) type as the water is in the external phase, and the dye will dissolve in it to give color. If the scattered globules appear red and continuous phase colorless, they are W/O (Water in

Oil) type. Likewise, if an oil-soluble dye such as Scarlet red or Sudan III is put on to an emulsion and the continuous phase appears red, it is w/o emulsion. Following the procedure, red color was observed; hence, it was O/W type of cream[66].

Dilution test

This method was applied from the work of Dhase and Team in the year 2014[66]. In this test, the cream is diluted either with oil or water. If the cream is o/w type and diluted with water, it will remain stable as water is the dispersion medium, but if it is diluted with oil, the cream will break as oil and water are not miscible. Oil in water emulsion can be diluted with an aqueous solvent, whereas water in oil emulsion can be diluted with an oily liquid. Following the procedure, it was found to be O/W type of cream as because the obtained product was stable[66].

The cream was the o/w type of emulsion. Due to the base material, the proper addition of surfactants to its proper quantity, and the proper combination of all the excipients, it was stable. The proper ratio of all ingredients of excipients with the active ingredients also reasons for the stability. During the formulation, the oil phase and water phase are mixed, and it was also responsible for the stability of that cream.

After the formulation of cream by checking all these different evaluation parameters, the 4 formulated creams showed good homogeneity when the creams were observed by touch and visual test. The color and physical appearance (color & odor) were not changed during storage; it may happen due to preservatives' helpful addition.

All the individual pH noted for the formulated herbal creams were F1 - 6.1, F2 - 5.7, F3 - 5.6, F4 - 5.9. The formulation F3 has shown the reading, which was matching to the

Time Interval (Day)	Homogeneity	Type of smear	Viscosity(cp)	Physical changes	pH
0	Excellent	Excellent	12.005	No change in color and odor	6.1
5	Good	Excellent	12.005	No change in color and odor	6.1
15	Good	Good	12.004	No change in color and odor	6.1
20	Good	Good	12.004	No change in color and odor	6.1
30	Good	Good	12.003	No change in color and odor	6.1

Table 6. Formulation 1.

Time Interval (Day)	Homogeneity	Type of smear	Viscosity(cp)	Physical changes	pH
0	Excellent	Excellent	12.521	No change in color and odor	5.7
5	Excellent	Excellent	12.500	No change in color and odor	5.7
15	Good	Good	12.510	No change in color and odor	5.7
20	Average	Good	12.512	No change in color and odor	5.7
30	Average	Good	12.515	No change in color and odor	5.7

Table 7. Formulation 2.

Time Interval (Day)	Homogeneity	Type of smear	Viscosity(cp)	Physical changes	pH
0	Excellent	Excellent	12.499	No change in color and odor	5.6
5	Excellent	Excellent	12.450	No change in color and odor	5.6
15	Good	Good	12.465	No change in color and odor	5.6
20	Good	Good	12.460	No change in color and odor	5.6
30	Average	Good	12.455	No change in color and odor	5.6

Table 8. Formulation 3.

Time Interval (Day)	Homogeneity	Type of smear	Viscosity(cp)	Physical changes	pH
0	Excellent	Excellent	12.008	No change in color and odor	5.9
5	Excellent	Excellent	12.005	No change in color and odor	5.9
15	Good	Good	12.002	No change in color and odor	5.9
20	Average	Good	12.006	No change in color and odor	5.9
30	Average	Good	12.008	No change in color and odour	5.9

Table 9. Formulation 4.

Sr. No.	Time (Sec)	Spread ability Studies (cm)			
		F1	F2	F3	F4
1	15	13.5	13.6	14.3	14.4
2	20	14.1	13.1	14.1	13.6
3	25	13.3	14.6	13.6	13.7

Table 10. Spread ability Test.

skin pH. As per the result, it was found that Trial F3 has better consistency of formulation of cream in the combination of different excipients in their quantities.

The prepared formulations showed no affirmation of phase separation, had good spread ability and had good consistency during the study period. Stability parameters like visual appearance, texture, viscosity, and fragrance of the formulations reflected no significant variation during the study period. The prepared formulations showed an acceptable pH range that was approximately pH 5.6; it confirms the compatibility of the formulations with skin secretions.

Conclusions

In this project work, the selected active ingredients are Punica leaf extract, carrot powder, Jamun powder, and neem oil. These all ingredients are cheap and readily available in the market, including all these ingredients, the selected excipients-beeswax, grape seed oil, almond oil, stearic acid, lanolin as base material; Sodium benzoate as a preservative; Cetyl alcohol as emollient and surfactants; peppermint oil as a flavoring agent for all type of formulation like F1, F2, F3 & F4. F3 stood out to be the better formulation concerning results obtained.

From the existing examination and acquired results, it could be concluded that it's possible to broaden poly natural cream containing natural extracts with anti-oxidants belongings, which may be formulated to act as a barrier or to defend skin and make cosmetic cream.

Acknowledgment

The authors would like to thank Mr. Mayukh Jana (Associate Professor, Department of Pharmaceutics, Bharat Technology, Uluberia) to help during this investigation.

Source of Funding

Nil

Conflict Of Interest

Nil

Bibliographic references

1. Watson REB, Ogden S, Cotterell LF, et al. A cosmetic 'anti-ageing' product improves photoaged skin: a double-blind, randomized controlled trial. Br J Dermatol. 2009;161(2):419-426. doi:10.1111/j.1365-2133.2009.09216.x
2. Kaur IP, Kapila M, Agrawal R. Role of novel delivery systems in developing topical anti-oxidants as therapeutics to combat photoageing. Ageing Res Rev. 2007;6(4):271-288. doi:10.1016/j.arr.2007.08.006
3. Matangi SP, Mamidi SA, Gulshan MD, Raghavamma STV, Nadendla RR. Formulation and Evaluation of Anti Aging Poly Herbal Cream. Int J Pharm Sci Rev Res. 2014;24(22):133-136.
4. Saraf S, Kaur C. Phytoconstituents as photoprotective novel cosmetic formulations. Pharmacogn Rev. 2010;4(7):1. doi:10.4103/0973-7847.65319
5. Draelos ZD, Thaman LA, eds. Cosmetic Formulation of Skin Care Products. In: Cosmetic Formulation of Skin Care Products. 0 ed. CRC Press; 2005:25-26. doi:10.3109/9781420020854-5
6. Chattopadhyay PK. Herbal Cosmetics & Ayurvedic Medicines (EOU). In: Herbal Cosmetics & Ayurvedic Medicines (EOU). 3rd Revised Edition. Niir Project Consultancy Services; 2013. https://books.google.co.in/books?id=cuCoDAAAQBAJ&printsec=frontcover&source=gbs_ge_summary_r&cad=0#v=onepage&q&f=false
7. Russell R. Cosmetics Use. In: Encyclopedia of Body Image and Human Appearance. Elsevier; 2012:366-371. doi:10.1016/B978-0-12-384925-0.00058-4
8. Datta HS, Paramesh R. Trends in aging and skin care: Ayurvedic concepts. J Ayurveda Integr Med. 2010;1(2):110-113. doi:10.4103/0975-9476.65081
9. Kumar D, Rajora G, Parkash O, Himanshu, Antil M, Kumar V. Herbal cosmetics: An overview. Int J Adv Sci Res. 2016;1(4):36-41.
10. Mishra A, Mishra A, Chattopadhyay P. Herbal Cosmeceuticals for Photoprotection from Ultraviolet B Radiation: A Review. Trop J Pharm Res. 2011;10(3). doi:10.4314/tjpr.v10i3.7
11. Geesin JC, Darr D, Kaufman R, Murad S, Pinnell SR. Ascorbic acid specifically increases type I and type III procollagen messenger RNA levels in human skin fibroblast. J Invest Dermatol. 1988;90(4):420-424. doi:10.1111/1523-1747.ep12460849
12. Dureja H, Kaushik D, Gupta M, Kumar V, Lather V. Cosmeceuticals: An emerging concept. Indian J Pharmacol. 2005;37(3):155. doi:10.4103/0253-7613.16211

13. Rajvanshi A, Sharma S, Khokra SL, Sahu RK, Jangde R. Formulation and evaluation of Cyperus rotundus and Cucumis sativus based herbal face cream. Pharmacologyonline. 2011;2:1238-1244.
14. Saraf S, Ashawat MS., Baghel M. Herbal Cosmetics: "Trends in Skin Care Formulation." Pharmacogn Rev. 2009;3(5):82-89.
15. Viswanatha G, Venkataranganna M, Prasad N, Ashok G. Evaluation of anti-epileptic activity of leaf extracts of Punica granatum on experimental models of epilepsy in mice. J Intercult Ethnopharmacol. 2016;5(4):415. doi:10.5455/jice.20160904102857
16. Basiri S. Evaluation of anti-oxidant and antiradical properties of Pomegranate (Punica granatum L.) seed and defatted seed extracts. J Food Sci Technol. 2015;52(2):1117-1123. doi:10.1007/s13197-013-1102-z
17. Wang D, Özen C, Abu-Reidah IM, et al. Vasculoprotective Effects of Pomegranate (Punica granatum L.). Front Pharmacol. 2018;9:544. doi:10.3389/fphar.2018.00544
18. Jurenka JS. Therapeutic applications of pomegranate (Punica granatum L.): a review. Altern Med Rev J Clin Ther. 2008;13(2):128-144.
19. Lee C-J, Chen L-G, Liang W-L, Wang C-C. Multiple Activities of Punica granatum Linne against Acne Vulgaris. Int J Mol Sci. 2017;18(1):141. doi:10.3390/ijms18010141
20. Fellah B, Bannour M, Rocchetti G, Lucini L, Ferchichi A. Phenolic profiling and anti-oxidant capacity in flowers, leaves and peels of Tunisian cultivars of Punica granatum L. J Food Sci Technol. 2018;55(9):3606-3615. doi:10.1007/s13197-018-3286-8
21. Lei F, Zhang XN, Wang W, et al. Evidence of anti-obesity effects of the pomegranate leaf extract in high-fat diet induced obese mice. Int J Obes. 2007;31(6):1023-1029. doi:10.1038/sj.ijo.0803502
22. Mohajer S, Taha RM, Azmi SZ. Phytochemical screening and potential of natural dye colourant from pomegranate (Punica granatum L.). Pigment Resin Technol. 2016;45(1):38-44. doi:10.1108/PRT-10-2014-0100
23. Kato K, Vo PHT, Furuyashiki T, Kamasaka H, Kuriki T. Co-ingestion of whole almonds and almond oil with carbohydrate suppresses postprandial glycaemia in mice in an insulin-dependent and insulin-independent manner. J Nutr Sci. 2019;8:e25. doi:10.1017/jns.2019.22
24. Mericli F, Becer E, Kabadayı H, et al. Fatty acid composition and anti-cancer activity in colon carcinoma cell lines of Prunus dulcis seed oil. Pharm Biol. 2017;55(1):1239-1248. doi:10.1080/13880209.2017.1296003
25. Musarra-Pizzo M, Ginestra G, Smeriglio A, Pennisi R, Sciortino MT, Mandalari G. The Anti-microbial and Antiviral Activity of Polyphenols from Almond (Prunus dulcis L.) Skin. Nutrients. 2019;11(10):2355. doi:10.3390/nu11102355
26. Franklin LM, Mitchell AE. Review of the Sensory and Chemical Characteristics of Almond (Prunus dulcis) Flavor. J Agric Food Chem. 2019;67(10):2743-2753. doi:10.1021/acs.jafc.8b06606
27. Ahmad Z. The uses and properties of almond oil. Complement Ther Clin Pract. 2010;16(1):10-12. doi:10.1016/j.ctcp.2009.06.015
28. Barreca D, Nabavi SM, Sureda A, et al. Almonds (Prunus Dulcis Mill. D. A. Webb): A Source of Nutrients and Health-Promoting Compounds. Nutrients. 2020;12(3):672. doi:10.3390/nu12030672
29. Buckle J. Clinical aromatherapy. Therapeutic uses for essential oils. Adv Nurse Pract. 2002;10(5):67-68, 88.
30. Lardos A. The botanical materia medica of the Iatrosophikon—A collection of prescriptions from a monastery in Cyprus. J Ethnopharmacol. 2006;104(3):387-406. doi:10.1016/j.jep.2005.12.035
31. Simon D, Nobbe S, Nägeli M, et al. Short- and long-term effects of two emollients on itching and skin restoration in xerotic eczema. Dermatol Ther. 2018;31(6):e12692. doi:10.1111/dth.12692
32. Gajera HP, Gevariya SN, Hirpara DG, Patel SV, Golakiya BA. Anti-diabetic and anti-oxidant functionality associated with phenolic constituents from fruit parts of indigenous black jamun (Syzygium cumini L.) landraces. J Food Sci Technol. 2017;54(10):3180-3191. doi:10.1007/s13197-017-2756-8
33. Aqil F, Gupta A, Munagala R, et al. Antioxidant and Antiproliferative Activities of Anthocyanin/Ellagitannin-Enriched Extracts From Syzygium cumini L. (Jamun , the Indian Blackberry). Nutr Cancer. 2012;64(3):428-438. doi:10.1080/01635581.2012.657766
34. Jagetia GC, Baliga MS, Venkatesh P. Influence of Seed Extract of Syzygium Cumini (Jamun) on Mice Exposed to Different Doses of γ-radiation. J Radiat Res (Tokyo). 2005;46(1):59-65. doi:10.1269/jrr.46.59
35. Ayyanar M, Subash-Babu P. Syzygium cumini (L.) Skeels: a review of its phytochemical constituents and traditional uses. Asian Pac J Trop Biomed. 2012;2(3):240-246. doi:10.1016/S2221-1691(12)60050-1
36. Benherlal PS, Arumughan C. Chemical composition and in vitro anti-oxidant studies on Syzygium cumini fruit: Composition and anti-oxidant studies on S. cumini fruit. J Sci Food Agric. 2007;87(14):2560-2569. doi:10.1002/jsfa.2957
37. Gajera HP, Gevariya SN, Patel SV, Golakiya BA. Nutritional profile and molecular fingerprints of indigenous black jamun (Syzygium cumini L.) landraces. J Food Sci Technol. 2018;55(2):730-739. doi:10.1007/s13197-017-2984-y
38. Sehwag S, Upadhyay R, Das M. Optimization and multivariate accelerated shelf life testing (MASLT) of a low glycemic whole jamun (Syzygium cumini L.) confection with tailored quality and functional attributes. J Food Sci Technol. 2018;55(12):4887-4900. doi:10.1007/s13197-018-3423-4
39. Ahmed R, Tariq M, Hussain M, et al. Phenolic contents-based assessment of therapeutic potential of Syzygium cumini leaves extract. Bakhsh A, ed. PLOS ONE. 2019;14(8):e0221318. doi:10.1371/journal.pone.0221318
40. Pérez Gutiérrez RM, Hernández Luna H, Hernández Garrido S. Antioxidant Activity Of Tagetes Erecta Essential Oil. J Chil Chem Soc. 2006;51(2):883-886. doi:10.4067/S0717-97072006000200010
41. Singh YP, Dwivedi R, Dwivedi SV. Effect of biofertilizers and graded dose of nitrogen on growth and flower yield of calendula (Callendula officinalis) ; 8 (2): 957-958. Plant Arch. 2008;8(2):957-958.
42. Karabacak ÇE, Karabacak H. Factors Affecting Carotenoid Amount In Carrots (Daucus Carota). E-J New World Sci Acad. 2019;14(2):29-39. doi:10.12739/NWSA.2019.14.2.5A0113
43. Dosti MP, Mills JP, Simon PW, Tanumihardjo SA. Bioavailability of β-carotene (βC) from purple carrots is the same as typical orange carrots while high-βC carrots increase βC stores in Mongolian gerbils (Meriones unguiculatus). Br J Nutr. 2006;96(2):258-267. doi:10.1079/BJN20061562
44. Bothra Nursery. Neem Tree. Bothra Nursery. Published 2015. Accessed 2 December, 2020. http://www.bothranursery.com/product/forest-and-roadside-plants/neem-tree/
45. Alravat Products. The Magnificent Neem Tree. Top-Tree-House Designs Tree House Designs. Published 10 May, 2016. Accessed 2 December, 2020. https://toptreehouse.wordpress.com/2016/05/10/30/
46. Alzohairy MA. Therapeutics Role of Azadirachta indica (Neem) and Their Active Constituents in Diseases Prevention and Treatment. Evid Based Complement Alternat Med. 2016;2016:1-11. doi:10.1155/2016/7382506
47. Paul R, Prasad M, Sah NK. Anti-cancer biology of Azadirachta indica L (neem): A mini review. Cancer Biol Ther. 2011;12(6):467-476. doi:10.4161/cbt.12.6.16850
48. Zanuncio JC, Mourão SA, Martínez LC, et al. Toxic effects of the neem oil (Azadirachta indica) formulation on the stink bug predator, Podisus nigrispinus (Heteroptera: Pentatomidae). Sci Rep. 2016;6(1):30261. doi:10.1038/srep30261
49. Lakshmi T, Krishnan V, Rajendran R, Madhusudhanan N. Azadirachta indica : A herbal panacea in dentistry - An update. Pharmacogn Rev. 2015;9(17):41. doi:10.4103/0973-7847.156337
50. Patel SM, Nagulapalli Venkata KC, Bhattacharyya P, Sethi G, Bishayee A. Potential of neem (Azadirachta indica L.) for prevention and treatment of oncologic diseases. Semin Cancer Biol. 2016;40-41:100-115. doi:10.1016/j.semcancer.2016.03.002
51. Ashokhan S, Othman R, Abd Rahim MH, Karsani SA, Yaacob JS. Effect of Plant Growth Regulators on Coloured Callus Formation and Accumulation of Azadirachtin, an Essential Biopesticide in Azadirachta indica. Plants. 2020;9(3):352. doi:10.3390/plants9030352

52. Gomes SA, Paula AR, Ribeiro A, et al. Neem oil increases the efficiency of the entomopathogenic fungus Metarhizium anisopliae for the control of Aedes aegypti (Diptera: Culicidae) larvae. Parasit Vectors. 2015;8(1):669. doi:10.1186/s13071-015-1280-9
53. Moga M, Bălan A, Anastasiu C, Dimienescu O, Neculoiu C, Gavriș C. An Overview on the Anticancer Activity of Azadirachta indica (Neem) in Gynecological Cancers. Int J Mol Sci. 2018;19(12):3898. doi:10.3390/ijms19123898
54. Jeba Malar TRJ, Antonyswamy J, Vijayaraghavan P, et al. In-vitro phytochemical and pharmacological bio-efficacy studies on Azadirachta indica A. Juss and Melia azedarach Linn for anti-cancer activity. Saudi J Biol Sci. 2020;27(2):682-688. doi:10.1016/j.sjbs.2019.11.024
55. Yilmaz Y, Toledo RT. Oxygen radical absorbance capacities of grape/wine industry by-products and effect of solvent type on extraction of grape seed polyphenols. J Food Compos Anal. 2006;19(1):41-48. doi:10.1016/j.jfca.2004.10.009
56. Shi J, Yu J, Pohorly JE, Kakuda Y. Polyphenolics in Grape Seeds—Biochemistry and Functionality. J Med Food. 2003;6(4):291-299. doi:10.1089/109662003772519831
57. Shivananda Nayak B, Dan Ramdath D, Marshall JR, Isitor G, Xue S, Shi J. Wound-healing Properties of the Oils of Vitis vinifera and Vaccinium macrocarpon: Wound Healing Activity Of Grape And Cranberry Oils. Phytother Res. 2011;25(8):1201-1208. doi:10.1002/ptr.3363
58. Micheli L, Mattoli L, Maidecchi A, Pacini A, Ghelardini C, Di Cesare Mannelli L. Effect of Vitis vinifera hydroalcoholic extract against oxaliplatin neurotoxicity: in vitro and in vivo evidence. Sci Rep. 2018;8(1):14364. doi:10.1038/s41598-018-32691-w
59. Chao CY, Mani MP, Jaganathan SK. Engineering electrospun multicomponent polyurethane scaffolding platform comprising grapeseed oil and honey/propolis for bone tissue regeneration. Mishra YK, ed. PLOS ONE. 2018;13(10):e0205699. doi:10.1371/journal.pone.0205699
60. Leparmarai PT, Sinz S, Kunz C, et al. Transfer of total phenols from a grapeseed-supplemented diet to dairy sheep and goat milk, and effects on performance and milk quality. J Anim Sci. 2019;97(4):1840-1851. doi:10.1093/jas/skz046
61. Oh JY, Park MA, Kim YC. Peppermint Oil Promotes Hair Growth without Toxic Signs. Toxicol Res. 2014;30(4):297-304. doi:10.5487/TR.2014.30.4.297
62. McKay DL, Blumberg JB. A review of the bioactivity and potential health benefits of peppermint tea (Mentha piperita L.). Phytother Res. 2006;20(8):619-633. doi:10.1002/ptr.1936
63. Chumpitazi BP, Kearns GL, Shulman RJ. Review article: the physiological effects and safety of peppermint oil and its efficacy in irritable bowel syndrome and other functional disorders. Aliment Pharmacol Ther. 2018;47(6):738-752. doi:10.1111/apt.14519
64. Sanders ER. Aseptic Laboratory Techniques: Plating Methods. J Vis Exp. 2012;(63):3064. doi:10.3791/3064
65. Hanley BP, Bains W, Church G. Review of Scientific Self-Experimentation: Ethics History, Regulation, Scenarios, and Views Among Ethics Committees and Prominent Scientists. Rejuvenation Res. 2019;22(1):31-42. doi:10.1089/rej.2018.2059
66. Dhase AS, Khadbadi SS, Saboo SS. Formulation and Evaluation of Vanishing Herbal Cream of Crude Drugs. Am J Ethnomedicine. 2014;1(5):313-318.
67. Chen MX, Alexander KS, Baki G. Formulation and Evaluation of Antibacterial Creams and Gels Containing Metal Ions for Topical Application. J Pharm. 2016;2016:1-10. doi:10.1155/2016/5754349

Received: 1 May 2021
Accepted: 4 July 2021

RESEARCH / INVESTIGACIÓN

Purificación parcial de péptidos del veneno de escorpión *Hadruroides charcasus* (Karsch, 1879) con actividad antimicrobiana

Partial purification of peptides from the scorpion venom *Hadruroides charcasus* (Karsch, 1879) with antimicrobial activity

Orlando Pérez-Delgado[1], Clara Andrea Rincon-Cortés[2], Nohora Angélica Vega-Castro[3], Edgar Antonio Reyes-Montaño[4], Marcela Gómez-Garzón[5]

DOI. 10.21931/RB/2021.06.03.6

Resumen: Los venenos de muchas especies de escorpiones son fuentes ricas en componentes biológicamente activos, como los péptidos antimicrobianos, biomoléculas que aún no han sido estudiados del veneno de *Hadruroides charcasus*. El objetivo de este artículo es evaluar la actividad antimicrobiana de los péptidos parcialmente purificados del veneno del escorpión *Hadruroides. asus*. A partir de 15,46 mg de proteína total del veneno del escorpión *H. charcasus* se purificaron parcialmente sus péptidos por medio de cromatografía de filtración en gel empleando sephadex G-75, consecutivo a una cromatografía de intercambio iónico en CM-Sephadex C-25. El peso molecular estimado de los péptidos se determinó mediante electroforesis PAGE-SDS-Tris-Tricina al 15% y la evaluación de la actividad antibacteriana y antifúngica se empleó el método de microdilución y Kirby-Bauer con cepas de *Escherichia coli* ATCC 25922, *Staphylococcus aureus* ATCC 29213, *Pseudomonas aeruginosa* ATCC 27853 y *Candida albicans* ATCC 10231. En la cromatografía de filtración en gel se obtuvieron 5 fracciones, de lo cual, la fracción IV presentó una concentración mínima inhibitoria de 3,6 mg/mL en *S. aureus* ATCC 29213 y en *C. albicans* ATCC 10231. De la cromatografía de intercambio se obtuvieron 7 fracciones, destacando la fracción OPDIV-5 con péptidos de 4 kDa; 5 kDa; 5,5 kDa y 6,4 kDa que presentó actividad antimicrobiana frente *S. aureus* ATCC 29213, *E. coli* ATCC 25922, *P. aeruginosa* ATCC 27853, *C. albicans* ATCC 10231.El veneno del escorpión *H. charcasus* presenta péptidos de naturaleza catiónica con actividad antibacteriana y antifúngica, según su actividad en las cepas evaluadas.

Palabras clave: Antibacteriano, antifúngico, cromatografía de filtración, cromatografía de intercambio iónico, electroforesis.

Abstract: Venoms of many scorpion species are rich sources of biologically active components, such as antimicrobial peptides, biomolecules that have not yet been studied from *Hadruroides charcasus* venom. The aim of this article is to evaluate the antimicrobial activity of partially purified peptides from the venom of the scorpion *Hadruroides charcasus. asus*. From 15.46 mg of total protein from *H. charcasus* scorpion venom, its peptides were partially purified by gel filtration chromatography using sephadex G-75, followed by ion exchange chromatography on CM-Sephadex C-25. The estimated molecular weight of the peptides was determined by 15% PAGE-SDS-Tris-Tricine electrophoresis and the evaluation of antibacterial and antifungal activity used the microdilution and Kirby-Bauer method with strains of *Escherichia coli* ATCC 25922, *Staphylococcus aureus* ATCC 29213, *Pseudomonas aeruginosa* ATCC 27853 and *Candida albicans* ATCC 10231. In gel filtration chromatography, 5 fractions were obtained, of which fraction IV showed a minimum inhibitory concentration of 3.6 mg/mL in *S. aureus* ATCC 29213 and *C. albicans* ATCC 10231. From the exchange chromatography, 7 fractions were obtained, highlighting the OPDIV-5 fraction with peptides of 4 kDa; 5 kDa; 5.5 kDa and 6.4 kDa that presented antimicrobial activity against *S. aureus* ATCC 29213, *E. coli* ATCC 25922, *P. aeruginosa* ATCC 27853, *C. albicans* ATCC 10231. *H. charcasus* scorpion venom presents peptides of cationic nat

Key words: Antibacterial, antifungal, filtration chromatography, ion exchange chromatography, electrophoresis.

Introducción

La resistencia a los antimicrobianos es un problema de salud mundial tanto en medicina humana como veterinaria donde los agentes antimicrobianos han sido ampliamente utilizados para tratar enfermedades bacterianas, por ejemplo, *Escherichia coli* es un microorganismo comensal común en personas y animales con ciertas cepas que son patógenas y se consideran excelentes indicadores de resistencia a los antimicrobianos[1].

También se conoce que *Pseudomonas aeruginosa* es una bacteria metabólicamente versátil que puede causar una amplia gama de infecciones oportunistas graves y a menudo muestran resistencia adaptativa, debido al estado de crecimiento de la bacteria en el paciente, incluida la capacidad del microorganismo para crecer como biopelícula y además que conducen a la mortalidad[2]. Otro de los ejemplos son reportes de *Staphylococcus aureus*, que está relacionada con su capacidad para adquirir y diseminar determinantes resistentes a los antimicrobianos en la naturaleza. En un estudio donde fueron positivos para *S. aureus* por PCR, más del 50% mostraron resistencia fenotípica a la meticilina, como también resistencia registrada a ampicilina y penicilina en un 96,7%, rifampicina y clindamicina 80%, oxacilina 73,3% y eritromicina 70%. También *S. aureus* reveló susceptibilidad variable a imipenem 96,7%, levofloxacina 86,7%, cloranfenicol 83,3%, cefoxitina 76,7%, ciprofloxacina 66,7%, gentamicina 63,3%, tetraciclina y sulfametoxazol-trimetoprima 56,7 % y vancomicina con doxiciclina en

[1] Universidad Señor de Sipán.
[2] Universidad de Ciencias Aplicadas y Ambientales.
[3] Universidad Nacional de Colombia.
[4] Fundación Universitaria de Ciencias de la Salud.

Corresponding author: operezd@gmail.com

un 50%[3]. Por otro lado, pero casos relacionados a las bacterias, son las infecciones fúngicas, las cuales han aumentado significativamente, lo que contribuye a la morbilidad y la mortalidad, como es el caso de *Candida albicans* caracterizado como un patógeno oportunista, a pesar de las terapias antifúngicas, ha llegado a ser letal por el aumento de la resistencia antimicrobiana, con una resistencia significativa frente a fluconazol e itraconazol a diferencia de otros antifúngicos que se reporta sensibilidad tales como para ketoconazol y anfotericina B[4].

Razones en las que actualmente se ha identificado un mecanismo intrínseco y la adquisición de resistencia antimicrobiana en muchas cepas bacterianas que son de gran importancia clínica por tal motivo ha puesto en grave peligro el uso de antibióticos y también ha provocado la propagación de microbios que son resistentes a los medicamentos efectivos de primera elección[5], Tal es así que la bacterias tanto gram positivas como gram negativas han logrado esta resistencia gracias a elementos genéticos móviles capaces de insertarse y transferirse de bacteria a bacteria[6]. Casos que han derivado el desarrollo de varios estudios experimentales, donde se ha logrado determinar que principios bioactivos tales como péptidos presentes en los venenos de escorpión logran desarrollar actividad antimicrobiana in vitro frente a diferentes microorganismos de importancia en el área de salud. Identificando actividades, independiente tanto de la especie de escorpión como del microorganismo evaluado. Uno de los reportes, es a partir del veneno del escorpión *Tityus discrepans* con una amplia actividad antibacteriana frente a bacterias Gram positivas y Gram negativas[7], mientras que los venenos de los escorpiones *Urodacus yaschenkoi martensii*[8] y *Buthus martensii*[9] y *Androctonus amoeruxi* son más efectivos con bacterias Gram positivas, entre ellas *S. aureus* meticilino resistente (MRSA), siendo una cepa multidrogorresistente[10]. Y el veneno de *Vaejovis punctatus* con actividad antifúngica[11]. Características tomadas en cuenta para determinar si el veneno de *H. charcasus* posee efecto antimicrobiano sobre microorganismos de interés clínico, se planteó en el presente estudio cuyo objetivo es, evaluar la actividad antimicrobiana de péptidos aislados del veneno del escorpión *H. charcasus* frente *E. coli* ATCC 25922, *S. aureus* ATCC 29213, *P. aeruginosa* ATCC 27853 y *C. albicans* ATCC 10231.

Materiales y métodos

Escorpiones y veneno

Los especímenes de *H. charcasus* fueron recolectados en el distrito de Chongoyape, ubicado en la latitud 6º 37' 40.0'' y longitud 79º 25' 21.4'', Chiclayo (Perú), la identificación de la especie por el Dr. José Ochoa Cámara, de la Universidad Nacional de San Antonio Abad del Cusco el veneno se obtuvo por estimulación eléctrica[12], luego se recolectó en tubos eppendorf, se liofilizó y se conservó a -20 °C hasta su uso, de 60 escorpiones se obtuvo 1,2 ml de veneno soluble.

Purificación de péptidos del veneno de *H. charcasus*

Para la cromatografía de filtración en gel, se aplicaron 15,46 mg de proteína del veneno a una columna de Sephadex G-75 (1,5 cm x 50 cm) en presencia de buffer acetato de amonio al 20 mmol/l, pH 4,7, a una velocidad de flujo de 500 µl/4min[13], las fracciones con actividad antimicrobiana, luego se separaron por cromatografía de intercambio iónico, en una columna de carboximetilcelulosa (CM-Sephadex C-25; 2 cm x 9 cm), equilibrada y desarrollada en presencia de buffer acetato de amonio, pH 4,7; con un gradiente continuo de 0 mol/l a 0,5 mol/l[14].

Composición del veneno y sus fracciones mediante método de electroforesis PAGE-SDS-Tricina

En condiciones desnaturalizantes fue realizada la electroforesis SDS-PAGE basados en el método de Schägger y Von Jagow[15], en una corrida a corriente constante y en gel de poliacrilamida al 15,0%. Para el buffer de corrida se empleó solución de tris-tricina-dodecil sulfato de sodio y como estándar de proteínas de rango bajo pre-teñidas (2 a 40 kDa) Thermo Scientific™.

Los geles obtenidos, se revelaron por el método de tinción con plata[16]. Finalmente, se registraron digitalmente los geles en el equipo ChemiDocTM XRS, Bio-Rad.

Actividad antimicrobiana del veneno H. charcasus

En esta parte de la metodología, se empleó el método de microdilución[17,18] con la fracción IV y V de la cromatografía de filtración, se realizaron diluciones dobles seriadas, con un total de siete concentraciones, para la fracción IV de 3,6 mg/ml hasta 0,056 mg/mL y para la fracción V de 6,3 mg/mL hasta 0,098 mg/ml.

Para la preparación del inóculo, se emplearon cepas de *E. coli* ATCC 25922, *S. aureus* ATCC 29213, *P. aeruginosa* ATCC 27853 y *C. albicans* ATCC 10231, se realizaron ensayos por triplicado sembrando 50 µL del inóculo conteniendo $5x10^4$ UFC/ml en cada pocillo, luego se repartieron 50 µl de cada dilución, después se incubaron a 37 ºC durante 24 horas. Los controles positivos fueron caldo más inóculo, y los controles negativos solo caldo. El crecimiento del control positivo se determinó por un botón de crecimiento de ≥ 2 mm o una turbidez definida. Se empleó el método Kirby-Bauer[19], para la sensibilidad antimicrobiana de las fracciones de la cromatografía de intercambio iónico, en las placas de agar Mueller-Hinton se sembraron con un inóculo de 1 a 2 x 10^8 UFC/ml.

El análisis de los datos se realizó usando el complemento MegaStat para Excel, con análisis varianza para determinar si los componentes proteicos purificados del veneno y las concentraciones empleadas si influyeron en el crecimiento microbiano.

Resultados

A partir de 15,46 mg de proteínas total del veneno de *H. charcasus*, se analizaron por el método de cromatografía de filtración en gel Sephadex G-75, obteniendo cinco fracciones bien definidas de la cromatografía de filtración Sephadex G-75 (Figura 1), en el análisis del gel de electroforesis de Poliacrilamida (PAGE-SDS-Tricina), presentó un número variable bandas proteicas para cada uno de las fracciones purificadas, asimismo reveló para la fracción IV la presencia de siete bandas con rango de pesos moleculares de 9,8 kDa, 12 kDa, 15,1 kDa, 18,3 kDa, 24,3 kDa, 30,2 kDa y 37,5 kDa y para la fracción V se obtuvieron 6 bandas con rango de peso entre 5,1 kDa, 5,7 kDa, 7,9 kDa, 8,5 kDa, 10,7 kDa y 12,2 kDa respectivamente (Figura 2).

En la evaluación de la actividad antimicrobiana se muestra en la fracción IV presentó una concentración mínima inhibitoria (CMI) de 3,6 mg/mL para las cepas de *S. aureus* ATCC 29213 y *C. albicans* ATCC 10231 y para las cepas de *E. coli* ATCC 25922 y *P. aeruginosa* ATCC 27853 no presentó inhibición total de

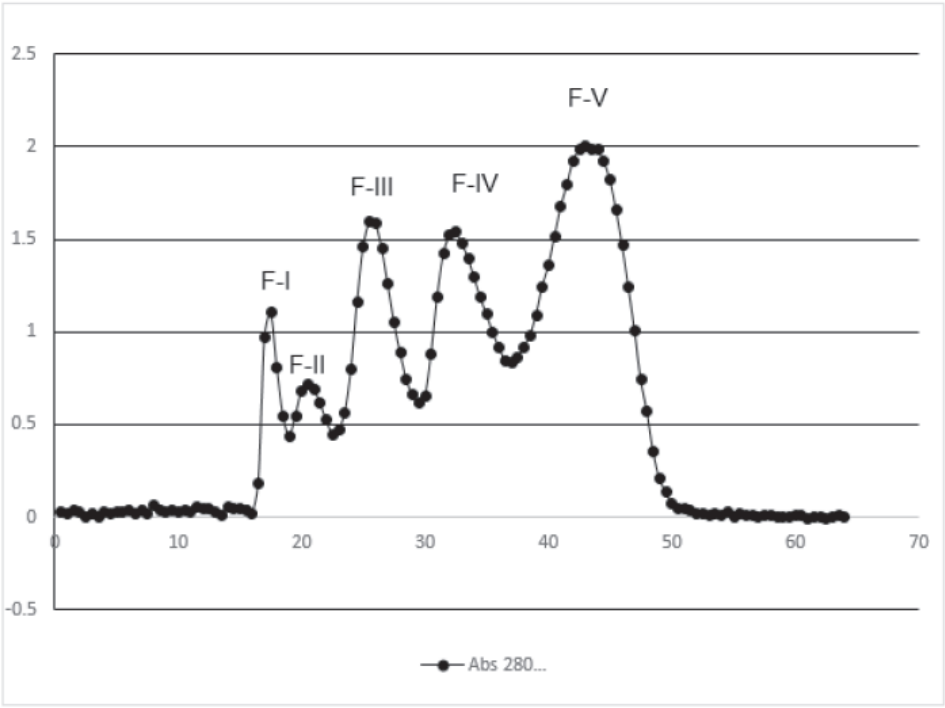

Figure 1. Purificación de las proteínas del veneno de *H. charcasus* por cromatografía de filtración en columna Sephadex G-75 con las fracciones (F-I, F-II, F-III, F-IV y F-V).

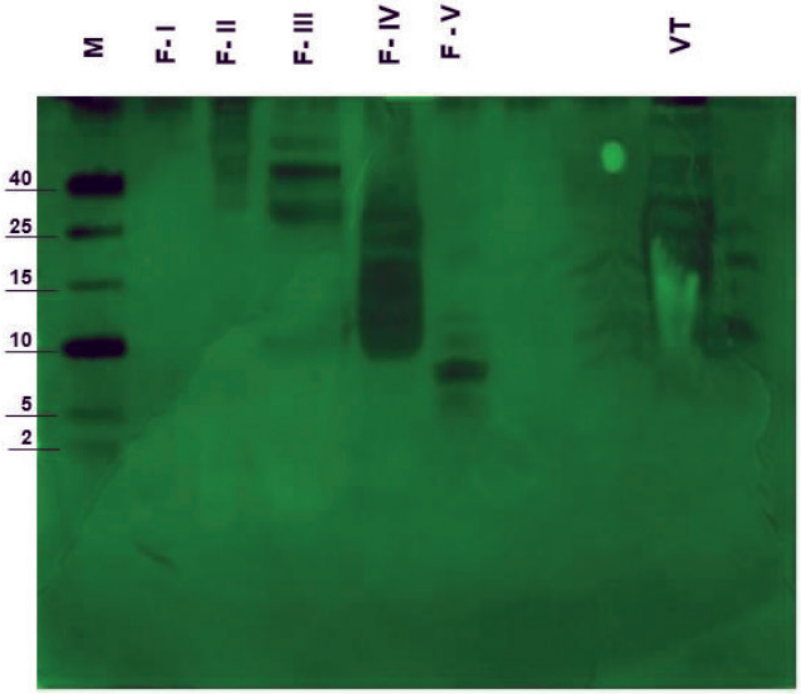

Figura 2. Electroforesis en gel de poliacrilamida con SDS - Tricina (PAGE-SDS-Tricina) de las proteínas purificadas, en el carril M marcador de peso molecular (2 – 40 KDa) (marcador de peso molecular) y fracciones de proteínas (FI - FV) y veneno total (VT).

crecimiento a las concentraciones empleadas respectivamente (Figura 3), para la fracción V no presentó inhibición total de crecimiento microbiano (Figura 4).

En la figura 5 se muestra el análisis de la separación de los péptidos por el método de cromatografía de intercambio iónico Sephadex C-25, se recuperaron al menos siete fracciones (OPDIV-1 a OPDIV-7), de los cuales al evaluar la actividad antimicrobiana mediante el método Kirby-Bauer, las cepas de *E. coli* ATCC 25922, *S. aureus* ATCC 29213, *C. albicans* ATCC 10231 y *P. aeruginosa* ATCC 27853 presentaron sensibilidad frente a la fracción OPDIV-5 a concentración de 1µg/mL (tabla 1) y en el análisis de PAGE-SDS-Tricina, la fracción OPDIV-5 presentó cuatro bandas de pesos moleculares de 7,5 kDa, 6,4 kDa, 5,5 kDa y 4 kDa (Figura 6).

Discusión

Actualmente los escorpiones son bien conocidos por sus picaduras peligrosas y sus venenos se han aplicado en la medicina tradicional, principalmente en Asia y África y se ha convertido en una valiosa fuente de moléculas biológicamente activas desde nuevos antibióticos hasta posibles terapias contra el cáncer[20], además de acuerdo a los reportes publicados el veneno de escorpión posee una fuente abundante péptidos antimicrobianos nuevos y potentes tanto como naturales o modificados químicamente con la finalidad ampliar su capacidad antibacteriana, antifúngica, antiparasitaria[21,22]. Los péptidos antimicrobianos son uno de los componentes del sistema inmune innato en una amplia gama de organismos eucariotas como hu-

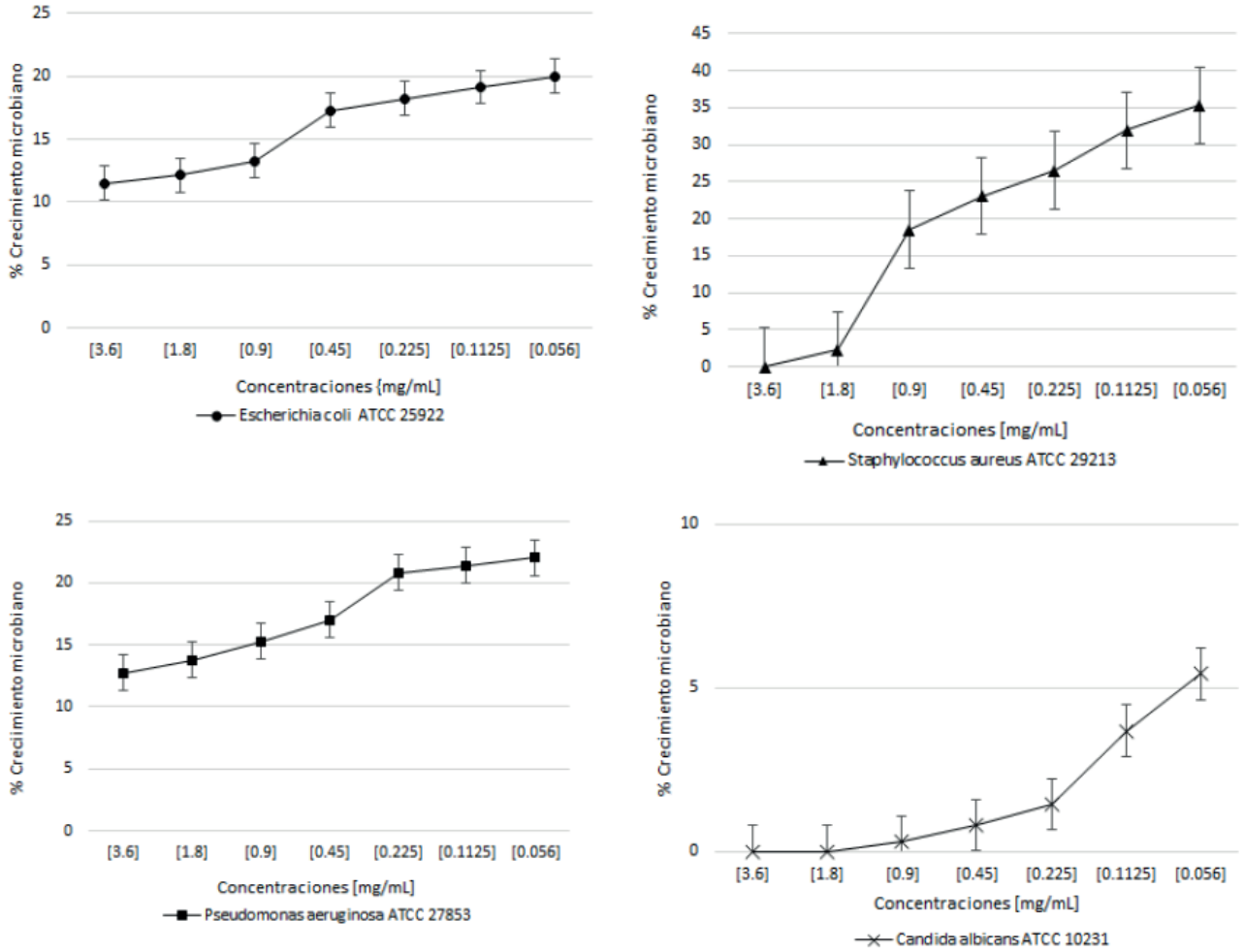

Figura 3. Actividad antimicrobiana de la fracción IV frente *Escherichia coli* ATCC 25922, *Staphylococcus aureus* ATCC 29213, *Pseudomonas aeruginosa* ATCC 27853 y *Candida albicans* ATCC 10231.

manos, plantas e insectos y que juegan un papel vital en los primeros mecanismos de defensa inmune contra los patógenos[23].

En el presente estudio se logró determinar la presencia péptidos antimicrobianos del veneno de *H. charcasus* esto es algo propio del veneno de los escorpiones tal como se evidencia de otras especies de escorpiones que demostraron e inclusive aislar péptidos con potencial acción antimicrobiana como las pantininas de *Pandinus imperator*[24], los péptidos TsAP-1 y TsAP-2 de *Tityus serrulatus*[25] péptidos del veneno de Scorpio *maurus palmatus*[26] y los péptidos HsAp del escorpión *Heterometrus spinifer*[27].

Además, en el presente trabajo mediante el empleo de dos métodos cromatográficos, uno de filtración en gel y otro de intercambio iónico permitió separar las proteínas en fracciones. Cuando el veneno crudo se separó por columna Sephadex G-75, se obtuvieron 5 fracciones, siendo evidente la fracción IV con actividad antibacteriana frente a *S. aureus* y antifúngica frente a *C. albicans*. Esta fracción relacionada con su actividad antimicrobiana fue purificada y analizada en CM Sephadex C-25, obteniendo 7 fracciones, de los cuales la quinta fracción denominada OPDIV-5 contiendo péptidos con pesos moleculares de 7,5 kDa, 6,4 kDa, 5,5 kDa y 4 kDa mediante el método Kirby–Bauer se encontró actividad frente *E. coli*, *S. aureus*, *P. aeruginosa* y *C. albicans*.

Esto es característico de los péptidos antimicrobianos que por lo general presentan peso molecular por debajo de 8,5 kDa como es el caso de las familias de las opiscorpinas del escorpión *Opistophthalmus carinatus*[28], vejonina de *Vaejovis mexicanus*[29] Heterinas de *Heterometrus spinifer*[30], demostrando su amplia acción antibacteriana y antifúngica.

La purificación parcial de la fracción OPDIV-5 conformado por cuatro péptidos con carga positiva que al interactuar con las cargas negativas de la CM Sephadex C-25, solo se pudo eluir aumentando la concentración del acetato de amonio, además, presentó actividad antibacteriana como actividad antifúngica. esto se debió al empleó mayor concentración del buffer acetato de amonio con la finalidad de recolectar péptidos de naturaleza catiónica y con mayor carga.

Los péptidos antimicrobianos del veneno de escorpión son péptidos anfipáticos cargados positivamente, se manifiesta en los péptidos meuVAP-6, meuAP-18-1 y meuPep34 de *Mesobuthus eupeus*[31], inclusive en los péptidos VpAmp de *Vaejovis punctatus*, por presentar acción contra bacterias gram positivas y contra *C. albicans* y frente a bacterias gram negativas[32], similar fue para los péptidos UyCT de *Urodacus yaschenkoi* por tener predilección por bacterias gram positivas[33], péptido antibacteriano de *Centruroides margaritatus*[34].

Conclusiones

El veneno de *H. charcasus*, posee péptidos de naturaleza catiónica, con capacidad antimicrobiana frente a microorganismos patógenos de importancia clínica.

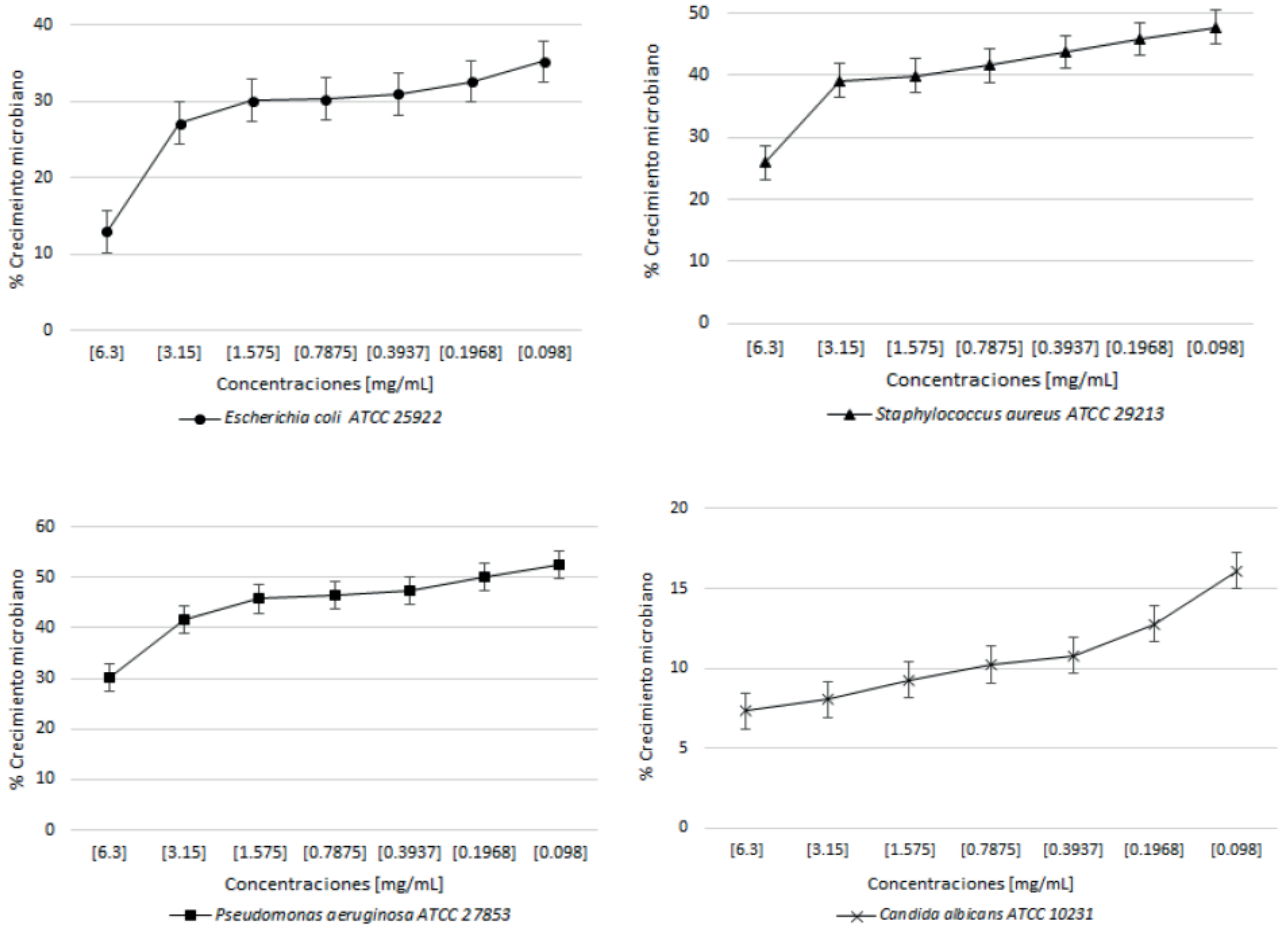

Figura 4. Actividad antimicrobiana de la fracción V frente a *Escherichia coli* ATCC 25922, *Staphylococcus aureus* ATCC 29213, *Pseudomonas aeruginosa* ATCC 27853 y *Candida albicans* ATCC 10231.

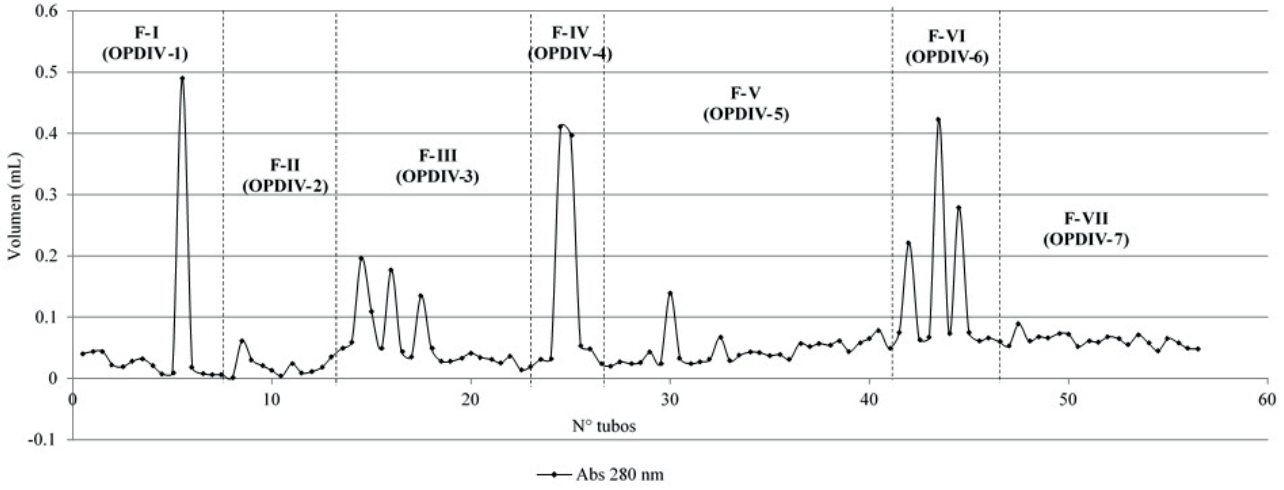

Figura 5. Purificación de la fracción IV (Sephadex G-75) con acción antimicrobiana, en cromatografía de intercambio iónico Carboximetilcelulosa Sephadex C-25.

Agradecimientos

Agradecimiento al Grupo de Investigación en Proteínas de la Universidad Nacional de Colombia sede en Bogotá, por la oportunidad para el desarrollo del trabajo de investigación.

Conflicto de interés

Los autores declaramos no presentar conflictos de interés potenciales con respecto a la investigación, autoría y/o publicación de este artículo.

Fracciones/ concentraciones	*E. coli* ATCC 25922	*S. aureus* ATCC 29213	*P. aeruginosa* ATCC 27853	*C. albicans* ATCC 10231
OPDIV-1 (4,96 ug/mL)	-	-	-	-
OPDIV -2 (14,5 ug/mL)	-	-	+	-
OPDIV -3 (3,42 ug/mL)	-	-	-	-
OPDIV -4 (3,02 ug/mL)	-	-	-	+
OPDIV -5 (1 ug/mL)	+	+	+	+
OPDIV -6 (7,72 ug/mL)	-	-	-	+
OPDIV -7 (2,24 ug/mL)	+	-	-	+

Con actividad +; Sin actividad -

Tabla 1. Sensibilidad antimicrobiana de las fracciones de la cromatografía de intercambio iónico (OPDIV-1 a OPDIV-7) frente a *Escherichia coli* ATCC 25922, *Staphylococcus aureus* ATCC 29213, *Pseudomonas aeruginosa* ATCC 27853 y *Candida albicans* ATCC 10231.

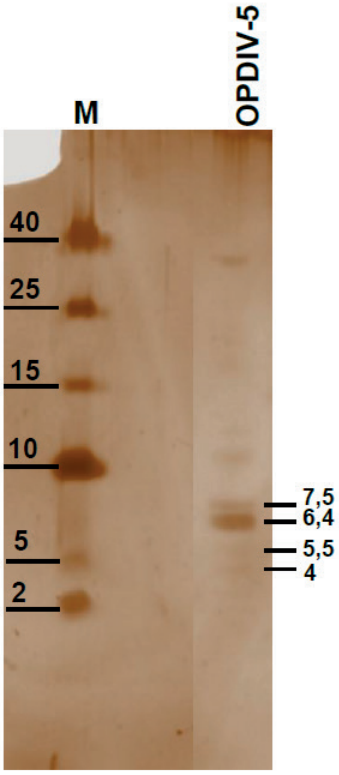

Figura 6. Electroforesis en gel de poliacrilamida con SDS - Tricina (PAGE-SDS-Tricina) de las proteínas purificadas de la fracción IV de la Cromatografía de intercambio iónico Sephadex C-25, en el carril M marcador de peso molecular (2 – 40 kDa) y fracción OPDIV-5.

Referencias bibliográficas

1. Yassin AK, Gong J, Kelly P, Lu G, Guardabassi L, Wei L, et al. Antimicrobial resistance in clinical Escherichia coli isolates from poultry and livestock, China. PLoS ONE. 2017; 12(9): e0185326. DOI: http://dx.doi.org/10.1371/journal.pone.0185326
2. Gellatly SL, Hancock REW. Pseudomonas aeruginosa: new insights into pathogenesis and host defenses. Path and Dis. 2013; 67: 159 – 173. DOI: http://dx.doi.org/10.1111/2049-632X.12033
3. Akanbi OE, Njom HA, Fri J, Otigbu AC, Clarke AM. Antimicrobial Susceptibility of Staphylococcus aureus Isolated from Recreational Waters and Beach Sand in Eastern Cape Province of South Africa. Int. J. Environ. Res. Public Health. 2017; 14: 1001. DOI: http://dx.doi.org/10.3390/ijerph14091001
4. Zaidi KU, Mani A, Parmar R, Thawani V. Antifungal Susceptibility Pattern of Candida albicans in Human Infections. Op. Biol. Scie. J. 2018; 4: 1 – 6. DOI: http://dx.doi.org/10.2174/2352633501804010001
5. Rayamajhi N, Bin Cha S, Yoo HS. Antibiotics Resistances: Past, Present and Future. J. Biomed Res. 2010; 11(2): 65 – 80. Disponible en: http://www.jbr.or.kr/journal/article.php?code=5527
6. Partridge SR, Kwong SM, Firth N, Jensen SO. Mobile genetic elements associated with antimicrobial resistance. Clin Microbiol Rev 2018; 31: e00088-17. DOI: https://doi.org/10 .1128/CMR.00088-17
7. Díaz P, D'Suze G, Salazar V, Sevcik C, Shannon JD, Sherman NE, Fox JW. Antibacterial activity of six novel peptides from Tityus discrepans scorpion venom. A fluorescent probe study of microbial membrane Na+ permeability changes. Toxicon. 2009; 54: 802 – 817. DOI: http://dx.doi.org/10.1016/j.toxicon.2009.06.014
8. Luna-Ramírez K, Quintero-Hernández V, Vargas-Jaimes L, Batista CVF, Winkel, KD, Possani LD. Characterization of the venom from the Australian scorpion Urodacus yaschenkoi: Molecular mass analysis of components, cDNA sequences and peptides with antimicrobial activity. Toxicon. 2013; 63: 44 – 54. DOI: http://dx.doi.org/10.1016/j.toxicon.2012.11.017
9. de la Salud R, Ross M, Luque LE. Synthesis of analogs of peptides from Buthus martensii scorpion venom with potential antibiotic activity. Peptides. 2015; 68: 228 – 232. DOI: http://dx.doi.org/10.1016/j.peptides.2014.10.008
10. Almaaytah A, Farajallah A, Abualhaijaa A, Al-Balas Q. A3, a Scorpion Venom Derived Peptide Analogue with Potent Antimicrobial and Potential Antibiofilm Activity against Clinical Isolates of Multi-Drug Resistant Gram Positive Bacteria. Molecules. 2018; 23: 1603. DOI: http://dx.doi.org/10.3390/molecules23071603
11. Ramírez S, Jiménez JM, Rivas B, Corzo G, Possani LD, Becerril B, Ortiz E. Peptides from the scorpion Vaejovis punctatus with broad antimicrobial activity. Peptides. 2015; 73: 51–59. DOI: http://dx.doi.org/10.1016/j.peptides.2015.08.014

12. Pérez-Delgado O, Espinoza-Vergara M, Castro-Vega N, Reyes-Montaño E. Evaluación preliminar de actividad antibacteriana in vitro del veneno de escorpión Hadruroides charcasus (Karsch, 1879) contra Pseudomonas aeruginosa y Staphylococcus aureus. Rev C Méd HNAAA, 2019; 12(1): 6 - 12. DOI: https://doi.org/10.35434/rcmhnaaa.2019.121.477
13. Possani LD, Dent MAR, Martin BM, Maelicke A, Svendsen I. The amino terminal sequence of several toxins from the venom of the Mexican scorpion Centruroides noxius Hoffmann. Carlsberg Res. Commun. 1981; 46: 207–214. DOI: https://doi.org/10.1007/BF02906498
14. Ramirez-Dominguez ME, Olamendi-Portugal T, Garcia U, Garcia C, Arechiga H, Possani LD. Cn11, the first example of a scorpion toxin that is a true blocker of Na(+) currents in crayfish neurons. The Journal of experimental biology. 2002; 205(Pt 6):869-76. Disponible en: https://jeb.biologists.org/content/205/6/869
15. Schägger, H.; von Jagow, G. 1987. Tricine–sodium dodecyl sulfate polyacrylamide gel electrophoresis for the separation of proteins in the range from 1–100 kDalton. Anal. Biochem. 166: 368 – 379. DOI: https://doi.org/10.1016/0003-2697(87)90587-2
16. Shevchenko A, Wilm M, Vorm O, Mann M. Mass Spectrometric Sequencing of Proteins from Silver-Stained Polyacrylamide Gels Anal. Chem. 1996; 68: 850 -858. DOI: https://doi.org/10.1021/ac950914h
17. National Committee for Clinical Laboratory Standards. Methods for dilution antimicrobial susceptibility tests for bacteria that grow aerobically. Document M07-A10. 2015. NCCLS, Wayne, PA. Recuperado a partir de: https://clsi.org/
18. Clinical and Laboratory Standars Institute. Reference Method for Broth Dilution Antifungal Susceptibility Testing Yeasts. Aprproved Estándar - tercera edición 2008 (28)14: 1 - 25. M27-A3. Recuperado a partir de: https://clsi.org/
19. Clinical and Laboratory Standars Institute. Performance Standards for Antimicrobial Disk Susceptibility Tests Document M02-A13. 2018. NCCLS, Wayne, PA. Recuperado a partir de: https://clsi.org/
20. Ortiz E, Gurrola GB, Ferroni E, Possani LD. Scorpion venom components as potential candidates for drug Development. Toxicon. 2015; 93: 125e135. DOI: http://dx.doi.org/10.1016/j.toxicon.2014.11.233
21. Luna-Ramirez K, Tonk M, Rahnamaeian M, Vilcinskas A. Bioactivity of Natural and Engineered Antimicrobial Peptides from Venom of the Scorpions Urodacus yaschenkoi and U. manicatus. Toxins. 2017; 9 (22): 1 -12. DOI: http://dx.doi.org/10.3390/toxins9010022
22. Borges A, Delgado O, Silva S, Bravo J, Velasco E, Rojas L, De Sousa L. Aislamiento y caracterización de un péptido del veneno de Tityus gonzalespongai (scorpiones, buthidae) con actividad sobre promastigotes de Leishmania (Leishmania) mexicana. Saber. 2013; 25 (4): 399 – 413. Disponible en: http://ve.scielo.org/scielo.php?script=sci_arttext&pid=S1315-01622013000400008&lng=es
23. arazi S. Scorpion venom as antimicrobial peptides (AMPs): A review article. Inter. arab. J. anti. age. 2015; 5(3): 1 – 5. Disponible en: https://imed.pub/ojs/index.php/IAJAA/article/view/1384/1134
24. Zeng CC, Zhou L, Shi W, Luo X, Zhang L, Nie Y, Wang J, Wu Sh, Cao B, Cao H. Three new antimicrobial peptides from the scorpion Pandinus imperator. Peptides. 2013; 45: 28–34. DOI: http://dx.doi.org/10.1016/j.peptides.2013.03.026
25. Guo X, Ma Ch, Du Q, Wei R, Wang L, Zhou M, Chen T, Shaw C. Two peptides, TsAP-1 and TsAP-2, from the venom of the Brazilian yellow scorpion, Tityus serrulatus: Evaluation of their antimicrobial and anticancer activities. Biochimie. 2013; 95: 1784 – 1794. DOI: http://dx.doi.org/10.1016/j.biochi.2013.06.003
26. Harrison PL, Abdel-Rahman MA, Strong PN, Tawfik MM, Miller K. Characterisation of three alpha-helical antimicrobial peptides from the venom of Scorpio maurus palmatus Toxicon. 2016;117: 30 - 6. DOI: http://dx.doi.org/10.1016/j.toxicon.2016.03.014
27. Nie Y, Chun X, Zeng XC, Yang Y, Luo F, Luo X, Wua S, Zhang L, Zhou J. A novel class of antimicrobial peptides from the scorpion Heterometrus spinifer. Peptides. 2012; 38: 389 – 394. DOI: http://dx.doi.org/10.1016/j.peptides.2012.09.012
28. Zhu S, Tytgat J. The scorpine family of defensins: gene structure, alternative polyadenylation and fold recognition. Cell. Mol. Life Sci. 2004; 61: 1751e1763. DOI: https://doi.org/10.1007/s00018-004-4149-1
29. Hernandez-Aponte CA, Silva-Sanchez J, Quintero-Hernandez V, Rodriguez-Romero A, Balderas C, Possani LD, Gurrola GB. Vejovine, a new antibiotic from the scorpion venom of Vaejovis mexicanus. Toxicon. 2011; 57: 84e92. DOI: https://doi.org/10.1016/j.toxicon.2010.10.008
30. Wu S, Nie Y, Zeng X-C, Cao H, Zhang L, Zhou L, Yang Y, Luo X, Liu Y. Genomic and functional characterization of three new venom peptides from the scorpion Heterometrus spinifer. Peptides. 2014; 53: 30-41. DOI: https://doi.org/10.1016/j.peptides.2013.12.012
31. Baradaran M, Jalali A, Naderi M, Galehdari H. A Novel Defensin-Like Peptide Associated with Two Other New Cationic Antimicrobial Peptides in Transcriptome of the Iranian Scorpion Venom. 2017; 21(3): 190 – 196. DOI: https://dx.doi.org/10.18869%2Facadpub.ibj.21.3.190
32. Ramírez S, Jiménez JM, Rivas B, Corzo G, Possani LD, Becerril B, Ortiz E. Peptides from the scorpion Vaejovis punctatus with broad antimicrobial activity. Peptides. 2015; 73: 51–59. DOI: http://dx.doi.org/10.1016/j.peptides.2015.08.014
33. Luna K, Sani MA, Silva J, Jiménez JM, Reyna F, Winkel KD, Wright CE, Possani LD, Separovic F. Membrane interactions and biological activity of antimicrobial peptides from Australian scorpion. Bioch. et Bioph. Ac. 2014; 1838: 2140 – 2148. DOI: http://dx.doi.org/10.1016/j.bbamem.2013.10.022
34. Rivera C, Flores L, Pantigoso C, Escobar E. Aislamiento y caracterización de un péptido antibacteriano del veneno de Centruroides margaritatus. Rev. Per. Biol. 2010; 17(1): 129 -132. Disponible en: http://www.scielo.org.pe/pdf/rpb/v17n1/a16v17n1.pdf

Received: 10 marzo 2021
Accepted: 5 julio 2021

RESEARCH / INVESTIGACIÓN

Trametes coccinea IDEA, un hongo súper productor de lacasa aislado de un lago natural de asfalto: Tolerancia y biotransformación de hidrocarburos policíclicos aromáticos

Trametes coccinea IDEA, a super laccase-producer fungus isolated from a natural asphalt lake: Tolerance and biotransformation of aromatics polycyclic hydrocarbons

Beatriz Pernía[1,2*], Hector Urbina[1,3], Meralys González[1], Lucia Sena[1], Yanet Villasana[4], Leopoldo Naranjo-Briceño[1,5]

DOI. 10.21931/RB/2021.06.03.7

Resumen: Los hidrocarburos policíclicos aromáticos (HPAs) son compuestos tóxicos que no se degradan fácilmente bajo condiciones naturales tales como fenómenos físicos (fotooxidación, volatilización), químicos (intercambio iónico, complejación, transformación) y biológicos (degradación por microorganismos autóctonos) que además, dependen de la temperatura, humedad y niveles de oxígeno. El objetivo del presente trabajo fue aislar, identificar y caracterizar fenotípicamente hongos hidrocarbono clásticos de ambientes extremos que sean capaces de tolerar HPAs, tales como *Trametes coccinea* IDEA, que se aisló del Lago de asfalto natural de Guanoco en Venezuela. A fin de estudiar su tolerancia a los HPAs, el hongo se expuso a diferentes concentraciones de naftaleno, fenantreno y pireno (0, 2.5, 25, 50, 100, 200, 400, 800 y 1600 mg/L). Posteriormente, en ensayo en medio de cultivo líquido, se procedió a estudiar el efecto de los HPAs sobre la actividad de enzimas del sistema enzimático de degradación de lignina (SEDL), así como sobre la posible variación en los niveles de toxicidad empleando *Lactuca sativa* como bioindicador. Los resultados mostraron una mayor tolerancia al pireno, seguido por el naftaleno y fenantreno. Se observó una fuerte inducción de la actividad lacasa en presencia de naftaleno (167.96 U/mgP) y pireno (124.89 U/mgP) con respecto al control, mientras que con fenantreno se obtuvo una baja actividad (88.67 U / mgP). De manera interesante, se evidenció una generación de sub-productos más tóxicos cuando el naftaleno y el fenantreno fueron biotratados por el hongo, mientras que el nivel de toxicidad del pireno disminuyó significativamente. *T. coccinea* IDEA tiene un alto potencial para ser utilizado en estrategias de biorremediación de hidrocarburos, las cuales deben ser monitoreadas mediante análisis ecotoxicológicos para detectar posibles variaciones de toxicidad de los productos parcialmente biotransformados.

Palabras clave: Micorremediación, biotransformación, ecotoxicidad, HPAs.

Abstract: Polycyclic aromatic hydrocarbons (HPAs) are toxic compounds that are not easily degraded under natural conditions. The goal of the present study was to isolate, identify and phenotypically characterize hydrocarbonoclastic fungi from extreme environments that are capable of tolerating HPAs, such as *Trametes coccinea* IDEA, that was isolated from the Natural Asphalt Lake of Guanoco in Venezuela. To study its tolerance to HPAs, the fungus was exposed to different concentrations of naphthalene, phenanthrene, and pyrene (0, 2.5, 25, 50, 100, 200, 400, 800, and 1600 mg/L). Subsequently, in a test in a liquid culture medium, the effect of these HPAs on the activity of enzymes of the lignin-degrading enzymes system (LDES) was studied, and the possible variations in toxicity levels using *Lactuca sativa* as bioindicator. The results showed a high tolerance to pyrene, followed by naphthalene and phenanthrene. Strong induction of laccase activity was observed at the presence of naphthalene (167.96 U/mgP) and pyrene (124.89 U/mgP) compared with the control, while with phenanthrene a low activity was obtained (88.67 U / mgP). Interestingly, a generation of more toxic byproducts was observed when naphthalene and phenanthrene were biotreated by the fungus, while the toxicity level of pyrene decreased significantly. *T. coccinea* IDEA has a high potential to be used in hydrocarbon bioremediation strategies, which must be monitored by ecotoxicological analysis to detect the possible toxicity levels variations in the partially biotransformed products.

Key words: Mycoremediation, biotransformation, ecotoxicity, PAHs.

Introducción

Los hidrocarburos policiclicos aromáticos (HPAs) son compuestos de origen natural y antropogénico, que se encuentran en el suelo, el aire y el agua. De estos compuestos, 16 han sido considerados por la Environmental Protection Agency (EPA) como tóxicos, recalcitrantes y cancerígenos[1,2]. Además, estos compuestos no se degradan fácilmente bajo condiciones naturales y su persistencia en el ambiente incrementa al aumentar su peso molecular. Se ha reportado que los HPAs se encuentran en todos los componentes del medio ambiente y se bioacumulan en los organismos[3].

Es por ello, que se han sumado esfuerzos para encontrar organismos que sean capaces de tolerar y degradar estos compuestos con la finalidad de emplearlos en nuevas estrategias biotecnológicas de saneamiento ambiental. La biorremediación emplea organismos para degradar, detoxificar o biotransformar compuestos tóxicos y convertirlos en menos tóxicos o

[1] Área de Energía y Ambiente, Fundación Instituto de Estudios Avanzados (IDEA), Caracas, Venezuela.
[2] Instituto de Investigaciones de Recursos Naturales, Facultad de Ciencias Naturales, Universidad de Guayaquil, Guayaquil, Ecuador.
[3] Division of Plant Industry, Florida Department of Agriculture, Gainesville, FL, USA.
[4] Grupo Biomass to Bioresources, Universidad Regional Amazónica Ikiam, CP, Tena, Ecuador.
[5] Grupo de Microbiología Aplicada, Universidad Regional Amazónica Ikiam, CP, Tena, Ecuador.

Corresponding author: beatriz.pernias@ug.edu.ec

inocuos[4]. Dentro de dichos organismos, se ha demostrado que los hongos cuentan con un sistema enzimático de degradación de lignina (SEDL) que, por su baja especificidad de sustrato, es capaz de biotransformar eficientemente HPAs[5]. Dentro del grupo de hongos, los hidrocarbonoclásticos extremófilos surgen como un grupo heterogéneo que vive de manera óptima en condiciones extremas y tiene una alta capacidad de usar hidrocarburos como única fuente de carbono y energía[5].

En este sentido, existen algunas especies de hongos capaces de tolerar y degradar estos hidrocarburos puesto que producen extracelularmente enzimas que catalizan reacciones oxidativas. Entre las enzimas con alto potencial en biocatálisis ambiental, han sido reportadas la citocromo P-450[6], la lignina peroxidasa (LigP)[7], la manganeso peroxidasa (MnP)[8,9], la cloroperoxidasa[10], la lacasa (Lac)[11] y las benzopireno hidroxilasa[12].

Dentro de éstas exoenzimas oxidativas, se destacan las lacasas (EC 1.10.3.2), las cuales son enzimas glicosiladas, multicobre, cuya función es catalizar la oxidación de compuestos fenólicos, polifenólicos y aminas aromáticas, mediante el acoplamiento con la reducción de oxígeno a agua[13]. Sin embargo, esta enzima presenta una amplia inespecificidad de sustrato, por lo que puede oxidar una gran variedad de compuestos, tales como colorantes, pesticidas, disrruptores endocrinos e HPAs[14]. La lacasa ha sido utilizada a nivel industrial para el análisis de drogas, el blanqueamiento en la industria papelera y textil, la síntesis de polímeros y en procesos de biorremediación y saneamiento de aguas residuales[15]. En el caso de los HPAs, se ha reportado que esta enzima es capaz de oxidar naftaleno, fenantreno, antraceno, benzopireno, 9 metilantraceno y 2 metilantraceno[16].

Sin embargo, aunque estas enzimas son capaces de degradar hidrocarburos, en algunos casos, en el proceso de biotransformación se podrían generar compuestos más tóxicos que los HPAs originales, por lo que deben realizarse pruebas de ecotoxicología a fin de verificar la posible generación de compuestos más tóxicos que el contaminante original[17].

En la búsqueda de hongos que sean capaces de sintetizar estas enzimas para su uso potencial en procesos de degradación de hidrocarburos, se han aislado hongos de ambientes extremos, tales como el caso del Lago de Asfalto de Guanoco, ubicado en el estado Sucre en Venezuela[18]. Este lago de asfalto tiene una superficie de 420 hectáreas, presenta una baja concentración de nutrientes debido a que está conformado casi en su totalidad por asfalto y se caracteriza por contener 83% carbono, 11% hidrógeno y 6% azufre[19].

En la presente investigación se aisló del Lago de Asfalto de Guanoco el hongo *Trametes coccinea*, el cual es un hongo de pudrición blanca, capaz de producir a nivel extracelular enzimas tales como celobiohidrolasas, glucanohidrolasas, β-glucosidasas, xilanasas, α-amilasa, lignina peroxidasa, manganeso peroxidasa, fenoloxidasa[20,21] y, adicionalmente, sintetiza grandes cantidades de la enzima lacasa[22]. También, se ha descrito que este hongo es capaz de degradar antraceno (67.5%), pireno (31.1%)[23], fenantreno (45.6%) y benzo[a]antraceno (90.1%) en 14 días a una temperatura de 28°C[24].

Los objetivos principales de este trabajo fueron: i) aislar e identificar un hongo con alta capacidad de degradar HPAs del Lago de Asfalto de Guanoco, ii) determinar la tolerancia del hongo a distintas concentraciones de HPAs, iii) identificar cambios en la actividad de las enzimas lacasas ante su exposición a distintos HPAs, y iv) analizar la variación en la toxicidad de los HPAs tras su biotransformación por el hongo.

Materiales y métodos

Aislamiento, caracterización taxonómica e identificación molecular

Un hongo Basidiomycota de identificación desconocida, el cual fue adoptado en nuestro Laboratorio de Petromicrobiología como el Soldado Desconocido, fue aislado de una raíz de una dicotiledónea que se encontraban inmersa en medio del Lago natural de Asfalto de Guanoco, ubicado en el estado Sucre en Venezuela, al Norte de América del Sur (Figura 1). La raíz se colocó en una bolsa plástica en oscuridad y fue conservada en el laboratorio a +4ºC. A los tres meses apareció el basidiocarpo creciendo sobre la raíz del árbol (Figura 2A).

Para su aislamiento, se seccionó un trozo del contexto del hongo en condiciones de esterilidad y se sembró en placas con medio Power[25] donde, tras sucesivos repiques, se obtuvo un cultivo axénico (Figura 2B).

La identificación taxonómica se realizó mediante la caracterización de su morfología macro y microscópica (color del basidiocarpo, hifas, conidias, clamidosporas, conidióforos y células conidiogénicas). La información fue recopilada en una descripción y se comparó con la literatura especializada.

La identificación molecular de este organismo se realizó inoculando esporas en medio MPPY según la metodología propuesta por Montenegro *et al.*[26] y Naranjo *et al.*[27] y fueron incubadas en un agitador a 30°C y 250 rpm durante 48 h. Posteriormente, el micelio fue recuperado por filtración utilizando un filtro Nytal, se lavó dos veces con NaCl al 0.9% (P/V), se congeló con nitrógeno líquido y se almacenó a -80°C. Luego, se tomaron 300-500 mg de micelio, se pulverizó con nitrógeno líquido y se añadieron 1 mL de tampón de rotura (0.18 M Tris/HCl pH 8.2, 10 mM EDTA, 1% SDS) y 1 mL de fenol, se incubó por 30 min a 50°C con agitación en Vórtex cada 5 min. Luego, se extrajo el ADN genómico con fenol/CIA (fenol:cloroformo:alcohol isoamílico, 25:24:1) y se repitió este procedimiento hasta que la interface quedó limpia. El ADN genómico fue precipitado con 2.5 vol de etanol y 0.1 vol de 3M acetato de sodio (pH 3.2) y se conservó durante la noche a -20 oC. Al día siguiente, la muestra se centrifugó a 14.000 rpm a RT, se hizo un lavado con ETOH al 70% y el ADN se resuspendió en buffer Tris-EDTA (TE)[28].

Para la identificación molecular se amplificó por PCR la región 26S rRNA, utilizando los cebadores: NL1(sentido): 5'...GCATATCAATAAGCGGAGGAAA AG...3' y NL4 (antisentido): 5'...GGTCCGTGTTTCAAGACGG...3'. Las reacciones de PCR se llevaron a cabo en un termociclador Applied Biosystems 2720 empleando una concentración final de los deoxiribonucleotidos trifosfatos (dNTP's) de 0.25 mM y 100-250 ng de ADN genómico como molde. Las condiciones de PCR fueron las siguientes: i) pre-desnaturalización a 95°C por 5 min, seguidos por 30 ciclos de ii) desnaturalización a 95°C por 5 min, iii) anillamiento a 52°C por 30 s, iv) extensión a 72°C por 1 min y, v) una extensión final a 72°C por 7 min.

El producto de PCR obtenido (600 pb) fue doblemente purificado utilizando el kit de purificación Wizard Genomic DNA Purification Kit Promega (Madison, WI). Posteriormente, las muestras de ADN fueron enviadas a secuenciar en UC Berkeley DNA Sequencing Facility (California, USA). El análisis *in silico* de las secuencias de nucleótidos se realizó utilizando los programas DNASTAR Programs (DNASTAR, Inc., UK), BLASTN[29] utilizando formato FASTA[30].

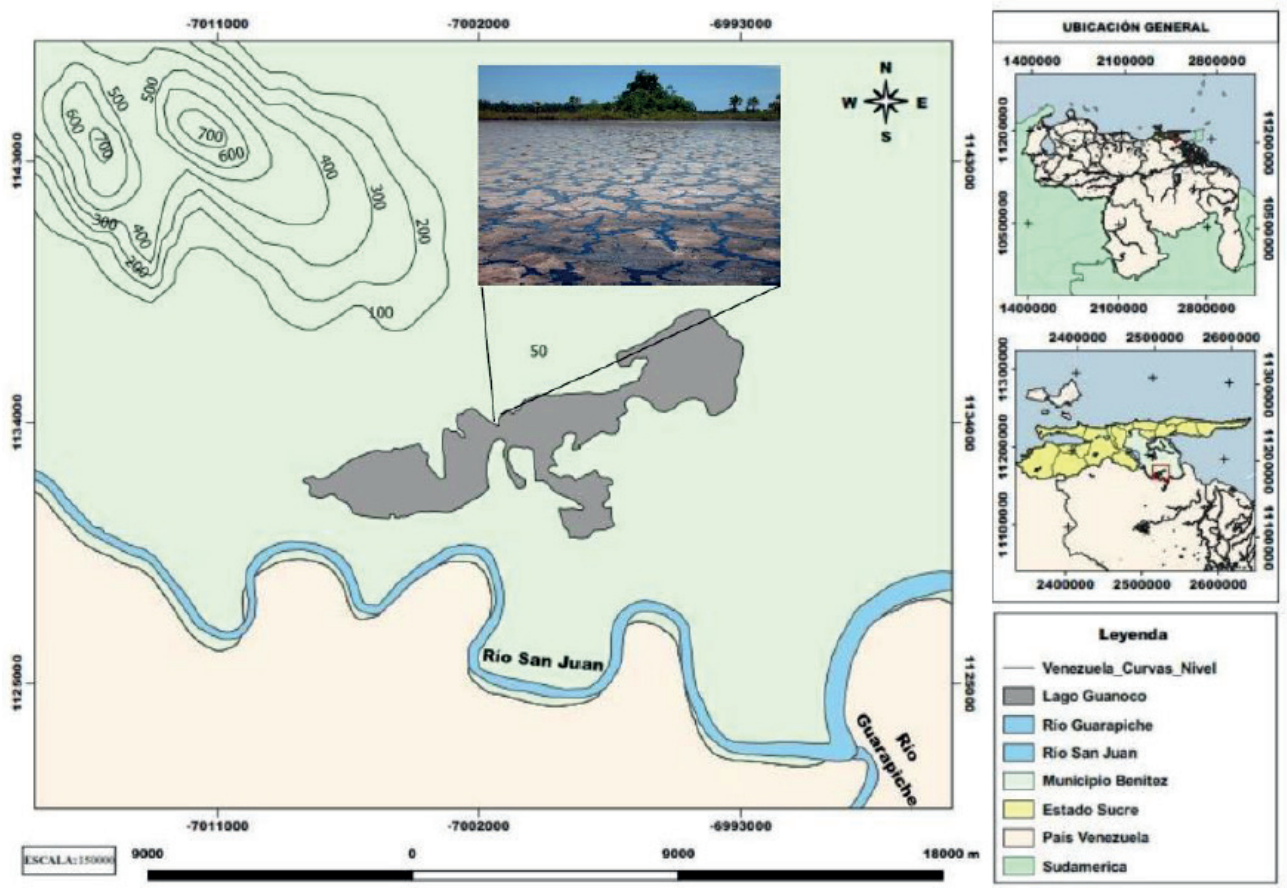

Figura 1. Localización espacial de Lago de Asfalto de Guanoco.

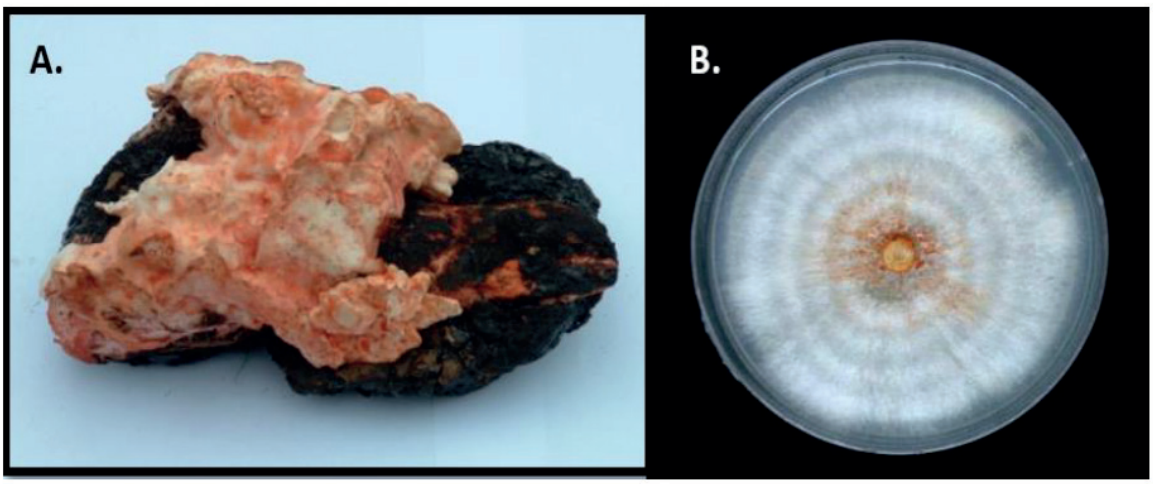

Figura 2. Soldado Desconocido creciendo en una raíz de dicotiledónea inmersa en el Lago natural de Asfalto de Guanoco (A). Cultivo axénico del Soldado Desconocido en medio Power (B).

Prueba de tolerancia del hongo a los HPAs en medio sólido BSM

Para determinar la tolerancia del hongo a los HPAs, en principio, se utilizó como base el medio salino básico (BSM)[31]. los HPAs se diluyeron inicialmente en una mezcla de 20 ml de acetona/ tween 80/agua y se ajustaron a las siguientes concentraciones: 12.5, 25, 50, 100, 200, 400, 800 y 1600 mg/L en medio BSM. Cada 24 horas y durante 8 días, se realizaron mediciones del diámetro de las colonias con un vernier calibrado a fin de determinar su tasa de crecimiento.

Índice de Tolerancia

El índice de tolerancia (IT) se determinó a los 8 días de incubación del hongo con los diferentes HPAs a 30°C, mediante la siguiente ecuación:

Donde:
LMt = es la longitud del micelio tratado con los HPAs.
LRc = es la longitud del micelio control.

Prueba de tolerancia del hongo a los HPAs en medio líquido BSM

Una vez conocida la concentración mínima inhibitoria de HPAs que no afectaba el crecimiento del hongo, se inocularon 95 ml de medio BSM con $20x10^4$ esporas de *T. coccinea* y se incubaron a 30ºC por 7 días. Al día 7 se procedió a añadir 5 mg/L de cada uno de los HPAs (naftaleno, fenantreno y pireno) diluidos en una mezcla tween-acetona con un volumen final de 100 ml. Se utilizó como control en hongo en medio BSM con el diluente tween-acetona. Todos los experimentos se realizaron por triplicado. Se tomaron muestras a los días 0, 1, 3 y 5.

Efecto de los HPAs sobre la actividad enzimática de las enzimas extracelulares guaiacol peroxidasa, lignina peroxidasa, manganeso peroxidasa y lacasa

Para determinar la actividad de la guaiacol peroxidasa se utilizó la metodología de Fielding y Hall (1978) citada por Chaoui *et al.*[32]. La actividad de la enzima se determinó siguiendo el incremento en la absorbancia a 470 nm por la polimerización del Guaiacol. Utilizando el coeficiente de extinción (26.6/mM x cm) se llevaron a unidades de enzima por g de peso fresco, definiéndose una unidad de enzima como la cantidad de enzima que produce 1 µmol de tetraguaiacol en 1 min a 25°C. Para llevar a cabo la reacción, se mezcló 25 mM de buffer fosfato (pH 7) con 10 mM de H_2O_2, 9 mM de guaiacol y 25 µl del cultivo enzimático.

La actividad de la LiP se midió siguiendo la metodología propuesta por Troller *et al.*[33] y fue analizada mediante la oxidación del alcohol veratrílico en una mezcla de reacción que contenía: alcohol veratrílico (20 mM) en un buffer 0.5 M de fosfato de sodio (pH 3.0), como agente oxidante peróxido de hidrógeno al 30 % y 0.025 mL del cultivo enzimático. La oxidación del alcohol veratrílico fue monitoreada de 0-200 s por medio del incremento de la absorbancia a 310 nm. La unidad de actividad enzimática (U) se definió como: 1 µM alcohol veratrílico oxidado por mL de sobrenadante en un min ($\varepsilon 310 = 9.3\ mM^{-1}.cm^{-1}$)

La actividad de la MnP se determinó según la metodología propuesta por Papinutti *et al.*[34] y fue analizada por medio de la oxidación del rojo de fenol, en una mezcla de reacción constituida por: 0.1 mL de rojo de fenol (0.1 %) en un buffer 0.5 M de fosfato de sodio (pH 5.0), cofactor 0.1 mL de sulfato de manganeso (1 mM) y 0.04 mL del cultivo enzimático. La oxidación del rojo de fenol fue monitoreada de 0-200 s por medio del incremento de la absorbancia a 610 nm. La unidad de actividad enzimática (U) se definió como: 1 µM rojo de fenol oxidado por mL de sobrenadante en un min ($\varepsilon 610 = 22.0\ mM^{-1}.cm^{-1}$).

La actividad de la Lac fue determinada según la metodología propuesta por Saparrat *et al.*[35] siguiendo la oxidación del ABTS en una mezcla de reacción constituida por: 0.01 mL de ABTS (25 mM) en un buffer 0.1 M de tartrato de sodio (pH 5.0) y 0.1 mL del cultivo enzimático. La oxidación del ABTS fue monitoreada de 0-200 s por medio del incremento de la absorbancia a 436 nm. La unidad de actividad enzimática (U) se definió como: 1 µM ABTS oxidado.

Estimación de proteínas totales

La concentración de proteínas se estimó en el sobrenadante utilizando el método de Bradford[36] y como estándar BSA.

Actividad de la enzima lacasa en un zimograma

Para observar la actividad de las isoenzimas de la lacasa por separado, se corrió un gel PAGE al 12 % bajo condiciones no denaturalizantes y, posteriormente, se fijó por 10 min con una solución 30% metanol y 10% ácido acético. El gel se incubó en una solución que contenía 5 mM de ABTS en buffer tartrato 0.5 M pH 5.0. Finalmente, se tiño el gel con azul de coomasie para verificar el peso molecular de las isoenzimas y para confirmar que la diferencia en la actividad no era debido a la concentración de la enzima sino a su activación por los HPAs.

Actividad de enzimas peroxidasas en gel

Para observar la actividad de las enzimas peroxidasas se utilizó el mismo protocolo anterior para el ABTS sólo que en este caso, en vez de ABTS, se utilizó 5 mM de Guaicol y 10 mM de H_2O_2.

Ensayos de toxicidad empleando Lactuca sativa como bioindicador

A fin de determinar variaciones en la toxicidad de los compuestos antes y después de haber sido biotratados con el hongo, se practicó una prueba de toxicidad según el protocolo propuesto por la USEPA EPA 00/3-88-029. En primer lugar, se estandarizó la concentración de medio de cultivo a utilizar, partiendo de la premisa de utilizar una dilución a la cual ni el medio de cultivo BSM ni el medio BSM en presencia del hongo fuese tóxico. En pruebas previas se determinó que la dilución óptima del sobrenadante era 1:15. Todos los extractos se conservaron durante la noche a -20°C previo a los ensayos con el fin de inactivar las enzimas ligninolíticas. Se calculó el Índice Integral de Fitotoxicidad (IIF) utilizando la fórmula propuesta por Pernía *et al.*[17]:

Donde:

SGM = número de semillas germinadas de la muestra, es el promedio del número de semillas germinadas en las cuatro réplicas para cada tratamiento (n = 4).

SGC = número de semillas germinadas del control, es el promedio del número de semillas germinadas en las cuatro réplicas del testigo (n = 4).

LRM = Longitud de la radícula de la muestra, es el promedio de la medición en centímetros de las radículas de 10 plántulas por réplica de cada tratamiento (n = 40).

LRC = Longitud de la radícula del control, es el promedio de la medición en centímetros de las radículas de 10 plántulas por réplica del testigo (n = 40).

LHM = Longitud del hipocótilo de la muestra, es el promedio de la medición en centímetros de los hipocótilos de 10 plántulas por réplica de cada tratamiento (n = 40).

LHC = Longitud del hipocótilo del control, es el promedio de la medición en centímetros de los hipocótilos de 10 plántulas por réplica del testigo (n = 40).

Este índice muestra los resultados de -100 a +100 pudiéndose interpretar en términos de porcentaje. También permite observar no solo los efectos de inhibición de crecimiento (valores positivos), sino también los efectos de estimulación de crecimiento (valores negativos).

Análisis estadísticos

Para el análisis estadístico se aplicó una prueba de Anderson-Darling para verificar la distribución normal de los datos. Con la finalidad de analizar la homocedasticidad de los tratamientos se aplicó una prueba de Levene. Para comparar entre las medias de crecimiento, concentración de proteínas, actividad enzimática y crecimiento de las plántulas se aplicó una prueba ANOVA de una vía con test a posteriori de Dunnet o Tukey ($p<0.05$). Todas las pruebas estadísticas se realizaron con el programa Minitab versión 19.

Resultados

La caracterización taxonómica y la identificación molecular del Soldado Desconocido determinaron que pertenece a la especie *Trametes coccinea*

El hongo Basidiomycota creciendo en una raíz de una dicotiledónea fue exitosamente aislado a partir de su micelio aéreo. La descripción taxonómica del Soldado Desconocido fue la siguiente: colonias blancuzcas cuando están jóvenes y a medida que maduran se tornan amarillentas con pigmentación anaranjada, crecen de forma zonada, superficial y con borde entero, algodonosas y superficiales (Figura 2B). Conidiogénesis tretrica, enteroblástica, baxautica. Las hifas son hialinas, de pared delgada y lisa, con fíbulas ramificadas. Los conidióforos no están diferenciados. Conidios hialinos, cilíndricos a globosos, algunos con una ligera constricción central, con extremos truncados cuando recién están escindidos de las hifas y con extremos redondeados cuando están maduros, de pared delgada y lisa, sin gútulas, aseptados, excisión esquizolítica. Clamidiosporas hialinas, obclavadas, solitarias, terminales a intercalares, algunas con un extremo truncado, de pared engrosada y lisa. Basidiocarpo, constituido por hifas esqueléticas, hialinas, y sin septos (Figura 3).

La caracterización taxonómica y la identificación molecular permitieron determinar que el Soldado Desconocido pertenecía a la especie *Pycnoporus sanguineus* (L.) Murrill 1904, Polyporaceae, el cual actualmente ha sido re-clasificado como *Trametes coccinea* (Fr.) según Li y He[38].

Tolerancia de *T. coccinea* a los HPAs estudiados

Los resultados mostraron que *T. coccinea* tiene tolerancia al naftaleno y al pireno, a excepción del fenantreno el cual fue tóxico para el hongo a bajas concentraciones. En cuanto al naftaleno pudimos observar un efecto tóxico a partir de 800 mg/L, donde el índice de tolerancia se redujo a 0.77 y 0.60 a 800 y 1600 mg/L, respectivamente. El porcentaje de crecimiento del hongo se redujo en el tratamiento con 800 mg/L a 77.25% y 59.61% a 1600 mg/L (F = 148.71; p = 0.000).

El fenantreno generó una reducción de crecimiento del hongo a partir de 25 mg/L, con una disminución de 78.43%, 70.20%, 72.55%, 66.67%, 66.27% y 61.96% a 25, 50, 100-200, 400, 800 y 1600 mg/L, respectivamente (F = 70.50; p = 0.000). De la misma manera, el índice de tolerancia se redujo al aumentar la concentración de fenantreno hasta 0.62 a 1600 mg/L.

El pireno fue el HPA menos tóxico para *T. coccinea*, ya que no presentó inhibición del crecimiento hasta los 800 mg/L de pireno. Solo se apreció una ligera reducción a altas concentraciones (1600 mg/L), donde hubo una disminución significativa del crecimiento de 20.78% (F = 70.50; p = 0.000), concomitante con una reducción del índice de tolerancia (0.78).

Una vez que se determinó el efecto tóxico de los HPAs sobre el crecimiento del hongo, se tomó la decisión de trabajar en medio líquido con una concentración mínima inhibitoria de 5 mg/L considerando el efecto tóxico del fenantreno, a fin de poder comparar los efectos de los distintos HPAs sobre las actividades enzimáticas del SEDL de *T. coccinea*, la concentración de proteínas totales y la fitotoxicidad.

Efecto de los HPAs sobre la concentración de proteínas totales y la actividad de las enzimas ligninolíticas: La isoenzima lacasa de 68 Kda se induce en presencia de HPAs

En cuanto a la concentración de proteínas totales en el sobrenadante, se observó un incremento en el tiempo para todos los tratamientos (Figura 5). Sin embargo, se encontró una reducción en la concentración de proteínas en el sobrenadante del hongo tratado con naftaleno desde el primer día de exposición. En el día 1, se observó una reducción significativa en la concentración de proteínas totales en el sobrenadante del tratamiento con naftaleno, de 0.093±0.001 mg/mL en el control a 0.068±0.002 mg/mL (F = 14.11; p = 0.001). En el día 5, también se apreció una disminución en el contenido protéico para los tratamientos con naftaleno y fenantreno según Anova de una vía y test a posteriori de Dunnet (F=26.64; p= 0.000). Se evidenció una reducción en el contenido de proteína en el tratamiento con naftaleno, de 0.121±0.006 mg/mL en el control a 0.085±0.011 mg/mL (F = 7.98; p = 0.000) y en el biotratado con fenantreno se redujo a 0.101±0.01 mg/mL.

Al estudiar el efecto sobre la síntesis de enzimas ligninolíticas, no se evidenció actividades de las enzimas guaiacol peroxidasa, LigP ni MnP. Sin embargo, se observó una fuerte inducción de la actividad lacasa en presencia de pireno y naftaleno. En la Figura 6A se observa un incremento en el tiempo para la actividad lacasa en todos los tratamientos la cual se vió fuertemente inducida en presencia de pireno y naftaleno. En el

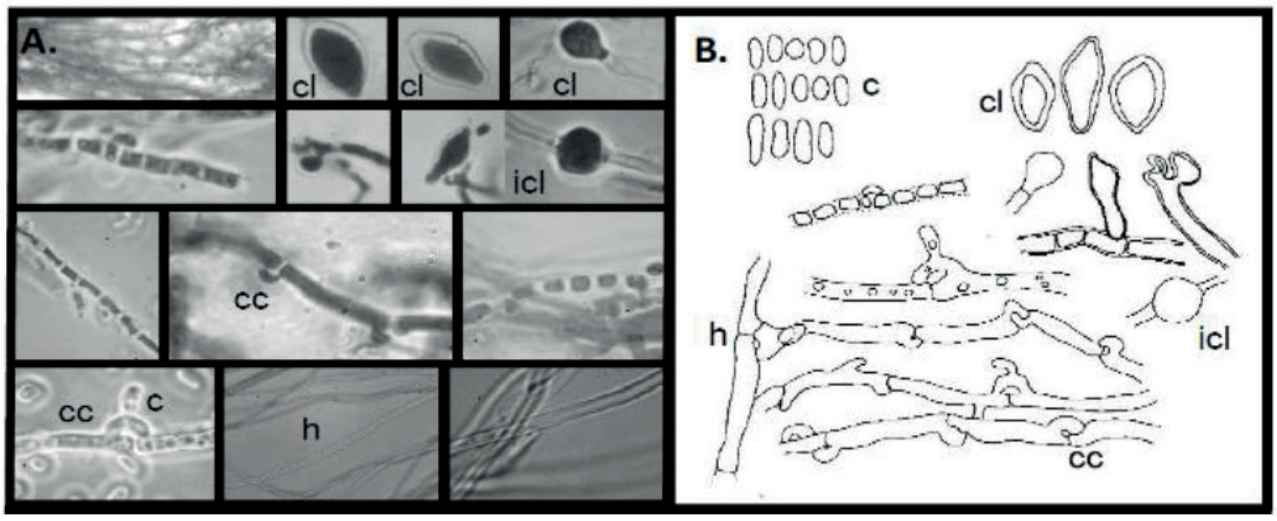

Figura 3. Fotografía y dibujos del Soldado Desconocido en medio de cultivo (A). Conidias (c), hifas productoras de conidias, clamidosporas (cl), clamidosporas intercalares (icl), fíbulas(cc) e hifas (h) en microscopio óptico1000X (B).

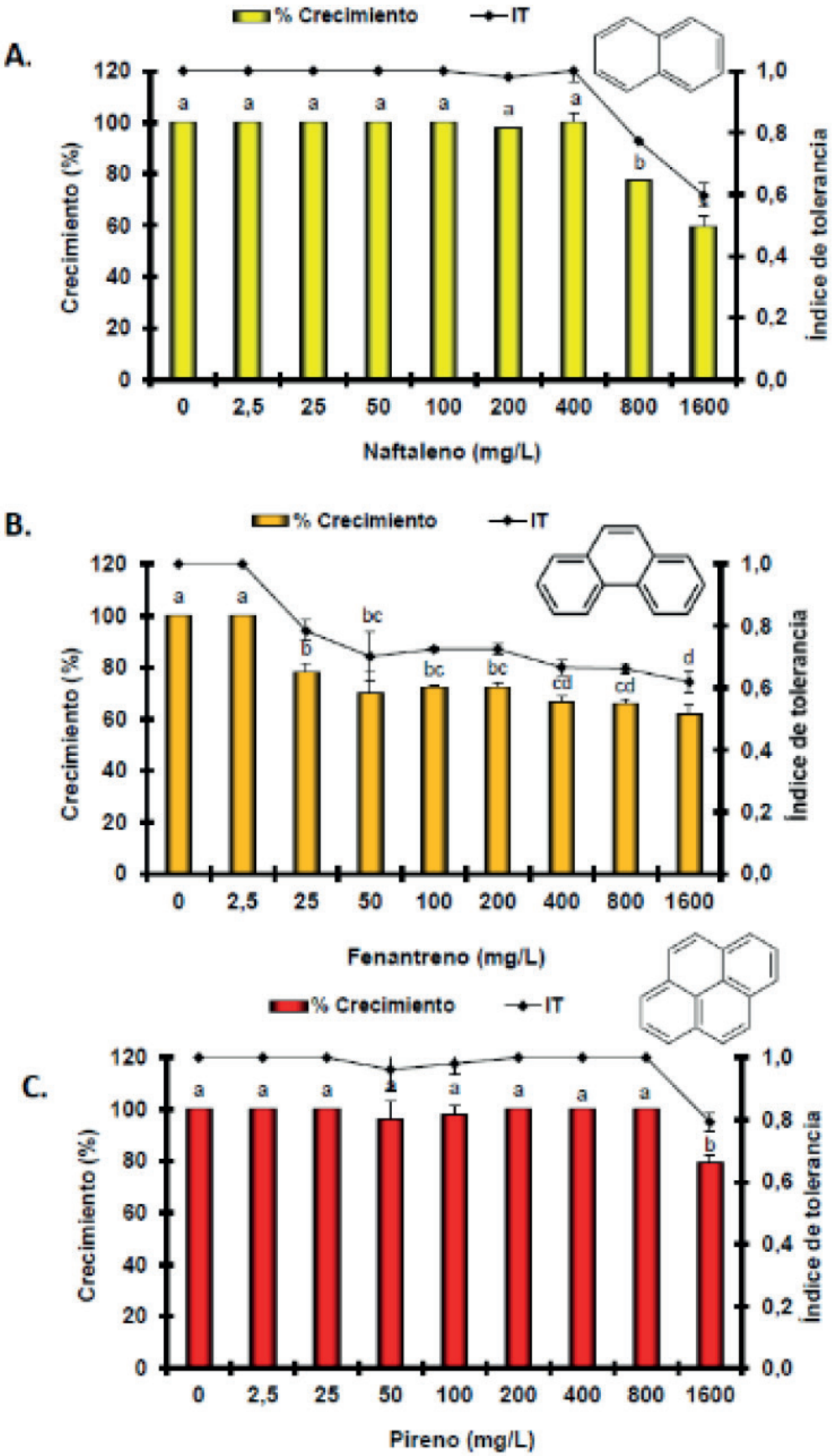

Figura 4. Porcentaje de tolerancia e inhibición del crecimiento del hongo *T. coccinea* en medio sólido BSM expuesto a distintas concentraciones de HPAs. Naftaleno (A), Fenantreno (B), Pireno (C). Las barras y puntos representan la media ± desviación estándar (n=3). Letras iguales señalan que no hay diferencias estadísticamente significativas según ANOVA de 1-vía $p<0.05$ y test a posteriori de Tukey.

día 1, se evidenció un aumento significativo de la actividad lacasa en el sobrenadante del tratamiento con pireno, incrementando de 5.95±4.96 U/mgP en el control hasta 96.90±51.10 U/mgP (F = 5.70; p = 0.027). Para el día 3, la actividad de la lacasa incrementó en el tratamiento con naftaleno de 18.81 a 104.91 U/mgP (F = 4.98; p = 0.039) y, para el día 5, se evidenció un fuerte estímulo de esta acividad enzimática en presencia de pireno (124.85±14.76 U/mgP) y naftaleno (167.95±16.23 U/mgP) (F = 22.45; p = 0.001).

Además, los zimogramas con ABTS (Figura 6B) muestran 3 isoenzimas de la lacasa con pesos moleculares estimados de 68, 58 y 56 KDa. De estas, la isoenzima que mostró una mayor actividad en presencia de los HPAs fue la de mayor peso molecular (68 KDa), especialmente, en presencia de naftaleno y pireno. En nuestro laboratorio se realizó esta misma prueba con un sobrenadante enriquecido con almidón y se vió un incremento en la actividad de las dos isoenzimas de menor peso molecular (datos no mostrados), de donde se desprende que la activación enzimática de las distintas isoenzimas depende del sustrato, en este caso, los HPAs estudiados.

Variación en la toxicidad de los HPAs tras su biotransformación por T. coccinea: La biotransformación de pireno estimula el crecimiento de las plántulas de L. sativa.

Se observó una variación en la toxicidad de los HPAs sobre el crecimiento de *L. sativa* luego de ser biotratados con el hongo. Con respecto al porcentaje de germinación, se observó una disminución ante la exposición a naftaleno (91.67 %), naftaleno biotratado con *T. coccinea* (93.33 %), fenantreno biotratado (91.67 %), pireno (96.67 %) y pireno biotratado (95.00 %). Sin embargo, esta disminución no fue significativa con respecto al control (100 %) (p>0.05).

Por otro lado, la longitud de las radículas de las plántulas se redujo ante la exposición a los HPAs (F = 15.54; p = 0.000). La longitud media de los controles fue de 2.01 cm el cual disminuyó en los tratamientos de naftaleno biotratado (1.34 cm), fenantreno biotratado (1,49 cm) y pireno (1.57 cm). En el caso del pireno biotratado (2.34 cm), mostró un estímulo de crecimiento en comparación al pireno solo (1.57 cm).

Las pruebas de fitotoxicidad mostraron que ocurrió un proceso de biotransformación de los HPAs al observarse diferencias en los niveles de toxicidad de los compuestos al exponerlos al hongo. En el caso del naftaleno y el fenantreno, el contacto con el hongo generó compuestos más tóxicos que el compuesto original mientras que, por el contrario, en el caso del pireno se generaron compuestos menos tóxicos, lo que se reflejó como un estímulo significativo en el crecimiento de las plántulas de *L. sativa*.

En este sentido, el IIF empleado en la presente investigación, mostró que el naftaleno promueve un estímulo de crecimiento con un valor de -6 y, luego del tratamiento con *T. coccinea*, genera una toxicidad con un valor de IIF de 17. De igual manera que el naftaleno, el fenantreno promueve un estímulo de crecimiento de -20 y, cuando es biotratado por el hongo, se evidenció una toxicidad de 16. Por el contrario, el pireno inicialmente fue tóxico para las plantas (2) y, luego de su exposición con el hongo, se observó un estímulo del crecimiento de -20, el cual pudiera deberse a la generación de sub-productos menos tóxicos que el original, en este caso, el pireno.

Discusión

El hongo *T. coccinea* aislado del Lago de Asfalto de Guanoco tiene la capacidad de tolerar ambientes extremos con altas temperaturas y contaminados con hidrocarburos recalcitrantes. En el presente trabajo, la cepa aislada fue capaz de crecer sobre bajas concentraciones de HPAs sin síntomas de toxicidad. Esta capacidad podría deberse a la presión adaptativa de esta cepa al vivir en presencia de asfalto y a bajas concentraciones de nutrientes. Además de ello, una cepa de esta misma especie fue aislada por Dantán-González *et al.*[38], creciendo en un tronco cubierto de crudo cercano a una refinería en Veracruz, México, lo que demuestra su alta tolerancia a los hidrocarburos.

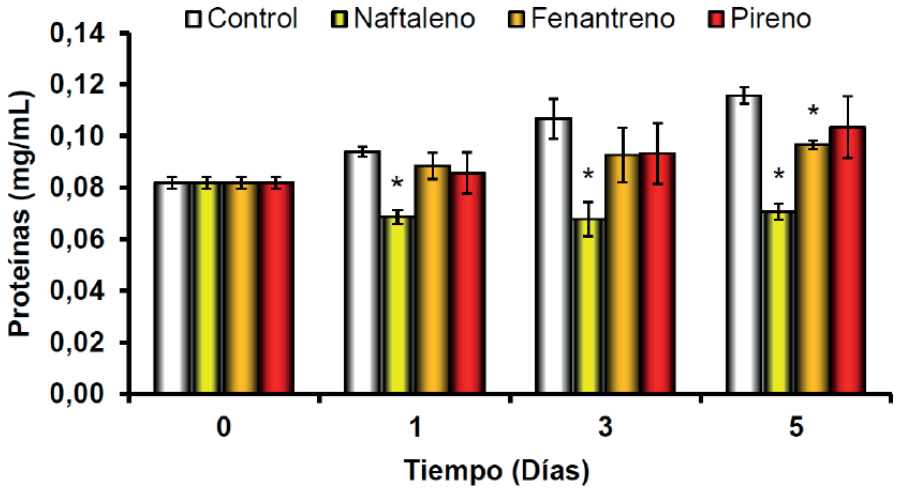

Figura 5. Concentración de proteínas totales de *T. coccinea* en medio líquido BSM y medio BSM suplementado con 5 mg/L de naftaleno, fenantreno y pireno, durante 5 días.

En el presente estudio no se observaron las actividades enzimáticas guaiacol peroxidasa, LigP ni MnP, resultados que coinciden con los reportados por otros autores que señalan que la principal enzima extracelular oxidtiva del SEDL de *P. sanguineus* (formalmente *T. coccinea*) es la lacasa[23,24]. Sin embargo, contrastan con los resultados obtenidos por Esposito *et al.*[20] quienes encontraron actividades LigP y MnP al exponer al hongo a extracto de malta, lo que sugiere que, aunque esta especie sintetize exoenzimas oxidativas en presencia de algunos sustratos como la malta, las mismas no se estimulan en presencia de los HPAs estudiados en la presente investigación (naftaleno, fenantreno y pireno) ni en los estudiados por Li *et al.*[24], quienes expusieron el hongo a fenantreno, benzo[a]antraceno y a antraceno.

Por otro lado, una posible explicación de la baja actividad lacasa los primeros días del experimento se debe a la presencia de glucosa en el medio, la cual, al irse consumiendo por el hongo, la actividad de la enzima incrementa proporcionalmente a la desaparición de la glucosa en el caldo de cultivo. A este respecto, Siqueira *et al.*[21] reportaron la inhibición de la

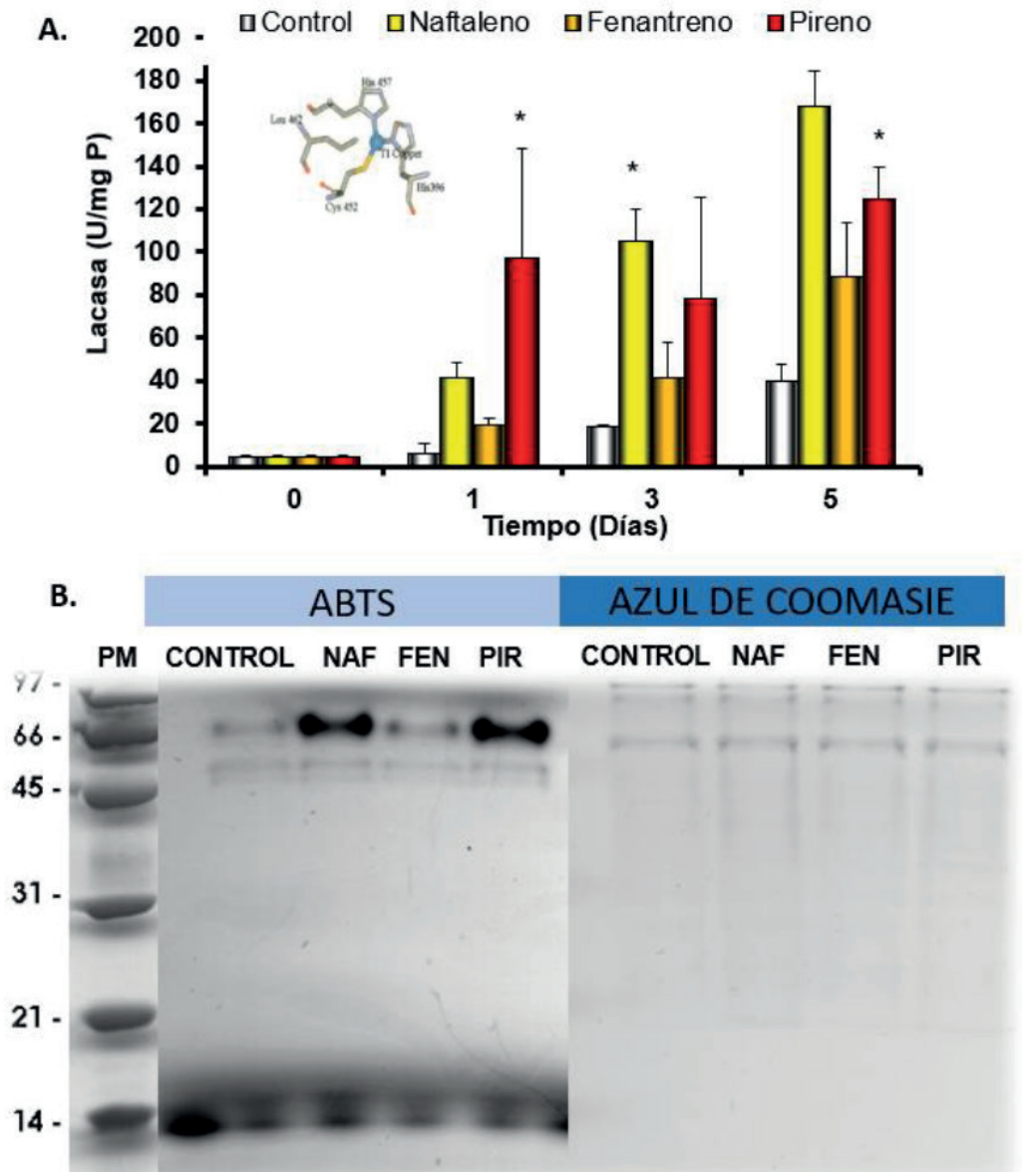

Figura 6. A. Actividad de la enzima lacasa en medio BSM control y suplementado con 5 mg/L de los diferentes HPAs B. Zimograma de los sobrenadantes de *T. coccinea* expuestos a los HPAs por 5 días y 5 mM de ABTS. Al lado, el mismo gel teñido con azul de coomasie. PM: peso molecular, Control: *T. coccinea* en medio BSM y medio BSM con 5 mg/L de NAF: naftaleno, FEN: fenantreno y PIR: pireno.

producción de la α-amilasa en presencia de glucosa, por lo que sugieren que esta fuente de carbono y energía pudiera generar represión catabólica.

Al igual que en el presente trabajo, otros trabajos reportan la presencia de varias isoenzimas de la lacasa. García *et al.*[39] encontraron 3 isoenzimas con distintos pesos moleculares, entre ellas una de 68 Kda, lo cual coincide con la isoenzima que se activó en T. coccinea en prencia de naftaleno y pireno en nuestro estudio. De igual manera, Litthauer *et al.*[40] encontraron una lacasa termoestable de 58 KDa, pH óptimo 3-5, que toleraba temperaturas de 50-75°C. Así mismo, Dantán-González *et al.*[38] aislaron dos isoenzimas de lacasa de 68 KDa con PI de 7.00 y 7.08, respectivamente. En nuestro caso, observamos la presencia de 3 isoenzimas de pesos moleculares distintos: 56, 58 y 68 KDa. Se pudiera sugerir, que la activación de las distintas isoenzimas lógicamente podría depender del sustrato utilizado, en este caso, por los HPAs ensayados.

En este sentido, la inducción de la actividad de la lacasa de 68 KDa de *T. coccinea* en presencia de naftaleno y pireno, sugiere que esta enzima podría reconocer estos compuestos como sustratos con una mayor especificidad. En otras pruebas realizadas en nuestro laboratorio, observamos que la actividad de la lacasa de *T. coccinea* en un medio rico en almidón se vio duplicada al añadir 5 mg/L de pireno, lo que confirma la inducción de esta enzima ante la exposición a este HPA.

La capacidad de la lacasa para degradar distintos compuestos orgánicos se debe a su baja especificidad de sustrato. Se ha demostrado que ciertos compuestos recalcitrantes tales como pesticidas, colorantes, bifenilos policlorados y diversos HPAs presentan una similaridad estructural con la lignina - sustrato original de la lacasa - y son degradados por la misma.

Con respecto a la toxicidad de los HPAs tratados con *T. coccinea*, se evidenció un incremento en la toxicidad del fenantreno al ser biotratado con el hongo. Según Li *et al.*[24], esta especie transforma el fenantreno en 9,10-fenantrenodiona mediado por la enzima lacasa y se conoce que las dionas son muy tóxicas.

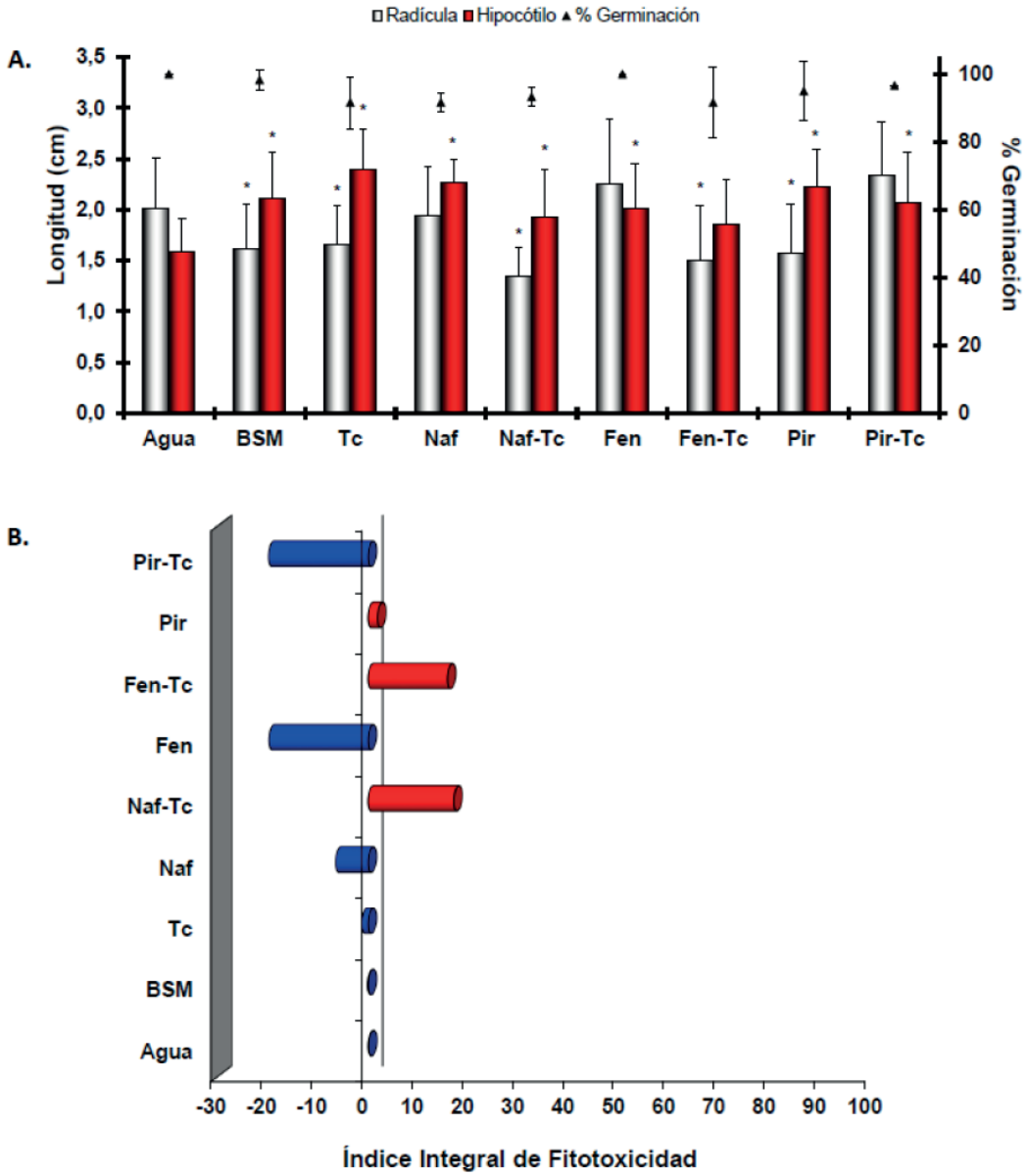

Figura 7. Efecto de los sobrenadantes de *T. coccinea* crecido en distintos HPAs sobre la germinación y el crecimiento de radículas e hipocótilos de plántulas de *L. sativa* expuestos a agua= control agua, BSM = control medio BSM, Tc = control hongo en medio BSM, NAF = medio BSM con 5 mg/L de naftaleno, Naf-Tc = medio BSM con naftaleno y *T. coccinea*, Fen = medio BSM con naftaleno, Fen-Tc= medio BSM con naftaleno y *T. coccinea*, Pir = medio BSM con naftaleno, Pir-Tc = medio BSM con naftaleno y *T. coccinea* durante 5 días. Los resultados se muestran como medias ± desviación estándar (n=30). *Estadísticamente significativas en comparación al control agua, según ANOVA de 1-vía y test de Dunnet p<0.05. B. Índice Integral de Fitotoxicidad (IIF) para las plantas de *L. sativa* expuestas a los distintos sobrenadantes.

Además, se ha demostrado que esta especie degrada el fenantreno via lacasa y también por la enzima citocromo P450, donde se genera el metabolito secundario 2-methyl- phenol[24].

Aunque *T. coccinea* es capaz de degradar hidrocarburos y es promisorio para fines de biorremediación, se sugiere el uso de la enzima lacasa purificada (Ej. isoenzima lacasa de 68 Kda) debido a la posibilidad de generar compuestos más tóxicos al original, como en el caso de naftaleno y fenantreno. Por otro lado, se ha descrito que *T. coccinea* (previamente *P. sanguineus*) tiene propiedades antibióticas sobre varias especies bacterianas[41], lo cual podría ser contraproducente ya que, por un lado, no se pueden generar consorcios con bacterias con fines de biorremediación y, por otro lado, el hongo podría eliminar bacterias autóctonas presentes en los suelos contaminados con capacidad de mineralizar HPAs.

Conclusiones

El hongo *Trametes coccinea* fue aislado del Lago natural de Asfalto de Guanoco y demostró tolerancia hacia los hidrocarburos naftaleno, fenantreno y pireno. Además, se evidenció que estos HPAs estimulan a la enzima lacasa, especialmente la isoenzima de 68 kDa que podría estar implicada en la oxidación inicial en el proceso de degradación de hidrocarburos. También se observó una variación en la toxicidad de los hidrocarburos sobre la especie *L. sativa* al ser biotratados por *T. coccinea*, generándose una mayor toxicidad en el caso del naftaleno y el fenantreno, mientras que, en el caso del pireno, disminuyó su toxicidad. Se recomienda trabajar con la enzima lacasa purificada para fines de biorremediación de suelos y aguas contaminados con HPAs.

Referencias bibliográficas

1. Menzie CA, Potocki BB, Joseph S. Exposure to Carcinogenic PAHs in The Environment. Environ Sci Technol. 1992 Jul 1;26(7):1278–84.
2. Nadon L, Siemiatycki J, Dewar R, Krewski D, Gérin M. Cancer risk due to occupational exposure to polycyclic aromatic hydrocarbons. Am J Ind Med [Internet]. 1995 Sep 1 [cited 2020 Jun 8];28(3):303–24. Available from: http://doi.wiley.com/10.1002/ajim.4700280302
3. Arun a, Eyini M. Comparative studies on lignin and polycyclic aromatic hydrocarbons degradation by basidiomycetes fungi. Bioresour Technol [Internet]. 2011 Sep [cited 2012 Apr 18];102(17):8063–70. Available from: http://www.ncbi.nlm.nih.gov/pubmed/21683591
4. Gouma S, Fragoeiro S, Bastos AC, Magan N. Bacterial and Fungal Bioremediation Strategies. In: Microbial Biodegradation and Bioremediation [Internet]. Elsevier Inc.; 2014. p. 301–24. Available from: http://dx.doi.org/10.1016/B978-0-12-800021-2.00013-3
5. Naranjo-briceño L, Pernía B, Perdomo T, González M, Inojosa Y, Sisto Á De, et al. Potential Role of Extremophilic Hydrocarbonoclastic Fungi for Extra- Heavy Crude Oil Bioconversion and the Sustainable Development of the Petroleum Industry. In: S. M. Tiquia-Arashiro MG (eds. ., editor. Fungi in Extreme Environments: Ecological Role and Biotechnological Significance [Internet]. Springer Nature Switzerland; 2019. p. 559–86. Available from: http://link.springer.com/10.1007/978-3-030-19030-9
6. Baillie GS, Hitchcock CA, Burnet FR. Increased cytochrome P-450 activity in Aspergillus fumigatus after xenobiotic exposure. Med Mycol [Internet]. 1996 Jan 1 [cited 2020 Jun 8];34(5):341–7. Available from: https://academic.oup.com/mmy/article-lookup/doi/10.1080/02681219680000581
7. Vazquez-duhalt R, Westlake DWS, Fedorak PM. Lignin Peroxidase Oxidation of Aromatic Compounds in Systems Containing Organic Solvents. 1994;60(2):459–66.
8. Baborová P, Möder M, Baldrian P, Cajthamlová K, Cajthaml T. Purification of a new manganese peroxidase of the white-rot fungus Irpex lacteus, and degradation of polycyclic aromatic hydrocarbons by the enzyme. Res Microbiol. 2006;157:248–53.
9. Wang Y, Vazquez-duhalt R, Pickard MA. Manganese – lignin peroxidase hybrid from Bjerkandera adusta oxidizes polycyclic aromatic hydrocarbons more actively in the absence of manganese. Life Sci. 2003;682:675–82.
10. Allenmark SG, Andersson MA. Chloroperoxidase-Catalyzed Asymmetric Synthesis of a Series of Aromatic Cyclic Sulfoxides. Science (80-). 1996;7(4):1089–94.
11. Majcherczyk A, Johannes C, Hu A. Oxidation of polycyclic aromatic hydrocarbons (PAH) by laccase of Trametes versicolor. Enzyme. 1998;0229(97):335–41.
12. Dutta D, Ghosh DK, Mishra AK, Samanta TB. Induction of benzo(a)pyrene hydroxylase in Aspergillus ochraceus TS: Evidences of multiple forms of cytochrome P-450. Biochem Biophys Res Commun. 1983 Sep 15;115(2):692–9.
13. Gochev VK, Krastanov AI. Isolation of Laccase Producing Trichoderma Spp. Vol. 13, Bulgarian Journal of Agricultural Science. 2007.
14. Majeau JA, Brar SK, Tyagi RD. Laccases for removal of recalcitrant and emerging pollutants. Bioresour Technol [Internet]. 2010;101(7):2331–50. Available from: http://dx.doi.org/10.1016/j.biortech.2009.10.087
15. Mayer AM, Staples RC. Laccase: New functions for an old enzyme. Phytochemistry. 2002;60(6):551–65.
16. Pickard MA, Roman R, Tinoco R, Vazquez-Duhalt R. Polycyclic aromatic hydrocarbon metabolism by white rot fungi and oxidation by Coriolopsis gallica UAMH 8260 laccase. Appl Environ Microbiol. 1999;65(9):3805–9.
17. Pernía B, Rojas-Tortolero D, Sena L, De Sisto A, Inojosa Y, Naranjo L. Phytotoxicity of pah, extra-heavy crude oil and its fractions in Lactuca sativa: An integrated interpretation using a modified toxicity index. Rev Int Contam Ambient. 2018;34(1):79-91.
18. Naranjo L, Urbina H, Sisto ADE, Leon V. Isolation of Autochthonous Non-White Rot Fungi with Potential for Enzymatic Upgrading of Venezuelan Extra-Heavy Crude Oil Isolation of autochthonous non-white rot fungi with potential for enzymatic upgrading of Venezuelan extra-heavy crude oil. 2007;25(2-4):341-349.
19. González V, Vásquez P. La vegetación del Lago de Asfalto de Guanoco después de cuatro décadas. Un primer enfoque fisionómico y florístico | González. Acta Biologica Venezuelica. 2004; 24(2) [Internet]. [cited 2020 Jun 8]. Available from: http://saber.ucv.ve/ojs/index.php/revista_abv/article/view/4036/3860
20. Esposito E, Innocentini-Mei LH, Ferraz A, Canhos VP, Durán N. Phenoloxidases and hydrolases from Pycnoporus sanguineus (UEC-2050 strain): applications. J Biotechnol. 1993 Jun 1;29(3):219–28.
21. De Almeida Siqueira EM, Mizuta K, Giglio JR. Pycnoporus sanguineus: A novel source of α -amylase. Mycol Res. 1997 Feb 1;101(2):188–90.
22. Abrahão MC, Gugliotta ADM, Silva D, Fujieda Y. Ligninolytic activity from newly isolated basidiomycete strains and effect of these enzymes on the azo dye orange II decolourisation. Microbiol. 2008;58(3):32212393.
23. Zhang S, Ning Y, Zhang X, Zhao Y, Yang X, Wu K. Contrasting characteristics of anthracene and pyrene degradation by wood rot fungus Pycnoporus sanguineus H1. Int Biodeterior Biodegradation [Internet]. 2015;105:228–32. Available from: http://dx.doi.org/10.1016/j.ibiod.2015.09.012
24. Li X, Pan Y, Hu S, Cheng Y, Wang Y, Wu K, et al. Diversity of phenanthrene and benz [a] anthracene metabolic pathways in white rot fungus Pycnoporus sanguineus 14. Int Biodeterior Biodegrad [Internet]. 2018;134(May):25–30. Available from: https://doi.org/10.1016/j.ibiod.2018.07.012
25. Casqueiro J, Bañuelos O, Gutiérrez S, Hijarrubia MJ, Martín JF. Intrachromosomal recombination between direct repeats in Penicillium chrysogenum: Gene conversion and deletion events. Mol Gen Genet. 1999;261(6):994–1000.
26. Montenegro E, Fierro F, Fernandez FJ, Gutierrez S, Martin JF. Resolution of chromosomes III and VI of Aspergillus nidulans by pulsed- field gel electrophoresis shows that the penicillin biosynthetic pathway genes pcbAB, pcbC, and penDE are clustered on chromosome VI (3.0 megabases). Vol. 174, Journal of Bacteriology. J Bacteriol; 1992. p. 7063–7.
27. Naranjo L, De Valmaseda EM, Bañuelos O, Lopez P, Riaño J, Casqueiro J, et al. Conversion of pipecolic acid into lysine in Penicillium chrysogenum requires pipecolate oxidase and saccharopine reductase: Characterization of the lys7 gene encoding saccharopine reductase. J Bacteriol. 2001;183(24):7165–72.
28. Evans GA. Molecular cloning: A laboratory manual. Second edition. Volumes 1, 2, and 3. Current protocols in molecular biology. Volumes 1 and 2. Cell. 1990 Apr 6;61(1):17–8.
29. Altschul S, Madden T, Schäffer A, Zhang J, Zhang Z, Miller W, et al. A simple sequence repeat-based linkage map of Barley. Nucleic Acids Res. 1997;25(17):3389–402.
30. Pearson WR, Lipman DJ. Improved tools for biological sequence comparison. Proc Natl Acad Sci U S A. 1988;85(8):2444–8.
31. Kerem Z, Friesem D, Hadar Y. Lignocellulose degradation during solid-state fermentation: Pleurotus ostreatus versus Phanerochaete chrysosporium. Appl Environ Microbiol. 1992;58(4):1121–7.
32. Chaoui A, Ghorbal MH, El Ferjani E. Effect of cadmoium-zinc interactions on hydroponically grown bean (Phaseolus vulgaris L.). Plant Sci. 1997;126:21–8.
33. Troller J, Smit JDG, Leisola MSA, Kallent J, Winterhalter KH, Fiechter A. Crystallization of a lignin peroxidase from the white-rot fungus Phanerochaete chrysosporium. Bio/Technology. 1988;6(5):571–3.
34. Papinutti L, Forchiassin F. Optimization of manganese peroxidase and laccase production ´ v .) Cke in the South American fungus Fomes sclerodermeus (Le. FEMS Microbiol Lett. 2003;536–41.
35. Carlos M, Saparrat N, Martínez MJ, Cabello MN, Arambarri AM. Screening for ligninolytic enzymes in autochthonous fungal strains from Argentina isolated from different substrata. Culture. 2002;181–5.

36. Bradford MM. A rapid and sensitive method for the quantitation of microgram quantities of protein utilizing the principle of protein-dye binding. Anal Biochem. 1976 May 7;72(1–2):248–54.
37. Distefano S, Palma JM, Gómez M, Del Río LA. Characterization of endoproteases from plant peroxisomes. Biochem J. 1997 Oct 15;327(2):399–405.
38. Li H-J, He S-H. Three species of polypores new to China. Mycosistema. 2014 Sep 15;33(5):967–75.
39. Dantán-González E, Vite-Vallejo O, Martínez-Anaya C, Méndez-Sánchez M, González M, Palomares L, et al. Caracterización de la lacasa de una cepa termotolerante de Pycnoporus sanguineus. Int Microbiol. 2008;11(3):163-169.
40. Garcia TA, Santiago MF, Ulhoa CJ. Studies on the Pycnoporus sanguineus CCT-4518 laccase purified by hydrophobic interaction chromatography. Appl Microbiol Biotechnol. 2007 May 11;75(2):311–8.
41. Litthauer D, van Vuuren MJ, van Tonder A, Wolfaardt FW. Purification and kinetics of a thermostable laccase from Pycnoporus sanguineus (SCC 108). Enzyme Microb Technol. 2007 Mar 5;40(4):563–8.
42. Smânia A, Monache FD, Smânia EFA, Gil ML, Benchetrit LC, Cruz FS. Antibacterial activity of a substance produced by the fungus Pycnoporus sanguineus (Fr.) Murr. J Ethnopharmacol. 1995;45(3):177–81.

Received: 25 marzo 2021
Accepted: 6 julio 2021

RESEARCH / INVESTIGACIÓN

Comparison of Anxiety Levels in Patients with Coronavirus Disease (COVID-19) and their Families

Azin Chakeri[1*], Maryam Rostami Qadi[2*], Shima Haghani[3]

DOI. 10.21931/RB/2021.06.03.8

Abstract: Very little research has been done on the anxiety of the families of patients with covid-19. Considering the vital role of the family in the continuation of supportive-psychological therapies and the direct impact on the patient's anxiety level, in this study, we examined the anxiety level of the family of patients with Covid-19 and compared their with their patient's anxiety level. In this comparative study, the samples were 60 people who were given a definitive diagnosis of covid-19 in selected hospitals (Masih Daneshvari Hospital and Besat Hospital). From the family members, the person who, according to the patient, is most affected and has an emotional relationship with him (spouse-father-mother-child) was selected. The standard Spielberger Anxiety Questionnaire has been used to measure apparent (state) and hidden (trait) anxiety. The questionnaire was completed by both groups (patient-family) and compared with each other. The mean of evident anxiety in patients and caregivers was 70.82 and 74.2, respectively, which this difference was statistically significant (P = 0.023). It is also observed that the mean of hidden anxiety in patients and caregivers was 68.83 and 74.71, respectively, which the mean of hidden anxiety in patients was significantly less than caregivers (P = 0.006). After identifying anxiety, nurses can better and more effectively deal with these unwanted conditions in the patient and her family by providing appropriate and correct education.

Key words: Anxiety, COVID-19, Patient.

Introduction

In December 2019, a viral outbreak was reported in Wuhan, China. The cause of this disease was a new and genetically modified virus from the family of coronaviruses called SARS-COV, which was named Covid-19 disease[1]. Unfortunately, due to its very high prevalence, the virus spread rapidly throughout the world and infected almost all world countries in a short period (less than four months)[2,3]. The COVID-19 virus has spread easily in some affected areas of the community. The local spread of COVID-19 disease means that individuals are infected in this region. Some individuals are not sure how or where they became infected4. COVID-19 virus is developed quickly in diverse parts of Iran and instigated people to different levels of anxiety. The symptoms of this virus vary from mild to severe. Signs and symptoms of infection include fever, cough, and breathing difficulty[5]. Anxiety is a common sign in patients suffering from respiratory disorders and can significantly reduce patients' quality of life. The majority of the anxiety cases develop clinical symptoms associated with severe respiratory disease and side effects of medications[6]. Lung diseases, including pulmonary disorders, are highly associated with anxiety disorders. Illness with severe clinical signs and also duration caused more levels of anxiety[7].

Higher distribution of anxiety and depression in lung diseases has been reported compared to other cases. The previous survey showed that 20-40% of patients who suffered from Chronic Obstructive Pulmonary Disease (COPD) had symptoms of anxiety[8]. In a study of patients with asthma and COPD, Pietras et al. found a positive association between anxiety and dyspnea[9]. Clinical anxiety affects up to two-thirds of chronic respiratory patients and reduces the quality of life and physical function. Little research has been done on anxiety experiences in patients with severe respiratory symptoms[10]. Anxiety is common in cases of COVID-19 and appears to be due to the unknown and cognitive ambiguity of the virus. Anxiety caused a severe reduction in the immunity levels of humans has always been anxious for human[11]. At this time, people are looking for more information to relieve their anxiety. Anxiety can make people unable to distinguish right from wrong to be exposed to false news. Stress and anxiety can weaken the immune system and make them vulnerable to diseases such as Coronavirus[12].

Anxiety is a psychological condition that almost all human beings experience to varying degrees throughout their lives. But when it increases and reaches a level that causes distress and conflict, it is known as a disorder. Anxiety disorder is one of the most common disorders characterized by persistent, excessive, and unrealistic concerns about everyday issues[13]. This disorder can cause sleep problems, centralization, physical problems such as; burnout, headaches, tension, muscle pain, and many problems in the future for people[14]. Evidence shows that this disorder is more common in people who had crises in their lives. Li *et al.* conducted a study to investigate the psychological consequences of COVID-19 in China through an online survey and concluded that the disease increased anxiety, stress, and decreased happiness among people. Given the global (pandemic) status of Covid-19 disease, which affects almost all essential economic, political, social, and even military aspects of all countries of the world, in other words, paralyzed, the psychological effects of this viral disease on mental health is very important for people at different levels of society[15]. Due to this virus's pathogenicity, spread rate, and high mortality rate, individuals' mental health status, including patients, health care workers, families, children, students, psychiatrists, and staff of various occupations, may be endangered[16,17]. It is essential to pay attention to this fact that in connection with the observance of protocols and training given to patients to reduce anxiety, the family plays a decisive and vital role. The family is the context of each person who plays a crucial role in guiding him.

Effective communication between the treatment team

[1] Department of Nursing, Garmsar branch, Islamic Azad University, Garmsar, Iran.
[2] Department of nursing sari bu-Ali sina Therapeutic and Education center Mazandaran University of medical science, Sari, Iran.
[3] Master of Biostatistics, Nursing Care Research Center, Iran University of Medical Sciences, Tehran, Iran.

Corresponding author: m.rostami.234@yahoo.com

and the patient's family members is critical to provide safe care and prevent further injury to the patient[18]. This is especially important for providing quality care services in stressful and unknown diseases such as Covid-19. Infection of one member of the family with this disease causes anxiety and psychological problems in other family members. Therefore, it is necessary to know the level of anxiety in patients' families due to their direct impact on increasing or decreasing the level of patient's anxiety and follow-up and continuation of supportive therapies[19]. When a patient enters the emergency department, the patient's family usually experiences psychological conditions such as anxiety and worry, such as fear or response to an unknown threat, which is a general reaction to stressful situations such as illness or life-threatening situations[20]. The patient's family members play an essential role in supporting the patient and cause the desired therapeutic response in the patient. However, when anxiety is high in family members, they may not play an effective supportive role[21]. Very little research has been done on the anxiety of the families of patients with covid-19. Considering the vital role of the family in the continuation of supportive-psychological therapies and the direct impact on the patient's anxiety level, in this study, we examined the anxiety level of the family of patients with Covid-19 and compared their with their patient's anxiety level.

Methods

Participants

This study was a comparative study. The research environment of this study included the emergency departments of selected hospitals for admission of patients with covid-19 (Masih Daneshvari Hospital and Besat Hospital). The study samples consisted of 60 people (men and women) who were given a definitive diagnosis of covid-19 by performing a corona test with a CT scan of the lungs, and the treating physician quarantined them at home and received medication and continued treatment at home with their family, which were selected by continuous sampling from the research environment. From the family members, the person who, according to the patient, is most affected and has an emotional relationship with him (spouse-father-mother-child) was selected.

Data collection tools

The questionnaire used to collect data in this study consists of two parts. The first part was a researcher-made questionnaire containing demographic information (age, level of education, marital status, and occupation). The second part was the standard Spielberger Anxiety Questionnaire, which showed patients' current level of anxiety and their families. This questionnaire has been used extensively in research and clinical practice and includes separate self-assessment scales to measure obvious and hidden anxiety. The questionnaire has been translated into 30 languages of the world and has been adapted to Iranian culture, in other words, it has been standardized[22]. Mehram, in 1373 calculated the reliability of this test through Cronbach's alpha on the average population (=0.9452). In general, scores (20-42) of mild anxiety, scores (43-64) of moderate anxiety, and scores (65-80) are classified as severe anxiety[23].

Data collection

All samples of the study that met the inclusion criteria (corona test and positive lung scan) were selected by continuous sampling with a selected person from their family (responsible for patient care) informed consent to participate in the study researcher. Then the standard Spielberger anxiety questionnaire was completed by both groups (patient-family) and compared with each other.

Results

The results showed that the mean age of the patients was 43.25 with a standard deviation of 11.18 years, and 76.7% of them were married, and the educational level was 36.7% at the diploma level. The mean age of the caregiver was 42.8 years with a standard deviation of 10.77 years, and 80% of them were married, and the educational level was 40% at the bachelor level (Table 1).

Table 2 shows that none of the patients and their caregivers had apparent (state) anxiety at a superficial level, and the apparent anxiety of all caregivers and 98.3% of patients was high. The mean of evident anxiety in patients was 70.82 with a standard deviation of 7.59, and the mean of evident anxiety in caregivers was 74.2 with a standard deviation of 4.24. Based on

Demographic Characteristics	Family	Patient
Age(years); Mean (S.D)	42.8 (10.77)	43.25 (11.18)
Sex; n (%)		
Female	20 (33.3)	20 (33.3)
Male	40 (66.7)	40 (66.7)
Marital Status; n (%)		
Married	48 (80)	46 (76.7)
Single	12 (20)	14 (23.3)
Education Status; n (%)		
High school	12 (20)	8 (13.3)
Diploma	18 (30)	22 (36.7)
Bachelor	24 (40)	19 (31.7)
Master	6 (10)	11 (18.3)

Table 1. Frequency Distribution of Demographic Characteristics of the Participants.

Anxiety	Family (n=60)	Patient (n=60)	†P
State anxiety; Mean (S.D)	74.20 (4.24)	70.82 (7.59)	0.023
Low n (%)	0 (0)	1 (1.7)	
High n (%)	60 (100)	59 (98.3)	
Trait anxiety; Mean (S.D)	74.71 (2.91)	68.83 (10.72)	0.006
Very Low n (%)	0 (0)	2 (3.3)	
Moderate n (%)	0 (0)	5 (8.3)	
High n (%)	60 (100)	53 (88.4)	

*Significance level: $P < 0.05$ † wilcoxon Test

Table 2. Frequency Distribution of Anxiety of the Participants.

the result of the Kruskal-Wallis test, this difference was statistically significant, and the mean of evident anxiety of patients was significantly less than caregivers (P = 0.023). It is also observed that all caregivers' hidden (trait) anxiety was high, and 88.4% of patients had hidden anxiety at a high level. The mean of hidden anxiety in caregivers was 74.71 with a standard deviation of 2.91 and in patients was 68.83 with a standard deviation of 10.72. Based on the result of the Kruskal-Wallis test, this difference was statistically significant, and the mean of hidden anxiety in patients was significantly less than caregivers (P = 0.006).

Discussion

COVID-19 is a pandemic disease with high mortality rates and distribution globally[24-27]. In this study, it was found that this disease (COVID-19) is anxious for most patients and causes more anxiety in the family (patient caregivers) than the patient. The mean of state anxiety in patients was 70.82, and the mean of state anxiety in caregivers was 74.2. Also, the mean of trait anxiety in patients was 68.83, and this means in caregivers was 74.71. Given the importance of the role of the family in the treatment of patients, and considering that most of the educational programs related to corona in medical centers are held only for patients, this study recommends that in addition to the patient, appropriate educational programs should also be considered for their family. The most appropriate providers of education in hospital wards are the nurses of such wards, who, in addition to frequently encountering similar patients and their families, also have the most time to communicate with them[28]. After identifying anxiety, nurses can better and more effectively deal with these unwanted conditions in the patient and her family by providing appropriate and correct education[29,30].

Conclusions

This research showed that the COVID-19 pandemic diseases caused severe effects on patients and their families mental and nervous systems. The majority of cases were faced with apparent anxiety. As anxiety in COVID-19 patients and their families may cause weakening of mood, despair, and hopelessness and finally encouraging the patient not to fail the disease; thus, it is essential to use antidepressant therapeutic agents to reduce the rate of anxiety among patients and their families. This is the first report comparing anxiety levels in patients with Coronavirus Disease (COVID-19) and their families globally. Thus, further investigations should perform to find more aspects of the COVID-19 mental disorders.

Bibliographic references

1. Zhu, H., Wei, L. and Niu, P. 2020. The novel coronavirus outbreak in Wuhan, China. Global Health Research and Policy, 5(1), 1-3.
2. Remuzzi, A. and Remuzzi, G. 2020. COVID-19 and Italy: what next? Lancet (London, England).
3. Zangrillo, A., Beretta, L., Silvani, P., Colombo, S., Scandroglio, A. M., Dell'Acqua, A., Fominskiy, E., Landoni, G., Monti, G. and Azzolini, M. L. 2020. Fast reshaping of intensive care unit facilities in a large metropolitan hospital in Milan, Italy: facing the COVID-19 pandemic emergency. Critical Care and Resuscitation, 22(2), 91.
4. Jernigan, J. A., Low, D. E. and Helfand, R. F. 2004. Combining clinical and epidemiologic features for early recognition of SARS. Emerging Infectious Diseases, 10(2), 327.
5. Wu, Z. and McGoogan, J. M. 2020. Characteristics of and important lessons from the coronavirus disease 2019 (COVID-19) outbreak in China: summary of a report of 72 314 cases from the Chinese Center for Disease Control and Prevention. JAMA, 323(13), 1239-1242.
6. Dong, X.-Y., Wang, L., Tao, Y.-X., Suo, X.-l., Li, Y.-C., Liu, F., Zhao, Y. and Zhang, Q. 2017. Psychometric properties of the Anxiety Inventory for Respiratory Disease in patients with COPD in China. International Journal of Chronic Obstructive Pulmonary Disease, 12, 49-58.
7. Cassem, N. and Bernstein, J. 2004. Depressed Patients (5th ed.). Philadelphia, PA: Mosby/Elsevier.
8. Coventry, P. A. 2009. Does pulmonary rehabilitation reduce anxiety and depression in chronic obstructive pulmonary disease? Current Opinion in Pulmonary Medicine, 15(2), 143-149.
9. Pietras, T., Witusik, A., Panek, M., Hołub, M., Gałecki, P., Wujcik, R. and Górski, P. 2009. Anxiety and depression in patients with obstructive diseases. Polski Merkuriusz Lekarski: Organ Polskiego Towarzystwa Lekarskiego, 26(156), 631-635.
10. Willgoss, T. G., Goldbart, J., Fatoye, F. and Yohannes, A. M. 2013. The development and validation of the anxiety inventory for respiratory disease. Chest, 144(5), 1587-1596.
11. Alipour, A., Ghadami, A., Alipour, Z. and Abdollahzadeh, H. 2020. Preliminary validation of the Corona Disease Anxiety Scale (CDAS) in the Iranian sample.
12. Al-Rabiaah, A., Temsah, M.-H., Al-Eyadhy, A. A., Hasan, G. M., Al-Zamil, F., Al-Subaie, S., Alsohime, F., Jamal, A., Alhaboob, A. and Al-Saadi, B. 2020. Middle East Respiratory Syndrome-Corona Virus (MERS-CoV) associated stress among medical students at a university teaching hospital in Saudi Arabia. Journal of Infection and Public Health, 13(5), 687-691.

13. Yu, W., Singh, S. S., Calhoun, S., Zhang, H., Zhao, X. and Yang, F. 2018. Generalized anxiety disorder in urban China: Prevalence, awareness, and disease burden. Journal of Affective Disorders, 234, 89-96.
14. Rijn, B. v. and Wild, C. 2013. Humanistic and integrative therapies for anxiety and depression: Practice-based evaluation of transactional analysis, gestalt, and integrative psychotherapies and person-centered counseling. Transactional Analysis Journal, 43(2), 150-163.
15. Li, S., Wang, Y., Xue, J., Zhao, N. and Zhu, T. 2020. The impact of COVID-19 epidemic declaration on psychological consequences: a study on active Weibo users. International Journal of Environmental Research and Public Health, 17(6), 2032.
16. Bao, Y., Sun, Y., Meng, S., Shi, J. and Lu, L. 2020. 2019-nCoV epidemic: address mental health care to empower society. The Lancet, 395(10224), e37-e38.
17. Chen, Q., Liang, M., Li, Y., Guo, J., Fei, D., Wang, L., He, L., Sheng, C., Cai, Y. and Li, X. 2020. Mental health care for medical staff in China during the COVID-19 outbreak. The Lancet Psychiatry, 7(4), e15-e16.
18. Dawood, E., Misuta, R., Alharbi, M., Almurairi, A., Kanori, H. and Alsaiari, M. 2018. Relationship between Nurses' Communication and Levels of Anxiety and Depression among Patient's Family in the Emergency Department. Ann Psychiatry Ment Health, 6(1), 1125.
19. Hosieni, F., Ravari, A. and Akbari, A. 2017. The Effect of Communicating with Patients Using Peplau Model on Patients' Satisfaction with the Provided Nursing Cares at the Cardiac Intensive Care Unit. Iran Journal of Nursing, 29(104), 36-45.
20. Townsend, M. and Morgan, K. 2017 Psychiatric mental health nursing: Concepts of care in evidence-based practice. FA Davis.
21. Zarei, M., Keyvan, M. and Hashemizadeh, H. 2015. Assessing the Level of Stress and Anxiety in Family Members of Patients Hospitalized in the Special Care Units. International Journal of Review in Life Sciences, 5(11), 118-122.
22. Basam pour, S. 2004. The effect of preoperative training on the anxiety level of patients undergoing open heart surge. Payesh Journal, 2, 139-144.
23. Behrouz, m. 1994. Spielberger anxiety test norms in mashhad. M.SC Allameh Tabatabai University.
24. Ranjbar R, Mahmoodzadeh Hosseini H, Safarpoor Dehkordi F. A Review on Biochemical and Immunological Biomarkers used for Laboratory Diagnosis of SARS-CoV-2 (COVID-19). The Open Microbiology Journal. 2020;14(1).
25. Mirzaie A, Halaji M, Dehkordi FS, Ranjbar R, Noorbazargan H. A narrative literature review on traditional medicine options for treatment of corona virus disease 2019 (COVID-19). Complementary Therapies in Clinical Practice. 2020:101214.
26. Halaji M, Farahani A, Ranjbar R, Heiat M, Dehkordi FS. Emerging coronaviruses: first SARS, second MERS and third SARS-CoV-2: epidemiological updates of COVID-19. Infez Med. 2020;28(suppl 1):6-17.
27. Sheikhshahrokh A, Ranjbar R, Saeidi E, Dehkordi FS, Heiat M, Ghasemi-Dehkordi P, Goodarzi H. Frontier therapeutics and vaccine strategies for sars-cov-2 (COVID-19): A review. Iranian Journal of Public Health. 2020;49:18-29.
28. Arrebolaα Pajares, A., Tejidoα Sanchez, A., Jimenezα Alcaide, E., Medinaα Polo, J., Perezα Cadavid, S., Guerreroα Ramos, F. and Diazα Gonzalez, R. 2014. Survey of satisfaction in hospitalized patients at a urology department. Archivos Espanoles De Urologia, 67(7), 621–627.
29. Brunner, L., Smeltzer, S., Bare, B., Hinkle, P. and Cheever, K. 2017. Brunner & Suddarth's textbook of medicalα surgical nursing. Philadelphia: PA: Williams & Wilkins.
30. Dehkordi FS, Valizadeh Y, Birgani TA, Dehkordi KG. Prevalence study of Brucella melitensis and Brucella abortus in cow's milk using dot enzyme linked immuno sorbent assay and duplex polymerase chain reaction. J Pure Appl Microbiol. 2014;8(2):1065-9.

Received: 15 April 2021
Accepted: 20 May 2021

RESEARCH / INVESTIGACIÓN

Usage of *Cicer Arietinum* as a local and eco-friendly natural coagulant in sewage treatment and its ability to increase the formation of floc process

Amera Marey Mohammed Hassanien (A.Marey)

DOI. 10.21931/RB/2021.06.03.9

Abstract: Cicer Arietinum (CA) or chickpea seeds were used as a local natural coagulant, cheap and cultivable which available in Egypt that can be used to reduce turbidity from wastewater, especially sewage water instead of chemical coagulant that causes different diseases like intestinal constipation, loss of memory, convulsions, so this paper represents the use of chickpea as a natural coagulant and eco-friendly in the environment because it assumed to be safe for the human health and efficient in sewage treatment, So the researchers advices now to use natural coagulant as coagulant aids which has a higher ability to raise the consistency of floc and prevent of the coagulation operation. The optimum removal conditions that applied on the research were temperature =25^{0}C, pH= 3, Contact time=120 min, agitation speed for 2 minutes =80 rpm (rapid mixing), (CA) dosage is 90 mg/L, and (95.89%) turbidity reduction was achieved on the studied area.

Key words: Turbidity, Cicer Arietinum, Chickpea, Natural Coagulant.

Introduction

Water is the main element for life on the earth's surface; turbidity is a handy indicator for water quality so, there are new techniques for sewage and water treatment, but the coagulation/flocculation method is still the essential process for treatment and turbidity removal from water. Nowadays, natural coagulants are becoming better for treatment than other organic and inorganic coagulants like Alum and polyacrylamide, to reduce the human diseases and no human health danger also it is minimal expensive than the traditional chemicals.

The history of natural coagulants' utilization is extended, For more than 2000 years in India, Africa, and China as operative coagulants for turbidity water elevation. They are perhaps produced from plant seeds, leaves, and roots[14]. Many operative coagulants from plant origin have been specified: Nirmali, Okra, red bean, Sugar and red maize, *Moringa oleifera*, *Cactus latifera*, and seed powder of *Prosopis juliflora*[7,8,19]. Sewage / Wastewater recognized as an aggregation of water holding wastes from sewage is organic to consists of carbon compositions like human waste, paper, vegetable matter residences, institutions, commercial and industrial factories with groundwater, surface water, and stormwater probably exist[5]. Sewage consists of 99.9% water and 0.1% solids, etc.; even after 1990, to increase scientific knowledge and a developed information base, wastewater treatment has initiated to focus on the health-related toxic chemicals emitted into the environment. The water quality progress objectives of 1970 have continued, but the assurance has shifted to the definition and elimination of toxic and trace compounds, which could cause long-term health wares and opposite environmental influences. As a significance, However, the early treatment objectives stay helpful today, the required degree of treatment has risen significantly, and further treatment objectives and goals have been added, like especially natural coagulants[17,18,20]. Chickpea seeds can reduce the turbidity in the wastewater. Natural coagulants have shown their coagulation efficiency and are reported in many research articles. Natural coagulants applications in removing turbidity from the water industry are still low. *Cicer Arietinum* (CA) belongs to the family Leguminosae, which is an annual plant that used as a coagulant for water treatment which contains various species of monosaccharides such as glucose, ribose, galactose, and fructose and disaccharides like maltose and sucrose likewise oligosaccharides like ciceritol, stachyose, verbascose and raffinose[15]. Medically, *C. arietinum* exhaustion minimizes the level of inveterate diseases such as heart troubles and minimizes the cholesterol rates, reducing the hazard of colorectal cancer. (CA) has an efficient weight loss and decreases obesity, so it considers as minimal-Gl food[6]. Cicer Arietinum is locally available in Egypt, so we used it as an effective natural coagulant to reduce turbidity from wastewater(sewage) in the studied area, Ismailia canal (Mostorod refinery site) then becoming easier in household applications. We noticed that natural coagulants have a bright future to their considerable origin, ecofriendly in the surrounding, and biodegradable from the previous information concerned by many researchers. The impartial tools of that research to estimate the efficiency of (CA) to reduce turbidity from natural wastewater by measuring the parameters (pH, turbidity).

Materials and methods

Cicer arietinum (chickpea is a commercial name): is locally available in the market, was ground to fine powder, which kept approximate size less than 600 µm to achieve solubilization of effective components in the seed filtered water was added to the powder to make suspension by about 1%. The suspension was busily shaken until 45 minutes by utilizing a magnetic stirrer to elevate water extraction of the coagulant proteins, while that was after that push through filter paper (Whatman no. 42, 125 mm dia.). The refine portions were utilized until seeked potion of natural coagulants. Fresh solutions were intended every day and preserved to prevent longevity effects (such as changing pH, viscosity, and coagulation action)[3]. Whole coagulation tests were held out utilizing wastewater from the outlet of Ismailia Canal (Mostourd refinery site) as a water source. pH= (7.34), (TDS) is (100.7) NTU and Temperature= (29^{0}C). Hardness was measured by titration with EDTA. TS (Total solid), TSS (Total suspended solid), and heavy metals were measured corresponding to Standard processes[7]. Overall solids are measured by evaporating the whole of the water outside of a specimen and weighing the residual solids. Unsettled so-

[1] Department of Basic Science, The Valley Higher Institute for Engineering and Technology, Egypt.

Corresponding author: amera_muhammad@hotmail.com

lids are measured by thread sample water through a filter. The solids held by the filter, once dried, are the suspended solids: Pekin Elmer, Analyst atomic absorption, measured heavy metals. Turbidity was recorded on a 2100N IS Turbidimeter (Hach). The color was decided by absorption scan (190-350 nm) using UV/ Vis-Spectrophotometer (LLG-UniSPEC 2)[2]. All Experiments were carried out in the laboratory. The eligible analysis was utilized to seek the best combination of variables to obtain optimum values due to elimination of responses and thus acquire clear wastewater to be reused for irrigation or in the same industrial methods. Eligibility varies from zero to one owing to every specified response. A significance of one exemplifies a perfect state; however, zero suggests that one or more answers fall outgoing the eligible boundaries[1].

Preparing Cicer Arietinum (CA)

The seeds were washed with a significant amount of water to remove impurities, then dried in the sun for 2 days. This was shown in Figure (1); after that (CA), a mixer (Oster) was ground to obtain an excellent powder then storage in a plastic vacuum container. To get a stock of solution, we added 10 grams of natural coagulant in 1000 ml distilled water, obtaining the solution of 10,000 mg/L at room temperature ~ 20-25^{0}C (cool place) and stirred at high speed 120 rpm for 1 hour, to be homogenous and ready for use in the treatment of sewage water.

Methodology and Coagulation Test

In the laboratory, we applied the jar test, which is the extreme close method for coagulation-flocculation, Like in Figure (2), We prepare six beakers filled with 300 ml wastewater respectively; before operating the test, the samples were mixed for measuring turbidity, then we added different concentrations of natural coagulant (CA) into the beakers with wastewater at room temperature ~ 20-25^{o}C. In this test, we used different pH of wastewater from 1 to 10. The beakers were agitated at several speed and mixing times, which the suspension was stirred at 200 rpm for 2 minutes of rapid mixing and followed by slow mixing at 60 rpm for 12 minutes. This mixing let flocs particles suspend finally removed from the samples in the beakers to be ready for measuring (turbidity, TSS, TDS, COD, BOD) (physicochemical parameters). All those experiments were carried out at a temperature in the zone between (25-45^{o}C), Turbidity test was conducted by nephelometric turbidity unit (NTU). Standard procedures measured BOD and COD. Hardness was measured by titration with EDTA. TDS was measured by weighting the filtrate before and after the drying. The reduction of turbidity can be calculated for each sample from the equation:

Lowering of turbidity (NTU)= Primary Turbidity (NTU)- Final Turbidity (NTU)

Results and discussion

Effectiveness of Dosage (CA) on Physicochemical Parameters

The results of the jar test at various Cicer. Arietinum concentrations (50, 30, and 20 mg/L). The optimum concentration of (CA) is 50 mg/L, which reduced turbidity from (97 to 93.16 %) and TSS from (110 to 55.6).

Effectiveness of Various pH Values

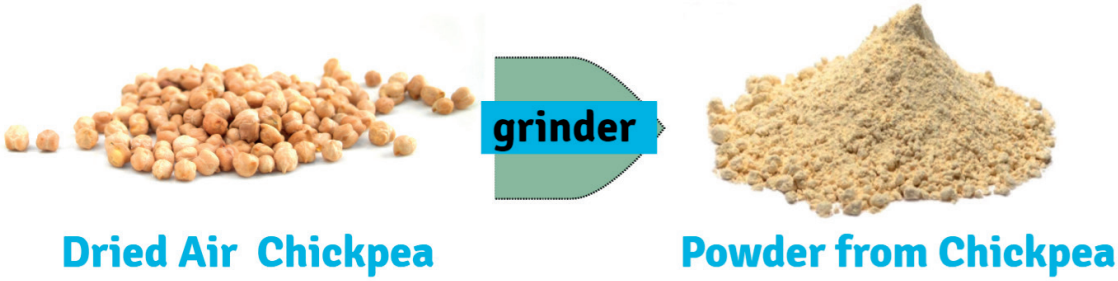

Figure 1. Preparation of *Cicer arietinum* (CA)

Figure 2. A traditional jar test device was owing for the treatment of turbid water.

The coagulation achievement of Cicer arietinum for reducing turbidity in wastewater preferred the acidic condition; in this experiment, the variation in pH was applied from (3-10), which works best at pH=3, we noticed that the water appeared clearer and the flocs were observed after the settling process, but when the pH increased more than 6 the water turned cloudier and fewer flocs were found and gave lower turbidity % at pH=10 because the conditions turned alkaline, all these data were noticed in Figure (3).

Reduction of Turbidity Using Different Doses of (CA)

Before we studied the effect of different doses on turbidity, the raw wastewater turbidity was found 97 NTU, using various *Cicer Arietinum* doses (50,60,70,80,90,100) mg/ L. It was observed that C. arietinum highly efficient to higher dosage and lower dosage, but increasing in dosage caused again increase in turbidity as shown in Figure (4).

Effectiveness of Contact time on the turbidity ratio

In Figure (5), Different values of contact time were examined from (40 to 160 minutes). The test showed turbidity elimination raised when the time increased from 100 to 120 minutes, then decreased when the contact time was increased up to 120 minutes because the coagulant (CA) efficiency in absorbing the colloids decreased flocs were broken. So, from the previous study, further increase for mixing escalates micro flocs breakage in primary particles, slowing down floc's growth during flocculation[10]. The highest turbidity removal was achieved at 120 minutes.

The efficiency of Temperature on Turbidity Reduction

In this experiment, we used different temperature values were (25,30,35,40), which the optimum temperature for removal turbidity was 25^{0}C as observed in Figure (6), Which by increasing temperature, the turbidity removal efficiency decreased.

Optimization of Agitation Speed on Turbidity Reduction

Mixing speed is one of the most substantial roles for obtaining turbidity removal competence or failure of the flocculation, different values were used beginning from (20-140), So Figure 7 indicates that the high evaluation at 80 rpm with 95% removal. From the following data, we observed that this case was especially which by higher agitation speed, the turbidity removal efficiency became very weak and minimized to the flocs created in the coagulation-flocculation operation was facilely destroyed[13]. A traditional flocculation unit operation contains three separate steps: 1-quick or flash blending: the convenient chemicals (flocculation and if required pH adjusters) are poured to the wastewater stream, stirred, and emphatically blended at rising speed. 2-Slow mixing (flocculation): the wastewater is only reasonably stirred to compose large flocs readily settled out. 3- Sedimentation: the floc created through flocculation is authorized to settle and is separated from the current flow[9,19,21].

Conclusions

The application of natural coagulant (*Cicer arietinum*) on surface water treatment was checked in this research. The surface water was described by the concentration elevation of suspended particles. On varying the coagulant dosage, pH, and settling time, these particles get readily dissolved and settled along with the coagulants added[4]. Based on the fact that Cicer arietinum (CA) being the most economical and environment-friendly alternative natural coagulant, so we used it for removing colloids and decrease turbidity by jar test method instead of chemical coagulants which have inherent disadvantages affecting on human health, from the parameters that were discussed in the experiment as atrial to remove or decreased turbidity efficiency from wastewater (Mostourd refinery area), we reach to a result that the optimal dose of Cicer arietinum (CA) for higher efficiency of turbidity and color removal is 90 mg/L, with other constant parameters like (Temperature =25^{0}C, pH= 3, Contact time=120 min, and agitation speed for 2 minutes =80 rpm (rapid mixing), from These all other optimal water quality parameters have a very significant effect on improving turbidity reduction percentage by 95.89%. Since we have collected the wastewater from the outlet of Ismailia Canal (Mostourd refinery site) as a water source; we suggest that instead of using chemical coagulants that has Avery terrible side effects on health, we must and restricted on using natural coagulants like (Cicer arietinum (CA) as an alternative method for the treatment process.

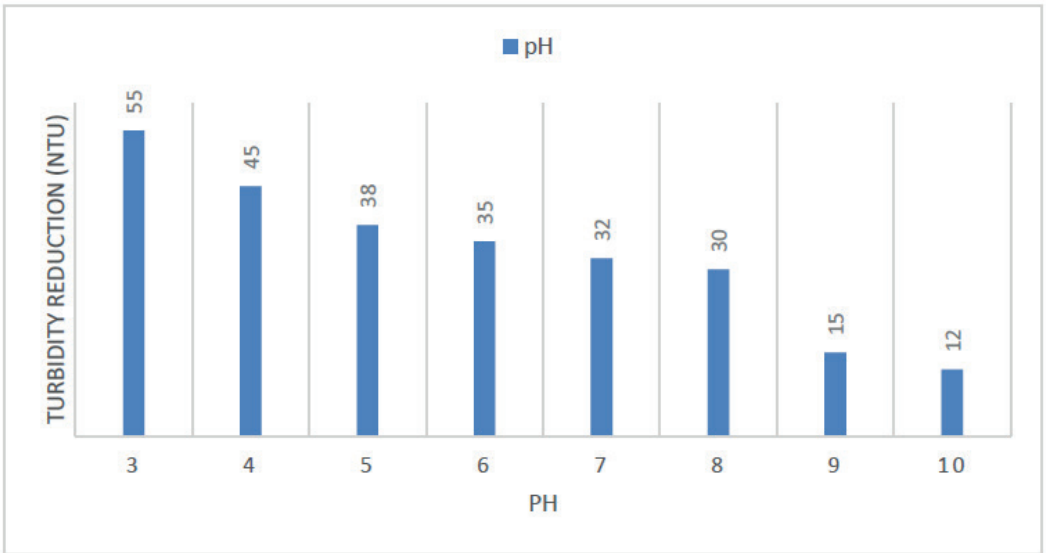

Figure 3. Turbidity reduction at different pH of the wastewater.

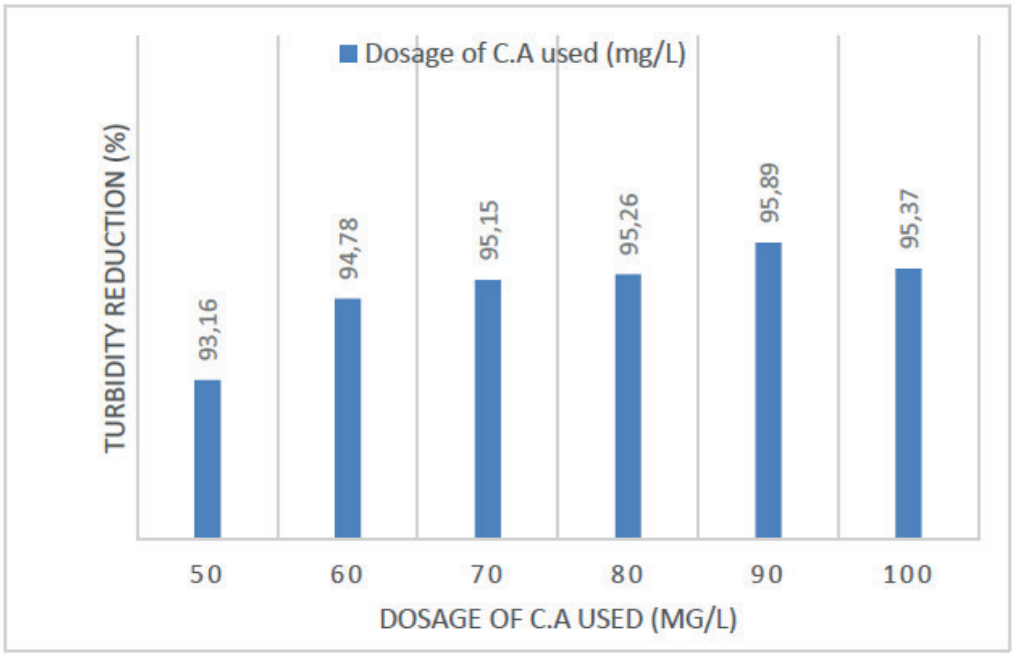

Figure 4. Elimination of turbidity using various dosages of *Cicer Arietinum*.

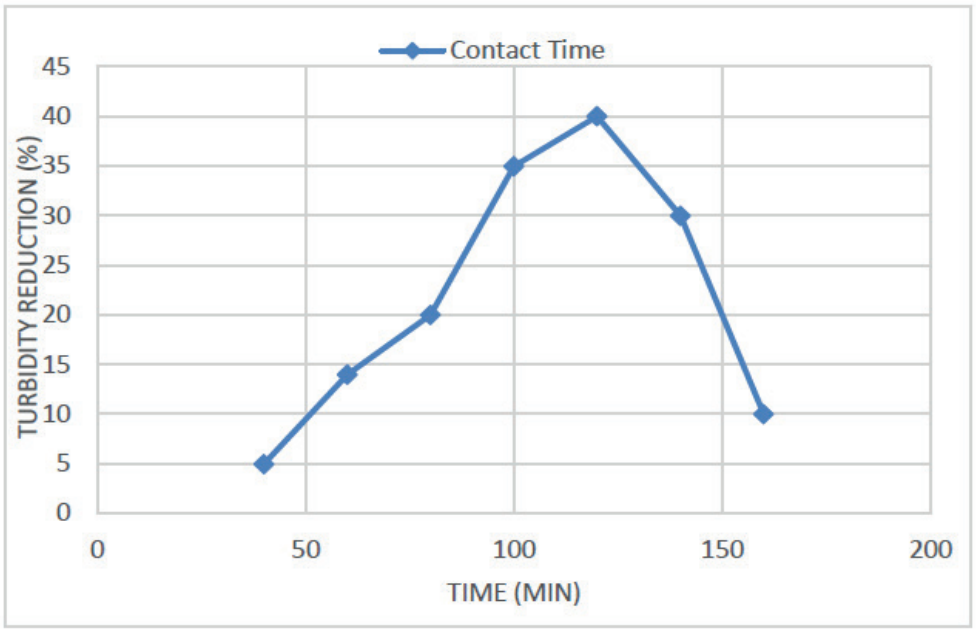

Figure 5. Shows the effects of various contact time on the efficiency of turbidity removal.

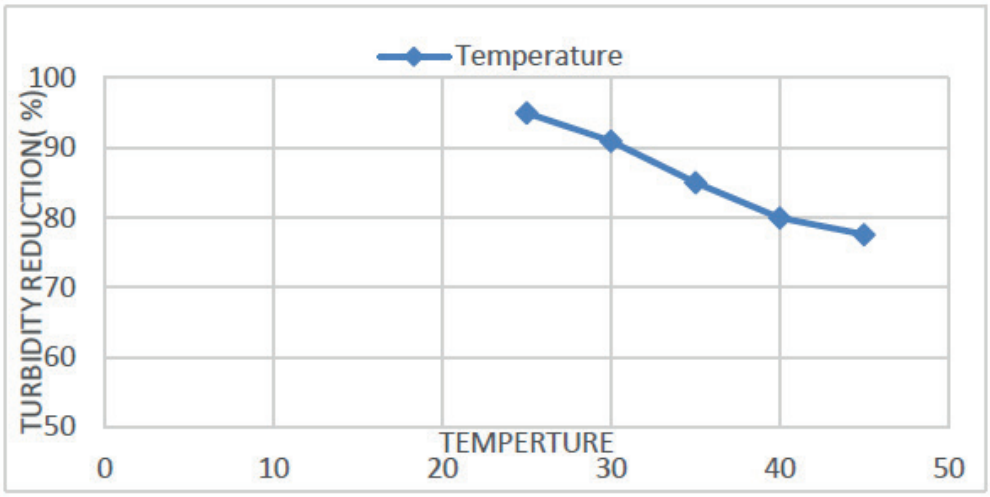

Figure 6. Shows the Effects of Various Temperatures on the Removal of Turbidity

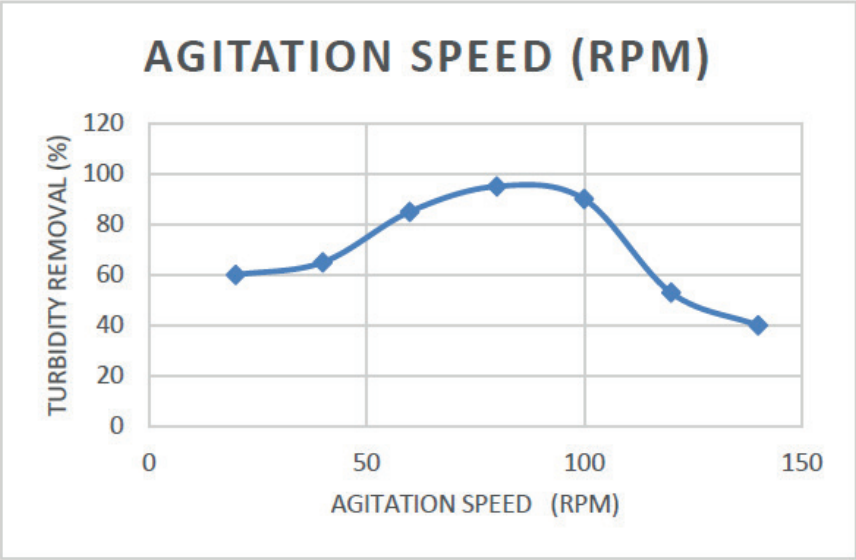

Figure 7. The influences of various mixing speeds on turbidity reduction.

Bibliographic references

1. Ebeling, JM, Sibrell PL, Ogden SR, Summerfelt ST. Summerfelt Evaluation of chemical coagulation-flocculation aids for the removal of suspended solids and phosphorus from intensive recirculating aquaculture effluent discharge, Aquacultural Engineering. 29(2003) 23-44.
2. McGhee TJ, Water Supply and Sewerage. McGraw-Hill, New York, 260 (1991) 287.
3. Francois RJ, Ageing of aluminum hydroxide flocs, Water Research. 21(1987) 523-531.
4. Gunaratna KR, Garcia B, Andersson S, Dalhammar G, Screening and evaluation of natural coagulants for water treatment, Water Science and Technology .7(2007) 19-25.
5. AE Clecerils, Greenberg and Eaton AD, Standard Methods for the Examination of water and wastewater, 20th Ed. American Public Health Association, USA, Washington DC. (1998).
6. Diaz A, Rincon N, Escorihuela A, Fernandez N, Chacin E, Forster CF. A preliminary evaluation of turbidity removal by natural coagulants indigenous to Venezuela" 1999, Process Biochemistry. 35(1999) 391-395.
7. Cheremisinff NP, Hank Book of Water and Wastewater Treatment Technologies, An Overview of Water and Water Treatments. Butterworth-Heinemann Publication, 3 (2002)1-60.
8. Rowe DR, Abdel- Magid IH, Handbook of Wastewater Reclamation and Reuse, Boca Raton, Lewis. 3 (1995)167-181.
9. Apha, Standard Methods for Examination of water and wastewater, 17th Ed. Washington DC. 3(1) (1992) 501-517.
10. Metcalf, Eddy, Wastewater Engineering Treatment, Disposal and Reuse New York, McGraw Hill. 3(1991) 35-40.
11. Asrafuzzaman Md, Fakhruddin ANM, Alamgir Hossain Md. Reduction of Turbidity of Water Using Locally Available Natural Coagulants. International Scholarly Research Notices.10 (2011) 1-7.
12. Abdel-Kalek MA, Abdel Rahman MK, Francis AA. Experimental Design and Desirability Analysis for Optimizing the Bio-sorption of Liquid Paint-related Wastes onto Solid Eggshell Wastes. Environmental Processes. 7(2) (2020) 493-508.
13. Jaoudi M, Amdouni N, Coagulation Treatment by Al2 (SO4) 3 and Residual Al Determination in Medjerda Water Dam (Tunisia), Journal de la Société Chimique de Tunisia.15 (2013) 175-181.
14. Marey A, Synthesis Composite of Tio2/ Chitosan and Tio2 / Bentonite for removing turbidity from Ismailia Canal as Water Treatment Plant, African Journal of Chemical Education (AJCE). 10(1) (2020)124-134.
15. Jahn SAA, Using Moringa seeds as coagulants in developing countries, Journal of the American Water Works Association. 80 (1988) 43-50.
16. Yarar B, Evaluation of Flocculation and Filtration Procedures Applied to WSRC Sludge, Report no, DE-AC09-96SR 18500, Colorado School of Miness.34 (2001) 234-244.
17. Choubey S, Rajput SK, Bapat, KN. Comparison of Efficiency of some natural coagulants-Bioremediation. International Journal of Emerging Technology and advanced Engineering. 2 (2012) 159-168.
18. Rossini M, Garrido J, Garcia, Galluzzo M, Optimization of the coagulation-flocculation treatment influence of rapid mix parameters, Water Research. 33(8) (1999)1817-1826.
19. Babitha Merlin S, Abirami S, Suresh Kumar R. Studies on the treatment of surface water using rajma seeds. Journal of Civil Engineering, 10 (2018) 10-15.
20. Kawamura S, Effectiveness of natural polyelectrolytes in water treatment. Journal of the American Water Works Association, 83 (1991) 88-91.
21. Liu MM, The Effectiveness of the Natural Polymers Chitosan, Polyglutamic Acid, and Moringa Oleifera Seeds in Water Purification, California State Science Fair. 3(2014) 2-14.

Received: 16 March 2021
Accepted: 10 July 2021

RESEARCH / INVESTIGACIÓN

Assessment of the diagnostic value of CEA, CA125, and CRP and their cut-off point for discrimination of exudative pleural effusions

Hanie Raji[1], Seyed Hamid Borsi[1], Mehrdad Dargahi MalAmir[1], Ahmad Reza Asadollah Salmanpour* DOI. 10.21931/RB/2021.06.03.10

Abstract: Pleural effusion is divided into exudative and transudative effusion, and the distinction between exudate and transudate requires multiple investigations of biochemical parameters and their comparison in pleural fluid and serum. This study aimed to assess the diagnostic value of CEA, CA125, and CRP and their cut-off point for discrimination of exudative pleural effusions. This epidemiological and cross-sectional study was performed on 50 patients aged between 18 to 90 years with the diagnosis of exudative pleural effusion referred to Imam Khomeini Hospital in Ahvaz in 2018 and 2019. Demographic and clinical information of patients were collected. The pleural effusion was diagnosed based on physical examination and chest radiography. Pleural effusion was confirmed by thoracentesis. A pleural fluid sample was taken from all patients, and the levels of CEA, CA125, and CRP markers were measured in the pleural fluid. Differentiation of transudate and exudate pleural effusions was performed using Light criteria. The mean CEA and CA125 level of pleural fluid were significantly higher, and the mean CRP level of pleural fluid was significantly lower in patients with malignant diagnoses (P <0.05). Cut-off value with highest sensitivity and specificity in differentiating types of exudative pleural effusions was obtained for CEA tumor marker (greater than 49.8), CA125 tumor marker (greater than 814.02), and CRP marker (less than 7.56). Also, in differentiating types of exudative pleural effusions, CEA tumor marker had sensitivity (89.03%) and specificity (78.42%); CA125 tumor marker had sensitivity (53.18%) and specificity (62.44%), and CRP marker had sensitivity (82.16%), and specificity (89.05%) were. Although the tumor markers had high specificity in the present study, the low sensitivity of some of these tumor markers reduced their diagnostic value. On the other hand, given the numerous advantages of tumor markers, such as low cost and non-invasive, combining them with another can increase the diagnostic value and accuracy.

Key words: Pleural effusion, Exudative, Transudative, Tumor markers.

Introduction

Pleural effusion is one of the most common clinical manifestations associated with some chest diseases[1], which is the accumulation of fluid in the pleural cavity and is often caused by a systemic or intrathoracic process. The prevalence varies by clinical setting, but 90% of all pleural effusions are caused by heart failure, malignant processes, and pneumonia and can lead to serious health problems if not properly treated or diagnosed[2]. The fluid that enters the pleural space can be of the origin of the pleural capillaries, interstitial lung space, intra-aortic lymphatics, intrathoracic blood vessels, or peritoneal cavity[3,4]. The pleural effusion is divided into two types of exudative and transudative effusions[3,5]. The distinction between exudate and transudate requires multiple investigations of biochemical parameters and their comparison in pleural fluid and serum[6-9]. Recently, to help differentiate the etiologies of pleural effusion, several studies have investigated tumor markers as a potential alternative to invasive procedures[10-13]. Different studies have investigated the diagnostic value of different tumor markers to differentiate different types of pleural effusion. However, the wide range of sensitivity, specificity, and cut-off values and the inconsistency in the results have made their diagnostic accuracy still questionable[14-18]. CEA has been the most common marker tumor studied for the diagnosis of malignant pleural effusion[19]. It has recently been reported that serum and fluid levels of pleural effusion CA-125 can be used to diagnose pleural effusion malignancy[20,21]. In addition, CRP is often produced by the liver, and CRP levels in pleural effusions can be used to differentiate parapneumonic effusions from other types of effusions[22,23]. Since no high sensitivity and specificity, the marker has been identified for the diagnosis of exudative effusion pleural effusions and due to inconsistency in the results of our studies, the aim of the present study was to evaluate the biomarker value of CEA, CA-125 and CRP tumor biomarkers in differentiation between exudative effusion pleural effusions.

Materials and methods

Study designs

Following approval of the study in the Ethics Committee of Ahvaz Jundishapur University of Medical Sciences (Code of Ethics: IR.AJUMS.REC.1397.950), this study is an epidemiological and cross-sectional study on 50 patients aged 18 to 90 years with the diagnosis of exudative pleural effusion who referred to Imam Khomeini Hospital in Ahvaz in 2018 and 2019. Initially, the goals, benefits of participating in the study, and how to conduct the research were explained to participants. Eligible patients were then enrolled in the study, if desired, with written consent.

At first, demographic data and clinical history of all patients were obtained and collected in a checklist. Required information about the underlying disease and the cause of pleural effusion was also collected and recorded based on the patient's medical record findings. Patients with exudative pleural effusion with different etiologies were included in the study, and biomarkers were measured before any treatment. Patients with unknown pleural effusion origin were excluded.

The diagnosis of pleural effusion was made after a physical examination and chest imaging. Pleural effusion was confirmed by thoracentesis. Microbiological, biochemical, and cytological studies were also performed for all patients. Di-

[1] Air Pollution and Respiratory Diseases Research Center, Faculty of Medicine, Ahvaz Jundishapur University of Medical Sciences, Ahvaz, Iran.

Corresponding author: dr_salmanpour@yahoo.com

fferentiation of transudate and exudate pleural effusions was performed using light criteria. Accordingly, the presence of one of the following indicated exudative pleural effusion.

- Pleural protein/serum protein ratio > 0.5
- Serum LDH/pleural LDH ratio > 0.6
- Pleural LDH activity exceeds two-thirds of the highest normal level for serum LDH[10,24,25].

A pleural fluid sample was obtained from all patients, and the supernatants were collected after centrifugation (3500 rpm for 10 minutes) and stored at -20°C for final testing. The pleural fluid sample was inserted through a needle between the rib cage based on examination and percussion, and auscultation (sound reduction and dullness). The samples were sent to the laboratory after collection and the levels of CEA, CA125, and CRP markers in the pleural fluid of the patients were measured.

CEA and CA125 measurements were performed on pleural specimens by electrochemical luminescence (ECL) and CRP measurements by turbidometric technique. All biomarkers were analyzed according to the manufacturer's instructions. Finally, all data collected were analyzed statistically to evaluate the diagnostic value of each tumor marker in different types of exudative pleural effusion.

Statistical analysis

The data are analyzed by descriptive statistics, including mean, standard deviation, frequency, and percentage. Data were analyzed using the Kolmogorov-Smirnov test and Q–Q plot and variance homogeneity by Leven test. Independent t-test (or Mann-Whitney nonparametric test), chi-square (or Fisher exact test), and logistic regression were used for data analysis. The ROC curve was used to determine the diagnostic value of tumor markers, and the area under the ROC diagram (AUC) was considered as the diagnostic value of the biomarker. Sensitivity, specificity, accuracy, positive and negative predictive values of each tumor marker were also calculated. All analyses were performed using SPSS software version 22, and the significance level was considered less than 0.05.

Results

The distribution of patients by gender was approximately similar, and the percentage of male and female patients was similar (48% vs. 52%). Patients older than 60 years had the highest frequency (72%) compared to other age groups. The etiology of the disease in most patients was adenocarcinoma and parapneumonic (Table 1).

To determine the diagnostic value of CEA, CA125, and CRP markers in differentiating different types of exudative pleural effusions, patients were divided into three groups according to the etiology of the disease. The mean level of CEA in pleural fluid was significantly higher in patients with malignancy (P <0.05). This rate was also higher in patients with the etiology of tuberculosis than in patients with the parapneumonic diagnosis. The mean CA-125 level of pleural fluid was significantly higher in patients with malignancy (P <0.05). This rate was also higher in patients with the etiology of tuberculosis than in patients with the parapneumonic diagnosis. The mean pleural fluid CRP level was significantly lower in patients with malignancy (P <0.05). Also, this rate was lower in patients with tuberculosis than in patients with parapneumonic diagnosis (Table 2).

The cut-off value with the highest sensitivity and specificity for CEA tumor marker differentiation in exudative pleural effusions was more significant than 49.8. According to this cut-off value, the sensitivity of the CEA tumor marker in differentiating different types of exudative pleural effusions was 89.03%, specificity was 78.42%, positive predictive value was 82.01, and negative predictive value was 64.36%.

The cut-off value with the highest sensitivity and specificity for CA125 tumor marker in the differentiation of exudative pleural effusions was greater than 814.02. Accordingly, CA125 tumor marker sensitivity in differentiating pleural effusions was 53.18%, specificity was 62.44%, positive predictive value was 67.34%, and negative predictive value was 59.19%.

The value of highly sensitive and specific cut-off for the

Variables		N (%)
Gender	Female	24 (48%)
	Male	26 (52%)
Age (year)	15 - 29	1 (2%)
	30 - 44	5 (10%)
	45 - 59	8 (16%)
	60 - 74	22 (44%)
	75 - 90	14 (28%)
Etiology	Para pneumonic	18 (36%)
	Adenocarcinoma	27 (54%)
	Mesothelioma	2 (4%)
	Tuberculosis	3 (6%)

Table 1. Demographic information of the patients.

Group	Pleural fluid CEA (mg/l)	Pleural fluid CA125 (mU/mL)	Pleural fluid CRP (mg/l)
Malignancy	46.11±35.80	782.45±314.05	6.12±2.89
Parapneumonic	4.67±2.09	351.32±189.14	21.56±11.83
Tuberculosis	11.32±5.45	544.19±264.10	17.02±5.31
P-Value	0.008*	0.007*	0.001*

Data are expressed as mean±SD.
The statistical test used was ANOVA.
*P<0.05 was considered as a significance level.

Table 2. Comparison of pleural fluid CEA levels based on disease etiology.

CRP marker differentiating different types of exudative pleural effusions was less than 7.56. Accordingly, CRP marker sensitivity in differentiating pleural effusions was 82.16%, specificity was 89.05%, positive predictive value was 64.32%, and negative predictive value was 59.71%.

Discussion

Malignant pleural effusion is a common problem in cancer patients that can be both a symptom and a complication of a previously diagnosed malignancy. Despite the combination of pleural fluid cytology and pleural biopsy, it is not possible to obtain a diagnosis in many cases[24]. Researchers have been researching to evaluate the value of pleural fluid analysis in the differential diagnosis of pleural effusions on different tumor markers[24,25].

In our study, 26 patients were male, and 24 were female. Also, in the present study, out of 50 people studied, 18 patients were parapneumonic, 27 patients were adenocarcinoma, 2 patients were mesothelioma, and 3 patients were tuberculosis.

Based on our results, mean levels of pleural fluid CEA and CA125 were significantly higher in patients with malignancy (P<0.05). It also indicated that the rate is higher in patients with tuberculosis etiology than in patients with the parapneumonic diagnosis. The threshold for identifying exudative pleural effusion with the highest sensitivity and specificity for CEA tumor markers is more remarkable than 49.8. consequently, the sensitivity of the CEA tumor marker was 89.83%, the specificity was 78.42%, the positive predictive value was 82.01%, and the negative predictive value 64.36%, which shows and highlights high biomarker effectiveness in the diagnosis of benign and malignant.

Also, the highest sensitivity and specificity for the cut-off value of the CA125 tumor marker when differentiating types of exudative pleural effusion was greater than 814.02. therefore, the sensitivity of the CA125 tumor marker when differentiating exudative pleural effusions was 53.18%, the specificity was 62.44%, the positive predictive value was 67.34%, and the negative predictive value was 59.19%, as obtained from the study.

Owing to the chronic nature of the disease, the approach on individuals affected by unclassical and even unidentified pleural effusion is applied. Additionally, using this method eases the distinguish of malignant cases of tuberculosis with lower costs of the experiment[26].

In the study done by Nguyen et al., who determined the diagnostic value of tumor antigens for malignant pleural effusions, the sensitivity and specificity were 54.9% and 96.2% for CEA tumor markers and 57.5% 92.8% for CA-125, respectively[15]. In another study done by Zhai et al., who investigated the diagnostic accuracy of CEA and CA-125 tumor markers in the differentiation of malignant pleural effusions, The results indicated that the serum levels of both tumor markers were significantly higher in the types of malignant pleural effusions than in benign pleural effusions. The CEA and CA15-3 levels were more stable than the CA-125 and CA19-9 tumors. CEA was also the best marker to distinguish between benign and malignant pleural effusions. The sensitivity and specificity of CEA were 84.7% and 90.9% in the pleural and 64.0% and 88.0% in the serum. The sensitivity and specificity for the CA-125 tumor marker were 49% and 73.1% in the pleural and 60.4% and 54.8% in the serum[14]. Tozzoli et al. compared the diagnostic value of pleural fluid CEA in patients with pleural effusion with histological findings.

The results indicated that the sensitivity and accuracy of pleural fluid CEA were significantly higher than that of pleural cytology, and the sensitivity of diagnosis of benign and malignant cases was high. They deduced that measuring pleural fluid CEA in patients with unexplained etiology of a pleural effusion is a safe and reasonably priced way for doctors to select patients for further examination. Increased pleural CEA values in patients with pleural effusion with negative cytology indicate the need for further invasive examinations, whereas people with low pleural CEA values should only be examined again[12]. In a study by Antonangelo *et al.*, A comparison of tumor markers in benign and malignant pleural effusions with positive, suspicious, and negative cytology showed that the CEA and CA125 markers were significantly higher in malignant effusions with positive cytology. Only the CA125 marker tumor score was significantly higher in the negative or suspected cytological results than in the benign effusions in the pleural fluid. As a result of this study, it could be shown that a tumor sensitivity and specificity of up to 60% can be used as a parameter for the assessment of patients with a suspected malignancy or cancer in the history[27]. The results of a study by Shalaby et al. showed that the CA-125 tumor marker was significantly higher in patients with exudative effusion than in patients with transudative effusion. This tumor marker was also more common in malignant effusions than benign effusions and tuberculosis compared to other infections. As a result, the highest CA125 level of pleural fluid was observed in malignancy and then in tuberculosis, and thus the level of this

marker tumor in the pleural fluid could be used as a diagnostic marker for pleural effusion[21]. In the present study, the mean CRP of pleural fluid was significantly lower in patients with malignancy (P <0.05). This rate was also lower in patients with tuberculosis etiology than in patients with the parapneumonic diagnosis.

The limit with the highest sensitivity and specificity for CRP markers when distinguishing different types of exudative pleural effusions was less than 7.56. Accordingly, the sensitivity of the CRP markers when differentiating pleural effusions was 82.16%, the specificity 89.05%, the positive predictive value 64.32%, and the negative predictive value 59.71%. In a study by Ji et al. To investigate the role of three markers of procalcitonin (PCT), CRP, and CEA in the differential diagnosis of malignant and benign pleural effusions, the CRP and PCT levels were significantly higher in benign pleural effusions than in malignant cases, while the CEA levels were lower were in benign cases. They concluded that the use of a biomarker is not only suitable for the diagnosis of pleural effusion and is not accurate enough. The combination of pleural CRP, pleural CEA and sPCT can effectively support the diagnosis of pleural effusions[1,28].

Conclusions

Based on the present study results, the tumor markers examined in this study had high specificity, but the low sensitivity of some of these tumor markers decreased their diagnostic value. However, since tumor markers in the diagnosis of malignant pleural effusion have many advantages, such as low cost and invasive use, the combination of tumor markers can significantly increase the value and diagnostic accuracy.

Acknowledgment

This research was supported by grants (APRD-9710) from Air Pollution and Respiratory Diseases Research Center, Ahvaz Jundishapur University of Medical Sciences, Ahvaz, Iran. This study is the residency thesis of Dr. Ahmad Reza Asadollah Salmanpour.

Bibliographic references

1. Ji M, Zhu X, Dong J, Qian S, Meng F, Gu W, et al. combination of procalcitonin, C-reaction protein and carcinoembryonic antigens for discriminating between benign and malignant pleural effusions. Oncology letters. 2018; 16(2): 1727-35.
2. Trapé J, Sant F, Franquesa J, Montesinos J, Arnau A, Sala M, et al. Evaluation of two strategies for the interpretation of tumour markers in pleural effusions. Respiratory research. 2017; 18(1): 103.
3. Na MJ. Diagnostic tools of pleural effusion. Tuberculosis and respiratory diseases. 2014; 76(5): 199-210.
4. Light RW. Pleural diseases. Lippincott Williams & Wilkins(2007).
5. Light RW. Pleural effusions. Medical Clinics. 2011; 95(6): 1055-70.
6. Ferreiro L, Toubes ME, Valdés L. Contribution of pleural fluid analysis to the diagnosis of pleural effusion. Medicina Clínica (English Edition). 2015; 145(4): 171-77.
7. Braunschweig T, Chung J-Y, Choi CH, Cho H, Chen Q-R, Xie R, et al. Assessment of a panel of tumor markers for the differential diagnosis of benign and malignant effusions by well-based reverse phase protein array. Diagnostic pathology. 2015; 10(1): 1-10.
8. Porcel JM, Light RW. Pleural effusions. Disease-a-month: DM. 2013; 59(2): 29.
9. Thomas R, Lee YG. Causes and management of common benign pleural effusions. Thoracic surgery clinics. 2013; 23(1): 25-42.
10. Gu Y, Zhai K, Shi H-Z. Clinical value of tumor markers for determining cause of pleural effusion. Chinese medical journal. 2016; 129(3): 253.
11. Volarić D, Flego V, Žauhar G, Bulat-Kardum L. Diagnostic value of tumour markers in pleural effusions. Biochemia medica: Biochemia medica. 2018; 28(1): 73-83.
12. Tozzoli R, Basso SM, D'Aurizio F, Metus P, Lumachi F. Evaluation of predictive value of pleural CEA in patients with pleural effusions and histological findings: A prospective study and literature review. Clinical biochemistry. 2016; 49(16-17): 1227-31.
13. Yoon DW, Cho JH, Choi YS, Kim J, Kim HK, Zo JI, et al. Predictors of survival in patients who underwent videoα assisted thoracic surgery talc pleurodesis for malignant pleural effusion. Thoracic cancer. 2016; 7(4): 393-98.
14. Zhai K, Wang W, Wang Y, Liu J-Y, Zhou Q, Shi H-Z. Diagnostic accuracy of tumor markers for malignant pleural effusion: a derivation and validation study. Journal of Thoracic Disease. 2017; 9(12): 5220.
15. Nguyen AH, Miller EJ, Wichman CS, Berim IG, Agrawal DK. Diagnostic value of tumor antigens in malignant pleural effusion: a meta-analysis. Translational Research. 2015; 166(5): 432-39.
16. Gu P, Huang G, Chen Y, Zhu C, Yuan J, Sheng S. Diagnostic utility of pleural fluid carcinoembryonic antigen and CYFRA 21α 1 in patients with pleural effusion: a systematic review and metaα analysis. Journal of clinical laboratory analysis. 2007; 21(6): 398-405.
17. SHI HZ, LIANG QL, Jiang J, QIN XJ, YANG HB. Diagnostic value of carcinoembryonic antigen in malignant pleural effusion: A metaα analysis. Respirology. 2008; 13(4): 518-27.
18. Liang Q, Shi H, Qin X, Liang X, Jiang J, Yang H. Diagnostic accuracy of tumour markers for malignant pleural effusion: a meta-analysis. Thorax. 2008; 63(1): 35-41.
19. Hammarström S. The carcinoembryonic antigen (CEA) family: structures, suggested functions and expression in normal and malignant tissues. Seminars in cancer biology 1999; 9(2): 67-81.
20. Shokouhi S, Samanabadi M, Gachkar L. Pleural fluid CA-125 in patients with pleural effusion. Tanaffos. 2005; 4(23–27.
21. Shalaby AED, Moussa HA, Nasr A, Samad MA. A study of CA-125 in patients with pleural effusion. Egyptian Journal of Bronchology. 2015; 9(3): 283-83.
22. Yang Y, Xie J, Guo F, Longhini F, Gao Z, Huang Y, et al. Combination of C-reactive protein, procalcitonin and sepsis-related organ failure score for the diagnosis of sepsis in critical patients. Annals of intensive care. 2016; 6(1): 51.
23. Izhakian S, Wasser WG, Fox BD, Vainshelboim B, Kramer MR. The diagnostic value of the pleural fluid C-reactive protein in parapneumonic effusions. Disease Markers. 2016; 2016(
24. Hackner K, Errhalt P, Handzhiev S. Ratio of carcinoembryonic antigen in pleural fluid and serum for the diagnosis of malignant pleural effusion. Therapeutic Advances in Medical Oncology. 2019; 11(1758835919850341.
25. Yang Y, Liu Y-L, Shi H-Z. Diagnostic accuracy of combinations of tumor markers for malignant pleural effusion: an updated meta-analysis. Respiration. 2017; 94(1): 62-69.
26. Shen Y, Liang Y, Cheng X, Lu W, Xie X, Wan X. Ovarian fibroma/fibrothecoma with elevated serum CA125 level: A cohort of 66 cases. Medicine. 2018; 97(34):
27. Antonangelo L, Sales R, Corá A, Acencio M, Teixeira L, Vargas F. Pleural fluid tumour markers in malignant pleural effusion with inconclusive cytologic results. Current Oncology. 2015; 22(5): e336.
28. Dehkordi FS, Valizadeh Y, Birgani TA, Dehkordi KG. Prevalence study of Brucella melitensis and Brucella abortus in cow's milk using dot enzyme linked immuno sorbent assay and duplex polymerase chain reaction. J Pure Appl Microbiol. 2014;8(2):1065-9.

Received: 30 February 2021
Accepted: 15 May 2021

RESEARCH / INVESTIGACIÓN

Tips for a reduction of false positives in manual RT-PCR diagnostics of SARS-CoV-2

Francisco J. Alvarez, Mariela Perez-Cardenas, Marco Gudiño, Markus P. Tellkamp
DOI. 10.21931/RB/2021.06.03.11

Abstract: RT-PCR is the standard gold technique for testing the presence of RNA of the coronavirus causing Severe Acute Respiratory Syndrome (SARS-CoV-2) due to its high specificity and sensitivity. Despite its general use and reliability, no lab in the world is immune to the generation of false positives. These errors cause a loss of confidence in the technique's power and damage the image of laboratories. More importantly, they can take a toll on tested individuals and have economic, psychological, and health-associated effects. Most false positives are caused during a manual operation inside the laboratory. However, not much has been published about the errors associated with particular laboratory techniques used to detect the virus since the beginning of the actual pandemic. This work precisely reflects on events that occur during manual RT-PCR diagnostics in a COVID-19 laboratory, providing tips for reducing false-positive results.

Key words: SARS-CoV-2, false positives, RNA extraction, RT-PCR.

Introduction

In COVID-19 diagnostics labs, most errors in reporting consist of false negatives due to the low viral load that escapes detection. Therefore, the sampling time is significant: a sample taken too early after the person has been infected may have too low a viral load to be detected[1]. Likewise, a sample taken after the patient has cleared the virus almost wholly would result in a very low viral titer. The skills of the doctor or nurse in charge of taking the samples from patients can also contribute to generating false negatives. In addition, the choice of transport medium where the sample is carried to the labs for analysis, whether the sample contains blood, and the temperature during storage and/or transportation can make a difference in the quality of the sample before its processing. False negatives are of great concern for public health management, but the impact of false positives has come to the fore recently due to the distress they can cause in the lives of patients and public health.

The RT-PCR (Reverse Transcriptase Polymerase Chain Reaction) is the standard gold technique for detecting the SARS-CoV-2 virus. It is routinely used for samples from diverse origins, such as nasopharyngeal and throat swabs, sputum, broncho-alveolar lavages[2], and anal swabs[3]. It can detect as few as 5 copies of the virus in a sample[4] and is, therefore, the technique of choice to reveal which individuals are contagious at any time of their infection period. They outcompete serological tests, which need a higher viral load to produce a positive result or indirectly measure the virus's presence in the organism. The RT-PCR has a sensitivity (ability to detect true positives) of 70% and a specificity (ability to report well true negatives) close to 100%[5,6]. Having such sensitivity, the technique can easily amplify contaminating virus particles that don't belong to the actual samples to be tested. Hence, RT-PCR can generate false positives with a significant likelihood. Although few studies report on rates of false positives for COVID-19, some estimates of false-positive rates suggest them to be in a range of about 0.3-4%[7-9]. For SARS-CoV and MERS-CoV, the rate oscillated between 0.3-6.9%[10].

False positives can also arise due to errors in reporting the results and uncertainties regarding the cycle-threshold (Ct) value used as a diagnostic criterium[11]. The former point can be addressed by judicious data entry; however, the latter poses a true challenge when Ct values are close to the cut-off. Here, the likelihood of a false positive or false negative is highest. For instance, if a Ct of 40 is chosen as the diagnostic criterium, does a Ct of 39.5 necessarily mean that 1) the true Ct is indeed below 40 and 2) is the patient still infectious?[11,12]

A false positive report on healthy people can have dramatic consequences, varied and challenging to quantify. A politician may be deprived of a critical meeting for the citizens he represents. A skilled celebrity may be deprived of a significant sports competition. Worse even, the economic distress caused to those belonging to low-income groups in the society is more significant, for they may have to stop working, may have dependents, and no savings. The stigma of being called positive and the fear of suffering complications can also be detrimental psychologically for many. Besides, healthy but wrongly diagnosed positive, people may be put at risk of real contagion when moved to areas in a hospital with infected patients or may suffer the delay of an essential medical procedure[10,13]. Unfortunately, due to the severity of the current pandemic, it is not feasible to perform confirmatory PCRs for every patient whose sample yielded a positive result. Instead, current guidelines by international and national public health agencies recommend evaluating every PCR result on a case by case basis in combination with the evaluation of local infection rates, clinical signs and symptoms, lung CT scans, and history of exposure[10]. The consequences for the labs that report false positives and negatives can also be dramatic. With their image damaged, contracts for private labs may be postponed, and potential customers' confidence can vanish. Public labs are also questioned when reports of false positives appear. However, false positives are unavoidable and cannot be eliminated in any laboratory. However, it should be possible to reduce them to a minimum to better comply with the targets of national regulatory agencies.

The standard laboratory workflow for COVID-19 testing goes in one direction and has multiple barriers to prevent cross-contamination. Laboratory technicians have routinely tested themselves for covid, for apparent reasons. Still, the laboratory is the primary source of false positives, mainly

[1] Yachay Tech University, School of Biological Sciences and Engineering, Hda. San José s/n y Proyecto Yachay, Urcuquí, Ecuador

Corresponding author: falvarez@yachaytech.edu.ec

cross-contamination due to human error[10]. In this review, we'll discuss working habits that reduce the occurrence of false-positive reports of coronavirus infection while navigating the manual processing of nasopharyngeal swabs in all phases of the workflow. The tips provided are based on personal experience of false positives while working in a COVID-19 test lab at Yachay Tech University, using typical kits and equipment.

Reduction of false positives in the RNA extraction area

The manual processing of samples during RNA extraction constitutes the highest source of false positives in the laboratory, but there is much room for improvement. The processing of samples in the RNA extraction area starts with setting the laminar flow hood under UV light for several minutes while the airflow stabilizes[14]. A small centrifuge should be located inside the hood, and it should be left open during UV irradiation to expose the rotor. The space under the hood should not be crowded to help the airflow exert its function and allow the UV light to reach most surfaces. If more than one batch of samples is going to be processed in the day, it is advisable to have rounds of UV irradiation in between batches. Next, parts and equipment to be used to process the samples are cleaned with 70% ethanol. Only filtered tips are used for the extraction and must be changed for every sampling step of the extraction process. Tube racks should be stable to avoid spills. Reagents should be aliquots of the original kit contents to minimize costs if contamination (reagent contamination is a significant source of false positives but easy to identify because most likely, all samples of the same batch would come out positive and with similar Ct values). Lab technicians must wear protective gear with very fit pairs of gloves, without folds on the surface of their fingertips. Once the site is clean, the lab technician starts preparing a master mix that ensures that all the samples get the same initial buffer solution. Fig. 1 shows the process of RNA extraction for a typical commercial kit, with few modifications of the original protocol. Similar steps apply to many other commercial kits. Double arrows A to C at the bottom indicate the times at which different contamination types can occur.

The master mix contains an extraction control that helps verify whether the extraction process has been optimal for every individual sample. As an example, this control can be the RNA of a cellular household gene such as actin. This will later appear as a specific curve in the PCR reaction since the primers for that gene will be included in the primer mix used for the PCR reaction. The signal generated during PCR amplification will appear in a different channel than that of the SARS-CoV-2 target gene of interest. The absence of the extraction control curve in all the samples of the batch in the PCR would indicate that it was probably not added to the master mix. If absent in only one or a few samples, it could indicate the presence of inhibitors of the PCR reaction such as ethanol, and the extraction of those particular samples should be repeated.

Once the master mix has been added to all the microcentrifuge tubes, it is time to place the nasopharyngeal swab samples inside the hood, which had been kept in a refrigerator upon arrival. Careless manipulation of swab samples can generate mix-ups leading to false positives. The manipulation of patient samples entails a high risk of contamination (arrow A, bottom of Fig. 1) that can then be passed down throughout the extraction process. Tubes should ideally be opened with a hand that does not hold the micropipette to avoid contaminating it. A brief vortex ensures a good mix for every sample and potentially generates aerosols that can contaminate the working area. That is why it is essential to work under the hood, with the airflow removing those aerosols. Aerosols can also adhere to the shaft of the micropipettes, especially when they are introduced deep into the patient's sample tubes or touch the swabs that usually come within. If that happens, the parts suspected of being contaminated should be wiped with 70% ethanol between pipetting samples. Once the micropipette tip is loaded with the sample, keeping it at an angle instead of vertically prevents dripping of the content for a sufficiently long time before adding it to the microcentrifuge tube. Also, it is common practice in molecular biology or microbiology labs to eject the residual volume of the tip with an extra push of the micropipette plunger. This, however, is an essential source of

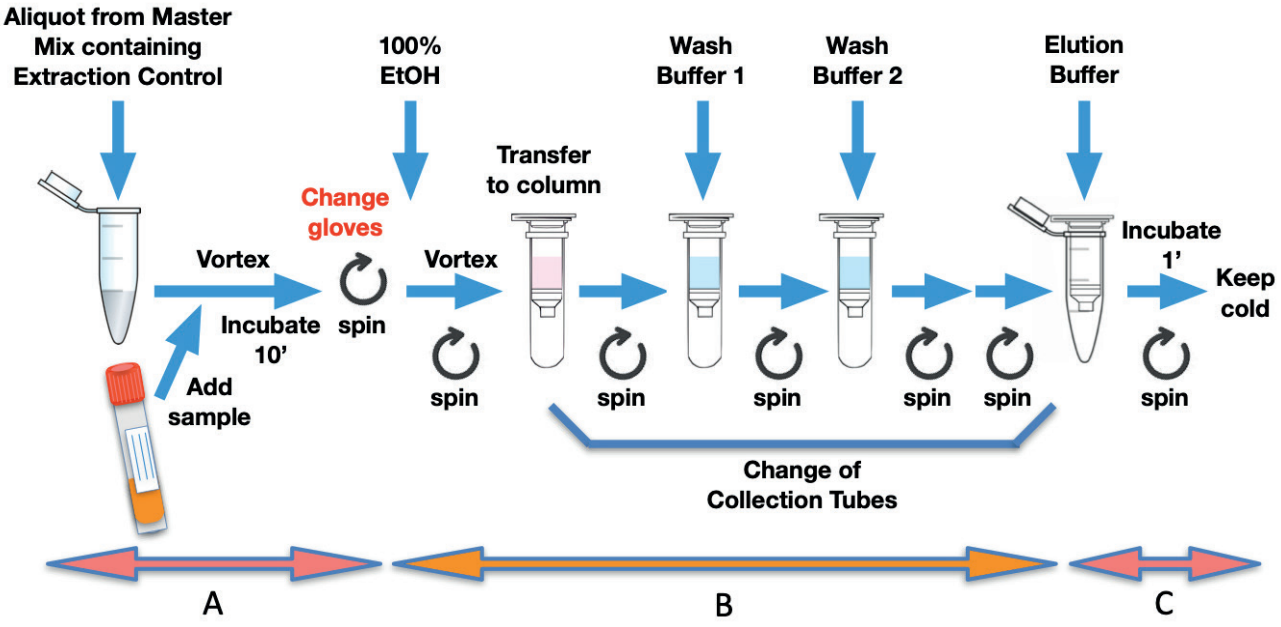

Figure 1. Diagram showing the steps for viral RNA isolation using a standard commercial kit (QIAamp® Viral RNA Mini Kit, Qiagen), with few modifications. Letters A-C at the bottom indicate different types of contamination for the different steps of sample processing mentioned in the text.

aerosols. Therefore, it is desirable to avoid ejecting that residual volume to avoid cross-contamination during the extraction of SARS-CoV-2 viral RNA.

The negative control of the extraction (NCE) must be the last microcentrifuge tube of every batch of samples to ensure that contamination is appropriately detected. Nuclease-free water is added to the tube instead of the viral sample. Being the last tube of the batch, the NCE will help identify cross-contamination events from aerosols of a positive sample of the same batch. In the PCR, the NCE should only yield the curve corresponding to the extraction control. In the case the NCE produced the curve corresponding to the SARS-CoV-2 gene being tested, the extraction of the whole batch should be repeated. Fig. 2A shows the fluorescence profile of the extraction control in the amplification plot of a positive sample.

Finally, many extraction kits require a few minutes to inactivate the virus. That time can be used to clean surfaces in contact with patient samples, tip boxes, micropipettes, and the microcentrifuge tubes' exterior. Once the samples have been inactivated in the first steps of the RNA extraction process, the risk of acquiring floating virus particles is significantly reduced, and many labs continue their work on the bench. However, the risk of cross-contamination among samples is higher on the bench than on the laminar flow hood. Hence, although not deemed necessary for the protection of the lab technician, a laminar flow hood helps avoid the generation of false positives among samples. During the intermediate steps of the extraction process, errors during pipetting and handling of samples and reagents account for additional cross-contamination risks (arrow B, bottom of Fig. 1). It is advisable always to assume that aerosols from positive samples are present in the air to increase the sense of alertness and carefulness during the handling of microcentrifuge tubes, buffer solutions, and micropipettes. When using the micropipette, the tips should not enter too deep into solutions because that facilitates the carryover of the solution and its posterior dripping. Very importantly, buffer solutions should be opened only when needed, keeping tubes closed in the meantime.

Most extraction kits require the use of small centrifuges for several steps. The centrifuges are challenging to clean from aerosols generated from positive samples during the manipulation of the tubes. A high risk of contamination occurs in the elution step (arrow C, bottom of Fig. 1) when a column is commonly placed inside an open microcentrifuge tube. Having it open, the lid of the microcentrifuge tube sometimes breaks during the final elution spin. Again, it is essential to use tightly fitting gloves when picking up the tubes and columns from the centrifuge. Centrifuges should be cleaned thoroughly after the processing of every batch of samples.

The use of automatized systems for RNA extraction improves the processing speed enormously and reduces the chances of cross-contamination. During manual feeding of patient samples to the robot in the laminar flow hood, errors can still happen at the initial step of the process. If possible, the operator should close all the wells that are not being used. To avoid pipetting errors, it is advised to mark during the loading process the wells of the plate where the sample has been already added. Once the work under the laminar flow hood has ended, it must be cleaned, and UV irradiated to inactivate any virus particles that could have escaped in aerosols during the extraction process[15]. Automatized systems also need to be UV irradiated after use.

Reduction of false positives in the pre-PCR area

The most common method for producing reliable test results involves the use of an RT-PCR thermocycler. The conversion of the extracted RNA into DNA is carried out by a retro transcriptase, while a DNA polymerase does further amplification of that DNA. Both enzymes can be part of the same mix (one-step RT-PCR) or separate reactions (two-step RT-PCR). The PCR mix must include primers and fluorescent probes for a SARS-CoV-2 gene and for the extraction RNA target gene that was added during viral RNA extraction as a control. These reagents are added in the pre-PCR area, space physically separated from the room in which the thermocycler is used. In the pre-PCR area, the lab technician will aliquot the PCR mix in the wells of PCR plates or tubes and then add the extracted RNA and controls.

There is absolutely no risk for the lab technicians in the pre-PCR area to be contaminated with active viruses. They can, however, bring contamination to the sample preparation area on her clothes. To avoid carrying over amplicons or viral RNA on their clothes, personnel who work in the pre-PCR area

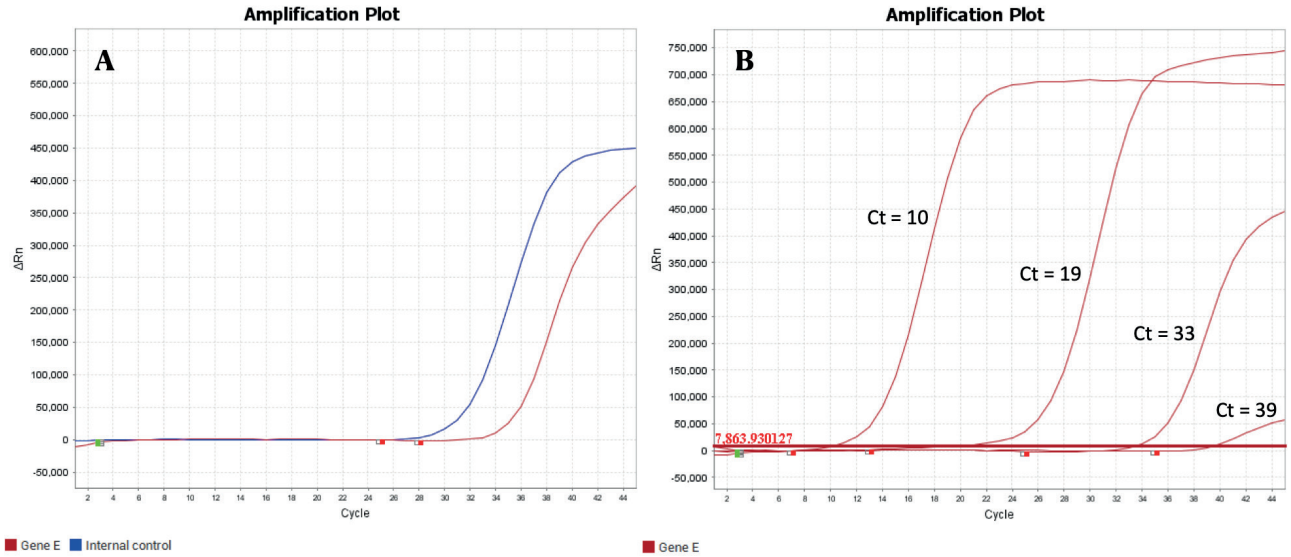

Figure 2. A) Amplification plot of a positive sample showing the extraction control (blue line) and the amplification of the SARS-CoV-2 gene (red line); B) Comparison of the amplification plots of two samples with low Ct (left) and two with high Ct (right). The horizontal line indicates the threshold of the PCR reaction.

must use a different lab coat and gloves than those used in other areas of the laboratory. Although in principle, the assembling of the PCR can take place on the bench, it is advisable to use a laminar flow hood for that purpose, similar to what was recommended for the extraction area, to prevent aerosols from positive RNA samples contaminating the wells of the PCR strips or plates. In Ecuador, a laminar flow hood is a mandatory requirement for this area. We must never forget how sensitive the PCR technique is and detect as few as 5 copies of viral cDNA[4]. Similar to what is done in the extraction area, the laminar flow hood must be irradiated for 10-20 minutes with UV light until the airflow stabilizes before assembling the PCR reaction.

Despite working under the laminar flow hood, we must assume that aerosols containing RNA from positive samples could still be present and cause false positives. Hence, a good piece of advice for the assembly of the PCR is to keep all the wells in the PCR strips or plates covered at all times and only lift the caps (strips) or optical film (plates) when a new sample must be added to the appropriate well. Keeping nearby a log of the position of the samples in the wells helps to prevent mistakes during sample loading. Again, to prevent the spread of aerosols, it is essential to use very fit gloves, without folds on the surfaces of the fingertips, to properly open and cap the tubes (strips) or hand the optical film (plates). The closing of the caps of PCR tubes may require applying great force, which can cause vibrations on the cold rack that supports the strips and make them move or fall off the rack. For that reason, it is good to write a small number or another type of code on top of each PCR strip that indicates the orientation and position of wells in the PCR to be run. Another suggestion to avoid aerosols is to not pipet the sample up and down to mix in with the PCR reagents in each tube. This common practice is not needed since the PCR strips or plates will be spun down in a centrifuge before taking them to the thermocycler. Combined with the high temperatures of the PCR process itself, the homogeneity of the reagent solution is assured.

The PCR reaction's assembly, a negative and one positive control, respectively, needs to be included. The negative control (Non-Template Control, NTC) contains the mix with the buffer, polymerase, and primers for the PCR reaction but nuclease-free water is added instead of extracted RNA. The control also lacks the extraction control added to the samples processed in the RNA extraction area. At the end of the PCR run, the NTC profile should be a flat line for all the channels. The positive control (PC) has the same content as the NTC, but instead of water, the same gene of the SARS-CoV-2 virus that the primers detect in the actual patient samples. The PC also lacks the extraction control added to the samples in the extraction process, and it also emits fluorescence in a different channel. Fig. 2A shows the fluorescence profile from a positive sample for SARS-CoV-2 at the end of the PCR run.

Both NTC and PC must be placed at the end of the assembly of the PCR reaction after all the other samples have been loaded. In this way, the NTC will serve the purpose of letting us know whether cross-contamination has taken place during the assembly process. If the NTC yields a positive signal for the gene of interest, the PCR should be repeated because either the master mix was contaminated or aerosols from a positive sample were spread during the assembly process to other samples. If possible, the negative controls from the RNA extraction step (NCEs) should not be added at the end to the PCR strips or plates to minimize their possible contamination with aerosols from positive samples during the assembly process. In this way, if the NCEs yield a positive signal for the viral gene of interest but the NTC produces a negative signal, we could be confident that the cross-contamination event has taken place during the RNA extraction steps and not in the pre-PCR area. If, on the other hand, one suspects contamination events taking place in the pre-PCR area, it is advisable to aliquot known negative samples or NTCs to the PCR plate and check afterward whether they yield a positive signal.

Although we focus mainly on the events that can generate false-positive results, there is also a chance of generating false negatives in the pre-PCR area. One way is to accidentally not pipetting up any liquid from the RNA sample. This can happen, for example, if there is an air bubble in the microcentrifuge tube and the tip of the micropipette just absorbs air instead of sample. That is why it is important not to lower the concentration during work on the bench and always look at the tips to make sure the liquid is absorbed and again check after centrifugation that every tube in the strip or plate has the same volume. Staying focused and being mindful of every movement of the hands above the wells in the strips or plate helps minimize the risk of contamination at every step of the process. Where available, the use of multichannel pipettes also greatly helps to speed up the PCR assembly process. However, they can also fail to acquire the desired volume in some of the channels and be a source of false negatives.

Reduction of false positives in the PCR area

An essential source of false positives that can originate in the PCR area is amplicon contamination. This occurs when the products of a previous PCR are accidentally released and migrate to other parts of the laboratory. The tubes with positive samples contain trillions of copies of the amplified genes that could easily contaminate future extraction processes and PCR assemblies. Even an initially slightly positive sample with a low viral load whose manipulation would not represent much risk during the extraction process can cause significant problems once the target genes have been exponentially multiplied[16]. To avoid this type of risk, PCR tubes or plates should be disposed of outside the PCR room at the end of the PCR run. Both the pre-PCR and PCR rooms must be physically separated and have independent air extraction systems. It is recommended not to cross from the PCR room to the extraction and pre-PCR rooms wearing the same protective clothing. Another possible source of false positives occurs when tube strips or plates are not adequately balanced during the centrifugation before the PCR run. This causes vibrations that can disperse the contents of the PCR tubes onto their walls, leading to underestimated readings by the thermocycler.

The best way to prevent amplicon contamination is the implementation of a regular cleaning protocol for all surfaces in the lab-based on 10% (w/v) sodium hypochlorite -a chemical amplicon oxidizer- followed by a rinse with 70% ethanol (to avoid the corrosive effect of the bleach on equipment)[17,18]. Commercial products abound that include diluted NaOH in their formulations. The use of UV irradiation in Class II biosafety cabinets[14] or portable UV lights can also be of great help. Inactivating enzymatic methods such as degradation by uracyl-N-glycosylase[19,20] can be included in the PCR reaction mix. On the other hand, inactivation protocols that require the opening of the PCR tubes after amplification are to be avoided.

The Ct (cycle threshold) is the cycle number when the fluorescence of the amplicons surpasses the threshold fluorescence during the PCR run. In our lab, based on the experience of other labs using the same diagnostics kits, a Ct value of 40 or earlier is interpreted as a positive result for COVID-19.

The Ct value also measures how many copies of the target gene were in the original sample. The smaller the Ct, the more viral copies the sample has. Fig. 2B shows the amplification plots of four samples, two of them with low Ct values indicating high titers of the target gene. A sample with Ct 10 contains thousands of more copies in origin than a sample of Ct 20. Extraction of samples with high viral titers constitutes a vital source of contamination for the subsequent samples in the batch due to the unintended release of aerosols[20]. One can never know beforehand which sample has a high viral titer; this is learned after the PCR. Automatic extraction reduces the risk of cross-contamination from high viral titer samples.

In the analysis post-PCR analysis, the lab personnel must decide in every case whether the sample is positive or negative, looking both at the Ct values and the curves. False positives can appear due to the presence of inviable viral particles in patients who are in the process of clearing the remains of the virus from their bodies. If the data look sound, the lab must report those results as positives and let the clinicians make the final decision based on the patients' medical history, local rates of COVID-19 infections, patient's signs and symptoms of the disease, or serological analysis[6,10,21].

When the signal of the SARS-CoV-2 gene in the PCR appears with a Ct value close to (above or below) 40 (like the sample with Ct 39 in Fig. 2B), a definite diagnosis should not yet be made by the lab processing the samples. Such a profile could result from contamination with aerosols of a close sample with a very low Ct value. The fastest solution is to repeat the extraction of that particular sample on the same day. Alternatively, one can request another sample of the same patient within 2-3 days: if the patient happened to be at the beginning of the infection process, she will appear positive in the second PCR, while a negative result would mean clearance of the virus at the end of the infection period. On average, the best time to get a sample that results in a lower chance of false-negative is eight days after infection or three days after the onset of symptoms[1].

All lab members in charge of the analysis post-PCR should be using precisely the same criteria. For that, an algorithm like the one in Fig. 3 can be devised and agreed upon. That way, based on the PCR results, any user can quickly troubleshoot unusual results, find the cause of false positives, and make amendments before reporting the results. Note that despite all the controls being correct at the bottom of Figure 3, one must still be wary of an unusual number of positive samples, especially if they appear grouped. In this case, we recommend that a subset of the samples that also includes negatives be subjected to another round of viral RNA extraction and PCR. As an internal quality control measure, a small fraction of the daily samples arriving at the lab can be randomly selected for retesting. The selection of samples should be made before knowing the results of the PCR test, allowing for the inclusion of both positive and negative samples.

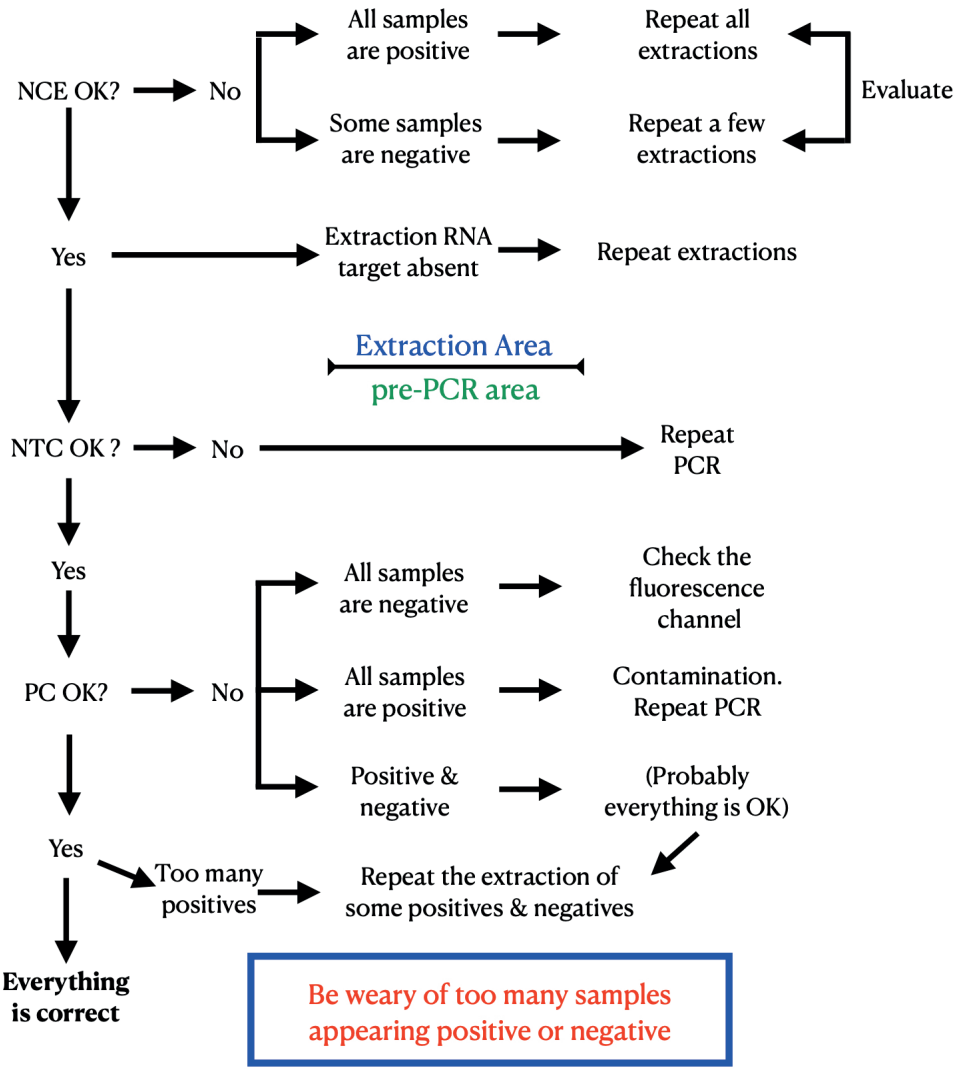

Figure 3. Algorithm post-PCR for the evaluation of the results. NCE, negative control of the extraction; NTC, negative control of the PCR; PC, positive control of the PCR.

Discussion

Having navigated through all the steps of manual sample processing in a laboratory of COVID-19 testing, one must not forget the importance of selecting the best personnel for the different tasks to be performed. Good leadership is necessary to be aware of the strengths and weaknesses of every person working in the lab and get the best out of everyone. False positives are mainly produced through unintentional errors during viral RNA extraction, the assembly of the PCR, and even data management. Hence, a tremendous amount of focus and manual dexterity is expected in laboratory workers to avoid pipetting errors. Maintaining focus is essential in the COVID-19 testing laboratory since many everyday tasks can be repetitive, and the operator may easily engage in detrimental mind-wandering behavior for brief periods of time[21]. At times the amount of COVID-19 samples arriving at the lab is too tremendous, and several shifts are required to process them. The schedules must be made to avoid too much strain on the workers, thus ensuring that the workers enjoy what they do and maintain a positive attitude in the lab. Remembering that sample numbers are numbers and represent people and their families can be another source of motivation.

It is common practice to interpret PCR results in the context of the pretest probability of the disease[13]. For example, a patient that appears positive for COVID-19 by PCR but has no symptoms or medical history of the disease has no antibodies and was not exposed to the disease could be considered a false positive. In our opinion, that is a call that doctors should make but not be the labs reporting their results. In case of doubt, it is always better to repeat the RNA extraction or PCR or ask for a new sample. Similarly, a positive result in someone already known to have contracted the disease weeks ago is still positive, although she may not be infectious anymore and is probably just shedding inviable virus particles[22].

Samples with low Ct values cause more trouble in the lab in terms of the production of false positives than those of high Ct values during the manual processing of samples. Although sampling introduces a great deal of variability in the first place, low Ct values reflect high titers of the SARS-CoV-2 gene. This seems associated with a high viral load in the original patient samples, for those with low Ct values are more culture-positive than those with high Ct values[23] and correlate with the risk of intubation and in-hospital mortality[12,24]. Hence, it could seem that reporting the Ct value would be very useful for physicians. However, the issue is up for debate nowadays, mainly due to the high Ct values between and within methods[11] and during sampling.

Conclusions

From our experience, it is virtually impossible to eliminate false positives in the COVID-19 diagnostics lab completely. Manual processing requires multiple manipulations of samples and reagents, which translates easily into events of contamination. Automatized systems can significantly reduce (but not eliminate) the appearance of false-positive results. Contamination from samples with very low Ct values is more likely to occur during the extraction process than during the assembly of the PCR. It is advisable to routinely repeat the extraction of positive samples from a batch in which very high viral titer samples were included, especially when too many positives appear clustered together. Also, as an internal quality control measure to gain confidence in their results, labs can temporarily keep a small fraction of their daily samples, chosen randomly, for retesting. With the comments of this article, we hope to contribute to a reduction in the rate of false positives in labs dedicated to similar tests elsewhere during the manual processing of COVID-19 samples.

Declarations

Funding: No funds, grants, or other support was received.

Conflicts of interest/Competing interests: Francisco Alvarez, Mariela Perez, Marco Gudiño, and Markus Tellkamp declare that they have no conflicts of interest.

Ethics approval: Not applicable.

Consent to participate: Not applicable.

Consent for publication: Not applicable.

Availability of data and material: Not applicable.

Code availability: Not applicable.

Authors' contributions: Francisco J. Alvarez wrote the manuscript and created the figures. Mariela Perez-Cardenas, Marco Gudiño-Gomezjurado and Markus P. Tellkamp edited the manuscript.

Acknowledgments

We want to thank GIZ (Deutsche Gesellschaft für Internationale Zusammenarbeit) for their support, providing equipment, detection kits, and reagents for the majority of tests at Yachay Tech University. We also want to thank the Prefecture of Imbabura, local governments, and enterprises for their help in adapting our university labs for COVID-19 testing.

We also want to acknowledge the rest of the team COVID at Yachay Tech University: Karla Miño, Abigail Montero, Daniela Navas-León, María Paula Romero, Carlos Pazmiño, Karen Sánchez and Alexandra Yépez.

Bibliographic references

1. Kucirka LM, Lauer SA, Laeyendecker O, Boon D, Lessler J (2020) Variation in False-Negative Rate of Reverse Transcriptase Polymerase Chain Reaction-Based SARS-CoV-2 Tests by Time Since Exposure. Ann Intern Med 173(4):262-267. https://doi.org/10.7326/M20-1495
2. Wang W, Xu Y, Gao R, Lu R, Han K, Wu G, Tan W (2020) Detection of SARS-CoV-2 in different types of clinical specimens. JAMA. https://doi.org/10.1001/jama.2020.3786
3. Kipkorir V, Cheruiyot I, Ngure B, Misiani M, Munguti J. Prolonged SARS-CoV-2 RNA detection in anal/rectal swabs and stool specimens in COVID-19 patients after negative conversion in nasopharyngeal RT-PCR test. J Med Virol. 2020 Nov;92(11):2328-2331. doi: 10.1002/jmv.26007. Epub 2020 2 August. PMID: 32401374; PMCID: PMC7272912.
4. Corman VM, Landt O, Kaiser M, Molenkamp R, Meijer A, Chu DKW, Bleicker T, Brünink S, Schneider J, Schmidt ML, Mulders DGJC, Haagmans B, van der Veer B, van den Brink S, Wijsman L, Goderski G, Romette JL, Ellis J, Zambon M, Peiris M, Goossens H, Reusken C, Koopmans MPG, Drosten C (2020) Detection of 2019 novel coronavirus (2019-nCoV) by real-time RT-PCR. Euro Surveill 25(3):2000045. https://doi.org/10.2807/1560-7917.ES.2020.25.3.2000045

5. Sethuraman N, Jeremiah SS, Ryo A (2020) Interpreting Diagnostic Tests for SARS-CoV-2. JAMA. 323(22):2249–2251. https://doi.org/10.1001/jama.2020.8259
6. Watson J, Whiting PF, Brush JE (2020) Interpreting a covid-19 test result. BMJ. 369:m1808. https://doi.org/10.1136/bmj.m1808
7. Albendín-Iglesias H, Mira-Bleda E, Roura-Piloto AE, Hernández-Torres A, Moral-Escudero E, Fuente-Mora C, Iborra-Bendicho A, Moreno Docón A, Galera Peñaranda C, García Vázquez E (2020) Usefulness of the epidemiological survey and RT-PCR test in pre-surgical patients for assessing the risk of COVID-19. J Hosp Inf 105(4):773-5. https://doi.org/10.1016/j.jhin.2020.06.009
8. Katz AP, Civantos FJ, Sargi Z, Leibowitz JM, Nicolli EA, Weed D, Moskovitz AE, Civantos AM, Andrews DM, Martinez O, Thomas GR (2020) False-positive reverse transcriptase polymerase chain reaction screening for SARS-CoV-2 in the setting of urgent head and neck surgery and otolaryngologic emergencies during the pandemic: Clinical implications. Head & Neck 42:1621-8. https://doi.org/10.1002/hed.26317
9. Cohen AN, Kessel B (2020) False positives in reverse transcription PCR testing for SARS-CoV-2. medRxiv preprint https://doi.org/10.1101/2020.04.26.20080911
10. Cohen AN, Kessel B, Milgroom MG (2020) Diagnosing SARS-CoV-2 infection: the danger of over-reliance on positive test results. medRxiv preprint https://doi.org/10.1101/2020.04.26.20080911
11. Rhoads D, Peaper DR, She RC, Nolte FS, Wojewoda CM, Anderson NW, Pritt BS (2020) College of American Pathologists (CAP) Microbiology Committee Perspective: Caution must be used in interpreting the Cycle Threshold (Ct) value. Clin Infect Dis. https://doi.org/10.1093/cid/ciaa1199
12. Magleby R, Westblade LF, Trzebucki A, Simon MS, Rajan M, Park J, Goyal P, Safford MM, Satlin MJ (2020) Impact of Severe Acute Respiratory Syndrome Coronavirus 2 Viral Load on Risk of Intubation and Mortality Among Hospitalized Patients With Coronavirus Disease 2019. Clinical Infectious Diseases. https://doi.org/10.1093/cid/ciaa851
13. Surkova E, Nikolayevskyy V, Drobniewski, F (2020) False-positive COVID-19 results: hidden problems and costs. The Lancet. https://doi.org/10.1016/S2213-2600(20)30453-7
14. Padua R, Parrado A, Larghero J, Chomienne C (1999) UV and clean air result in contamination-free PCR. Leukemia 13:1898–1899. https://doi.org/10.1038/sj.leu.2401579
15. Storm N, McKay LGA, Downs SN, Johnson RI, Birru D, de Samber M, Willaert W, Cennini G, Griffiths A (2020). Rapid and complete inactivation of SARS-CoV-2 by ultraviolet-C irradiation. Sci Rep 10, 22421. https://doi.org/10.1038/s41598-020-79600-8
16. Persing DH (1990) Polymerase chain reaction: trenches to benches. J Clin Microbiol 29:1281-1285
17. Hayatsu H, Pan S, Ukita T (1971) Reaction of sodium hypochlorite with nucleic acids and their constituents. Chem Pharm Bull (Tokyo). 19(10):2189-92. https://doi.org/10.1248/cpb.19.2189
18. Kampmann ML, Børsting C, Morling N (2017) Decrease DNA contamination in the laboratories. Forensic Science International: Genetics Supplement Series 6:e577-e578. https://doi.org/10.1016/j.fsigss.2017.09.223
19. Longo MC, Berninger MS, Hartley JL (1990) Use of uracil DNA glycosylase to control carry-over contamination in polymerase chain reactions. Gene 93(1):125-8. https://doi.org/10.1016/0378-1119(90)90145-h
20. Sefers S, Stratton CW, Tang YW (2013) Amplification Product Inactivation. In: Tang YW., Stratton C. (eds) Advanced Techniques in Diagnostic Microbiology. Springer, Boston, MA. https://doi.org/10.1007/978-1-4614-3970-7_26
21. McVay, J. C., & Kane, M. J. (2012). Drifting from slow to "d'oh!": Working memory capacity and mind wandering predict extreme reaction times and executive control errors. Journal of Experimental Psychology: Learning, Memory, and Cognition, 38(3), 525–549. doi:10.1037/a0025896
22. Wölfel R, Corman VM, Guggemos W, Seilmaier M, Zange S, Müller MA, Niemeyer D, Jones TC, Vollmar P, Rothe C, Hoelscher M, Bleicker T, Brünink S, Schneider J, Ehmann R, Zwirglmaier K, Drosten C, Wendtner C (2020) Virological assessment of hospitalized patients with COVID-2019. Nature. https://doi.org/10.1038/s41586-020-2196-x
23. Jaafar R, Aherfi S, Wurtz N, Grimaldier C, Van Hoang T, Colson P, Raoult D, La Scola B (2020) Correlation Between 3790 Quantitative Polymerase Chain Reaction–Positives Samples and Positive Cell Cultures, Including 1941 Severe Acute Respiratory Syndrome Coronavirus 2 Isolates. Clinical Infectious Diseases. https://doi.org/10.1093/cid/ciaa1491
24. Rao SN, Manissero D, Steele VR, Pareja J (2020) A Systematic Review of the Clinical Utility of Cycle Threshold Values in the Context of COVID-19. Infect Dis Ther. 9(3):573-586. https://doi.org/10.1007/s40121-020-00324-3. Erratum in: Infect Dis Ther. PMID: 32725536

Received: 10 February 2021
Accepted: 8 March 2021

RESEARCH / INVESTIGACIÓN

Comparative study between lumpy skin disease virus and sheep pox virus vaccines against recent field isolate of lumpy skin disease virus

Nermeen G Shafik[1], Heba A Khafagy[1], Amal AM[1], Ayatollah I Bassiuony[2], Farid Fouad Zaki[1], Christine A Mikhael[2] and Mohamed Samy Abousenna[1]

DOI. 10.21931/RB/2021.01.03.12

Abstract: Lumpy Skin Disease (LSD) is a vector born disease of cattle, caused by Lumpy Skin Disease Virus (LSDV), there is antigenic relationship between LSDV, Sheeppox virus (SPPV) and Goat pox virus GTPV within a genus Capripoxvirus, accordingly it can be used homologous or heterologous Capripoxvirus strains for vaccination of cattle against LSD. This study compare the efficacy of live attenuated Neethling LSDV vaccine and live attenuated Romanian SSPV Vaccine against recent circulating LSDV field isolate. The evaluation was done in calves as the main host of LSD, through using three different batches for each vaccine type. Experimental calf groups were vaccinated with vaccines batches, and after 21 days serum samples were collected for evaluation of humoral immune response by using SNT and commercial ELISA technique, then the vaccinated calves were challenged by virulent LSDV field isolate. The results of SNT for vaccinated calves by LSDV vaccines indicated mean neutralizing antibody titer 1.2, 1.6 and1.5 log10 for the batches 1, 2 and 3 respectively, while vaccinated calves by SPPV vaccines indicated 1.05, 1.05 and 1.5 log10 for the batches 1,2 and 3 respectively; the ELISA mean sample to positive (S/P) percentage for the vaccine batches 1, 2 and 3 of LSDV were 40, 45 and 42% respectively and for SPPV vaccine batches 1,2 and 3 were 35, 37 and 40 % respectively, the challenge test indicated mean difference titer for the groups of calves vaccinated with LSDV vaccine were 4.2, 4.5 and 3.8 log10 and for groups vaccinated with SPPV vaccine were 2.6, 2 and 2.65 log10 respectively, it was concluded that potential using of Neethling LSDV vaccine against LSD is superior for combating and prevention of the lumpy skin disease.

Key words: Lumpy Skin Disease Virus, Sheep Pox Virus, Challenge test, Serological test.

Introduction

The genus Capripoxvirus (CaPV) within the subfamily Chordopoxvirinae, family Poxiviridae contains three closely related viruses, namely Sheep pox (SPPV) and lumpy skin disease (LSD) which are diseases of sheep and cattle respectively in addition to Goat pox virus (GTPV) which causes goat pox disease. The Virus strains affecting sheep and cattle are totally host specific and this is reflecting in the different geographic distribution of lumpy skin disease[1]. All strains of *Capripoxvirus* are antigenically closely related and cross-react serologically[2], because of the antigenic homology among all strains, the probability to use a single vaccine strain like sheep pox virus to protect cattle and sheep[3]. Lumpy skin disease is a vector born disease transmitted by biting insects such as mosquitoes and biting flies, its clinical signs include persistent fever, wide spread skin nodules (lumps) and enlarged peripheral lymph nodes complications include but are not limited to sever emaciation and death, LSD also has pulmonary form especially in young calves with high mortality rate[4],The disease has highly economic impacts as it affects the milk production and the leather industry[5].

The disease's first appear ance was in Africa in 1929, reported from Zambia given the name 'Ngamiland Cattle Disease'. The disease continued to spread and resulted in a panzootic; the first appearance of the disease in Egypt was during two outbreaks in Suez and Ismalia governorates in 1989. In early 2006, a severe LSD outbreak struck foreign (imported from Ethiopia) and local cattle in different Egyptian governorates, causing enormous economic losses; the disease also reappeared in 2012 and 2013[6].

Controlling lumpy skin disease depends mainly on vaccination and vector control. Capripoxviruses are cross-reactive within the genus. Consequently, it is possible to protect cattle against LSD using strains of capripoxvirus derived from sheep or goats in the vaccine[7]. Live attenuated strains of capripoxvirus vaccines have been explicitly used for the control of LSD[8]. According to these, there are three types of vaccine used against lumpy skin disease, attenuated LSDV (Lumpy Skin Disease) vaccines which provide good protection in cattle, attenuated SPPV (Sheep pox virus) vaccines which have been used in cattle against LSDV in those regions where LSD and SPP are both present as it believed in providing partial protection against lumpy skin disease, and Attenuated Gorgan GTPV vaccine containing GTPV Gorgan strain, this vaccine has been used in those countries where GTP and LSD overlap[9,10]. However, it is recommended to carry out evaluation trials using the most susceptible breeds before introducing a vaccine strain for vaccination into the field.

In Egypt, the control of LSD was applied by vaccination of cattle with SPPV using a Romanian strain for long time which proved to partially tackle the LSD outbreaks with partial cross protection with some notices on its duration of immunity as recommendation for revaccination after 8 months[11], and recently live attenuated LSDV vaccines containing Neethling strain were introduced to be use in Egypt.

The humoral immune response of vaccinated cattle against LSD either by SPPV and LSD vaccines can be evaluated using virus neutralization test (VNT) and ELISA[1,4,12], in this study we compare the efficacy of live attenuated lumpy skin disease vaccine and live attenuated sheep pox vaccine against lumpy skin disease virus field isolate, using serological and challenge tests.

[1] Central Laboratory for Evaluation of Veterinary Biologics (CLEVB), Agricultural Research Center, Cairo, Egypt.
[2] Veterinary Serum and Vaccine Research Institute, Pox department, Agricultural Research Center, Cairo, Egypt.

Corresponding author: Mohamedsamy2020@hotmail.com

Materials and methods

Vaccines

a- Live attenuated Lumpy skin disease virus vaccine (Neethling strain).

Three batches (one imported and two local batches[AGO13]).

b- Live attenuated Sheep pox virus vaccine (Romanian strain).

Three local batches.

These vaccine batches were delivered to Central Laboratory for Evaluation of Veterinary Biologics (CLEVB), Abbassia-Cairo, and evaluated last year for sterility, safety, and potency.

Virus

Lumpy skin disease virus (LSDV):

- Animal Health Research Institute supplied virulent circulating field strain; the virus was isolated in 2018[13]. It was used for the challenge test for vaccinated calves.
- Tissue culture adapted strain, the virus was propagated on Madin-Darby bovine kidney (MDBK) cells with a titer $10^{5.5}$ $TCID_{50}$ as shown in Figure (1 & 2), it was used for the serum neutralization test.

Cells

The Reference Strain Bank Department supplied Madin-Darby bovine kidney (MDBK) cells in the Central Laboratory for Evaluation of Veterinary Biologics (CLEVB). It was used for the serum neutralization test.

Animals and vaccination

Twenty four susceptible mixed breed apparently clinically healthy calves 6-12 months old free from specific antibodies against LSD virus, were supplied by CLEVB, these calves were divided into eight groups, each group contain three calves, six groups of them were used for vaccination and the other two groups kept as positive control and negative control groups. The six vaccinated groups were divided as follow, three groups of them were vaccinated with field dose of the three batches of live attenuated lumpy skin disease vaccine (one group for each vaccine batch), and the other three groups were vaccinated with field dose of the three batches of live attenuated sheep pox virus vaccine (one group for each vaccine batch), the route of vaccination followed as instruction of manufacture. After 21 days post vaccination serum samples were collected from vaccinated and unvaccinated calves for serological tests (SNT and commercial ELISA).

Challenge of vaccinated calves

After 21 days from vaccination, the vaccinated groups and positive control (non vaccinated) group were challenged with lumpy skin disease virulent virus according to OIE[1], the animals were shaved at flank region then six log_{10} dilutions were prepared for inoculation, each dilution inoculated intradermally at four sites for each shaved part (0.1 ml per each inoculum). The challenged animals were kept under observation for seven days after challenge, after that the titer of the challenge virus was calculated for vaccinated and control animals through recording number of lesions per each dilution at inoculated sites (the lesion developed as inflammation and necrotizing fibrinoid cutaneous nodules), the difference in titer between control and vaccinated animals was calculated for each vaccine batch. The negative control was kept without vaccination or challenge.

Serum Neutralization Test (SNT)

It measures the humoral immune response against lumpy skin disease Virus for sera of vaccinated calves, it was applied according to the method described in OIE[1], the neutralizeng titer was calculated according to Reed and Muench[14]. The samples neutralizing antibody titer ≥ 1.10 is considered positive[15].

ELISA IDVIT KIT

ID screen® Capripox Double Antigen Multi-species, REF CPVDA-5A, LOT E83. was used to detect specific antibodies against capripoxvirus. The test was carried out according to the manufacturer's instructions insert. The results of each sample were calculated as aggregate to positive control ratio S/P[AGO20] percentage (S/P %) in (Formula 1). The samples less than 30% are considered negative, while samples higher than or equal to 30% are considered positive.

$$S/P \equiv \frac{test\ sample\ OD - negative\ control\ OD}{positive\ control\ OD - negative\ control\ OD} \times 100$$

Results

The mean titers of the live attenuated lumpy skin disease virus vaccine batches and the live attenuated sheep pox virus vaccine batches on tissue culture were recorded. The titer was expressed as log_{10} tissue culture infective $dose_{50}$ ($TCID_{50}$)/ dose, indicated the titers for the three live attenuated lumpy skin disease virus vaccine batches and the three live attenuated sheep pox virus vaccine batches, as shown in table No.1.

The humoral immune response against lumpy skin disease virus for the sera collected from vaccinated calves after 21 days post vaccination was determined by SNT and ELISA, the lumpy skin disease virus was adapted on MDBK cells for using in serum neutralization test, Figure 1 (A) showing normal MDBK cells and Figure 1 (B) showing cytopathic effect of lumpy skin disease virus on MDBK cells which represent by clustering, cell rounding and degeneration, the results of SNT for serum samples of calves vaccinated by live attenuated lumpy skin disease virus vaccines and live attenuated sheep pox virus vaccine indicated mean neutralizing antibody titer indicated as shown in table No. (2), while the results of ELISA test were calculated as S/P percentage, the mean percentage for the sera of vaccine batches of live attenuated lumpy skin disease virus vaccines and for live attenuated sheep pox virus vaccine batches recorded in table No.(3).

Vaccine potency in cattle; the challenge of vaccinated groups and positive control group by virulent lumpy skin disease virus was done, and after seven days, the difference in titer between vaccinated and positive control group was calculated for each group (reading the lesion in inoculated sites), the mean titer for the groups of calves vaccinated with live attenuated lumpy skin disease vaccine and for groups vaccinated with local and imported live attenuated sheep pox vaccines as shown in table No. 4.

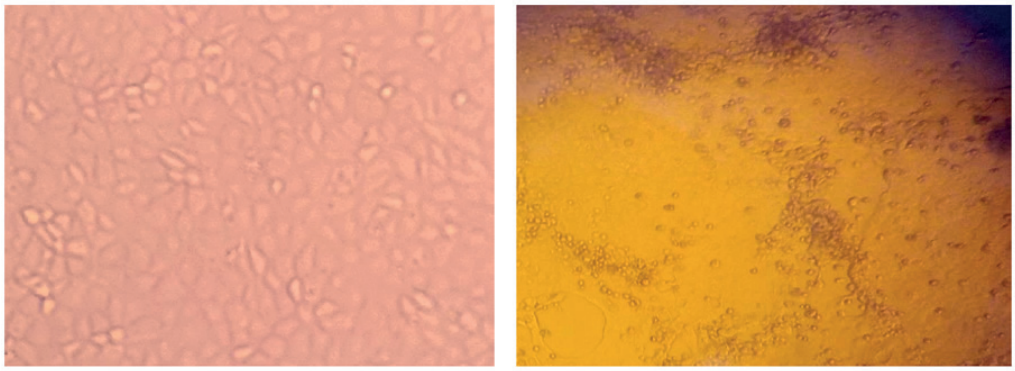

A- Normal MDBK cells

B- Cytopathic effect (CPE) of LSDV on MDBK cells

Figure 1. (A and B):Normal MDBK cells and adapted Lumpy skin disease effect on MDBK cell line

Batch Vaccine	Virus Vaccine titer on MDBK tissue culture(log_{10} $TCID_{50}$)	
	**LSDV vaccine	*SPPV vaccine
Batch 1	3.5	3.5
Batch 2	4.1	3.5
Batch 3	3.7	3.7

Table 1. The titer of virus vaccine batches on tissue culture.

*Recommended field dose titer of sheeppox virus vaccine in cattle[2] = 3.0 $TCID_{50}$

**Recommended dose of lumpy skin disease virus vaccine[2] = 3.5 $TCID_{50}$

Table 2. Evaluation of humoral immune response in the sera of vaccinated calves by using SNT.

Batch Vaccine	SNT Antibody titer(Log10)	
	LSDV vaccine	SPPV vaccine
Batch 1	*1.2	1.05
Batch 2	1.6	1.05
Batch 3	1.5	1.5

*Neutralization index ≥ 1.5 is considered positive.

Batch Vaccine	ELISA S/P%	
	LSDV vaccine	SPPV vaccine
Batch 1	*40	35
Batch 2	45	37
Batch 3	42	40

Table 3. Evaluation of humoral immune response in the sera of vaccinated calves using ELISA Kit against Capripox.

*S/P percentage (S/P %). ≥30% are considered positive.

Table 4. Challenge of vaccinated calves by LSDV.

Batch Vaccine	Challenge titer (log10)	
	LSDV vaccine	SPPV vaccine
Batch 1	*4.2	2.6
Batch 2	4.5	2
Batch 3	3.8	2.65

*difference in titre(>log_{10} 2.5 is taken as evidence of protection).

Discussion

In Egypt and Middle East live attenuated sheep pox vaccine is used to protect against LSD, although some researches recorded the effectiveness of this vaccine against LSD[16], there are some other recorded that it may offer incomplete protection against LSD[17,18,19,20], recently live attenuated LSD vaccine was introduced to be applied in Egypt, but we still need many researches to investigate and compare the efficacy and adverse reactions between live attenuated LSD virus vaccine and other Capripox virus vaccines.

In this study we compare the efficacy of live attenuated LSDV vaccine and live attenuated sheep pox virus vaccine against LSD in calves as the main host for the disease, using three batches for each vaccine type, showing the vaccines batches titer, evaluate humoral immune response of vaccinated calves (using SNT and ELISA) and challenge vaccinated calves by virulent strain of LSDV.

The titers of live attenuated LSDV vaccine batches per dose were satisfactory where the recommended field dose for LSDV in the vaccine is $\log_{10}$ 3.5 $TCID_{50}$ and minimum protective dose is $\log_{10}$ 2.0 $TCID_{50}$. The titers of live attenuated SPPV vaccine batches were also satisfactory where the recommended dose of sheep pox virus in the vaccine for cattle is $\log_{10}$ 3 $TCID_{50}$[1].

The SNT was carried out to detect the neutralizing antibody titer against LSDV for sera of vaccinated calves after 21 days post vaccination, the results for live attenuated LSDV vaccine batches indicated that all the three batches reached to positive neutralizing antibody titer ≥1.10[15], and the results for the live attenuated SPPV vaccine batches indicated that only the batch (3) reached positive neutralizing antibody titer ≥1.10 while the other two batches (1 and 2) didn't record the positive titer. These results reflect that live attenuated LSDV vaccine achieved best results in titer and number of batches reaching the positive titer, but we must put in consideration if the antibody is low it doesn't reveal that the animal isn't definitely protected as commented by OIE[1] which clarify the conflict in results of SNT and challenge test as this disease mainly depend on cellular immunity and the VNT or SNT only tests the positivity. Neutralization test is used for evaluation of humoral immune response for LSDV as recommended by OIE, as it was applied by other similar studies for evaluation of serum samples of cattle vaccinated by live attenuated SPPV vaccine against LSDV[16], also applied by Christine[21] who used it in evaluation calves vaccinated by Attenuated Sheep Pox and Inactivated Lumpy Skin Disease Vaccines against Lumpy Skin Disease, and used in evaluation of the cross-protection between Sheep pox and bovine Lumpy skin vaccines in vaccinated sheep[22].

ELISA kit against Capripox is also used in the evaluation of humoral immune response for the sera of vaccinated calves (this kit is not specific for LSDV only but it against genus capripox, on the other hand the SNT is specific against LSDV only), the results for live attenuated LSDV vaccines batches indicated positive results ≥30% (as mentioned in ELISA kit) for the three batches, also live attenuated SPPV vaccine indicated results ≥ 30% for the three batches, but we noticed that the percentages for live attenuated LSDV vaccines batches is higher than percentages of live attenuated SPPV vaccine batches. Although the neutralization test is the standard test for evaluation of humoral immune response for LSDV as recommended by OIE, there are other studies recommending to use commercial ELISA, commercial Capripox Double Antigen ELISA (ID.Vet) was used in evaluation of serological tests for detection of antibodies against LSDV and find strong correlation between VNT/MDBK and ELISA[23], also ELISA method and neutralization test were used for detection antibodies against LSDV[24].

Challenge test is used for testing potency of the vaccines, and it was carried out in vaccinated calves (as a main host for LSDV) by calculating the difference in titer (between control positive and vaccinated challenged calves in each group) of the inoculum (virulent LSDV) which developed specific lesion, the results for live attenuated LSDV vaccines batches indicated a protective titer for the three batches where the minimum protective result is >$\log_{10}$ 2.5 as recommended by OIE[1], and for the live attenuated SPPV vaccine batches indicated only first and third batches are protective with border titer limit but second batch didn't reach protective titer, and that indicated that live attenuated LSDV vaccine is more protective than live attenuated SPPV vaccine against LSDV. These results agreed with Hamdi[22] who used virulent LSDV in challenge of two groups of calves, one group vaccinated with Romanian SPPV vaccine and the other with Neethling LSDV vaccine and reported that Romanian SPPV vaccine provide partial protection against LSDV while Neethling LSDV vaccine provide fully protection against LSDV, also recombinant LSDV vaccine (LSD-Rift Valley Fever.mf vaccine) was used in two groups of calves, one group challenged by virulent LSDV and other group by virulent Rift Valley Fever Virus and recorded that tested vaccine is safe and protective for both diseases[25], and Neethling vaccine is reported significantly more effective than x10 RM65 Sheep Pox vaccine strain in preventing LSD morbidity[26].

Conclusions

It was believed that the wide cross protection within Capripoxvirus genus allows using of any Capripoxvirus isolate as an effective vaccine against LSDV, otherwise and avoiding this confirmation bias, it is clear from the relevant results that the potential using of Neethling LSDV vaccine against LSDV is superior for combating and prevention the Lumpy skin disease. Also it was be recommended to evaluate both homologous or heterologous virus strain vaccines against LSD in cattle, as it the main host of the lumpy skin disease.

Conflict of interest

The authors certify that they have no affiliations with or involvement in any organization or entity with any financial interest (such as honoraria; educational grants; participation in speakers' bureaus; membership, employment, consultancies, stock ownership, or other equity interest; and expert testimony or patent-licensing arrangements), or non-financial interest (such as personal or professional relationships, affiliations, knowledge or beliefs) in the subject matter or materials discussed in this manuscript.

Ethical approval

Institutional Animal Care and Use Committee at Central Laboratory for Evaluation of Veterinary Biologics acknowledge the research manuscript, and it has been reviewed under our research authority and is deemed compliance with bioethical standards in good faith.

Author Contributions

NGS designed experiments, AAM and MSA the experiments were performed HAK, AAM AIB, CAM, and MSA. Data

analysis was accomplished by NGS, FFZ, HAK, AAM, and MSA. AAM,AIB and MSA wrote the manuscript.

Funding

This study received no specific grant from any funding agency in the public, commercial, or not-for-profit sectors.

Data Availability

All data generated or analyzed during this study are included in this published article.

Bibliographic references

1. OIE. Organization for Animal Health. Lumpy Skin Disease. En: OIE. World Organization for Animal Health. Manual of diagnostic tests and vaccines for terrestrial animals (mammals, birds, bees). Paris:OIE; 2018. p. 1158-1171. Available from: https://www.oie.int/.
2. FAO (Food and Agriculture Organization of the United Nation) (2017): FAO Animal Production and Health (20), Lumpy Skin Disease, a field manual for veterinarians.
3. Norian RN, Afzal NA, Varshovi HR , and Azadmehr A. Comparative efficacy of two heterologous capripox vaccines to control lumpy skin disease in cattle, Bulgarian Journal of Veterinary Medicine, 2019, 22, No 2, 171–179.
4. Yasser FE, El-Tholoth M, Saher S, EL- Said A.A, Mohamed AS, and Younis EE. Investigation of lumpy Skin Disease virus infection in young calves from cows vaccinated with sheep poxvirus vaccine..(2015); 5thinternational conference of virology 112.
5. Tuppurainen ES, Stoltsz WH, Troskie M, Wallace DB, Oura CA, Mellor PS, Coetzer JA, Venter EH. A potential role for ixodid (hard) tick vectors in the transmission of lumpy skin disease virus in cattle. Transbound Emerg Dis. 2011 Apr;58(2):93-104. doi: 10.1111/j.1865-1682.2010.01184.x. Epub 201030 November0. PMID: 21114790.
6. FAO Regional Office for the near east (FAO-RNE) .Emergence of lumpy skin disease in the eastern Mediterranean Basincountries . VOL. 29. (2013) Rome. Available at: http://www.fao.org/3/a-i6155e.pdf.
7. Coakley W. & Captickp B. Protection of cattle against lumpy skin disease. Factors affecting small scale production of tissue culture propagated virus vaccine. Res. Vet. Sci.,(1961); 2, 369–371.
8. Brenner J, Haimovitz M, Oron E, Stram Y, Fridgut O, Bumbarov V, Kuznetzova L, Oved Z, Waserman A, Garazzi S, Perl S, Lahav D, Edery N. & Yadin H. Lumpy skin sease (LSD) in a large dairy herd in Israel. Isr. J. Vet. Med.(2006), 61, 73–77.
9. Tuppurainen ES, Pearson CR, Bachanek-Bankowska K, Knowles NJ, Amareen S, Frost L, Henstock MR, Lamien CE, Diallo A, Mertens PP. Characterization of sheep pox virus vaccine for cattle against lumpy skin disease virus. Antiviral Res. 2014 Sep;109(100):1-6. doi: 10.1016/j.antiviral.2014.06.009. Epub 201425 June5. PMID: 24973760; PMCID: PMC4149609.
10. Abutarbush, S.M. Lumpy Skin Disease (Knopvelsiekte, Pseudo-Urticaria, Neethling Virus Disease, Exanthema Nodularis Bovis). In: Bayry J (eds.) Emerging and Re-emerging Infectious Diseases of Livestock. Springer International Publishing, Gewerbestrasse 11, 6330 Cham, Switzerland, pp: 309-326. (2017).
11. Ayatollah IB, Christine AM and Amal A. Comparison between field and laboratory immune response of cattle vaccinated with sheep pox vaccine against lumpy skin disease. Egypt vet. Med. Assoc. Journal (2015):Vol 75, no (4):649-662.
12. Christine AM, Ibrahim MM, Manal A, Soad MS and Michael A. Comparative study on the efficacy of some capripox vaccines in protection against Lumpy Skin Disease. SCVMJ,(2014); XIX (2):177-189.
13. Hodhod A, Elgendy E, Abd El-Moniem MI and Ibrahim MS. ISOLATION AND MOLECULAR CHARACTERIZATION OF LUMPY SKIN DISEASE VIRUS IN EGYPT DURING 2017- 2018, ejpmr, (2020),7(1), 96-103.
14. Reed LJ and Muench H . A simple method of estimating fifty per cent endpoints. Am. J. Hyg.(1938). 27: 493-497.
15. Shaimaa El-gbily, Emad M. Al-Ebshahy, Heba A. AbdelHady, AboulSoud, E.A. and Samy A. Khalil. Evaluation of Humoral Immune Response Against Lumpy Skin Disease Virus in Cattle Vaccinated with Sheep Pox Virus Vaccine. AJVS. (2019).Vol. 61 (1): 128-132.
16. Ali AA, Esmat M, Attia H, Selim A and Abdelhamid YM. Clinical and pathological studies on lumpy skin disease in Egypt. Vet. Rec. (1990) 127, 549–550.
17. Omyma ME. Recent isolation and identification of lumpy skin disease virus from cattle in Egypt. Egypt J.Comp. Path and Clin. Path. (2008).21,(1): 139-147.
18. Brenner J, Bellaiche M, Gross E, Elad D, Oved Z, Haimovitz M, Wasserman A, Friedgut O, Stram Y, Bumbarov V, Yadin H. Appearance of skin lesions in cattle populations vaccinated against lumpy skin disease: statutory challenge. Vaccine. 2009 Mar;27(10):1500-1503. DOI: 10.1016/j.vaccine.2009.01.020.
19. Somasundaram MK. An outbreak of lumpy skin disease in a holstein dairy herd in Oman: a clinical report. Asian J. Anim. Vet. Adv.2011; 6, 851–859.
20. Christine AM, Ibrahim MM and Saad MA.. Efficacy of Alternative Vaccination with Attenuated Sheep Pox and Inactivated Lumpy Skin Disease Vaccines against Lumpy Skin Disease. SCVMJ,(2016) XXI (2), 125-142.
21. Hamdi J, Zahra B, Mohammed J, Zineb B, Khalid O T, Ouafaa FF and Mehdi E. Experimental evaluation of the cross-protection between Sheep pox and bovine Lumpy skin vaccines. J. Scientific Reports (2020) 10, Art. No.8888, P.1-9. https://doi.org/10.1038/s41598-020-65856-7.
22. Krešić N, Šimić I, Bedeković T and Acinger-Rogić Ž Lojkić I. Evaluation of Serological Tests for Detection of Antibodies against Lumpy Skin Disease Virus. J Clin Microbiol. 2020 Aug 24;58(9):e00348-20. doi: 10.1128/JCM.00348-20. PMID: 32434783; PMCID: PMC7448653.
23. Samojlović M, Polaček V, Gurjanov V, Lupulović D, Lazić G, Petrović T, and Lazić S. Detection of antibodies against Lumpy skin disease virus by Virus neutralization test and ELISA methods. Acta Veterinaria (2019) 69, 1, 47-60, Available From: Sciendo https://doi.org/10.2478/acve-2019-0003.
24. Wallace DB, Mather A, Kara PD, Naicker L, Mokoena NB, Pretorius A, Nefefe T, Thema N, Babiuk S. Protection of Cattle Elicited Using a Bivalent Lumpy Skin Disease Virus-Vectored Recombinant Rift Valley Fever Vaccine. Front Vet Sci. 202019 May9;7:256. doi: 10.3389/fvets.2020.00256. PMID: 32509806; PMCID: PMC7248559.
25. Ben-Gera J, Klement E, Khinich E, Stram Y, Shpigel NY. Comparison of the efficacy of Neethling lumpy skin disease virus and x10RM65 sheep-pox live attenuated vaccines for the prevention of lumpy skin disease - The results of a randomized controlled field study. Vaccine. 2015 Sep 11;33(38):4837-42. doi: 10.1016/j.vaccine.2015.07.071. Epub 20151 August1. PMID: 26238726.

Received: 1 May 2021
Accepted: 9 July 2021

RESEARCH / INVESTIGACIÓN

Differences between preterm infants receiving a dose for lung maturation and those receiving an additional rescue dose of corticosteroids

Sandra Liliana Medina Poma[1], Fabricio González-Andrade[1,2]
DOI. 10.21931/RB/2021.06.03.13

Abstract: It is unknown if there is a difference between preterm infants with a history of receiving pulmonary corticosteroid maturation or using an additional rescue dose of corticosteroid. This paper aims to determine the difference between infants with pulmonary maturation and infants who received a rescue dose of corticosteroid. We performed an epidemiological, observational, and cross-sectional study. We analyzed time of stay, the requirement of mechanical ventilation, the use of surfactant, and neurological complications in newborns hospitalized in Neonatology of the Isidro Ayora Gyneco-Obstetric Hospital, 2019. We analyzed 204 preterm infants of 28-37 weeks who received a total lung maturation dose versus an added rescue dose. We analyzed the information with the statistical program SPSS v 22.0. With rescue dose the stay time was 28.4±21.6 days (p <0.05), days of invasive mechanical ventilation 3±5.7 days (p <0.05); Surfactant use 33.3% (p>0.05). We found neurological complications in 6.9% of patients (p> 0.05). In group 2 with not rescue dose use, the stay time was 21.5±16.6 days (p<0.05), days of invasive mechanical ventilation 1.8 ± 4.1 days (p <0.05). Surfactant use was 24.5% (p>0.05), and neurological complications 2% (p> 0.05). Preterm males weighing <1000 g from 30 to 32 weeks, who used rescue doses of corticosteroids, showed an increase in intraventricular hemorrhage (13.7%), seizures (6.9%), and leukomalacia (13.7%), associated with the fact that in the group with rescue dose they are younger and had lower weight.

Key words: Preterm birth; Respiratory Distress Syndrome, Pulmonary surfactants; Obstetric Labor, Preterm; prenatal exposure to corticosteroids.

Introduction

A single cycle of prenatal corticosteroids administered to mothers with early preterm birth improves survival, reduces respiratory distress syndrome, necrotizing enterocolitis, and intraventricular hemorrhage. It was not associated with any significant adverse effects for the mother or the unborn child in the short term[1].

Prenatal corticosteroid therapy recommends all pregnancies with threatened preterm birth before 34 weeks of gestation, where the newborn's ongoing care is anticipated. Although there are limited data from randomized studies in infants with <25 weeks gestation, observational studies suggest that prenatal corticosteroids and other active treatment practices diminish pregnancy mortality to 22 weeks[2]. In pregnancies between 34 and 36 weeks of gestation, prenatal corticosteroids also reduce the risk of short-term respiratory morbidity but not mortality, and there is an increased risk of neonatal hypoglycemia[3].

Given the potential for long-term side effects, it does not recommend corticosteroids for women in spontaneous preterm labor after 34 weeks. When administered before elective cesarean section, up to 39 weeks, reduce the risk of admission to the Neonatal Intensive Care Unit (NICU)[4], although follow-up data on term newborns exposed to prenatal corticosteroids lack[5].

The optimal interval between treatment and delivery is more than 24 hours and less than seven days after the start of corticosteroid treatment; beyond 14 days, the optimal interval between treatment and delivery is more than 24 hours and less than seven days after the start of corticosteroid treatment; beyond 14 days, the benefits decrease. The beneficial effects of the first dose of prenatal corticosteroids begin in a few hours, advanced dilation should not be a reason to refrain from therapy, and the same can happen with magnesium sulfate (MgSO4)[6]. Corticosteroids should be repeated one to two weeks after the first course for women with the threat of preterm delivery. A repeated course reduces the risk of respiratory assistance. However, fetal growth decreases and repeated doses do not reduce mortality[7].

It observed no effect on neurosensory disability at follow-up, but data on possible longer-term adverse effects are lacking. The WHO recommends that a single corticosteroid cycle be used if preterm delivery does not occur within seven days after the initial course, and there is a high risk of preterm delivery within the next seven days. Repeated courses administered after 32 weeks of gestation do not improve the results[8].

Indeed corticosteroids are medications with several side effects, such as impaired fetal and placental growth, apoptosis in the brain, and increased infection, but when properly managed, they are safe. The use of corticosteroids should be reduced by an adequate assessment of the risk of preterm delivery and avoiding unnecessary early elective cesarean section, which is the obstetrician's decision to terminate the pregnancy in a woman with a history of previous cesarean section. In some cases, when an early cesarean section is needed, the establishment of fetal lung maturity may be better than administering corticosteroids to all women. There is little evidence that cesarean delivery of preterm newborns instead of allowing vaginal delivery improves outcomes[9]. However, the recommendations of the European consensus guidelines for the prevention of hyaline membrane disease in preterm infants are summarized below[10]: Mothers with a high risk of preterm birth <28-30 weeks gestation should transfer to perinatal centers with experience in the treatment of respiratory distress syndrome. A single cycle of prenatal corticosteroids should offer all women at risk of preterm birth when pregnancy is considered potentially viable until 34 weeks of gestation, ideally at least 24 hours before birth. A single cycle of corticos-

[1] Universidad San Francisco de Quito USFQ, Colegio Ciencias de la Salud, Quito, Ecuador.
[2] Universidad Central del Ecuador, Facultad de Ciencias Médicas, Unidad de Medicina Traslacional, Quito, Ecuador.

Corresponding author: fabriciogonzaleza@gmail.com

teroids might be administered in the threat of preterm delivery before 32 weeks of gestation at least 1 to 2 weeks before. Magnesium sulfate should be administered to women in imminent labor before 32 weeks of gestation[11].

In women with preterm birth symptoms, cervical length and fibronectin measures should consider avoiding unnecessary tocolytic medications and prenatal corticosteroids. Short-term use of tocolytic drugs should be considered in early pregnancies to complete a corticosteroid cycle and transfer the uterus to a specialized perinatal center[12].

There are differences between European and national clinical practice guidelines for newborn care with respiratory distress. They recommend administering prenatal corticosteroids, in risky pregnancies, between 26 and 34 weeks, for two days and, it is not advisable to use repeated doses if the birth has not occurred after one week of the last dose since It has not shown additional benefits. The medications recommended in these guidelines are Betamethasone[12,13]. Despite the available evidence on the use of pulmonary maturation with corticosteroids in the threat of preterm birth, there is a possibility of using the rescue dose if the birth has not occurred after seven days of the last dose.

It observed a 17% reduction in respiratory distress and 16% in severe complications associated with prematurity in infants with corticosteroid rescue doses. Besides, the use of rescue dose is associated with non-significant reductions in the newborn's weight and size, which disappear at discharge and have no implications in early childhood[14]. McKinlay *et al.*[2] studied the results for one or more repeated doses of corticosteroids in newborns and pregnant women, demonstrating that corticosteroids decrease the incidence of neonatal death, respiratory distress syndromes, intraventricular hemorrhage, necrotizing enterocolitis, and early sepsis. Prenatal corticosteroid therapy increases the effectiveness of postnatal surfactant therapy. Corticosteroids can induce the maturation of fetal organs and improve the transition to life after childbirth.

In another systematic review, Hutchinson and Hodgden[15] showed that women with preterm labor who received a cycle of corticosteroids and are still at risk of preterm delivery after seven days might benefit from a rescue dose. Studies discovered neonatal outcomes immediately after childbirth and no long-term risks in childhood by comparing growth, cardiovascular and endocrine functions. It also considered that maternal risks are not different between groups. Therefore, it considered additional corticosteroid therapy.

Indeed, preterm birth is the leading cause of death in children under five years of age worldwide; the rates of preterm infants' survival increase in high-income countries, neonates still die due to lack of attention or necessary supplies in middle and low-income countries. On the other hand, preterm birth remains a critical problem in infant mortality; it used antenatal corticosteroids to improve maternal and neonatal care quality. Despite this, inequality in survival rates is very different; in low-income countries, 32-week-old preterm newborns die due to lack of feasible and cost-effective care, while in high-income countries, almost all preterm neonates survive[16].

It is possible to say that after the administration of prenatal corticosteroids between weeks 24 and 34, the structural and biochemical changes that the pneumocytes both I and II undergo; fetal lung maturity accelerate by increasing the production of natural surfactant; These changes, in turn, improve lung mechanics, which results in a decrease in respiratory distress, use of exogenous corticosteroids.

Knowing that the maximum benefit is obtained after the first 24 hours post-administration until seven days, years ago, the administration of repeated treatments was used as a daily practice, a practice that has become deprecated due to the adverse effects that the affected products presented both in its growth as fetal development[14].

Prenatal corticosteroid administration is used to prevent respiratory distress syndrome in fetuses less than 34 weeks gestation in newborns who are still preterm newborns until birth and receive a rescue dose of corticosteroids. The purpose is to determine if there is a difference in the length of stay, the requirement for mechanical ventilation, the use of surfactant, and neurological complications[17] to establish a new pharmacological regimen.

This new approach to prenatal therapy in patients with risk factors for preterm birth may increase infant survival with light birth weight[18,19]. The aim is to contribute to the neonatal population to improve birth conditions and avoid neonatal complications that affect the individual, family, and society[20].

This work aims to determine the difference between infants with pulmonary maturation and those who received a rescue dose of corticosteroid concerning their time of stay, the requirement of mechanical ventilation, use of surfactant, and neurological complications in hospitalized newborns in the Neonatology Service of the Isidro Ayora Gyneco-Obstetric Hospital in 2019.

Methods

Study design

Epidemiological, observational, and cross-sectional study.

Context

Gyneco-Obstetric Hospital Isidro Ayora (HGOIA), in Quito, Ecuador. The analyzed period was from 14 November, 2019, to 29 January, 2020.

Sample size

204 newborns.

Participants

The population under study was from 28 to 37 weeks of gestational age, divided into two groups; one: received the total dose of corticosteroid lung maturation, and group two: complete lung maturation plus rescue dose.

Inclusion criteria

Preterm newborns with gestational age at birth from 28 to 37 of gestational age and history of prenatal corticosteroid use; that merited or not ventilatory support, use of surfactant, whether or not it presented neurological complications; of both sexes and any ethnic group. Group one received a total dose of fetal lung maturation with Betamethasone or Dexamethasone, while group two received a rescue dose before birth with Betamethasone or Dexamethasone.

Exclusion criteria

We excluded newborns referred to HGOIA with gestational age at birth over 37 and below 27 weeks of gestational age.

Elimination criteria

There were newborns with congenital malformations incompatible with life who died during the study.

Variables

It developed a sheet with socio-demographic characteristics: sex, ethnicity, gestational age, classification of prematurity, birth weight. Regarding prenatal factors: week in which lung maturation was administered. Postnatal factors were the use of mechanical ventilation, surfactant use, number of surfactant doses, trans fontanel ultrasound, neurological complications, seizures, days of mechanical ventilation, and days of hospitalization. The diagnosis at admission and discharge: the degree of prematurity, birth weight, size for gestational age, respiratory pathology, neurological, infectious, metabolic, hematological, cardiac, and hemodynamic pathology.

Sources, data, and measurements

From the beginning of the study, it revised the medical records of preterm patients admitted to HGOIA to identify the necessary data for analysis and interpretation. It is essential to mention that gynecologists did not influence the therapeutic decision regarding preterm deliveries concerning prenatal corticosteroid therapy. We identified a pregnant mother who received pulmonary maturation and a rescue dose of corticosteroid before week 37 of gestation for the preterm newborn's follow-up during his hospital stay.

Biases avoidance

It collected information from complete medical records and by the same person consistently.

Statistical methods

The information obtained was stored in an Excel database and then analyzed with the SPSS® software version 22.0, licensed: 4-2E097 I. We used descriptive statistics: frequencies, percentages, average, standard deviation, and inferential: Chi-square test, a p-value less than 0.05, which was accepted as statistical significance. We performed a multivariate analysis.

Ethical criteria

This research was approved by the Research Ethics Committee on Human Beings (CEISH) of the San Francisco University of Quito. It was dated 14 November of 2019, and coded with the number P2019-155TPG.

Results

Table 1 shows that, for both study groups, the variables that reached statistical significance using corticosteroid rescue doses were gestational age and the degree of prematurity ($p < 0.05$). There was no statistical significance between sex, ethnicity, or birth weight using rescue doses of corticosteroids ($p > 0.05$). See table 1. It included 204 preterm patients in this research, is divided into two patient groups, according to the

Socio-demographic characteristics	Rescue dose lung maturation (n; %)[1]		X^2	$p<0,05$
	Yes	No		
Sex			0,729	0,393
Male	57 (55,9)	63 (61,8)		
Female	45 (44,1)	39 (38,2)		
Ethnicity			5,247	0,263
Afro-Ecuadorian	3 (2,9)	1 (1,0)		
Native American	0 (0,0)	2 (2,0)		
Mestizo	97 (95,1)	94 (92,2)		
Caucasian	2 (2,0)	3 (2,9)		
Gestational Age (weeks)			15,243	<0,001
< 30	12 (11,8)	0 (0,0)		
30,1-33,6	50 (49,0)	45 (44,1)		
34 - 36,6	40 (39,2)	57 (55,9)		
Prematurity classification			11,67	0,003
Very preterm	32 (31,4)	12 (11,8)		
Moderate	28 (27,5)	34 (33,3)		
Late	42 (41,2)	56 (54,9)		
Birth weight (g)				
Mean±DE	1571± 362	1833 ± 431	170,0	0,094
Min-MAX	890-2340	855-2835		
Total	102 (100,0)	102 (100,0)		

Source: Medical records, Isidro Ayora Gyneco-Obstetric Hospital
Prepared by: authors (2020).

Table 1. Distribution of socio-demographic characteristics according to the rescue dose of pulmonary maturation. Preterm newborns, Isidro Ayora Gyneco-Obstetric Hospital, 2019.

use of a rescue dose of lung maturation, and it split each group of 102 patients.

Table 2 shows that there were significant differences between the time when lung maturation in both groups (p <0.001); it was administered later among patients who did not receive rescue dose (31.3 ± 2.1 weeks), compared to the group in which rescue dose was administered (30.5 ± 2.9 weeks). There was also statistical significance between mechanical ventilation and hospitalization days in both study groups (p <0.05). There was no statistical significance between mechanical ventilation modality, surfactant use, surfactant dose number, trans fontanelar ultrasound, neurological complications, seizures, or days of mechanical ventilation in both study groups (p> 0.05).

Table 3 shows the time of admission; there was statistical significance for the association between the use of rescue doses of corticosteroids with the degree of prematurity and the newborn's size (p <0.05). There was no statistical significance for the association between birth weights, the presence of respiratory, neurological, infectious, metabolic, hematological, or renal pathologies using rescue doses of corticosteroids (p> 0.05).

Table 4 shows that, at the time of discharge, there was a

Prenatal	Rescue dose lung maturation (n; %)[1]		X^2	$p<0,05$
	Yes	No		
Week in which lung maturation was administered				
Mean ± SD	30,5 ± 2,9	31,3 ± 2,1	50,94	<0,001
Min-MAX	25-35,4	25-35		
Postnatal				
Mechanic ventilation			4,738	0,094
No	39 (38,2)	41 (40,2)		
Non-invasive	20 (19,6)	31 (30,4)		
Invasive + non-invasive	43 (42,2)	30 (29,4)		
Use of pulmonary surfactant			1,932	0,165
Yes	34 (33,3)	25 (24,5)		
No	68 (66,7)	77 (75,5)		
Number of surfactant dose			5,152	0,076
A dose	23 (22,5)	22 (21,6)		
> 1 dose	11 (10,8)	3 (2,9)		
Not use surfactant	68 (66,7)	77 (75,5)		
Ecografía transfontanelar			9,499	0,147
No	29 (28,4)	32 (31,4)		
Intraventricular hemorrhage	14 (13,7)	11 (10,8)		
Leukomalacia	14 (13,7)	5 (4,9)		
Choroid cyst	7 (6,9)	4 (3,9)		
Hydrocephalus	0 (0,0)	3 (2,9)		
Normal	38 (37,3)	47 (46,1)		
Neurological complications			2,906	0,085
Yes	7 (6,9)	2 (2,0)		
No	95 (93,1)	100 (98,0)		
Seizures				
Yes	7 (6,9)	2 (2,0)	2,906	0,085
No	95 (93,1)	100 (98,0)		
Days of Invasive Mechanical Ventilation			29,9	0,023
Mean ± DE	3 ± 5,7	1,8 ± 4,1		
Min-MAX	0-30	0-26		
Days of Non-invasive Mechanical Ventilation			17,00	0,523
Mean ± DE	3,5 ± 4,5	2,5 ± 3,6		
Min-MAX	0-22	0-17		
Hospitalization days			67,6	0,015
Mean ± DE	28,4 ± 21,6	21,5 ± 16,6		
Min-MAX	4-104	3-85		
Total	102 (100,0)	102 (100,0)		

Source: Medical records, Isidro Ayora Gyneco-Obstetric Hospital
Prepared by: authors (2020).

Table 2. Distribution of prenatal and postnatal history according to the rescue dose of pulmonary maturation. Preterm newborns, Isidro Ayora Gyneco-Obstetric Hospital, 2019.

Diagnosis at admission	Rescue dose lung maturation (n; %)[1]		X^2	$p<0.05$
	Yes	No		
Recién nacido según prematuridad			9,522	0,023
RNpT (mp)	14 (13,7)	3 (2,9)		
RNpT (m)	53 (52,0)	52 (51,0)		
RNpT (t)	35 (34,3)	47 (46,1)		
Newborn according to prematurity			2,974	0,226
Adequate weight	5 (4,9)	10 (9,8)		
Low weight	92 (90,2)	90 (88,2)		
Very low weight	5 (4,9)	2 (2,0)		
Newborn according to size			9,202	0,002
Small for gestational age	36 (35,3)	17 (16,7)		
Suitable for gestational age	66 (64,7)	85 (83,3)		
Respiratory pathology			4,053	0,542
Respiratory distress syndrome	54 (52,9)	58 (56,9)		
Hyaline Membrane Disease	23 (22,5)	14 (13,7)		
Adaptive syndrome	2 (2,0)	2 (2,0)		
Transient tachypnea of the newborn	5 (4,9)	4 (3,9)		
Several	0 (0,0)	1 (1,0)		
Neurological pathology			4,223	0,238
Initial depression	5 (4,9)	6 (5,9)		
Prenatal asphyxia	0 (0,0)	1 (1,0)		
Malformations of the neural tube	0 (0,0)	3 (2,9)		
Infectious Pathology			5,552	0,475
RPM sepsis risk	10 (9,8)	10 (9,8)		
Risk of sepsis due to chorioamnionitis	4 (3,9)	2 (2,0)		
Risk of sepsis due to septic delivery	4 (3,9)	1 (1,0)		
Risk of sepsis due to urinary tract infection or bacterial vaginosis	22 (21,6)	16 (15,7)		
Perinatal exposed	0 (0,0)	1 (1,0)		
TORCH exposed	3 (2,9)	2 (2,0)		
Metabolic pathology			4,601	0,203
Hypoglycemia	7 (6,9)	4 (3,9)		
Asymmetric RCIU	10 (9,8)	4 (3,9)		
Symmetric RCIU	3 (2,9)	6 (5,9)		
Hematological pathology			5,021	0,285
Jaundice of prematurity	0 (0,0)	2 (2,0)		
Multifactorial jaundice	2 (2,0)	0 (0,0)		
ABO incompatibility	3 (2,9)	3 (2,9)		
Polycythemia	3 (2,9)	1 (1,0)		
Renal pathology				…
No	102 (100,0)	102 (100,0)		
Total	102 (100,0)	102 (100,0)		

Source: Medical records, Isidro Ayora Gyneco-Obstetric Hospital
Prepared by: authors (2020).
RNpT (mp): very preterm newborn; RNpT (m): moderate preterm newborn; RNpT (t): late preterm newborn; RPM: the preterm rupture of membranes; RCIU: intrauterine growth retardation.

Table 3. According to rescue dose of pulmonary maturation in preterm infants, distribution of diagnosis at admission, Isidro Ayora Gyneco-Obstetric Hospital, 2019.

Diagnosis at discharge	Rescue dose lung maturation (n; %)[1]		X^2	$p<0,05$
	Sí	No		
Newborn according to prematurity			6,862	0,032
RNpT (mp)	12 (11,8)	3 (2,9)		
RNpT (m)	53 (52,0)	51 (50,0)		
RNpT (t)	37 (36,3)	48 (47,1)		
Newborn according to prematurity			1,332	0,514
Adequate weight	2 (2,0)	2 (2,0)		
Low weight	95 (93,1)	98 (96,1)		
Very low weight	5 (4,9)	2 (2,0)		
Newborn according to size			14,87	<0,001
Small for gestational age	38 (37,3)	14 (13,7)		
Suitable for gestational age	64 (62,7)	88 (86,3)		
Respiratory pathology			14,23	0,162
Respiratory distress syndrome	18 (17,6)	26 (25,5)		
Hyaline Membrane Disease	39 (38,2)	30 (29,4)		
Adaptive syndrome	0 (0,0)	2 (2,0)		
Taquipnea transitoria del recién nacido	7 (6,9)	10 (9,8)		
Displasia broncopulmonar	2 (2,0)	0 (0,0)		
Transient tachypnea of the newborn	12 (11,8)	6 (5,9)		
Several	3 (2,9)	5 (4,9)		
Neurological pathology			3,81	0,283
Initial depression	5 (4,9)	9 (8,8)		
Seizures	5 (4,9)	1 (1,0)		
Malformations of the neural tube	2 (2,0)	2 (2,0)		
Infectious Pathology			16,46	0,05
Risk of sepsis due to preterm rupture of ovular membranes	5 (4,9)	5 (4,9)		
Risk of sepsis due to chorioamnionitis	0 (0,0)	2 (2,0)		
Risk of sepsis due to septic delivery	2 (2,0)	0 (0,0)		
Risk of sepsis due to urinary tract infection or bacterial vaginosis	7 (6,9)	4 (3,9)		
Perinatal exposed	0 (0,0)	1 (1,0)		
TORCH exposed	3 (2,9)	0 (0,0)		
Septic shock	8 (7,8)	2 (2,0)		
Early sepsis	33 (32,4)	27 (26,5)		
Late sepsis	3 (2,9)	2 (2,0)		
Metabolic pathology			5,342	0,254
Hypoglycemia	7 (6,9)	4 (3,9)		
Asymmetric RCIU	16 (15,7)	8 (7,8)		
Symmetric RCIU	7 (6,9)	6 (5,9)		
Hematological pathology			5,77	0,450
Jaundice of prematurity	17 (16,4)	14 (13,7)		
Multifactorial jaundice	34 (33,3)	24 (23,5)		
ABO incompatibility	10 (9,8)	10 (9,8)		
Anemia	12 (11,8)	12 (11,8)		
Several	0 (0,0)	2 (2,0)		
Cardiac and hemodynamic pathology			6,159	0,188
Persistence of the ductus arteriosus	2 (2,0)	7 (6,9)		
Inter earphone communication	2 (2,0)	1 (1,0)		
Cardiogenic shock	2 (2,0)	0 (0,0)		
Patent Oval Trench	0 (0,0)	1 (1,0)		
Total	102 (100,0)	102 (100,0)		

Source: Medical records, Isidro Ayora Gyneco-Obstetric Hospital
Prepared by: authors (2020).

Table 4. According to the rescue dose of pulmonary maturation in preterm infants, the distribution of diagnosis at discharge is determined by Isidro Ayora Gyneco-Obstetric Hospital, 2019.

statistically significant association between the degree of prematurity, the size of newborns, and the presence of infectious diseases, using rescue doses of corticosteroids (p <0.05). There was no statistical significance between birth weights, respiratory, neurological, metabolic, hematological, cardiovascular, or renal pathologies, using rescue doses of corticosteroids at discharge (p> 0.05). See table 4.

Table 5 shows the model summary. We used for the multivariate analysis a binomial logistic regression model. The variables that obtained statistical significance were included in the bivariate analysis. A 50% probability of success was obtained with this model, which is very low, and a Negelkerke statistic = 28.4%. The goodness of fit test of Hosmer and Lemeshow obtained statistical significance (p <0.05), thereby increasing the probability of prediction to 71.1%. The only variable associated with corticosteroid rescue doses was the newborn size (p<0.05).

	B	Standard error	Wald	gl	Sig.	Exp(B)
Small for gestational age	1,181	0,411	8,241	1	0,004	0,307

Source: Medical records, Isidro Ayora Gyneco-Obstetric Hospital
Prepared by: authors (2020).

Table 5. Multivariate análisis.

Discussion

We analyzed the behavior of two groups of infants with prematurity. In the first group, we included those who had received rescue doses of corticosteroids. In the second group, newborns who had not received this rescue dose, applying a new dose of corticosteroids when birth did not occur after seven days of completing the pulmonary maturation scheme.

In both study groups, male sex predominated, which accounted for 55.9% of cases. This factor explains in male fetuses an increased risk of prematurity, low birth weight, probability of complications, and death. This variable explains fetal testosterone's action on the pituitary hypothalamus axis, with an adverse feedback action, which affects the secretion hormones that prolong pregnancy. It knows that fetal sex influences the risk of adverse outcomes in response to prenatal corticosteroid therapy. It states that the chromosomal differences in both sexes' placenta are essential in determining fetal responses to prenatal noxas and prematurity. Female preterm infants respond more effectively to prenatal betamethasone exposure than their male counterparts, with lower respiratory distress syndrome rates, by the action of female hormones.

On the other hand, gestational age was statistically significantly related to corticosteroid rescue doses (30.1-33.6 weeks: 49%), so in the group of patients in the corticosteroid rescue dose was used, the most frequent gestational age was 30.1 to 33.6 weeks. This variable explains that lung immaturity in these neonates is higher due to the respiratory system's formation not completed. The few alveoli that exist do not produce pulmonary surfactant in sufficient quantity and quality. Therefore, the risk increases bronchopulmonary dysplasia and respiratory distress. Besides, since these are newborns in whom the risk was identified early, they were given lung maturation more than seven days before birth occurred.

On the other hand, the patients' degree of prematurity was also significantly associated with the rescue dose of corticosteroids. In this group, late preterm patients (41.2%) predominated, and, at the time of admission, there was a higher percentage than was classified as moderate preterm, with statistically significant differences (p <0.05) indicating that it was administered early lung maturation. For this reason, the dose of corticosteroids was repeating, but it could also be patients with significant respiratory dysfunction or with a high risk of complications such as bronchopulmonary dysplasia. Also, it accepts that preterm infants' respiratory complications decrease as gestational age increases, and the survival benefits of using additional doses of corticosteroids after 33 weeks have been discussed. However, we reported that yes, It is beneficial due to adaptive syndrome in late preterm infants.

Another finding was that the birth weight was lower in infants who received rescue doses of corticosteroids [1571±362 g], the minimum weight was 890 g, and the maximum weight was 2340 g; however, not was statistically significant. The criteria for using the rescue dose of corticosteroids are based on their administration when labor has not occurred within seven days after the first dose of corticosteroids. There is sufficient evidence to conclude that, after this period, lung maturation benefits increase the risk of perinatal death and maternal infections.

On the other hand, the size of the infants was significantly different in both study groups. 35.3% of those who received the rescue dose were classified as small for gestational age, significantly higher than the other group (16.7%). The impact of corticosteroids on fetal growth has been explained by inhibiting fetal growth and DNA replication due to cortisol, accompanied by lower birth weight and possible intrauterine growth restrictions. This factor also manifests itself in smaller head circumference and skull volume; therefore, it suggested the careful use of exogenous corticosteroids in fetuses with stress and restricted growth.

The gestational age at which lung maturation in the group where rescue dose was used was significantly lower than the other study group [□: 30.5 ± 2.9]. Besides, there is evidence that corticosteroids are beneficial after 26 weeks of gestation in reduced neonatal morbidity, including intraventricular hemorrhage. This variable explains because, when administered before birth, a binding occurs to the transporter proteins, such as the corticoid transport globulin (CTG) of the pregnant woman and the fetus, which favors the action on the respiratory system, which consists of increase the levels of surfactant and its action, lung compliance, clearance of intrapulmonary fluids, as well as reduce the permeability of blood vessels.

The postnatal history found that the use of mechanical ventilation in the invasive and non-invasive modality was superior among infants who had received the rescue dose of corticosteroids, although without statistical significance (p> 0.05). Similarly, the days of invasive mechanical ventilation were significantly longer in this study group [3±5.7 days] (p<0.05). In very preterm or moderately preterm newborns, the degree

of the respiratory system's immaturity and the surfactant deficit was higher than in other newborns. Sphingomyelin, another component of the surfactant, has a constant production throughout pregnancy, but other components such as lecithin and phosphatidylglycerol begin to occur after 25 weeks would explain its deficit in the very preterm.

The use of surfactants among infants with corticosteroid rescue doses was higher and the other newborns. However, without statistical significance (p>0.05), which shows that offering another dose of corticosteroids, Prenatal, did not have an important influence on preventing hyaline membrane disease, which is the consequence of lung immaturity the absence of pulmonary surfactant. This factor complements the lack of usefulness of the rescue dose of corticosteroids in preventing respiratory complications, which in these cases depends more on the degree of prematurity and lung immaturity than on the pulmonary maturation scheme offered. It was also more frequent in patients with corticosteroid rescue than additional doses of surfactant (10.8%) compared to the group without corticosteroid rescue, indicating no improvement in respiratory distress in patients' first six hours surfactant administered.

On the other hand, when analyzing the trans fontanel ultrasound and corticosteroid rescue dose results, it was obtained that intraventricular hemorrhage (13.7%), leukomalacia, and choroidal cysts were more frequent in neonates with a rescue dose of corticosteroids, although it was not statistically significant. The effect of corticosteroids on preterm infants' central nervous system is substantial, with intraventricular hemorrhage complications. Indeed, an increase in central venous pressure, which usually occurs during labor, and when respiratory complications occur, which increased with the use of corticosteroids, which is assigned an essential role in the appearance of periventricular leukomalacia, which is related to an increase in interleukin 6, which is due to a local inflammatory process, which can subsequently bleed.

Intraventricular hemorrhage of the neonate is associated with increased cerebral blood flow and blood pressure, which is complicated by the vascular alterations that accompany hypoxemia and metabolic acidosis of neonates with respiratory distress. The use of additional doses of corticosteroids can contribute to weakening the capillary wall.

Seizures among infants who had received the rescue dose of corticosteroids were also more frequent than in other newborns. The cause of these seizures is probably due to the higher frequency of intraventricular hemorrhage in preterm infants with rescue doses of corticosteroids. Numerous mechanisms make immature brains hyperexcitable. First, the neonatal period is a period of physiological synaptogenesis, and both the synapse and the density of the dendritic spine are at their peak. Secondly, glutamatergic neurons, the primary excitation mechanism of both the neonatal brain, are excessively abundant. Their receptors have subunits that allow relative hyperexcitability; with the up-regulation mechanism, the number of receptors increases, and with the down-regulation mechanism, the number of receivers decreases.

Third, gamma-amino-butyric acid (GABA), the primary inhibitory mechanism of the adult brain, can exert a paradoxical exciting action on the developing brain due to the preponderance of the sodium, potassium, and chloride cotransporter (NKCC1) and the Delayed expression of KCC2 chloride cotransporters, which leads to a high concentration of intracellular chloride and depolarization in response to GABAergic agents.

There was a significant difference in the patients' group with corticosteroid rescue doses [28.4±21.6] and the others. It could correspond to the higher frequency of days of mechanical ventilation, due to the pulmonary immaturity associated with the higher degree of prematurity in this group, with the neurological and infectious complications, which were in this study group, compared to infants who did not receive the rescue dose of corticosteroids. Other factors that could have influenced the more magnificent hospital stay of these patients are the lower birth weight and gestational age in this group than the other, which also predisposes to the appearance of multiple complications.

Also, within respiratory complications, upon admission: hyaline membrane disease was present in 22.5% of infants who received rescue doses of corticosteroids and in 13.7% of those who did not receive it without statistical significance (p> 0.05). Similarly, at the time of discharge from the NICU, no statistically significant intergroup differences were obtained, an essential effect of the rescue dose of corticosteroids on the prognosis, and the reduction of complications of infants who received it. Corticosteroids accelerate the morphological differentiation of epithelial cells in type II cells, increase the rate of phosphatidylcholine synthesis and cause the accumulation of messenger RNAs for B-surfactant proteins (Mr=7000) and C (Mr=5000). Induction of phospholipid surfactants and mRNA proteins occurs rapidly, reverses, and appears to be mediated by receptors.

However, no significant effect was found in reducing hyaline membrane disease in this work, probably due to this group's infants' great prematurity. The production of surfactants mediates not all the effects of prenatal corticosteroids in the prevention of respiratory distress. A rapid removal of fluid from the lung to allow efficient gas exchange at the alveolar surface is key to the fetus's transition to other uterus life. The signaling of cellular corticosteroid receptors influences the function of several proteins involved in the mediation of alveolar fluid clearance; they include a subunit of the epithelial sodium channel (aENaC) and the a1 and b1 subunits of the adenosine triphosphate-based basolateral pump (ATP), both expressed in the respiratory epithelium.

Therefore, at the time of admission, neurological pathology was more frequent among infants in whom the rescue dose of corticosteroids, but this difference was very discrete and did not obtain statistical significance. At the time of discharge, neurological complications did not have statistical significance among the study groups (p>0.05), indicating that the rescue dose of corticosteroids did not interfere; Although there is evidence that links the use of corticosteroids with neurological disorders such as intra-parenchymal hemorrhage and neonatal seizures. These complications were more frequent in the group that received the rescue dose, but it was not statistically significant.

Besides, neonatal infections at the time of admission had no significant differences between the two study groups (p>0.05), although they were more frequent in the group that received the rescue dose, within these, the risk for urinary tract infection (21.6%). However, at the time of discharge from neonatal ICU, there were essential differences between the two groups (p<0.05), with a clear predominance in neonates who received the rescue dose, where early sepsis predominated (32.4 %) and septic shock (7.8%). The immunosuppressive effect of corticosteroids predisposes to the appearance of infections at all levels.

The use of rescue doses of corticosteroids in the neonatal period is associated with a higher probability of developing prenatal infections, such as chorioamnionitis and endometritis. It also increases the risk of early neonatal sepsis due to its suppressive effect on cellular and humoral immunity and

decreases the production of lymphocytes, interleukins, and tumor necrosis factors, through a decrease in the stability of messenger RNA.

There were no significant differences between the two study groups when admission or discharge concerning metabolic pathologies. At admission, intrauterine growth restriction affected 9.8% of infants on corticosteroid rescue doses. This percentage was 15.7% at discharge. It associates corticosteroids' action on fetal growth with reduced size and weight at birth and intrauterine growth restriction.

Nor was an essential relationship between hematological pathologies and the use of rescue doses of corticosteroids at the time of admission or discharge. The most frequent cases were multifactorial jaundice in the group of those who received rescue doses (33.3%) but without statistical significance ($p>0.05$). In this case, jaundice seems to correspond to the interaction of several factors related to enzymatic immaturity, the use of antibiotics, or neonatal sepsis.

Similarly, cardiovascular and hemodynamic conditions did not have a significant difference in both study groups; at discharge from the NICU, infants in whom the rescue dose was not used had a higher incidence of this type of complications, significantly the persistence of the ductus arteriosus, which is a malformation in which the use of rescue doses of prenatal corticosteroids is not involved.

In summary, the most critical findings were, in the group that received rescue doses, which included very preterm newborns, there was an increase in the number of days of mechanical ventilation and infectious complications, which at the same time was associated with an increase in hospitalization days.

Limitations

The sample was adequate but could be extended to another population group from other hospitals and provinces.

Generalization

It is possible to generalize this research following a multicenter and prospective design.

Conclusions

Preterm males weighing <1000 g from 30 to 32 weeks, who used rescue doses of corticosteroids, showed an increase in intraventricular hemorrhage (13.7%), seizures (6.9%), and leukomalacia (13.7%), associated with the fact that in the group with rescue dose they are younger and had lower weight.

Acknowledgments

Authors thanks Gonzalo Mantilla, Luis Eguiguren, Hugo Burgos, Ana María Merchán-Tamariz, Alonso Herrera, and Humberto Navas López, for their support to this work.

Funding

Authors self-funding.

Conflict of interest

The authors report NO conflict of interest.

Ethical approval

This research was approved by the Research Ethics Committee on Human Beings (CEISH) of the San Francisco University of Quito. It was dated 14 November of 2019, and coded with the number P2019-155TPG.

Informed consent

It obtained Informed consent from all individual participants included in the study.

Consent for publication

The institutions cited in this document gave their consent to use this information.

Bibliographic references

1. Roberts D, Brown J, Medley N, Dalziel SR. Antenatal corticosteroids for accelerating fetal lung maturation for women at risk of preterm birth. Cochrane Database Syst Rev. 2017 21 March;3(3):89-104. DOI: 10.1002/14651858.CD004454.pub3.
2. McKinlay CJD, Crowther CA, Middleton P, Harding JE. Repeat antenatal Corticosteroids for women at risk of preterm birth: A Cochrane Systematic Review. Am J Obstet Gynecol. 2012 Mar;206(3):187-194. DOI: 10.1016/j.ajog.2011.07.042.
3. Ehret DEY, Edwards EM, Greenberg LT, Bernstein IM, Buzas JS, Soll RF, et al. Association of Antenatal Steroid Exposure With Survival Among Infants Receiving Postnatal Life Support at 22 to 25 Weeks' Gestation. JAMA Netw Open. 2018 Oct 5;1(6):e183235. DOI: 10.1001/jamanetworkopen.2018.3235.
4. Sotiriadis A, Makrydimas G, Papatheodorou S, Ioannidis JPA, Mcgoldrick E. Corticosteroids for preventing neonatal respiratory morbidity after elective cesarean section at term. Cochrane Database Syst Rev. 2018 3 August;8(8): CD006614. DOI: 10.1002/14651858.CD006614.pub3.
5. Kamath-Rayne BD, Rozance PJ, Goldenberg RL, Jobe AH. Antenatal corticosteroids beyond 34 weeks gestation: What do we do now? Am J Obstet Gynecol. 2016 1 October;215(4):423-430. DOI: 10.1016/j.ajog.2016.06.023.
6. Norman M, Piedvache A, Børch K, Huusom LD, Bonamy AKE, Howell EA, et al. Association of short antenatal corticosteroid administration-to-birth intervals with survival and morbidity among very preterm infants results from the EPICE group. JAMA Pediatr. 2017 1 July;171(7):678-686. DOI: 10.1001/jamapediatrics.2017.0602.
7. Cartwright RD, Crowther CA, Anderson PJ, Harding JE, Doyle LW, McKinlay CJD. Association of Fetal Growth Restriction With Neurocognitive Function After Repeated Antenatal Betamethasone Treatment vs. Placebo: Secondary Analysis of the ACTORDS Randomized Clinical Trial. JAMA Netw Open. 2019 Feb 1;2(2):e187636. DOI: 10.1001/jamanetworkopen.2018.7636.
8. Asztalos E V., Murphy KE, Willan AR, Matthews SG, Ohlsson A, Saigal S, et al. Multiple courses of antenatal corticosteroids for preterm Birth study outcomes in children at 5 years of age (MACS-5). JAMA Pediatr. 2013 Dec;167(12):1102-1110. DOI: 10.1001/jamapediatrics.2013.2764.
9. Besnard AE, Wirjosoekarto SAM, Broeze KA, Opmeer BC, Mol BWJ. Lecithin/sphingomyelin ratio and lamellar body count for fetal lung maturity: A meta-analysis. Eur J Obstet Gynecol Reprod Biol. 2013;169(2):177-183. DOI: 10.1016/j.ejogrb.2013.02.013.
10. Shanks AL, Grasch JL, Quinney SK, Haas DM. Controversies in antenatal corticosteroids. Semin Fetal Neonatal Med. 2019 1 June;24(3):182-188. DOI: 10.1016/j.siny.2019.05.002.
11. Jobe AH, Kemp MW, Kamath-Rayne B, Schmidt AF. Antenatal corticosteroids for low and middle-income countries. Semin Perinatol. 2019 1 August;43(5):241-246. DOI:10.1053/j.semperi.2019.03.012.
12. The American College of Obstetricians and Gynecologists. Antenatal Corticosteroid Therapy for Fetal Maturation. Obstet Gynecol [Internet]. 2017;140(3):102-109. DOI: 10.1542/peds.2017-2082. Available from: https://www.acog.org/-/media/Committee-Opinions/Committee-on-Obstetric-Practice/co713.pdf?dmc=1&ts=20200125T1631437144
13. Watterberg KL, Ballard PL. Optimizing antenatal corticosteroid therapy for improving the outcome of preterm infants. Pediatr Res. 2019 Nov 1;86(5):556-557. DOI: 10.1038/s41390-019-0538–x.

14. Crowther CA, McKinlay CJ, Middleton P, Harding JE. Repeat doses of prenatal corticosteroids for women at risk of preterm birth for improving neonatal health outcomes. Cochrane Database Syst Rev. 2011 15 June;6:CD003935. DOI: 10.1002/14651858.CD003935.pub3.
15. Hutchinson M, Hodgden JD. Clinical Question: In women with preterm labor, do repeated courses of prenatal corticosteroids improve neonatal outcomes compared to a single course? J Okla State Med Assoc [Internet]. 2018 Jan [cited 2020 Jan 3];111(1):498-499. ISBN: 0030-1876. Available from: http://www.ncbi.nlm.nih.gov/pubmed/30532343
16. Frey HA, Klebanoff, MA. The epidemiology, etiology, and costs of preterm birth. Semin Fetal Neonatal Med. 2016 1 April;21(2):68-73. DOI: 10.1016/j.siny.2015.12.011.
17. Kemp MW, Schmidt AF, Jobe AH. Optimizing antenatal corticosteroid therapy. Semin Fetal Neonatal Med. 2019 1 June;24(3):176-181. DOI: 10.1016/j.siny.2019.05.003.
18. Kamath-Rayne BD, Defranco EA, Marcotte MP. Antenatal steroids for treatment of fetal lung immaturity after 34 weeks of gestation: An evaluation of neonatal outcomes. Obstet Gynecol. 2012 May;119(5):909-916. DOI: 10.1097/AOG.0b013e31824ea4b2.
19. McKinlay CJ, Manley BJ. Antenatal and postnatal corticosteroids: A swinging pendulum. Semin Fetal Neonatal Med. 2019 1 June;24(3):167-169.DOI: 10.1016/j.siny.2019.05.007.
20. Haviv HR, Said J, Mol BW. The place of antenatal corticosteroids in late preterm and early term births. Semin Fetal Neonatal Med. 2019 1 February;24(1):37-42. DOI: 10.1016/j.siny.2018.10.001

Received: 19 February 2021
Accepted: 17 April 2021

RESEARCH / INVESTIGACIÓN

Determination of pro-oxidant-antioxidant balance (PAB) assay in mothers with spontaneous abortion

Faezeh Ghasemi[1], Alireza Kamali[2], Maryam Shokrpour[3*]
DOI. 10.21931/RB/2021.06.03.14

Abstract: Oxidative stress has been identified to play a vital role in the pathogenesis of spontaneous abortion were characterized as an imbalance between the generation of pro-oxidants, free radicals, and reactive species, and enzymatic and non-enzymatic antioxidant defenses in favor of the former. In the present study, the pro-oxidant-antioxidant balance was assessed in women with spontaneous abortion and compared with healthy age-matched controls. A group of 50 females with spontaneous abortion were considered patients, and a group of age-matched healthy pregnant women was considered controls. The pro-oxidant-antioxidant balance (PAB) assay was carried out on participants' serum samples. The mean age of the spontaneous abortion group was 30.84 ± 3.82, and controls were 26.53 ± 4.05 years. The obtained PAB values were 236.74 ± 11.37 HK and 148.69 ± 76.50 HK in patients and controls. Our results demonstrate the significant rise of PAB values in subjects with spontaneous abortion compared to healthy controls ($p< 0.0001$). Our study showed that the PAB values might be involved in the termination of spontaneous abortion.

Key words: Spontaneous abortion, Oxidative stress, Antioxidants, PAB assay.

Introduction

Spontaneous abortion is considered as the fetus's natural death before 20 gestations. Based on scientific declarations, spontaneous abortion defines by pregnancy termination before complete 20 weeks gestational period while the fetal weight is less than a half kilogram[1,2]. Massive investigation showed that the rate of spontaneous abortion depends on pregnancy age and miscarriage[3,4]. According to the Cardone *et al.* rate of spontaneous abortion increased in elder females compare with younger cases. In North American pregnant females, spontaneous abortion happened in 17%- 20% cases younger than 25 years old whereas increased to 30%-35% in those with 35-45 years old[3].

Cramer and Wise published data demonstrated that miscarriage increase spontaneous abortion risk. The incidence of spontaneous abortion in females with no miscarriage is approximately 13 percent and increased to 25%, 30 %, and 35 % in those who suffered from 1, 2, and 3 miscarriages, respectively[3]. Further investigation illustrated the various spontaneous abortion risk factors. Dickey RP and colleagues represented the higher incidence of spontaneous abortion in one-fourth of females treated with human gonadotropin and clomiphene[5].

Moreover, fragmentation of sperm DNA, hyperhomocysteinemia, immunological disorders, and insufficient antioxidant defenses have also been observed in females with spontaneous abortion[4].

Oxidative stress, a profound imbalance between pro-oxidants, reactive oxygen specious, free radicals, and enzymatic and non-enzymatic antioxidants in favor of the former, plays the leading role in disorders and deficiencies[6,7]. Despite the essential role of oxygen in metabolism and life persistency, its toxic derivatives can be caused severe damage to cellular compartments[7].

Reactive species damage DNA, mitochondria, and cell membrane, which affects the cellular compartments pathologically and leads to ultimate cellular demise[8,9]. In response to oxidative damage, the antioxidant system neutralizes the excess pro-oxidants, maintains physiological balance, and establishes cellular homeostasis[10,11]. Simsek *et al.* uncovered the essential role of oxidative damage, higher level of lipid peroxidation, and reactive oxygen specious immediately before abortion[12,13].

Although the exact causes of spontaneous abortion are not clearly understood, immunological alterations and profound disruption of oxidative stress seem to be involved etiologically. Our study aims to characterize the prooxidant-antioxidant balance (PAB) in patients with spontaneous abortion.

Materials and methods

Subjects

The presented study was conducted on 80 pregnant females (50 with spontaneous abortion history as a patient group and 30 normal age-matched healthy women without a history of abortion as controls) hospitalized between March 2017 and October 2018 in Taleghani Hospital Arak, Iran. The first day of gestation was determined based on ultrasound obtained data, and obstetricians evaluated the risk of spontaneous abortion in participants. Females who had been exposed to teratogenic drugs were excluded, whereas the participants who have had at least 1 terminated abortion before complete 20 weeks gestation were categorized as the patients. Moreover, all participants were signed the written consent to contribute to the survey that the ethics committee approved of Arak Medical School.

Sample collection

For all subjects, the age, history of spontaneous abortion, gestational time, deliveries, and abortions were recorded. To carrying out the PAB assay, 2 ml arterial-venous mixed cord

[1] Blood Transfusion Research Center, High Institute for Research and Education in Transfusion Medicine, Next to Milad Tower, Tehran, Iran.
[2] Departments of Anesthesiology and Critical Care, Arak University of Medical Sciences, Arak, Iran.
[3] Department of Gynecology, Faculty of Medicine, Arak University of Medical Sciences, Arak, Iran

Corresponding author: ghasemi_808@yahoo.com

blood was collected after delivery and abortion. The collected blood samples were centrifuged at 3600 rpm for 10 minutes after clotting to separate sera. To measure the oxidative stress parameters in the rapid, accurate method, the obtained sera were kept at -80°C until analysis. The hemolytic samples were excluded from the PAB assay.

Chemicals

The chemicals were used in our survey include TMB powder (3, 3′, 5, 5′-Tetramethylbenzidine, Fluka), chloramine T trihydrate (AppliChem: A4331, Darmstadt, Germany), peroxidase enzyme (AppliChem: 230 U/mg, A3791, 0005, Darmstadt, Germany), hydrogen peroxide (Merck). Double distilled water was applied for dissolving molecular biology grade reagents that need further preparation.

The pro-oxidant antioxidant balance (PAB) assay

PAB assay was carried out based on our previous studies[14,15]. Standard solutions were prepared by blending the exact proportion of 250 M H2O2 (0-100%) and uric acid 3 mM and added to the NaOH (10 mM). To prepare TMB cation, 60 mg TMB powder was dissolved in 10 ml dimethyl sulfoxide (DMSO) and was added to 20 ml acetate buffer (0.05 M, pH 4.5). After that, well-mixed 70 µl freshly chloramine T solution (100 mM) was added to the previously prepared solution, shacked immediately, and incubated for 2 hours at room temperature (23°C-27°C) in the dark places.

The horseradish peroxidase working solution was prepared by blending the 25-unit peroxidase enzyme solution into the 20 ml TMB cation and aliquoted into 1 ml microtubes and stored at -20, respectively. TMB working solution was prepared by gently blending 200 µl TMB/DMSO into the 10 ml acetate buffer (0.05 M, pH 5.8).

To determine the PAB values in the subjects' sample, 200 µl working solution was added to each well of 96-well ELISA. Then, 10 µl participants' sera, distilled H_2O (blank well), and standard solutions were added and mixed gently as well as the plates were incubated in the dark place at 37°C for 15 minutes. The 50 µl of 2 N HCl was recruited as the stop solution, and the PAB was measured at 450 nm wavelength.

The PAB values were demonstrated in arbitrary HK units, the percentage of H_2O_2 in the standard solution. Meanwhile, unknown samples were then calculated based on the obtained values from the standard drowning curve.

Statistical analysis

The Statistical Package for Social Sciences (SPSS version 20.0, IBM, USA) was used for data analysis while the P-value < 0.05 was considered statistically significant. The Kolmogorov-Smirnov test was carried out to determine the data's normality, and unpaired sample T-tests were applied for evaluating the statistical analysis.

Results

The mean age of participants with spontaneous abortion and controls were 30.84±3.82 and 26.53±4.05 years, respectively. The higher range and lower range of participants' PAB value shows 214 – 253.74 HK in females with spontaneous abortion and 2.50 – 264.03 in the standard group. Our obtained data revealed a significantly raised level of PAB values in spontaneous abortion participants compared to the standard group (p-value <0.0001) (figure 1).

No abortion was seen in controls, while in the spontaneous abortion group, 21 cases had had one abortion, and 5 cases had had 3 abortions. Furthermore, 29 cases had delivered at least one normal childbirth (Table 1).

Discussion

Massive investigations demonstrate the role of oxidative stress in the pathogenesis of spontaneous abortion, pre-eclamptic pregnancy, and related pregnancy hypertensive

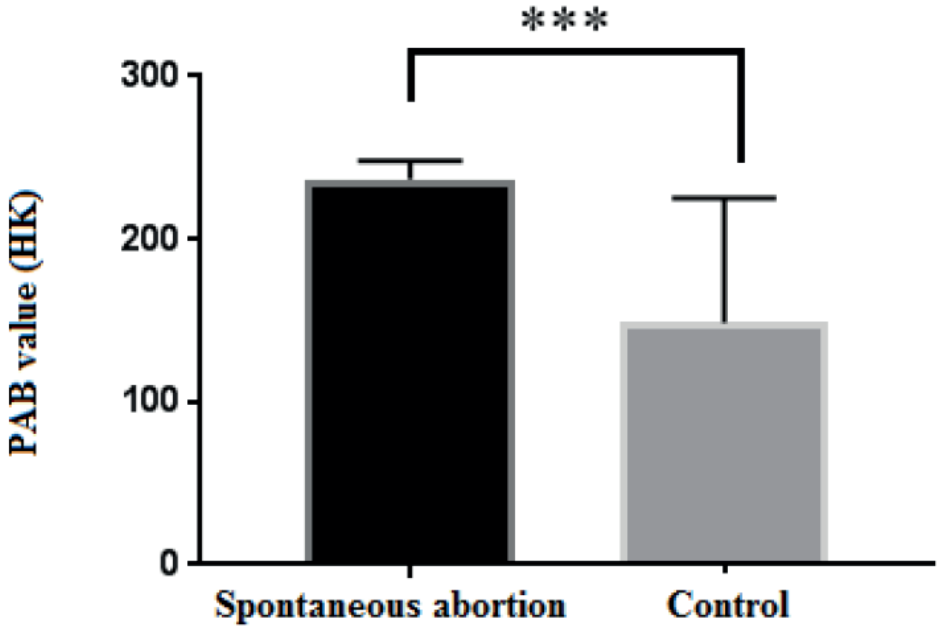

Figure 1. Evaluation of the PAB values between two groups. Results showed a significant increase in PAB values in the spontaneous abortion group 236.74±11.37 HK compared to the control group 148.69±76.50 (p<0.0001).

Delivery-abortion /Group		Frequency	Mean	S.D	Max	Min
Delivery	Spontaneous abortion	50	2.76	0.77	5	2
	control	30	1.03	0.18	2	1
abortion	Spontaneous abortion	50	1.7	0.73	4	1
	control	30	0	0	0	0
Gestation (week)	Spontaneous abortion	50	26.54	11.10	40	6
	control	30	38.06	2.86	41	28

Table 1. Comparison the delivery, abortion and gestational time between spontaneous abortion group and controls.

disorders[16-18]. Higher levels of oxidants such as malondialdehyde, protein carbonyl, erythrocyte glutathione peroxidase, and erythrocyte superoxide dismutase were observed in placentation, miscarriage, and recurrent pregnancy loss[19]. Our results indicate that a significant increase in pro-oxidants in subjects with spontaneous abortion compared to controls.

Despite the suggestion of published reports that show the beneficial effects of antioxidants in vitro fertilization (IVF), rare of them demonstrate the role of antioxidants in miscarriage[20,21]. Recent investigations demonstrate that the proper fetus implantation seriously depends on low oxygen concentration to complete 10 gestational weeks[22]. It may protect fetal development and differentiation against reactive specious, free radicals, and immunological reactions[19]. Compelling evidence uncovered the deficient trophoblastic invasion that occurred following the spontaneous abortions[23]. Therefore, in the same direction as our obtained data, oxidative stress may raise the spontaneous abortions before complete 10 weeks of gestation, which might be the consequence of maternal blood-flow disorders[19].

Higher lipid peroxidation and oxidative stress biomarkers such as malondialdehyde increase in females with spontaneous abortion[24]. Sugino *et al.* published a report that showed the higher concentration of lipid peroxidation in females with spontaneous abortion suffered from vaginal bleeding[25]. These observations boost our hypothesis about the role of oxidative stress in spontaneous abortion. In other words, higher levels of reactive specious, free radicals and consequent oxidative damages lead to placenta oxidation, spontaneous abortion, and fetal termination. A higher level of lipid peroxides such as malondialdehyde may involve in urine evacuation.

The corpus luteum activity is fundamental for embryogenesis and fetal development. The early stages of pregnancy and trophoblast implantation are dependent on corpus luteum activity which relies upon superoxide dehydrogenase-enzyme activity. In the ovary, superoxide dehydrogenase prevents the restrictive reaction of hydrogen peroxide-derived peroxide and superoxide ions on gonadotropin hormones and affects the ovary's follicular function[26], demonstrating the role of superoxide dehydrogenase-enzyme activity in early gestation.

Interestingly, Umaoka and colleagues demonstrate that in vitro fetal development was restricted during the high level of oxygen. Likewise, reactive oxygen specious and superoxide ions cause severe damage to embryogenesis and trophoblast expansion. Superoxide dehydrogenase can prevent the harmful effects of superoxide ions[27].

Conclusions

A significant increase in pro-oxidants and oxidative stress were reported in several investigations. Based on our data, profound disruption of oxidative stress may involve spontaneous abortion even though more surveys are needed.

Bibliographic references

1. Kwegyir-Afful E, Adu G, Spelten ER, Räsänen K, Verbeek J. Maternity leave duration and adverse pregnancy outcomes: An international country-level comparison. Scandinavian journal of public health. 2018; 46(8): 798-804.
2. Blencowe H, Cousens S, Oestergaard MZ, Chou D, Moller A-B, Narwal R, et al. National, regional, and worldwide estimates of preterm birth rates in 2010 with time trends since 1990 for selected countries: a systematic analysis and implications. The lancet. 2012; 379(9832): 2162-72.
3. Gupta S, Agarwal A, Banerjee J, Alvarez JG. The role of oxidative stress in spontaneous abortion and recurrent pregnancy loss: a systematic review. Obstetrical & gynecological survey. 2007; 62(5): 335-47.
4. Cramer DW, Wise LA. The epidemiology of recurrent pregnancy loss. Seminars in reproductive medicine 2000; 18(04): 331-40.
5. Dickey RP, Taylor SN, Curole DN, Rye PH, Pyrzak R. Infertility: Incidence of spontaneous abortion in clomiphene pregnancies. Human reproduction. 1996; 11(12): 2623-28.
6. Pouya VT, Hashemy SI, Shoeibi A, Tirkani AN, Tavallaie S, Avval FZ, et al. Serum Pro-Oxidant-Antioxidant Balance, Advanced Oxidized Protein Products (AOPP) and Protein Carbonyl in Patients With Stroke. Razavi International Journal of Medicine. 2016; 4(2):
7. Avval FZ, Mahmoudi N, Tirkani AN, Jarahi L, Alamdari DH, Sadjadi SA. Determining Pro-Oxidant Antioxidant Balance (PAB) and Total Antioxidant Capacity (TAC) in Patients with Schizophrenia. Iranian journal of psychiatry. 2018; 13(3): 222.
8. Sharif ME, Mohamedain A, Ahmed AA, Nasr AM, Adam I. Folic acid level and preterm birth among Sudanese women. Maternal health, neonatology and perinatology. 2017; 3(1): 25.
9. Ronnenberg AG, Goldman MB, Chen D, Aitken IW, Willett WC, Selhub J, et al. Preconception folate and vitamin B6 status and clinical spontaneous abortion in Chinese women. Obstetrics & Gynecology. 2002; 100(1): 107-13.
10. Agarwal A, Allamaneni SS. Role of free radicals in female reproductive diseases and assisted reproduction. Reproductive biomedicine online. 2004; 9(3): 338-47.
11. Lu J, Wang Z, Cao J, Chen Y, Dong Y. A novel and compact review on the role of oxidative stress in female reproduction. Reproductive Biology and Endocrinology. 2018; 16(1): 80.

12. Şimşek M, Naziroα lu M, Şimşek H, Cay M, Aksakal M, Kumru S. Blood plasma levels of lipoperoxides, glutathione peroxidase, beta carotene, vitamin A and E in women with habitual abortion. Cell Biochemistry and Function: Cellular biochemistry and its modulation by active agents or disease. 1998; 16(4): 227-31.
13. Mohd Mutalip S, Ab-Rahim S, Rajikin M. Vitamin E as an antioxidant in female reproductive health. Antioxidants. 2018; 7(2): 22.
14. Pouya VT, Hashemy SI, Shoeibi A, Tirkani AN, Tavallaie S, Avval FZ, et al. Serum Pro-Oxidant-Antioxidant Balance, Advanced Oxidized Protein Products (AOPP) and Protein Carbonyl in Patients With Stroke. Razavi International Journal of Medicine. 2016; 4(2):
15. Alamdari DH, Ghayour-Mobarhan M, Tavallaie S, Parizadeh MR, Moohebati M, Ghafoori F, et al. Prooxidant–antioxidant balance as a new risk factor in patients with angiographically defined coronary artery disease. Clinical biochemistry. 2008; 41(6): 375-80.
16. Vanderlelie J, Venardos K, Clifton V, Gude N, Clarke F, Perkins A. Increased biological oxidation and reduced antioxidant enzyme activity in pre-eclamptic placentae. Placenta. 2005; 26(1): 53-58.
17. Scholl TO, Leskiw M, Chen X, Sims M, Stein TP. Oxidative stress, diet, and the etiology of preeclampsia. The American journal of clinical nutrition. 2005; 81(6): 1390-96.
18. Bulgan Kilicdag E, Ay G, Celik A, Ustundag B, Ozercan I, Simsek M. Oxidant-antioxidant system changes relative to placental-umbilical pathology in patients with preeclampsia. Hypertension in pregnancy. 2005; 24(2): 147-57.
19. Ozkaya O, Sezik M, Kaya H. Serum malondialdehyde, erythrocyte glutathione peroxidase, and erythrocyte superoxide dismutase levels in women with early spontaneous abortions accompanied by vaginal bleeding. Medical Science Monitor. 2008; 14(1): CR47-CR51.
20. Olson S, Seidel Jr G. Culture of in vitro-produced bovine embryos with vitamin E improves development in vitro and after transfer to recipients. Biology of Reproduction. 2000; 62(2): 248-52.
21. Peng Y, Kwok K, Yang P-H, Ng SS, Liu J, Wong O, et al. Ascorbic acid inhibits ROS production, NF-α B activation and prevents ethanol-induced growth retardation and microencephaly. Neuropharmacology. 2005; 48(3): 426-34.
22. Burton GJ, Watson AL, Hempstock J, Skepper JN, Jauniaux E. Uterine glands provide histiotrophic nutrition for the human fetus during the first trimester of pregnancy. The Journal of Clinical Endocrinology & Metabolism. 2002; 87(6): 2954-59.
23. Burton GJ, Jauniaux E. Placental oxidative stress: from miscarriage to preeclampsia. Journal of the Society for Gynecologic Investigation. 2004; 11(6): 342-52.
24. Sane A, Chokshi SA, Mishra V, Barad D, Shah V, Nagpal S. Serum lipoperoxides in induced and spontaneous abortions. Gynecologic and obstetric investigation. 1991; 31(3): 172-75.
25. Sugino N, Nakata M, Kashida S, Karube A, Takiguchi S, Kato H. Decreased superoxide dismutase expression and increased concentrations of lipid peroxide and prostaglandin F2α in the decidua of failed pregnancy. Molecular human reproduction. 2000; 6(7): 642-47.
26. MARGOLIN Y, ATEN RF, BEHRMAN HR. Antigonadotropic and antisteroidogenic actions of peroxide in rat granulosa cells. Endocrinology. 1990; 127(1): 245-50.
27. Umaoka Y, Noda Y, Narimoto K, Mori T. Effects of oxygen toxicity on early development of mouse embryos. Molecular reproduction and development. 1992; 31(1): 28-33.

Received: 22 March 2021
Accepted: 21 May 2021

RESEARCH / INVESTIGACIÓN

Molecular characterization of *net*B and *tpe*L virulence factors and antimicrobial resistance genes of *Clostridium perfringens* isolated from herbs and spices

Ashraf A. Abd El-Tawab[1], Fatma I. El-Hofy[1], Mohamed A. Abdelmonem[2], Hend S. Youssef[2*]
DOI. 10.21931/RB/2021.06.03.15

Abstract: The present study aimed to determine some virulence-associated genes and antimicrobial multidrug resistance of *Clostridium perfringens* recovered from herbs and spices widely distributed in the Egyptian market. *C. perfringens* virulence and resistance factors were determined using PCR targeting the *net*B, *tpe*L, *erm*B, *bla* and *tetK* genes. Thirty three out of 392 samples (8.42%) from herbs and spices submitted to our laboratory for bacteriological screening were positive for presence *C. perfringens*. PCR results for the *tpe*L gene in isolated *C. perfringens* revealed 9 out of 33 (27.3 %) of isolates, while *net*B was not detected. The isolates were resistant to Clindamycin, Vancomycin, tetracycline, and erythromycin with inhibition zones of 6.28 ± 0.63, 8.78 ± 0.41, 9.63 ± 0.63, and 9.84 ± 0.66 mm, respectively. The genes mentioned above were selected to correspond to the ineffective antimicrobials; *erm*B for erythromycin, *tetK* for tetracycline, and *bla* for the remainder. PCR results for antibacterial resistant genes in isolated *C. perfringens* revealed their presence. From 33 isolates, *bla* gene was detected in 21 (63.4 %), *tetK* in 13 (39.4 %) and *erm*B in only one isolate (3.03 %). Sequencing analysis was done for the *bla* gene as an example for the detected genes as detected at the highest incidence (63.4%). No cross-relationship was detected upon comparing incidence data of both studied virulence genes and those of antimicrobial resistance. The present findings may explain the resistance of *C. perfringens* to the examined antibacterials and recommend avoiding the application of them to control the microbe. In addition, the authors recommend following strict hygienic procedures during the industry of herbs and spices to ensure their clearance from *Clostridium perfringens* before distributing the products as food additives into the markets.

Key words: *Clostridium perfringens*, Herbs, Spices, Antibiotic Susceptibility Test, Resistance, Genes.

Introduction

Among food additives, herbs and spices are considered as severe vectors for foodborne microorganisms, including *C. perfringens*[1,2]. Incidence of *C. perfringens* in herbs and spices has been checked worldwide, including India[3], Turkey[4], the United Kingdom[5], Italy[6], Lebanon[7], Saudi Arabia[8], and Egypt[9].

Abundant toxin production and multidrug resistance are considered as the two major problems caused by *Clostridium perfringens*. This microbe is Gram-positive eubacteria, a rod-shaped, spore-forming anaerobe widely distributed elsewhere in nature, including soil, surfaces, sewage, feces, foods, and food additives[10].

C. perfringens is a highly toxicogenic bacterium as it can produce various toxins (at least 17) that are considered to be its pathogenic virulence factors[11]. Four among these toxins are commonly categorized as significant as they may cause lethality; these are α-, ß-, £-, and i-toxins. Each strain with its particular toxins is associated with a particular disease in humans and animals[12]. For this, most studies are focused on looking at these toxins from bacterial isolates, including one carried out by our team (El-Tawab *et al.*, 2021, under publishing). On the other hand, some other genes were considered minor ones because they are thought not to be pivotal for *C. perfringens* pathogenesis. Among these genes are found *net*B and *tpe*L toxins. However, recently, these genes were suggested to contribute to disease pathogenesis. For many years, α-toxin was thought to be the major virulence factor involved in necrotic enteritis, but a clostridial strain cloned for deactivation of α -toxin still able to produce lesions in broilers. This study led to the discovery of the pathogenicity of a new toxin, NetB[13]. In addition, it was discovered that inoculation of broilers with strains positive for both *net*B and *tpe*L were associated with greater severity of gross lesions over strains with only *net*B[14], a fact that supports the idea of the pathogenicity of tpeL too.

Even though a relatively limited number of studies focused on investigating these two toxins and their driving genes, no study has looked at these two virulence factors in clostridial isolates from herbs and spices.

The second major problem of the studied microbe is its resistance to drugs. In a previous study, we have conducted the antibiotic susceptibility test and detected the resistance of clostridial isolates to Clindamycin, Vancomycin, tetracycline, and erythromycin. However, the underlying mechanism of this resistance was not investigated[9].

The present study aimed to investigate the *net*B and *tpe*L toxin/gene positivity of *C. perfringens* isolated from herbs and spices retailed all over the Egyptian markets and to determine the molecular mechanisms underlying the antimicrobial drug resistance by investigating the positivity to *bla*, *tet*K, and *erm*B genes. To fulfill this aim, PCR and sequencing, and phylogenetic analyses have been conducted on *C. perfringens* isolates from herbs and spices.

Methods

Samples and isolates

The study was applied to 392 samples obtained from the top herbs and spices suppliers in Egypt. The samples have been screened for the incidence of *C. perfringens*. Thirty-three *C. perfringens* isolates were obtained from these samples following ISO 6887-2, ISO 6887-3, ISO 6887-4, or ISO 8261[9]. The isolates were resistant to Clindamycin, Vancomycin, tetracycline, and erythromycin[9].

[1] Department of Microbiology, Faculty of Veterinary Medicine, Benha University, 13736 Moshtohor, Egypt.
[2] Department of Microbiology, Central Lab of Residue Analysis of Pesticides & Heavy Metals in Food, Agricultural Research Center, Ministry of Agriculture, Giza, Egypt.

Corresponding author: hend.micro@outlook.com

DNA extraction

DNA was extracted from the pure isolated colonies using the QIAamp DNA Mini kit purchased from Qiagen® (Hilden, Germany) following the manufacturer's instructions with some modifications. The kit provides silica-membrane-based nucleic acid purification from different types of samples. The spin-column procedure does not require mechanical homogenization; thus, the total hands-on preparation time is only 20 minutes. The DNA concentration was determined using NanoDrop ND-1000 Spectrophotometer from Thermo-scientific (Waltham, MA, USA) by reading absorbances at 260 and 280 nm. The extracted samples were stored at –20 °C until used as templates for PCR amplification.

PCR

The conventional PCR was applied to screen *net*B and *tpe*L toxin-encoding genes and those of resistance, namely, *bla*, *tet*K and *erm*B in the 33 isolates of *C. perfringens*, using Emerald Amp GT PCR Master Mix kit, Code No. RR310A was purchased from Takara Bio Inc.® (Shiga, Japan). The amplification process was performed according to the manufacturer's instructions, using specific primers from Midland® (TX, USA) and a thermal cycler from Biometra® (Jena, Germany). The thermal cycling conditions are briefly described in tables 1, 2, and 3.

Agarose gel electrophoresis

Thirty µl of each PCR test product, negative and positive controls, and 100-bp DNA ladder (purchased from Fermentas®, Massachusetts, USA; cat. no. SM0243) were loaded to agarose gel 1.5 % and the process was conducted according to (20) following instructions of the manufacturer. The power supply was adjusted between 1~5 volts/cm of the tank length. The run was stopped after about 30 min, and then the gel was transferred to the UV cabinet. A gel documentation system photographed the gel, and the data was analyzed through computer software.

Sequencing reaction of bla gene

Uniplex PCR products of five *C. perfringens* isolates positive of *bla* gene were taken randomly and purified using the QIAquik PCR product purification protocol (Qiagen®, Hilden, Germany) provided by the manufacturer. The purified PCR products were sequenced in the forward and reverse directions on an Applied Biosystems 3130 automated DNA Sequencer (ABI, 3130, USA), using a ready reaction Bigdye Terminator V3.1 cycle sequencing kit, Cat. No. 4336817 (Perkin-Elmer / Applied Biosystems, Foster City, CA). The master mix using Big dye Terminator V3.1 cycle sequencing kit is described below (Table 4).

Toxin	Primer	Sequence	Amplified product	Reference
netB toxin	F	GCTGGTGCTGGAATAAATGC	560 bp	[15]
	R	TCGCCATTGAGTAGTTTCCC		
tpeL toxin	F	ATATAGAGTCAAGCAGTGGAG	466 bp	[16]
	R	GGAATACCACTTGATATACCTG		
bla	F	ATGAAAGAAGTTCAAAAATATTTAGAG	780 bp	[17]
	R	TTAGTGCCAATTGTTCATGATGG		
tetK	F	TTATGGTGGTTGTAGCTAGAAA	382 bp	[18]
	R	AAAGGGTTAGAAACTCTTGAAA		
ermB	F	GAA AAG GTA CTC AAC CAA ATA	638 bp	[19]
	R	AGT AAC GGT ACT TAA ATT GTT TAC		

Table 1. Oligonucleotide primers for the 5 targeted genes.

Component	Volume/reaction
Emerald Amp GT PCR mastermix (2x remix)	25 µl
PCR grade water	5 µl
Forward primer (20 pmol)	1 µl each
Reverse primer (20 pmol)	1 µl each
Template DNA	10 µl
Total	50 µl

Table 2. Preparation of 5 *Clostridium* genes uniplex PCR Master Mix.

Gene	Primary denaturation	Secondary denaturation	Annealing	Extension	No. of cycles	Final extension
netB	94°C 5 min.	94°C 30.	58°C 45 sec.	72°C 45 sec.	35	72°C 10 min.
tpeL	94°C 5 min.	94°C 30.	55°C 45 sec.	72°C 45 sec.	35	72°C 10 min.
bla	94°C 5 min.	94°C 30 sec.	50°C 45 sec.	72°C 45 sec.	35	72°C 10 min.
tetK	94°C 5 min.	94°C 30 sec.	50°C 40 sec.	72°C 40 sec.	35	72°C 10 min.
ermB	94°C 5 min.	94°C 30 sec.	57°C 45 sec.	72°C 45 sec.	35	72°C 10 min.

Table 3. Cycling conditions of the different primers for cPCR and RAPD.

Reagent	Amount
Big dye terminator v.3.1	2 µl
Primer	1 µl
Template according to quality of band and concentration of DNA	From 1 to 10 µl
Deionized water or PCR grade	Complete till to total volume become 20 µl
Total volume	20 µl (Well mixed and briefly spinned)

Table 4. Preparation of master mix using Bigdye Terminator V3.1 cycle sequencing kit.

Phylogenetic analysis

The nucleotide sequences of *bla* gene were compared with the sequences available at public domains using BLAST (Basic Local Alignment Search Tool) server to establish sequence identity to GenBank accessions[21]. A comparative analysis of sequences was performed using the CLUSTAL W multiple sequence alignment program, version 1.83 of MegAlign module of Lasergene DNAStar software Pairwise, designed by (22) and phylogenetic analyses done using maximum likelihood, neighbor-joining, and maximum parsimony in MEGA6[23].

GenBank submission

The sequences of the bla gene have been deposited in the GenBank database under the following accession numbers: HY1 MT891107; HY2 MT891108; HY3 MT891109; HY4 MT891110; HY5 MT891111.

Data management

The obtained results were statistically analyzed using EXCEL® software version 16. The number of positive samples for each gene against the total number of examined samples was calculated as a percentage from the total.

Results and discussion

C. perfringens was first isolated by William Welch and George Nuttall at a Hospital in Baltimore, USA, following a postmortem autopsy from a dead patient and was termed as *Bacillus aerogenes capsulatus*[24]. The microbe can secrete various toxins of pore-forming nature by causing conformational change and barrel formation through the lipid bilayer of the affected host cells[25]. Among those toxins, 4 types are considered as significant, which are alpha, beta, epsilon, and iota; and according to the ability of a clostridial strain to secrete one or more of such significant toxins, *C. perfringens* was subtyped into five types, A, B, C, D and E[26].

Identification and characterization of *C. perfringens* isolated from various sources have been made by many researchers. In the present work, 33 positive isolates for the studied bacteria were obtained from herbs and spices (33 isolates/392 samples) commonly distributed in the Egyptian market[9]. Newer virulence factors, including *net*B and *tpe*L have been raised[13,27]. Relatively to the major ones (α-, ß-, £-, and i-toxins), these two factors have limited the number of studies on some source materials, especially poultry affected with necrotic enteritis. Moreover, no information is available about them from herbs and spices; therefore, we have encouraged to look at *net*B and *tpe*L from this source.

Irrational antimicrobial use has increased the antimicrobial resistance among bacterial pathogens, including *C. perfringens*. Moreover, an antimicrobial may also contribute positively or negatively to virulence factors of a bacterium[28].

In the present study, electrophoresis of the obtained multiplex PCR products confirmed the amplification of the target primer sequences for the positive controls of *net*B (560 bp) and *tpe*L (466 bp) gene fragments, while no bands were detected in the lanes of the negative controls. Bands corresponding to the *tpe*L fragments were detected in 27.3 % (9 out of 33) of the tested isolates, and no bands were detected for the *net*B fragments (Table 5 and Figures 1 & 2). The results may indicate the low prevalence of *tpe*L positive clostridial strains isolated from herbs and spices and the absence of those with *net*B genes. Although no similar studies were conducted on herbs and spices in Egypt, the absence of *net*B may be supported by the fact that this gene is only found in *C. perfringens* strains of poultry and exceptionally in one isolate recovered from a cow in the USA[29]. Comparatively, the presence of *tpe*L in about one-third of the obtained *C. perfringens* colonies may be partially consistent with (30), where was reported a 37 % of prevalence of clostridial strains positive for tpeL genes from ostriches. Low prevalence of both genes, netB, and *tpe*L in Alabama farms was also reported in (31). No studies have been conducted on herbs and spices regarding these genes to discuss. Generally, *net*B has a similar molecular size to beta-toxin, hence the name *net*B (necrotic enteritis toxin B-like), which has cytotoxic activity in chicken[13]. While *tpe*L is a member of the large clostridial toxins that is still poorly understood and needs further investigations, it also has cytotoxicity[27].

PCR data of the present study detected the presence of *bla*, *tet*K and *erm*B genes in *C. perfringens* isolates from herbs and spices. From 33 isolates, *bla* gene was detected in 21 (63.4 %), *tet*K in 13 (39.4 %) and *erm*B in only one isolate (3.03 %) (Table 5 and Figures 3, 4 & 5). This assay was aimed at exploring the genetic basis of our previous findings of antibiotic susceptibility test (AST) that found *C. perfringens* isolates resistant to Clindamycin, Vancomycin, tetracycline, and erythromycin with inhibition zones of 6.28 ± 0.63, 8.78 ± 0.41, 9.63 ± 0.63 and 9.84 ± 0.66 mm, respectively[9]. The finding of *bla* may explain the resistance of *C. perfringens* to Clindamycin and Vancomycin based on its highest presence (about 64%), but the susceptibility to Penicillin-G (inhibition zone = 16.6 ± 1.16 mm) remains to be understood. The highest susceptibility of the microbe to Ampicillin-Salbactam (19.4 ± 0.98 mm) could be explained post-transcriptionally, where sulbactam inhibits beta-lactamase after its production from the bacterial cell. These findings may be in partial consistency with (32) who reported zero % resistance of *C. perfringens* to Penicillin, Cefoxitin, Meropenem, and piperacillin with 3.8 % of resistance to Clindamycin. However, our finding of resistance to vancomycin may be inconsistent with that of (33,34) who reported that *C. perfringens* to vancomycin, is low (0–5.6 %) because of the limited use of this antibiotic in farms. The finding of amplified bands of *tet*K gene fragments in *C. perfringens* isolated from herbs (39.4 %) may partially explain and parallel with the recorded resistance of isolates to tetracycline (8.8 ± 0.4 mm inhibition zone). In contrast, the finding of only 3 % of *erm*B-positive strains is not parallel with and cannot

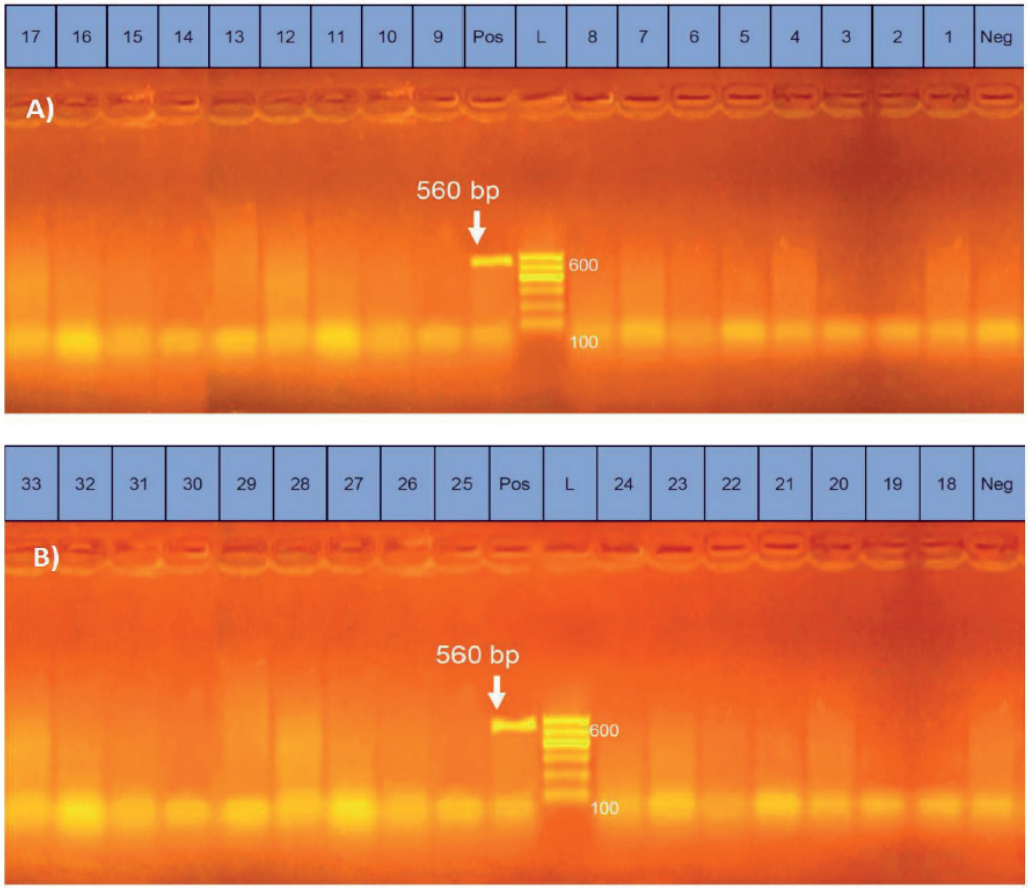

Figure 1. Uniplex PCR results of *net*B gene of *C. perfringens* isolated from herbs and spices in samples from 1~17 (A) and 18~33 (B); *net*B gene band was detected at 560 bp in control positive lane only.

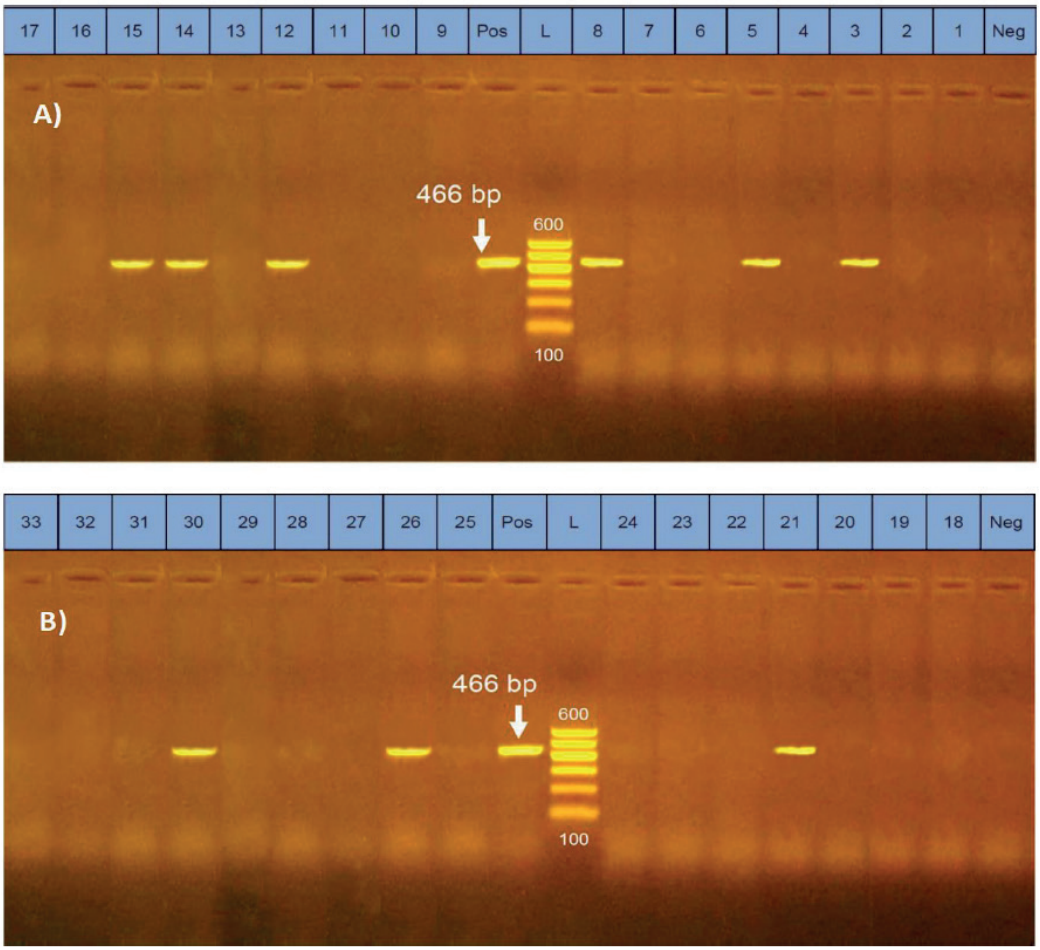

Figure 2. Uniplex PCR results of *tpe*L gene of *C. perfringens* isolated from herbs and spices in samples from 1~17 (A) and 18~33 (B); netB gene band was detected at 466 bp.

Sample #	Virulence genes		Resistance genes		
	netB	*tepL*	*bla*	*tetk*	*ermB*
1	-	-	+	+	-
2	-	-	-	+	-
3	-	+	+	+	-
4	-	-	+	+	-
5	-	+	+	+	-
6	-	-	+	+	-
7	-	-	+	+	-
8	-	+	+	-	-
9	-	-	-	-	-
10	-	-	+	-	-
11	-	-	+	-	-
12	-	+	-	+	+
13	-	-	-	-	-
14	-	+	+	-	-
15	-	+	+	-	-
16	-	-	+	-	-
17	-	-	+	-	-
18	-	-	-	-	-
19	-	-	-	-	-
20	-	-	-	-	-
21	-	+	+	+	-
22	-	-	+	-	-
23	-	-	+	+	-
24	-	-	+	-	-
25	-	-	+	+	-
26	-	+	-	-	-
27	-	-	-	-	-
28	-	-	-	-	-
29	-	-	+	+	-
30	-	+	-	-	-
31	-	-	+	-	-
32	-	-	+	+	-
33	-	-	-	-	-

Table 5. Virulence (*net*B and *tpe*L) and multidrug resistance (*bla*, *tet*K and *erm*B) genes of *C. perfringens* isolated from herbs and spices.

explain the resistance of isolates to erythromycin (9.8 ± 0.7 mm inhibition zone). This might refer to the presence of other mechanisms exhibited by the bacterium for resistance against erythromycin. The findings of resistance to Tetracycline and Erythromycin are consistent with (35) who reported resistance of *C. perfringens* isolates to these two antibiotics by 50.8 and 29.2 %, respectively. However, our finding may not agree with 36, who reported that the most probable mechanism of resistance against macrolides is modifying a target site by a methylase encoded by the *erm*B gene. The authors added that the *erm*B genotype exhibits the highest level of resistance against all macrolides, the statement does not match our findings as the *erm*B gene was detected in only one isolate among all the resistant isolates.

Taken together, it could be speculated that *net*B toxin does not correlate with the resistance of *C. perfringens* to the tested antibiotics because it was absent in all resistant isolates. However, *tpe*L toxin might contribute to the antimicrobial resistance as it was detected in about 40 % of the resistant isolates. Although this hypothesis needs more in-depth investigations, it could be in agreement with (35) who reported that the *tpe*L gene was more common among *C. perfringens* isolates susceptible to tetracycline. From our previous studies, it could be stated that the antimicrobial resistance profiles of *C. perfringens* varies significantly according to sources, countries, other bacterial factors rather than the resistance-driving genes.

Despite its apparent minimal contribution to antimicrobial resistance, yet, *bla*- gene was detected in 21 out of 33 isolates (63.4 %) of *C. perfringens* isolated from herbs and spices; therefore, its sequencing analysis becomes essential to map the epidemiology of *C. perfringens* infections caused by herbs and spices or food containing them. In the present study, sequence analysis was done for bla gene to detect its genetic diversity. The obtained sequences were analyzed using BLAST tool of GenBank. The BLAST result showed maximum identity ranging from 100% down to 97.3% with *C. perfringens bla*-gene. Our data (Figures 6 A & B) show the sequence alignment of the first 80 nucleotides from a total of 770 and the deduced amino acids of the first bla fragment, firstly isolated from herbs and spices. The overall sequence has high similarity and conservation with little divergences compared with those of *bla*-gene sequence of other global strains listed in GenBank.

Figure 7 depicts the phylogenetic analysis of *bla*-gene sequence, which shows a great degree of sequence conservation with slight divergence. The tree showed that the sequences of our local strain from herbs and spices have the same ancestors. There are no other sequencing studies conducted on isolates from herbs and spices to discuss our results with them.

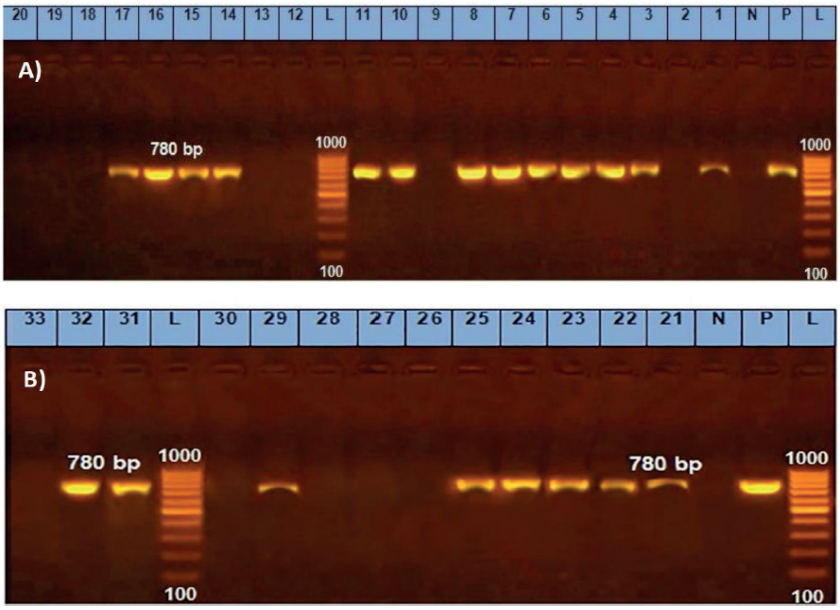

Figure 3. Uniplex PCR results of *bla* gene of *C. perfringens* isolated from herbs and spices in samples from 1~20 (A) and 21~33 (B); *bla* gene band was detected at 780 bp.

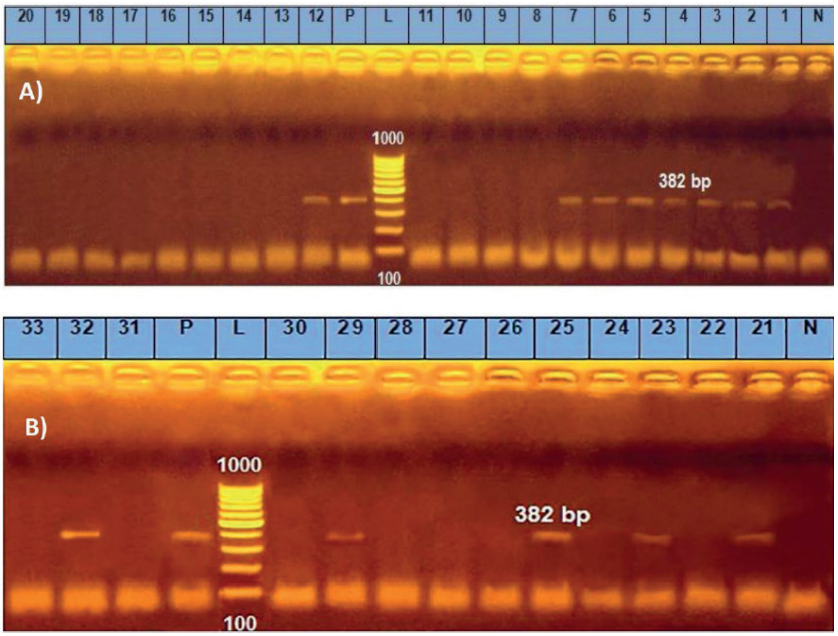

Figure 4. Uniplex PCR results of *tet*K gene of *C. perfringens* isolated from herbs and spices in samples from 1~20 (A) and 21~33 (B); *bla* gene band was detected at 382 bp.

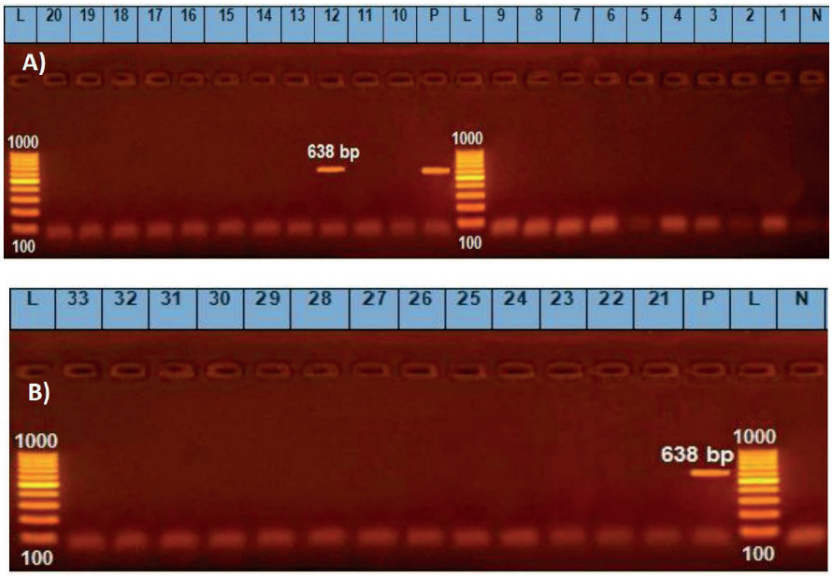

Figure 5. Uniplex PCR results of *erm*B gene of *C. perfringens* isolated from herbs and spices in samples from 1~20 (A) and 21~33 (B); *bla* gene band was detected at 638 bp.

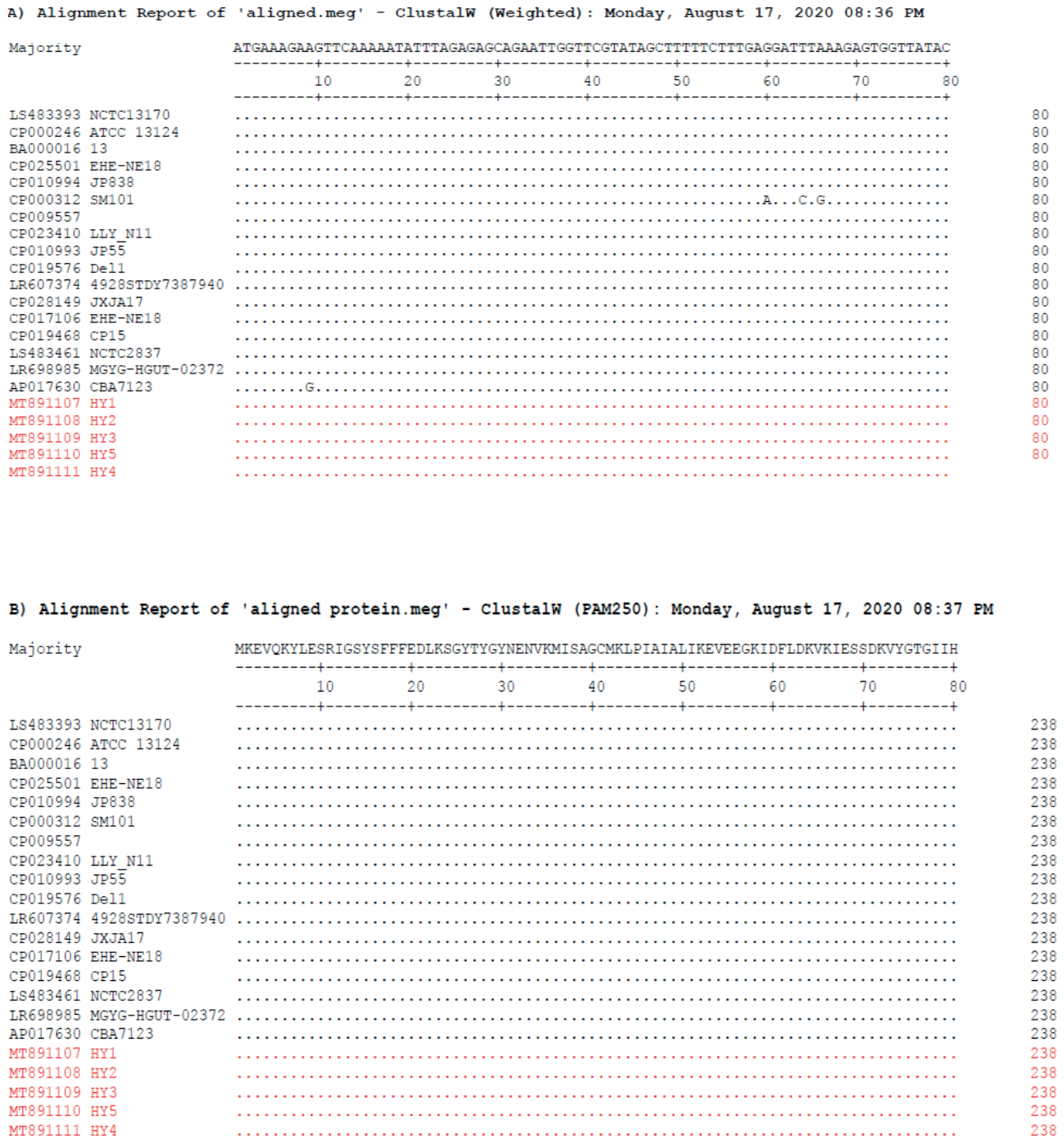

Figure 6. Nucleotides (A) and amino acid (B) graphic view of *bla* sequencing analysis showing similarities represented by dots and diversities represented by letters. Gene sequences submitted by the authors are colored red.

Conclusions

From the data presented above, it could be concluded that strains of *C. perfringens* isolated from herbs and spices retailed in the Egyptian market have a higher occurrence of *tpe*L but not *net*B toxin coding genes. Resistance of *C. perfringens* to tetracycline is partially dependent on the presence of *tet*K gene. At the same time, sensitivity to Penicillin is evident despite the presence of *bla*-gene at a high rate among isolates that has a high similarity to the sequences submitted to GenBank among global isolates of epidemiological concern. These findings expand knowledge about *C. perfringens* isolated from herbs and spices as food additives, which provide the scientific basis for efficient prevention and intervention of *C. perfringens*-caused problems in man and animals.

Acknowledgments

Not applicable.

Declaration

Conflict of interest: There is no actual or potential conflict of interest concerning this article.

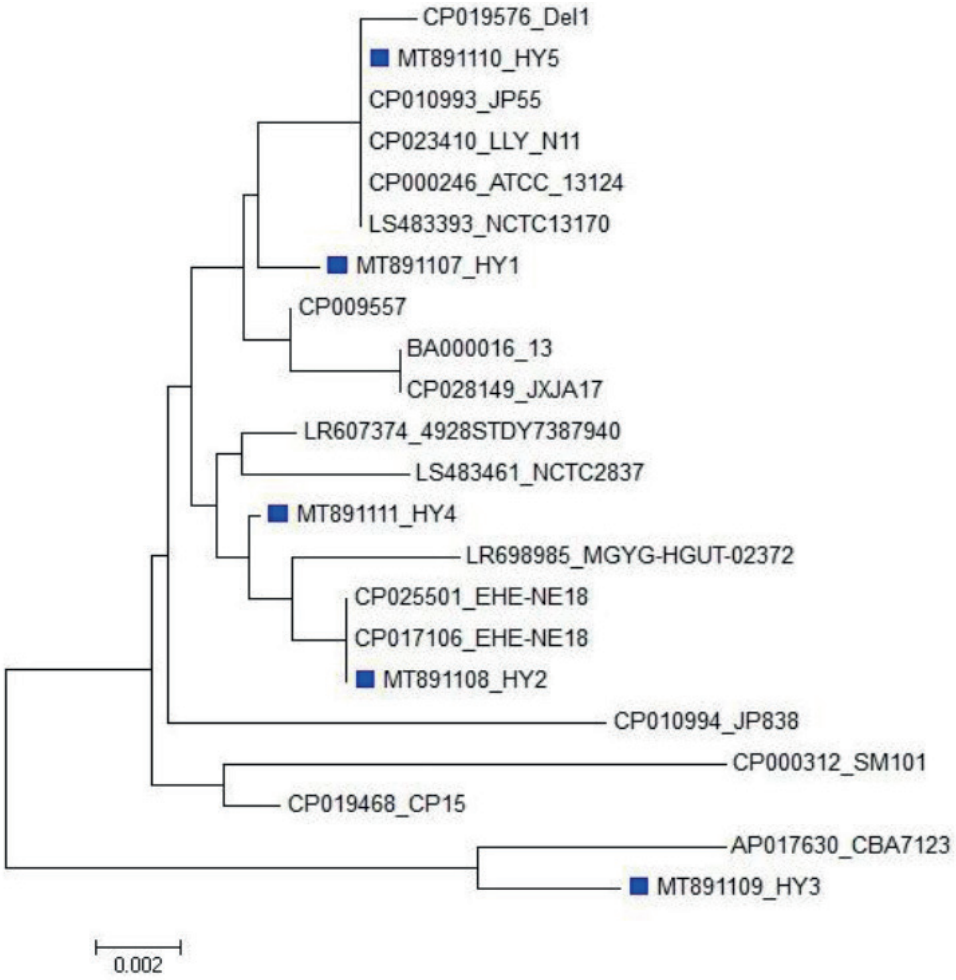

Figure 7. Phylogenetic analysis of nucleotide/amino acid sequences of *bla* coding gene of *C. perfringens* isolated from herbs and spices, the sequences of the present study are marked by blue squares among the sequences of GenBank.

Bibliographic references

1. Banerjee M, Sarkar PK. Growth and enterotoxin production by sporeforming bacterial pathogens from spices. Food Control 2004;15(6):491-496.
2. Aguilera MO, Stagnitta PV, Micalizzi B, de Guzmán AMS. Prevalence and characterization of Clostridium perfringens from spices in Argentina. Anaerobe 2005;11(6):327-334.
3. Banerjee M, Sarkar PK. Microbiological quality of some retail spices in India. Food Research International 2003;36(5):469-474.
4. Hampikyan H, Bingol EB, Colak H, Aydin A. The evaluation of microbiological profile of some spices used in Turkish meat industry. Journal of Food, Agriculture & Environment 2009;7(3&4):111-115.
5. Sagoo S, Little C, Greenwood M, et al. Assessment of the microbiological safety of dried spices and herbs from production and retail premises in the United Kingdom. Food microbiology 2009;26(1):39-43.
6. Vitullo M, Ripabelli G, Fanelli I, Tamburro M, Delfine S, Sammarco M. Microbiological and toxicological quality of dried herbs. Letters in applied microbiology 2011;52(6):573-580.
7. Debs-Louka E, El Zouki J, Dabboussi F. Assessment of the Microbiological Quality and Safety of Common Spices and Herbs Sold in Lebanon. J Food Nutr Disor 2 2013;4:2.
8. Hassan S, Altalhi A. Safety Assessment of Spices and Herbs Consumed In Saudi Arabia: Microbiological Quality and Toxin Production. Life Sci J 2013;10:2819-2827.
9. El-Tawab A, Abdallah M, Yusuf H. Incidence and antibiogram of Clostridium perfringens isolated from herbs and spices widely distributed in the Egyptian market. Benha Veterinary Medical Journal 2017;32(1):198-206.
10. Chen J, McClane BA. Characterization of Clostridium perfringens TpeL toxin gene carriage, production, cytotoxic contributions, and trypsin sensitivity. Infection and immunity 2015;83(6):2369-2381.
11. Bokori-Brown M, Savva CG, da Costa SPF, Naylor CE, Basak AK, Titball RW. Molecular basis of toxicity of Clostridium perfringens epsilon toxin. The FEBS journal 2011;278(23):4589-4601.
12. Van Immerseel F, Rood JI, Moore RJ, Titball RW. Rethinking our understanding of the pathogenesis of necrotic enteritis in chickens. Trends in microbiology 2009;17(1):32-36.
13. Keyburn AL, Boyce JD, Vaz P, et al. NetB, a new toxin that is associated with avian necrotic enteritis caused by Clostridium perfringens. PLoS pathog 2008;4(2):e26.
14. Coursodon C, Glock R, Moore K, Cooper K, Songer J. TpeL-producing strains of Clostridium perfringens type A are highly virulent for broiler chicks. Anaerobe 2012;18(1):117-121.
15. Datta S, Rakha N, Narang G, Arora D, Mahajan N. Prevalence of α, β and netb toxin producing strains of Clostridium perfringens in broiler chickens in Haryana. Haryana Vet 2014;53(1):39-42.
16. Bailey MA, Macklin KS, Krehling JT. Use of a Multiplex PCR for the Detection of Toxin-Encoding Genes netB and tpeL in Strains of Clostridium perfringens. International Scholarly Research Notices 2013;2013.
17. Catalán A, Espoz M, Cortés W, Sagua H, González J, Araya J. Tetracycline and penicillin resistant Clostridium perfringens isolated from the fangs and venom glands of Loxosceles laeta: its implications in loxoscelism treatment. Toxicon 2010;56(6):890-896.

18. Gholamiandehkordi A, Eeckhaut V, Lanckriet A, et al. Antimicrobial resistance in Clostridium perfringens isolates from broilers in Belgium. Veterinary research communications 2009;33(8):1031-1037.
19. Soge O, Tivoli L, Meschke J, Roberts M. A conjugative macrolide resistance gene, mef (A), in environmental Clostridium perfringens carrying multiple macrolide and/or tetracycline resistance genes. Journal of applied microbiology 2009;106(1):34-40.
20. Sambrook J, Fritsch E, Maniatis T. Gel electrophoresis of DNA and pulsed-field agarose. Molecular cloning: a laboratory manual 1989;1:441-542.
21. Altschul SF, Gish W, Miller W, Myers EW, Lipman DJ. Basic local alignment search tool. Journal of molecular biology 1990;215(3):403-410.
22. Thompson JD, Higgins DG, Gibson TJ. CLUSTAL W: improving the sensitivity of progressive multiple sequence alignment through sequence weighting, position-specific gap penalties and weight matrix choice. Nucleic acids research 1994;22(22):4673-4680.
23. Tamura K, Stecher G, Peterson D, Filipski A, Kumar S. MEGA6: molecular evolutionary genetics analysis version 6.0. Molecular biology and evolution 2013;30(12):2725-2729.
24. Welsh W, Nuttall G. A Gas Producing Bacillus (Bacillus aerogenes capsulatus, nov, spec.) Capable of Rapid Development in the Blood Vessels after Death. Johns Hopkins Hospital Bulletin 1892;3:81-91.
25. Popoff MR. Clostridial pore-forming toxins: powerful virulence factors. Anaerobe 2014;30:220-238.
26. Songer JG. Clostridial enteric diseases of domestic animals. Clinical microbiology reviews 1996;9(2):216.
27. Amimoto K, Noro T, Oishi E, Shimizu M. A novel toxin homologous to large clostridial cytotoxins found in culture supernatant of Clostridium perfringens type C. Microbiology 2007;153(4):1198-1206.
28. Beceiro A, Tomás M, Bou G. Antimicrobial resistance and virulence: a successful or deleterious association in the bacterial world? Clinical microbiology reviews 2013;26(2):185-230.
29. Martin TG, Smyth JA. Prevalence of netB among some clinical isolates of Clostridium perfringens from animals in the United States. Veterinary microbiology 2009;136(1-2):202-205.
30. Mirzazadehghassab A, Razmyar J, Kalidari GA, Tolooe A. Prevalence of netb and Tpel Genes among Clostridium perfringens Isolates Obtained from Healthy and Diseased Ostriches (Struthio camelus). the 12th biennial Congress of the Anaerobe Society of the Americas2014.
31. Bailey M, Macklin K, Krehling J. Low prevalence of netB and tpeL in historical Clostridium perfringens isolates from broiler farms in Alabama. Avian diseases 2015;59(1):46-51.
32. Marchand-Austin A, Rawte P, Toye B, Jamieson FB, Farrell DJ, Patel SN. Antimicrobial susceptibility of clinical isolates of anaerobic bacteria in Ontario, 2010–2011. Anaerobe 2014;28:120-125.
33. Yanagihara K, Akamatsu N, Matsuda J, Kaku N, Katsumata K, Kosai K. Susceptibility of Clostridium species isolated in Japan to fidaxomicin and its major metabolite OP-1118. Journal of infection and chemotherapy 2018;24(6):492-495.
34. Li J, Zhou Y, Yang D, et al. prevalence and antimicrobial susceptibility of Clostridium perfringens in chickens and pigs from Beijing and Shanxi, China. Veterinary Microbiology 2021;252:108932.
35. Wei B, Cha S-Y, Zhang J-F, et al. Antimicrobial Susceptibility and Association with Toxin Determinants in Clostridium perfringens Isolates from Chickens. Microorganisms 2020;8(11):1825.
36. Roberts MC, Sutcliffe J, Courvalin P, Jensen LB, Rood J, Seppala H. Nomenclature for macrolide and macrolide-lincosamide-streptogramin B resistance determinants. Antimicrobial agents and chemotherapy 1999;43(12):2823-2830.

Received: 11 March 2021
Accepted: 10 July 2021

RESEARCH / INVESTIGACIÓN

Investigate workers' health in the western industrial region, Mosul, Iraq

Salim Rabeea Znad[1], Mazin Nazar Fadhel[1], Ayça Erdem Ünşar[2]

DOI. 10.21931/RB/2021.06.03.16

Abstract: The current study aims to determine the level of heavy metal contamination in the Western Industrial Region of Mosul City, northern Iraq. Heavy metals such as(Pb ،Co ،Hg) are measured In the blood serum of 40 workers in the main industrial areas of Mosul City. It was compared with the control group of (40) people from Mosul university, Where is Far away from the industrial areas and all activities.

The results indicated a highly significant increase of P<0.001 in the serum of the workers in the industrial areas compared with the control group. The study investigates the impact of heavy metals on the workers' health in the industrial areas who are in direct contact with them.

Key words: Investigation, Heavy metals Pollution, Blood Serum, industrial Region.

Introduction

Industry areas are often associated with positive economic benefits such as job creation and increased standard of living; however, Industrial activities may also negatively impact the environment and human health. Industrial activities are dangerous to human health, as heavy metals, mainly Hg, Pb, and Cobalt (Co), are often released into the environment[1].

Metals such as lead (Pb), Cobalt (Co), mercury (Hg) are unknown Function in the environment[2].

These metals are quickly released into the environment via anthropogenic activities, e.g., metal plating facilities, mining, and agricultural activities[3].

Some of these metals are known to act as human mutagens and carcinogens and are associated with various human ailments such as cardiovascular, nervous system, blood and bone diseases, kidney failure, gingivitis, and tremors, among others[4].

Mercury (Hg) is present in the Earth's crust. Although present in the environment and atmosphere in small quantities, it is release through anthropogenic emissions. Mercury toxicity is not limited to humans; it is also toxicity to animals and plants[5].

Natural sources of mercury in the environment include mercury vapor from volcanoes and forest fires. More recent anthropogenic sources include burning coal and fossil fuels, mining mercury, precious metal refinement, electrical and automotive part manufacture, chemical processing, and release through waste incineration, landfills, and industrial contamination of water systems[6].

Cobalt (Co) is a typical toxic trace metal that is widely found in Industrial Waste. Environmental exposure to this toxic trace metal occurs primarily through smoking and industrial plant emissions, and contaminated food and water[7]. (Co) has a half-life period of 15-30 years and accumulates in the liver as the primary target tissue[1]. This toxic trace metal can cause liver or renal cell apoptosis in a low dose of exposure[8].

Lead (Pb) is the third most abundant metal on the planet and is highly available in soil and water. Due to its impacts on the environment and human health, the scientific community is interested in investigating both issues, especially when considering that humans are mainly exposed to) Pb) through drinking water, household goods, cosmetics, and drugs[9]. Then, the (Pb) ability to cross the blood-brain barrier features its tropism for the central nervous system[10]. Modulating cell biochemistry and tissue integrity and may drive behavioral dysfunctions[11].

Researchers such as (12) indicated in their study about measuring the concentrations of heavy metals (Pb, Ni, Co, Fe Cu, Zn) in serum blood comparison of The industrial workers with the control group (employees of the University of Mosul), that there are Hight significant increase og Heavy metals in the serum of the workers who are in the industrial areas compared with the control group.

Materials and methods

Study Area

The study area is the city of Mosul, which is located in the western part of Iraq, between the longitude of 41° - 44° and the latitude of 35°-37°. In particular, the industrial region of the city is the manufacture of the Wadi Okab on the right side (the western part) (Figure 1).

Study Design

The blood samples were taken from (40) industrial agents randomly and from two main areas, namely the manufacture of the Wadi Okab (right side) industry. In addition to taking blood samples from (40) people as a control group working at Mosul University and without a history of industrial activity. The control group is not different from workers in terms of gender and age groups.

Demographic information

Participant demographic information was collected using a researcher-made questionnaire. Information was further verified by cross-checking with medical records (age, gender, number of years spent at work, smoking cases)[13].

Ethics approval

All participants in the study approved the study gave their permission to access their medical records, blood sampling, and anonymous use of their samples.

[1] College of Environmental Sciences and Technology, Depart. Of Environmental Sciences, University of Mosul.
[2] Faculty of Engineering. Department of Environmental Engineering. Akdeniz University.

Corresponding author: salim.znad@yahoo.com

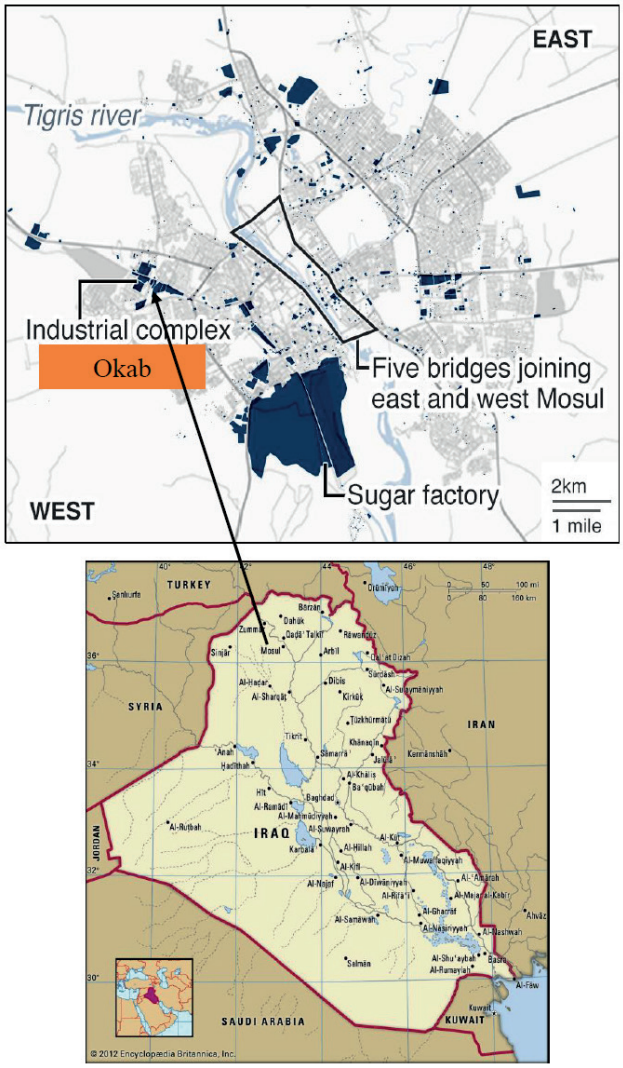

Figure 1. Location of Study Area in the western industrial region, Mosul, Iraq.

Blood samples

Samples were taken from (40) workers in (plastic recycling plant, mechanics, car thighs). (40) samples were taken of those working at Mosul University as a control group. 5 mL of vein has been withdrawn and placed into a test tube with information for each person. They were transferred to the laboratory and separated by centrifuge at 4,000 rpm for 15 minutes, then isolated serum samples and kept samples at -4 until analyzed. The serum samples were then diluted by 5:1 with ions-free water. The Atomic Absorption (flame) device was used to estimate the Heavy Metals in the serum.

Statistical analysis

The data is analyzed with some statistical processes by SPSS in its copy 16 and expressed in the mean ± Standard Deviation (SD). The value of 0.05 was considered to indicate the existence of statistically significant differences.

Results and discussion

The results show that there is a clear mental difference of ($P<0.001$) for elements (Pb, Co, Hg) element. There is an apparent increase in the mix of elements measured in the control group's industrial workers' serum (Table 1) and (Figure 2).

The toxicity of heavy metals occurs when they build up in the body's soft tissue and are not metabolic[14]. The human body enters through food, water, air, or absorption by the skin when direct contact is made with it in agricultural environments and industrial areas that are the general path of exposure of adults to the risk of these elements[15].

Environmental pollution poses a health threat to the entire world[16]. The concentration of heavy metals in serum above 1 µg/L indicates that there are potential environments to which the individual is exposed, and the concentration above 5 µg/L indicates that toxic substances already exist[17].

Conclusions

The study results indicate a high increase in the concentration of heavy metals in the blood of workers in the industrial area (paint workers, mechanics, plastic recycling workers, blacksmiths) For those who do not work in this field. In the future, this may cause severe health and general environmental problems. The Iraqi environment is contaminated with heavy metals, especially in industrial places, where its members are exposed to many dangers of these elements, which cause many health problems.

Recommendation

Current workplaces in industrial zones are unsafe for workers or their families. Professionals and workers need more secure support by providing and introducing other alternatives in less polluted and safer industrial processes. More heavy metals risk awareness workshops are also required for its harm to the general environment.

Bibliographic references

1. Dooyema CA, Neri A, Lo YC, Durant J, Dargan PI, Swarthout T, Biya O, Gidado SO, Haladu S, Gwarzo NS, Nguku PN, Akpan A, Idris S, Bashir AM, Brown. Outbreak of fatal childhood lead poisoning related to artisanal gold mining in northwestern Nigeria, 2010. Environ Health Perspect [Internet]. 2012 Apr [cited 2015 May 25].
2. Zheng J, Chen KH, Yan X, Chen SJ, Hu GC, Peng XW, Yuan JG, Mai BX, Yang ZY. Heavy metals in food, house dust, and water from an e-waste recycling area in South China and the potential risk to human health. Ecotoxicol Environ Safety [Internet]. 2013 Oct 1 [cited 2015 May 25];96:205-12.
3. Matović, V., Buha, A., Đukić-Ćosić, D., Bulat, Z., . Insight into the oxidative stress induced by lead and/or cadmium in blood, liver and kidneys. Food Chem. Toxicol. 2015; 78, 130-140.
4. Olujimi O, Steiner O, Goessler W. Pollution indexing and health risk assessments of trace elements in indoor dusts from classrooms, living rooms and offices in Ogun State, Nigeria. J Afr Earth Sci [Internet]. 2015 Jan [cited 2015 May 25]; 101:396-404.
5. Bose-O'Reilly. Mercury exposure and children's health. Curr Probl Pediatr Adolesc Health Care. 2010;40(8):186–215.
6. Bernard, A.,. Renal dysfunction induced by cadmium: biomarkers of critical effects. Biometals2004; 519-523.
7. Eisler R .Mercury hazards from gold mining to humans, plants, and animals. Rev Environ Contam Toxicol. 2004; 181:139–98.
8. Eck, P. and Wilson, L., Toxic Metal In Human Health And Disease. Applied Nutrition and Bioenergetics, Ltd., 1989; 8650 N.
9. Tower, S. S., . Cobalt Toxicity in Two Hip Replacement Patients. Bulletin.2010; No. (14): 28.
10. Fernandez-Lorenzo JR . Aluminum contents of human milk, cow's milk, and infant formula. J Pediatr Gastroenterol Nutr 1999; 28(3):270–275

Elements	Grouping	N	Mean ± SD (ppm)	p-Value
Pb	Workers Control	40 40	1.4050 ± 0.66872 0.7095 ± 0.71500	p<0.001
Co	Workers Control	40 40	0.9890 ± 0.49871 0.5545 ± 0.50351	p<0.001
Hg	Workers Control	40 40	0.5590 ± 0.69120 0.3835 ± 0.20709	p<0.001

P< 0.05 Significant P> 0.05 No significant

Table 1. Determination of heavy metals in Area of workers & controls groups.

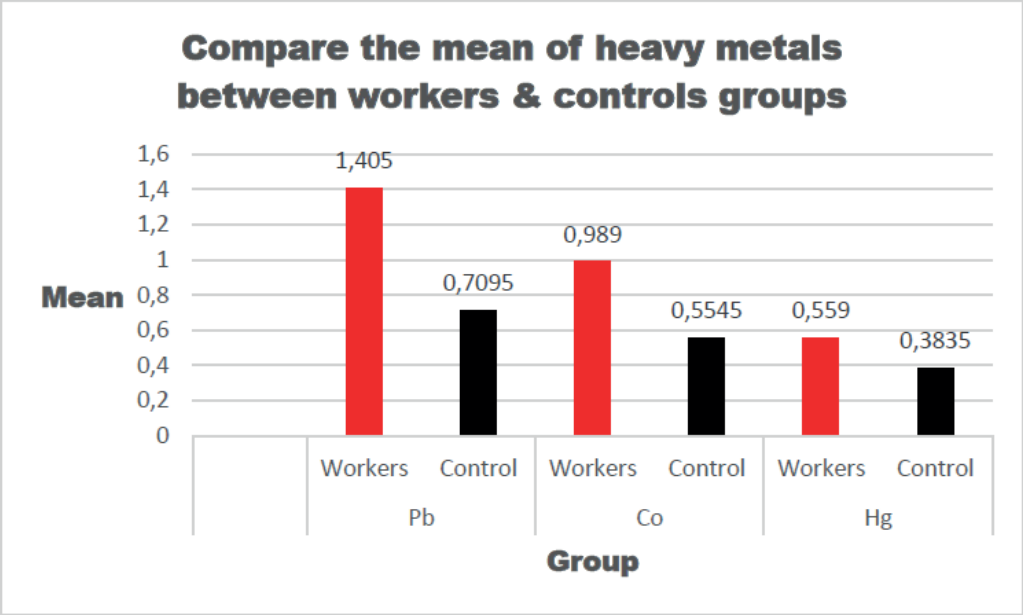

Figure 2. Compare the mean of heavy metals between workers & controls groups.

11. Gauthier E, Fortier I, Courchesne F, Pepin P, Mortimer J,Gauvreau D. Aluminum forms in drinking water and risk of Alzheimers disease. Environ Res2000; 84(3):234–246.
12. Znad, Salim Rabee. and Al-Sinjary, MazinNazar . The vital accumulation of some Heavy metals in the blood serum of industrial zone workers in Mosul city. Plant Archive journal volume 2020; 20. Supplement 1 , pp 3194- 3200 .
13. Kozlowski H, Brown DR, Valensin G . Metallochemistry of neurodegeneration: biological, chemical and genetic aspects.Royal Society of Chemistry,2007; London
14. Rashed MN. Total and extractable heavy metals in indoor, outdoor and street dust from Aswan City, Egypt. Clean – Soil, Air, Water [Internet]. 2008 Nov [cited 2015 May 25];36(10-11):850-7.
15. Satarug, S., Moore, M.R.. Adverse health effects of chronic exposure to low-level cadmium in foodstuffs and cigarette smoke. Environ Health Perspect 2004; 112, 1099-1103.
16. Sun G, Li Z, Bi X, Chen Y, Lu S, Yuan X. Distribution, sources and health risk assessment of mercury in kindergarten dust. Atmospheric Environ [Internet]. 2013 Jul [cited 2015 May 25];73:169-76.
17. Verougstraete, V., Lison, D., Hotz, P.,. Cadmium, lung and prostate cancer: a systematic review of recent epidemiological data. J Toxicol Environ Health B Crit Rev 2003; 6, 227-255.

Received: 11 March 2021
Accepted: 10 July 2021

RESEARCH / INVESTIGACIÓN

Synthesis, *in silico* studies and antibacterial assessment of α-amino phosphonates derivatives

Bouchra El Khalfi[1], Boutaina Addoum[1], Suhayla Harrati[1], Abdelhakim Elmakssoudi[2] and Abdelaziz Soukri[1]

DOI. 10.21931/RB/2021.06.03.17

Abstract: The widespread of multi-resistant strains due to the lack of specific treatment and the propagation of infectious diseases requires all resources to remedy this scourge. This study is therefore aimed to assess the antibacterial activity of four synthetic α-Aminophosphonate 4(a-d). Methods: Firstly, α-Aminophosphonate has been synthesized and characterized, then molecular docking of these compounds 4(a-d) into the active binding site of *Escherichia coli* MurB enzyme (PDB Id: 1MBT) was performed to gain a comprehensive understanding of their biological activity. These compounds have been subjected to in vitro antibacterial screening against three multi-resistant strains *E. coli*, *S. aureus*, and *L. monocytogenes*. These compounds showed crucial antibacterial behavior against all studied strains. Thus, their docking estimation supported the in vitro results and showed that the 4c derivative has considerable binding energy towards the active site of *Escherichia coli* MurB. These findings provide critical information for the exploration of α-amino phosphonates as novel antibacterial agents.

Key words: α-Aminophosphonate, Docking, Antibacterial.

Introduction

The emergence and widespread bacterial resistance to antibiotics dramatically sapped our ability[1] to remedy this infection and precipitate an alarming public health dilemma[2]. Nowadays, the new obsession of researchers is to innovate new therapeutic approaches able to overcome these microbial diseases[3]. Several studies have been focused on the synthesis of eco-friendly substances[4]. Among these molecules, α-amino phosphonates take a leading position[5], especially in biological and environmental applications[6–9].

These compounds attracted the renewed interest of biologists due to their wide-ranging activities; they are recognized as an overwhelming inhibitor of enzymes like serine[10], UDP-galactopyranose mutase[11], and the viral enzyme human immunodeficiency virus protease. Likewise, they limited metastatic progression, activated different apoptosis pathways, and induced anti-tumoral cytotoxicity.

In this regard, the current study pertains to the synthesis and characterization of some α-amino phosphonates derivatives 4(a-c), then we evaluated *in silico* their antimicrobial potential[12] based on a computer-aided simulation[13]. Then, we tested their antibacterial behavior on resistant strains and their synergistic effect with some standard antibiotics.

All this investigation is essential to understand better the mechanism of action of these molecules, which could offer an exceptional framework that may lead us to the discovery of new potent antibiotics.

Methods

The general protocol of α-amino phosphonates synthesis

The multicomponent synthesis of the 4 derivatives of α-amino phosphonates was carried out through the well-established literature protocol[14,15]. We grafted an aromatic aldehyde (1a), aniline (2), and diethyl phosphite (3) in the presence of $Na_2CaP_2O_7$ as a catalyst[16]. A plausible reactional mechanism of the one-pot domino reaction is illustrated in Scheme S1of ESI.

Characterization of th α-aminophosphonates 4(a-d)

Characterization of the Diethyl(phenyl)-N-(phenyl) aminomethylphosphonate 4a

^{1}H-NMR (CDCl3) δ: 1.2 (3H, J_{HH}= 7.2 Hz, t, OCH_2CH_3); 1.4 (3H, J_{HH}= 7.2 Hz, t, OCH_2CH_3); 3.73-4.3 (4H, m, OCH_2CH_3); 4.9 (1H, J_{HP}= 24.6 Hz, d, CHP), 5 (1H, s, NH); 6.6-7.8 (10H, m, HAr).13C-NMR (CDCl3) δ: 16.46 (d, 3JCP= 6.03 Hz, OCH_2CH_3); 16.7 (d, 3JCP= 6.03 Hz, OCH_2CH_3); 56.35 (d, 1JCP = 149 Hz, CHP); 63.5 (d, 2JCP = 6.79Hz, OCH_2CH_3); 63.53 (d, 2JCP = 6.79 Hz, OCH_2CH_3); 114.13 (s); 118.64 (s); 128.1 (s); 128.85 (s); 129.43 (s); 136.2 (s); 146.6 (s). IR (KBr) υ 3304(NH), 2985(CH), 1605 (C=C), 1514 (C=C), 1240 (P=O),1020 (P-O) cm^{-1}.

Diethyl(4-methoxyphenyl)-N-(phenyl) aminomethylphosphonate 4b

^{1}H-NMR ($CDCl_3$) δ : 1.25 (3H, J_{HH}= 7.2 Hz, t, OCH_2CH_3); 1.4 (3H, J_{HH}= 7.2 Hz, t, OCH2CH3); 2.45 (3H, s, $C_6H_4CH_3$);3.79-4.31 (4H, m, OCH_2CH_3); 4.87 (1H, JHP= 24.6 Hz, d, CHP), 5 (1H, s, NH); 6.71-7.5 (9H, m, HAr).13C-NMR (CDCl3) δ: 16.5 (d, 3JCP= 5.8 Hz, OCH_2CH_3); 16.71 (d, 3JCP= 5.8 Hz, OCH_2CH_3); 21.4 (s, C6H4CH3); 56 (d, 1JCP = 150 Hz, CHP); 63.48 (d, 2JCP = 6.94 Hz, OCH_2CH_3); 114.14 (s); 118.57 (s); 128 (s); 129.4 (s); 129.55 (s); 129.58 (s); 133 (s); 137.8 (s);146.8 (s). IR (KBr) υ 3325 (NH), 2980 (CH), 1604 (C=C), 1498 (C=C), 1234 (P=O), 1016 (P-O) cm^{-1}.

Characterization of the Diethyl(2-hydroxyphenyl)-N phenyl) Aminomethylphosphonate 4c

^{1}H-NMR ($CDCl_3$) δ : 1.25 (3H, J_{HH}= 7.2 Hz, t, OCH_2CH_3); 1.39 (3H, J_{HH}= 7.2 Hz, t, OCH_2CH_3); 3.86 (3H, s, $C_6H_4OCH_3$);3.8-4.26

[1] Laboratory of Physiopathology, Genetics, Molecular and Biotechnology (PGMB), Department of Biology, Faculty of Sciences Aïn Chock, Research Center of Health and Biotechnology, Hassan II University of Casablanca, B.P 5366 Maarif, Casablanca, Morocco.

[2] Laboratory of Organic Synthesis, Extraction, and Valorization, Department of Chemistry, Faculty of Sciences Aïn Chock, Hassan II University of Casablanca, B.P 5366 Maarif, Casablanca, Morocco.

Corresponding author: addoum636@gmail.com

(4H, m, OCH_2CH_3); 4.85 (1H, J_{HP}= 23.1 Hz, d, CHP), 4,95 (1H, s, NH); 6.7-7.53 (9H, m, HAr).^{13}C-NMR ($CDCl_3$) δ: 16.53 (d, $^3J_{CP}$= 5.7 Hz, OCH2CH3); 16.72 (d, $^3J_{CP}$= 5.7 Hz, OCH_2CH_3); 55.44 (s, $C_6H_4OCH_3$); 55.62 (d, $^1J_{CP}$ = 151,2 Hz, CHP); 63.43 (d, $^2J_{CP}$ = 6.9 Hz, OCH_2CH_3); 63.47 (d, $^2J_{CP}$= 6.9 Hz, OCH_2CH_3);114.15 (s); 114.32 (s); 118.57 (s); 128 (s); 129.2 (s); 129.33 (s); 146.67 (s); 159.56 (s). IR (KBr) υ 3300 (NH), 2983 (CH), 1600 (C=C), 1510 (C=C), 1232 (P=O), 1020 (P-O) cm^{-1}.

Characterization of the Diethyl(4-methylphényl)-N(phenyl)aminomethylphosphonate 4d

^{1}H-NMR ($CDCl_3$) δ : 1.25 (3H, J_{HH}= 7.2 Hz, t, OCH_2CH_3); 1.39 (3H, J_{HH}= 7.2 Hz, t, OCH_2CH_3); 3.86 (3H, s, $C_6H_4OCH_3$);3.8-4.26 (4H, m, OCH_2CH_3); 4.85 (1H, J_{HP}= 23.1 Hz, d, CHP), 4,95 (1H, s, NH); 6.7-7.53 (9H, m, H_{Ar}).^{13}C-NMR ($CDCl_3$) δ: 16.53 (d, $^3J_{CP}$= 5.7 Hz, OCH_2CH_3); 16.72 (d, $^3J_{CP}$= 5.7 Hz, OCH_2CH_3); 55.44 (s, $C_6H_4OCH_3$); 55.62 (d, $^1J_{CP}$ = 151,2 Hz, CHP); 63.43 (d, $^2J_{CP}$ = 6.9 Hz, OCH_2CH_3); 63.47 (d, $^2J_{CP}$= 6.9 Hz, OCH_2CH_3);114.15 (s); 114.32 (s); 118.57 (s); 128 (s); 129.2 (s); 129.33 (s); 146.67 (s); 159.56 (s). IR (KBr) υ 3300 (NH), 2983 (CH), 1600 (C=C), 1510 (C=C), 1232 (P=O), 1020 (P-O) cm^{-1}.

Biological experimental data)

Computational studies

Determination ADMET parameters

The ADMET parameters (absorption, distribution, metabolism, excretion, and toxicity of the synthesized compounds 4(a-d) were calculated using the freely accessible web server Swiss ADME (http://swissadme.ch/index.php#undefined)[17]

Protein-Ligand Docking calculations

After preparing protein/ligands structures, we stimulated the docking interaction using the software AutoDock 1.5.6 (MGL tools- 1.5.6)[18]. Polar hydrogen atoms and Kollman united charges were added to all target proteins, and the resulting file has been saved in pdbqt extension. For the docking calculation, a grid box of 60×60×60 Å in x, y, z directions were created to cover the active site of the target. The default grid points spacing was fixed to 0.375 Å and centred at x = 42.527 y = -46.679, z = 65.559. We used in this work the Lamarckian Genetic Algorithm (LGA) for flexible docking calculations. The LGA parameters including size, energy screening, mutation rate, and crossover rate. After the calculation procedure, we selected the best conformations of the complex from the 10 calculated based on their binding energy scores. Then the complex interaction map was displayed using Discovery Studio Visualizer[17,19].

Microbiology

Bacterial strains

Three bacterial strains *E. coli*, *S. aureus*, and *L. monocytogenes* have been used in this study. The media used for antibacterial screening was the LB and the Brain Heart Infusion (BHI).

Preparation of stock solutions

To prepare a final concentration of 5 µg / ml, we solubilized the selected compounds in DMSO (16.66 µg / ml). Then the stock solutions were stored in sterile containers in obscurity.

Antibiotics

Stocks of antibiotics: ampicillin (100 mg / ml), chloramphenicol (34 mg / ml) and rifampicin (50 mg / ml) were prepared, filtered and stored at -20 ° C until microbiological assays. The chloramphenicol is prepared in ethanol and rifampicin was formulated in methanol.

Antibacterial sensitivity test

The compounds 4(a-d) were tested for their antibacterial activity against *E.Coli*; *S.aureus*, and *L.monocytogene* by using the agar well diffusion method[20]. To explore the antibacterial effect of these compounds, we subculture the different strains by streaking the supercooled media (LB and BHI) with bacterial inoculum adjusted to 10^6 CFU (bacteria/ml) then poured into Petri dishes. After 15 minutes, wells of 6mm were made on each plate by using a sterile cone. Under aseptic conditions, we injected separately 50 µl of the tested molecule; positive control (antibiotic), and negative control (DMSO) in each well. The Petri dishes were incubated at 30 - 37 ° C for 24h. All tests were performed in triplicate.

Test of synergistic effect

We used the diffusion assay described previously to study the synergistic effect between standard antibiotics and the target compounds. Firstly, wells were produced in each plate and filled with 50 µl of the tested samples containing the mixture of molecules and antibiotics. The Petri dishes are maintained at 30 ° - 37 ° C for 24 hours. The use of antibiotics singly serves as a positive control and DMSO is considered a negative control. All tests were obtained in triplicate.

Results

ADMET studies

The ADMET data provides information on the lipophilicity of the ligands, which is predicted by the MIlog P parameter, the hydrogen bonding potential of the compounds, and their molecular flexibility[21]. The different drug-likeness proprieties for all selected compounds were in harmony with Lipinski's rule of five[12] (see table 1).

Binding energy evaluation

Modeling studies are essential to understand the mechanism of action of these designed compounds. Our Docking investigation has been confirmed that the highest energies of binding (ΔG) observed are -6.44 and -6.45 K. cal/mol for the 4c and the 4a (see table 2), which can reflect the good affinity between the protein targeted and ligand in contrast to the ligand of reference (ciprofloxacin).

All the docked molecules were subjected to 2D protein-ligand interaction analysis and the obtained conformations compared to the Ciprafloxin have been reported in Figures 3. The selected compounds complex to the target enzyme (MurB) represented at least two H-bonds. Accordingly, the docking studies of α-amino phosphonates gathered previously in table 2 revealed their free energy of binding to *E. coli* UDP-N-acetylenolpyruvoylglucosamine reductase (MurB) was higher for all compounds than the score obtained for standard antibiotic (Ciprofloxacin). Hence, we can conclude that *E. coli* MurB is the putative target responsible for the antibacterial activity of these compounds[22]. Their interaction with the target was stabilized by forming hydrogen bonds, hydrophobic interactions, Van der walls Pi-sulfur and Pi-alkyl interactions (Figure 1).

Additionally, the binding mode of the most active compound 4c (binding energy: -6.45 kcal/mol) showed two hydro-

Compounds	MW [a]	MLogP[b]	nHBA [c]	nHBD [d]	nRB [e]	TPSA [f]	Lipinski
Rules	<500	≤4.15	<≤10	≤5	≤10	<160 Å	
4a	319.34 g/mol	4	3	1	8	57.37	Yes; 0 violation
4b	333.36 g/mol	3.65	3	1	8	57.37	Yes; 0 violation
4c	349.36 g/mol	3.28	4	1	9	66.60	Yes; 0 violation
4d	336.34 g/mol	2.42	5	1	6	82.64	Yes; 0 violation

[a]Molecular Weight; [b] Calculated Lipophilicity (MLog Po/w); [c] Number of Hydrogen Bond Acceptor; [d] Number of Hydrogen Bond Donor; [e] Number of Rotatable Bond; [f] Topological Polar Surface Area.

Table 1. Determination of pharmacokinetic parameters for good oral bioavailability of synthesized compounds 4(a-d).

Ligand	Energie (KJ/mol)	Residue involved	RSM(Å)
4a	**-6.44**	**Gly 219 and Ser 64**	**1.52**
4b	-5.59	Arg 207 Ile 59 Val 181 Gly 61	1.54
4c	**-6.45**	**Val 181 and Ile 59**	**1.16**
4d	-6.29	Arg 207 Pro 123 Cyst 218	1.84
Ciprafloxin	**-5.4**	**Arg 207 Pro 123 Val 181 Ile 59 Ser 64**	**0.9**

Table 2. The binding score of the tested compounds docked into the active site of 1MBT.

gen bonds formed between the oxygen atom and the amino acid Ile 59. We also detected the formation of close interaction with Val 181 via a hydrogen bond. Moreover, Pi-alkyl and Pi-sulfur interactions are formed with the residues Leu 80Lys 292 and Met 132. These amino acids reside at the enzyme's active site and are crucial in the biosynthesis of peptidoglycan; any modifications in these amino acids could down-regulate the enzyme activity, which induces bacterial cell death23.

In vitro studies

The antibacterial effect of the four synthesized compounds against the three strains was investigated by using the diffusion method, and the results are reported in Table 3. The obtained data showed clearly that the 4c compound possesses significant activity against the whole strains compared to the other derivatives. We also observed that the 4a and 4b were more actives against *E. coli* and *S. aureus*, while the 4d compound showed a substantial activity only against *L. monocytogenes*. On the other side, no inhibition zone was detected with vehicle control (DMSO).

Synergistic Test

The effect of the combination between the 4 synthesized products and antibiotics viz ampicillin, chloramphenicol, and rifampicin on the viability of the strain are summarized in figures 2 and 3.

By comparing the above results, it's exciting to underline that the synergistic effect of the synthesized products varies as a function of the studied strain and the antibiotic used. The potent inhibition was detected against *S. aureus* and *L. monocytogenes* after rifampicin to the 4 b and 4c compounds. Nevertheless, when we combine ampicillin/4b, chloramphenicol/4b, and chloramphenicol/4c we obtain a sizable activity only against *E. coli* (G- bacteria).

Discussion

The *in silico* data have been supported our study *in vitro* performed previously against Multi-resistant strains. According to our docking finding, all the selected compounds had H-bond interactions with the MurB enzyme indicating that the binding affinity increased significatively with the number of the H-bond, which reflects the stability of the complex ligand-protein.

We also observed that the studied compounds fulfill Lipinski's rule requirements and represent a high binding score with an RSM (root square mean) value < 2Å, which confirms their antibacterial inhibiting activity and the reliability of our virtual screening[24]. Based on molecular docking analysis, we can conclude that the putative mechanism of antibacterial activity observed *in vitro* is probably the inhibition of the *E. coli* MurB enzyme. This enzyme catalyzed the second step in forming muramyl sugar[22], which is essential for peptidoglycan biosynthesis[25,26].

On the other side, the sensitivity of the studied strains against these molecules provides their antibacterial potency estimated using an inhibition zone formed around the well. If we should classify these molecules as a function of their increasing antibacterial potential order: the 4c compound takes the place position due to their great effect against the three multi-resistant strains viz *S. aureus*, *E. coli* et *L. monocytogenes*(4c>4b> 4a >4d). At the same time, the three other compounds possessed a variable antibacterial activity as a function of the strain used. For example, the 4a and 4b derivatives possess antibacterial activity against gram-negative strains (*E. coli*); Nevertheless, the 4d derivative is more efficient against gram-positive strains(*L. monocytogenes* and *S.aureus*). It's gratifying to elucidate that this antibacterial sensitivity presu-

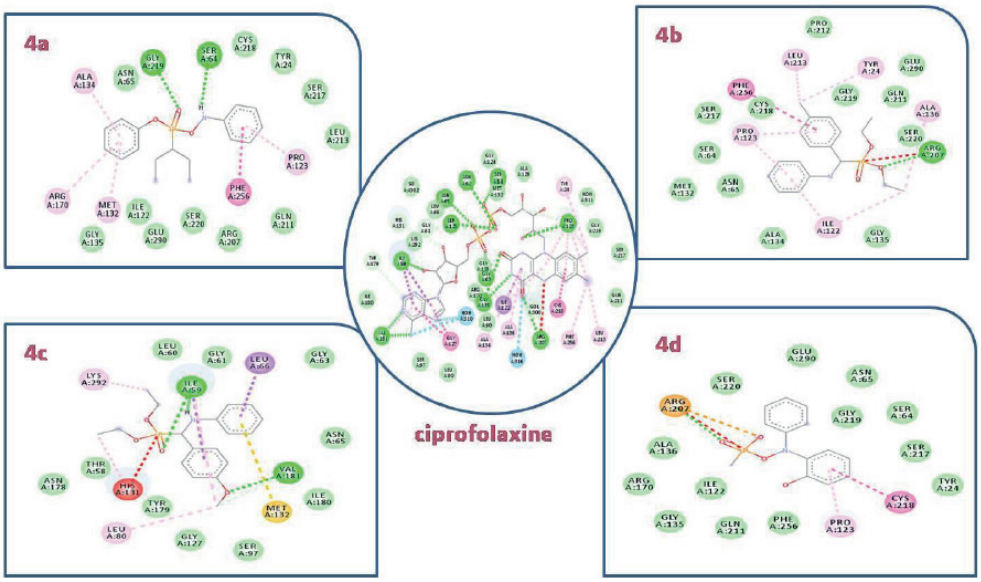

Figure 1. 2D docking diagrams of compounds 4a, 4b, 4c and,4d at the active site of MurB.

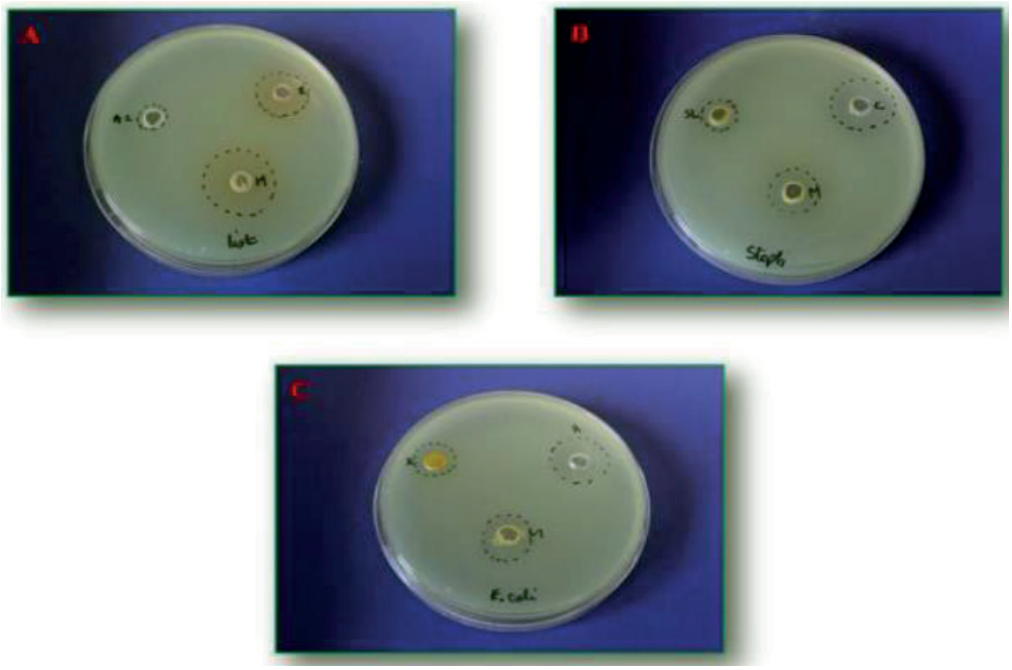

Figure 2. Synergistic effect between α-amino phosphonates and commercial antibiotics. A: a mixture between rifampicin and compound 4b, B: chloramphenicol supplemented to 4c, and C: ampicillin added to the compound 4c. *M: molecule/antibiotic, List: L. *monocytogenes*, Staph: *S. aureus.*

mably related to the structure of the tested compounds, as described the substitution of bioactive motive such methyl previously; methoxy, or metoxybenzaldhyde in the phenyl ring enhance this activity[27]; as results when the aromatic aldehyde is replaced with hydroxyl scaffold, we notice a slight and inconspicuous antibacterial activity[28,29].

Our results are in harmony with some previous studies. It's gratifying to cite the research work published in 2011[30], and they showed the excellent antibacterial and antifungal behavior of these compounds[30]. Another research work achieved in 2020[5] also confirmed their main antibacterial activity against a panel of gram-positive and harmful strains.

Despite their excellent antibacterial effects, in some cases, these pathogens strains can escape from the effect of these substances[31,32]. This new situation compelled the researchers to develop new promising strategies. Our study selected a simple method by combining the synthesized compounds and some antibiotics of references.

The approach adopted herein has given a satisfactory result. On the one hand, we noticed an increase in antibacterial activity. On the other hand, we obtained a powerful effect with a lower concentration of antibiotics.

Conclusions

In this study, four derivatives of α-amino phosphonates were successfully synthesized, then assessed for their antibacterial activity *in vitro* and *silico*.

The obtained data revealed that all studied compounds are biologically active and possess potent antibacterial activities, especially the 4*a* derivative.

With biological evaluation and docking results in hand, we

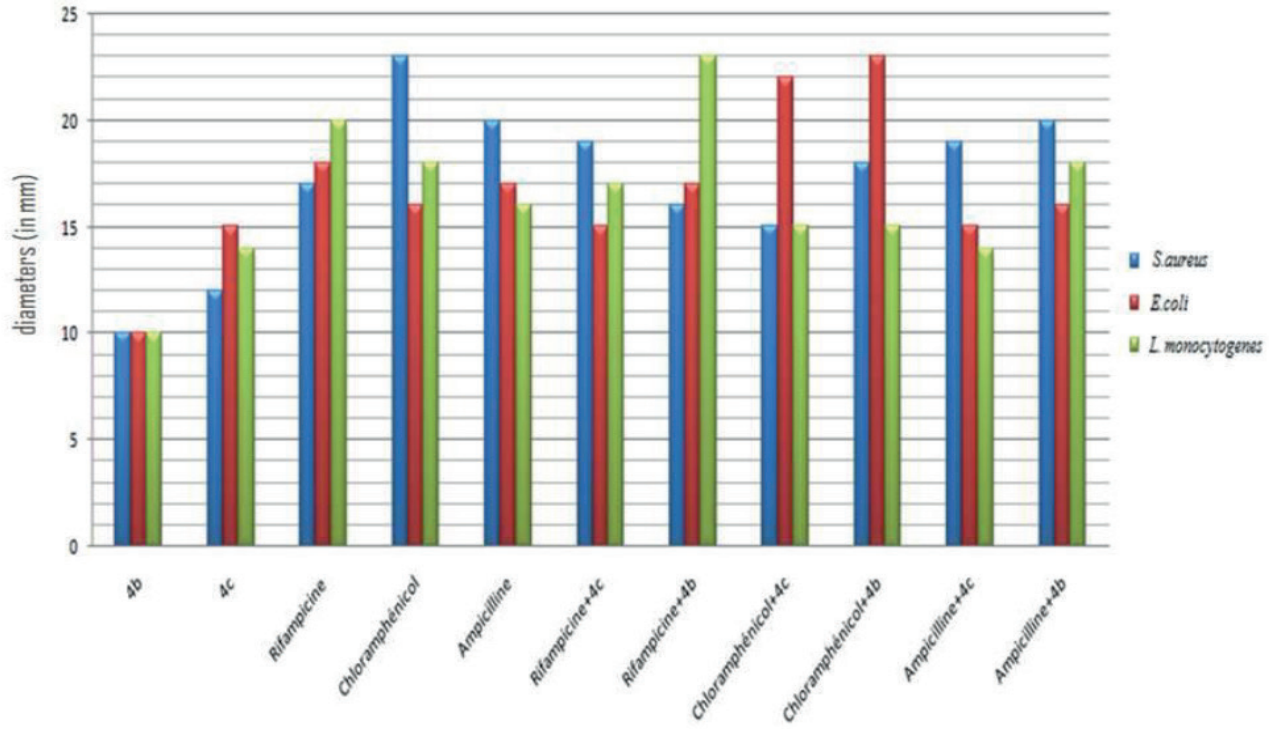

Figure 3. The plot of a synergistic effect of α -amino phosphonates/antibiotic on the growth inhibition of studied strains.

Stains	*E. coli*			*L. monocytogenes*			*S. aureus*		
	IZD* expressed in mm								
	1\2	1\4	1\8	1\2	1\4	1\8	1\2	1\4	1\8
4a	**12**	**10**	**9**	**10**	**9**	**8**	**11**	**9**	**7**
4b	**11**	**12**	**11**	**10**	**8**	**6**	**10**	**8**	**6**
4c [a]	**19**	**17**	**14**	**18**	**17**	**14**	**18**	**17**	**16**
4d	**10**	**8**	**7**	**12**	**12**	**10**	**10**	**8**	**6**

*IZD is the inhibition zone diameter calculated in mm.

Table 3. Antibacterial activity of the synthesized compounds 4(a-d).

can propose a plausible mode of action of these compounds before evaluating their biological activity *in vitro* and *in vivo*.

Limit of studies

Given the above facts, a single bioassay is not able to reflect the full picture of the derivatives' effects on multi-resistant bacteria.

Recommendations for future studies

We recommend using another bacterial species (Gram- and Gram+) to provide broad information about the antibacterial potential of these compounds.

Acknowledgments

This work was supported by the CNRST (Moroccan research center of science and technology) under the Research Excellence Scholarship Program.

Finding statement

This research was conducted within the university research plans and benefited from the general funds granted to the physiopathology, molecular genetics, and biotechnology laboratories.

Conflicts of Interest

None

Author contributions

B. Addoum, A. Soukri, B. El Khalfi, and H. Elmakssoudi contributed to the study's design. S. Harrati wrote and reviewed the draft of the manuscript.

Bibliographic references

1. Vouga M, Greub G. Emerging bacterial pathogens: The past and beyond. Clin Microbiol Infect [Internet]. 2016;22(1):12–21. http://dx.doi.org/10.1016/j.cmi.2015.10.010
2. Bonneaud C, Weinert LA, Kuijper B. Understanding the emergence of bacterial pathogens in novel hosts. Philos Trans R Soc B Biol Sci. 2019;374(1782).
3. Kenawy ERS, Azaam MM, Saad-Allah KM. Synthesis and antimicrobial activity of α -aminophosphonates containing chitosan moiety. Arab J Chem. 2015 May 1;8(3):427–32.
4. Reddy GM, Garcia JR, Reddy VH, Kumari AK, Zyryanov G V., Yuvaraja G. An efficient and green approach: One pot, multi component, reusable catalyzed synthesis of pyranopyrazoles and investigation of biological assays. J Saudi Chem Soc. 2019 Mar 1;23(3):263–73.

5. Poola S, Nagaripati S, Tellamekala S, Chintha V, Kotha P, Yagani JR, et al. Green synthesis, antibacterial, antiviral and molecular docking studies of α -aminophosphonates. Synth Commun [Internet]. 2020;0(0):1–18. Available from: https://doi.org/10.1080/00397911.2020.1753079
6. Abdel-Megeed MF, Badr BE, Azaam MM, El-Hiti GA. Antimicrobial activities of a series of diphenyl (4-(aryldiazenyl)biphenyl- 4-yl-amino)(pyridin-3-YL)methylphosphonates. Phosphorus, Sulfur Silicon Relat Elem. 2012 Oct 1;187(10):1202–7.
7. Addoum B, El Khalfi B, Daouda Mar P, Ansari NF, Elmakssoudi A, Soukri A, et al. Synthesis, Characterization of Some α -aminophosphonate Derivatives and Comparative Assessment of their Antioxidant Potential in-vivo and in-vitro. Vol. 2, Acta Scientific Pharmaceutical Sciences. 2018.
8. Rezaei Z, Firouzabadi H, Iranpoor N, Ghaderi A, Reza M. Design and one-pot synthesis of a -aminophosphonates and bis (a -aminophosphonates) by iron (III) chloride and cytotoxic activity. Eur J Med Chem. 2009;44:4266–75.
9. Subba G, Uma K, Rao M, Syama C, Suresh C. Neat synthesis and antioxidant activity of a -aminophosphonates. Arab J Chem [Internet]. 2014;7(5):833–8. Available from: http://dx.doi.org/10.1016/j.arabjc.2013.01.004
10. Sieńczyk M, Oleksyszyn J. Irreversible Inhibition of Serine Proteases - Design and In Vivo Activity of Diaryl alpha- Aminophosphonate ... Irreversible Inhibition of Serine Proteases – Design and In Vivo Activity of. Curr Med Chem. 2009;16:1673–87.
11. Aissa R, Guezane-Lakoud S, Kolodziej E, Toffano M, Aribi-Zouioueche L. Diastereoselective synthesis of bis(α -aminophosphonates) by lipase catalytic promiscuity. New J Chem. 2019;43(21):8153–9.
12. Rauhamäki S, Postila PA, Niinivehmas S, Kortet S, Schildt E, Pasanen M, et al. Structure-activity relationship analysis of 3-phenylcoumarin-based monoamine oxidase B inhibitors. Front Chem. 2018 Mar 1;6:3–18.
13. Bouchentouf S, Noureddine M. Identification of Compounds from Nigella Sativa as New Potential Inhibitors of 2019 Novel Coronasvirus (Covid-19): Molecular Docking Study . ChemRxiv. 2020;(April).
14. Addoum B, El Khalfi B, Derdak R, Sakoui S, Elmakssoudi A, Soukri A. The one-pot synthesis of some bioactive pyranopyrazoles and evaluation of their protective behavior against extracellular H2O2 and SNP in T. Thermophila. Jordan J Biol Sci. 2021;14(1):31–9.
15. Zahouily M, Elmakssoudi A, Mezdar A, Rayadh A, Sebti S, Lazrek H. Three Components Coupling Catalysed by Na2CaP2O7: Synthesis of α-Amino Phosphonates Under Solvent-Free Conditions at Room Temperature. Lett Org Chem. 2005 Jul 9;2(5):428–32.
16. Zahouily M, Elmakssoudi A, Mezdar A, Rayadh A, Sebti S, Lazrek H. Three Components Coupling Catalysed by Na2CaP2O7: Synthesis of α-Amino Phosphonates Under Solvent-Free Conditions at Room Temperature. Lett Org Chem. 2005 Jul 9;2(5):428–32.
17. Jouimyi MR, Bounder G, Essaidi I, Boura H, Zerouali K, Lebrazi H, et al. Molecular docking of a set of flavonoid compounds with helicobacter pylori virulence factors CagA and VacA. J HerbMed Pharmacol. 2020;9(4):412–9.
18. da Silva FMA, da Silva KPA, de Oliveira LPM, Costa E V., Koolen HHF, Pinheiro MLB, et al. Flavonoid glycosides and their putative human metabolites as potential inhibitors of the sars-cov-2 main protease (Mpro) and rna-dependent rna polymerase (rdrp). Mem Inst Oswaldo Cruz. 2020;115(9):1–8.
19. Ramesh DMK V. Binding site analysis of potential protease inhibitors of COVID-19 using AutoDock. VirusDisease. 2020;2(31):1–6.
20. Filali OA, Soukri A, Khalfi B El. Evaluation of Antibacterial Effect of Some Essential Oils by Contact and Volatile Methods. 2019;9(4):81–90.
21. Kumar MH, Jones CS, Ravi A. Molecular docking studies of interaction between protease activated inhibitor receptor as the crucial protein and hydroxyl cinnamic acid as ligands. Asian J Pharm Pharmacol. 2019;5(1):137–42.
22. El Zoeiby A, Sanschagrin F, Levesque RC. Structure and function of the Mur enzymes: Development of novel inhibitors. Mol Microbiol. 2003;47(1):1–12.
23. Demeester KE, Liang H, Jensen MR, Jones ZS, D'Ambrosio EA, Scinto SL, et al. Synthesis of Functionalized N-Acetyl Muramic Acids to Probe Bacterial Cell Wall Recycling and Biosynthesis. J Am Chem Soc. 2018;140(30):9458–65.
24. Nadiveedhi MR, Nuthalapati P, Gundluru M, Yanamula MR, Kallimakula SV, Pasupuleti VR, et al. Green Synthesis, Antioxidant, and Plant Growth Regulatory Activities of Novel α -Furfuryl-2-alkylaminophosphonates. ACS Omega. 2021;6(4):2934–48.
25. Yang Y, Severin A, Chopra R, Krishnamurthy G, Singh G, Hu W, et al. 3,5-Dioxopyrazolidines, novel inhibitors of UDP-N- acetylenolpyruvylglucosamine reductase (MurB) with activity against gram-positive bacteria. Antimicrob Agents Chemother. 2006;50(2):556–64.
26. Yao G, Ye M, Huang R, Li Y, Pan Y, Xu Q, et al. Bioorganic & Medicinal Chemistry Letters Synthesis and antitumor activities of novel rhein a -aminophosphonates conjugates. Bioorg Med Chem Lett [Internet]. 2014;24(2):501–7. Available from: http://dx.doi.org/10.1016/j.bmcl.2013.12.030
27. Maleki B, Nasiri N, Tayebee R, Khojastehnezhad A, Akhlaghi HA. Green synthesis of tetrahydrobenzo[b] pyrans, pyrano[2,3-c] pyrazoles and spiro[indoline-3,4α -pyrano[2,3-c] pyrazoles catalyzed by nano-structured diphosphate in water. RSC Adv. 2016;6(82):79128–34.
28. Kunjapur AM, Tarasova Y, Prather KLJ. Synthesis and accumulation of aromatic aldehydes in an engineered strain of escherichia coli. J Am Chem Soc. 2014;136(33):11644–54.
29. Manolov I, Danchev ND. Synthesis, toxicological, and pharmacological assessment of some oximes and aldehyde condensation products of 4-hydroxycoumarin. Arch Pharm (Weinheim). 1999;332(7):243–8.
30. Rezaei Z, Khabnadideh S, Zomorodian K, Pakshir K, Nadali S, Mohtashami N, et al. Design , Synthesis , and Antifungal Activity of New $α $ -Aminophosphonates. 2011;2011.
31. Feleke T, Eshetie S, Dagnew M, Endris M, Abebe W, Tiruneh M. Multidrug - resistant bacterial isolates from patients suspected of nosocomial infections at the University of Gondar Comprehensive Specialized Hospital , Northwest Ethiopia. BMC Res Notes [Internet]. 2018;1–7. Available from: https://doi.org/10.1186/s13104-018-3709-7
32. Li B, Webster and TJ. Bacteria antibiotic resistance: New challenges and opportunities for implant-associated orthopedic infections. J orthopeadic Res. 2018;36(1):22–32.

Received: 18 May 2021
Accepted: 12 July 2021

RESEARCH / INVESTIGACIÓN

Código de barras de ADN de tres especies de árboles frutales con potencial económico del valle de Huaura, Lima, Perú

DNA barcoding of three species of fruit trees with economic potential from the Huaura Valley, Lima, Peru

Hermila Belba Díaz-Pillasca, Angel David Hernández-Amasifuen*, Miguel Machahua, Alexandra Jherina Pineda-Lázaro, Alexis Argüelles-Curaca, Brayan Lugo

DOI. 10.21931/RB/2021.06.03.18

Resumen: El Perú presenta una gran diversidad de recursos genéticos, pero a la vez se desaprovechan especies por desconocimiento o bajo rendimiento económico. Situación que se refleja en el valle de Huaura con los árboles frutales de cansaboca (*Bunchosia armeniaca*), palillo (*Campomanesia lineatifolia*) y naranja agria (*Citrus aurantium*), especies con gran importancia en la gastronomía tradicional local, pero en la actualidad catalogadas en peligro crítico. Con el fin de conservar estas especies se planteó como objetivo establecer código de barras de ADN de tres especies amenazadas con potencial económico del valle de Huaura. Se extrajo ADN de las tres especies con el método CTAB y para las amplificaciones en PCR se emplearon los cebadores de código de barras de ADN universales pertenecientes a cloroplastos: *matK*, *rbcL* y *trnH-psbA*. A partir de los productos purificados y cuantificados se realizó el secuenciamiento de las muestras. Las secuencias fueron analizadas, alineadas y agrupadas con los programas Bioedit, Codon Code Aligner y MEGA respectivamente. Las concentraciones de ADN fueron: palillo (457 ng/µl), cansaboca (433 ng/µl) y naranja agria (442 ng/µl). La amplificación de los cebadores produjo productos de PCR entre 357 y 810 pb. Las secuencias de NCBI que presentaron mayor porcentaje de identidad con cada especie en estudio fueron sometidas a análisis filogenético, los cuales colocaron a las especies en grupos distintos y revelando diferencia genética con las muestras estudiadas. Se proporcionaron las herramientas básicas para implementar códigos de barras de ADN en tres especies de árboles frutales en el valle de Huaura.

Palabras clave: *Bunchosia armeniaca*, *Campomanesia lineatifolia*, *Citrus aurantium*, palillo, naranja agria.

Abstract: Peru has a great diversity of genetic resources, but at the same time, species are wasted due to ignorance or low economic performance. The situation reflected in the Huaura valley with the fruit trees of cansaboca (*Bunchosia armeniaca*), palillo (*Campomanesia lineatifolia*) and sour orange (*Citrus aurantium*), species with great importance in the traditional local gastronomy, but currently classified as endangered critically. To conserve these species, the objective was to establish DNA barcoding of three threatened species with economic potential in the Huaura Valley. DNA from the three species was extracted with the CTAB method, and universal DNA barcode primers belonging to chloroplasts were used for the PCR amplifications: *matK*, *rbcL*, and *trnH-psbA*. Samples were sequenced from the purified and quantified products. The sequences were analyzed, aligned, and grouped with the Bioedit, Codon Code Aligner, and MEGA programs. The DNA concentrations were: cansaboca (457 ng / µl), palillo (433 ng / µl) and sour orange (442 ng / µl). Amplification of the primers produced PCR products between 357 and 810 bp. The NCBI sequences that presented the highest percentage of identity with each species under study were subjected to phylogenetic analysis, which placed the species in different groups and revealed genetic differences with the studied samples. The essential tools were provided to implement DNA barcoding in three species of fruit trees in the Huaura valley.

Key words: *Bunchosia armeniaca*, *Campomanesia lineatifolia*, *Citrus aurantium*, palillo, sour orange.

Introducción

El Perú presenta gran riqueza biológica por la alta diversidad genética, debido a esto es considerado como uno de los países más importantes en recursos genéticos[1]. Estos recursos pueden permitir un mayor desarrollo económico y social, siempre que se incluya una alta responsabilidad con respecto a especies endémicas y rescate de especies domesticadas[2]. El desaprovechamiento de especies por desconocimiento o bajo rendimiento económico conlleva a la perdida de material genético valioso, situación que en la actualidad se refleja en el valle de Huara, provincia de Huaura, departamento de Lima; con árboles frutales como cansaboca o ciruela del fraile (*Bunchosia armeniaca* Cav. DC), palillo (*Campomanesia lineatifolia* Ruiz & Pav.) y naranja agria (*Citrus aurantium* L.), especies con gran demanda en décadas pasadas e importancia en la gastronomía tradicional local[3]. Pero en la actualidad existe una baja o nula presencia en mercados locales, mientras que en campos de cultivo es difícil encontrar estas especies, presentándose muy pocos individuos en huertas por herencia familiar, debido a esto son catalogadas en peligro crítico[4,5].

Estas especies vegetales, así como muchas especies de otras regiones del país presentan gran potencial socio-económico. Por lo que el Perú, viene desarrollando objetivos estratégicos como parte del Convenio sobre la Diversidad Biológica, de las cuales se ha trazado el país la meta de evitar la extinción de especies mediante el avance de conocimientos, con una gran base científica y tecnológica para aumentar la valoración y funcionalidad de estas especies[6]. Como parte del avance científico se están desarrollando técnicas avanzadas relacionadas a biología molecular, tales como estudios de código de barras, genómica, proteómica, metabolómica, transcriptómica[2].

[1] Universidad Nacional José Faustino Sánchez Carrión, Facultad de Ciencias, Laboratorio de Biotecnología Vegetal, Huacho, Perú.

Corresponding author: adhernandz@hotmail.com

El código de barras de ADN es un método para identificar las especies de todo tipo de organismo vivo empleando una secuencia corta de ADN (<1000 pb) que evoluciona lo suficientemente rápido como para diferir entre especies estrechamente relacionadas[7]. Cuando se recupera una secuencia de código de barras de una muestra desconocida, se utiliza un algoritmo para compararla con una base de datos de referencia que contiene códigos de barras de muestras de especies identificadas, lo que permite su comparación y posible identificación de manera rápida y clara[6,8,9]. En otras palabras, los códigos de barras de ADN funcionan como identificadores moleculares para cada especie, de la misma manera que los códigos de barras en blanco y negro legibles por máquina se utilizan en la industria minorista para identificar productos comerciales[10,11,12].

Las secuencias para código de barras que se emplean en las investigaciones están relacionadas a sus alineamientos múltiples y número de variaciones, las cuales permiten distinguir las especies emparentadas sin influir en su asignación correcta a través de la variación intraespecífica[13]. Estas secuencias de ADN son: ribulosa-bisfosfato carboxilasa (*rbcL*), maturasa K (*matK*) y el espaciador intergénico *trnH-psbA* (*trnH-psbA*). Cada uno de las secuencias presenta diferencias en sus regiones codificantes, es así como *rbcL* presenta una región de codificación universal que no evoluciona rápidamente, *matK* presenta una región de codificación que evoluciona bastante rápido y *trnH-psbA* es un espaciador intergénico que evoluciona rápidamente[14,15].

La identificación molecular de especies mediante código de barras de ADN facilita la selección de material vegetal desde plántulas, permitiendo la conservación de especies amenazadas. Por lo tanto, en la investigación se planteó el objetivo de establecer el código de barras de ADN de tres especies con potencial económico del valle de Huaura, para facilitar su identificación a nivel molecular.

Métodos

Material vegetal y extracción de ADN

Se emplearon muestras de hojas de las especies *Bunchosia armeniaca*, *Campomanesia lineatifolia* y *Citrus aurantium*, las cuales fueron colectadas de la campiña de Huacho y transportadas al Laboratorio de Biotecnología Vegetal de la Universidad Nacional José Faustino Sánchez Carrión – Huacho. La extracción de ADN se realizó según el protocolo de bromuro de cetiltrimetilamonio (CTAB)[16]. Se tomaron alrededor de 100 mg de tejido de hojas frescas, se añadieron 2,85 µl de β-mercaptoetanol y 1.000 µl de tampón de extracción CTAB 2% (100 mM Tris, 28 mM EDTA, 2% CTAB, 1,4 M NaCl y 2,5% PVP), las muestras se trituraron de forma mecánica y se incubó a 65º C durante 45 min y. Posteriormente, se añadió 900 µl de cloroformo-alcohol isoamílico (24:1) y se mezcló suavemente durante 5 min. Las muestras se centrifugaron a 14.000 rpm durante 5 min. Después de la centrifugación, se recogió la fase acuosa y se adicionaron 60 µl de CTAB al 10% y se incubó a 65° C por 5 min. Se añadió 900 µl de cloroformo-alcohol isoamílico (24:1) y se mezcló suavemente durante 5 min y centrifugo a 14.000 rpm durante 5 min, se retiró el sobrenadante y se adiciono isopropanol frio en el mismo volumen que el sobrenadante obtenido. Las muestras fueron colocadas a -20° C durante 30 min. Posteriormente, se centrifugó a 14.000 rpm durante 20 min, se decantó el sobrenadante y se invirtieron los tubos sobre papel toalla durante 1 min. Seguidamente, se lavó con etanol al 70% y se centrifugo a 14.000 rpm por 5 min. Se añadió 300 µl de CH3CO2K 5 M frio y se incubó a -20° C durante 10 min. Luego se centrifugó a 14.000 rpm por 5 min, se eliminó el sobrenadante y se realizó un lavado con etanol al 90%. Seguidamente se eliminó el etanol y se invirtieron los tubos sobre papel toalla estéril. Una vez seco el pellet se añadió 100 µl de agua libre de nucleasas, posterior se adicionó 3 µl de RNAsa al 2% y se incubó a 37° C durante 60 min. A continuación, las muestras se centrifugaron a 14.000 rpm durante 5 min y los sedimentos de ADN se lavaron dos veces con etanol al 70% y se invirtieron los tubos sobre papel toalla estéril durante 30 min. Los sedimentos de ADN se diluyeron con 50 µl de agua libre de DNAsa y posteriormente se cuantifico en Nanodrop ND-1000 (NanoDrop Technologies, USA) y estimo la calidad mediante electroforesis en gel de agarosa al 1%. El ADN extraído se almacenó a -20 ° C hasta su posterior uso.

Amplificación por PCR y secuenciamiento.

Se emplearon los siguientes cebadores de código de barras de ADN universales pertenecientes a cloroplastos: *matK, rbcL* y *trnH-psbA* (Tabla 1). Las reacciones de PCR se realizaron en un volumen de 25 µl que contenía 12.5 µl master mix (10 mM Tris HCl, 50 mM KCl, 2 mM de MgCl2, 0,2 mM de dNTP, 0,02 U/µl de Taq Polimerasa), 0.5 µl de cada cebador (forward y reverse), 1 µl de ADN genómico y 10,5 µl de agua pura estéril.

Se utilizaron los siguientes parámetros del termociclador: desnaturalización inicial de 94° C durante 5 min, seguido de 40 ciclos a 94° C durante 30 s, hibridación a 52° C para los cebadores *rbcL* y *matK* durante 30 s, 55° C para cebadores de *trnH-psbA* durante 30 s y extensión a 72° C durante 1 min, seguido de una extensión final a 72° C por 10 min. Las amplificaciones se realizaron en el termociclador PCRMax (BioSystems, UK).

Los productos de amplificación por PCR se sometieron a

Código de barra	Cebador	Secuencia de ADN (5' a 3')
matK	Matk_3F	GTT ATG CAT GAS CGT AAT GCT C
	Matk_1R	ACC CAG TCC ATC TGG AAA TCT TGG TTC
rbcL	rbcLa_F	ATG TCA CCA CAA ACA GAG ACT AAA GC
	rbcLa_R	ACC CAG TCC ATC TGG AAA TCT TGG TTC
trnH-psbA	PsbA3f	GTT ATG CAT GAS CGT AAT GCT C
	trnHf_05	CGC GCA TGG TGG ATT CAC AAT CC

Tabla 1. Secuencia de cebadores para código de barras de ADN.

electroforesis en geles de agarosa al 1% durante 30 minutos a 40 V, detectados por tinción con azul de bromofenol, los resultados se observaron bajo luz ultravioleta (UV) mediante un sistema de documentación de geles con transiluminador UV (Illuminyx, USA). El tamaño de los productos de PCR se determinó utilizando DNA ladder de 100 pb (Promega, Madison). Los productos de PCR purificados se cuantificaron usando un espectrofotómetro Nanodrop ND-1000 (NanoDrop Technologies, USA). El secuenciamiento de los productos de PCR se realizó en la empresa MACROGEN (Corea del Sur).

Análisis de datos

Las secuencias obtenidas fueron analizadas con el programa Bioedit y alineadas con el programa Codon Code Aligner. La identificación de códigos de barras desconocidos a partir de hojas se realizó básicamente mediante datos de la Herramienta de búsqueda de alineación local básica (BLAST) con un corte mínimo de 98% de identidad para una coincidencia superior[7]. Estos resultados se verificaron mediante agrupación y análisis filogenéticos en los que comparamos las ramas de especímenes desconocidos con secuencias de especies de referencia, para ello las secuencias de ADN se alinearon y curaron empleando el algoritmo MUSCLE del programa MEGA 7.0. Los árboles filogenéticos se construyeron en MEGA 7.0 utilizando el método de Neighbor-Joining (NJ) con 1.000 bootstraps basado en el modelo de parámetros de Kimura 2[17]. Se construyeron árboles filogenéticos con los fragmentos combinados.

Resultados

Los resultados obtenidos permitieron establecer que, la técnica de CTAB fue eficiente para la extracción de ADN en las tres especies; lo cual se comprobó con la verificación de la integridad del ADN extraído. La relación de absorbancia 260/280 fue cercana a 1,80, lo que significa ADN altamente puro para el análisis de códigos de barras. Las concentraciones de ADN en diferentes accesiones fueron: *Bunchosia armeniaca* (457 ng/µl), *Campomanesia lineatifolia* (433 ng/µl) y *Citrus aurantium* (442 ng/µl). La amplificación exitosa de los tres cebadores de códigos de barras produjo productos de PCR entre 300 y 800 pb (Figura 1).

Las secuencias de nucleótidos obtenidas mostraron diferencias en longitud y contenido de guanina-citocina (GC) en las muestras analizadas con cada cebador de código de barras (Tabla 2). En el caso del cebador *matK*, la longitud de secuencia más alta de *Bunchosia armeniaca* (810 pb). Se observó una variación de longitud de secuencia en *Citrus aurantium* (357 pb) con el cebador *matK*. La longitud media de la secuencia de *rbcL* fue casi uniforme (573 pb). *Citrus aurantium* presento la menor longitud (373 pb) y contenido de GC (26,27 %) con el cebador *trnH-psbA*.

Las secuencias obtenidas de este estudio se compararon con el banco de datos de ADN publicados en BLAST de NCBI (Tabla 3, 4 y 5), presentando en algunos casos una identidad superior al 98% con las secuencias NCBI de especies de plantas conocidas y podrían estar emparentadas a ellas.

Las especies que han logrado presentar mayor porcentaje de identidad con *Bunchosia armeniaca* del valle de Huaura, se encontraron en el rango de 99,75% hasta 98,28% de identidad (Tabla 3), manteniendo una baja variabilidad entres especies del mismo género. Las comparaciones de *Campomanesia lineatifolia* muestran un descenso en el porcentaje de identidad con las demás especies, mientras se van alejando del género, pero manteniendo en común la familia (Myrtaceae) (Tabla 4). En el caso de *Citrus aurantium* se logró encontrar porcentajes de identidad de 99,83% hasta 99,47%, dentro del mismo género con 99% de cubierta de consulta (Tabla 5), así mismo dentro de la lista se presentan tres accesiones de *Citrus aurantium* de otras partes del mundo, mostrándose que no comparten tantos porcentajes de identidad debido posiblemente a una evolución necesaria al habitad de cada región.

Las secuencias de NCBI que presentaron mayor porcentaje de identidad con cada especie en estudio (*Campomanesia lineatifolia*, *Bunchosia armeniaca* y *Citrus aurantium*) fueron sometidas a análisis filogenético.

La alineación combinada de las secuencias de las especies en estudio (Figura 2) con secuencias de 13 (*Citrus aurantium*) y 15 (*Bunchosia armeniaca* y *Campomanesia lineatifolia*) especies de mayor porcentaje de similitud y cubierta de consulta, descargadas de NCBI mostró una variabilidad las posiciones de nucleótidos. De manera similar, se construyó un árbol filogenético combinado de máxima verosimilitud mediante la concatenación de datos de secuencia de tres cebadores de códigos de barras (*matK*, *rbcL* y *trnH-psbA*) para estimar las divergencias evolutivas entre cada especie en estudio con las especies

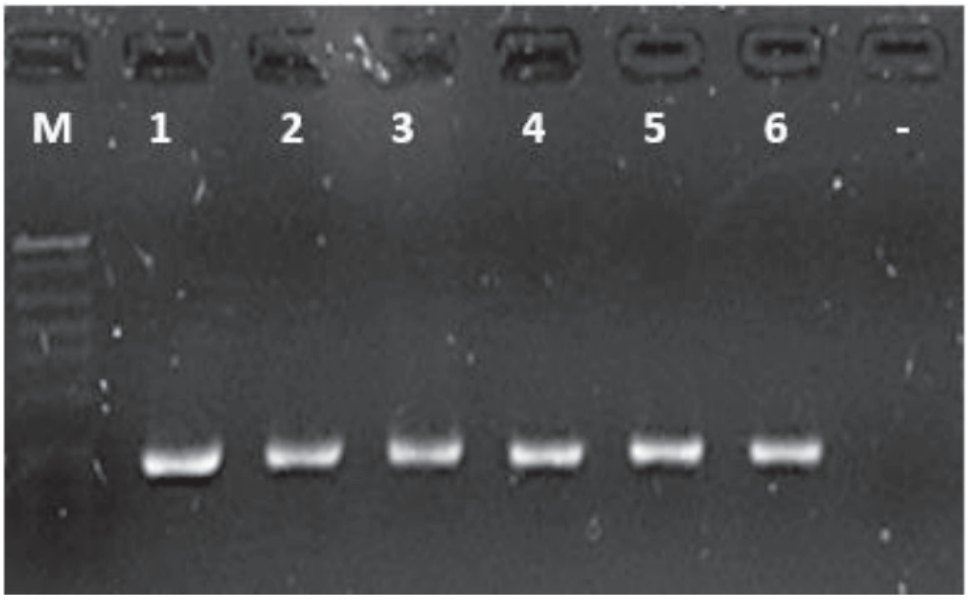

Figura 1. Productos de PCR amplificados con los cebadores *trnH-psbA* en las tres especies en peligro de extinción del valle de Huaura. La posición de las muestras en el gel de agarosa (1-2) *Campomanesia lineatifolia*, (3-4) *Bunchosia armeniaca*, (5-6) *Citrus aurantium* y (-) control negativo; M: DNA ladder de 100 pb para la determinación del tamaño de las muestras.

Especie	Cebadores de código de barras de ADN					
	matK		*rbcL*		*trnH-psbA*	
	Longitud (pb)	Contenido GC (%)	Longitud (pb)	Contenido GC (%)	Longitud (pb)	Contenido GC (%)
Bunchosia armeniaca	810	31,73	573	44,15	475	27,58
Campomanesia lineatifolia	799	32,92	545	43,85	562	32,21
Citrus aurantium	357	45,66	573	46,25	373	26,27

Tabla 2. Características de secuencia de nucleótidos de marcadores de código de barras de ADN.

Especie	Secuencia ID	Cubierta de consulta	Porcentaje de Identidad
Bunchosia cestrifolia	KM197241.1	100%	99,75%
Bunchosia deflexa	HQ247224.1	100%	99,75%
Bunchosia polystachia	HQ247232.1	100%	99,63%
Bunchosia decussiflora	HQ247223.1	100%	99,38%
Bunchosia paraguariensis	KM197250.1	100%	99,38%
Bunchosia angustifolia	HQ247220.1	100%	99,26%
Bunchosia pilocarpa	HQ247231.1	100%	99,14%
Bunchosia pernambucana	KM197251.1	100%	99,14%
Bunchosia pallescens	KM197248.1	100%	99,14%
Bunchosia matudae	KM197245.1	100%	99,14%
Bunchosia lindeniana	KM197243.1	100%	99,14%
Bunchosia cruciana	KM197242.1	100%	98,89%
Bunchosia swartziana	HQ247233.1	100%	99,89%
Bunchosia armeniaca	HQ247222.1	100%	98,28%
Bunchosia armeniaca	AF344533.1	100%	98,28%

Tabla 3. Especies de mayor homología en BLAST con muestras de *Bunchosia armeniaca* del valle de Huaura.

de mayor porcentaje de identidad descargadas de NCBI.

En el árbol filogenético de *Bunchosia armeniaca* (Figura 3) se reveló que la muestra en estudio es genéticamente diferente a las especies de referencia determinadas por BLAST y se colocan en grupos distintos. Se consideró secuencias de la misma especie (*Bunchosia armeniaca*) localizadas en México y se mostró una diferencia genética con la muestra estudiada en Huaura, Perú.

En el caso de *Campomanesia lineatifolia* no se encontró alguna secuencia de ADN de la misma especie en BLAST, por lo que se presenta los primeros resultados de secuenciamiento relacionada a esta especie. El árbol filogenético revelo que se encuentra muy emparentado con *Campomanesia xanthocarpa*, agrupados en un solo clado con 100% de soporte de arranque (Figura 4).

Mientras que el árbol filogenético de la naranja agria reveló una diferencia genética con las muestras de *Citrus aurantium* de referencia determinadas por BLAST situadas en Canadá, Estados Unidos e Italia, colocándose en grupos separados y distintos. Con la muestra de naranja agria de referencia de Grecia se revelo una menor diferencia al estar en un grupo cercano con 87% de soporte de arranque (Figura 5).

Especie	Secuencia ID	Cubierta de consulta	Porcentaje de Identidad
Campomanesia xanthocarpa	KF421071.1	100%	99,29%
Campomanesia xanthocarpa	KY392760.1	100%	99,29%
Campomanesia pubescens	AM489822.1	98%	99,64%
Campomanesia velutina	MF954284.1	97%	99,27%
Campomanesia adamantium	MF954283.1	97%	99,09%
Myrcia variabilis	JN091439.1	99%	97,33%
Myrcia spectabilis	JN091432.1	99%	97,15%
Myrcia guianensis	JN091415.1	99%	97,15%
Campomanesia guazumifolia	AM489821.1	97%	97,81%
Myrcia tenuivenosa	JN091437.1	98%	97,46%
Myrcia vestita	JN091440.1	98%	97,11%
Myrcia subverticillaris	JN091435.1	99%	96,30%
Myrcia guianensis	JN091416.1	99%	96,12%
Myrcia decorticans	JN091412.1	99%	95,77%
Myrcia laruotteana	AM489856.1	98%	96,40%

Tabla 4. Especies de mayor homología en BLAST con muestras de *Campomanesia lineatifolia* del valle de Huaura.

Especie	Secuencia ID	Cubierta de consulta	Porcentaje de Identidad
Citrus maxima	KR073282.1	99%	99,83%
Citrus reticulata	MH714105.1	99%	99,83%
Citrus aurantium	MT106672.1	99%	99,82%
Citrus polytrifolia	NC_045403.1	99%	99,65%
Citrus depressa	LC218435.1	99%	99,82%
Citrus limon	KY085897.1	99%	99,82%
Citrus platymamma	KR259987.1	99%	99,82%
Citrus japonica	MN495932.1	99%	99,82%
Citrus hindsii	MN073195.1	99%	99,82%
Citrus sunki	MN895042.1	99%	99,82%
Citrus aurantium	MT702983.1	99%	99,82%
Citrus aurantiifolia	KJ865401.1	99%	99,65%
Citrus aurantium	KY626925.1	99%	99,47%

Tabla 5. Especies de mayor homología en BLAST con muestras de *Citrus aurantium* del valle de Huaura.

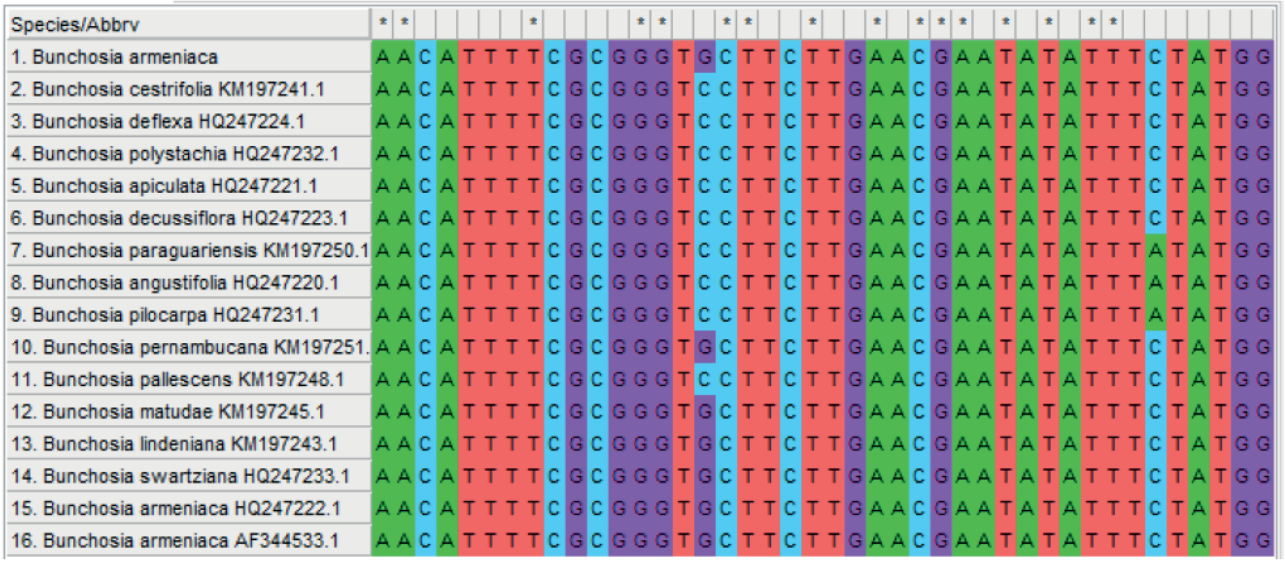

Figura 2. Alineamiento combinado de las secuencias con el programa MEGA.

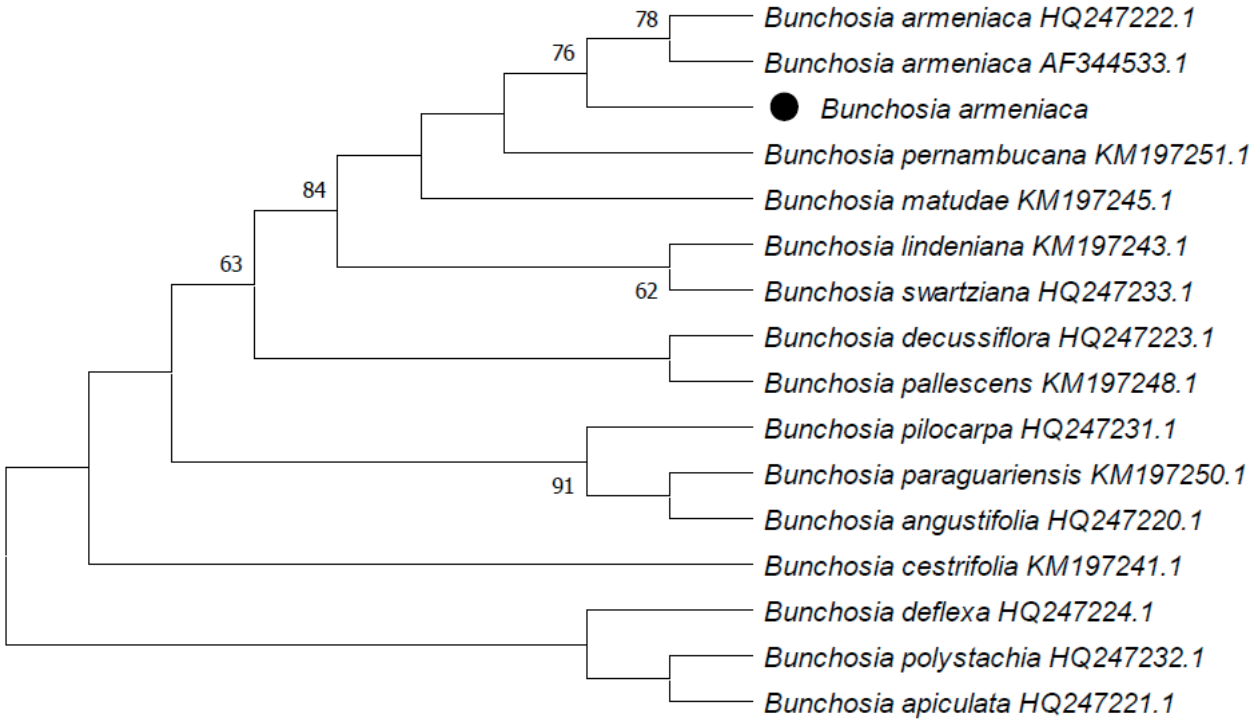

Figura 3. Árbol filogenético de máxima probabilidad de evolución divergente en *Bunchosia armeniaca* del valle de Huaura.

Discusión

Se ha aplicado con éxito un método que utiliza secuencias cortas de ADN, conocidas como "códigos de barras de ADN", para identificar especies de plantas, especialmente loci en el genoma de los plástidos como *matK, rbcL*, y *trnH-psbA*[8,13].

La evaluación de la aplicabilidad universal mediante la cuantificación por PCR y el éxito de la secuencia es el primer paso para determinar la idoneidad de un fragmento de ADN dado como código de barras. A este respecto, todas las regiones analizadas (*matK*, *rbcL* y *trnH-psbA*) se amplificaron de manera efectiva, lo que permitió una secuenciación simple y de alta calidad. Por lo que, los cebadores empleados en las tres especies en estudio presentaron características ideales para código de barras de ADN tales como capacidad de amplificación, alta eficiencia de amplificación y secuenciación, también variación genética suficientemente alta para distinguir secuencias a nivel de especie, pero también suficientemente conservadora entre individuos de la misma especie[6,18].

La amplificación de la región *trnH-psbA* fue exitosa, con amplicones más cortos (aproximadamente 570 pb) que permitió una secuenciación efectiva, al ser fácilmente amplificable usando cebadores universales y sus niveles de discriminación de especies son generalmente más altos que para otras regiones, considerándose un marcador valioso[8,19,20,21]. Los resultados obtenidos presentan similitud con otros grupos de plantas, donde la amplificación de la región *trnH-psbA* y la calidad de secuenciación fue lo suficientemente alta como para consi-

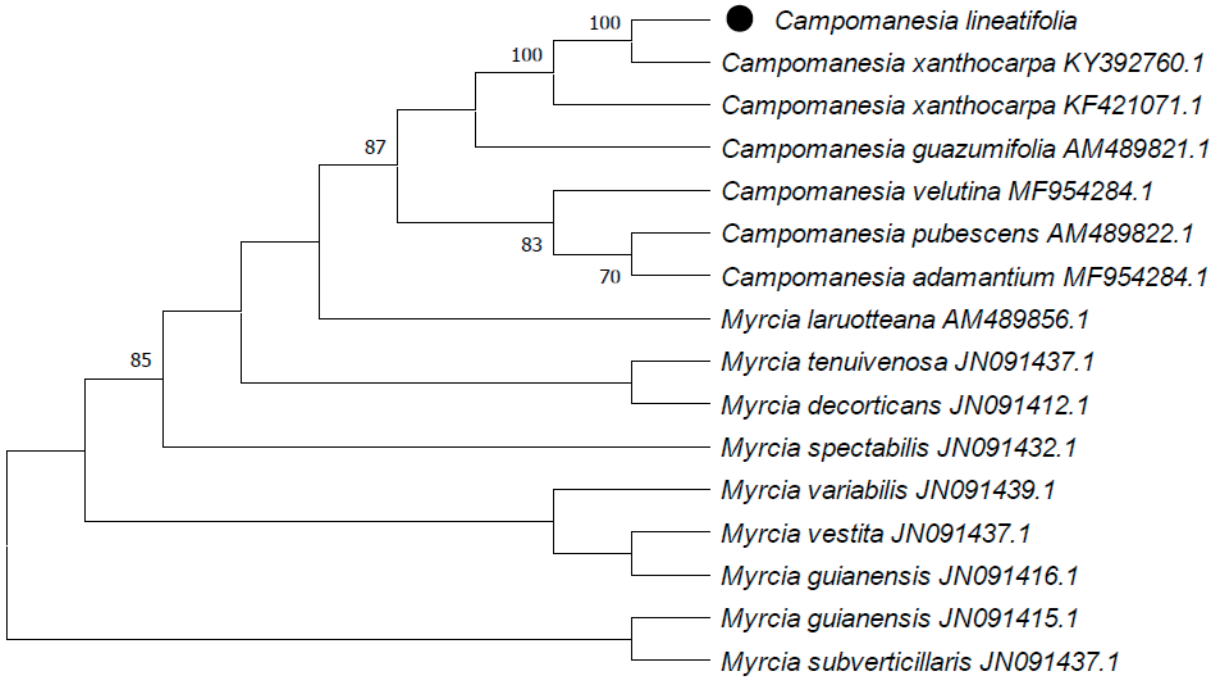

Figura 4. Árbol filogenético de máxima probabilidad de evolución divergente en *Campomanesia lineatifolia* del valle de Huaura.

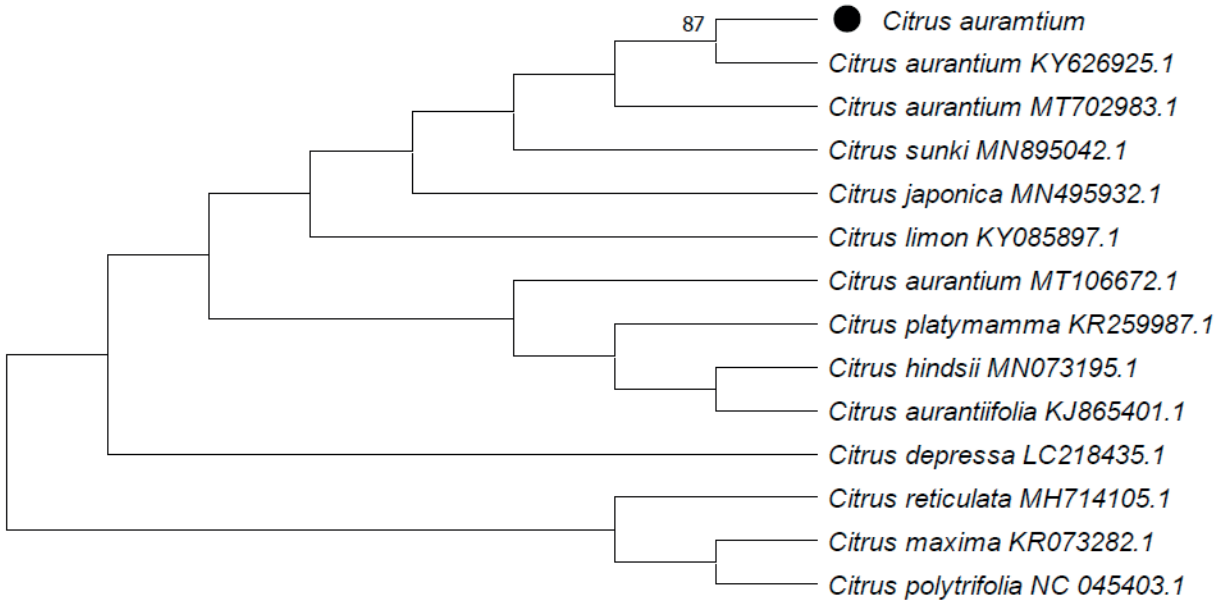

Figura 5. Árbol filogenético de máxima probabilidad de evolución divergente en *Citrus aurantium* del valle de Huaura.

derarlo un código de barras[7,21,22]. Pero algunos grupos taxonómicos presentan limitaciones que han reducido severamente la utilidad de *trnH-psbA* como código de barras. Su alta frecuencia de variación de longitud resultante de sus numerosas inserciones y eliminaciones dificulta la construcción de una alineación precisa de estas secuencias[8].

En el presente estudio *Bunchosia armeniaca* del valle de Huara se separó en otro grupo con *Bunchosia armeniaca* de referencia de México, esto podría demostrar una combinación de dispersión temprana de larga distancia entre América del Sur y México, aunque no podemos determinar la ubicación geográfica precisa donde estos clados comenzaron a diversificarse. Pero esto podría relacionarse al predominio de la dispersión en la formación de un grupo de especies regionales[23]. El marcador *matK* presento 810 pb de longitud y 31,73% de contenido GC, mostrando el marcador con mayor longitud en comparación con *rbcL* y *trnH-psbA*, pero presenta variaciones entre especies respeto a su amplificación y longitud; es por ello que el marcador *matK* presenta división entre investigadores respecto a su universalidad como cebador. Presentándose estudios donde se indican que este marcador es clave en el código de barras de ADN, al discriminar grupos específicos[11,24]. Pero también están otros autores que cuestionan la utilidad de este gen como código de barras debido a la pobre amplificación y secuenciación. eficiencia y problemas relacionados con la universalidad de los cebadores[25,26].

Campomanesia lineatifolia no ha presentado antecedentes en relación al secuenciamiento de su cloroplasto, como si encontraron de *Campomanesia xanthocarpa* secuencias parciales con el espaciador intergénico *trnH-psbA*, con una

longitud de 569 pb y con menos del 1% de gaps[27]. Con la secuencia de *matK* se obtuvo una longitud de 799 pb, la misma longitud obtenida por (28) empleando la misma secuencia en *Campomanesia xanthocarpa*; mientras que en el mismo estudio empleando *rbcL* obtuvieron una longitud mayor (645 pb) que la del presente estudio (546 pb), así mismo se presenta mucha similitud con las tres secuencias con 99% de identidad, a partir de las investigaciones realizadas en *Campomanesia xanthocarpa* de Brasil. Demostrando que la diversificación es claramente un contribuyente importante a la riqueza de especies existentes en esta región. La secuencia que fue más conservadora (entre las tres regiones analizadas) en términos de variabilidad molecular fue *rbcL*, proporcionando una amplia información para la selección de cebadores específicos de orden apropiado. Esto indica que *rbcL* tiene el menor número de sitios variables y que la secuencia de cebador seleccionada tiene una fuerte universalidad. Por lo tanto, es recomendable *rbcL* como un fragmento efectivo para el código de barras de ADN en especies arbóreas. Esto también fue confirmado por (6) y otros autores[11,19], quienes recomiendan *rbcL* y *matK* para el código de barras de ADN central para plantas.

El espaciador intergénico *trnH-psbA* en *Citrus aurantium* de la presente investigación presento una menor longitud en comparación a *Citrus aurantium* de referencias de otras partes del mundo, pero con la secuencia *rbcL* se obtuvo la misma longitud, llegando a presentar una identidad de casi 100%[29,30]. Finalmente, con la secuencia de *matK* no se presentaron identidades dentro del género *Citrus*. La separación de grupos de esta misma especie podría estar relacionada a la diversificación general de especies introducidas de manera individual permitiendo explicar el patrón de dispersión frecuente y continua de nuevos linajes, esto plantea la posibilidad de que la caracterización de grupos de especies esté dominada por linajes únicos que se trasladaron a una región, lo que parece haber brindado a individuos el tiempo necesario para adaptarse a nuevas condiciones abióticas[23]. Así mismo la alta frecuencia de las variantes de longitud de *trnH-psbA* en algunas especies impactó la identificación de especies utilizando métodos basados en la alineación, así como la comparación con las especies del presente estudio mediante el análisis de distancia, que tuvo un efecto mínimo en las búsquedas de BLAST[8,20].

El análisis filogenético a partir del código de barras de ADN permite mejorar la identificación de especies, al proporcionar caracteres adicionales que pueden estar conducidas por variaciones variación intraespecífica e inversiones interespecíficas que pueden confundir las relaciones entre especies estrechamente relacionadas[31,32]. Permitiendo identificar a las especies exactas que se encuentra en peligro de extinción en el valle de Huaura, y, además, mostrando un distanciamiento entre la misma especie ubicada en otras partes del mundo.

De esta manera se puede emplear estos métodos como base de cualquier estudio científico de identificación completamente perfecta de material vegetal, conjuntamente con la enorme biblioteca digital en línea de códigos de barras de ADN, que sirve como información para buscar muestras (no identificadas o identificadas) utilizando uno o unos pocos loci de códigos de barras de ADN[20].

Conclusiones

El presente estudio es el primero en analizar especies frutales con potencial económico en peligro de extinción del valle de Huaura para facilitar la identificación a nivel molecular. Nuestros resultados proporcionan las herramientas básicas para implementar códigos de barras de ADN en especies nativas en el valle de Huaura, y pueden ayudar a elegir un código de barras de ADN apropiado para aplicaciones de alta productividad. Dichas aplicaciones de alto rendimiento podrían mejorar en gran medida los protocolos de monitoreo de la biodiversidad que se utilizan para estudiar la ecología y conservación de especies en peligro de extinción.

Agradecimientos

A la Universidad Nacional José Faustino Sánchez Carrión, por el financiamiento del estudio mediante fondos del área prioritaria FOCAM: Preservación de la biodiversidad, identificación y desarrollo de las potencialidades económicas de la zona de impacto del Proyecto de Camisea; con Resolución Vicerrectoral N° 0044-2013-VTR-UNJFSC. Así como al Blgo. Fernando Serna y Blgo. Alfredo Martin por sus sugerencias en la culminación de la investigación.

Referencias bibliográficas

1. León B, Pitman N, Roque J. Introducción a las plantas endémicas del Perú. Revista Peruana de Biología 2006, 13(2): 9-22. DOI: https://doi.org/10.15381/rpb.v13i2.1782
2. von May R, Catenazzi A, Angulo A, Venegas P, Aguilar C. Investigación y conservación de la biodiversidad en Perú: importancia del uso de técnicas modernas y procedimientos administrativos eficientes. Revista Peruana de Biología 2012, 19(3): 351-358. DOI: https://doi.org/10.15381/rpb.v19i3.1055
3. Ministerio del Ambiente (MINAM). Estrategia Nacional de Diversidad Biológica al 2021 y su Plan de acción 2014-5018. Ministerio del Ambiente, Dirección General de Diversidad Biológica. Lima, Perú. 2014. Consultado 19 jul. 2020. Disponible en https://sinia.minam.gob.pe/documentos/estrategia-nacional-diversidad-biologica-2021-plan-accion-2014-2018
4. Mostacero J, Mejía F, Gastañadui D, De La Cruz J. Inventario taxonómico, fitogreográfico y etnobotánico de frutales nativos del norte del Perú. Scientia Agropecuaria 2017, 8(3): 215-224. DOI: http://dx.doi.org/10.17268/sci.agropecu.2017.03.04
5. Díaz H, Honorio Z, Hernández A, Durand M, Gózalo A, Domínguez G. Identificación de especies frutícolas nativas con potencialidad productiva en peligro de extinción en la provincia de Huaura. Aporte Santiaguino 2020, 13(2): 78-91. DOI: https://doi.org/10.32911/as.2020.v13.n2.700
6. CBOL Plant Working Group. A DNA barcode for land plants. Proceedings of the National Academy of Sciences of the United States of America 2009, 106: 12794-12797. DOI: https://doi.org/10.1073/pnas.0905845106
7. Kress WJ, García-Robledo C, Uriarte M, Erickson DL. DNA barcodes for ecology, evolution, and conservation. Trends in Ecology & Evolution 2015, 30(1): 25-35. DOI: https://doi.org/10.1016/j.tree.2014.10.008
8. Kress JW, Wurdack KJ, Zimmer EA, Weigt LA, Janzen DH. Use of DNA barcodes to identify flowering plants. Proceedings of the National Academy of Sciences 2005, 102(23): 8369-8374. DOI: https://doi.org/10.1073/pnas.0503123102
9. Little DP, Stevenson DW. A comparison of algorithms for the identification of specimens using DNA barcodes: examples from gymnosperms. Cladistics 2007, 23(1): 1–21. DOI: https://doi.org/10.1111/j.1096-0031.2006.00126.x
10. Lahaye R, van der Bank M, Bogarin D, Warner J, Pupulin F, Gigot G, Maurin O, Duthoit S, Barraclough TG, Savolainen V. DNA barcoding the floras of biodiversity hotspots. Proceedings of the National Academy of Sciences 2008, 105(8): 2923-2928. DOI: https://doi.org/10.1073/pnas.0709936105
11. Newmaster SG, Grguric M, Shanmughanandhan D, Ramalingam S, Ragupathy S. DNA barcoding detects contamination and substitution in North American herbal products. BMC Medicine 2013, 11(1): 222. DOI: https://doi.org/10.1186/1741-7015-11-222

12. Michel CI, Meyer RS, Taveras Y, Molina J. The nuclear internal transcribed spacer (ITS2) as a practical plant DNA barcode for herbal medicines. Journal of Applied Research on Medicinal and Aromatic Plants 2016, 3(3): 94–100. DOI: https://doi.org/10.1016/j.jarmap.2016.02.002
13. Hollingsworth PM, Graham SW, Little DP. Choosing and using a plant DNA barcode. PLoS One 2011, 6: e19254. https://doi.org/10.1371/journal.pone.0019254
14. Group CP, Hollingsworth PM, Forrest LL, Spouge JL, Hajibabaei M, Ratnasingham S, van der Bank M, Chase MW, Cowan RS, Erickson DL. A DNA barcode for land plants. Proceedings of the National Academy of Sciences 2009, 106(31): 12794-12797. DOI: https://doi.org/10.1073/pnas.0905845106
15. de Groot GA, During HJ, Maas JW, Schneider H, Vogel JC, Erkens RH. Use of rbcL and trnL-F as a two-locus DNA barcode for identification of NW-European ferns: an ecological perspective. PLoS One 2011, 6(1): e16371. DOI: https://doi.org/10.1371/journal.pone.0016371
16. Doyle JJ, Doyle JL. A rapid DNA isolation procedure for small quantities of fresh leaf tissue. Phytochemical Bulletin 1987, 19: 11-15.
17. Kumar S, Stecher G, Li M, Knyaz C, Tamura K. MEGA X: Molecular Evolutionary Genetics Analysis across computing platforms. Molecular Biology and Evolution 2018, 35:1547-1549. DOI: https://doi.org/10.1093/molbev/msy096
18. Cowan RS, Chase MW, Kress WJ, Savolainen V. 300 000 species to identify: problems, progress, and prospects in DNA barcoding of land plants. Taxon 2006, 55(3): 611–616. DOI: https://doi.org/10.2307/25065638
19. Bieniek W, Mizianty M, Szklarczyk M. Sequence variation at the three chloroplast loci (matK, rbcL, trnH-psbA) in the Triticeaetribe (Poaceae): comments on the relationships and utility in DNA barcoding of selected species. Plant Systematics and Evolution 2015, 301(4):1275-1286. DOI: https://doi.org/10.1007/s00606-014-1138-1
20. Kress WJ, Erickson DL. DNA barcodes: genes, genomics, and bioinformatics. Proceedings of the National Academy of Sciences 2008, 105(8): 2761–2762. DOI: https://doi.org/10.1073/pnas.0800476105
21. Pang XH, Song JY, Zhu YJ, Xu HX, Huang LF, Chen SL. Applying plant DNA barcodes for Rosaceae species identification. Cladistics 2010, 27(2): 165–170. DOI: https://doi.org/10.1111/j.1096-0031.2010.00328.x
22. Pang XH, Liu C, Shi LC, Liu R, Liang D, Li H, Cherny S, Chen S. Utility of the trnH–psbA intergenic spacer region and its combinations as plant DNA barcodes: a metaanalysis. PLoS ONE 2012, 7(11): e48833. DOI: https://doi.org/10.1371/journal.pone.0048833
23. Willis C, Franzone B, Xi Z, Davis C. The establishment of Central American migratory corridors and the biogeographic origins of seasonally dry tropical forests in Mexico. Frontiers in Genetics 2014, 5:433. DOI: http://dx.doi.org/10.3389/fgene.2014.00433
24. De Mattia F, Bruni I, Galimberti A, Cattaneo F, Casiraghi M, Labra M. A comparative study of different DNA barcoding markers for the identification of some members of Lamiaceae. Food Research International 2011, 44: 693-702. DOI: https://doi.org/10.1016/j.foodres.2010.12.032
25. Du ZY, Qimike A, Yang CF, Chen JM, Wang Q. Testing four barcoding markers for species identification of Potamogetonaceae. Journal of Systematic and Evolution 2011, 49(3):246-251. DOI: https://doi.org/10.1111/j.1759-6831.2011.00131.x
26. Yan HF, Hao G, Hu CM, Ge XJ. DNA Barcoding in closely related species: A case study of Primula L. sect. Proliferae Pax (Primulaceae) in China. Journal of Systematics and Evolution 2011, 49: 225-236. DOI: http://dx.doi.org/10.1111/j.1759-6831.2011.00115.x
27. Bolson M, Smidt-Ede C, Brotto ML, Silva-Pereira V. ITS and trnH-psbA as Efficient DNA Barcodes to Identify Threatened Commercial Woody Angiosperms from Southern Brazilian Atlantic Rainforests. PLoS One 2015, 10(12): e0143049. DOI: https://doi.org/10.1371/journal.pone.0143049
28. Lima RA, Oliveira AA, Colletta GD, Flores TB, Coelho RL, Días P, Frey GP, Iribar A, Rodrigues RR, Souza VC, Chave J. Can plant DNA barcoding be implemented in species-rich tropical regions? A perspective from São Paulo State, Brazil. Genetics and Molecular Biology 2018, 41(3): 661-670. DOI: https://doi.org/10.1590/1678-4685-GMB-2017-0282
29. Kress WJ, Erickson DL. A two-locus global DNA barcode for land plants: the coding rbcL gene complements the non-coding trnH-psbA spacer region. PLoS One 2007, 2(6): e508. DOI: https://doi.org/10.1371/journal.pone.0000508
30. Cornara L, Borghesi B, Canali C, Andrenacci M, Basso M, Federici S, Labra M. Smart drugs: green shuttle or real drug?. Int J Legal Med. 2013, 127(6): 1109-1123. DOI: https://doi.org/10.1007/s00414-013-0893-9.
31. Whitlock BA, Hale AM, Groff PA. Intraspecific inversions pose a challenge for the trnH-psbA plant DNA barcode. PLoS ONE 2010, 5(7): e11533. DOI: https://doi.org/10.1371/journal.pone.0011533
32. Degtjareva GV, Logacheva MD, Samigullin TH, Terentieva EI, Valiejo-Roman CM. Organization of chloroplast psbA-trnH intergenic spacer in dicotyledonous angiosperms of the family Umbelliferae. Biochemistry (Moscow) 2012, 77(9): 1056-1064. DOI: https://doi.org/10.1134/S0006297912090131

Received: 21 April 2021
Accepted: 20 June 2021

RESEARCH / INVESTIGACIÓN

Role of *Candida glabrata* as nosocomial pathogen and its susceptibility to Fluconazole, Voriconazole, Caspofungin, Micafungin and Amphotericin B

Teeba Hashim Mohammed[1], Mohsen Hashim Risan[1], Mohammed Kadhom[2], Emad Yousif[3*]

DOI. 10.21931/RB/2021.06.03.19

Abstract: Candida has different types that could cause bloodstream infections. A total number of 150 samples were collected from candidemia patients and examined. The *Candida spp.* Species isolated from blood samples were analysed. These were identified by culturing the species using different media, namely the chromogenic agar test. Then, the virulence factors of all samples were tested. *The Candida* glabrata isolates were tested with six commercial antifungal drugs. *C. glabrata* 67 (44.6%), *C. albicans* 34 (22.6%), *C. krusei* 18 (12%), *C. tropicalis* 17 (11.3%), and *C. parasilosis* 14 (9.3%). the production of phospholipase ranged between 0.63-0.99 mm. It was found that 96% of the species showed phospholipase activity in aerobic conditions. The protease activities of *Candida spp.* Isolates were experimentally tested by area of inhibition around the colonies, where 59.3% had the double (++) protease activity, 31.4% with (+) grade, and 9.3% had (–) grade or clear zone around the colony. The hemolytic capacity ranged from 0.69-0.89 in the optimum aerobic environments. Finally, 38.33% of the isolated *Candida spp.* were positive and 61.67% negative for biofilm formation. Out of the total positive *Candida spp.* for biofilm formation, 21.73% were strong biofilm producers, and 78.27% were weak. Minimum fungicidal concentration (MFC) of Fluconazole for *C. glabrata* isolates was not appropriate (NA) due to the occurrence of low inhibition tested for species. Micafungin exhibited the lowest fungicidal activity against *C. glabrata* ranging from 0.03 - 0.125, while Fluconazole showed the highest.

Key words: Candidemia, chromogenic agar, *Candida glabrata*, Antifungal.

Introduction

Candida is a significant genus of Ascomycete fungi, commonly called yeast, consisting of approximately 150 species, more than 20 of them of clinical importance[1]. *Candida spp.* became the fourth most public reason for bloodstream infections (BSI) more than two decades ago[2,3]. The highest occurrence rate was described in the USA[4], where candidemia signifies an essential danger for hospital patients[5]. Hence, *C. albicans* and *C. glabrata* remain the primary cause of aggressive candidiasis, responsible for 50% of all cases followed by other species of *Candida*, such as *C. tropicalis* and *C. parapsilosis*[6,7].

The effect of *Candida* species is presented by interrupting BSI incidents; their phospholipase and protease activity and the sensitivity towards the main antifungal agents were available[8]. Described mortality data comprised the age, period of hospitalization, skin infection, severe renal failure, preservation of the dominant venous line, and mechanical ventilation[9,10]. The germs become active at 37 °C, where protease and phospholipase are produced and facilitated adherence to the surfaces of host cell membranes; these were measured to be significant factors in starting the infection. Proteinase and phospholipase release can prime the membranes dysfunction or uniform rupture that assists the microbe to adhere to the host[11]. The communication in the pathogenesis of aggressive candidiasis, proliferation in fungal colonization is the best significant factor in the invasive candidiasis for pathogenesis. The density and colonized apparent area are responsible for the strength of the infection. Precise identification of *Candida* species helps control the hazards of candidemia infections and transmission from exogenous sources in certain patients[12]. Virulence factors are also associated to a great degree with the antifungal resistance shown by the microorganisms.

Furthermore, the capabilities of *Candida* species to produce drug-resistant virulence factors are significant in their development of human disease[13]. Recognition of *Candida* to the type's level is significant to improve the range of the antifungal agent to be prescribed. On the other hand, essential and developing resistance to azoles characterizes a significant trial for experimental, therapeutic, and prophylactic approaches. The range of candidemia has altered with the appearance of *C.glabrata* species, a strain with the hazard of increased transience and antifungal treatment of drug resistance, particularly in immunocompromised and very ill patients. The situation is very significant to recognize *Candida* to the type's level to improve the range of the antifungal agent[14].

Materials and methods

Collection of samples

Samples were collected from 150 patients with leukaemia and dialysis who were hospitalized at Madinat Al-tib hospital. The collection continued over four months, from September 2019 to January 2020. Processes of blood culturing and yeast segregation were conducted in the fungus laboratory at the College of Biotechnology/ Al-Nahrain University. The blood samples were inoculated on an SDA medium with chloramphenicol. All plates were incubated at 37°C±1 for 24, 48 hrs. Later, samples were examined and biochemical tests were performed to confirm the diagnosis of the species; the approval was obtained to take blood samples from the hospital administration and the discharged patients.

Isolation of *Candida spp*

Samples were inoculated on the appropriate culture medium containing sabouraud dextrose agar with chloramphenicol. All plates were incubated in aerobic conditions of 37 °C for 48 h[15].

[1] College of Biotechnology, Al-Nahrain University, Baghdad, Iraq.
[2] Department of Renewable Energy, College of Energy and Environmental Sciences, Alkarkh University of Science, Baghdad, Iraq.
[3] Department of Chemistry, College of Science, Al-Nahrain University, Baghdad, Iraq

Corresponding author: emad_yousif@hotmail.com

Identification of *Candida spp.* Isolates

First, single colonies were separated from the prime positive cultures; then, they were isolated according to published protocols[16] that involved the following examination. All isolates were grown on sabouraud dextrose agar and incubated at 37 ºC for 48 hrs. Pure isolates of *Candida* colonies were examined to explore their form, size, color, and surface. Chromogenic agar plates were inoculated by streaking. *Candida* colonies using sterile loop then incubated at 37 Cº±1 for 48 hrs. The growth and color of colonies were observed.

The medium was prepared by dissolving 45.9 grams of the standard medium in one liter of purified water, mixed well, and melted by heating with repeated agitation. The mixture was boiled for 2 minutes until the complete dissolution and was not autoclaved[17].

Virulence Factor Tests

The quick preliminary medical identification of *Candida spp.* usually depends on the detection of germ tubes from *Candida* cells, where their width or length is about three to four times the size of the cell. *Candida spp.* cells were added to 1000 µl of human serum with a sterilized loop, and incubated aerobically for three hours at 37 ºC. Then, cells were visualized under a microscope[18].

The egg yolk agar technique is used to test the phospholipase activity[19]. The culture medium contained of 1 L of SDA comprising (1M NaCl, 0.005 M CaCl2, and 10% egg yolk). From prepared yeast suspension, 10 microliters were taken to one McFarland (3×10^8 CFU/ml) inoculated at 37 Cº for 48 hr. in the petri dish, 3 replicates per sample. After that, it was incubated at 37 °C for 3 days in aerobic conditions; the significance of phospholipase action was calculated with this formula: (Pz value= Colony diameter/ (Colony diameter + zone of precipitation)[20]. To test the proteinase activity, bovine-serum albumin agar was used. The prepared agar consisted of 0.1% KH_2PO_4, 0.05% $MgSO_4$, 2% agar, and 1% bovine serum albumin at a final pH of 4.5. Similar inoculation aerobic conditions as above were applied for 48 h. The existence of the proteinase activity test was determined by observing a clear zone around the *Candida spp.* colonies[21]. Regarding the structural haemolytic action, SDA consisted of 7 ml human blood, 3g glucose, and 90 ml of sterile media was prepared using an autoclave with a final pH of 5.6 ± 0.2. 10 microliters were taken to one McFarland (3×108 CFU/ml) inoculated onto a dish; this was replicated 3 times per sample. Then, it was incubated at 37 °C for five days in aerobic conditions. After incubation, a clear/semi-clear zone around the yeast colony was detected as a positive haemolytic activity. The significance of hemolysis activity (Hz) was tested according to the equation: Hz rate = Colony diameter / (Colony diameter + Zone of precipitation) Agreeing to this scheme, activity kinds were recognized allowing to the Hz catalogue: Hz<0.69= very strong (++++), Hz = 0.70- 0.79= strong (+++) , Hz = 0.80- 0.89= slight (++), Hz = 0.90- 0.99=frail (+), and Hz =1 that is to say "Negative" results[22]. Biofilm production was tested using different recognition tests for *Candida spp.*, which needs the use of a specifically prepared brain heart infusion broth (BHI), solid medium supplemented (agar) with glucose and Congo red indicator. The medium contained BHI (37 gm/L), agar no.1 (10 gm/L), glucose (80 gm/L), and Congo red stain (0.8 gm/L) as an indicator[23].

Determination of minimum inhibitory concentration (MIC) of several antifungals for *Candida glabrata*

The MIC of Fluconazole, Voriconazole, Caspofungin, Micafungin, Amphotericin B, and Flucytosine against *Candida glabrata* was determined broth microdilution method established on the Clinical and Laboratory Standards Institute (CLSI) natural resistance + base (bioMerieux, USA). Manufacturers' recommendations were strictly followed to obtain adequate measurements, which confirmed sterility and efficacy of the prepared media and used mixtures. Card type AST-YS07 of a barcode no. 287 (bioMerieuxm, USA) was used with an analysis time of 24 hours[24].

Determination of MFC for *Candida glabrata*

For MFC determination, samples with different concentrations of MIC and *C. glabrata* were subcultured in Petri dishes containing SDA and incubated at 37 °C for 48 hours. The MFC is the minimum product concentration that stops apparent growth; it is the minor concentration capable of killing the yeast[25].

Results

Group's classification

In this study, 150 samples were taken from three groups. The first group comprised 50 infected patients (women and men), as illustrated in Table 1; the second group comprised 50 patients of children with leukemia (Table 2); the third group comprised 50 patients with dialysis (women and men), as listed in Table 3. The first and third groups were divided into five categories, while the second group contained three subcategories. Generally, it was found that the total number of infected patients with *Candida* present in the bloodstream were isolated as follows: 67(44.6%) with *C. glabrata*, 34 (22.6%) with *C. albicans*, 18 (12%) with *C. krusei*, 17 (11.3%) with *C. tropicalis*, and 14 (9.3%) with *C. parapsilosis*.

Determination of *Candida* species by Chromogenic agar Medium

Candida spp was cultivated in a chromogenic agar medium plates and the characteristic dyed colonies were obtained after incubation; the medium supported the development of all isolates. *C. albicans* isolates produced green colonies when incubation for 48 h, while *C. glabrata* formed light pink smooth colonies and *C. krusei* colonies were pink; the distribution graduated from a light surrounding to a dark center. Also, *C. tropicalis* color was dark blue and *C. parapsilosis* formed pale colored colonies[26] as shown in Figure 1.

Determination of Virulence Factors for *Candida* Species

The development of germ tubes was achieved, as long tubes, within 2 hours, and positive results of *Candida albicans* isolates were observed, while no *C. tropicalis* production within that time was detected, as shown in Figure 2.

The germ tubes were grown in an incubator, and a particular diagnostic was used for distinguishing the *C. albicans* by separating it from other yeasts. Other species of yeasts, in general, did not produce germ tubes during this 2-hour incubation period. The Pz value varied between 0.63–0.99 mm when species were measured. It was found that 144 (96%) *Candida spp.* isolates expressed phospholipase activity in aerobic conditions, whereas the rest did not. *Candida spp.* possibly vary depending on the species and basis of isolates; Figure 3 shows the phospholipase activity of different *Candida* types on egg yolk agar medium.

The protease activities of *Candida spp.* isolates were tes-

Age group	No. of infected in women/25	(%)	No. of infected in men/25	(%)
> year 20	4	16	3	**12**
20-30 year	2	8	1	**4**
31-40 year	5	20	8	**32**
41-50 year	7	28	7	**28**
51-75 year	7	28	6	**24**
Total	25	100	25	**100**

Table 1. Age group relationship with the number (and percentage) of infected patients with *Candida spp* from blood samples for adults (women and men).

Age group	No. of infected Children/ 50	(%)
4-8 years	21	**42**
8-10 years	12	**24**
10-12 years	17	**34**
Total	50	**100**

Table 2. Age group relationship with the number (and percentage) of infected patients with *Candida spp* from blood samples for children.

Age group	No. of infected women/25	(%)	No. of infected men/25	(%)
> year 20	-	0	1	**4**
20-30 year	1	4	3	**12**
31-40 year	2	8	4	**16**
41-50 year	5	20	6	**24**
51-75 year	17	68	11	**44**
Total	25	100	25	**100**

Table 3. Age group relationship with the number (and percentage) of infected patients with *Candida spp* from blood samples of patients with dialysis for women and men.

ted for 3 days after an inoculation loop on bovine-serum albumin agar by the inhibition area around the colony. Eighty-nine (59.3%) isolates had the double (++) protease activity, while the grade (+) of protease activity was for forty-seven (30%) of isolates and fourteen (9.3%) had the grade (–) or clear zone around the colony as shown in Figure 4.

Commonly, the hemolytic index is 0.69–0.89 in optimal aerobic environments. In this study, all experimental *Candida spp* isolations from blood samples had hemolysis activity when cultivated on SDA involving 7% human blood and 3% glucose.

Out of all *Candida spp.* isolates, the biofilms were 81(54.4%) negative, 28(18.6%) strong positive, and 41(27%) weak positive resulted from patients with leukemia and dialysis who are lying in hospital. The number of recovered *Candida spp.* from experimental samples was *C. glabrata* 34(49.2%), followed by *C albicans* (15.8%), *C. krusei* (12.5%), *C.tropicalis* (11.6%), and *C. parapsilosis* (10.9%). Among all *Candida isolates*, 46% were positive biofilm, and 54% cases were harmful biofilm. However, within the positive *Candida* biofilm, 21.73 % were strong biofilm producers, and 78.27% were weak; Figure 5 shows the biofilms.

Determination of MICs for Candida glabrata

The results of the susceptibility analysis of *Candida glabrata* isolates are summarized in Table 7. In all examinations, the minimum inhibitory concentrations (MICs) of the control *C. glabrata* isolated yeast were within the recognized limits (data are not shown). However, the CLSI's wild-brand MIC distributions were tested against six commercial antifungal drugs, namely: Fluconazole, Voriconazole, Caspofungin, Micafungin, Amphotericin B, and Flucytosine. The results showed that Fluconazole was the most active antifungal against *Candida glabrata* with different concentrations, whereas micafungin was the lowest antifungal resistance against *Candida glabrata*.

The MFC ranges for the six drugs though significant change for the different organisms. Fluconazole, Voriconazole, and Flucytosine showed fungicidal activity against *C. glabrata* (MFC50s where appropriate ≥1 g/mL). MFCs of Fluconazole for this yeast was not appropriate (NA) due to the occurrence of small inhibitions tested number for species; table 8 illustrates this.

DISCUSSION

Hospitalization (especially in cancer cases), location of central venous dialysis, and who preceding antimicrobial therapies control the number of candidemia infections. Candidemia in this concept was related to the prolonged stay (more than 15 days) of patients[27]. It is essential to mention that el-

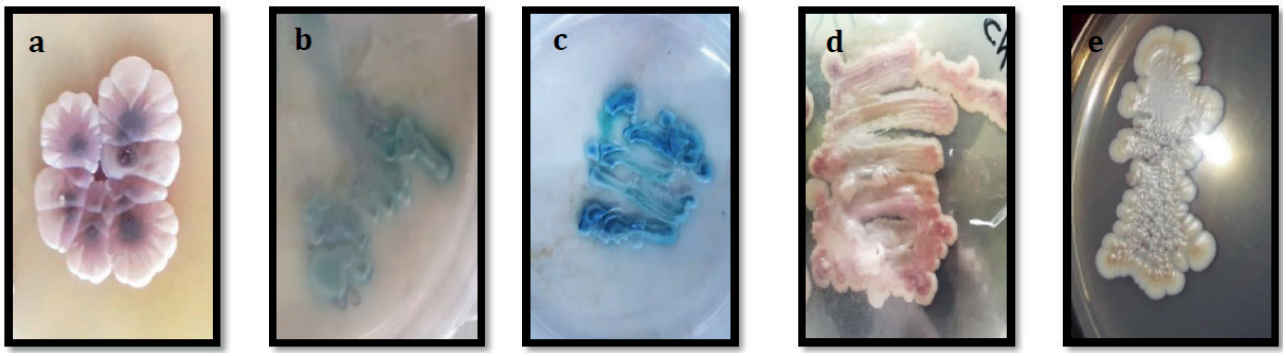

Figure 1. Observation of *Candida spp.* in Chromogenic agar media, (a) *C. krusei*, (b) *C. albicans*, (c) *C. tropicalis*, (d) *C. glabrata*, and (e) *C. parapsilosis*.

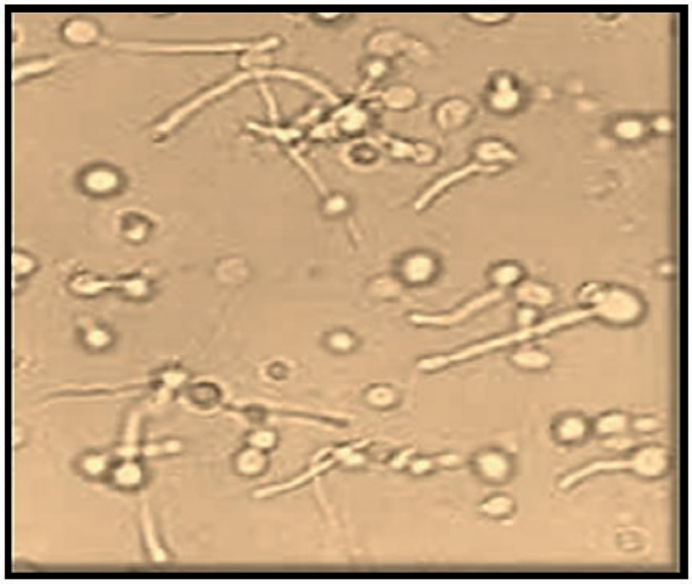

Figure 2. Germ tube of *C. albicans* growth on human serum at 37°C for 2hrs (40 X)..

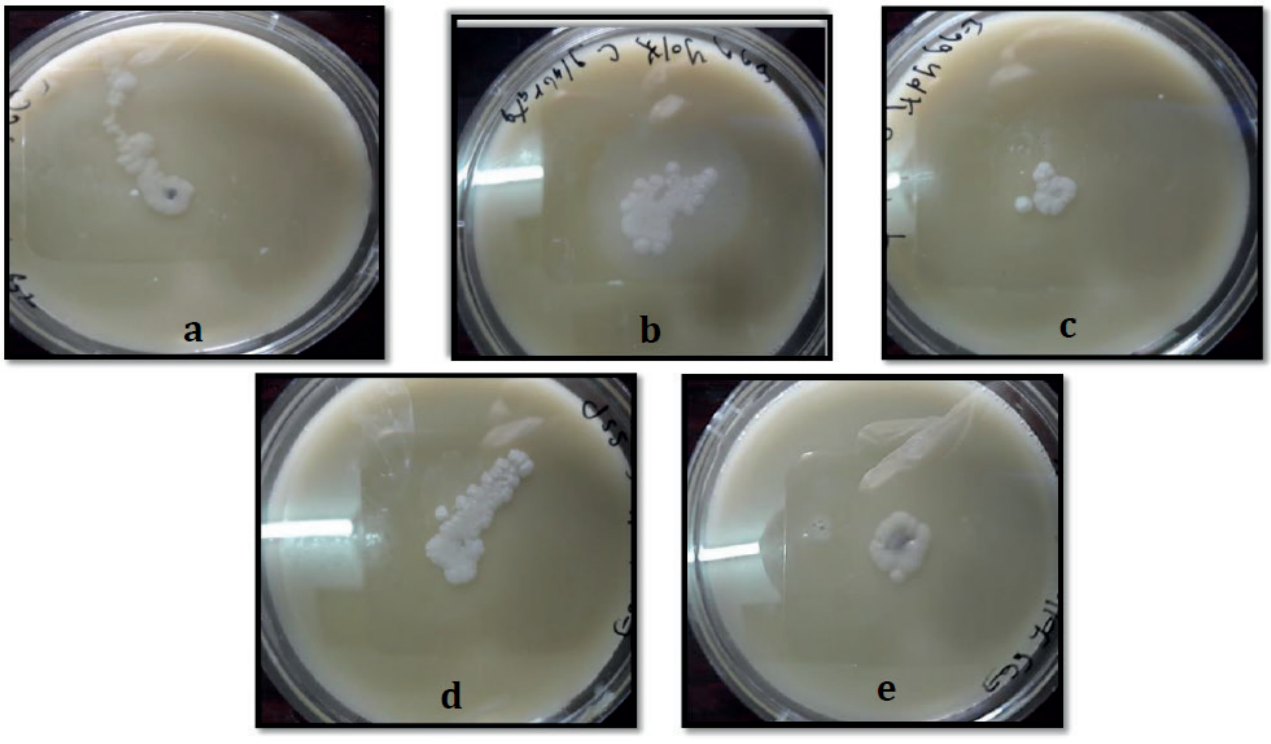

Figure 3. Phospholipase activity of (a) *C. krusei*, (b) *C. albicans*, (c) *C. tropicalis*, (d) *C. glabrata*, and (e) *C. parapsilosis* on egg yolk agar medium at 37 °C for (24-48) hrs.

Candida spp.	Number of Isolates (%)			Total
	Negative	Moderate (++)	Large (+++)	
C glabrata	3	22	42	67
C. albicans	0	11	23	34
C. krusei	1	12	5	18
C. tropicalis	0	6	11	17
C. parapsilosis	2	9	3	14
Total	6(4%)	60(40%)	84(56%)	150

Table 4. Phospholipase activity of *Candida spp* on egg yolk agar medium at 37 °C for (24-48) hrs.

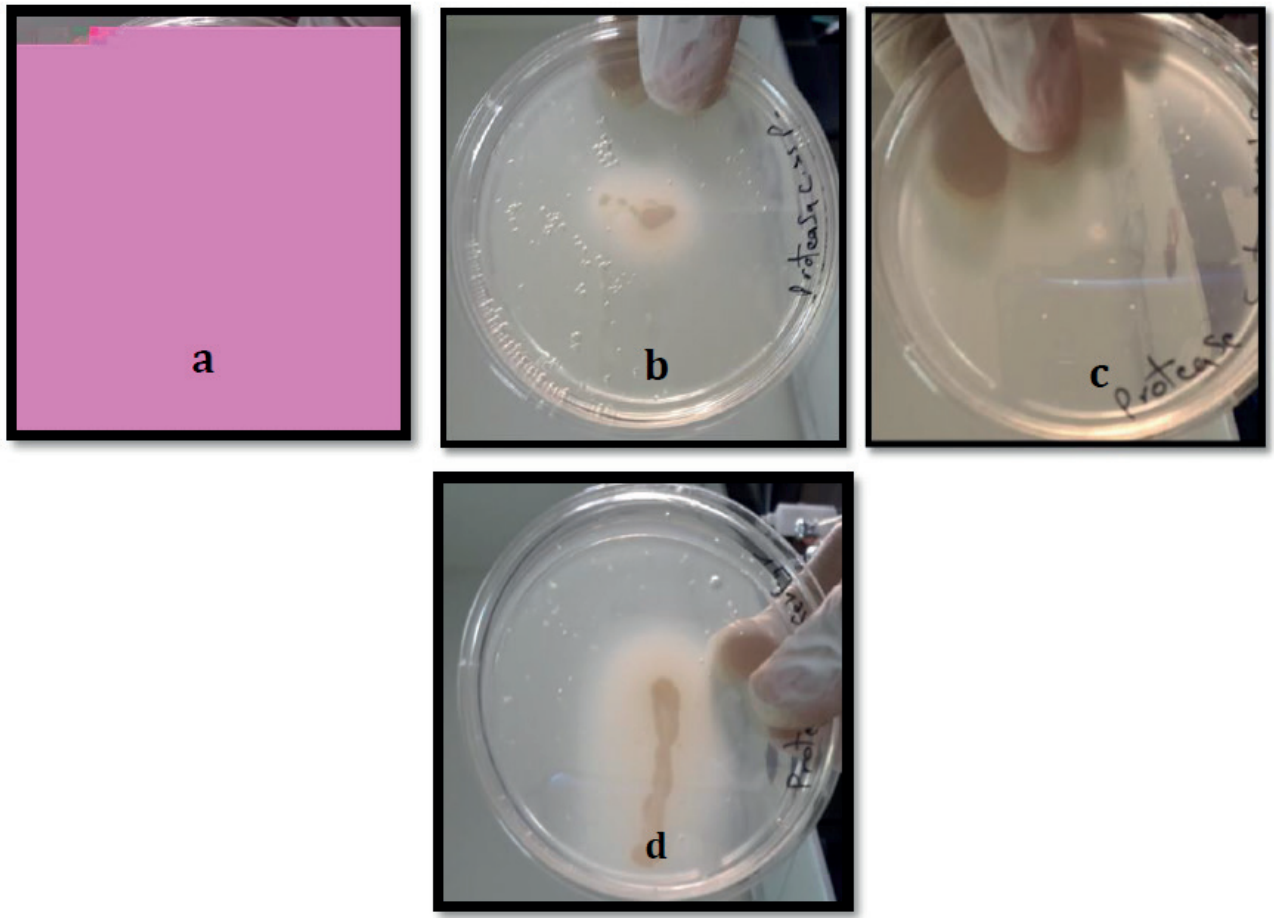

Figure 4. Protease activity from (a) *C. krusei*, (b) *C. albicans*, (c) *C. tropicalis*, (d) *C. glabrata*, and (e) *C.parapsilosis* on bovine-serum albumin agar at 37°C for (24-48) hrs.

Candida ssp.	Number of Isolation (%)			Total
	grade (–)	grade (+)	The double-positive (++)	
C glabrata	4	10	53	67
C. albicans	2	13	19	34
C. krusei	5	9	4	18
C. tropicalis	1	4	12	17
C. parapsilosis	2	11	1	14
Total	9.3%	% 31.4	59.3%	150

Table 5. Protease activity from *Candida spp* on bovine-serum albumin agar at 37°C for (24-48) hrs.

Candida spp.	Biofilm negative no. (%)	Positive biofilm no. (%)		
		Strong	Weak	Total of positive (%)
C. glabrata	33(40.7%)	16(57.1%)	18(43.9%)	34(49.2%)
C.albicans	27(33.3%)	3(10.7%)	4(9.7%)	7(10.1%)
C.krusei	8(9.8%)	4(14.2%)	6(14.6%)	10(14.4%)
C.tropicalis	9(11.1%)	2(7.1%)	6(14.6%)	8(11.5%)
C. parapsilosis	4(4.9%)	3(10.7%)	7(17%)	10(14.4%)
Total	81(54%)	28(18.6%)	41(27.3%)	69(46%)

Table 6. Biofilm formation results of 150 *Candida* isolated by Congo red agar.

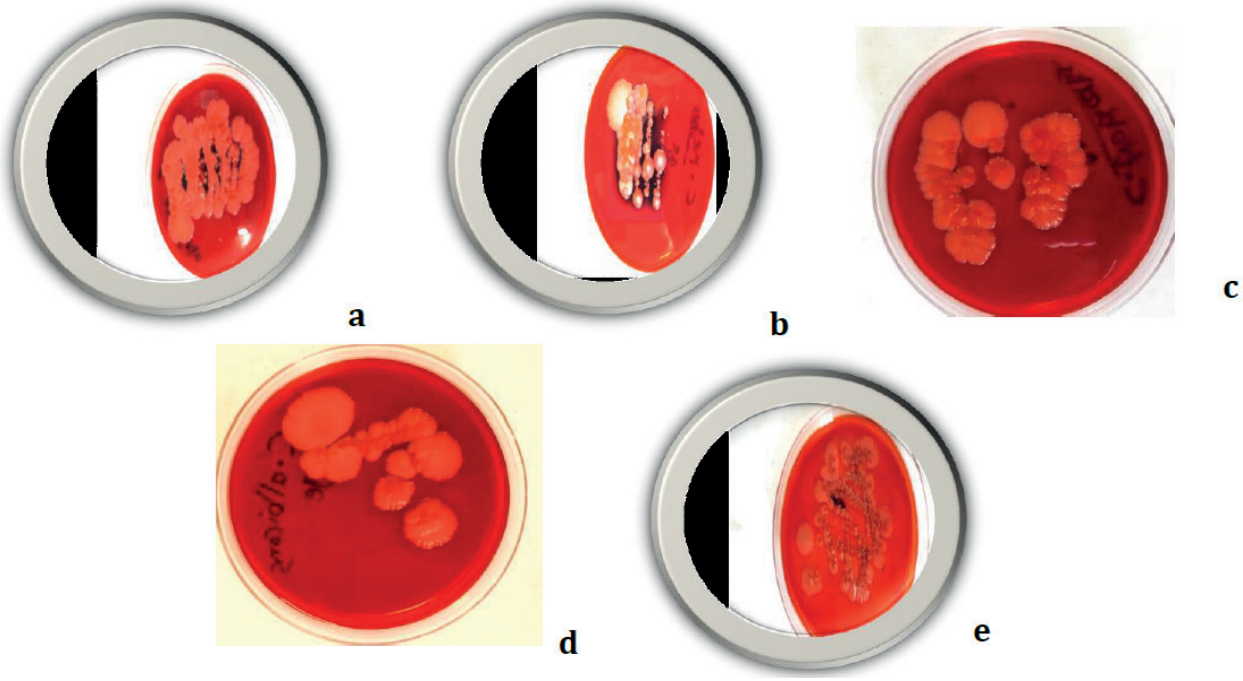

Figure 5. Biofilm formation resulted by (a) *C. krusei*, (b) *C. albicans*, (c) *C. tropicalis*, (d) *C. glabrata* and (e) *C. parapsilosis* on Congo red agar

Antifungal for *C.glabrata* (67)	MIC (mg/L)							
	0.03	0.06	0.125	0.25	0.5	1	S%	R%
	S							
Fluconazole	4	3	6	9	19	23	95.5%	4.5%
Voriconazole	1	2	6	15	17	9	74.6%	25.4%
Caspofungin	-	-	2	7	12	9	44.7%	55.3%
Micafungin	-	2	-	6	8	3	28.3%	71.7%
Amphotericin B	-	4	10	11	14	20	88%	12%
Flucytosine	2	4	8	11	18	19	92.5%	7.5%

S: sensitive; R: resistant

Table 7. Minimum Inhibitory Concentration (MIC) for *C. glabrata* isolates.

Candida spp.	Antifungal Agent	MFC (mg/mL)	
		MFC50	Range
C. glabrata	Fluconazole	0.03 -1	NA
	Voriconazole	0.03 -1	NA
	Caspofungin	0.03 - 0.125	0.125
	Micafungin	0.03 - 0.125	0.125
	Amphotericin B	≥ 0.06	0.06
	Flucytosine	0.03-1	NA

Table 8. Minimum Fungicidal Concentrations (MFC) for *C. glabrata*.

NA.: not-appropriate

der patients were more likely to receive insufficient antifungal therapy. Candidemia is connected with high mortality rates, increasing the hospitalization staying period, and raising therapeutic care[28]. The production test of the germ-tube has the benefit of being simple, effective, inexpensive, and fast to identify the *Candida spp*[29]. The chromogenic agar media are different; a selective medium was used to identify Candida spp fast. As a result, the capability to distinguish these species macroscopically was achieved[30].

The impact of the phospholipase enzyme was presented by digesting the cells' membrane of the host, producing cell lysis, and altering the external structures that increase adherence and result in infection. Therefore, phospholipase is possibly used as one of the limits to distinguish virulent hostile strains from non-hostile colonizers[20]. Mohandas and Ballal, (2008)[31] was referred that *Candida spp.* isolated from blood has more phospholipase activity. In two different studies from Turkey *Candida* isolates from blood culture, phospholipase activity resulted was (60.3% - 100%). The differences in results were retained because of distinctions in the sources of yeast isolates and the percentage of occurrence of isolates[32].

The essential protease enzyme of *Candida spp.* evades the attack of host tissues. The majority of tested *Candida spp.* had a positive protease activity. These conclusions propose that generating the protease may play a significant role in the pathogenesis of candidemia produced by *Candida spp.* It has been testified that more than 90% of Candida spp isolates proteinase products[33]. Proteinase production was identified in 74.56% of *Candida spp*. It was also testified that 88% of *Candida spp.* isolated from blood-linked intense proteinase action.

Moreover, *Candida spp.* atmospheric environments did not damage isolates testifying strong proteinase action. The alterations between studies may include product from differences in the sources of incubation, isolates and times[34].

Sachin *et al.* (2012)[35] reported that 94.8% of *C. albicans* samples presented hemolysis activity, whereas hemolysis activity of additional non-*C.albicans* extended from 7% to 60%; similarly, Sathiya *et al.* (2015)[36] described 100% of *Candida spp.* isolates exhibited β-hemolytic.

Form biofilms are associated with pathogenicity and should be considered an important virulence determinant during candidiasis. Biofilms may help fungi maintain the role of commensal and pathogen by evading host immune mechanisms, resisting antifungal treatment, and withstanding the competitive pressure from other organisms[37].

Our results are in good agreement with Khan's *et al.* results (2012)[38], where amphotericin B and Fluconazole showed vigorous antifungal activity against *Candida* due to their MIC standards of under 100 µg/ml. Also, the antifungal proved to be an active inhibitor against *C. glabrata*[39]. According to Hafidh *et al.* (2011)[40], the MFC/MIC relation is used to identify the influence of the antifungal effect against a specific pathogen. When the percentage of MFC:MIC result is between 1:1 and 2:1, the biochemical analysis measured fungicidal. In addition, Mohamadi *et al.* (2014)[41] also testified the fungicidal action of strain, using the destroy time technique in *C. albicans* and expending agar disc diffusion test, for example *C. albicans*, *C. tropicalis*, and *C. glabrata*. Fungicidal action is clinically more significant than fungistatic action. The prophylactic usage of fungistatic treatments has been related to an increased rate of innate or acquired immunity in clinical isolates[24-44].

Conclusions

Candida samples vary in their ability to form virulence factors, such as the production of phospholipase, proteinase, biofilms, and hemolysis when taken from leukemia patients. *Candida spp* samples were more sensitive to Fluconazole followed by Flucytosine, Amphotericin B, Voriconazole, Caspofungin, and Micafungin.

Funding

Not applicable.

Acknowledgments

The authors like to thank the Department of Molecular and Medical Biotechnology at the College of Biotechnology/ Al-Nahrain University and the Department of Chemistry at the College of Science/Al-Nahrain University for partially supporting this work.

Conflicts of Interest

The authors declare no conflict of interest.

Bibliographic references

1. Saikkonen K. Forest structure and fungal endophytes. Fungal Biol. Rev. 2007; 21: 67–74. doi:10.1016/j.fbr.2007.05.001
2. Risan M H. Molecular Identification of Yeast Candida glabrata from Candidemia Patients in Iraq. Iraqi J. Sci. 2016; 808-813.
3. Mei-Yin L, Jen-Fu H , Shih-Ming C , Hsyuan W, Hsuan-Rong H, Ming-Chou C, Ren-Huei F, Ming-Horng T. Risk Factors and Outcomes of Recurrent Candidemia in Children: Relapse or Re-Infection. J. Clin. Med. 2019; 8: 99. doi:10.3390/jcm8010099
4. Cleveland A A, Harrison L H, Farley M M, Hollick R, Stein B, Chiller T M , Lockhart S R, Park B J. Declining incidence of candidemia and the shifting epidemiology of Candida resistance in two US metropolitan areas 2008–2013: Results from Population-Based Surveillance. Microb. Pathog 2018; 117: 128-13. https://doi.org/10.1371/journal.pone.0120452
5. Blot S I, Vandewoude K H, Hoste E A. Colardyn F A. Effects of nosocomial candidemia on outcomes of critically ill patients. A.M. J. Med. 2002; 113: 480-485. doi: 10.1016/s0002-9343(02)01248-2

6. Ruan S Y, Hsueh P R. Invasive candidiasis: an overview from Taiwan. J. Formos. Med. Assoc.2009; 108: 443-451. doi: 10.1016/S0929-6646(09)60091-7
7. Chih-Cheng L, Wang C Y, Wei-Lun Liu W L, Huang, Y T, Hsueh P R. Time to positivity of blood cultures of different Candida species causing fungaemia. J. Med. Microbiol. 2012; 61: 701-704. DOI 10.1099/jmm.0.038166-0
8. Mohandas V, Ballal M. Proteinase and phospholipase activity as virulence factors in Candida species isolated from blood. Rev Iberoam Micol 2008; 25: 208-10. doi: 10.1016/s1130-1406(08)70050-0
9. Zaoutis T E, Argon J, Chu J, Berlin J A, Waish, T J, Feudtner C. The epidemiology and attributable outcomes of candidemia in adults and children, hospitalized in the United States: a propensity analysis. Clin. Infect. Dis. 2005; 41 (9): 1232-1239. doi: 10.1086/496922
10. Labelle A J, Micek S T, Roubinian N, Koilef M H . Treatment-related risk factors for hospital mortality in Candida bloodstream infections. Crit.Care Med. 2008; 36 (11): 2967-2972. DOI: 10.1097/CCM.0b013e31818b3477
11. Costa C R, Passos X S, Hasimoto L K, Lucena F O, Silva M. Differences in exoenzyme P. production and adherence ability of Candida spp. isolates from catheter, blood and oral cavity. Rev. Inst. Med. Trop. Sao Paulo 2010; 52 (3): 139-143. http://dx.doi.org/10.1590/S0036-46652010000300005
12. Suleyman G, Alangaden G J. Nosocomial fungal infections: epidemiology, infection control, and prevention. Infect. Dis. Clin. North Am. 2016; 30: 1023-1052. doi: 10.1016/j.idc.2010.11.003
13. Rodrigues C F, Silva S, Henriques M. Candida glabrata: A review of its features and resistance. Eur. J. Clin. Microbiol. Infect. Dis. 2014; 33: 673–688. doi: 10.1007/s10096-013-2009-3
14. Garcia-Cuesta C, Sarrion-Perez M G, Bagan J V. Current treatment of oral candidiasis: A literature review. J. Clin. Exp. Dent. 2014; 6: 576–582. doi:10.4317/jced.51798
15. Colle J G, Fraser A G, Marmion B P, Simmons A. Pactical medical microbiology.14th ed. Curchill living stone 1996; USA.
16. Emmons C W, Binford C H, Uts J P, Kwonchung, K J. Medical Mycology. 1977; 3rd Ed. Lea and Febiger. Philadelphia.
17. Willinger B, Hillowoth C, Selitsch B, Manafi M. Performance of Candida ID, a new chromogenic medium for presumptive identification of Candida species, in comparison to CHROMagar Candida, J. Clin. Microbiol 2001; 39: 3793-3795. DOI: 10.1128/JCM.39.10.3793–3795.2001
18. Murray P R. Manual of Clinical Microbiolog. 9th Ed. American Society for Microbiology 2007; Washington, D.C.
19. Janaina C O, Duque C, Flávia S, Iza T A, José F, Reginaldo B. Candida spp. in periodontal disease: a brief review. J. Oral Sci. 2010; 52 (2): 177-185. doi: 10.2334/josnusd.52.177
20. Deepa K, Jeevitha T, Michael A. In vitro evaluation of virulence factors of Candida species isolated from oral cavity. J. Microbiol. Antimicrob 2015; 7(3):28-32. https://doi.org/10.5897/JMA2015.0337
21. Mohandas V, and Ballal M, . Proteinase and phospholipase activity as virulence factors in Candida species isolated from blood. Rev Iberoam Micol., 2008; 25: 208-10.
22. Akcağlar S, Ener B, Tore O. Acid proteinase enzyme activity in Candida albicans strains: a comparison of spectrophotometry and plate methods. Turk. J. Biol. 2001; 67-559:35. doi:10.3906/biy-1002-39
23. Yenişehirli G, Bulut Y, Tunçoglu E, . Phospholipase proteinase and hemolytic activities of Candida albicans isolates obtained from clinical specimens. Mikrobiyol Bul. 2010; 44: 71-7.
24. Gültekin B, Eyigör M, Tiryaki Y, Kırdar S, Aydın N, . Investigation of antifungal susceptibilities and some virulence factors of Candida strains isolated from blood cultures and genotyping by RAPD-PCR. Mikrobiyol Bul. 2011; 45: 306-17.
25. Melek I, Mustafa A A, Ayse N K, Erkan Y, Omar E, Suleiman D, Gonca D. Investigating virulence factors of clinical Candida isolates in relation to atmospheric conditions and genotype. Turk .J. Med. Sci. 2012; 42(2):1476-1483. doi:10.3906/sag-1204-119
26. Naveen S, Deepak M, Divya D, Savita S. Evaluation of congo red agar for detection of biofilm production by various clinical Candida isolates. J. of Evolution of Med. and Dent. Sci 2014; 3 (59): 2278-4748. DOI: 10.14260/jemds/2014/3761
27. Andrew M B, Fraser M, Michael D P, Szekely A, Houldsworth M, Patterson Z, Elizabeth M J. MIC Distributions and Evaluation of Fungicidal Activity for Amphotericin B, Itraconazole, Voriconazole, Posaconazole and Caspofungin and 20 Species of Pathogenic Filamentous Fungi Determine Using the CLSI Broth Microdilution Method. J. Fungi 2017; 3: 27. doi: 10.3390/jof3020027
28. Rex J H, Pfaller M A, Walsh T J, Chaturvedi V, Espinel-Ingroff A et al. Antifungal susceptibility testing: Practical aspects and current challenges. Clin. Microbiol. Rev. 2001; 14: 643-658. DOI: 10.1128/CMR.14.4.643–658.2001
29. Ghelardi E, Pichierri G, Castagna B, Barnini S, Tavanti A, Campa M. Efficacy of Chromogenic Candida Agar for isolation and presumptive identification of pathogenic yeast species. Clin Microbiol Infect. 2007; 1469-0691. doi: 10.1111/j.1469-0691.2007.01872.x
30. Wisplinghoff H, Bischoff T, Tallent S M, Seifert H, Wenzel R P, Edmond M B. Nosocomial bloodstream infections in US hospitals: analysis of 24,179 cases from a prospective nationwide surveillance study. Clin. Infect. Dis. 2004; 39: 309-317. doi: 10.1086/421946
31. Motta-Silva A C, Aleva N A, Chavasco, J K, Armond M C, França J P, Pereira L J . Erythematous Oral Candidiasis in Patients with Controlled Type II Diabetes Mellitus and Complete Dentures, Mycopathologia. 2010; 169: 215-223. https://doi.org/10.1007/s11046-009-9240-6
32. Chakrabarti A, Shivaprakash M, Ghosh A. Standard Operating procedures, Mycology Laboratories. Indian Council of Medical Research 2016; 5-47.
33. Baillie G S, Douglas L J. Candida biofilm and their susceptibility to antifungal agents. Methods Enzymol 1999; 310: 644-56. doi: 10.1016/s0076-6879(99)10050-8
34. Silva J O F S, Lavrador M A, Candido R C. Performance of selective and differential media in the primary isolation of yeasts from different biological samples.Mycopathologia. 2004; 151(1):29-36. https://doi.org/10.1023/B:MYCO.0000012223.38967.7d
35. Sachin C D, Ruchi K, Santosh S. In vitro evaluation of proteinase, phospholipase and haemolysin activities of Candida species isolated from clinical specimens. Int. J. Med. Bio Res. 2012; 1(2):153-157. DOI: 10.14194/ijmbr.1211
36. Sathiya T, Arul Sheeba M S, Moorthy K, Punitha T, Vinodhini R, Saranya, A S. Candida albicans non-albicans species: Astudy of biofilm production and putative virulence properties. J. Harmo. Res. Pham. 2015; 4(1): 64-75. DOI: 10.1007/s11046-013-9638-z
37. Khan S M A, Malik A, Ahmad I. Anti-candidal activity of essential oils alone and in combination with amphotericin B or Fluconazole against multi-drug resistant isolates of Candida albicans. Med Mycol 2012; 50: 33 - 42. doi: 10.3109/13693786.2011.582890
38. Espinel-Ingroff A, Chaturvedi V, Fothergill A, Rinaldi M G. Optimal testing conditions for determining MICs and minimum fungicidal concentrations of new and established antifungal agents for uncommon molds: NCCLS collaborative study. J. Clinic Microbiol 2002; 40: 3776 - 3781. DOI: 10.1128/JCM.40.10.3776–3781.2002
39. Mohamadi J, Motaghi M, Panahi J, Havasian M R, Delpisheh A, Azizian M, Pakzad I. Anti-fungal resistance in candida isolated from oral and diaper rash candidiasis in neonates. Bioinformation 2014; 10:667-70. DOI: 10.6026/97320630010667
40. Hafidh R R, Abdulamir A S, Vern L S, Bakar F A, Abas F, Jahanshiri F, Sekawi Z. Inhibition of growth of highly resistant bacterial and fungal pathogens by a natural product. Open Microbiol. J. 2011; 5: 96 -106. doi: 10.2174/1874285801105010096
41. Monk B C, Goffeau A. Outwitting multidrug resistance to antifungals. Science 2008; 321: 367 - 369. DOI: 10.1126/science.1159746
42. Luksamijarulkul P, Aiempradit N, Vatanasomboon P. Microbial contamination on used surgical masks among hospital personnel and microbial air quality in their working wards: A hospital in Bangkok. Oman Med J 2014; 29(5):346-350. DOI: 10.5001/omj.2014.92
43. Mohammad T, Risan M, El-Hiti G, Ahmed D, Yousif E. Successful in-vivo treatment of mice infected with Candida glabrata using silver nanoparticles. Bionatura 2020, 5(4), 1340–1345. DOI. 10.21931/RB/2020.05.04.10

Received: 4 April 2021
Accepted: 25 June 2021

RESEARCH / INVESTIGACIÓN

Conjugation strategies on functionalized iron oxide nanoparticles as a malaria vaccine delivery system

Aswan Al-Abboodi[1], Hussain A. Mhouse Alsaady[1], Shaima R. Banoon[1], Mohammed Al-Saady[2]
DOI. 10.21931/RB/2021.06.03.20

Abstract: Vaccination has been used effectively to protect from infectious diseases and non-infectious diseases such as cancer and allergies. Different forms of particulate arrangements, including nanoparticles, virus-like particles (VLPs), and virosomes, have been built recently depending on the type of pathogen to be targeted. The ability to conjugate the recombinant *Plasmodium yoelii*, 19-kDa C-terminal fragment of merozoite surface protein 1 ($PyMSP1_{19}$) on the surface of superparamagnetic magnetite nanoparticles (SPIONs) was explored as a new technique of enhancing vaccination against malaria. Different conjugation strategies were performed to correlate the effects of nanoparticle chemistry surfaces to bind later with the malaria protein. (SPIONs) were prepared by chemical coprecipitation method and coated with 3-aminopropyltriethoxysilane (APTS) alone (as a surface coater), or with both APTS and polyethylene glycol (PEG) (as a shield to protect the malaria protein from proteolytic enzymes) by using a modified silanisation method.

X-ray powder diffraction (XRD, Philips Model) patterns indicated that the SPIONs were of high purity with an inverse spinal structure. Fourier Transform Infrared Spectroscopy (FTIR) was collected using PerkinElmer Spectrum 100 Series; spectra of uncoated and coated magnetite nanoparticles confirmed that the silane layer had been coated on the surface Fe_3O_4. The SPIONs were superparamagnetic as investigated by Vibrating Sample Magnetometry (VSM, Princeton Applied Research, model ISS) and relatively stable in aqueous phase at room temperature and could also be quickly recovered from suspension using an external magnet. Introduce the carboxyl groups onto the SPIONs surfaces, resulting in a relatively high protein binding capacity onto the nanoparticle surfaces.

The bare particles had a mean size of around 20 nm with a relatively narrow size distribution. 82% of African Green Monkey fibroblast (COS-7) were alive in nanoparticle suspension using the MTT assay method. The quantity of protein explicitly bound to particles was determined using Sodium Dodecyl Sulfate (SDS) - Polyacrylamide Gel Electrophoresis (PAGE). SDS–PAGE. When the conjugation blend was prepared in EDC, there was approximately 100% binding between $PyMSP1_{19}$ and the Fe_3O_4-COOH particles because no protein band was apparent at the expected molecular weight for $PyMSP1_{19}$ (45 kDa).

The current study investigates the theory that the gradual, persistent release of the malaria antigen may stimulate and maintain an elevated level of immune response for an extended period *in vivo*, which will be the scope of future work.

Key words: Malaria vaccine, Superparamagnetic nanoparticles, protein functionalization.

Introduction

Iron oxide nanoparticles such as magnetite Fe_3O_4 or maghemite γ- Fe_2O_3 are promising materials for applications in biomedicine and bioengineering areas[1-3,30] These nanoparticles have attracted great interest due to their unique properties[4, 31] such as narrow size distribution, biocompatibility, non-toxicity, and ability to be detected and manipulated with an external magnetic field. Both are generally appropriate and safe for in vivo biomedical applications[4]. However, the utilization of these nanoparticles is still subject to many limitations, including surfaces containing hydroxyl groups that cannot bond covalently with biomolecules. Therefore, examining the best method to conjugate high protein binding capacity is an urgent issue because the most excellent technique for increasing vaccine efficiency still needs investigation since many diseases are still without effective vaccines, such as malaria disease.

The Coprecipitation technique is the most common method to prepare iron oxide nanoparticles. Both sodium hydroxide (NaOH) and ammonium hydroxide (NH_4OH) have been used to detect whether the basicity manipulates the crystallization process during particle formation[8,32]. Various surface modification techniques have been used to enhance nanoparticles' diagnosis and therapeutics potential in biomedicine applications[6]. Successful conjugation of biomolecules to the surface of magnetic particles is critical to their applicability[5]. Therefore, a versatile method of surface functionalization of SPIONs is often required, which sensitively balances the intermolecular forces concerning biomolecules such as proteins and antibodies attached to the particles' outer layer. However, conjugation of a desired functional group at the right orientation on the nanoparticle surface remains a significant challenge[7,33,44]. The method of surface modification of iron oxide by using organosilane reagent [amino-silane reagent (3-aminopropyltriethoxysilane, APTS)] is relatively robust, with many parameters such as silane concentration, temperature, time, and solvent type that can be optimized to create diffused functionalized magnetic particles for consequent tagging with biomolecules[6].

Some vaccines are still challenged and need effective strategies to obtain good control for malaria vaccines. Protein vaccine is one strategy that can generate both humoral and cellular immune responses, primarily when it supports by promoter injections[12,34]. Magnetofection is a suitable device for protein delivery, gene therapy, and gene expression[14,42,43]; therefore, magnetic nanoparticles have been chosen for this study to prove its achievability as a proposed protein delivery carrier of malaria vaccine to use it later as a vaccine carrier for other some parasitic diseases that their vaccines are underdeveloped until now. Substantial development in the malaria vaccine field has been presented in the current study; the key to this

[1] Department of Biology, College of Science, University of Misan, Misan, Iraq.
[2] Department of Mechanical and Aerospace Engineering, Monash University, Clayton, Australia.

Corresponding author: aswan.abboodi@uomisan.edu.iq

success is iron oxide nanoparticles' use to deliver malaria protein (antigen) in an effectual technique to where it matters.

Materials

Analytical grade reagents for magnetite nanoparticles synthesis included Fe (III) chloride hexahydrate ($FeCl_3.6H_2O$ >99%) from Ajax Finechem (NSW Australia), Fe (II) sulfate ($FeCl_2.7H_2O$ >99%) from Ajax Chemical (Sydney, Australia), sodium hydroxide (NaOH), and trisodium citrate dihydrate ($C_6H_5Na_3O_7.2H_2O$) from Sigma Aldrich (Sydney, Australia). All materials including 3-aminopropyltriethoxysilane (APTS, 95%), Polyethyleneglycol (PEG), absolute ethanol (C_2H_5OH, 99.5%) glutaraldehyde (10%), succinic anhydride, phosphate buffered saline (PBS, 0.01M, pH 7.4), and the conjugating agents N-hydroxysulfosuccinimide (NHS), 1-ethyl-3-(3-dimethylaminopropyl) carbodiimide (EDC), N, N-dimethylformamide (DMF) were supplied by Sigma Aldrich (Sydney, Australia). African green monkey kidney cells (COS-7 cell lines) were kindly provided by staff at Prof. Ross Coppel's laboratory (Department of Microbiology, Monash University, Australia), Dimethylsulfoxude (DMSO), 3-(4,5-87-90% dimethyl-2-thiazol-2-yl-2, 5-diphenyltetra-zolium bromide (MTT), penicillin/ streptomycin, foetal calf serum and other related reagent grade chemicals were acquired from Invtrogen (Carlsbad, California, USA) and used to measure the toxicity of the as-synthesised nanoparticles.

Methods

Synthesis and coating of Magnetite nanoparticles

Magnetite nanoparticles were prepared using the procedure reported in (8), in which a chemical coprecipitation method was used with some modification. Trisodium citrate was used as an electrostatic stabilizer to create an electrostatic double layer and reduced the extent of agglomeration[12,13,41]. In a typical experiment, ferric chloride (0.005 mol) and ferrous chloride (0.0025 mol) (molar ratio 2:1) were dissolved in deionized water (50 ml). To raise the pH value, sodium hydroxide solution (20 ml, 1.5 M, including 0.005 mol trisodium citrate) was added to a 100 ml three-necked flask. The precipitation was done by drop-by-drop addition of iron salts solution to the mixture of NaOH and trisodium citrate under vigorous stirring (homogenization string rate was 1500 rpm) for 1h at 80 º C in a nitrogen (N_2) atmosphere. The color of the bulk solution immediately turned from orange to black. The nanoparticles were then split from the solution by a permanent magnet and cleaned several times with ethanol and distilled water before re-suspended in water.

APTS is an amino-functional silane-coupling agent used to immobilize physiologically active molecules. The hydroxyl groups on the magnetite surface can be easily coupled with silanes by forming covalent bonds through condensation reaction to give a siloxane linkage, as Scheme 1 shows. In this work, ethanol was used to change the medium from water. 0.43g of Fe_3O_4 nanoparticles were dispersed in 9.7ml ethanol by sonication for 10 min. 0.3ml of 3-aminopropyltriethoxysilane (APTS) was added, and the resulting solution was transferred into a round-bottomed flask to carry out the silanisation reaction at 25 ºC under N_2 atmosphere overnight in a Schlenk system. The Fe_3O_4 – APTS magnetic nanoparticles were recovered from the reaction mixture using a permanent magnet. The supernatant was removed, and the precipitates were washed several times with ethanol and then with water. The high molecular weight of PEG polymer was mixed with silane to possibly improve the biocompatibility and dispersibility of Fe_3O_4 nanoparticles[15,16].

SPIONs Characterisations

Powder X-Ray diffraction (XRD)

X-ray powder diffraction (XRD) measurements were used to identify the crystalline phase of the particles before and after coating. XRD was performed on a Philips PW 1140/90 diffractometer using monochromatized x-ray beams from CuKα, λ = 1.54 Å radiation at a scan rate of 1° min^{-1} from 5° to 60° with a step size of 0.02°. The scanning voltage was 50KV, and the scanning current was 20 mA.

Vibrating Sample Magnetometry (VSM)

The particular values for the inundation magnetization measurements were directly acquired on a predetermined weight of SPIONs before and after coating using Vibrating Sample Magnetometry (VSM, Princeton Applied Research, model ISS) working at room temperature. A recognized weight of the samples was placed into the VSM sample holder. A top magnetic field of approximately 15KOe was used. The saturation magnetization values were standardized to the mass of samples to yield specific magnetization, M_s (emu g^{-1}).

Fourier Transform Infrared Spectroscopy (FTIR)

FTIR spectra of the nanoparticles were collected on an FTIR spectrophotometer using PerkinElmer Spectrum 100 Series FT-IR spectrometer in a wave number varying from 4000 to 400 cm^{-1} with a resolution accuracy of 4 cm^{-1} under ambient conditions. Before compacting, all samples were dried at 70 ºC for 48h. A small amount of each sample dry powder was thoroughly mixed and crushed with dried KBr using a mortar and pestle. The mixture was pressed into pellets using 8 tons/cm^2 of pressure for 2 minutes to form discs for analysis.

Transmission Electron Microscope (TEM)

TEM was used to determine the size and morphology of the nanoparticles. The nanoparticle suspension was diluted, and a few drops were put on a carbon-stabilized grid (200 meshes). The grids were left in the oven at 50ºC overnight. Sample grids were attached to the sample holder on a Hitachi H7500 TEM instrument at an accelerating voltage of 120 kV microscope. The mean diameter of the size distribution was determined by measuring more than 150 particles from TEM images using *Image J*[9].

MTT assay

To evaluate whether the particles could be used for biomedical applications, a non-radioactive colorimetric MTT assay[10] was performed to measure the cell cytotoxicity. African Green Monkey Fibroblast (COS-7) cells were seeded on a 96-well microtiter plate at a concentration of 2* 10^4 /well and cultured in a complete RPMI (C-RPMI) medium supplemented with 10% fetal calf serum (FCS). The plate was incubated at 37ºC and 5% CO_2 overnight. Three different concentrations of bare and coated nanoparticles (0.1 mg/ml, 1 mg/ml and 10 mg/ml) were added for a further 24h incubation. The control well group was a culture medium with no particles. All samples and the control were tested in triplicate, with the results conveyed as mean ± standard deviation shown as error bars in the MTT plots. 5µl of a solution of 5mg/ml MTT (3-(4,5- dimethylthiazol-2-yl-2, 5-diphenyltetra-zolium bromide) dissol-

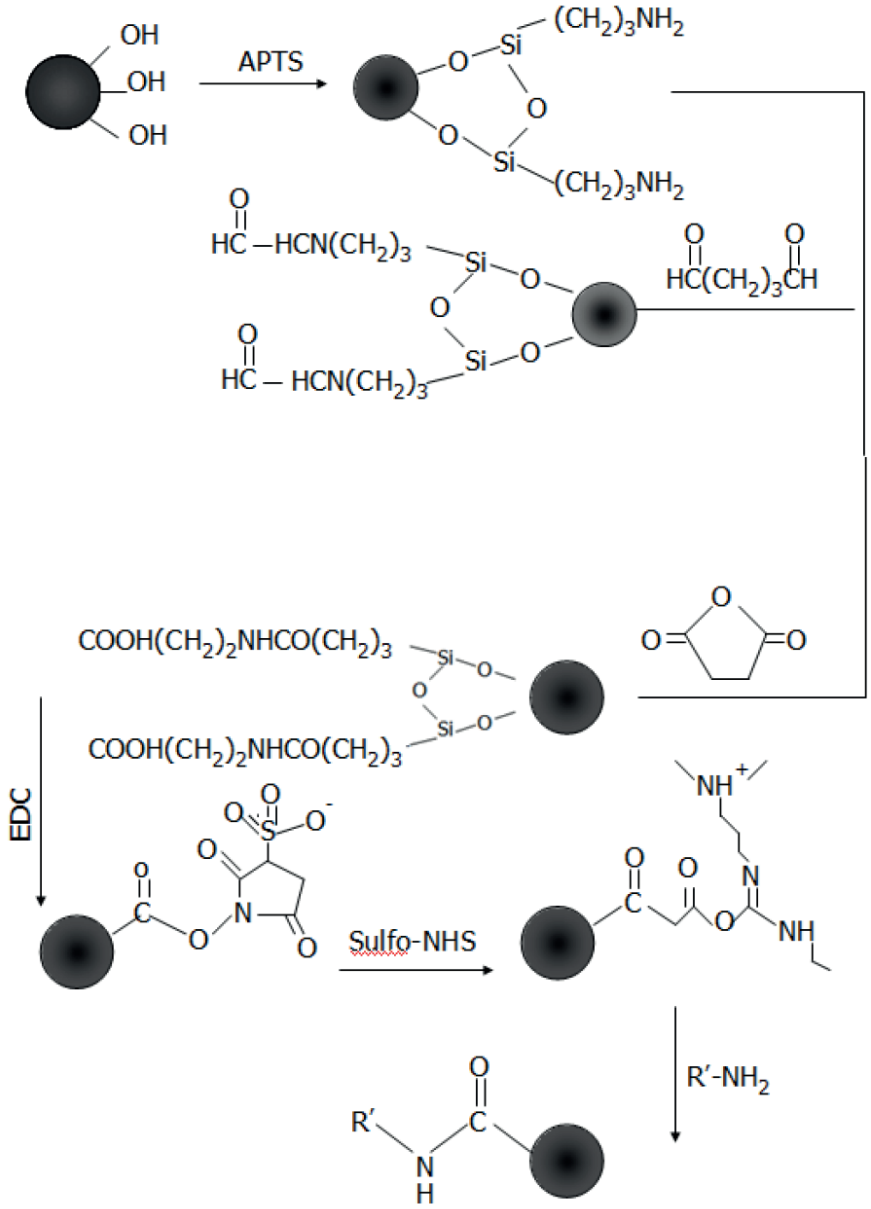

Scheme 1. Silane chemistry approaches to functionalize Fe_3O_4 particles with $-NH_2$, –CHO, and –COOH.

ved in PBS pH 7.4 was added to each well and incubated for 4h at 37ºC in the 5% CO_2 incubator. After incubation for 4h, the medium was removed from the plate and rinsed with PBS. MTT is a yellow-colored, water-soluble, and tetrazolium salt. Living cells can metabolize this salt in their mitochondria by active mitochondrial reductase enzyme into a water-insoluble and dark blue ring, Formazan derivative. Dead cells can now reduce tetrazolium salt; thus, the conversion can be related to the amount of Formazan crystals formed. Subsequently, ring Formazan crystals can be dispersed in an organic solvent such as dimethyl sulfur oxide (DMSO). Therefore, 100 µl of 5mg/ml of (DMSO) was added to each well in the plate to dissolve the crystals, and the plate was incubated for 1h. The absorbance of each well was read on a microplate reader (Magellan, Tecan, Australia) at wavelengths of 570nm and 690nm. The net absorbance was calculated by (A_{570}-A_{690}) (A refers to the area means absorbance). The relative cell viability (%) was calculated as ([A_{sample}] / [$A_{control}$]*100%, with the resultant value representing the number of living cells.

Surface functionalization of Fe_3O_4 – APTS nanoparticles

The particles were modified to introduce aldehyde or carboxylic functional groups. 20 ml of 10% glutaraldehyde was added to the precipitate of silane-coated magnetic particles (Fe_3O_4 – APTS) prepared previously, and the reaction mixture was left under gentle agitation for 3hrs at room temperature (25ºC) to introduce aldehyde functional groups. After 3hrs, the Fe_3O_4 – CHO particles were steadied with a magnet and then cleaned several times with PBS via magnetic parting and then re-dispersed. To create the carboxyl functional groups, succinic anhydride was added to the Fe3O4 – APTS nanoparticles (1:20 wt/ wt) suspended in DMF. The mixture was agitated for 3hrs under an N_2 atmosphere. Subsequently, the Fe_3O_4 – COOH derivatized particles were washed two times with DMF followed by PBS. The washed particles were suspended in PBS and stored at 4ºC for further use.

Results

Characterization of nanoparticles

X-ray powder diffraction (XRD) was performed to characterize the crystal phase of as-synthesized nanoparticles

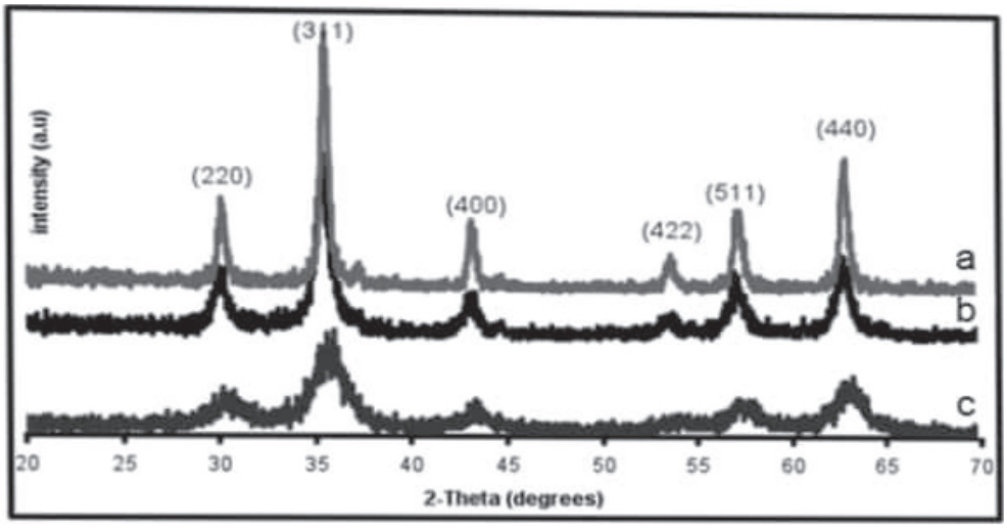

Figure 1. Indexed X-ray diffractograms of (a) Fe_3O_4, (b) Fe_3O_4 – APTS, and (c) Fe_3O_4 – APTS+PEG nanoparticles.

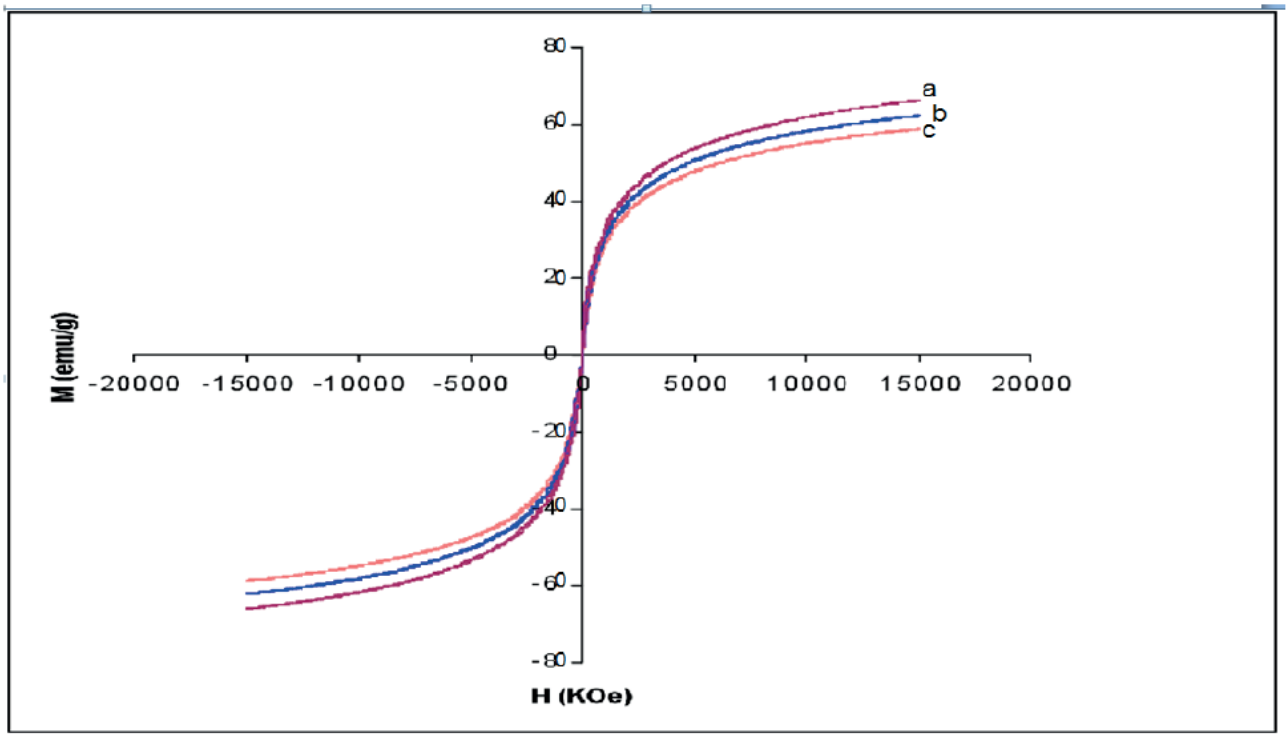

Figure 2. Magnetization curves of (a) Fe_3O_4, (b) Fe_3O_4 – APTS and (c) Fe_3O_4 – APTS+PEG nanoparticles. (H) Applied magnetic field (KOe); (M) Magnetization (emu/g).

(Fig. 1). The different peaks of Fe_3O_4 marked by their indices: (220), (311), (400), (422), (511), and (440) at 2θ can be referred to as the cubic structure of Fe_3O_4. Magnetic features of the as-synthesized nanoparticles were investigated by VSM measurement at room temperature (Fig. 2). The bare Fe_3O_4 displayed relatively high magnetization (67 emu/g) at 15KOe. The magnetization of silane-coated Fe_3O_4 – APTS nanoparticles was calculated to be 63.3 emu/g (Fig. 2b), slightly diminished in comparison to bare Fe_3O_4 due to the non-magnetic silane layer. In addition, Fe_3O_4 – APTS+PEG nanoparticles have a magnetization of 58.9 emu/g, due to the thickness of the silane and PEG coating.

TEM images of bare and silane-coated nanoparticles were taken to investigate the particles' size, shape, and uniformity. The bare particles had a mean size of around 20 nm with a relatively good size distribution (Fig. 3a). Scanning electron micrograph images for magnetic nanoparticles before and after silanisation are shown in Fig. 3, confirming the size of bare Fe_3O_4 of around 20nm. FTIR spectra of uncoated and coated magnetite nanoparticles are shown in Fig. 4. The wide band of 3600 – 3300 cm^{-1} paralleled the O-H stretching tremor of a trace amount of water due to physisorbed water and surface hydroxyls. After silanisation, the characteristic bands of Si-O-C at 1086 and 1155 cm^{-1} appeared (Fig. 4b), confirming that silane layer had been coated on the surface of Fe_3O_4.

In vitro cytotoxicity evaluation

To investigate the percentage of cell viability due to the introduction to nanoparticles, the viabilities of African Green Monkey fibroblast (COS-7) cells in models with both bare and coated magnetite were studied by the MTT assay method to evaluate whether these nanoparticles are suitable for biomedical applications. This method measures the mitochondrial dehydrogenase activity of viable cells, with materials inducing

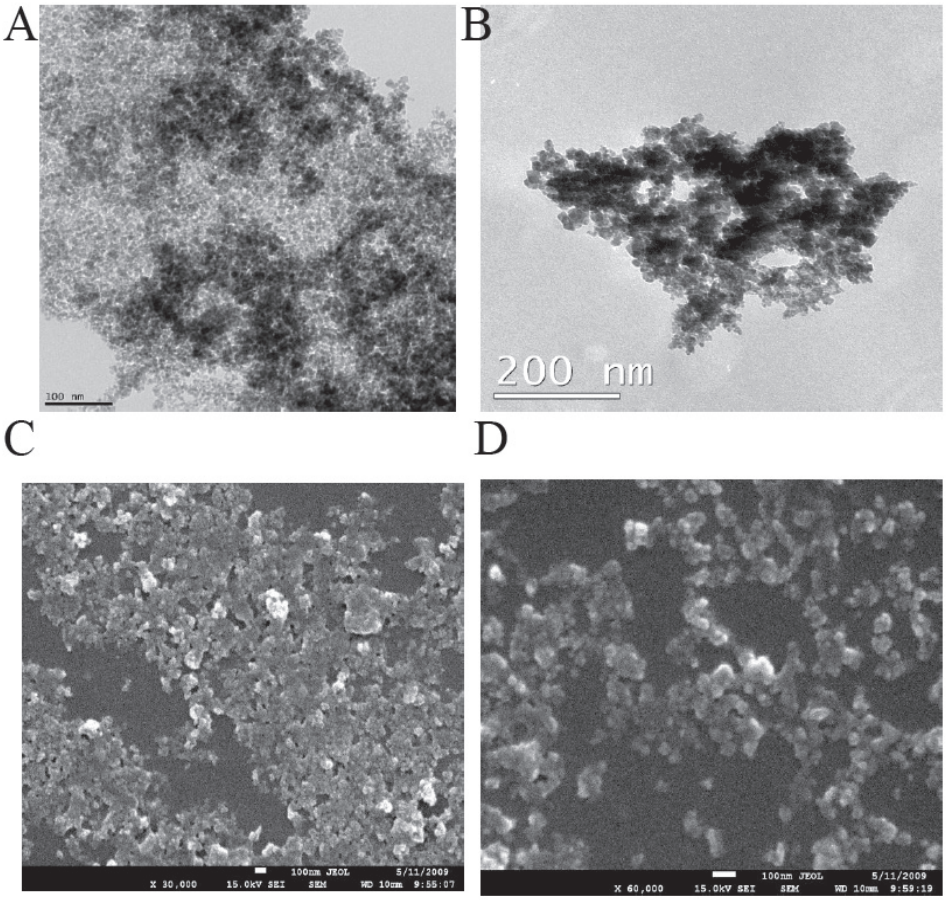

Figure 3. TEM images showing the morphology of (a) Fe_3O_4; (b) Fe_3O_4 – APTS, SEM images of (c) Fe_3O_4; (d) Fe_3O_4 – APTS.

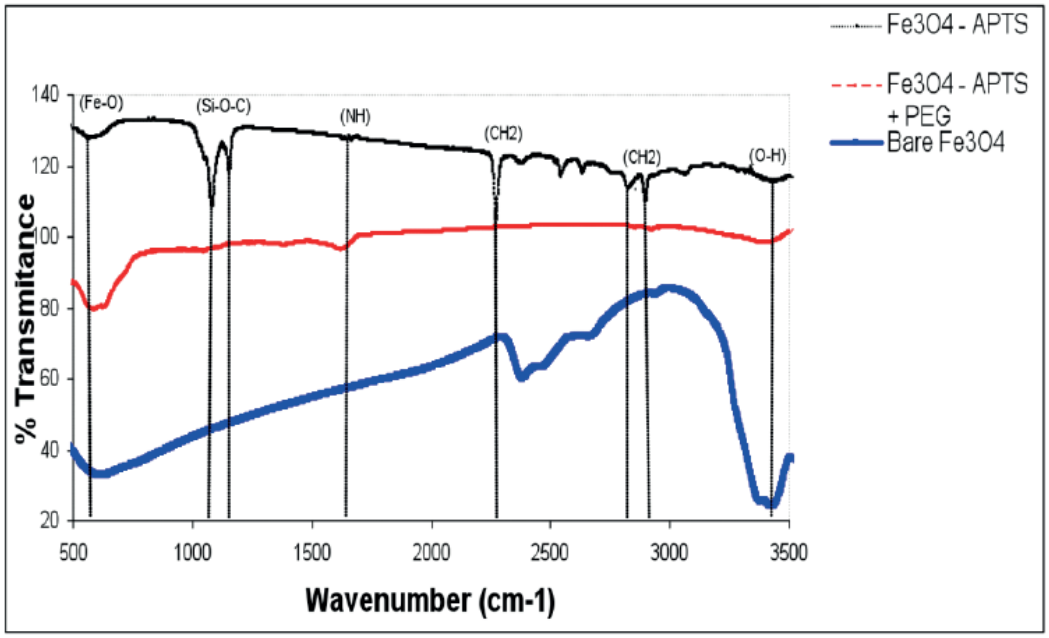

Figure 4. FTIR spectra of Fe_3O_4, Fe_3O_4 – APTS, and Fe_3O_4 – APTS+PEG.

cell viability of more than 80%, often recognized as biocompatible[22]. All the nanoparticles samples (three different concentrations for each sample) from a 24 h incubation led to a decrease in the viability of COS-7 cell lines compared to the control. As shown in Fig. 5, when the cells were incubated with 0.1 mg/ml bare Fe_3O_4 solution, more than 82% of cells remained alive, whereas the cell viability decreased to 34% and 12.5% with increasing concentrations to 1 mg/ml and 10 mg/ml, respectively.

Surface functionalization of Fe_3O_4 – APTS nanoparticles

The introduction of –COOH and –CHO groups on the magnetite surface was confirmed with FTIR spectroscopy (Fig. 6). The spectrum of the functionalized SPIONs with –COOH showed the characteristic absorption peak at 1634 cm^{-1} corresponding to the symmetric COO- stretching. The characteristic absorption peak –C-O-C– at 2993.4 cm^{-1} was observed in the spectrum of the –COOH group activated on the silane-coated Fe_3O_4 nanoparticles.

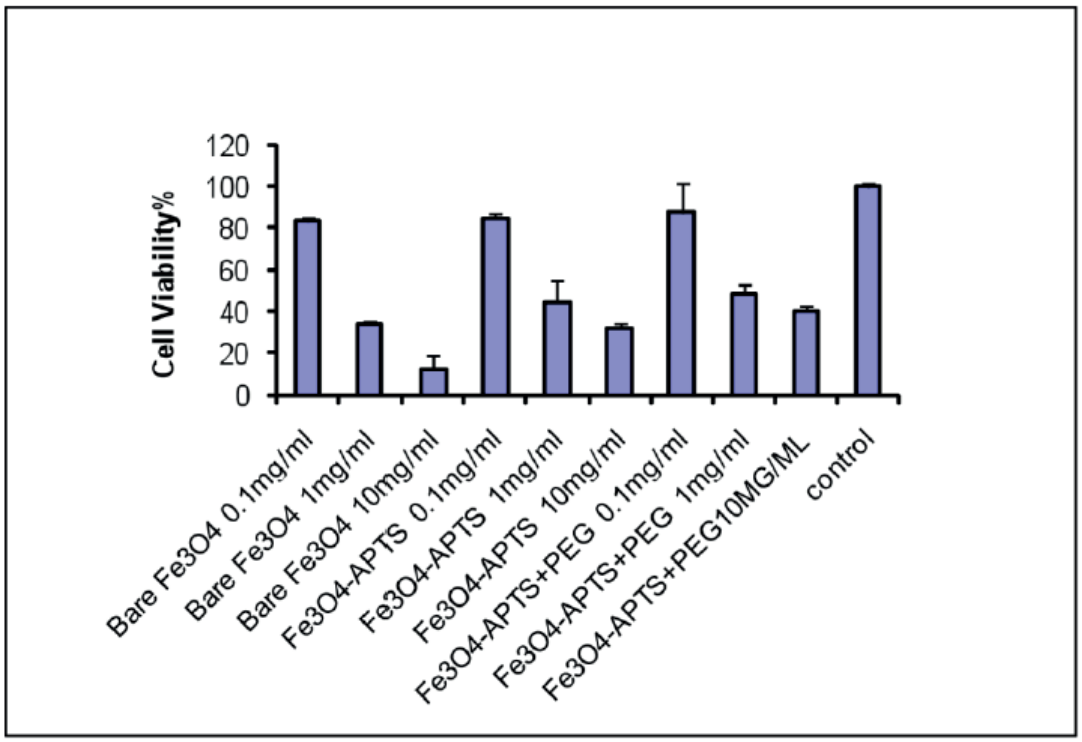

Figure 5. MTT assay of Fe_3O_4, Fe_3O_4 – APTS, and Fe_3O_4 – APTS+PEG.

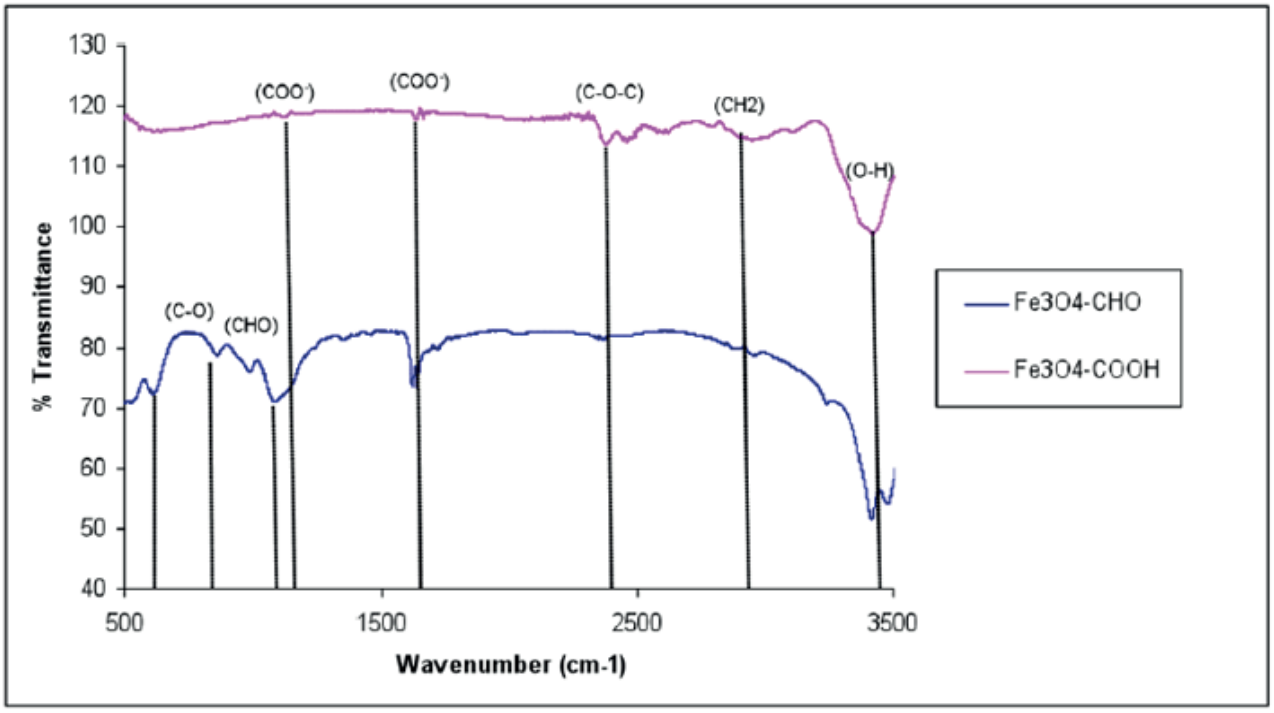

Figure 6. FTIR spectra of functionalized Fe_3O_4 – COOH and Fe_3O_4 – CHO nanoparticles.

DISCUSSION

Characterization of nanoparticles

The X-ray diffraction results showed in (Fig. 1) are in good agreement with the theoretical values (JCPDS 19-629) of the standard XRD reference pattern of pure magnetite. A clean Fe_3O_4 cubic spinel phase can be confirmed. Generally, there was no significant shift in the highest position due to the presence of amino silane. The broader peak that appeared at about 23.4º in the coated particles Fe_3O_4 – APTS+PEG attributed to the existence of an amorphous layer possibly due to the presence of polymer. The magnetic properties presented in (Fig. 2), in all cases, the magnetization plots exhibited zero remanence and coercivity with no hysteresis loop, indicating that these nanoparticles were superparamagnetic[17,18,35], due to their sizes rendering single magnetic domains[19]. The TEM images illustrated in (Fig 3) revealed a thin silane layer favorable

to keep the high magnetization and stability, while it was also convenient for modification on the nanoparticles surface[29]. In the three presented samples in (Fig. 4), the presence of Fe_3O_4 core could be seen by the strong assimilation bond 579 cm-1, corresponding to the Fe-O bond of Fe_3O_4[20,21,36]. The strong C-O-C, CH2, and –CH peaks indicated that PEG was bonded to the surface through a reaction of PEG-silane with –OH group on the nanoparticle's surface[11].

In vitro cytotoxicity evaluation

Fig. 5 showed the results of the MTT assay. This result proved the biocompatibility of the synthesized magnetite nanoparticles at minimal concentrations (<0.1 mg/ml), comparable to the standard dosage for particulate vaccine typically measured in micrograms[23]. The toxicity of SPIONs may correlate to the capability of these nanoparticles to damage DNA via magnetite oxidation. Karlsson *et al.*[24] indicated that magnetite nanoparticles could cause a minimal amount of toxicity (examined with a comet assay) due to the effectiveness in causing oxidative DNA lesions in cultured A549 cells (the human lung epithelial cell line). A small adverse effect on cell viability at low concentrations suggested that citrate groups on the surface of Fe_3O_4 play an essential role in providing some protection against cell toxicity and reducing the toxic effect of magnetic solution[25,26,37]. The coated SPIONs with silane alone and silane with PEG showed slightly reduced toxic effects at the highest concentrations. This may be due to the different properties and surface reactivity of their surfaces. The toxicity of silane has been well-reviewed by Iler *et al.*[27]. Addition of –NH2 groups (Fig. 6) denote less accessible sites for biomolecules to attach in comparison to the uncoated SPIONs. The reduced toxicity of the Fe_3O_4 – APTS+PEG nanoparticles may be attributed to the high solubility of PEG in the cell membranes[28,38]. However, there were still toxic effects on the soluble factors present in these nanoparticles, including detergents and monomers from the preparation procedure or the breakdown of products during incubation.

Surface functionalization of Fe_3O_4 – APTS nanoparticles

The peaks that appeared in (Fig.6) provide evidence that –COOH groups were attached to the surface through a reaction of –NH2 and succinic anhydride at a transmittance of 119%[29,39,40]. As the amine-terminated surface was converted to the aldehyde group, the characteristic band for HC=O vibration appeared at 1711 cm^{-1} and CH_2-CHO at 1414 cm^{-1}, and CHO at 1374 cm^{-1} indicating that the aldehyde group had been introduced to the SPION surfaces. The findings illustrated in (Fig. 6) indicated that the size of Fe_3O_4 – APTS+PEG was the largest, possibly either due to the high molecular weight of the polymer or due to the agglomerate of these particles.

Conclusions

Multifunctional magnetite nanoparticles have been successfully prepared by a co- precipitation method. By surface modification with APTS and subsequent functionalization with glutaraldehyde and succinic anhydride, these nanoparticles should have a high active binding to $PyMSP1_{19}$ malaria protein molecules (which is currently under study). XRD patterns indicated the high purity of the synthesized SPIONs, FTIR spectra confirmed that silane layer had been coated on the surface of Fe_3O_4. The SPIONs were superparamagnetic and were stable in aqueous phase at room temperature. VSM displayed relatively high magnetization (67 emu/g) at 15Koe of the iron oxide nanoparticles. TEM images of bare and silane-coated nanoparticles were taken to investigate the size, shape and uniformity of the particles. The bare particles had a mean size of around 20 nm with relatively slim size distribution which also confirmed by Scanning Electron Micrograph (SEM). The fabricated nanoparticles were non-toxic which indicated by MTT assay. The particles can potentially be used as a platform to conjugate with other proteins including those targeting specific parasites. With the advantage of narrow size properties, relatively low toxicity, and ease of coupling with other biomolecules, we envision that these nanoparticles could be used as particulate vaccine in biomedical application.

Bibliographic references

1. Halavaara J, Tervahartiala P, Isoniemi H, Höckerstedt K. Efficacy of sequential use of superparamagnetic iron oxide and gadolinium in liver MR imaging. Acta radiologica. 2002 Mar;43(2):180-5.
2. Liberti PA, Rao CG, Terstappen LW. Optimization of ferrofluids and protocols for the enrichment of breast tumor cells in blood. Journal of magnetism and magnetic materials. 2001 1 January;225(1-2):301-7.
3. Lübbe AS, Alexiou C, Bergemann C. Clinical applications of magnetic drug targeting. Journal of Surgical Research. 2001 Feb 1;95(2):200-6.
4. Dormann JL, Fiorani D, Tronc E. Advances in chemical physics. Vol. XCVII, Eds. I. Prigogine y Stuart A. Rice, John Wiley and Sons. 1997.
5. Tartaj P, Morales MP, Gonzalez-Carreno T, Veintemillas-Verdaguer S, Serna CJ. Advances in magnetic nanoparticles for biotechnology applications. Journal of Magnetism and Magnetic Materials. 2005 Apr 1;290:28-34.
6. Li D, Teoh WY, Gooding JJ, Selomulya C, Amal R. Functionalization strategies for protease immobilization on magnetic nanoparticles. Advanced Functional Materials. 2010 9 June;20(11):1767-77.
7. Cannon WR, Danforth SC, Flint JH, Haggerty JS, Marra RA. Sinterable Ceramic Powders from Laser-Driven Reactions: I, Process Description and Modeling. Journal of the American Ceramic Society. 1982 Jul;65(7):324-30.
8. He R, You X, Shao J, Gao F, Pan B, Cui D. Core/shell fluorescent magnetic silica-coated composite nanoparticles for bioconjugation. Nanotechnology. 2007 6 July;18(31):315601.
9. Rasband WS. US National Institute of Health. http://rsb. info. nih. gov/ij. 2006.
10.
11. Gupta AK, Wells S. Surface-modified superparamagnetic nanoparticles for drug delivery: preparation, characterization, and cytotoxicity studies. IEEE transactions on nanobioscience. 2004 Mar 15;3(1):66-73.
12. Liu X, Ma Z, Xing J, Liu H. Preparation and characterization of amino–silane modified superparamagnetic silica nanospheres. Journal of Magnetism and magnetic Materials. 2004 Mar 1;270(1-2):1-6.
13. Liu X, Xing J, Guan Y, Shan G, Liu H. Synthesis of amino-silane modified superparamagnetic silica supports and their use for protein immobilization. Colloids and Surfaces A: Physicochemical and Engineering Aspects. 2004 4 May;238(1-3):127-31.
14. Sun J, Zhou S, Hou P, Yang Y, Weng J, Li X, Li M. Synthesis and characterization of biocompatible Fe3O4 nanoparticles. Journal of biomedical materials research Part A. 2007 Feb;80(2):333-41.
15. Zaitsev VS, Filimonov DS, Presnyakov IA, Gambino RJ, Chu B. Physical and chemical properties of magnetite and magnetite-polymer nanoparticles and their colloidal dispersions. Journal of Colloid and Interface Science. 1999 Apr 1;212(1):49-57.
16. Harris LA, Goff JD, Carmichael AY, Riffle JS, Harburn JJ, St. Pierre TG, Saunders M. Magnetite nanoparticle dispersions stabilized with triblock copolymers. Chemistry of Materials. 2003 25 March;15(6):1367-77.
17. Saravanan P, Alam S, Mathur GN. Comparative study on the synthesis of γ-Fe 2 O 3 and Fe 3 O 4 nanocrystals using high-temperature solution-phase technique. Journal of materials science letters. 2003 Sep;22(18):1283-5.

18. Kim DK, Zhang Y, Voit W, Rao KV, Muhammed M. Synthesis and characterization of surfactant-coated superparamagnetic monodispersed iron oxide nanoparticles. Journal of magnetism and Magnetic Materials. 2001 1 January;225(1-2):30-6.
19. Montagne F, Mondain-Monval O, Pichot C, Mozzanega H, Elaıssari A. Preparation and characterization of narrow sized (o/w) magnetic emulsion. Journal of magnetism and magnetic materials. 2002 Sep 1;250:302-12.
20. Cornell RM, Schwertmann U. The iron oxides: structure, properties, reactions, occurrences and uses. John Wiley & Sons; 2003 17 October.
21. Yamaoka T, Tabata Y, Ikada Y. Distribution and tissue uptake of poly (ethylene glycol) with different molecular weights after intravenous administration to mice. Journal of pharmaceutical sciences. 1994 1 April;83(4):601-6.
22. Weissleder R, Bogdanov A, Neuwelt EA, Papisov M. Long-circulating iron oxides for MR imaging. Advanced Drug Delivery Reviews. 1995 Sep 1;16(2-3):321-34.
23. Karlsson HL, Cronholm P, Gustafsson J, Moller L. Copper oxide nanoparticles are highly toxic: a comparison between metal oxide nanoparticles and carbon nanotubes. Chemical research in toxicology. 2008 Sep 15;21(9):1726-32.
24. Lacava ZG, Azevedo RB, Martins EV, Lacava LM, Freitas ML, Garcia VA, Rebula CA, Lemos AP, Sousa MH, Tourinho FA, Da Silva MF. Biological effects of magnetic fluids: toxicity studies. Journal of magnetism and magnetic materials. 1999 Jul 1;201(1-3):431-4.
25. Häfeli UO, Pauer GJ. In vitro and in vivo toxicity of magnetic microspheres. Journal of magnetism and magnetic materials. 1999 Apr 1;194(1-3):76-82.
26. Iler KR. The chemistry of silica. Solubility, polymerization, colloid and surface properties and biochemistry of silica. Wiley, New York.1979: 89.
27. Jarrell BE, Williams SK, Stokes G, Hubbard FA, Carabasi RA, Koolpe E, Greener D, Pratt K, Moritz MJ, Radomski J. Use of freshly isolated capillary endothelial cells for the immediate establishment of a monolayer on a vascular graft at surgery. Surgery. 1986 1 August;100(2):392-9.
28. Liu C, Wu X, Klemmer T, Shukla N, Weller D, Roy AG, Tanase M, Laughlin D. Reduction of sintering during annealing of FePt nanoparticles coated with iron oxide. Chemistry of materials. 2005 8 February;17(3):620-5.
29. Feng B, Hong RY, Wang LS, Guo L, Li HZ, Ding J, Zheng Y, Wei DG. Synthesis of Fe3O4/APTES/PEG diacid functionalized magnetic nanoparticles for MR imaging. Colloids and Surfaces A: Physicochemical and Engineering Aspects. 2008 Oct 1;328(1-3):52-9.
30. Ajinkya N, Yu X, Kaithal P, Luo H, Somani P, Ramakrishna S. Magnetic Iron Oxide Nanoparticle (IONP) Synthesis to Applications: Present and Future. Materials. 2020 Jan;13(20):4644.
31. Cheah P, Cowan T, Zhang R, Fatemi-Ardekani A, Liu Y, Zheng J, Han F, Li Y, Cao D, Zhao Y. Continuous growth phenomenon for direct synthesis of monodisperse water-soluble iron oxide nanoparticles with extraordinarily high relaxivity. Nanoscale. 2020;12(16):9272-83.
32. Velázquez-Herrera FD, Fetter G. Hydrotalcites with heterogeneous anion distributions: a first approach to producing new materials to be used as vehicles for the successive delivery of compounds. Clay Minerals. 2020 Mar;55(1):31-9.
33. Yong KW, Yuen D, Chen MZ, Porter CJ, Johnston AP. Pointing in the right direction: controlling the orientation of proteins on nanoparticles improves targeting efficiency. Nano letters. 2019 Feb 18;19(3):1827-31.
34. Li X, Yang Y, Yang F, Wang F, Li H, Tian H, Wang G. Chitosan hydrogel loaded with recombinant protein containing epitope C from HSP90 of Candida albicans induces protective immune responses against systemic candidiasis. International Journal of Biological Macromolecules. 2021 Mar 15;173:327-40.
35. Nkurikiyimfura I, Wang Y, Safari B, Nshingabigwi E. Temperature-dependent magnetic properties of magnetite nanoparticles synthesized via coprecipitation method. Journal of Alloys and Compounds. 2020 15 December;846:156344.
36. Mostafaei M, Hosseini SN, Khatami M, Javidanbardan A, Sepahy AA, Asadi E. Isolation of recombinant Hepatitis B surface antigen with antibody-conjugated superparamagnetic Fe3O4/SiO2 core-shell nanoparticles. Protein expression and purification. 2018 1 May;145:1-6.
37. Yew YP, Shameli K, Miyake M, Khairudin NB, Mohamad SE, Naiki T, Lee KX. Green biosynthesis of superparamagnetic magnetite Fe3O4 nanoparticles and biomedical applications in targeted anticancer drug delivery system: A review. Arabian Journal of Chemistry. 2020 1 January;13(1):2287-308.
38. Sharma A, Jyoti K, Bansal V, Jain UK, Bhushan B, Madan J. Soluble telmisartan bearing poly (ethylene glycol) conjugated chitosan nanoparticles augmented drug delivery, cytotoxicity, apoptosis and cellular uptake in human cervical cancer cells. Materials Science and Engineering: C. 2017 1 March;72:69-76.
39. Shagholani H, Ghoreishi SM, Sharifi SH. Conversion of amine groups on chitosan-coated SPIONs into carbocyclic acid and investigation of its interaction with BSA in drug delivery systems. Journal of Drug Delivery Science and Technology. 2018 1 June;45:373-7.
40. Ikonen T, Kalidas N, Lahtinen K, Isoniemi T, Toppari JJ, Vázquez E, Herrero-Chamorro MA, Fierro JL, Kallio T, Lehto VP. Conjugation with carbon nanotubes improves the performance of mesoporous silicon as Li-ion battery anode. Scientific reports. 2020 27 March;10(1):1-8.
41. Filipczak P, Borkowski M, Chudobinski P, Bres S, Matusiak M, Nowaczyk G, Kozanecki M. Sodium citrate stabilized Ag NPs under thermal treatment, electron-beam and laser irradiations. Radiation Physics and Chemistry. 2020 1 April;169:107948.
42. Albukhaty S, Naderi-Manesh H, Tiraihi T, Sakhi Jabir M. Poly-l-lysine-coated superparamagnetic nanoparticles: a novel method for the transfection of pro-BDNF into neural stem cells. Artificial cells, nanomedicine, and biotechnology. 2018 Nov 12;46(sup3):S125-32.
43. Albukhaty S, Al-Musawi S, Abdul Mahdi S, Sulaiman GM, Alwahibi MS, Dewir YH, Soliman DA, Rizwana H. Investigation of Dextran-Coated Superparamagnetic Nanoparticles for Targeted Vinblastine Controlled Release, Delivery, Apoptosis Induction, and Gene Expression in Pancreatic Cancer Cells. Molecules. 2020 Jan;25(20):4721.
44. Banoon SR, Ghasemian A. The Characters of Graphene Oxide Nanoparticles and Doxorubicin Against HCT-116 Colorectal Cancer Cells In Vitro. Journal of Gastrointestinal Cancer. 2021 Mar 19:1-5.

Received: 10 April 2021
Accepted: 15 July 2021

RESEARCH / INVESTIGACIÓN

Molecular Exploring of Plasmid-mediated Ampc beta Lactamase Gene in Clinical Isolates of *Proteus mirabilis*

Israa Abdul Ameer Al-Kraety[1], Sddiq Ghani Al-Muhanna[1], Shaima R. Banoon[2]

DOI. 10.21931/RB/2021.06.03.21

Abstract: Between September to December 2020, thirteen isolates of *Proteus mirabilis* were recovered among one hundred fifty; MacConkey agar was utilized to purify Gram-negative bacteria isolated from infections of the urinary tract. The primary identification of *Proteus mirabilis* isolates was relied on "colonial morphology, microscopic examination, and biochemical "tests; however, the confirmation of identification of antimicrobial susceptibility of isolates was conducted utilizing an automated VITEK-2 compact system. The result showed that *Proteus mirabilis* isolates were highly resistant to most antibiotics, making them multi-drug resistant (MDR). Phenotype methods were used to detect AmpC beta-lactamase. Initial and confirmatory methods showed that eight isolates were AmpC producers. Polymerase Chain Reaction (PCR) was employed to detect the bla_{ampC} gene.

Key words: *Proteus mirabilis*, β-lactamase, blaampC, VITEK-2, PCR.

Introduction

Urinary tract infection (UTI) is a form of infection that affects the urinary tract. Microorganisms infecting or colonizing the urinary tract. The most common bacterial are pathogens in UTIs are *P. aeruginosa*, *S. saprophyticus*, *E .coli*, and *P. mirabilis*[1]. Infections of the urinary tract can take place throughout the body. Urinary tract infections, such as cystitis, pyelonephritis, urethritis, prostatitis, and perinephritis[2-5], affect people of all ages and are among the most widespread infectious diseases. *Proteus mirabilis* represents a Gram-negative bacterium famous for its ability to spread rapidly within a pattern resembling bulls' eyes. This organism is most commonly a urinary tract pathogen in clinical settings, especially in long-term catheterization patients. *P. mirabilis* uses urease and stone formation, fimbriae and other adhesives, iron and zinc conquest, proteases and toxins such as hemolysin and its function in pore formation, biofilm formation, and pathogenesis regulation to enter and colonize the host urinary tract[6,7]. The continuous usage of antibiotics produces the spread of antibiotic impedance and, in particular, to the progress of antibiotic resistance genes in gram-negative organisms, which are considered the most severe medical problems. For *P. mirabilis* the resistance to antimicrobials is growing[8,9], including the resistance to expanded spectrum cephalosporin according to the production of expanded-spectrum β-lactamases (ESBLs)[10]. Although antibiotics are so valuable for treating many bacterial diseases, they are considered environmental contaminants in infected animals and humans for a long time[38]. This study aimed to detect Plasmid-mediated Ampc beta Lactamase Gene in Clinical Isolates of Proteus mirabilis at the molecular level.

Methods

Sample's collection and identification

During the study period from September to December 2020, the whole 150 midstream urine samples were obtained. The samples were taken from patients in Al-Najaf province hospitals who had urinary tract infections. Suspected *P. mirabilis* isolates were retrieved from clinical samples after purification on MacConkey agar and incubated aerobically overnight at 37°C and confirmed by biochemical tests. The definite identification was carried out using Gram-Negative - Identification (GN-ID) cards and VITEK 2 compact devices.

Antibiotic Susceptibility Testing

Using the automated VITEK-2 compact device and AST-N093 cards (bioMérieux, France), the Minimum Inhibitory Concentration (MIC) technique was calculated. This card composed the following antibiotics: Amikacin, Aztreonam, Cefepime, Ceftazidime, Ciprofloxacin, Colistin, Imipenem, Isepamicin, Gentamicin, Meropenem, Minocycline, Pefloxacin, Piperacillin, Piperacillin-Tazobactam, Rifampicin, Ticarcillin, Ticarcillin-Clavulanic acid, Tobramycin, Trimethoprim-Sulfamethoxazole.

Exploring AmpC β-Lactamase

Initial Examination for AmpC β-Lactamase Production

Employing the standard disk diffusion process, all *P. mirabilis* isolates were checked for cefoxitin susceptibility using cefoxitin disk 30 µg/ml (CLSI, 2019)[11]. Initially 14mm inhibition zone diameter) were thought to be AmpC lactamase producers[12].

Confirmatory Test for AmpC β-Lactamase Product

To detect plasmid-mediated AmpC B-lactamase, the AmpC disk test was used. The test involves permeabilizing a bacterial cell with Tris-EDTA and releasing β-lactamases into the surrounding medium. AmpC disks (i.e., filter paper disks consisting of Tris-EDTA) were made via immerse sterile filter paper disks with 20 µl of a 1:1 mixture of normal saline and 100X Tris-EDTA, allowing the disks to dry, and storing them at 2 to 8 ˚C. Using the typical disk diffusion process, a lawn of cefoxitin susceptible *E. coli* ATCC 25922 was spread on the surface of a Mueller-Hinton agar plate (CLSI, 2019). AmpC disks were rehydrated with 20 µl of normal saline immediately before use, and several colonies of each research organism were added to the disk. On the inoculated surface of the Mue-

[1] Department of Medical Laboratory Techniques, Faculty of Medical and Health Techniques, University of Alkafeel, Najaf, Iraq.
[2] Department of Biology, College of Science, University of Misan, Maysan, Iraq.

Corresponding author: sddiq.g@gmail.com

ller-Hinton agar, a 30 g cefoxitin disk occurred. After that, the inoculated AmpC disk was mounted on top of the antibiotic disk, with the inoculated disk face touching the agar base. After that, the plate was switched over and left to incubate at 37°C in ambient air overnight. After incubation, the plate was inspected, indicating the enzyme inactivation of cefoxitin or lack of distortion, indicating no apparent inactivation of cefoxitin (negative result) for indentation or flattening of the inhibition zone (negative result)[13].

Molecular Identification

The bla_{ampC} gene for *P.mirabilis* was detected using a PCR assay, as shown in Table (2). As shown in Table (1), this primer was developed by Alpha DNA Company in Canada. To estimate the size of the PCR products, 1% agarose gel electrophoresis was used to validate amplified products. The gel was stained with 5 µL of 10 mg/mL ethidium bromide (Promega, USA) and run for 1.5 hours at 85 volts. On an ultraviolet light transilluminator (Cleaver, UK), one band was viewed at the required place; bands were produced employing a gel registration method "Cleaver, UK." The molecular weights of amplified items were calculated using a 100bp ladder "Bioneer, South Korea"[14].

Results and discussion

Initial identification of bacterial isolates obtained from clinical samples was based on cultural morphology, microscopic characteristics, and biochemical examinations. The colonial morphology was employed to define the cultural identity of *P. mirabilis* from those isolates. *P. mirabilis* colonies are grown on blood agar and nutrient agar swarm in waves, while colonies grown on MacConkey agar[15] do not swarm and form smooth colorless colonies, suggesting that *P. mirabilis* cannot ferment lactose sugar. P. mirabilis was Gram-negative bacilli organized separately, in couples, or short chains under microscopic examination. Table (3) displays the results of biochemical tests used to perform the initial identification of P. mirabilis insulates. The isolates shared oxidase-negative and catalase-positive characteristics in common. They were motile, methyl red, and gelatin liquefication positive for urease, catalase, citrate, urease, and gelatin. The isolates could sour glucose on Kliger iron agar, resulting in (Alkaline) red color on the slant and lower (acidic) yellow color with gas and H2S production[16]; oxidase, indole, and vogues-Proskauer were all negative[17,18].

The automated VITEK-2 compact device was utilized to complete the identification, including 47 biochemical tests and one negative control well on GN-ID cards. The findings show that only thirteen of 150 suspected isolates were emphasized as *P.mirabilis*, with ID message confidence levels varying from very good to excellent (Eventually from 93% to 99%).

Antibiogram Testing and Minimum Inhibitory Concentration

The automated VITEK-2 compact device was employed to test antibiograms. The analysis findings showed that all *P. mirabilis* isolates tested were resistant to at least three groups of antibiotics. As a result, all isolates were deemed multi-drug resistant (MDR). The findings showed that (100%) of isolates were resistant to penicillins (piperacillin and ticarcillin), while (64.7%) were resistant to both. Resistance to β-lactam- β-lactamase inhibitor was found in 100% of piperacillin/tazobactam and (47%) of ticarcillin_clavulanic acid moreover resists to ceftazidime, cefepime, and cefoxitin" were identified in (100%), (94.1%) and (64.7%), correspondingly, in the sample. Aztreonam resistance was 100 percent in all isolates. Low resistance was observed in the carbapenem community, which included imipenem and meropenem (the efficient β-lactam antibiotics), with the resistance of (5.9%) for each. This finding was confirmed by (19), who found that *P.mirabilis* is (97.2%) sensitive to this antimicrobial. Some *Proteus mirabilis* isolates have reduced resistance to imipenem for various reasons, including the lack of outer film porins, reduced expression of PBP1a, and decreased imipenem combining by PBP2[20]. Because of the lack of 24 kDa OMP, *Proteus mirabilis* has developed resistance to imipenem. Amikacin (70.5%), isepamicin (64.7%), tobramycin (53%), and gentamicin (23.5%) of the aminoglycoside population all had a significant intermediate effect on *P.mirabilis* insulates. These mechanisms of transmission effectively accelerate the spread of MDR bacteria causing nosocomial outbreaks worldwide[21-23]. Amikacin represents an aminoglycoside antibiotic that can be used to combat several bacterial infections. It works by interacting with the 30s ribosomal subunit of bacteria, triggering mRNA misreading and preventing the bacterium from synthesizing important proteins for development. This finding agrees with (24), who found that (88.2%) of insulates were resistant to pefloxacin and (64.7%) of isolates were resistant to ciprofloxacin. (76.5%) of insulates were impedance to trimethoprim-sulfamethoxazole, while (94.1%) were impedance to minocycline, (25) observed that all insulates were impedance to both colistin and rifampicin. Susceptibility testing showed that none of the insulates were completely immune or susceptible to any of the antibiotics examined.

Gene name	Primer Sequence (5'-3')	Product Size bp	Reference
AmpC	F:ATCAAAACTGGCAGCCG R: GAGCCCGTTTTATGCACCCA	510	36

Table 1. Primers employed in the current investigation.

Gene Name	Temperature (°C) / Time					Cycles Number
	Initial Denaturation	Cycling conditions			Final Extension	
		Denaturation	Annealing	Extension		
*bla*AmpC	94/5 mint	94/30 sec.	60/30 sec.	72/30 sec.	72/10 mint	30

Table 2. PCR program of ampC gene that applies in the thermocycler.

No.	Test	Result
1.	Oxidase	-
2.	Catalase	+
3.	Motility	+
4.	Indole	-
5.	Citrate Utilization	+
6.	Methyl Red	+
7.	Voges-Proskauer	-
8.	Klingler iron agar	+
9.	Urease	+
10.	gelatin liquefaction	+

Table 3. Conventional biochemical tests results of *P.mirabilis* suspected isolates.

Exploring Phenotypic of Plasmid-Mediated AmpC β-Lactamase (PMABL)

Producing insulates phenotypic detection cefoxitin impedance was an initial screening marker for AmpC β -lactamase producers. The basic Kirby-Bauer disk diffusion approach was employed to test *P.mirabilis* insulates for cefoxitin susceptibility. Cefoxitin zone diameter less than 14 mm yielded Such impedance insulates were classified as AmpC β-lactamase producers, due to the Clinical and Laboratory Standards Institute's (2019) recommendation. According to the phenotypic data collected in this study, 10 (76.9%) insulates were resistant to cefoxitin, while 2 (15.3%) were intermediate, and 1 (7.6%) was susceptible. The development of AmpC β-lactamase was screened in all isolates using the AmpC disk test, that AmpC producer was found in five (38.4%) of the thirteen isolates with 5 (62.5%) isolates resistant to cefoxitin, 2 (25%) intermediate resistant isolates, and 1 (12.5%) isolate susceptible to cefoxitin (Figure 1). The detection of plasmid-mediated AmpC-lactamases was calculated employing the AmpC disk test. The AmpC disk examination had 100% responsively and 98% mainly for detecting plasmid-mediated AmpC β-lactamases.

On the other hand, the phenotypic data revealed that the whole AmpC positive insulates had previously been identified as cefoxitin resistant[26] However, this test was in cefoxitin susceptible, and intermediate resistant insulates not able to demonstrate the possibility of AmpC development. This may be because the AmpC disk test relies on the permeabilization of the cell membrane and the release of β-lactamases into the system. This examination may not identify low-level expression enzymes. According to (27) (22%) of AmpC producers, insulates were susceptible to cefoxitin. The development of amps in these insulates may be according to a mechanism close to that of ESBL production organisms susceptible to ceftazidime when tested using the disc diffusion approach. Cefoxitin impedance in non-producers of AmpC may be following several mechanisms, including a lack of porin permeation (27). Occasionally, rather than AmpC enzyme activity, cefoxitin impedance results from producing several carbapenemases and a few forms of class A β-lactamases[28].

Molecular Exposure of Plasmid-Mediated AmpC β-Lactamase (PMABL) Producing Insulates

The existence of the bla_{ampC} gene was investigated in thirteen isolates of *P.mirabilis*, with the results indicating that only 5 (38.4%) isolates yielded bla_{ampC} gene amplification products using specific primers (Table1). The identification of these isolates by PCR is depicted in (Figure 2). Several cellular functions[29-32]. Some Enterobacteriaceae family members such as "Enterobacter, Shigella, Providencia, Citrobacterfreundii, Morganellamorganii, Serratiamarcescens, and Escherichia coli"[33-35] have AmpC β-lactamase genes on their chromosomes. As a consequence of this shift, plasmid-mediated ampC-lactamases have arisen. Plasmid-mediated AmpC-lactamases are a novel task since they impart carbapenem tolerance in strains missing outer membrane porins, have cephamycin impedance and are unaffected by commercially available -lactamase inhibitors. This mechanism of resistance has been discovered all over the world and has the potential to cause nosocomial outbreaks. It seems to be increasing, so more research is required to evaluate the best detection and treatment options[37].

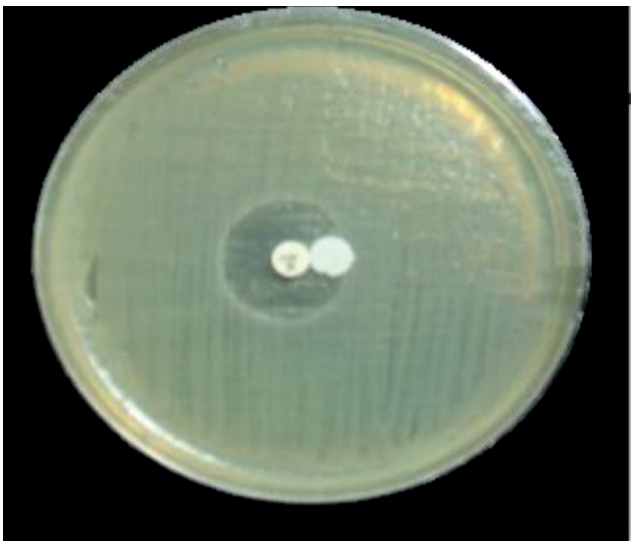

Figure 1. A positive result of a phenotypic confirmatory test for AmpC.

Conclusions

According to our knowledge, the present study revealed that chromosome *ampC* gene was detected on a plasmid of local *Proteus mirabilis* isolates. Show the result that *Proteus mirabilis* isolates were highly resistant to most antibiotics, making them multi-drug resistant (MDR). Meropenem and imipenem were highly active against *P.mirabilis* isolates. The simultaneous presence of ESBLs and AmpC β-lactamase was seen in several *P.mirabilis* isolates. The results indicating that only 5 (38.4%) isolates yielded blaAmpC gene amplification products.

Bibliographic references

1. Foxman B. Urinary tract infection syndromes: occurrence, recurrence, bacteriology, risk factors, and disease burden. Infectious disease clinics of North America. 2013 Dec 8;28(1):1-3.
2. O'Hara CM, Brenner FW, Miller JM. Classification, identification, and clinical significance of Proteus, Providencia, and Morganella. Clinical microbiology reviews. 2000 1 October;13(4):534-46.
3. Nicolle LE. Catheter-related urinary tract infection. Drugs & aging. 2005 Aug;22(8):627-39.
4. Jacobsen SÁ, Stickler DJ, Mobley HL, Shirtliff ME. Complicated catheter-associated urinary tract infections due to Escherichia coli and Proteus mirabilis. Clinical microbiology reviews. 2008 1 January;21(1):26-59.

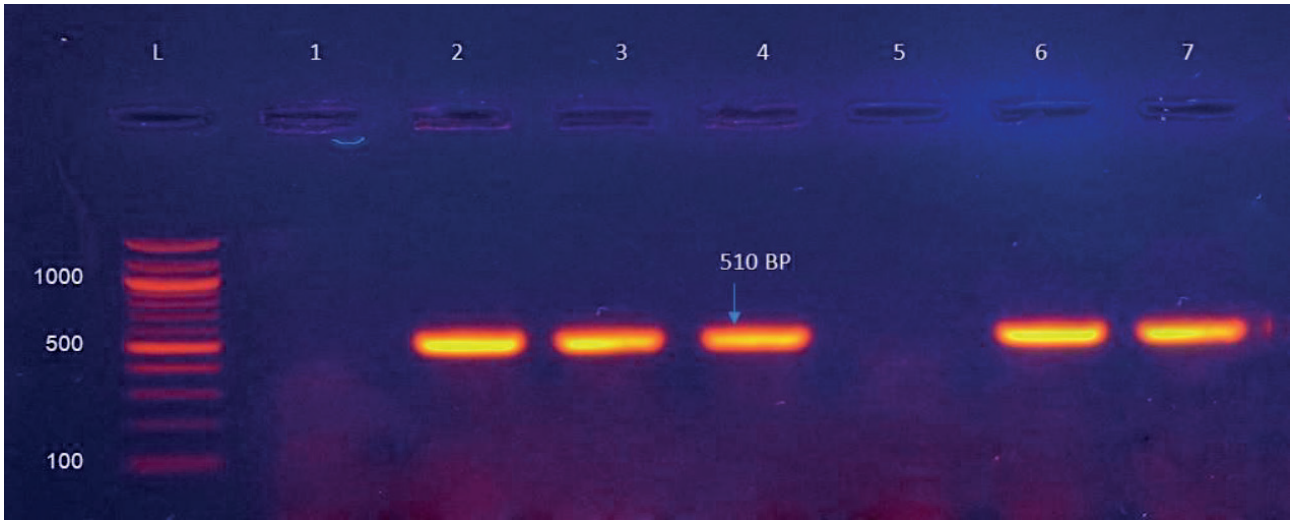

Figure 2. PCR production of *P.mirabilis* isolates dilated with bla$_{ampC}$ primary genes, with a product size of 510 bp. (L): 100-bp ladder; Lanes (2, 3, 4, 6, and 7): positive bla$_{ampC}$ gene results; Lanes (1, 5, 8, and 9): negative bla$_{ampC}$ gene results.

5. O'Brien VP, Hannan TJ, Schaeffer AJ, Hultgren SJ. Are you experienced? Understanding bladder innate immunity in the context of recurrent urinary tract infection. Current opinion in infectious diseases. 2015 Feb;28(1):97.
6. Massad G, Bahrani FK, Mobley HL. Proteus mirabilis fimbriae: identification, isolation, and characterization of a new ambient-temperature fimbria. Infection and immunity. 1994 1 May;62(5):1989-94.
7. Zunino P, Geymonat L, Allen AG, Legnani-Fajardo C, Maskell DJ. Virulence of a Proteus mirabilis ATF isogenic mutant is not impaired in a mouse model of ascending urinary tract infection. FEMS Immunology & Medical Microbiology. 2000 Oct 1;29(2):137-43.
8. Paterson DL, Yu VL. Editorial response: extended-spectrum α -lactamases: a call for improved detection and control. Clinical Infectious Diseases. 1999 Dec 1;29(6):1419-22.
9. Bradford PA. Extended-spectrum α -lactamases in the 21st century: characterization, epidemiology, and detection of this important resistance threat. Clinical microbiology reviews. 2001 1 October;14(4):933-51.
10. Sohn KM, Kang CI, Joo EJ, Ha YE, Chung DR, Peck KR, Lee NY, Song JH. Epidemiology of ciprofloxacin resistance and its relationship to extended-spectrum α -lactamase production in Proteus mirabilis bacteremia. The Korean journal of internal medicine. 2011 Mar;26(1):89.
11. Nasim K, Elsayed S, Pitout JD, Conly J, Church DL, Gregson DB. New method for laboratory detection of AmpC α -lactamases in Escherichia coli and Klebsiella pneumoniae. Journal of clinical microbiology. 2004 Oct 1;42(10):4799-802.
12. Coudron PE, Hanson ND, Climo MW. Occurrence of extended-spectrum and AmpC beta-lactamases in bloodstream isolates of Klebsiella pneumoniae: isolates harbor plasmid-mediated FOX-5 and ACT-1 AmpC beta-lactamases. Journal of Clinical Microbiology. 2003 Feb 1;41(2):772-7.
13. Black JA, Moland ES, Thomson KS. AmpC disk test for detection of plasmid-mediated AmpC α -lactamases in Enterobacteriaceae lacking chromosomal AmpC α -lactamases. Journal of clinical microbiology. 2005 1 July;43(7):3110-3.
14. Levy H, Diallo S, Tennant SM, Livio S, Sow SO, Tapia M, Fields PI, Mikoleit M, Tamboura B, Kotloff KL, Lagos R. PCR method to identify Salmonella enterica serovars Typhi, Paratyphi A, and Paratyphi B among Salmonella isolates from the blood of patients with clinical enteric fever. Journal of clinical microbiology. 2008 1 May;46(5):1861-6.
15. Mahillon J, Chandler M. Insertion sequences. Microbiology and molecular biology reviews. 1998 Sep 1;62(3):725-74.
16. Matsen JM, Blazevic DJ, Ryan JA, Ewing WH. Characterization of indole-positive Proteus mirabilis. Applied microbiology. 1972 1 March;23(3):592-4.
17. Kishore J. Isolation, identification & characterization of Proteus penneri-a missed rare pathogen. The Indian journal of medical research. 2012 Mar;135(3):341.
18. Kamga HL, Nsagha DS, Assob JC, Njunda AL, Tchape GN. Epidemiological studies on proteeae isolates from clinical specimens in the Laquintinie Hospital in Douala, Cameroon. African Journal of Clinical and Experimental Microbiology. 2012;13(2):118-26.
19. Al-Jumaily E, Zgaer SH. Multi-drug resistant Proteus mirabilis isolated from urinary tract infection from different hospitals in Baghdad City. Int. J. Curr. Microbiol. App. Sci. 2016;5(9):390-9.
20. Girlich D, Dortet L, Poirel L, Nordmann P. Integration of the bla NDM-1 carbapenemase gene into Proteus genomic island 1 (PGI1-Pm PEL) in a Proteus mirabilis clinical isolate. Journal of Antimicrobial Chemotherapy. 2015 1 January;70(1):98-102.
21. Koehn FE, Carter GT. The evolving role of natural products in drug discovery. Nature reviews Drug discovery. 2005 Mar;4(3):206-20.
22. Molinari G. Natural products in drug discovery: present status and perspectives. Pharmaceutical Biotechnology. 2009:13-27.
23. Hayashi MA, Bizerra FC, Da Silva Junior PI. Antimicrobial compounds from natural sources. Frontiers in microbiology. 2013 15 July;4:195.
24. Al-Muhanna AS, Al-Muhanna S, Alzuhairi MA. Molecular investigation of extended-spectrum beta-lactamase genes and potential drug resistance in clinical isolates of Morganella morganii. Annals of Saudi medicine. 2016 May;36(3):223-8.
25. Al-Muhanna SG, Banoon SR, Al-Kraety IA. Molecular detection of integron class 1 gene in proteus mirabilis isolated from diabetic foot infections. Plant Archives. 2020 Apr; 20(1): 3101-3107.
26. Black JA, Moland ES, Thomson KS. AmpC disk test for detection of plasmid-mediated AmpC α -lactamases in Enterobacteriaceae lacking chromosomal AmpC α -lactamases. Journal of clinical microbiology. 2005 1 July;43(7):3110-3.
27. Mohamudha PR, Harish BN, Parija SC. AmpC beta lactamases among Gram negative clinical isolates from a tertiary hospital, South India. Brazilian Journal of Microbiology. 2010 Oct;41(3):596-602.
28. Jacoby GA. AmpC α -lactamases. Clinical microbiology reviews. 2009 1 January;22(1):161-82.
29. Schmitzova J, Klaudiny J, Albert Š, Schröder W, Schreckengost W, Hanes J, Judova J, Šimúth J. A family of major royal jelly proteins of the honeybee Apis mellifera L. Cellular and Molecular Life Sciences CMLS. 1998 Sep;54(9):1020-30.
30. Albert S, Bhattacharya D, Klaudiny J, Schmitzová J, Simúth J. The family of major royal jelly proteins and its evolution. Journal of Molecular Evolution. 1999 1 August;49(2):290-7.
31. Kupke J, Spaethe J, Mueller MJ, Rössler W, Albert Š. Molecular and biochemical characterization of the major royal jelly protein in bumblebees suggest a non-nutritive function. Insect biochemistry and molecular biology. 2012 Sep 1;42(9):647-54.

32. Buttstedt A, Moritz RF, Erler S. Origin and function of the major royal jelly proteins of the honeybee (Apis mellifera) as members of the yellow gene family. Biological Reviews. 2014 May;89(2):255-69.
33. Medeiros AA. Evolution and dissemination of α -lactamases accelerated by generations of α -lactam antibiotics. Clinical Infectious Diseases. 1997 1 January;24(Supplement_1):S19-45.
34. Subha A, Devi VR, Ananthan S. AmpC beta-lactamase producing multi-drug resistant strains of Klebsiella spp. & Escherichia coli isolated from children under five in Chennai. Indian Journal of Medical Research. 2003 1 January;117:13-8.
35. Mohamudha PR, Harish BN, Parija SC. AmpC beta lactamases among Gram negative clinical isolates from a tertiary hospital, South India. Brazilian Journal of Microbiology. 2010 Oct;41(3):596-602.
36. Messai Y, Benhassine T, Naim M, Paul G, Bakour R. Prevalence of α -lactams resistance among Escherichia coli clinical isolates from a hospital in Algiers. Rev Esp Quimioter. 2006 Jun 1;19(2):144-51.
37. Tan TY, Ng LS, He J, Koh TH, Hsu LY. Evaluation of screening methods to detect plasmid-mediated AmpC in Escherichia coli, Klebsiella pneumoniae, and Proteus mirabilis. Antimicrobial agents and chemotherapy. 2009 1 January;53(1):146-9.
38. Banoon S, Ali Z, Salih T. Antibiotic resistance profile of local thermophilic Bacillus licheniformis isolated from Maysan province soil. Comunicata Scientiae. 2020 13 July;11:e3921-.

Received: 10 April 2021
Accepted: 15 July 2021

RESEARCH / INVESTIGACIÓN

Risk factors in bacterial colonization of internal ureteral stent

Ekremah K. Shaker[1], Fatima A. Chaloob[2]
DOI. 10.21931/RB/2021.06.03.22

Abstract: A ureteral stent is most broadly used to manage upper urinary tract disorders such as obstruction and prevent post-endoscopic complications. However, the stent may become a niche for bacterial colonization. This study aimed to determine the rate of bacterial colonization and type of bacteria in internal ureteral stents and the risk factors associated with bacterial colonization. This prospective cross-sectional study included 100 consecutive adult patients who had temporary ureteral stenting as preparation for a secondary ureterorenoscopy at Al-Yarmook Hospital/ Baghdad. All included patients were negative for bacterial culture before stenting.

Stent and urine culture were performed at the time of stent removal. The colonization rate and bacteriuria in patients with internal ureteral stent were 19% and 9%, respectively. The most common bacteria in-stent and urine were *E. coli* accounting for 31.58% and 33.33%. *Pseudomonas aeruginosa* was common in stent culture, representing 21.05%. Positive bacterial culture was confirmed in 19 stents and 9 urine samples. All cases with positive urine samples were also positive for culture. Thus, the sensitivity and specificity of urine culture for detection of stent colonization were 47.37% and 100%, respectively. Diabetes mellitus, chronic renal failure, and prolonged stenting were significantly associated with increased stent colonization. The ureteral stent could be a source of urinary tract infection. The most pathogenic bacteria associated with the ureter stent are *E. coli* and *Pseudomonas aeruginosa*. Risk factors associated with stent colonization are diabetes mellitus, chronic renal failure, and prolonged indwelling time.

Key words: Ureteral stent colonization, urine culture, bacterial profile, urinary tract infection.

Introduction

Ureteral Double-J (DJ) stents are broadly employed to treat obstruction in upper urinary tract and avoid post-endoscopic complications. Moreover, these stents are also used to decrease the possible risk of obstruction resulting in stone fragmentation after extracorporeal shock-wave lithotripsy (ESWL), especially in patients with relatively large stones[1]. On the other hand, a ureteral stent is generally associated with several complications, including dysuria, hematuria, lumbar or suprapubic pain[2], stent migration, fragmentation, and encrustation. However, the most severe complication possibly involves the biofilm formation on the stent and infection, which may be associated with bacteremia, renal worsening, pyelonephritis, or even mortality because of the development of sepsis[3].

The biofilms that form on the ureteral stent can originate from urinary tract microbiota or contamination of the stent during insertion of the device[4]. Moreover, the internal ureteral stents offer a perfect medium for bacterial adhesion, colonization, and biofilm formation[5]. Regardless of its origin, biofilm formation on the stent indicates that even very small numbers of bacteria can rapidly benefit from the niche-altering non-self material to grow and increase their population. Previous studies in stented patients have indicated that 70% to 90% of those patients developed bacterial colonization[6].

The present study aimed to determine the rate of bacterial colonization and type of bacteria in an internal ureteral stent and determine the risk factors associated with bacterial colonization of these stents.

Materials and methods

Patients

This is a single prospective center observational study including all consecutive adult patients who had ureteral stenting as part of management for a secondary ureterorenoscopy (URS) due to urolithiasis during the period from April 2020 to May 2021 in the department of Urology/ Al-Yarmook Teaching Hospital, Baghdad, Iraq. Patients positive for urine bacterial culture, immune suppression, pregnant women, those with previous surgery for lower urinary tract, and those who refused to give consent were excluded from the study. Demographic data, including age, gender, body mass index (BMI), the presence of comorbidities, and stent dwelling time, were extracted through direct interviews or from patient records. The study was approved by the Institutional Review Board (IRB) of Al-Dewaniyah Technical Institute, Al-Furat Al-Awsat Technical University. Written consent from each participant was obtained at the time of sample collection after explaining the aim of the study. Each patient was given the complete unconditioned choice to withdraw anytime. The patients were assured that data will be used for research purposes only. Based on inclusion and exclusion criteria, the eligible patients who give the consent form were 100 patients.

Bacterial Isolation from Stents and Urine

At the time of stent removal, Midstream urine from all patients was collected. The stents were removed under antiseptic conditions with the aid of a cystoscope and foreign body forceps. All stent segments (inner and outer surface and the stent tip) were splashed with 1 mL sterile tryptic soy broth solution. The resultant liquid was vortexed for 1 minute, then diluted (1/100) with phosphate buffer saline. Both urine samples and diluted stent preparation were immediately transferred to a Brain heart infusion (BHI) medium. The medium was incubated at 37°C overnight. The samples were then subcultured aerobically on MacConkey agar, while chocolate agar me-

[1] Medical Laboratory Technique, Al-Rasheed University College, Iraq.
[2] Al-Dewaniyah Technical Institute, Al-Furat Al-Awsat Technical University, Iraq

Corresponding author: aa98414@yahoo.com

dia was used for incubation under CO_2 conditions. The growth of microorganisms on the agar was evaluated quantitatively (growth of >1000 colony-forming units/mL was considered positive)[7]. Api20E system was used to identify Enterobacteriaceae, while Api Staph System was used to identify staphylococci (bio-Merieux, France). These systems can detect bacteria to species level. For other bacteria, routine biochemical tests were used for identification. These included the oxidase test, catalase test, CAMP test, motility agar, and urease test.

Statistical Analysis

All statistical analyses were performed using SPSS Statistics Windows, Version 25.0 (Armonk, NY: IBM Corp.). Data were expressed as mean and standard deviation (for quantitative variables) and frequency and percentage (for binomial variables). Student t-test or Chi-square as required was used to compare the association between different factors and the stent colonization. The level of significance was set at $p < 0.05$.

Demographic and Clinical Characteristics of the Patients

The mean age of the patients was 53.01±9.67 years (range 26-82 years). About three-quarters of the patients were males. The mean BMI was 26.44±3.57 kg/m^2. Most patients (60%) had no comorbidity, while 25% and 24% of them were suffering from DM or hypertension, respectively. The mean stent indwelling time was 42.32±9.9 days (range 24-66 days), as shown in table 1.

Microbiology

Out of 100 stents, positive culture was confirmed in 19 stents (19%). On the other hand, only 9 urine samples had a positive culture. Interestingly, all positive urine samples were positive for stent culture. On the other hand, 10 positive stent cultures had negative urine cultures. Thus, urine culture's sensitivity and specificity for stent colonization detection are 47.37% and 100%, respectively (Table 2).

The most common bacterium was *E. coli* encountered in 31.58% and 33.33% of stent and urine cultures. *P. aeruginosa* came next accounted for 21.05% of stent colonization but was not detected in urine samples. *Staphylococcus epidermidis* and *Klebsiella pneumoniae* were detected in 10.53% and 11.11% of stent and urine culture, respectively (Table 3). None of the stent or urine cultures had mixed infection.

Variables	Value
Age, years	
Mean±SD	53.01±9.67
Range	26-82
Gender	
Male	76(76%)
Female	24(24%)
Body mass index, kg/m^2	
Mean±SD	26.44±3.57
Range	18.4-35.45
Comorbidities	
No comorbid	60(60%)
DM	25(25%)
Hypertension	24(24%)
Chronic renal failure	6(6%)
Malignancy	5(5%)
Stent indwelling, days	
Mean±SD	42.32±9.9
Range	24-66

DM: diabetes mellitus, HTN: hypertension, URS: ureterorenoscopy

Table 1. Patients' characteristics and demographic data (n=100).

Urine culture	Stent colonization		Total
	positive	Negative	
Positive	9	0	9
Negative	10	81	91
Total	19	81	100

Table 2. Relationship of stent colonization with urine culture.

Association of Demographic and Clinical Characteristics with Stent Colonization

Two factors were significantly associated with stent colonization: comorbidities and stent indwelling. A 47.37% of patients in the bacterial colonization group had DM compared with 19.75% among patients without colonization with a significant difference. Similarly, chronic renal failure was more common among patients than without colonization (15.79% vs. 3.7%), with a significant difference. The mean time for indwelling stent patients with colonization was 47.68±9.63 days compared with 41.06±9.59 days in patients without colonization, with a highly significant difference (Table 4).

Discussion

According to the result of the present study, 19% and 9% of internal ureteral stents and urine samples were positive for bacterial colonization. A speedy result was obtained by Ulkar *et al.*[8], in which bacterial colonies were demonstrated in 20%. Also, Lojanapiwat[9] reported that bacterial colonization and growth in-stent culture was detected in 7 of 35 patients (20%). A much higher rate was reported in other studies. Kehinde *et al.*[10] reported that about 42 % of patients with indwelled stent had their stent colonized, while 17% developed bacteriuria. Lifschitz *et al.*[11] reported that 45 of their patients had positive stent culture, and 15% suffered from bacteriuria. In Bangladesh, Rahman *et al.*[6] investigated 100 adult patients who had ureteral stent placement for different urinary tract operations. Bacterial colonies were found in 45% of the stent, while bacteriuria was found only in 21% of patients. On the other extreme, as high as 90% of stent colonization was reported in an earlier series of 30 patients[12].

These discrepancies in the colonization rate may be attributed to several factors, the most important of which are the polymer characteristic of the stent, indwelling times, different patient populations, and technical issues. The relatively low rate of colonization in the present study reflects the high standard of hygiene followed by the operative team, and maybe some prophylactic antibiotics were taken by the patients.

In the present study, the sensitivity and specificity of bacteriuria in the detection of stent colonization were 47.37% and 100%, respectively. In a similar study, Lifshitz *et al.*[11] demonstrated that the sensitivity and specificity of urine culture were 31% and 97%, respectively. Thus, in most cases, urine culture had low sensitivity and very high specificity because mostly urine gives negative results when there is no stent colonization, but not all stent colonization results in bacteriuria.

According to the present study, *E. coli* and. *P. aeruginosa* was the most predominant pathogen in-stent and urine culture. In this regard, different studies disclosed different bacterial profiles of stent and urine colonization. In many previous studies, *E. coli* and *Enterococci spp* were found to be the most prevalent[13-14]. In a Turkish study, the most frequently isolated bacteria were *Staphylococcus epidermidis*, *Escherichia coli*,

Bacteria	Stent culture (N=19)	Urine Culture (N=9)
E. coli	6(31.58%)	3(33.33%)
P. aeruginosa	4(21.05%)	0(0%)
Enterococcus spp	3(15.8%)	0(0%)
Staphylococcus epidermidis	2(10.53%)	1(11.11%)
Klebsiella pneumoniae	2(10.53%)	1(11.11%)
Enterococcus fecalis	1(5.26%)	1(11.11%)
Achromobacter sp.	1(5.26%)	1(11.11%)
Proteus mirabilis	0(0%)	2(22.22%)

Table 3. Bacterial isolates from stent and urine samples.

Variables	With bacterial colonization (n=19)	Without bacterial colonization (n=81)	*p*-value
Age, years	54.26±10.8	52.72±9.43	0.533
Gender			
Male	13(68.42%)	63(77.78%)	0.390
Female	6(31.58%)	18(22.22%)	
BMI, kg/m²	25.68±3.7	26.62±3.54	0.308
Comorbidities			
DM	9(47.37%)	16(19.75%)	**0.012**
Hypertension	7(36.84%)	17(20.99%)	0.125
Chronic renal failure	3(15.79%)	3(3.7%)	**0.046**
Malignancy	0(0%)	5(6.17%)	0.267
Stent indwelling, days	47.68±9.63	41.06±9.59	**0.008**

Table 4. Bacterial isolates from stent and urine samples.

and *Enterococcus faecalis*[8]. In Rahman's *et al.*'s study, *E. coli* was the common organism isolated from both stent and urine[6]. Lojanapiwat *et al.*[9] found that *Staphylococcus epidermidis* is the predominant bacteria responsible for stent colonization. Two other recent studies described gram-positive pathogens, particularly *Staphylococcus*, as predominant bacterium[15-16]. Farsi *et al.*[13] reported that *P. aeroginosa* was most commonly isolated from both stents and urine. Paick *et al.*[17] isolated *Enterococcus* species from 6 stents out of 25, followed by *E. coli* (5 of 25). They indicated that Gram-positive and gram-negative bacteria were similarly distributed in-stent cultures; nevertheless, only gram-negative bacteria were established in urine cultures. Another study demonstrated that *Acinetobacter sp.* and *R. pickettii* were the most common pathogens, followed by *Staphylococci* and *Pseudomonas* species in-stent culture[7].

Therefore, it seems that each study has its peculiar conditions regarding antibiotic use, isolation, stent material, and study population that result in specific bacterial profiles.

There was almost complete agreement between stent and urine in the types of bacterial isolates. These data suggest that colonization in the stent is a crucial step of UTI and precedes colonization in the urine.

In the present study, DM and chronic renal failure, as comorbidities, were significantly associated with an increased stent colonization rate. Furthermore, the meantime for indwelling stent patients with colonization was significantly longer than in patients without colonization. Following these results is the outcome of many previous studies worldwide. Akay *et al.*[14] investigated risk factors for UTI and stent colonization in 190 patients with ureteral stents. The independent risk factors for the development of UTI were DM, chronic renal failure, and pregnancy. Altuna *et al.*[18] demonstrated that UTI was more common in patients with ureteral stents with DM and chronic renal failure.

Diabetes is known to hurt the immune system. Besides, the presence of sugar in the urinary tract enhances bacterial growth. On the other hand, chronic renal failure is associated with urinary stagnation, alkalization of urine, and absence of flushing action[19]. All these factors increase the likelihood of bacterial colonization.

The association of prolonged stent dwelling with stent colonization is beyond dispute. Most studies in this regard demonstrated that stent dwelling periods were significantly correlated with stent colonization rates[10]. The longer the indwelling period, the higher rate of stents colonized. Rahman *et al.*[6] disclosed that the colonization rate was 71.4% in stents that exist for 6 weeks compared to 33.3% in those that exist for 4-6 weeks and 23.5% for stents removed before 4 weeks. In a prospective study, Farsi *et al.*[13] investigated stent colonization in 266 patients for 2 weeks to 27 months. A linear correlation was disclosed between the indwelling time and stent colonization rate. Coskun *et al.*[20] emphasized that prompt removal of the stent can significantly decrease the rate of UTI. Shabenaa *et al.*[21] did not find bacterial colonization in the first two weeks of stent employment.

As dwelling time increases, there will be more chance for different bacterial strains to adhere and colonize the stent regardless of the stent material. Eventually, a biofilm is formed, and most bacteria find their way to the urine.

The study has some limitations. Firstly, it was a single-center study with a limited number of patients, and the result cannot be generalized. Therefore, multicenter studies with a larger sample size are required for more solid conclusions. Secondly, the study did not link stent colonization with clinical symptoms and patients' quality of life. That is because the study was intended to be a microbiological rather than a clinical study. However, this study provides a clear insight into the risk of bacterial colonization of internal ureteral stent.

Conclusions

The study findings indicate the importance of internal ureteral stent as a source for UTI. The most pathogenic bacteria associated with the ureter stent are *E. coli* and *Pseudomonas aeruginosa*. Risk factors associated with stent colonization are DM, chronic renal failure, and indwelling time. Thus, the use of ureter stents should be reduced to a short dwelling time. Otherwise, every measure should be taken to reduce the sent colonization, especially in diabetics and patients with chronic renal failure, such as regular urine analysis and prophylactic broad-spectrum antibiotics.

Conflict of interest

The authors declare no conflict of interest.

Authors' Declaration

The authors at this moment declare that the work presented in this article is original and that they will bear any liability for claims relating to the content of this article.

Bibliographic references

1. Shinde S, Al Balushi Y, Hossny M, Jose S, Al Busaidy S. Factors Affecting the Outcome of Extracorporeal Shockwave Lithotripsy in Urinary Stone Treatment. Oman Med J. 2018;33(3):209-217.
2. Joshi HB, Stainthorpe A, Keeley FX, MacDonagh R, Timoney AG. Indwelling ureteral stents: evaluation of quality of life to aid outcome analysis. J Endourol. 2001;15:151-154.
3. Ranganathan M, Akbar M, Ilham MA, Chavez R, Kumar N, Asderakis A. Infective complications associated with ureteral stents in renal transplant recipients. Transplant Proc. 2009;41(1):162-4.
4. Bossa L, Kline K, McDougald D, Lee BB, Rice SA. Urinary catheter-associated microbiota changes in accordance with treatment and infection status, PLoS One. 2017;12(6):e0177633.
5. Valentin Z, Patrick B, Werner A, Matthias B, Qun R, Hans-Peter S, Dominik A. Biofilm formation on ureteral stents – incidence, clinical impact and prevention. Swiss Med Wkly. 2017;147:w14408.
6. Rahman MA, Alam MM, Shamsuzzaman SM, Haque ME. Evaluation of bacterial colonization and bacteriuria secondary to internal ureteral stent. Mymensingh Med J. 2010;19, 366–371.
7. Ozgur BC, Ekıcı M, Yuceturk CN, Bayrak O. Bacterial colonization of double J stents and bacteriuria frequency. Kaohsiung J Med Sci. 2013;29(12):658-61.
8. Ulkar V, Yilmaz N, Agus N, Can E, Cakmak O, Yucel C, Celik O, Libey YO. Bacterial colonization of ureteral double-J stents in patients with negative urine culture. J Urological Surg 2019;2:125-129.
9. Lojanapiwat B. Colonization of internal ureteral stent and bacteriuria. World J Urol. 2006;24(6):681-683.
10. Kehinde EO, Rotimi VO, Al-Hunayan A, Abdul-Halim H, Boland F, Al-Awadi KA. Bacteriology of urinary tract infection associated with indwelling J ureteral stents. J. Endourol. 2004;18:891-896.
11. Lifshitz DA, Winkler HZ, Gross M. Predictive value of urinary cultures in assessment of microbial colonization of ureteral stents. J Endourol. 1999;13:735–738.
12. Reid G, Denstedt JD, Kang YS, Lam D, Nause C. Microbial adhesion and biofilm formation on ureteral stents in vitro and in vivo. J Urol. 1992;148:1592-1594.
13. Farsi HM, Mosli HA, Al-Zemaity MF, Bahnasy AA, Alvarez M. Bacteriuria and colonization of double-pigtail ureteral stents: long-term experience with 237 patients. J Endourol. 1995;9:469–472 2.

14. Akay AF, Aflay U, Gedik A. Risk factors for lower urinary tract infection and bacterial stent colonization in patients with a double J ureteral stent. Int Urol Nephrol. 2007;39:95-98.
15. Aydin HR, Irkilata H, Aydin M, Gorgun S, Demirel HC, Adanur S, Keles M, Atilla A, Atilla MK. Incidence of bacterial colonisation after indwelling og double-J ureteral stent. Arch Ital Urol Androl. 2016;87:291-294.
16. Nevo A, Mano R, Schreter E, Lifshitz DA. Clinical implications of stent culture in patients with indwelling ureteral stents prior to ureteroscopy. J Urol. 2017;198:116-121.
17. Paick SH, Park HK, Oh SJ, Kim HH. Characteristics of bacterial colonization and urinary tract infection after indwelling of double-J ureteral stent. Urol. 2003;62(2):214-217.
18. Altunal N, Willke A, Hamzaoğlu O. Ureteral stent infections: a prospective study. Braz J Infect Dis. 2017;21(3):361-364.
19. Richa C, Bhushan CS, Kumar SP, Dev PN, Nabaraj P. Bacteriology of Urinary Tract Infection of Chronic Renal Failure Patients Undergoing for Hemodialysis. J Microbiol Exp. 2016;3(3): 00089.
20. Coskun AK, Harlak A, Ozer T, Eyitilen T, Yigit T, Demirbas, S. Is removal of the stent at the end of 2 weeks helpful to reduce infectious or urologic complications after renal transplantation? Transplant Proc. 2011;43:813e5.
21. Shabenaa KS, Bhargava R, Manzoor MAP, Mujeeburahiman M. Characteristics of bacterial colonization after indwelling double-J ureteral stents for different time duration. Urol Ann. 2018;10:71-75.

Received: 20 April 2021
Accepted: 15 July 2021

RESEARCH / INVESTIGACIÓN

Investigation about contamination of some food items in local markets, Mosul, Iraq

Ammar Nafea Alnema, Mazin Nazar Fadhel

DOI. 10.21931/RB/2021.06.03.23

Abstract: Results of enzyme-linked immunoassay (ELISA), which was conducted on 58 samples of dried fruits and nuts available in the local market in Mosul city that there were samples that are contaminated with aflatoxins with rates higher than the tolerated level permitted by the European Union (4 parts per billion) in the human-consumed foodstuff products as the percentages were 40%, 40, 70% and 10% for almond, cashew, pistachio, and walnut respectively, which are beyond the permitted level. At the same time, the percentages were 66% and 10% for dried apricot and figs, respectively, and more than the permitted level. The average quantity of aflatoxins in the nuts samples was (1.6, 3.8. 4.1 and 6.1 ppb) for walnut, cashew, almond, and pistachio, respectively, while in the dried fruits (3.3, 1.4, and 6.9 ppb) for raisin, figs, and apricot respectively.

Key words: Aflatoxin pollution, (ELISA), Mycotoxins.

Introduction

Aflatoxins are secondary metabolites with relatively low molecular weights produced by genus *Aspergillus* that affect the human-consumed foodstuff and animal fodders[1]. The United Nations Foods and Agriculture Organization (FAO) estimated that about 25% of foodstuff and fodders worldwide are polluted with aflatoxins[2].

The foodstuff that is more subject to aflatoxins is cereals, spices, rice, corn, nuts, and dried fruits[3]. The term was used for the first time in 1952 when animal diseases were studied[4].

In general, toxins affect the foods in various stages: transport, storage, or affecting the various crops in the growth stage before the harvest. The effect of these poisons is associated with the quantities consumed, as having them for long periods with small quantities in foods and fodder causes chronic diseases to humans and animals, while having large quantities for short periods leads to acute cases and might result in death in most of the cases[5].

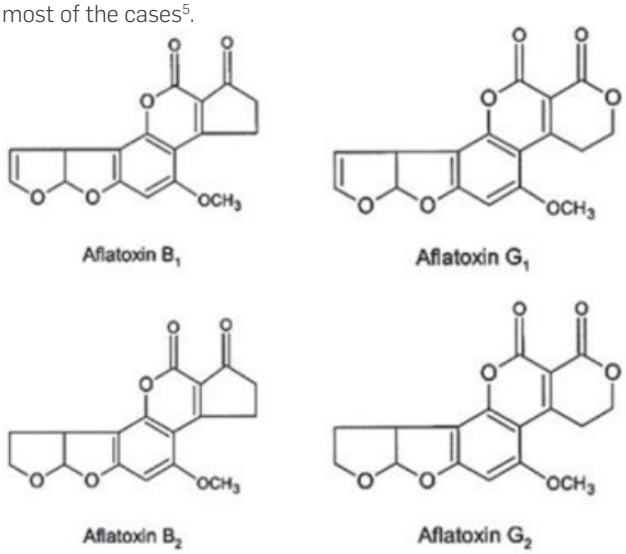

Figure 1. Chemical structure of aflatoxin B (AFB1 and AFB2), aflatoxin G (AFG1 and AFG2)[8].

Aflatoxins stand for a set of metabolites, which are severely poisonous and produced by certain types of Aspergillus species, including Aspergillus flavus, Aspergillus parasitic us, and Aspergillus nomius during their growth on foods and fodders[6].

The most critical main aflatoxins types are (G2, G1, B2, and B1). Aspergillus flavus produces type B only, whereas the other two (*Aspergillus parasiticus* and *Aspergillus nomius*) produce G and B. The two letters "B" and "G" refer to the two colors, blue and green, produced when subjected to the ultraviolet rays on the TLC plates, while the numbers 1 and 2 refer to the main ad the secondary compounds, respectively[7].

Aflatoxin B1 is considered the most poisonous, and it was identified as the most carcinogenic chemical that occurs naturally in the liver.

The International Agency classified AFB1 for Cancer Researches as a first-class carcinogen, and several epidemics studied demonstrated a relationship between aflatoxins and stomach, intestine, and liver tumors in Africa, the Philippines, and China[9]. Therefore, regulations were adopted by many countries to control the concentrations of Aflatoxin in foods as the concentration of Aflatoxins was restricted to the highest concentration in nuts and dried fruits to be (4 µg/kg)[10].

The primary purpose of this work is to test the level of AFs in samples of dried fruits and nuts which are available in the local markets in Mosul city, Iraq, that are consumed in huge quantities and on a wide range.

Materials and methods

Sampling

Samples were collected in January 2021and they were 58 samples (n=58). These samples included dried fruits and nuts Included: (6 samples of dried grapes, 6 samples of dried apricot, 6 samples of dried figs, 10 samples of walnut, 10 samples of almonds, 10 samples of cashews, and 10 samples of Allepo pistachios), which were all bought from the local market in Mosul city. Each sample was ground to a volume of 250 grams, put in plastic bags, taken to the laboratory, and analyzed immediately in search of AFs[11].

Chemical and reagents

The number of Aflatoxins in the samples was measured according to Ela science American company using Enzyme (ELISA).

[1] Department of Environmental Sciences, College of Environmental Sciences and Technology, Mosul University, Iraq.

Corresponding author: ammer.abd.technology@gmail.com

Reagents: Methanol, N-hexane, were obtained from Merck (Darmstadt, Germany), Methanol (V): Deionized water (V) =7: 3

The extraction procedure

Sample uniformity using an electrical blender. A quantity of 2 grams of the homogeneous sample was weighted, put in the 50 ml-capacity centrifuge tube. Then 8 ml of N-hexane and 10 ml of methanol 70% and they are shacked well for 5 minutes and then they are put in the centrifuge at 4000 round per minute for 10 minutes at the room temperature. The upper liquid is removed, and 0.5 ml of the lower liquid is taken to another centrifuge tube. After that, 0.5 ml of deionized water is added and thoroughly mixed. A quantity of 50 µl is taken for analysis and detection. The test is conducted. All the reagents and samples are prepared at room temperature before using them.

Sample's numbering: The samples are numbered in order, and records of standard well and wells samples are kept.

Sample's addition: a volume of 50 microliters is added to each well, and then 50 µl of conjugated HRP is added to each well, and then 50 µl of antibody action solution is added. After that, the plate is sealed with a plate stopper; it is shacked for 5 seconds to get a good mixture and put in the incubator for 30 minutes at 25 Cº.

Wash, examine carefully, and remove the liquid. Immediately add 300 µl of wash buffer to each well, and the process is repeated 5 times with intervals of 30 seconds. The plate is reversed and fixed on a thick, clean, and absorbent paper (if there were bubbles in the wells, clean tips are used to pierce them).

Color development: 50 µl of substrate reagent A is added to each well, and then 50 µl of the substrate reagent B is added and shake gently until a good mixture is obtained and after that, it is incubated for 15 minutes in the slight shade (the time of the reaction can be extended according to the fundamental change in the color). Suspension of the reaction: 50 µl of the suspension solution is added to each well and shaken gently for good mixing.

OD measurement: Determining the optical density (OD value) for each well at 450 nanometers (the standard wavelength is 630 nanometers) using the microplate reader. This step should be completed within 10 minutes after the suspension of the reaction[12].

Results

The Aflatoxins quantitative measurement of dried fruit and nuts samples in the local markets in Mosul city showed that they are highly polluted with these poisons, and several samples were polluted at a rate higher than the accepted limit stipulated by the European Union.

Dried fruits

Results of the test, as shown by table (1), that apricot contains the least quantity of Aflatoxin (1.948 per billion) and the highest was (12.295 per billion) due to the long period of storage of the samples and this is because the low demand on it during January and this conforms with what was found by (13). in their study of 20 samples of dried apricot, as they found that 4 sample was highly polluted.

The Results Shown that figs dried is polluted with the Aflatoxin with the highest value (13.694 per billion) and the lowest value (0.296 per billion), and the average quantity of Aflatoxin (3.354 per billion) as shown in figure 2.

As for raisin, the analysis results showed that the samples included concentrations of Aflatoxin at the accepted range as the highest pollution with Aflatoxin was (3.096 per billion), while the lowest was (0.000 per billion). The average quantity of Aflatoxin was (1.456 per billion).

Nuts

The analysis showed that several samples of nuts exceeded the acceptable limit, as shown in Table 2. These results demonstrated that the pollution was (40%) in the almonds samples and the pollution levels between (1.838 to 8.726 per billion) and the average quantities of Aflatoxin was (4.017 per billion), as displayed in figure 3.

Results of the walnuts test also revealed that one of the samples exceeded the tolerated limit of the European Union (4 per billion) for the total AF in the foodstuff and its concentration was (11.529 per billion) due to the lousy storage, high humidity, and the long period of storage and the average quantity in the samples was (1.687 per billion).

AFL concentrations in cashew samples ranged between (2.701 per billion), and this value lies within the tolerated limit. The average quantities in the sample were (3.857 per billion).

For the AFL concentrations in measured pistachio samples, the highest values were (9.761 per billion) and the most negligible value was (1.814 per billion), and the average quantity of Aflatoxin was (6.195 per billion) as shown in table 2 and figure 3.

Discussion

Through the qualitative and quantitative detection of Aflatoxins in the samples of the nuts and the dried fruits used in the study that used the ELISA technique, results showed that some samples were polluted with Aflatoxins[11,12] found that the pollution of nuts with Aflatoxin with a percentage of 43% with concentrations that range between 0.58-15.2 µl per billion. The reason behind that was inadequate storage, extended storage, and humidity, which led to increased Aflatoxins in the samples.

Dried fruits	The number of samples	Average values (µg/kg)	The lowest value (µg/kg)	highest value (µg/kg)	Samples exceeded the limit (4µg/kg)
Dried grapes	6	1.456	0.000	3.096	0
Dried figs	6	3.354	0.296	13.694	1
Dried apricot	6	6.941	1.948	12.295	4

Table 1. Results of the occurrence of AFs in the analyzed dried fruit samples.

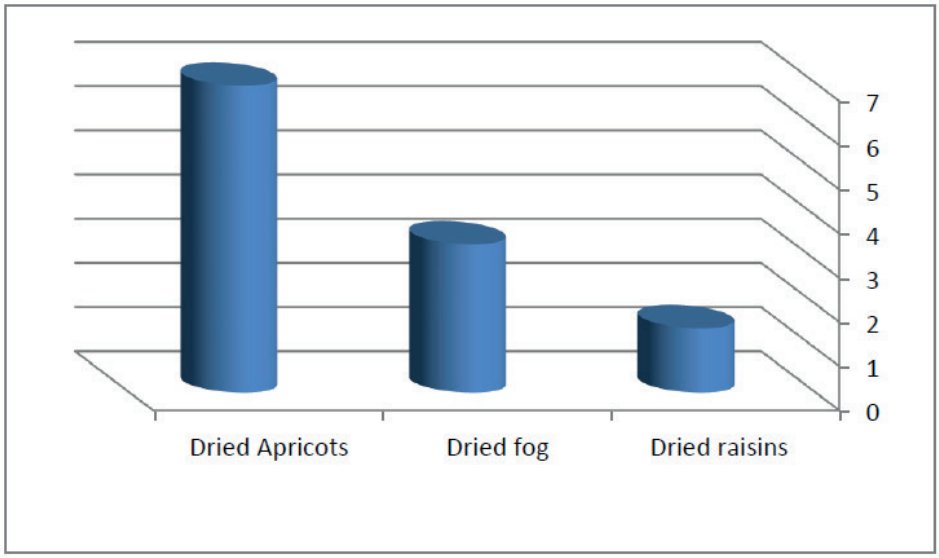

Figure 2. Average concentrations of AFLA in dried fruit samples.

Dried fruits	The number of samples	Average values (µg/kg)	The lowest value (µg/kg)	highest value (µg/kg)	Samples exceeded the limit (4µg/kg)
Pistachio	10	6.195	1.814	9.761	7
cashew	10	3.857	2.701	5.721	3
Almonds	10	4.017	1.838	8.726	4
walnuts	10	1.687	0.000	11.529	1

Table 2. Results of the occurrence of AFs in the analyzed nuts samples.

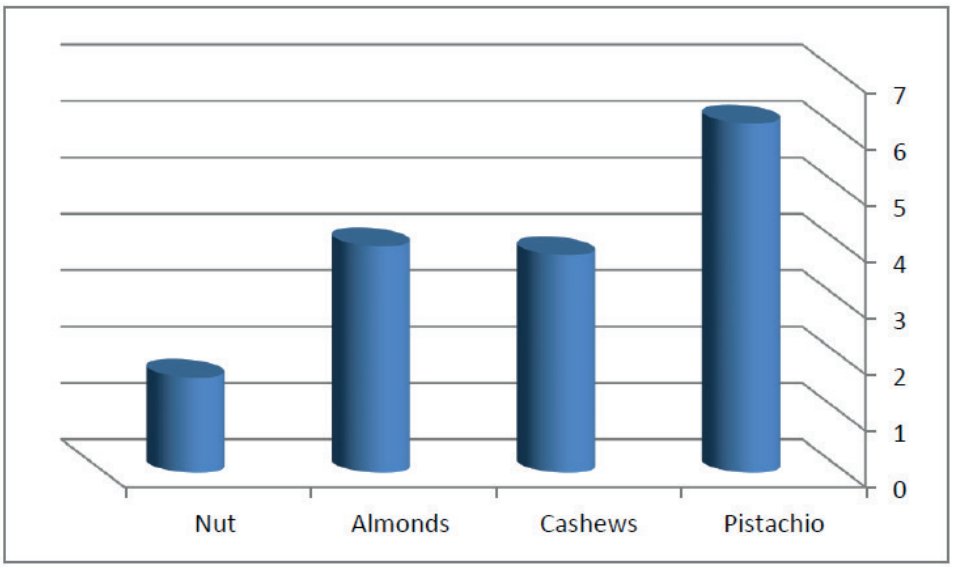

Figure 3. Average AFLA Concentrations in Nuts Samples.

The current research recommends that several actions should be taken to limit the occurrence of mycotoxins in foods. First of all, storing the foods in good conditions and also conducting coordinated studies with the Colleges of Medicine and other relevant specializations to diagnose the fungi and the diseases they cause in an attempt to limit them and also symposiums should be held to raise the awareness of the society about the risks of these poisons and the ways to avoid them.

Conclusions

It is concluded that Aflatoxins highly pollute the samples of nuts and dried fruits in question, and this implies a high risk of cancers incidence, especially liver cancer.

Acknowledgments

We, the authors, bear witness that what has been mentioned in this research in terms of results and everything is our own, and we bear responsibility in the event of any problem.

Author's conflict

We researchers acknowledge that there is no conflict with our interests.

Bibliographic references

1. Calderari, T.O., Iamanaka, B.T., Frisvad, J.C., Pitt, J.I., Sartori, D., Pereira, J.L., Fungaro, M.H.P., et al.,. The biodiversity of Aspergillus section Flavi in Brazil nuts: from rainforest to consumer. Int. J. Food Microbiol.2013; 160 (3), 267–272.
2. Park ,O.L.H. Niapau , E.Boutrif. Minimizing risks posed by mycotoxins utilizing the HACCP concept .2009; 17 November, Available from .
3. Smith, M. C., Madec, S., Coton, E., & Hymery, N. Natural co-occurrence of mycotoxins in foods and feeds and their in vitro combined toxicological effects. Toxins,2016; 8(4), 94
4. Dhanasekaran, D., Shanmugapriya, S., Thajuddin, N., & Panneerselvam, A.Aflatoxins and aflatoxicosis in human and animals. Aflatoxins-Biochemistry and Molecular Biology,2011; 221-254 .
5. Chukwuka,O.K. ; Okoli ,I.C. ; Opara,M. N. ; Ogbuewu ,I.P . and Iheshiulor, O.O.M.The growing proplems of mycotoxin in animal feed industry .Asian.J.Poultry.Sci.,2010; 4:122-134
6. Kumar, P., Mahato, D. K., Kamle, M., Mohanta, T. K., & Kang, S. G.Aflatoxins: a global concern for food safety, human health and their management. Frontiers in microbiology,2017; 7, 2170.α
7. A Saadullah, A., & K Abdullah, S. Detection of Aspergillus species in dried fruits collected from Duhok market and study their aflatoxiginic properties. Rafidain journal of science,2014; 25(1), 12-18.
8. Zain, M. E. Impact of mycotoxins on humans and animals. Journal of Saudi chemical society,2011; 15(2), 129-144.
9. Marchese, S., Polo, A., Ariano, A., Velotto, S., Costantini, S., & Severino, L. Aflatoxin B1 and M1: Biological properties and their involvement in cancer development. Toxins, 2018; 10(6), 214.
10. Commission Regulation (EC) n.1881/2006 of 19 December 2006 Setting Maximum Levels for Certain Contaminants in Foodstuffs. Official Journal of the European Union,2006; 364, 5-24. α α
11. Commission, E. Commission Regulation (EC) No 401/2006 of 23 February 2006 laying down the methods of sampling and analysis for the official control of the levels of mycotoxins in foodstuffs. Off. J. Eur. Union.2006; 12–34.
12. Commission, E. Commission Regulation (EC) No 165/2010 of 26 February 2010 amending Regulation (EC) No 1881/2006 setting maximum levels for certain contaminants in foodstuffs as regards aflatoxins. Off. J. Eur. Union.2010; 8–12 .
13. Luttfullah, G., & Hussain, A. Studies on contamination level of aflatoxins in some dried fruits and nuts of Pakistan. Food Control,2011; 22(3-4), 426-429 .

Received: 11 May 2021
Accepted: 25 June 2021

RESEARCH / INVESTIGACIÓN

Modelo de regresión de Cox para análisis de supervivencia en pacientes con cáncer de mama en la provincia de Manabí, Ecuador

Cox regression model for survival analysis in patients with breast cancer in the province of Manabí, Ecuador

Cecilia Bucheli Giler[1], Daniel Fabricio Alarcón Cano[2], Karime Montes Escobar[3]

DOI. 10.21931/RB/2021.06.03.24

Resumen: El cáncer de mama es un problema de salud pública, que ha venido incrementándose, ubicándose como el cáncer de mayor incidencia en las mujeres, su repercusión en la población en general ocupaba el segundo lugar a nivel mundial, siendo la neoplasia maligna más frecuente en la población femenina y en relación a los decesos por cáncer y afecta con más frecuencia a los países del primer mundo y en vías de desarrollo. Estudio observacional, descriptivo y retrospectivo realizado a pacientes diagnosticados con cáncer de mama en el Hospital Oncológico de Manabí, Ecuador. La supervivencia global y libre de enfermedad a seis años se estableció a partir del tiempo trascurrido desde el diagnóstico hasta la ocurrencia de un evento o fecha del último contacto, con límite a diciembre de 2015. De los 403 pacientes, los límites de edad fueron 15 y 90 años, con media de 56.08 años. Se considero el tamaño del tumor, donde (T1) representa el 26.55%, (T2) representaron 45.66%, la supervivencia global fue de 80% a 6 años. Los pacientes en etapas avanzadas tuvieron menores probabilidades de supervivir con un porcentaje del 43%. Con el modelo de regresión de Cox, fue posible demostrar asociación estadísticamente significativa entre el tamaño del tumor y la supervivencia. El estudio demuestra que los pacientes en etapas avanzadas tienen menores probabilidades de supervivir, por lo que es imperativo que se continúen esfuerzos en promoción de la salud hasta conseguir que la detección sea en etapas curables.

Palabras clave: Modelo de Riesgos Proporcionales de Cox, supervivencia, cáncer de mama, Ecuador.

Abstract: Breast cancer is a public health problem, which has been increasing, ranking as cancer with the highest incidence in women, its impact on the general population ranked second worldwide, being the most frequent malignant neoplasm in the female population and concerning deaths from cancer and affects more frequently the first world and developing countries. Observational, descriptive, and retrospective study carried out in patients diagnosed with breast cancer at the Oncological Hospital of Manabí, Ecuador. The six-year global and disease-free survival was established from the time elapsed from the diagnosis to the occurrence of an event or the date of the last contact, with a limit to December 2015. Of the 403 patients, the age limits were 15 and 90 years, with a mean of 56.08 years. The tumor size was considered, where (T1) represents 26.55%, (T2) represented 45.66%, the overall survival was 80% at 6 years. Patients in advanced stages were less likely to survive with a percentage of 43%. With the Cox regression model, it was possible to demonstrate a statistically significant association between tumor size and survival. The study shows that patients in advanced stages are less likely to survive, so efforts in health promotion must continue until detection is in curable stages.

Key words: Cox Proportional Hazards Model, survival, breast cancer, Ecuador.

Introducción

Según cifras de Globocan, el cáncer de mama es un problema de salud pública, que desde el año 2012 ha venido incrementándose, ubicándose como el cáncer de mayor incidencia en las mujeres[1]; para el año 2018 su repercusión en la población en general ocupaba el segundo lugar a nivel mundial, alcanzando el 11.6%; siendo la neoplasia maligna más frecuente en la población femenina y en relación a los decesos por cáncer, ocupa el cuarto lugar con un 6.6%. El cáncer de mama afecta con más frecuencia a los países del primer mundo y en vías de desarrollo, la edad con más recurrencia a la mortalidad es en mujeres de 60 a 74 años[2].

Para la Organización mundial de la salud, el desafío de la problemática de esta enfermedad es detectarla a tiempo. En Ecuador, según registros del Ministerio de Salud Pública, hasta junio de 2018 se realizaron 1.287 nuevas atenciones con diagnóstico de cáncer de mama, de las cuales 1.254, corresponden a mujeres representando el 97,6% de los casos presentados por esta patología, de acuerdo a datos obtenidos del Registro Diario Automatizado de Consultas y Atenciones Ambulatorias (RDACAA 2018) Y Plataforma de Registro de Atención en Salud (PRAS 2018)[3].

Seguidamente el Instituto de Estadísticas y Censos (INEC), en el año 2015, Manabí era la provincia que ocupaba el cuarto puesto a nivel nacional en decesos provocados por el cáncer de mama y el tercer puesto a nivel nacional en tasa de mortalidad por la misma enfermedad[4]. En Manabí el cáncer de mama ocupa el primer lugar entre los diferentes tipos de cáncer que existen; siendo esta una de las principales provincias de nuestro país, donde se encuentran estadísticas que puntúan al cáncer de mama como la principal causa de mortalidad femenina. En total, 235 casos en el 2018, que representan el 14,28%, según estadística emitida por Solca (Sociedad de Lucha contra el Cáncer)[5].

Con base en lo anterior se han desarrollado Modelos de Riesgos Proporcionales de Cox, para predecir la supervivencia de cáncer de mama, que han conllevado a estimar la super-

[1] Maestría en Estadística, Instituto de Posgrado, Universidad técnica de Manabí, Portoviejo, Ecuador.
[2] Docencia e investigación, Solca Manabí, Ecuador.
[3] Departamento de Matemáticas y Estadística. Instituto de Ciencias Básicas. Universidad Técnica de Manabí, Portoviejo, Ecuador y Departamento de Estadística. Universidad de Salamanca, Salamanca, España.

Corresponding author: karime.montes@gmail.com

vivencia personalizada a largo plazo en función de las características demográficas del paciente, los factores tumorales y tratamiento entregado[6]; este modelo permite identificar los factores clínicamente significativos asociados con el cáncer de mama y esto puede ayudar a predecir el riesgo de enfermedad, por lo tanto sirve para obtener una evaluación adecuada de los factores clínicos relevantes para el pronóstico del cáncer, lo que contribuye particularmente en la selección de eficientes estrategias terapéuticas[7].

Es por ello que el presente estudio tiene como objetivo realizar un análisis de supervivencia en pacientes con cáncer de mama de la Provincia de Manabí, mediante el Modelo de Riesgos proporcionales de Cox que permita determinar la supervivencia a los 6 años de los pacientes diagnosticados con la enfermedad y su relación con las variables como edad, género y estadio del tumor, sobrevida y meses de tratamiento, que proporcionen información útil a la toma de decisiones del médico con el paciente.

Métodos

El presente trabajo es un estudio Transversal, Retrospectivo, Descriptivo, Analítico y observacional; comprendido durante el periodo 2010 hasta 2015 en el Hospital Oncológico "Dr. Julio Villacreses Colmont"; de la Sociedad de Lucha contra el cáncer SOLCA Manabí, Ecuador. Los pacientes con cáncer de mama en este periodo ascendieron a 403, que fueron objetos del análisis de supervivencia. El estudio se realizó utilizando una matriz de información sobre los pacientes con cáncer de mama, obtenida del departamento de estadística, de SOLCA, Manabí, donde se elaboró una tabla de análisis descriptivo para un examen lo más completo posible sobre el cáncer de mama, sin buscar ni causas ni consecuencias de éste. Se midió las características de manera porcentual y se observó la configuración y los procesos que componen esta enfermedad, sin detenerse a valorarlos.

Se realizó un análisis de la matriz de información, sobre las variables o características de los pacientes con cáncer de mama, consiguiendo priorizarlas en los pacientes que reunieron las características como: género, edad, estadio del tumor en relación al tamaño del mismo, la sobrevida y meses de tratamiento constituyendo esta última en la variable respuesta, en sentido de dar una mejor utilidad para el análisis de supervivencia; en ellas se analizó la relación con características clínicas o covariables que intervienen en el tiempo hasta la ocurrencia del evento o no, es decir el tiempo de censura. Este análisis de supervivencia general se efectuó mediante el programa RStudio versión 3.2.2.[8].

Seguidamente se efectuó un análisis de supervivencia mediante el Modelo de Riesgos Proporcionales de Cox, donde se desarrolló el concepto de probabilidad marginal, una función de probabilidad que se caracteriza por los coeficientes de β, que miden los efectos de las covariables en la función de tasa de falla[9].

El modelo de Riesgos Proporcionales de Cox, constituye un modelo multivariado que puede ponderar el efecto de una serie de covariables, variables explicativas, predictores, factores de riesgo, variables de confusión[10], como también de variables cualitativas o cuantitativas sobre un desenlace dicotómico en función del tiempo y que puede definir al individuo en estudio mediante la ecuación[11]:

$$\lambda\left(t; Z_i(t)\right) = \lambda_0\,(t)e^{\beta' Zi(t)} \quad \text{Ó} \quad \lambda_i(t) = \lambda_0(t)e^{xi(t)\beta}$$

La finalidad del Modelo de Riesgos Proporcionales de Cox es facilitar un método de análisis de supervivencia sin necesidad de especificar o estimar una función de riesgo basal, mediante el desarrollo del concepto de probabilidad marginal, una función de probabilidad que solo depende de los coeficientes del modelo; al usar este modelo, el resultado se expresa por medio de una estadística llamada hazard ratio (HR), que es una división de riesgo (h) entre grupos y se define como la probabilidad de tener el desenlace en un periodo de tiempo determinado, donde hay la posibilidad de que uno de los grupos llegue antes al evento de interés al compararlo con otro grupo[11].

El Modelo de Riesgos Proporcionales de Cox se basa en considerar la prueba de significación que será la variable de agrupación o de tratamiento, la misma cuyo efecto se probará con la prueba de Wald, que proporciona un valor de p; además se considera la obtención del estimador del efecto, que es el Hazard ratio, y la obtención del intervalo de confianza de 95% para el Hazard ratio, que permite evaluar la significancia estadística de la relación de las variables del estudio y sus efectos en el desenlace del evento de interés; en este sentido el primer supuesto que debe cumplirse será sobre los datos censurados que no están relacionados con la probabilidad que ocurra el evento, es decir, que los individuos que no llegan al evento, no abandonaron el estudio por razones relacionadas a la variable de agrupación, este supuesto se corrobora investigando las posibles razones por las que abandonaron el estudio, y el segundo supuesto seria que las curvas de supervivencia para cada uno de los estratos deben tener funciones de riesgos que sean proporcionales en el tiempo entre las etapas del problema estudiado, aplicándose a las variables cuantitativas y ordinales, en donde se logre evidenciar los riesgos con incrementos constantes de un valor a otro y que siga la misma dirección[11]. Este análisis de supervivencia se efectuó mediante el programa SPSS versión 25[12].

Esta investigación no buscó lograr un estudio profundo sobre el Cáncer de mama en el aspecto de la medicina científica; lo que se pretendió fue lograr un análisis de supervivencia a la enfermedad de acuerdo con las variables intervinientes en el estudio en función a la tasa de muerte.

Resultados

De los 403 pacientes analizados, se observó que el 98.76%, son mujeres y el 1.24% son hombres, los límites de edad fueron 15 y 90 años, con media de 56.08 años. El 45.66%, presentan un tamaño del tumor T2 y el 16.63%, en T4. El 30.27%, tienen menos de un año padeciendo la enfermedad y el 4.96% más de cinco años. El 87.10%, estaban vivos y el 12.90% fallecieron (Tabla 1).

$$HR = \frac{\dfrac{\text{Sucesos ocurridos en el instante t en el grupo 1}}{\text{Sujeto en riesgo en el instante t en el grupo 1}}}{\dfrac{\text{Sucesos ocurridos en el instante t en el grupo 2}}{\text{Sujeto en riesgo en el instante t en el grupo 2}}} = \frac{h1}{h2}$$

DESCRIPCION DE VARIABLES			
VARIABLE	DESCRIPCIÓN	CODIFICACIÓN	%
Género	Género	Femenino (1)	98,76
		Masculino (2)	1,24
Edad	Edad en años	15-30 años	2,23
		31-40 años	12,16
		41-50 años	23,33
		51-60 años	26,55
		61-70 años	17,12
		71-80 años	11,41
		81-90 años	7,2
Sobrevida	Sobrevida	Vivo (0)	87,1
		Muerto (1)	12,9
Estadío del Tumor	TNM	Tamaño 1 (1)	26,55
		Tamaño 2 (2)	45,66
		Tamaño 3 (3)	11,17
		Tamaño 4 (4)	16,63
Meses	Meses de Tratamiento	0-12	30,27
		13-24	21,84
		24-36	18,86
		37-48	17,37
		49-60	6,7
		61-72	4,96

Tabla 1. Descripción de las Variables.

Se procedió a realizar el análisis de supervivencia general, considerando el tiempo de censura y el tiempo de fallas, ubicándose a la variable meses de tratamiento como la variable respuesta del presente estudio, la misma que se mide en meses considerando la fecha del primer diagnóstico hasta la fecha del fin del estudio o la ocurrencia del evento de interés que sería la muerte del paciente con cáncer de mama. El mayor tiempo de supervivencia de los 52 pacientes que llegaron al evento, es de 40 meses para 15 pacientes (Figura 1).

En el estudio del tiempo de supervivencia en los pacientes con cáncer de mama se evidenciaron observaciones incompletas o parciales, es decir censuras múltiples de tipo I a la derecha (tiempo censurado); en donde el inicio del tiempo de supervivencia se realizó en diferentes fechas y a la fecha fin de estudio no se observó el evento de interés (muerte) en 351 pacientes; los mismos que no abandonaron el estudio por razones relacionadas con el tratamiento o la variable de agrupación, ya que algunos pacientes fallecieron después de la fecha fin de estudio. Entre 0 a 20 meses existe la mayor cantidad de pacientes que no llegaron al evento de interés (muerte) (Figura 2).

La Tabla 2, indica los valores de beta (B) que se encuentran asociados al hazard ratio y resultan positivos para los estadios del tumor (T3 y T4), estos estadios según los resultados representan los principales factores de riesgo de la enfermedad, esto significa, que los pacientes con estadio del tumor (T3), con un 95% de confianza (IC95%:2.841-56.051) tienen 12.6 veces el riesgo de haber fallecido en el mes 72 de seguimiento, en relación con el estadio del tumor T1, y los pacientes con estadio del tumor T4 (IC95%:2.902-52.900), tienen 12.4 veces el riesgo de haber fallecido en el mes 72 de seguimiento en relación con el estadio del tumor T1. Seguidamente el estadístico chi cuadrado modificado de Wald es significativo con valores p> 0.001, para los tamaños del tumor T3 y T4 respectivamente, el resto de covariables como edad y género resultan con un valor no significativo en cuanto al riesgo de la enfermedad, por lo tanto no contribuyen con la ocurrencia del evento de interés; lo que significa que los pacientes que llegan con un tamaño del tumor en categoría T3 y T4 tienen menor tiempo de supervivencia al cáncer de mama sin incidir el género y la edad del paciente.

La curva de supervivencia global (Figura 3), en la que se representa gráficamente cómo van llegando al desenlace los 403 casos analizados conforme pasa el tiempo. La probabilidad de supervivencia global a 6 años fue de 80%, esto significa que para el mes 72 de seguimiento, el 80% de los pacientes continúa con vida. El tiempo medio de supervivencia está cerca a los 54 meses.

Las curvas de supervivencia ajustadas por edad y género para cada uno de los estadios de la enfermedad reflejan cómo va incrementando la mortalidad en los pacientes en los tamaños del tumor (T1, T2, T3 y T4) de la enfermedad. Es claro que los pacientes en tamaño (T3 y T4) viven menos que los pacientes en estadios menos avanzados. Para el mes 72 cerca del 57% de los pacientes en estadio 3 y 4 habrán fallecido mientras que más del 90% de los pacientes con estadio I continúan con vida (Figura 4).

La figura 5, muestra la curva para los estadios del tumor T1, T2, T3 Y T4, donde puede verse que los estadios T3 y T4 se incrementan con mayor proporción en los intervalos del tiempo de manera que a mayor tamaño del estadio del tumor, mayor es el riesgo de supervivencia al cáncer de mama.

Discusión

En relación a los hallazgos encontrados, el Modelo de Riesgos Proporcionales de Cox ha sido de gran importancia para el presente estudio, ya que genera una descripción precisa y clara sobre la incidencia de las variables en el análisis de supervivencia del cáncer mama, considerando la variable respuesta al tiempo transcurrido desde la fecha del primer diagnóstico del paciente, hasta la fecha fin de estudio u ocurrencia del evento del interés (muerte), frente a covariables como sobrevida, estadio del tumor, edad y género; estos resultados guardan relación con lo que señala (11) que el modelo multivariante de Riesgos Proporcionales de Cox, es muy útil en el campo de la salud, cuando se trata de enfermedades graves como el cáncer, ya que el exponente de Beta o hazard ratio proporciona la significancia de la covariable más representativa en el análisis de supervivencia y así se obtiene un análisis que ayuda a la toma de decisiones sobre el tratamiento de la enfermedad entre el médico tratante con el paciente que la padece.

Así mismo los resultados del presente estudio guardan relación con lo que manifiesta (7), que el modelo de Riesgos Proporcionales de Cox genera una evaluación adecuada de los factores clínicos relevantes para el pronóstico del cáncer, lo que contribuye particularmente en la selección de eficientes

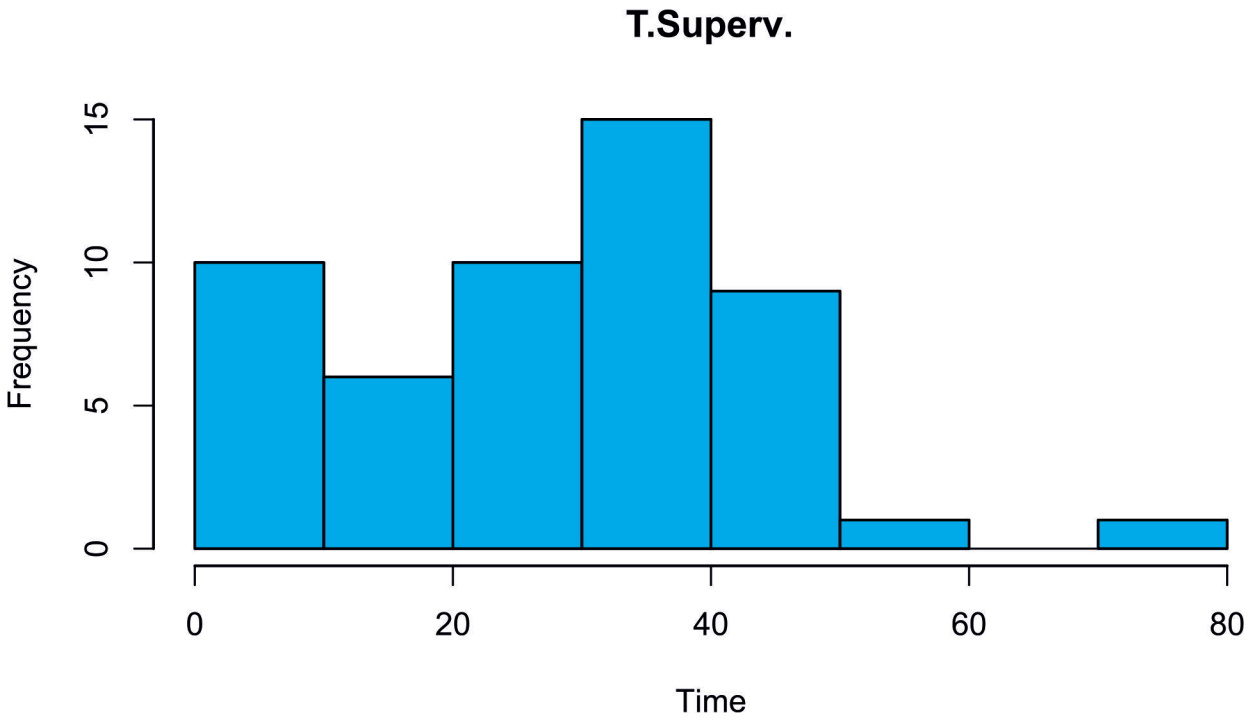

Figura 1. Tiempo de supervivencia.

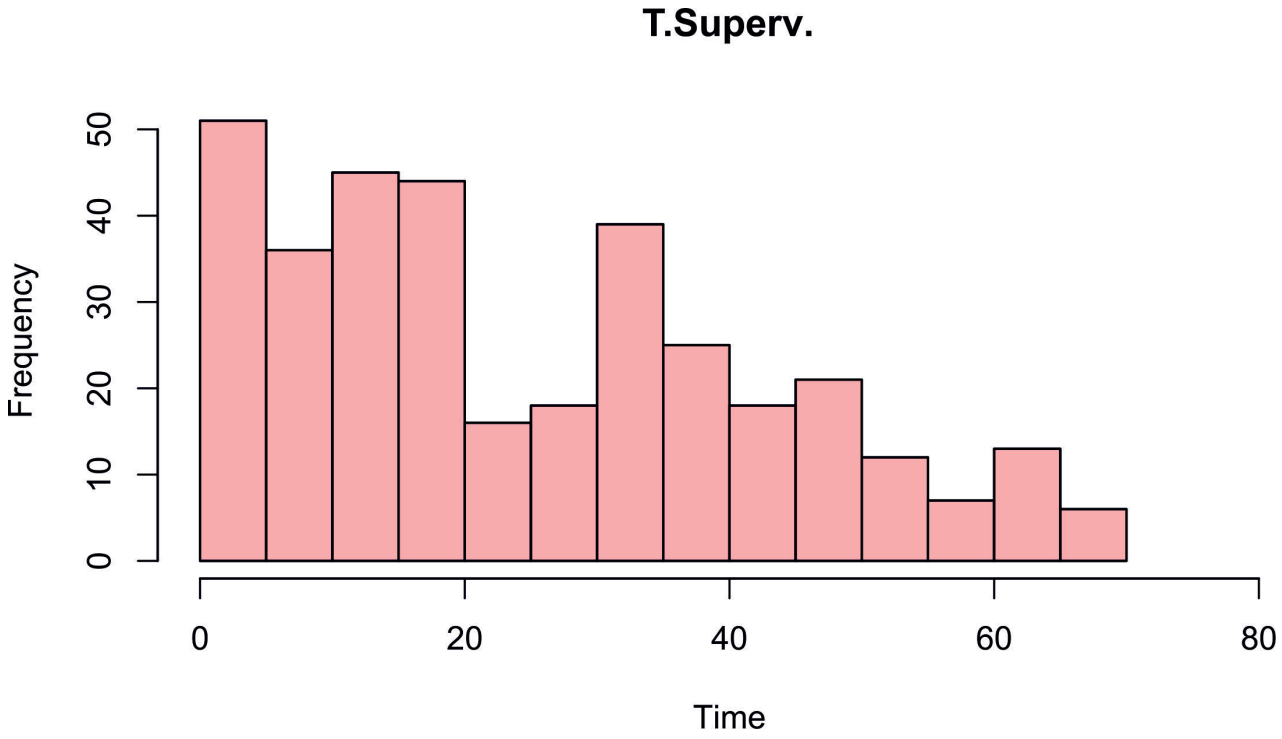

Figura 2. Tiempo censurado.

estrategias terapéuticas; pero este no concuerda con (2) ya que los pacientes con menor edad presentaran una mejor supervivencia global al cáncer de mama.

Por lo tanto en lo que se refiere a la variable edad no se pudo demostrar relación con la supervivencia, lo que tampoco coincide con estudios realizados (13), a 1113 pacientes con cáncer de mama en un periodo de estudio de cinco y diez años donde el aumento de la edad en el momento del diagnóstico se asoció con un mayor riesgo de muerte en los pacientes, así mismo en la investigación hecha por (14), a 767 pacientes con cáncer de mama, en donde se analizó la edad con la supervivencia, este encontró que los pacientes más jóvenes y mayores parecen tener una supervivencia más corta al cáncer de mama, sin embargo en este estudio no hay significancia en esta covariable edad, y por consiguiente el riesgo de que ocurra el evento no discrimina la edad del paciente.

La supervivencia global encontrada en el presente trabajo, en 6 años fue del 80%, semejante a la reportada en el estudio de (15), que se efectuó a 119 pacientes con cáncer de mama atendidas durante el 2010 al 2015 en el Hospital Militar de Especialidades de la Mujer y Neonatología en la Ciudad de México, donde la supervivencia global se situó en 81%. En lo que

	B	SE	Wald	df	Sig.	Exp(B)	95,0% CI para Exp(B)	
							Inferior	Superior
TNM			24,22	3	0			
TNM(1)	1,306	0,753	3,007	1	0,08	3,691	0,844	16,153
TNM(2)	2,535	0,761	11,1	1	0	12,62	2,841	56,051
TNM(3)	2,517	0,741	11,55	1	0	12,39	2,902	52,9
Género	-10,69	423,82	0,001	1	0,98	0	0	.
Edad	0,001	0,009	0,009	1	0,93	1,001	0,983	1,019

Tabla 2. Factores predictores de supervivencia de los pacientes con cáncer de mama.

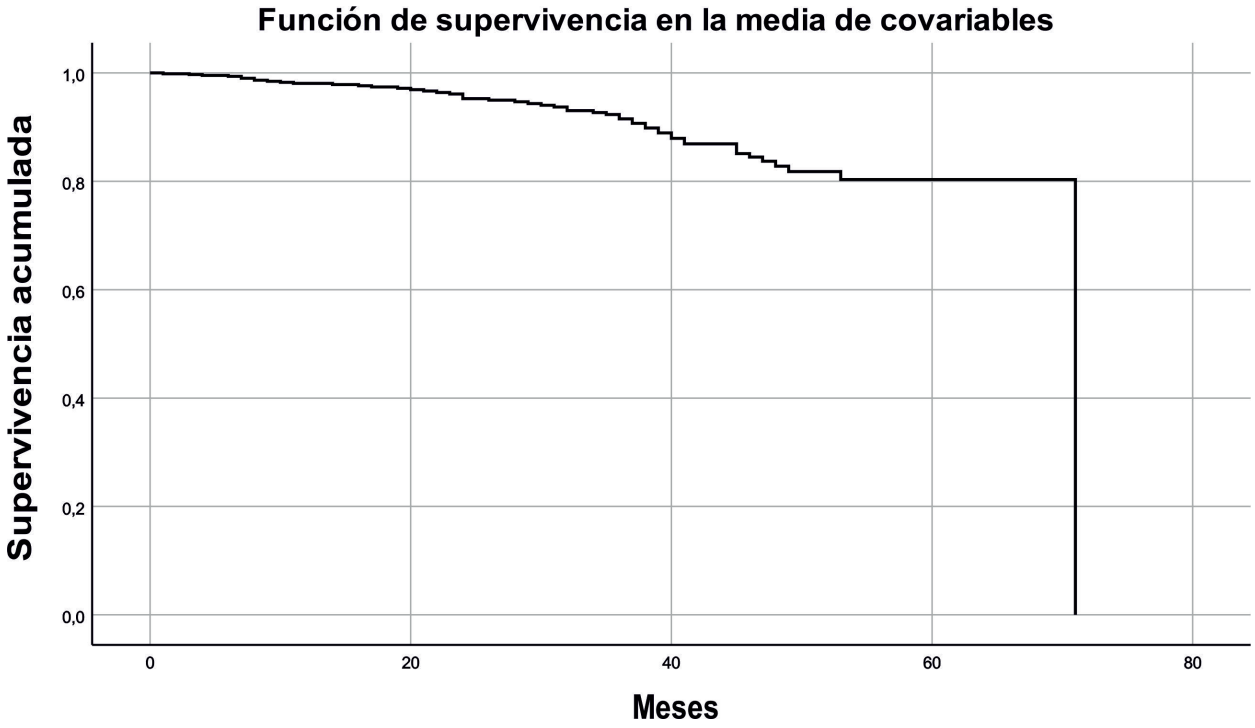

Figura 3. Curva de supervivencia ajustada por los cofactores.

no concuerda con la investigación citada, es que en esta no se pudo demostrar que la supervivencia se relaciona con otras variables como estadio del tumor (tamaño), ya que precisamente es la variable significativa relacionada con la supervivencia en los pacientes con cáncer de la presente investigación, donde tamaño del tumor T1 y T2, demostraron que a menor tamaño del tumor, mayor supervivencia a la enfermedad.

Conclusiones

En Ecuador los reportes de supervivencia son pocos, por ello se realiza esta investigación la cual significa un gran logro y esfuerzo entre instituciones, teniendo en cuenta los reportes de supervivencia a 6 años. Se demostró en este estudio, que los pacientes diagnosticados en etapas avanzadas son aquellos que su probabilidad de sobrevida es mucho menor, con base en lo anterior cabe resaltar que es de gran importancia seguir investigando en pro de la salud, esto con el fin de detectar a tiempo y en etapas curables a los pacientes.

Agradecimientos

Este estudio fue apoyado por el Departamento de Matemáticas y Estadística. Instituto de Ciencias Básicas. Los autores desean agradecer a SOLCA Portoviejo por su apoyo y facilitar los datos.

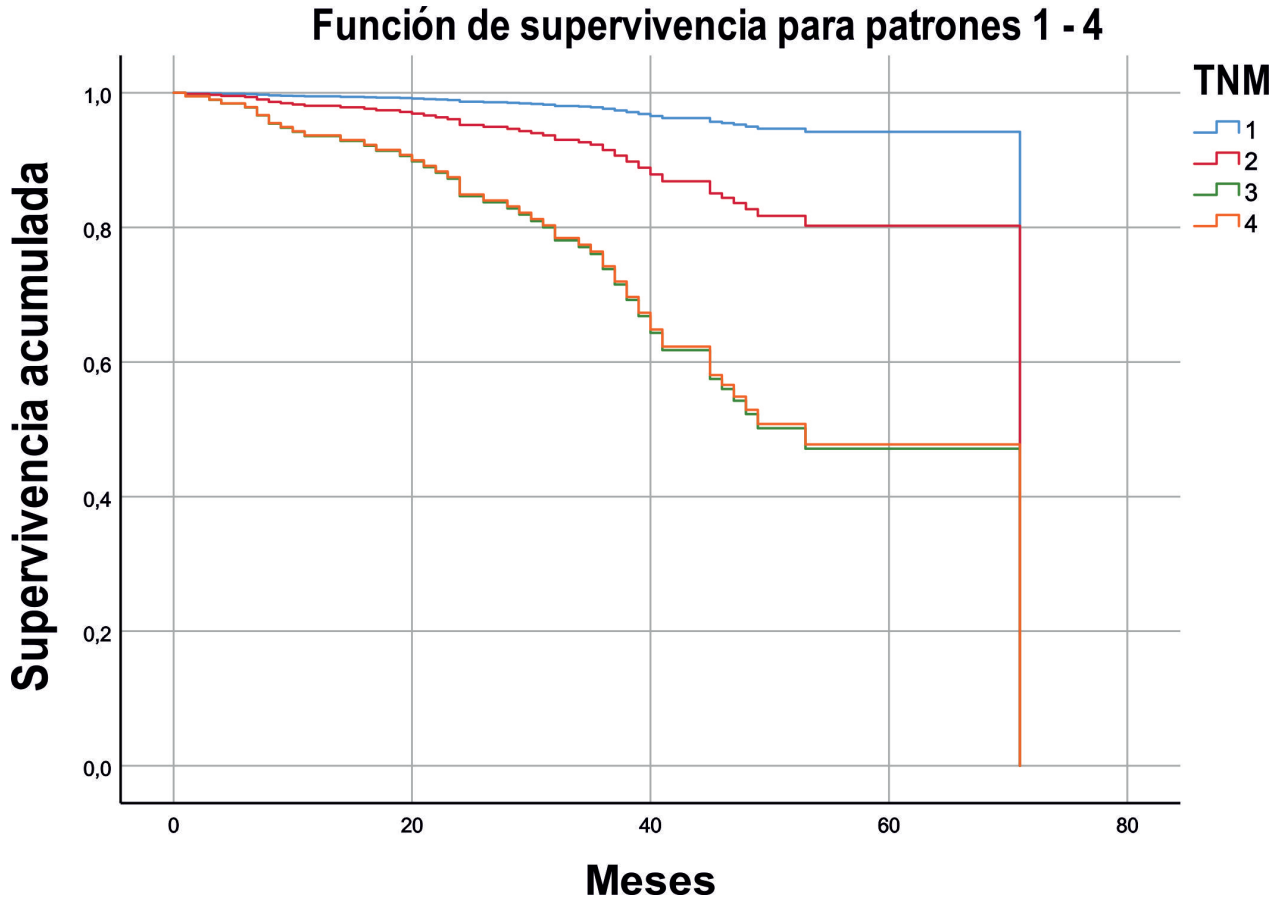

Figura 4. Curva de supervivencia por estadio de la enfermedad.

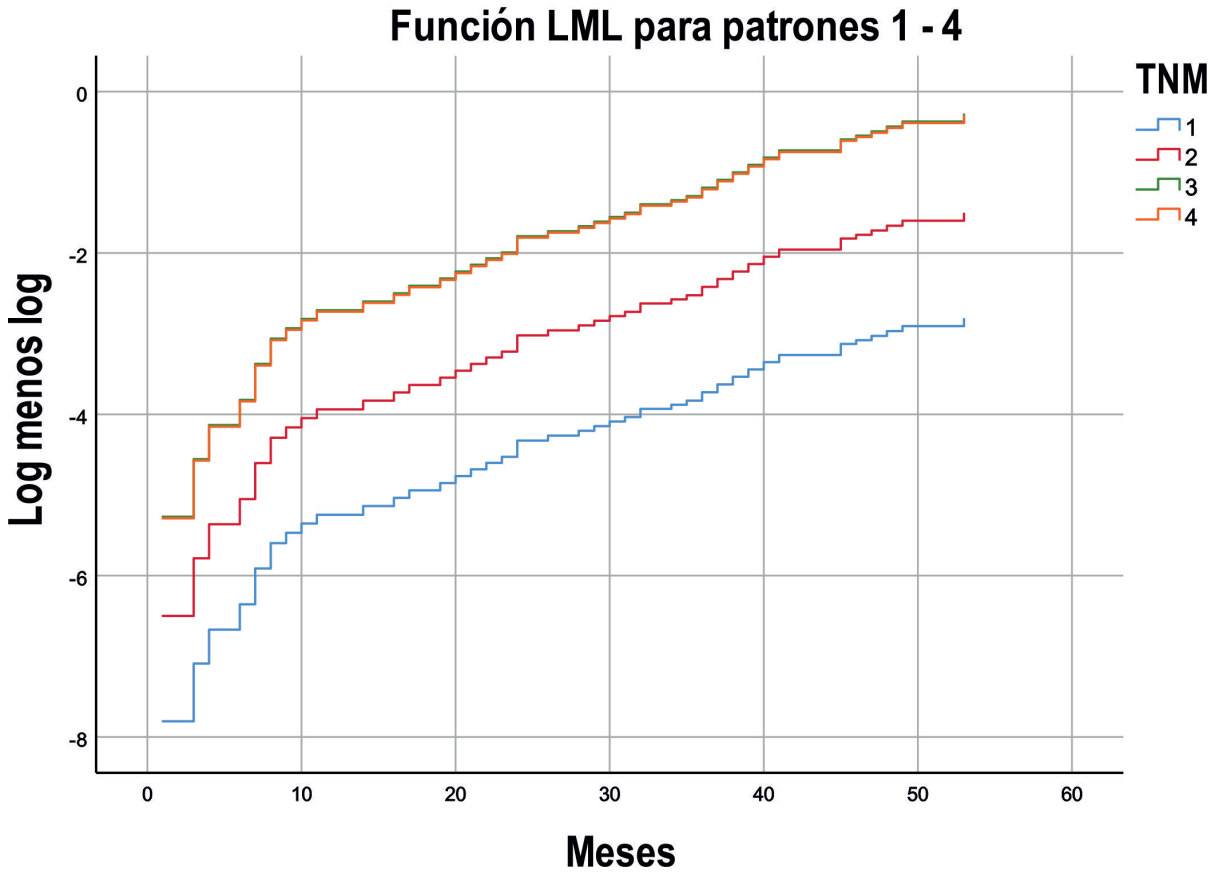

Figura 5. Evaluación de la función de riesgos proporcionales.

Referencias bibliográficas

1. Ministerio de Salud Pública. Estrategia Nacional para la atención integral del cáncer en el Ecuador. (2017).
2. Ulloa, P., Ronquillo, S. & Sánchez, K. Sobrevida en pacientes con cáncer de mama según su inmunohistoquímica experiencia del Instituto Oncológico Nacional - Sociedad de Lucha Contra el Cáncer, Guayaquil Ecuador. Rev. Medica Sinerg. 5, e542 (2020).
3. Ministerio de Salud Publica del Ecuador. Instructivo para el llenado del Automatizado de Consultas y Atenciones Ambulatorias (RDACAA). Minist. Salud Pública Ecuador 10–60 (2013).
4. Arreaga, A. & Torres, L. Visualización geográfica de la tasa de mortalidad por cáncer de mama, cérvix y de próstata en el Ecuador. (2017).
5. Risco, J. Nosotros – REVISTA DE MANABÍ.. Se dieron 'un toque' para prevenir el cáncer de mama. (2019).
6. Asare, E. A. et al. Development of a model to predict breast cancer survival using data from the National Cancer Data Base. Surg. (United States) 159, 495–502 (2016).
7. Tang, W. et al. Screening of Clinical Factors Related to Prognosis of Breast Cancer Based on the Cox Proportional Risk Model. J. Comput. Biol. 27, 1–10 (2020).
8. Team, R. r studio - Google Académico. RStudio: integrated development for R. RStudio, Inc. Boston, MA (2018).
9. Rebaza, D. "MODELOS SEMIPARAMÉTRICOS DE EVENTOS RECURRENTES: CASO APLICACIÓN A PACIENTES CON CANCER DE MAMA". 67 (2017).
10. Boj del Val, E. El modelo de regresión de Cox. El modelo de regresión de Cox (2017).
11. Pérez-Rodríguez, M., Rivas-Ruiz, R., Palacios-Cruz, L. & Talavera, J. O. XXII. Del juicio clínico al modelo de riesgos proporcionales de Cox. Rev Med Inst Mex Seguro Soc 52, 430–435 (2014).
12. Spss, I. spss - Google Académico. IBM SPSS Statistics for Windows, version 25 Armonk, NY: IBM SPSS CORP. (2017).
13. Caleffi, M. et al. Breast cancer survival in Brazil: How much health care access impact on cancer outcomes? Breast 54, 155–159 (2020).
14. Balabram, D. Asociación entre edad y supervivencia en una cohorte de pacientes brasileñas con cáncer de mama operable Asociación entre edad y supervivencia en una cohorte de pacientes brasileñas con cáncer de mama operable Asociación entre edad y supervivencia en una. 31, 1732–1742 (2015).
15. Heredia, A. & Palacios, G. Supervivencia a 5 años pos tratamiento de cáncer de mama: experiencia institucional. Ginecol. Obstet. Mex. 86, 575–583 (2018).

Received: 18 marzo 2021
Accepted: 15 julio 2021

CASE REPORTS / REPORTE DE CASO

Infección metastásica por *Staphylococcus aureus* en neonatos: a propósito de un caso

Metastatic infection by *Staphylococcus aureus* in neonates: about a case

Laura Taylor[1], Carlos S. Mamani-García[2], Alexandra Gutiérrez-Pingo[3], Jerry K. Benites-Meza[4], Diego Chambergo-Michilot[5], Norma del Carmen Gálvez-Díaz[6], Joshuan J. Barboza[7]

DOI. 10.21931/RB/2021.06.03.25

Resumen: La infección metastásica como complicación infrecuente de bacteriemia por *Staphylococcus aureus* en neonatos es de difícil manejo por la limitada bibliografía. Comunicar el caso clínico de un neonato prematuro que desarrolló infección metastásica como complicación de bacteriemia por *S. aureus*. Presentamos el caso de un neonato prematuro que ingresó a Unidad de cuidados intensivos neonatal, diagnosticado de sepsis bacteriana, síndrome de dificultad respiratoria neonatal y afectación por ruptura prematura de membrana. Le insertaron catéter epicutáneo y fue tratado para bacteriemia por *E. coli* con éxito. Reingresó por sepsis tardía debido a infección de *S. aureus* multisensible en catéter epicutáneo. Aparece un absceso en la cara anterior del tórax por *S. aureus*, confirmando infección metastásica. Se realizó el drenaje del absceso con resolución favorable del cuadro clínico. En neonatos sometidos a procedimientos invasivos es importante vigilar la evolución clínica e identificación temprana de infección metastásica post-bacteriemia por *Staphylococcus aureus* y brindar tratamiento temprano para evitar secuelas.

Palabras clave: Bacteriemia, infección metastásica, infección relacionada a catéter, recién nacido, *Staphylococcus aureus*.

Abstract: Metastatic infection as an infrequent complication of *Staphylococcus aureus* bacteremia in neonates is challenging due to the limited literature. To report the clinical case of a premature neonate who developed a metastatic infection as a complication of *S. aureus* bacteremia. We present the case of a premature neonate admitted to the Neonatal Intensive Care Unit, diagnosed with bacterial sepsis, neonatal respiratory distress syndrome, and involvement by premature rupture of the membrane. A patch catheter was inserted, and he was successfully treated for *E. coli* bacteremia. He was re-admitted for late sepsis due to infection with multisensitive *S. aureus* in a patch catheter. An abscess appears on the front of the chest due to *S. aureus*, confirming metastatic infection. The abscess was drained with a favorable resolution of the clinical picture. In neonates submitted to invasive procedures, it is essential to monitor the clinical evolution and early identification of metastatic infection after *Staphylococcus aureus* bacteremia and provide early treatment to avoid sequelae.

Key words: Bacteremia, catheter-related infections, metastatic infection, newborn, *Staphylococcus aureus*.

Introducción

La bacteriemia es la presencia de bacterias en la sangre[1]. Al ser una infección grave, puede conducir a una morbilidad y mortalidad significativa si no se maneja adecuadamente[2]. La incidencia es variable por países y grupos de edad. En población pediátrica; el diagnóstico clínico puede ser un desafío debido a la presentación variable dependiendo de la edad, el sitio de infección y el organismo causal[3]; e incluso la bacteriemia por *Staphylococcus aureus* tiene variedad de presentaciones[4].

La bacteriemia por *S. aureus* provoca infecciones que incluyen infecciones de piel, tejidos blandos y neumonía. Ésta puede dar lugar a complicaciones como endocarditis infecciosa, complicaciones pulmonares e infecciones metastásicas[5]. La infección metastásica se define como la extensión de la infección que no presenta relación alguna con la infección del sitio primario[6]. Puede ser del tipo endocarditis infecciosa, osteomielitis vertebral, abscesos de tejidos blandos, artritis séptica, infección ocular, embolismo pulmonar séptico, entre otros[7,8].

La prevalencia de infección metastásica por *S. aureus* en recién nacidos es incierta, sin embargo, un estudio reportó la diseminación metastásica en el 13,4% de 112 episodios de bacteriemias por *S. aureus* relacionadas a catéter en pacientes pediátricos[9].

Según las guías, la duración del tratamiento en pacientes pediátricos con bacteriemia puede variar de 2 a 6 semanas según diversos factores[10]. Por ello, es importante identificar una infección metastásica en neonatos debido a que el tratamiento es diferente al de una bacteriemia no complicada, además de que un tratamiento insuficiente (por ejemplo, por una identificación tardía) para estas complicaciones graves se asocia con mal pronóstico, discapacidad y recaída.

Nuestro objetivo es reportar el caso de un neonato que desarrolló infección metastásica como complicación de bac-

[1] Médico Epidemiólogo, Clínica Palermo de Bogotá, Colombia.
[2] Estudiante de medicina, Facultad de Medicina, Universidad Nacional de San Agustín, Arequipa, Perú y Sociedad Científica de Estudiantes de Medicina Agustinos (SOCIEMA), Universidad Nacional de San Agustín, Arequipa, Perú.
[3] Estudiante de medicina, Escuela de Medicina, Universidad Nacional del Santa, Nuevo Chimbote-Ancash, Perú y Sociedad Científica de Estudiantes de Medicina de la Universidad Nacional del Santa (SOCEMUNS), Universidad Nacional del Santa, Nuevo Chimbote-Ancash, Perú.
[4] Estudiante de medicina, Facultad de Medicina, Universidad Nacional de Trujillo, Trujillo, Perú y Sociedad Científica de Estudiantes de Medicina de la Universidad Nacional de Trujillo (SOCEMUNT), Universidad Nacional de Trujillo, Trujillo, Perú.
[5] Estudiante de medicina, Facultad de Medicina, Universidad Científica del Sur, Lima, Perú y Tau-Relaped Group, Trujillo, Perú.
[6] Doctora en Enfermería, Escuela de Enfermería, Universidad Señor de Sipán, Chiclayo, Perú.
[7] Maestría en Investigación Clínica, Especialista en Cuidados Intensivos Neonatales, Tau-Relaped Group, Trujillo, Perú y Escuela de Medicina, Universidad Señor de Sipán, Chiclayo, Perú.

Corresponding author: jbarbozameca@relaped.com.

teriemia por *Staphylococcus aureus*; abordar aspectos diagnósticos y terapéuticos más importantes y revisar la literatura disponible.

Caso clínico

Neonato masculino, nacido a las 29,4 semanas por cesárea debido a ruptura prematura de membrana prolongada. Como antecedente se destaca: madre de 30 años, sin antecedentes patológicos, con 6 controles en la gestación y pruebas de infección congénitas negativas.

Se realizó maduración pulmonar y reanimación con presión positiva continua en vía aérea (CPAP). Presentó presión arterial de 56/25, Silverman 4/0, frecuencia cardiaca de 138 latidos por minuto, frecuencia respiratoria de 60 respiraciones por minuto, SaO_2 de 94%, FiO_2 de 35% y ventilación mediante tubo orotraqueal. Nació con bajo peso (1 540 g), talla adecuada (43 cm), perímetro cefálico de 29 cm, sin contacto piel con piel y no se inició lactancia materna en la primera hora. Ingresó a Unidad de cuidados intensivos neonatales (UCIN) con diagnóstico de sepsis bacteriana y síndrome de dificultad respiratoria (SDR) neonatal.

En su 2° día de vida se inserta catéter epicutáneo, inicia ventilación no invasiva (VNI) y posteriormente, por cánula nasal. Se administró 1 dosis de surfactante exógeno y fue retirado el tubo orotraqueal. Se inició antibioticoterapia. Luego del cultivo se reporta *Escherichia coli*, leucopenia y PCR positiva (Tabla 1); asimismo, por ictericia acentuada, se inició fototerapia, acompañado de nutrición parenteral y segunda dosis de surfactante exógeno. Al 6° día, ameritó paso de oxígeno por cánula nasal a VNI, pero fue retomado al día siguiente, además no presentó distermias y la PCR fue en descenso. Al 10° día, fue trasladado a cuidados intermedios, finalizó antibioticoterapia y los hemocultivos y PCR fueron negativos.

El 15° día, presentó polipnea y edemas periféricos, aumento del requerimiento respiratorio y tendencia a la taquicardia. Se retiró catéter epicutáneo y se ordenó cultivo de la punta y exámenes auxiliares (Tabla 1). Se inició tratamiento por sospecha de sepsis tardía (Tabla 2). El 16° día, los resultados de hemocultivo y punta de catéter fueron positivos, la causa de la sepsis tardía por *Staphylococcus aureus*, presentó lesión de tipo absceso en la cara anterior del tórax. El 17° día, presentó hipotensión, taquicardia, llenado capilar lento, gasto urinario aumentado. Se pasó bolo de solución salina y reingresó a UCIN. Posteriormente fue trasladado a cuidados básicos, con absceso del tórax limitado de 1 x 2 cm con calor local, cuya secreción reportó *S. aureus* multisensible, por lo que se iniciaron 10 días de antibioticoterapia (Tabla 2). Egresó el día 29 de vida con oxígeno domiciliario, plan canguro, absceso resuelto y con dosis de palivizumab.

Día	Examen	Resultado
2° Día	Radiografía de tórax	Sin infiltrados pulmonares
3° Día	Hemocultivo	*Escherichia coli* en 4 hemocultivos
	PCR*	Positivo
5° Día	Antibiograma	*Escherichia coli*, betalactamasa de espectro extendido sensible a amikacina
	Hemograma	Trombocitopenia
6° Día	LCR†	Sin gérmenes
	Radiografía de tórax	Normal
	Ecografía transfontanelar	Normal
7° Día	Hemocultivo	Negativo
	PCR*	En descenso
10° Día	Hemocultivo	Negativo
	PCR*	Negativo
	Hemograma	Recuento leucocitario de 8 900 leucocitos/ul y sin trombocitopenia
15° Día	PCR*	Muy elevado
	LCR†	Hiperproteinorraquia
	Radiografía de tórax	Normal
	Hemograma	Recuento leucocitario de 24 800 leucocitos/ul
16° Día	Hemocultivo	*Staphylococcus aureus* en 2 hemocultivos
17° Día	Ecografía transfontanelar	Normal
	Ecocardiografía	Estenosis relativa de las ramas pulmonares, no patológica y sin evidencia de vegetaciones
18° Día	Hemocultivo	*Staphylococcus aureus* multisensible
19° Día	PCR*	En descenso
	Hemograma	Descenso de recuento leucocitario a 14 220 leucocitos/ul
21° Día	Hemocultivo	Negativo
	Cultivo de LCR†	Negativo
	Urocultivo	Negativo

Tabla 1. Resultados de exámenes diagnósticos y auxiliares.

DÍA	TRATAMIENTO
2° Día	Ampicilina - amikacina (antibióticos de primera línea)
5° Día	Continúa con terapia por 7 días, pero se suspende ampicilina
15° Día	Vancomicina (ajustada a dosis meníngeas) y piperacilina - tazobactam,
16° Día	Pasó de piperacilina - tazobactam a cefepime, por desescalamiento por identificación de agente causal
18° Día	Se suspendió la vancomicina y se inició oxacilina
29° Día	Dosis de palivizumab al egreso

Tabla 2. Cambios en el tratamiento.

Discusión

Presentamos el caso de un neonato pretérmino, recuperado de una bacteriemia inicial por *E. coli*, con diagnóstico de bacteriemia por *S. aureus*, sospechada por signos y síntomas hemodinámicos inespecíficos y confirmada por hemocultivos, complicada por sepsis e infección metastásica (absceso) la cual se comprobó al identificar el origen en el catéter periférico. La bibliografía acerca de la infección metastásica en neonatos es escasa, por lo que reportamos este caso con el objetivo de ampliar los conocimientos sobre el tema.

Se realizó una búsqueda sistemática en dos bases de datos (Pubmed y Scopus). No se aplicaron restricciones de idioma o fecha de publicación. Las palabras clave usadas para formular las estrategias de búsqueda fueron "*Staphylococcus aureus*", "Metastatic infection", "Bacteremia", "Catheter-Related Infections" y "Newborn infant".

En este caso, el primer microorganismo aislado fue *E. coli*, el cual probablemente provino del tracto genitourinario de la madre considerando los 5 días de evolución de la ruptura prematura de membrana; pues la bacteria *Escherichia coli*, luego de *S. aureus*, es uno de los microorganismos más frecuentemente transferidos madre-hijo en pacientes con ruptura prematura de membrana y suele ocurrir antes de las 37 semanas de gestación[11].

La ruptura prematura de membrana es factor de riesgo materno para infección de aparición temprana por *Escherichia coli*. Así mismo la prematuridad y bajo peso predisponen a una infección que puede resultar en sepsis[12]. Una vez superada esa infección, hubo un episodio de inestabilidad hemodinámica con hemocultivos positivos para *S. aureus*, confirmándose la infección tardía. Esto dado que el acceso venoso central por catéter epicutáneo es factor de riesgo para infección de aparición tardía (después de los 3 a 7 días de vida) por *Staphylococcus aureus*[12].

Considerando que el paciente había sido sometido a procedimiento invasivo (colocación de un catéter epicutáneo) y haber descartado otro proceso infeccioso simultáneo, se considera como diagnóstico una infección del torrente sanguíneo asociada a catéter (ITS-AC). Con la ITS-AC de mínimo 6 días de evolución (periodo de suspensión de antibioticoterapia para la infección anterior) se procedió a retirar el catéter (lo recomendado en las guías de manejo)[13] e insertar uno nuevo. Los estudios recomiendan que se retire de manera inmediata, evitando una infección en sangre[14] dentro de las dos primeras semanas. Estas recomendaciones se basan en estudios observacionales, por los escasos o nulos ECA respecto a este tema[15]. Por ejemplo, un estudio realizado en la clínica privada de Sao Paulo[16], entre el 2010 y 2011 demostró que la ITS-AC es una complicación en neonatos que requiere la extracción no selectiva del catéter. Otro estudio, realizado por Beard, Lauren MD *et al.*[17], en el año 2019, demostró un valor significativo entre el tiempo de permanencia del catéter y el retiro no selectivo del mismo ($p< 0.0001$), siendo observado en menor frecuencia entre los 8 y 59 días de permanencia del catéter. Así se concluyó en el estudio que durante la primera semana y pasado los 59 días el retiro no selectivo del catéter conlleva mayores riesgos de complicaciones como la ITS-AC, acompañados de un periodo de estabilidad. Una particularidad en nuestro caso, es que se hace visible un absceso en la cara anterior del tórax, sin lesiones previas, en donde se aísla el mismo microorganismo. Esto confirma una infección metastásica a tejidos blandos por *S. aureus*, lo cual constituye una de las pocas metástasis reportadas[18]. En neonatos, la infección metastásica de origen en el catéter periférico ha sido poco estudiada[9,19]. De acuerdo a Murdoch F, *et al.*[20], en el 2017, en una población pediátrica menores de 15 años (mediana = 1 año) se reportaron un 4,8% (N=126) de casos que desarrollaron un absceso profundo. Asimismo, un reciente estudio de Falup-Pecurariu O, *et al.*[21], reportó un caso de un recién nacido de 3 semanas presentó un absceso profundo, pero fue en la región izquierda del cuello.

Ante la sospecha de sepsis tardía por bacteriemia, se administró tratamiento empírico (abarcando a *S. aureus* meticilino-resistente[SAMR]). Este consistió en vancomicina y piperacilina - tazobactam. Diferentes estudios muestran la eficacia mayor de administrar vancomicina junto a un betalactámico, comparado con tan sólo vancomicina. El betalactámico más usado para estas combinaciones fue piperacilina - tazobactam, similar a nuestro caso[22]. El desescalamiento de piperacilina - tazobactam es a menudo a ceftriaxona pero también es aceptable otro betalactámico[22]. En este caso, el desescalamiento fue a cefepime, una cefalosporina de cuarta generación. Algunos otros estudios han demostrado la efectividad de regímenes basados en daptomicina u otros basados en vancomicina; y en caso de que los regímenes basados en vancomicina y daptomicina no reviertan la bacteriemia, otros fármacos como ceftarolina sola, ceftarolina con trimetoprim - sulfametoxazol (TMP-SMX), linezolid, telavancina, fosfomicina con imipenem y quinupristina-dalfopristina, han mostrado eficacia[22]. Sin embargo, la IDSA recomienda usar vancomicina IV como tratamiento primario para las infecciones graves por SAMR en el período neonatal, a su vez; la decisión de combinar fármacos debe ser individualizada y que TMP-SMX no se use durante el período neonatal inmediato debido al mayor riesgo de kernícterus[10].

La duración del tratamiento desde la confirmación de *S.*

aureus como causa de la sepsis tardía (un día después del inicio del tratamiento empírico con vancomicina y piperacilina - tazobactam) hasta la resolución del absceso fue de 12 días. La Sociedad Americana de Enfermedades Infecciosas (en inglés, IDSA) recomienda que el tratamiento en bacteriemias complicadas dure entre 2-6 semanas dependiendo del caso[10]. Existen estudios que indican cuánto debe durar el tratamiento en caso de infección metastásica tipo endocarditis infecciosa, osteomielitis vertebral, artritis séptica, entre otros[7]; pero no existen en el caso de infección de tejidos blandos, probablemente debido a que este debe ser tratado de manera similar a una infección de tejidos blandos primaria (es decir, no infección metastásica). La IDSA recomienda vancomicina IV si se sospecha de SAMR[10]. En este caso, el absceso en los dos primeros días fue tratado con la misma combinación para la bacteriemia (vancomicina y cefepime) y una vez identificado que el *S. aureus* era multisensible, se suspendió la vancomicina y se inició oxacilina, por diez días, hasta resolución del absceso.

Conclusiones

Es importante la vigilancia de la evolución clínica, la sospecha e identificación temprana de una infección metastásica como complicación de una bacteriemia por Staphylococcus aureus en neonatos sometidos a procedimientos invasivos con el fin de iniciar un tratamiento adecuado y temprano para evitar las posibles secuelas.

Agradecimientos

Este estudio fue apoyado por el Departamento de Matemáticas y Estadística. Instituto de Ciencias Básicas. Los autores desean agradecer a SOLCA Portoviejo por su apoyo y facilitar los datos.

Contribuciones de autores

Laura Taylor y Joshuan J. Barboza: Revisión crítica del artículo, aprobación de la versión final, aporte de pacientes o material de estudio, garante.

Carlos S. Mamani-García, Alexandra Gutiérrez-Pingo, Jerry K. Benites-Meza: Redacción, revisión crítica y aprobación de la versión final.

Diego Chambergo-Michilot y Norma del Carmen Gálvez-Díaz: Revisión crítica del artículo, aprobación de la versión final

Información de financiación

El reporte ha sido autofinanciado.

Conflictos de interés

Los autores declaran que no tienen conflicto de intereses contrapuestos.

Referencias bibliográficas

1. Geier R, Liu S, Tilley P, Roberts A, Rassekh SR, Ting J, et al. Epidemiology of Antibiotic Resistant Gram-negative Bacteremia in a Hospital-Based Pediatric Population. Pediatrics 2018;142:567–567. https://doi.org/10.1542/PEDS.142.1_MEETINGABSTRACT.567.
2. Coon ER, Srivastava R, Stoddard G, Wilkes J, Pavia AT, Shah SS. Shortened IV antibiotic course for uncomplicated, late-onset group b streptococcal bacteremia. Pediatrics 2018;142. https://doi.org/10.1542/peds.2018-0345.
3. Pai S, Enoch DA, Aliyu SH. Bacteremia in children: Epidemiology, clinical diagnosis and antibiotic treatment. Expert Rev Anti Infect Ther 2015;13:1073–88. https://doi.org/10.1586/14787210.2015.1063418.
4. McMullan BJ, Bowen A, Blyth CC, Van Hal S, Korman TM, Buttery J, et al. Epidemiology and mortality of staphylococcus aureus Bacteremia in Australian and New Zealand children. JAMA Pediatr 2016;170:979–86. https://doi.org/10.1001/jamapediatrics.2016.1477.
5. Keynan Y, Rubinstein E. Staphylococcus aureus Bacteremia, Risk Factors, Complications, and Management. Crit Care Clin 2013;29:547–62. https://doi.org/10.1016/j.ccc.2013.03.008.
6. Khatib R, Riederer K, Saeed S, Johnson LB, Fakih MG, Sharma M, et al. Time to Positivity in Staphylococcus aureus Bacteremia: Possible Correlation with the Source and Outcome of Infection. Clin Infect Dis 2005;41:594–8. https://doi.org/10.1086/432472.
7. Horino T, Hori S. Metastatic infection during Staphylococcus aureus bacteremia. J Infect Chemother 2020;26:162–9. https://doi.org/10.1016/j.jiac.2019.10.003.
8. Fowler VG, Justice A, Moore C, Benjamin DK, Woods CW, Campbell S, et al. Risk Factors For Hematogenous Complications of Intravascular Catheter--Associated Staphylococcus aureus Bacteremia. Clin Infect Dis 2005;40:695–703. https://doi.org/10.1086/427806.
9. Carrillo-Marquez MA, Hulten KG, Mason EO, Kaplan SL. Clinical and Molecular Epidemiology of Staphylococcus aureus Catheter-Related Bacteremia in Children. Pediatr Infect Dis J 2010;29:410–4. https://doi.org/10.1097/INF.0b013e3181c767b6.
10. Catherine Liu 1, Arnold Bayer, Sara E Cosgrove, Robert S Daum, Scott K Fridkin, Rachel J Gorwitz, Sheldon L Kaplan, Adolf W Karchmer, Donald P Levine, Barbara E Murray, Michael J Rybak, David A Talan HFC. Clinical Practice Guidelines by the Infectious Diseases Society of America for the Treatment of Methicillin-Resistant Staphylococcus aureus Infections in Adults and Children | Clinical Infectious Diseases | Oxford Academic. Clin Infect Dis 2011;52:e18–9. https://doi.org/10.1097/INF.0b013e3181c767b6.
11. Zeng L nan, Zhang L li, Shi J, Gu L ling, Grogan W, Gargano MM, et al. The primary microbial pathogens associated with premature rupture of the membranes in China: A systematic review. Taiwan J Obstet Gynecol 2014;53:443–51. https://doi.org/10.1016/j.tjog.2014.02.003.
12. Shane AL, Sánchez PJ, Stoll BJ. Neonatal sepsis. Lancet 2017;390:1770–80. https://doi.org/10.1016/S0140-6736(17)31002-4.
13. Boussamet L, Launay E, Thomas E, Leguen CG, Lepelletier D. Should central venous catheters be rapidly removed to treat Staphylococcus aureus related-catheter bloodstream infection (CR-BSI) in neonates and children? An 8-year period (2010–2017) retrospective analysis in a French University Hospital. J Hosp Infect 2019;103:97–100. https://doi.org/10.1016/j.jhin.2019.03.015.
14. Serane T, Kothendaraman B. Incidence and risk factors of infections associated with peripheral intravenous catheters. J Infect Prev 2015;17:115–20. https://doi.org/10.1177/1757177416631415.
15. Gordon A, Greenhalgh M, Mcguire W. Early planned removal versus expectant management of peripherally inserted central catheters to prevent infection in newborn infants. Cochrane Database Syst Rev 2018;2018. https://doi.org/10.1002/14651858.CD012141.pub2.
16. Paiva ED, Costa P, Kimura AF, de Castro TE. Reasons for non-elective removal of epicutaneous catheters in neonates. Rev Da Esc Enferm 2013;47:1279–84. https://doi.org/10.1590/S0080-623420130000600004.
17. Beard L, Levek C, Hwang S, Grover T. Prediction of Nonelective Central Venous Catheter Removal in Medically Complex Neonates. Pediatr Qual Saf 2019;4:e179. https://doi.org/10.1097/pq9.0000000000000179.
18. Chuang YY, Huang YC, Lee CY, Lin TY, Lien R, Chou YH. Methicillin-resistant Staphylococcus aureus bacteraemia in neonatal intensive care units: An analysis of 90 episodes. Acta Paediatr Int J Paediatr 2004;93:786–90. https://doi.org/10.1080/08035250410028084.

19. Hakim H, Mylotte JM, Faden H. Morbidity and mortality of Staphylococcal bacteremia in children. Am J Infect Control 2007;35:102–5. https://doi.org/10.1016/j.ajic.2006.09.016.
20. Murdoch F, Danial J, Morris AK, Czarniak E, Bishop JL, Glass E, et al. The Scottish enhanced Staphylococcus aureus bacteraemia surveillance programme: the first 18 months of data in children. J Hosp Infect 2017;97:127–32. https://doi.org/10.1016/j.jhin.2017.06.017.
21. Falup-Pecurariu O, Leibovitz E, Pascu C, Falup-Pecurariu C. Bacteremic methicillin-resistant Staphylococcus aureus deep neck abscess in a newborn-Case report and review of literature. Int J Pediatr Otorhinolaryngol 2009;73:1824–7. https://doi.org/10.1016/j.ijporl.2009.09.008.
22. Lewis PO, Heil EL, Covert KL, Cluck DB. Treatment strategies for persistent methicillin-resistant Staphylococcus aureus bacteraemia. J Clin Pharm Ther 2018;43:614–25. https://doi.org/10.1111/jcpt.12743.

Received: 10 February 2021
Accepted: 10 May 2021

CASE REPORTS / REPORTE DE CASO

Common Peroneal Nerve Injury in a Patient with COVID-19 Infection

Zeynab Bossaghzadeh[1], Firoozeh Niazvand[2*], Medi Saneie[3], Shahram Rahimi-Dehgolan[4], Hooshan Sahariati Ghadikolaei[5], Sara Mobarak[6]

DOI. 10.21931/RB/2021.06.03.26

Abstract: This report described a 46-year man with the characteristic Computerized Tomography (CT) scan findings of Corona Virus Disease Infection 19 (COVID-19) who presented to the hospital with right ankle weakness three weeks after the pneumonitis. He had been initially hospitalized, complaining of fever, myalgia, cough, and dyspnea. Electromyogram (EMG) revealed obvious evidence of increased insertional activity (IA) and significant denervation potentials, including positive sharp waves (PSW) and fibrillation potentials, particularly in ankle dorsiflexor muscles. Moreover, no voluntary motor unit action potential (MUAP) was observed. Eventually, the patient was diagnosed with severe axonal mononeuropathy of the right CPN, which could be considered a rare complication of COVID-19.

Key words: Nerve injury, Electromyography, Coronavirus, COVID-19.

Introduction

A new beta coronavirus named COVID-19 was detected in December 2019 in Wuhan City, China, and shortly became a pandemic[1]. COVID-19 is fused with the angiotensin-converting enzyme II (ACE-II) receptor and enters the cells[2]. This new coronavirus can cause several systemic infections, among which respiratory complications are the most prevalent, quite similar to what earlier happened in severe acute respiratory syndrome coronavirus called SARS-CoV[3].

It has been previously proved that around one-third of patients with COVID-19 had neurological symptoms. Although several specific neurological presentations such as anosmia, other non-specific ones, including reduced consciousness level, dizziness, and headache, have also been detected[4]. In one study, 214 patients with COVID-19 were evaluated in terms of neurological symptoms[5]. According to their findings, 36.4% of the hospitalized patients showed nervous system manifestations such as hyposmia, hypogeusia, headache, muscle injury, dizziness, ischemic, and hemorrhage stroke. However, it is still unknown whether the neurological symptoms are associated with the virus's direct damage, an abnormal immune response, or secondary mechanisms, including systemic inflammation or multi-organ dysfunction.

It has been hypothesized that SARS-CoV-2 can be considered as a new neuropathogen. However, it has not yet been proven by solid evidence[6]. Before COVID-19, it had been well-defined that infectious peripheral neuropathy could happen secondary to other viruses, including varicella-zoster, hepatitis C and human immunodeficiency virus (HIV)[7]. Similarly, during a viral infection, immune-mediated neuropathies such as chronic inflammatory demyelinating polyneuropathy (CIDP), as well as Guillain-Barre syndrome (GBS), might occur[8]. Also, an extended stay in the hospital can cause peripheral nerves.

Damage resulting from prolonged pressure effect or even critical illness polyneuropathy[9]. Recently, in some case reports, a potential relationship between peripheral nerve injury and the SARS-CoV-2 infection preceding the onset of damage by up to 4 weeks. Thus, the most probable reason would be a SARS-CoV2-triggered dysregulation of the immune system[10-12]. This case report described a male patient infected with COVID-19 who showed a common peroneal nerve (CPN) injury as a rare complication.

Case presentation

On 2 December, 2020, a 46-year-old man complained of inability to dorsiflex the right ankle from 3 weeks ago. The patient has referred to the emergency ward about 6 weeks ago under the probable diagnosis of COVID-19 and symptoms including fever, body aches, cough, and shortness of breath. During hospitalization, the polymerase chain reaction (PCR) and computerized chest tomography (CT) scan were performed and confirmed the diagnosis (Figure 1).

The patient had been admitted for 2 weeks resulting in 20 kg weight loss during this period. One week after the patient came back home, he noticed paresthesia on the right foot's dorsum and the sudden weakness of the right ankle dorsiflexion while walking and during the affected limb's swing phase.

He was referred to the clinic of physical medicine and rehabilitation (PM&R) to perform electromyography (EMG) and nerve conduction studies (NCS). As a result, sensory nerve action potential (SNAP) of the right superficial peroneal nerve (SPN) was not present, and the compound muscle action potential (CMAP) of the deep peroneal nerve (DPN) nerve was absent at the right side. In the EMG analysis, some evidence of increased insertional activity (IA) and denervation potentials, including PSW and fibrillation potentials, were detected in Tibialis Anterior (TA), Peroneus Longus (PL), Extensor Hallucis Longus (EHL), and Extensor Digitorum Brevis (EDB) muscles. Moreover, no voluntary motor unit action potential (MUAP) was observed in these muscles. Therefore, he was diagnosed with severe acute mono-neuropathy of the right CPN. Lumbosacral spine magnetic resonance imaging (MRI) was performed to assess discopathy, which was reported to be expected.

[1] Assistant professor of Physical Medicine, Rehabilitation and Electrodiagnosis Department, School of Medicine Abadan Faculty of Medical Sciences, Abadan, Iran.
[2] Assistant Professor of Anatomical Science, School of Medicine, Abadan Faculty of Medical Sciences, Abadan, Iran.
[3] Department of Orthopedics, School of Medicine, Abadan Faculty of Medical Sciences.
[4] PM&R Department, Tehran University of Medical Sciences, Tehran, Iran.
[5] Department of Neurosurgery, School of Medicine, Abadan Faculty of Medical Sciences, Abadan, Iran.
[6] Assistant Professor of Infectious Disease, School of Medicine, Abadan Faculty of Medical Sciences, Abadan, Iran.

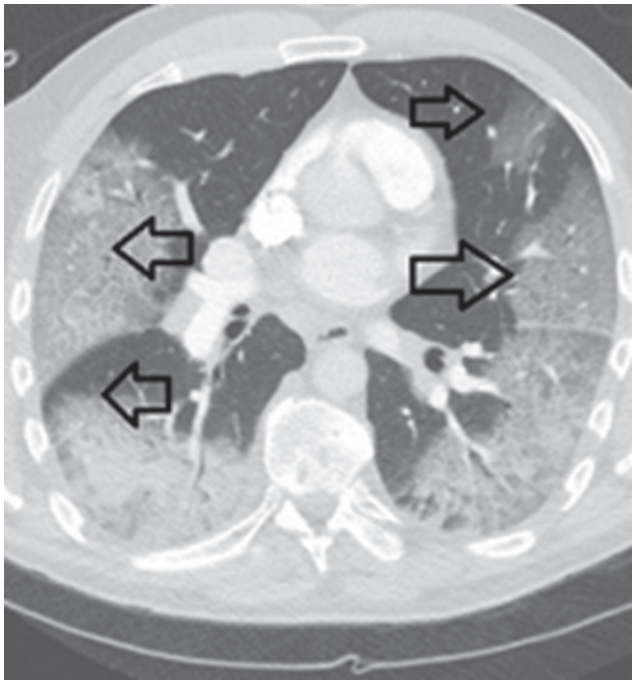

Figure 1. Findings of the CT scan of COVID-19 patient. Bilateral peripheral ground-glass opacities in a patient with cough and dyspnea.

Discussion

As we mentioned, as a post-infectious inflammatory response after SARS-CoV-2 infection, peripheral nerve injury can occur during the acute phase of resolution. This might be either the result of an abnormal hyper-immune response or treatment complications for COVID-19, such as nerve entrapment secondary to hematoma in the anticoagulation consumption setting or prolonged hospitalization that could be positional or critical illness-related polyneuropathy.

In the presented case, the patient was diagnosed with severe mononeuropathy of the right CPN after 3 weeks of developing symptoms such as fever, body aches, cough, and shortness of breath; compatible with COVID-19 pneumonia. The possibility of a direct neuropathic effect or an abnormal hyper-immune response in COVID-19 patients requires further research. There have been existed several case reports about GBS incidence among COVID-19 sufferers[10,13,16].

This case has been reported even though all neurological manifestations in severe COVID-19 are not fully understood yet; then, the peripheral neuropathic damage cannot be positively attributed to COVID-19 due to the lack of nerve biopsy. However, the EMG findings, along with the clinical neural image, indicated peripheral neuropathy. There are two main probabilities in this regard: 1) direct involvement of nerve by the virus and the following inflammatory response; 2) nerve compression after severe weight loss has also been reported in bariatric surgery and so on[17,18].

On the other hand, it has not clearly been understood how weight loss contributes to peroneal neuropathy. It is assumed that changes in metabolism followed by weight loss and mechanical compression of the peroneal nerve can play a significant role in this regard[17,21]. The adipose tissue depletion (inside and surrounding the nerve) results from weight loss; thus, the peroneal nerve's sensitivity to compression caused by the PL tendon on the lateral side and the adjacent fibular head medial side increases[22].

The ACE-II receptor is where COVID-19 and SARS have in common[19]. The receptor is found in the cell membrane of various organs in humans, such as the liver, kidney, lung, skeletal muscle, and nervous system[5]. However, the mechanisms involved in peripheral nerve injury incidence after COVID-19 infection have not yet been precisely studied. COVID-19 stimulates inflammatory cells, and different cytokines are generated, resulting in immune-mediated processes[19]. Therefore, peripheral nerve injury after SARS-CoV-2 infection is a theoretical consideration, and some COVID-19 patients have been reported to present with peripheral neuropathy and GBS[13,20]. Then, the cases of immune-mediated nerve injuries should be considered during this pandemic. According to the global pandemic of the SARS-COVID-1923-26, additional surveys should be conducted to find all epidemiological properties of disease[27].

Conclusions

To summarize, peripheral nerve injury should always be considered as a neurological complication that might occur in COVID-19. Probable post-infection peripheral nerve injury mechanisms include autoimmune response, direct neuro-invasion by the virus, and systemic disease complications. Further investigations are necessary to shed light on the exact pathophysiology of peripheral nerve involvement and high-risk patient determination. Given that, clinicians must be aware of these relationships to prevent delayed diagnosis from promoting treatment initiation at early stages and supportive care. This fact will be elucidated by further identified cases as well as longer time results.

Acknowledgments

The authors would like to thank the School of Medicine, Abadan Faculty of Medical Sciences, Abadan, Iran, for the clinical supports.

Author contributions

FN designed the study and carried out the case identification. ZB, MS, and SRD carried out the CT-Scan and PCR. HSG and SM carried out the history taking and electromyography. FN wrote and drafted the manuscript. All authors read and confirm the final manuscript.

Competing interests

The authors declared that they have no conflict of interest.

Data and materials availability

All data are available in the main text or supplementary materials.

Ethics statement

As noted on the journal's author guidelines page, the authors confirm that the journal's ethical policies have been adhered to. All identifying information of the patient presented in this study was kept secret.

Bibliographic references

1. Zhu N, Zhang D, Wang W. China Novel Coronavirus Investigating and Research Team. A novel coronavirus from patients with pneumonia in China, 2019 [published 24 January, 2020]. N Engl J Med.

2. Wan Y, Shang J, Graham R, Baric RS, Li F. Information: read & look at all below. 2020.
3. Zhou P, Lou YX, Wang X, Hu B, Zhang L, Zhang W. A pneumonia outbreak associated with a new coronavirus of probable bat origin. Nature [Internet]. 2020; 579 (7798): 270–3.
4. Zito A, Alfonsi E, Franciotta D, Todisco M, Gastaldi M, Cotta Ramusino M, et al. COVID-19 and Guillain-Barré Syndrome: A Case Report and Review of Literature. Front Neurol. 2020;11:909-.
5. Mao L, Jin H, Wang M, Hu Y, Chen S, He Q, et al. Neurologic manifestations of hospitalized patients with coronavirus disease 2019 in Wuhan, China. JAMA neurology. 2020;77:683-90.
6. Fernandez CE, Franz CK, Ko JH, Walter JM, Koralnik IJ, Ahlawat S, et al. Imaging Review of Peripheral Nerve Injuries in Patients with COVID-19. Radiology. 2020:203116.
7. Sindic CJ. Infectious neuropathies. Current opinion in neurology. 2013;26:510-5.
8. Katona I, Weis J. Diseases of the peripheral nerves. Handbook of clinical Neurology: Elsevier; 2018. p. 453-74.
9. Tsivgoulis G, Palaiodimou L, Katsanos AH, Caso V, Köhrmann M, Molina C, et al. <? covid19?> Neurological manifestations and implications of COVID-19 pandemic. Therapeutic Advances in Neurological Disorders. 2020;13:1756286420932036.
10. Toscano G, Palmerini F, Ravaglia S, Ruiz L, Invernizzi P, Cuzzoni MG, et al. Guillain–Barré syndrome associated with SARS-CoV-2. New England Journal of Medicine. 2020.
11. Bigaut K, Mallaret M, Baloglu S, Nemoz B, Morand P, Baicry F, et al. Guillain-Barré syndrome related to SARS-CoV-2 infection. Neurology-Neuroimmunology Neuroinflammation. 2020;7.
12. Farzi MA, Ayromlou H, Jahanbakhsh N, Bavil PH, Janzadeh A, Shayan FK. Guillain-Barré syndrome in a patient infected with SARS-CoV-2, a case report. Journal of neuroimmunology. 2020;346:577294.
13. Zhao H, Shen D, Zhou H, Liu J, Chen S. Guillain-Barré syndrome associated with SARS-CoV-2 infection: causality or coincidence? The Lancet Neurology. 2020;19:383-4.
14. Sedaghat Z, Karimi N. Guillain Barre syndrome associated with COVID-19 infection: a case report. Journal of Clinical Neuroscience. 2020.
15. Virani A, Rabold E, Hanson T, Haag A, Elrufay R, Cheema T, et al. Guillain-Barré syndrome associated with SARS-CoV-2 infection. IDCases. 2020:e00771.
16. Webb S, Wallace VC, Martin-Lopez D, Yogarajah M. Guillain-Barré syndrome following COVID-19: a newly emerging post-infectious complication. BMJ Case Reports CP. 2020;13:e236182.
17. Thaisetthawatkul P, Collazo-Clavell M, Sarr M, Norell J, Dyck PJB. A controlled study of peripheral neuropathy after bariatric surgery. Neurology. 2004;63:1462-70.
18. Clark N. Neuropathy following bariatric surgery. Seminars in neurology: © Thieme Medical Publishers; 2010. p. 433-5.
19. Huang C, Wang Y, Li X, Ren L, Zhao J, Hu Y, et al. Clinical features of patients infected with 2019 novel coronavirus in Wuhan, China. The lancet. 2020;395:497-506.
20. Abdelnour L, Abdalla ME, Babiker S. COVID 19 infection presenting as motor peripheral neuropathy. Journal of the Formosan Medical Association. 2020.
21. Sernik RA, Abicalaf CA, Pimentel BF, Braga-Baiak A, Braga L, Cerri GG. Ultrasound features of carpal tunnel syndrome: a prospective case-control study. Skeletal radiology. 2008;37:49-53.
22. Meylaerts L, Cardinaels E, Vandevenne J, Velghe B, Gelin G, Vanormelingen L, et al. Peroneal neuropathy after weight loss: a high-resolution ultrasonographic characterization of the common peroneal nerve. Skeletal radiology. 2011;40:1557-62.
23. Ranjbar R, Mahmoodzadeh Hosseini H, Safarpoor Dehkordi F. A Review on Biochemical and Immunological Biomarkers used for Laboratory Diagnosis of SARS-CoV-2 (COVID-19). The Open Microbiology Journal. 2020;14(1).
24. Mirzaie A, Halaji M, Dehkordi FS, Ranjbar R, Noorbazargan H. A narrative literature review on traditional medicine options for treatment of corona virus disease 2019 (COVID-19). Complementary Therapies in Clinical Practice. 2020:101214.
25. Halaji M, Farahani A, Ranjbar R, Heiat M, Dehkordi FS. Emerging coronaviruses: first SARS, second MERS and third SARS-CoV-2: epidemiological updates of COVID-19. Infez Med. 2020;28(suppl 1):6-17.
26. Sheikhshahrokh A, Ranjbar R, Saeidi E, Dehkordi FS, Heiat M, Ghasemi-Dehkordi P, Goodarzi H. Frontier therapeutics and vaccine strategies for sars-cov-2 (COVID-19): A review. Iranian Journal of Public Health. 2020;49:18-29.
27. Dehkordi FS, Valizadeh Y, Birgani TA, Dehkordi KG. Prevalence study of Brucella melitensis and Brucella abortus in cow's milk using dot enzyme linked immuno sorbent assay and duplex polymerase chain reaction. J Pure Appl Microbiol. 2014;8(2):1065-9.

Received: 20 April 2021
Accepted: 10 June 2021

CASE REPORTS / REPORTE DE CASO

Strongyloides stercoralis infestation in a pediatric patient

Ricardo Rubio-Sánchez[1], Esperanza Lepe-Balsalobre[2]
DOI. 10.21931/RB/2021.06.03.27

Abstract: Strongyloidiasis is a parasitic disease, very rare in countries like Spain, caused by the *Strongyloides stercoralis* nematode. We present a case of a 5-year-old patient from Ecuador who came to the Emergency Department due to fever, colicky abdominal pain, watery diarrhea, and occasional vomiting of several days of evolution. In laboratory studies, a marked leukocytosis with eosinophilia stands out, for which reason a microscopic study of the stool was carried out where larval forms compatible with *Strongyloides stercoralis* were observed. The diagnostic strategy of parasitic infection in developed countries is highly influenced by the low prevalence and diversity of the parasitic species, causing the diagnosis, on many occasions, to be a challenge. In the presence of eosinophilia and abdominal symptoms, it is recommended to orient the diagnosis towards a possible infection of parasitic origin to make an early diagnosis of the infection and avoid possible serious complications.

Key words: Diarrhea, eosinophilia, larva, microscopy, parasite, *Strongyloides stercoralis*.

Background

Strongyloidiasis is a parasitic disease caused by the *Strongyloides stercoralis* nematode that usually occurs asymptomatically but can manifest as a severe disseminated infection[1]. The necessary forms for the diagnosis of this parasitosis are the rhabditiform larvae present in the intestinal mucosa, characterized by a prominent esophageal bulb, and the filariform larvae present in the feces, which are the infecting forms, measuring about 600 µm in length and having elongated fusiform esophagus[1,2].

The biological cycle of *Strongyloides stercoralis* is unique and unusual since the females are parthenogenetic; that is, they can give rise to a progeny without being fertilized. Due to this, there can be two types of cycles, the free life cycle that occurs in the external environment without the need for a mammalian host and the parasitic cycle inside a mammalian host. The invasion of this parasite occurs by penetration through the skin of filariform larvae present in the soil or the water[3].

Figure 1. *Strongyloides stercoralis* larva in the stool.

Clinical case

A 5-year-old male patient from Ecuador with no relevant medical history came to the Emergency Department due to fever, colicky abdominal pain, watery diarrhea, and occasional vomiting of several days of evolution that intensified in the last two days. On physical examination, the abdomen was tender and painful on palpation, without masses or megaly, and increased peristalsis. The following complimentary tests were urgently requested: complete blood count, basic biochemistry with inflammatory markers (C-reactive protein), and urinary study. Laboratory results showed marked leukocytosis (24,000 leukocytes/µL) at the expense of 27% eosinophilia. The biochemistry and the study of the urinary sediment did not show alterations. Given the patient´s symptoms and origin, a microscopic study of parasites in feces was indicated, where larval forms compatible with *Strongyloides stercoralis* were observed (Figure 1).

Given this finding, treatment with oral ivermectin (200 mg/kg of body weight) was prescribed for two days, progressively decreasing diarrheal episodes and abdominal pain.

Discussion

The diagnosis of this disease is epidemiological, clinical, and laboratory, and it is based on the microscopic visualization of the larvae of *Strongyloides stercoralis* in feces but, except in cases of hyperinfestation, the elimination is usually scarce and sporadic; therefore, the sensitivity of standard concentration procedures is very low[4]. This, together with the fact that the diagnostic strategy of parasitic infection in countries such as Spain is highly influenced by the low prevalence and diversity of parasitic species, makes the diagnosis, on many occasions, a challenge[5,6].

Based on the above, many laboratories are replacing diagnostic methods based on conventional microscopy with enzyme immunoassay or molecular methods, which are techniques with higher sensitivity and specificity and less dependent on the observer. Thus, with more sensitive methods, work time is significantly reduced, and it is unnecessary to obtain the three classic fecal samples for parasitological examination. This approach would be similar to that already established for

[1] UGC de Análisis Clínicos, Hospital Universitario Virgen de Valme, Sevilla, España.
[2] Laboratorio de Análisis Clínicos, Hospital Universitario Virgen del Rocío, Sevilla, España.

Corresponding author: ricrubsan@gmail.com

detecting microorganisms that cause bacterial and viral diarrhea (molecular stool culture), giving an entirely new dimension to the differential laboratory diagnosis of diarrheal diseases[6,7].

Conclusions

Currently, there are initiatives to organize quality assessment schemes for the molecular diagnosis of intestinal parasites. However, these systems have not yet been widely adopted due to the high cost of traditional microscopy and the uncertainty regarding the clinical importance of the molecular detection of each of the parasites included in the panels. Therefore, its impact on clinical practice has yet to be assessed.

In short, in the presence of eosinophilia and abdominal symptoms, it is recommended to orient the diagnosis towards a possible infection of parasitic origin to make an early diagnosis of the infection and avoid possible serious complications.

Bibliographic references

1. Greaves D, Coggle S, Pollard C, Aliyu SH, Moore EM. Strongyloides stercoralis infection. BMJ 2013;347:f4610.
2. Buonfrate D, Gobbi F, Angheben A, Bisoffi Z. Strongyloides stercoralis: the need for accurate information. Lancet 2018;391:2322-23.
3. Morales ML, López M, Ly P, Anjum S, Fernández-Baca MV, Valdivia-Rodríguez AM, et at. Strongyloides stercoralis infection at different altitudes of the Cusco region in Peru. Am J Trop Med Hyg 2019;101:422-27.
4. Barroso M, Salvador F, Sánchez-Montalvá A, Bosch-Nicolau P, Molina I. Strongyloides stercoralis infection: A systematic review of endemic cases in Spain. PLoS Negl Trop Dis 2019;13:e0007230.
5. Meningher T, Boleslavsky D, Barshack I, Tabibian-Keissar H, Kohen R, Gur-Wahnon D, et al. Giardia lamblia miRNAs as a new diagnostic tool for human giardiasis. PLoS Negl Trop Dis. 2019;13(6): e0007398.
6. De Boer RF, Ott A, Kesztyus B, Kooistra-Smid AM. Improved detection of five major gastrointestinal pathogens by use of a molecular screening approach. Clin Microbiol. 2010; 48: 4140-6.
7. Verweij JJ, Stensvold CR. Molecular testing for clinical diagnosis and epidemiological investigations of intestinal parasitic infections. Clin Microbiol. 2014; 27: 371-418.

Received: 1 April 2021
Accepted: 10 June 2021

CASE REPORTS / REPORTE DE CASO

Reporte de caso de postcirugía de ligamento cruzado anterior

Case report of post-surgery anterior cruciate ligament surgery

Clara Gualotuña[1] y Thelvia I. Ramos[2]

DOI. 10.21931/RB/2021.06.03.28

Resumen: El ligamento cruzado anterior (LCA) es la lesión de la rodilla con mayor prevalencia en los atletas. Los avances en la técnica quirúrgica y la fijación de injertos han permitido a los pacientes participar en una rehabilitación funcional postoperatoria temprana. Este tratamiento está dirigido a lograr un mayor rango de movimiento, progresando hacia la movilización, fortalecimiento y control neuromuscular propioceptivo de la articulación. Existen varios protocolos de rehabilitación con variaciones en ejercicios específicos, progresión a través de fases y componentes claves que permiten la recuperación funcional. El objetivo final de la fisioterapia es devolver al paciente al nivel de rendimiento anterior a la lesión, incluidos el movimiento y la fuerza, sin dañar ni alargar el injerto. Presentamos el reporte de un caso con una lesión de LCA compleja, que recupero la funcionalidad de la articulación por aplicación de plan de tratamiento fisioterapéutico de forma inmediata a su intervención quirúrgica.

Palabras clave: Ligamento cruzado anterior, rehabilitación funcional, propiocepción, injerto, fuerza muscular y movimiento.

Abstract: An anterior cruciate ligament (ACL) is the most prevalent knee injury in athletes. Advances in surgical technique and graft fixation have allowed patients to participate in early postoperative functional rehabilitation. This treatment focuses on achieving a more excellent range of motion, progressing toward mobilization, strengthening, and proprioceptive neuromuscular control of the joint. Several rehabilitation protocols have variations in specific exercises, progression through phases, and critical components that allow functional recovery. The ultimate goal of physical therapy is to return the patient to the pre-injury level of performance, including motion and strength, without damaging or lengthening the graft. We present a case report of a patient with a complex ACL injury who recovered joint function by applying a physiotherapy treatment plan immediately after surgery.

Key words: Anterior cruciate ligament, functional rehabilitation, proprioception, grafting, muscle strength, and movement.

Introducción

La articulación de la rodilla es propensa a lesionarse debido a su complejidad y función de soporte de peso[1]. Está formado por la tibia, el fémur y la rótula, que están estabilizados por el ligamento colateral medial (LCM), el ligamento colateral lateral (LCL), el ligamento cruzado posterior (LCP) y el LCA[1]. Los meniscos medial y lateral actúan como amortiguadores, distribuyendo el peso uniformemente con cada paso o giro[1]. El LCA tiene una función importante en la estabilidad de la rodilla[2]. Esta estructura articular presenta dos porciones una antero medial y otra postero lateral, además sostiene el 90% del peso corporal[3]. Las fibras tendinosas del LCA tienen forma helicoidal dirigiéndose desde el área pre-espinal de la tibia hasta la superficie interna del cóndilo externo fémur[2]. Esté ligamento se considera la principal restricción pasiva de la traslación anterior de la tibia en el fémur[4,5] proporcionando estabilidad rotacional a la rodilla tanto en el plano frontal como en el transversal[1].

Las lesiones ligamentosas de la rodilla son frecuentes en las poblaciones jóvenes físicamente activas[3,5,6]. Se reporta una incidencia de estas lesiones de 1 por cada 3.000 personas en los Estados Unidos[7]. Solo en Norteamérica 250.000 personas sufren una ruptura de LCA cada año[6,8]. En un estudio de Li y colaboradores demostraron que la incidencia de lesiones por LCA ocurría de cuatro a cinco veces más entre los militares en referencia a la población general[9]. En un meta-análisis que reunió 25 estudios epidemiológicos encontraron una tasa de desgarro del LCA del 5% en mujeres que jugaban fútbol y baloncesto durante todo el año[10]. En esta investigación las mujeres tenían un riesgo tres veces mayor de desgarro del LCA que los hombres que practicaban el mismo deporte, reportándose un 42,3% cifra más alta reportada en la literatura para cualquier tipo de deporte[5,11].

Algunas actividades deportivas se han asociado a la ruptura de LCA ocasionados por la práctica de deportes profesionales como: baloncesto[12], fútbol[13] alpinismo[10], balonmano[14], fútbol americano[15], voleibol y lucha[16]. Estas lesiones tienen una mayor predisposición en los deportistas de fin semana, en el adulto mayor y en mujeres que presenta un valgo fisiológico[17].

Existen tres mecanismos principales de lesión del LCA: contacto directo, contacto indirecto y sin contacto[18]. Por contacto directo la lesión se ocasiona cuando una persona u objeto golpea directamente la rodilla; en el contacto indirecto la lesión aparece en las regiones no propias de la rodilla transfiriéndose una fuerza excesivas hacia la articulación y las lesiones sin contacto se producen cuando se aplica una fuerza de desaceleración o de cambio de dirección (pivote) sobre la rodilla[19]. Otros mecanismos asociados a LCA menos frecuentes son: los movimientos combinados de flexión de la articulación de la rodilla con valgo forzado, rotación medial excesiva de la espina tibial[20] y varo con rotación lateral[16].

En la evaluación clínica de una lesión por LCA los síntomas iniciales son: dolor intenso, crepitación, inflamación, tumefacción y pérdida de la movilidad[21]. La lesión en si suele provocar derrames articulares, alteraciones en la cinemática de la rodilla, afectaciones de la marcha, debilidad muscular y reducción del rendimiento funcional[6].También las personas afectadas manifiestan sensación de inestabilidad de las rodillas[22,6]. Otros autores fundamentan que existe ruptura de ligamento cruzado anterior en actividades de torsión-recorte-desaceleración aceleración en combinación con una carga en el valgo

[1] Sistema Integrado de Salud, Área de Fisioterapia Universidad de las Fuerzas Armadas ESPE, Sangolquí, Ecuador.
[2] Departamento Ciencias de la Vida y de la Agricultura, Universidad de las Fuerzas Armadas ESPE, Sangolquí, Ecuador.

Corresponding author: tiramos@espe.edu.ec

de rodilla[6,8]. Algunos pacientes manifiestan que escuchan o sienten un "estallido" en el momento de la lesión, acompañado en ocasiones de hemartrosis durante las dos primeras horas posteriores al daño[6].

En la exploración física se detecta la laxitud articular anteroposterior y antero externa, siendo las maniobras más importantes el test de subluxación excéntrica con un 98% de especificidad, considerada como la única prueba clínica y dinámica más específica para determinar la lesión de LCA[4,8,22]. Existen otras pruebas como el test de Lachman y la prueba de cajón anterior para determinar la ruptura del LCA[6], y para el diagnóstico definitivo se realiza exámenes de imagenología como la Resonancia Magnética Nuclear (RMN)[22,23].

El principal tratamiento para esta lesión es el quirúrgico dirigido a la reconstruir el LCA y considerando aspectos como: la edad, tipo de deporte que la ocasionó y el injerto, con el fin de evitar lesiones secundarias a la articulación[24]. Actualmente hay dos opciones para injertos del LCA: los autoinjertos y los aloinjertos[22]. El primero requiere la sustitución del LCA con tejido obtenido de otra parte del cuerpo[25], como cuando se utiliza un autoinjerto de tendones semitendinosos, cuádriceps y el gracilis[25]. El aloinjerto se obtiene a partir de donantes cadavéricos y tiene la ventaja de que no presenta morbilidad en el sitio donante, no es necesario tomar precauciones en el proceso de rehabilitación y presenta la misma fuerza que los autoinjertos[26]. Pero la curación del aloinjerto se retrasa con respecto a la incorporación y remodelación y puede transmitir enfermedades que no tienen la resistencia biomecánica de la intervención[27]. La literatura reciente sugiere el uso de autoinjertos biológicos, sobre todo en pacientes jóvenes, debido a su potencial para la remodelación, la curación del tendón al hueso[4].

Después de la cirugía de una lesión por LCA se requiere tratamiento fisioterapéutico que permita recuperar la funcionalidad de la articulación. En estas lesiones por lo general también se presentan secuelas clínicas a largo plazo asociados con desgarro del menisco medial, lesiones condrales y desarrollo de osteoartritis postraumática[6]. Otros factores a considerar es fallo articular, con subluxación femorotibial[28]. Aumento del grado de laxitud articular condicionando a un deterioro articular progresivo objetivable en los estudios radiográficos (aplanamiento del cóndilo, esclerosis subcondral, pinzamiento articular y formación de osteofitos)[29].

Es relevante presentar un programa de rehabilitación que se debe desarrollar en forma inmediata después de la cirugía del LCA, respetando todos los procesos fisiológicos de reparación de los tejidos afectados[30]. Los procedimientos fisioterapéuticos deben ir encaminados a restaurar la condición locomotora e identificar factores prexistente para prevenir futuras lesiones del LCA[31]. La locomoción normal depende, entre otros factores, de la estabilidad de la estructura ligamento capsular, el rango de movimiento de la articulación de la rodilla y un nivel de fuerza apropiado de los músculos así como de la propiocepción de esta articulación tan compleja[32]. El propósito en el programa de rehabilitación es restaurar la función completa sin restricciones y ayudar al paciente a regresar al 100% del nivel anterior a la lesión mientras logra excelentes resultados a largo plazo[33].

Presentamos un reporte de un paciente con una compleja ruptura del LCA, el cual tuvo una rehabilitación en el servicio de fisioterapia de la Universidad de las Fuerzas Armadas ESPE. Los resultados alcanzados son debidos a la combinación de técnicas de rehabilitación orientadas a una acelerada recuperación funcional, reflejada en el aumento de la movilidad articular y fuerza de los músculos extensores y flexores, así como de la restitución de la propiocepción de la rodilla y de todo el miembro inferior, permitiendo que pudiera incorporase a todas sus actividades de la vida diaria con normalidad.

Reporte de caso

Paciente de 33 años de edad, obrero, que tuvo un accidente en el año 2017 al levantar una puerta metálica, que traumatizó la cara anterior de la rodilla izquierda, presentando un dolor grado 4 en escala de EVA (Escala Visual Analógica) (Gonzales, Ana ;Ramos, Adriana; Rojas, 2018). El dolor persistió por 8 semanas y acudió a consulta médica de la empresa donde labora. El examen físico reveló un diagnóstico de sinovitis y hoffitis (inflamación de la grasa de la Hoffa)[35] y el tratamiento fue medicación con antiinflamatorios y 10 sesiones de fisioterapia, mejorando su sintomatología.

Dos años después, practicando fútbol (septiembre 2019) el paciente presenta nuevamente dolor en la cara anterior de la rodilla izquierda grado 5 en escala de EVA manifestando fatiga muscular durante el trote, limitando de manera parcial la funcionalidad biomecánica de la marcha. Al finalizar ese mismo año tiene un segundo accidente de trabajo armando una columna de 11 cajas plásticas con un peso de 1,5 kg, por cada caja. Un compañero provoca una colisión de una columna conformadas por 11 cajas que se impactaron sobre el cuerpo del paciente. Realiza una flexión de hombros con extensión de codos y muñeca quedando la cara palmar apoyada en las cajas y al mismo tiempo efectuó una flexión de cadera y rodilla derecha simultáneamente sobre la estructura para soportar el peso de 126 kg, el miembro inferior izquierdo se mantuvo apoyado en el piso provocando un movimiento de desplazamiento medial.

Inmediatamente inicio un dolor agudo intenso en la rodilla con un grado 8 en la escala de EVA, con limitación funcional al caminar e inestabilidad de la rodilla. Es valorado por el médico de la empresa quien diagnóstica una lesión de LCA e indica un tratamiento con antinflamatorios y reposo. El dolor persiste sin alivio durante un mes y es evaluado por fisioterapia, aplicándose la prueba de cajón anterior y la prueba de Lachman, siendo ambas positivas, remitiéndose a evaluación por traumatología[3,4].

El diagnóstico por el especialista se apoyó en la valoración clínica y una RMN de rodilla que reveló cambios en la intensidad del ligamento cruzado anterior, signos de ruptura intrasustancial 50%, desgarro a nivel de la base del menisco lateral y cambios de la intensidad de señal a nivel de cartílago articular y el tejido óseo subcondral hacia el borde lateral de la meseta tibial, edema óseo a este nivel e incremento de líquido articular (ver figura1. 2, 3 y 4).

Se practica la cirugía reparadora con la técnica de intervención hueso tendón hueso (HTH) cirugías más autoinjerto por representar un menor riesgo por la edad del paciente y la actividad laboral[4,25]. El autoinjerto fue extraído del tendón del músculo semitendinoso de la rodilla teniendo éxito la cirugía[36]. Este tipo de cirugía realizada permitió comenzar la fisioterapia de forma precoz, evitando la debilidad de la musculatura de los isquiotibiales, perdida de arcos de movimiento y perdida de la propiocepción, como describe la literatura[5].

Tratamiento fisioterapéutico

La rehabilitación estuvo dirigida a recuperar el rango de movimiento articular, la fuerza de los músculos flexores y extensores de la articulación de la rodilla (sartorio, gráciles, semitendinoso, semimembranoso, bíceps femoral, gastrocnemio

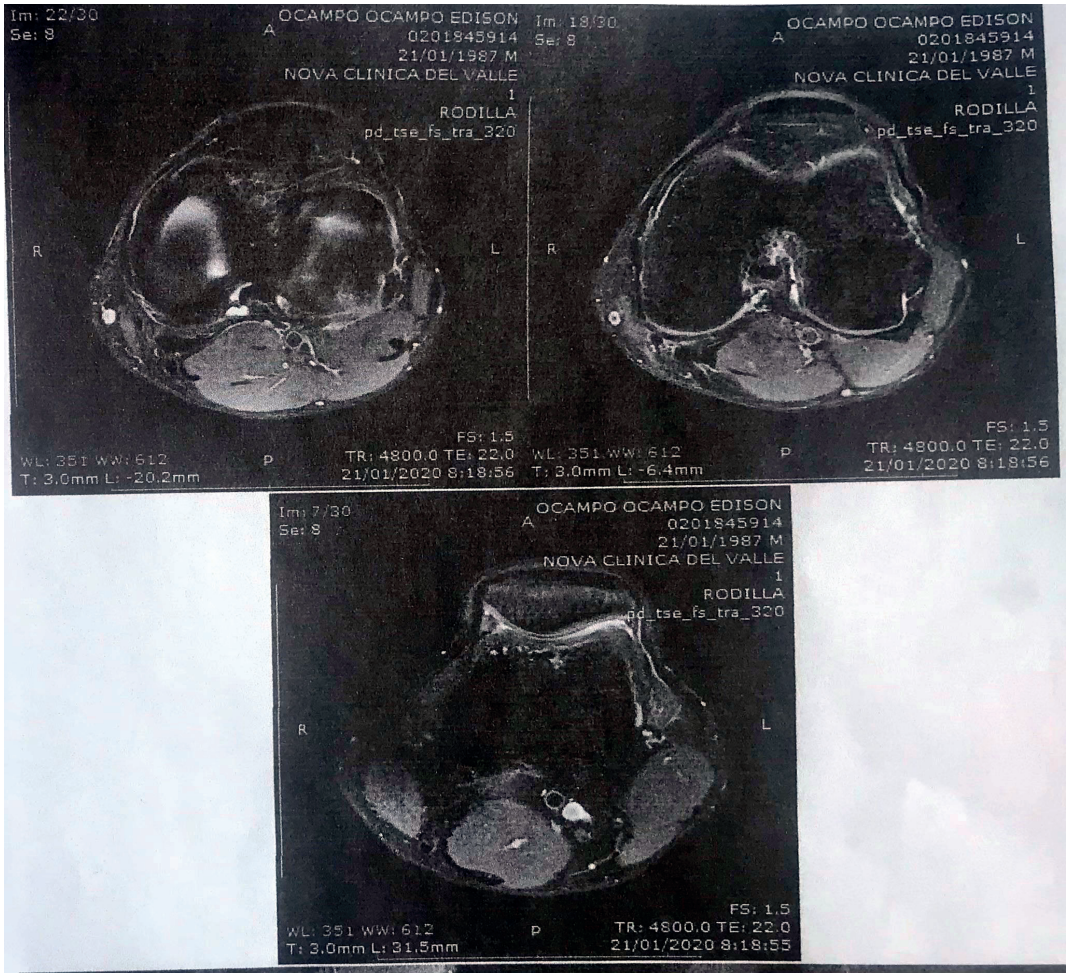

Figura 1. Corte sagital de resonancia magnética (RM), en T2 se puede visualizar que existe un proceso inflamatorio a la altura del ligamento cruzado anterior.

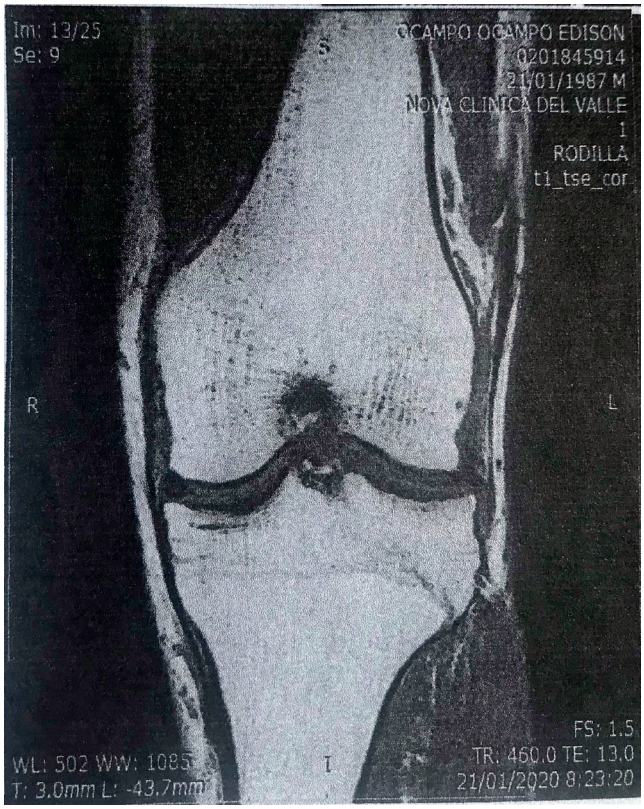

Figura 2. Corte coronal de RM potenciado de T1 se observa proceso inflamatorio.

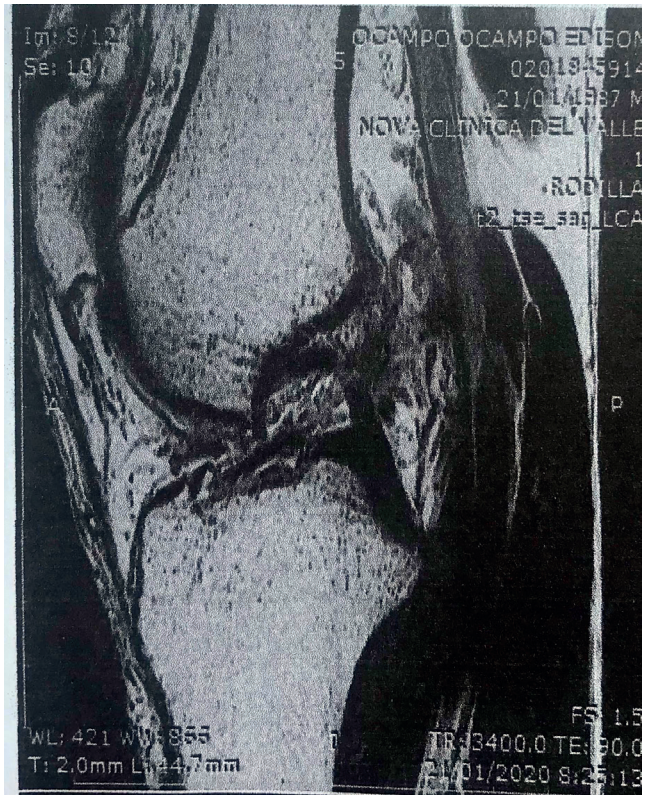

Figura 3. Corte sagital de resonancia magnética (RM) potenciado de T1 se puede visualizar que existe un proceso inflamatorio a la altura del ligamento cruzado anterior.

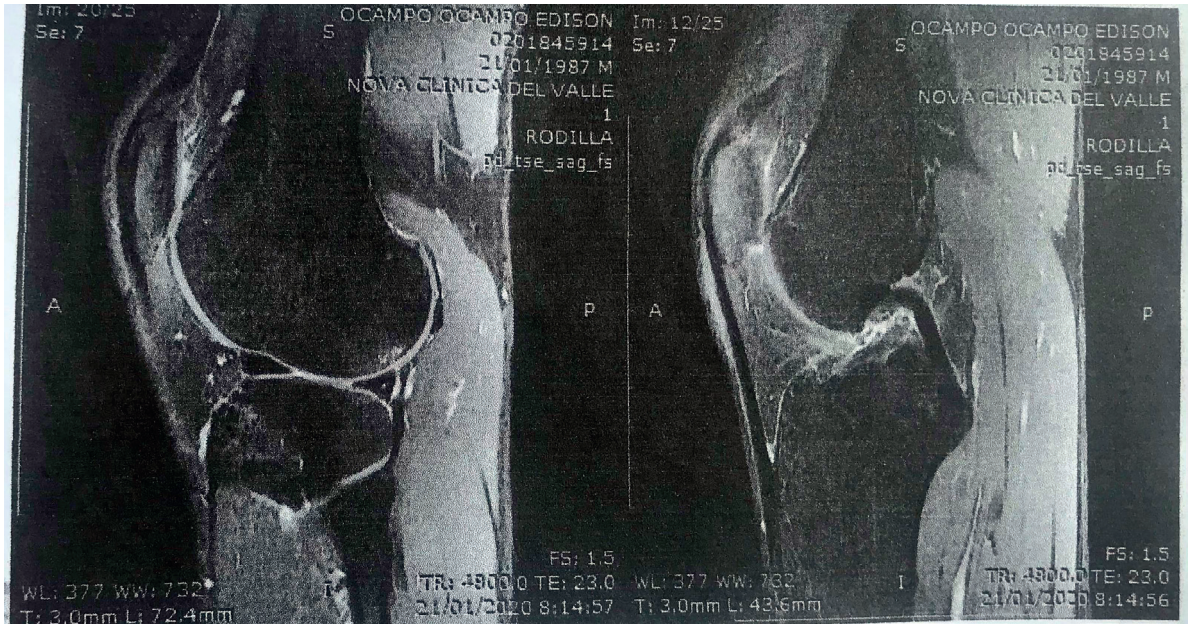

Figura 4. Corte sagital de RM potenciado en T1 se observa un leve incremento líquido articular, y proceso inicial de esclerosis. A nivel de la meseta tibial lesiones osteocondrales borde lateral y a nivel del cóndilo femoral lateral.

y el cuádriceps) tanto en condiciones estáticas como la dinámica articular, recuperar la amplitud y la propiocepción para lograr una adecuada funcionabilidad de la rodilla[23].

Se consideró además la selección de los ejercicios, la magnitud y el tiempo de aplicación de la carga, el proceso gradual de angiogénesis del autoinjerto en el nuevo ligamento[5]. Los procedimientos fisioterapéuticos se establecieron en diferentes etapas apoyados en los datos clínicos.

Diagnóstico fisioterapéutico

Postcirugía de ligamento cruzado anterior, con dolor en la cara posterior de los isquiotibiales, y cara anterior. Puntos de gatillo en el músculo tensor de la fascia lata y semitendinoso.

Sintomatología Clínica

El paciente acude con los puntos de sutura y presenta una marcha claudicante, apoyado con muletas. Presenta inflamación en todo el contorno de la rodilla, derrame en absorción en la parte anterior, equimosis en la parte posterior, piel brillante tersa, temperatura normal, atrofia de la masa muscular. Manifiesta dolor al flexionar la rodilla a partir de los 60 grados y al caminar en terreno irregular, en la cara anterolateral interna de la rodilla grado 5 de EVA y en la cara postero externa del muslo grado 7 de EVA, lugar de donde se extrajo el tendón para el autoinjerto.

Examen físico

Dolor a la palpación en la cara posterior un grado 8 en escala de EVA. Sensibilidad superficial alterada en la parte anterior de la rodilla (en la intervención quirúrgica). Sensibilidad profunda normal. Puntos de gatillo en el musculo semitendinoso y tensor de la fascia lata.

Valoración funcional

Goniometría

Rodilla	Izquierda	Derecha
Flexión	45	120
Extensión	0	0

Plan de tratamiento de rehabilitación consta de cuatro fases

Primera fase inflamatoria de 1 a 2 semanas

En esta fase se realizará el control del dolor e inflamación. Se aplicaron compresas frías a nivel local en la parte anterior de la rodilla durante la primera semana. Se emplearon bolsas de hielo, reemplazadas con crioterapia local. Se indican movimientos pasivos continuos[20]. Estimulación con electroestimulación percutánea (o transcutánea) de los nervios en la cara anterior de la rodilla, cuádriceps y en los músculos isquiotibiales del muslo. Utilizamos ultrasonido en la cara anterior de la rodilla con 1 w/cm2, al 20 % y 1 hz para obtener un efecto mecánico y alineamiento de las fibras de colágeno, evitando la formación de adherencias en el sitio de intervención quirúrgica. Ejercicios de activación muscular mediante movilidad activa asistida de la rodilla y ejercicios de fortalecimiento del otro miembro inferior. Se recurrió a la técnica Kinesio Tape (KT) o vendaje neuromuscular sobre los músculos isquiotibiales para mejorar la oxigenación y aporte de nutrientes disminuyendo de esta forma el dolor y acelerando el proceso de cicatrización, el uso del vendaje también se puede utilizar como estabilizador de la rodilla después de la poscirugía de LCA.

Segunda fase proliferativa de 3 a 6 semanas

En esta fase es importante realizar la movilidad y carga progresiva, por tal motivo se realizara movilización de la rótula en sentido céfalo caudal, transversal y oblicuo, electroestimulación para fortalecimiento del vasto medial[37]. Ejercicios de fortalecimiento progresivo de flexión y extensión de la rodilla con aumento gradual del rango de movimiento, en posición supina y con deslizamiento del talón sobre la camilla[38]. Se practicó al paciente técnicas de inducción miofascial, como: la técnica longitudinal y transversal para los isquiotibiales y para los cuádriceps.

Tercera fase de remodelación de 7 a 12 semanas

En esta fase se inicia el programa de entrenamiento de fuerza, coordinación y propiocepción en combinación con ejercicios en cadena cinemática cerrada en terreno plano, con ojos

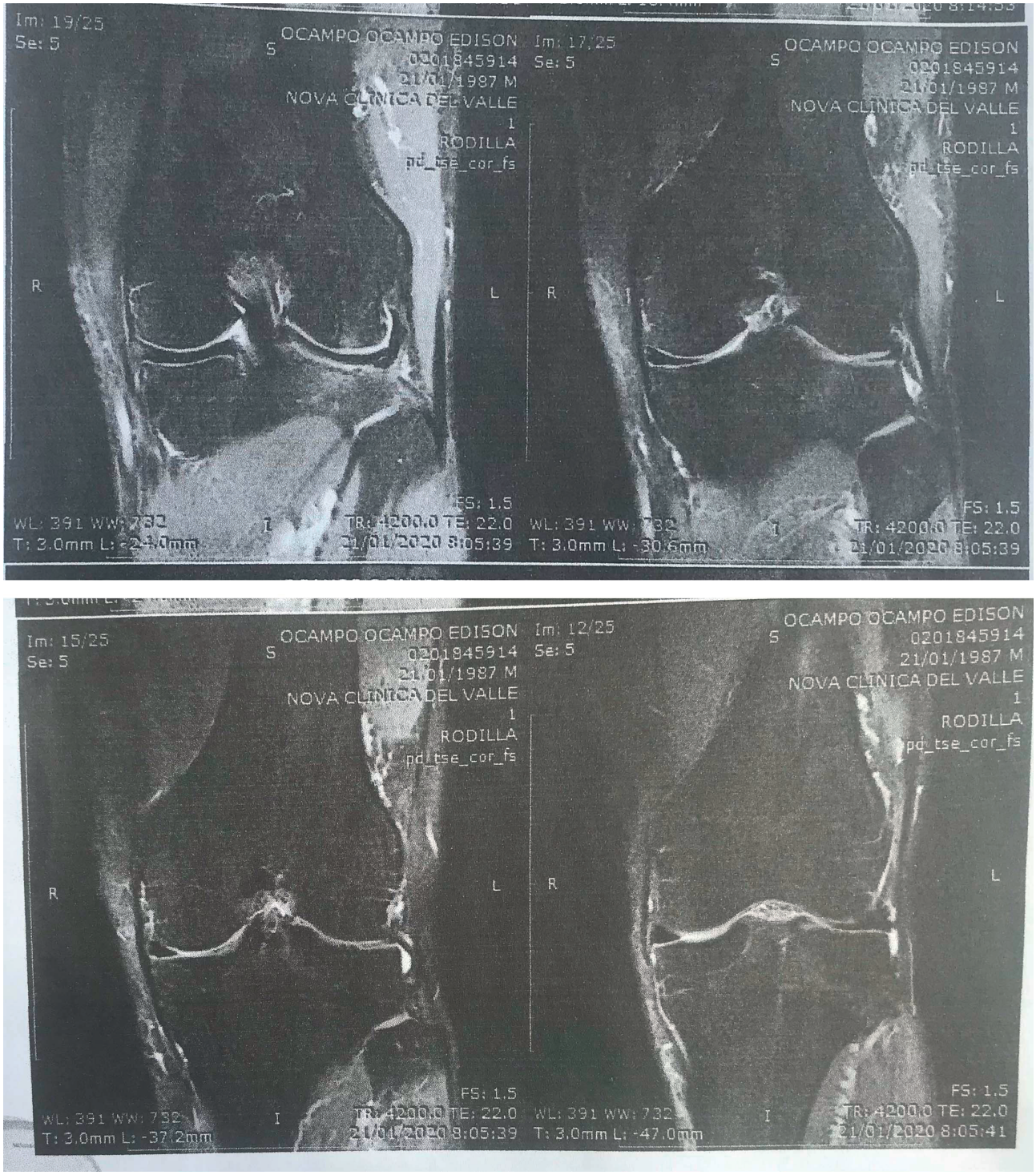

Figura 5. Corte coronal potenciado a T2, se visualiza ruptura intrasustancial de ligamento cruzado anterior aproximadamente un 50%, presencia de líquido inflamatorio.

abiertos y posteriormente con inhibición de ojos, pero en terreno plano. Es necesario trabajar ejercicios excéntricos, aeróbicos, equilibrio y control postural[39].

Se realizaron ejercicios del puente (paciente en posición supina con rodillas flexionadas y las plantas de los pies apoyadas en balancín.

Se efectuaron ejercicios de subir y bajar un solo escalón y sentadillas logrando aumentar gradualmente la fuerza de los músculos isquiotibiales y cuádriceps de la pierna operada en el plano sagital[20].

Fase final de 13 a 15 semanas

Dirigida a la recuperación total de la coordinación, fuerza y gestos deportivos, para lo cual se trabaja a nivel muscular mediante la técnica de facilitación neuromuscular para los miembros inferiores partiendo de extensión, abducción y rotación interna de cadera retornando con flexión, aducción y rotación externa de cadera con flexión de rodilla, también se ejecutó ejercicios de propiocepción con inhibición de ojos y en área inestable utilizando elementos externos de perturbación como ligas y balón medicinal.. Para finalizar está fase se aplicó ejercicios polimétricos, trote con desplazamientos en diferen-

tes direcciones y por último se practicó diferentes gestos deportivos (fútbol).

Discusión

El objetivo de la reconstrucción del LCA es restaurar las propiedades anatómicas y biomecánicas de este ligamento[40]. Algunos autores mencionan que para este tipo de lesión es necesario mantener la estabilidad de la articulación de la rodilla anteroposterior, anteromedial y recuperar la cinemática de la articulación[41].

La rehabilitación rigurosa después de la reconstrucción del ligamento cruzado anterior (LCA) es necesaria para un resultado quirúrgico exitoso[33], el fortalecimiento muscular acelerado[42], la rehabilitación en el hogar[43], la propiocepción con entrenamiento neuromuscular[37], pero sin excluir el rango de movimiento y los ejercicios funcionales[44]. Otro autor menciona que es importante recuperar la locomoción normal, entre otros factores, la estabilidad de la estructura ligamento capsular, el rango de movimiento y un nivel de fuerza apropiado de los músculos de la articulación de la rodilla y la propiocepción[45]. En nuestro trabajo consideramos la importancia de recuperar la estabilidad de la rodilla en conjunto con la fuerza, el arco de movimiento, la propiocepción y con el fin de integrarlo a la actividad laboral o deportiva.

La terapia de crio compresión se ha propuesto como un método para reducir el dolor y la respuesta inflamatoria en el período postoperatorio temprano después de la cirugía de reconstrucción de la articulación[46]. Otro estudio menciona que la aplicación de compresas frías sobre la lesión disminuye el dolor[32]. De acuerdo con la práctica cuando se aplicó las compresas químicas frías en la etapa inicial de la poscirugía de LCA, se determinó la disminución considerable del dolor y la inflamación permitiendo mejores rangos de movimientos con lo cual se confirma lo mencionado por Nabiyev V. N. y colaboradores (2018)[47].

La incorporación de estrategias efectivas para aliviar el dolor durante la rehabilitación de la cirugía de RLCA conduce a una mejor condición en la recuperación del rango de movimiento y la función de la rodilla. Al aplicar electroestimulación transcutánea se ocasiona una inhibición pre-sináptica con disminución del dolor, en combinación con ejercicios controlados en las cuatro primeras semanas que permitieron resultados positivos en la recuperación. Esto se corrobora también con el estudio de Forogh y colaboradores que aplica electroestimulación transcutánea sobre 70 deportistas en combinación con ejercicios controlados reportando disminución de los niveles de dolor en todos los individuos del estudio[48]. En otro estudio la utilización de electroestimulación transcutáneo manifiesta que sus efectos son relativos, obteniendo mejores resultados a nivel de cuádriceps con la aplicación de electroestimulación eléctrica funcional a partir de la cuarta semana[49].

El uso de KT tiene un efecto positivo sobre la propiocepción en pacientes con rotura del LCA. Por lo tanto, la aplicación puede mejorar el patrón de la marcha, así como la función subjetiva de la articulación de la rodilla afectada[50]. Liu menciona que el KT puede tener efectos beneficiosos sobre la propiocepción, el equilibrio y el rendimiento funcional en personas con ruptura LCA, pero no puede compensar por completo la pérdida de propiocepción[51]. En la práctica actual se aplicó el KT para disminuir la contractura que presentaban los músculos isquiotibiales y también se utilizó en la fase final del programa de fisioterapia como técnica para estabilizar la rodilla, solo durante la primera semana cuando retorno a la actividad laboral y deportiva, es decir, que el KT se puede utilizar como medio de apoyo temporal para estimular la propiocepción pero no como tratamiento permanente.

Se debe lograr la extensión completa de rodilla sobre las dos primeras semanas de rehabilitación y para esto se requieren técnicas de estiramiento de larga duración con poca carga[52]. La literatura científica indica la importancia de la marcha con extensión completa de la rodilla, para obtener una buena funcionabilidad de la articulación[44]. En la experiencia profesional es importante alcanzar durante las primeras semanas la extensión completa de la rodilla con el fin de recuperar la biomecánica funcional en forma correcta después de la postcirugía de LCA. Aplicando al paciente la rehabilitación con ejercicios selectivos, se obtiene la extensión completa de rodilla en el periodo inicial del tratamiento acompañado con movilización de la articulación patelofemoral el cual permite ganar rangos de movimiento durante el programa de fisioterapia establecida. La aplicación de masaje en la banda iliotibial y de la parte lateral del cuádriceps ayuda a mejorar la movilidad articular, con lo cual aumentan los arcos de movilidad y disminuyen las contracturas mejorando el proceso de oxigenación y aportes de nutrientes para obtener el proceso de cicatrización de manera óptima[32]. También contribuye la movilización de rotula con movimientos fisiológicos durante la primera semana y el masaje profundo en el muslo, para mejorar los rangos de movimientos y la irrigación sanguínea a nivel de la rodilla.

La rehabilitación acelerada y bien programada no ha mostrado efectos perjudiciales, iniciando con activación de cuádriceps mediante ejercicios isométricos, posteriormente ejercicios con carga progresiva, luego utilizando el propio peso, ejercicios de cadena cinética abierta y cerrada[53]. En la fase inicial de rehabilitación es seguro para los pacientes empezar inmediatamente después del postoperatorio con ejercicios isométricos, conforme va mejorando se incrementa en forma progresiva el peso para el fortalecimiento de los músculos que intervienen en la función de la rodilla, es necesario trabajar ejercicios de cadena cinética cerrada y abierta para ganar fuerza tanto en los músculos proximales y distales de miembros inferiores los mismos que se requieren para una buena reeducación de la marcha.

Cimino y colaboradores (2010) explican que al realizar el entrenamiento neuromuscular propioceptivo mejora la respuesta refleja de la articulación y la reacción voluntaria de los músculos que tiende a ser rápida para contrarrestar las fuerzas que actúan sobre la rodilla[1]. En otro estudio de Basar y colaboradores determina que el mecanismo propioceptivo de la rodilla da información sobre la posición y el movimiento de las articulaciones evitando de esa manera una segunda lesión de LCA[54]. Es necesario trabajar en la fase final de la fisioterapia el programa de entrenamiento neuromuscular propioceptivo para un aprendizaje motor mediante la utilización de movimientos de perturbación en combinación con acciones visomotoras en lesión de LCA[55]. Al aplicar el programa de propiocepción en el paciente con lesión de LCA se pudo observar un cambio importante en la funcionalidad estabilidad con mejor coordinación en las reacciones motoras y articulares de la rodilla, permitiendo integrar al paciente de forma óptima en la actividad deportiva y laboral. El trabajo de entrenamiento muscular propioceptivo permite constituir los factores sensoriales, visuales y motores con el fin de minimizar los riesgos acelerados de secuelas y reduciendo el riesgo de una segunda lesión de LCA.

En la fase final de la rehabilitación se deben realizar pruebas de salto después de completar los seis meses de tratamiento para el retorno a la actividad deportiva[52]. Otro estudio

menciona que todos los atletas a menudo son autorizados para regresar a las actividades cuando pueden realizar saltos en un solo pie sin dolor (periodo 6 meses) después de la reconstrucción del LCA[56]. Actualmente para autorizar el retorno a la actividad deportiva se ejecutó los ejercicios de saltos con los dos pies y con un pie es decir ejercicios polimétricos de baja y alta intensidad, también es importante que pueda correr y subir escaleras sin molestias para el retorno de la actividad laboral y deportiva.

Conclusiones

Los estudios presentados en este documento se centraron en mejorar la rehabilitación después de la reconstrucción del LCA, con el objetivo de retornar en forma segura con una fuerza muscular óptima para darle mayor estabilidad a la rodilla y evitar la aparición acelerada de la osteotritis con el fin de evitar limitaciones en la vida diaria.

Un programa de rehabilitación tradicional después de la cirugía es eficaz para mejorar la fuerza muscular de los músculos flexores de la rodilla. Esta intervención temprana puede incorporarse a la rehabilitación actual para facilitar la recuperación rápida de la fuerza en los pacientes con ruptura de LCA.

Referencias bibliográficas

1. Cimino, F., Naval Hospital, U., Bradford Scott Volk, J. & Setter, D. Anterior Cruciate Ligament Injury: Diagnosis, Management, and Prevention. American Family Physician vol. 82 (2010).
2. Amis, A. A. The functions of the fibre bundles of the anterior cruciate ligament in anterior drawer, rotational laxity and the pivot shift. Knee Surgery, Sports Traumatology, Arthroscopy vol. 20 613–620 (2012).
3. Seco, J. Afecciones medicoquirurgicas para fisioterapia. in 297,298,299,300,301 (2017).
4. Biz, C., Cigolotti, A., Zonta, F., Belluzzi, E. & Ruggieri, P. ACL reconstruction using a bone patellar tendon bone (BPTB) allograft or a hamstring tendon autograft (GST): A single-center comparative study. Acta Biomed. 90, 109–117 (2019).
5. Krause, M. et al. Operative versus conservative treatment of anterior cruciate ligament rupture a systematic review of functional improvement in adults. Dtsch. Arztebl. Int. 115, 855–862 (2018).
6. Filbay, S. R. & Grindem, H. Evidence-based recommendations for the management of anterior cruciate ligament (ACL) rupture. Best Practice and Research: Clinical Rheumatology vol. 33 33–47 (2019).
7. Herzog, M. M. et al. Trends in Incidence of ACL Reconstruction and Concomitant Procedures Among Commercially Insured Individuals in the United States, 2002-2014. Sports Health 10, 523–531 (2018).
8. Ayala,J; Gracia ,G;Alcocer, L. Lesión de ligamneto cruzado anterior. Acta Ortopédica Mexicana 1,21 (2014).
9. Li, W. et al. Biomechanical Evaluation of Preoperative Rehabilitation in Patients of Anterior Cruciate Ligament Injury. Orthop. Surg. 12, 421 (2020).
10. Westin, M., Harringe, M. L., Engström, B., Alricsson, M. & Werner, S. Risk Factors for Anterior Cruciate Ligament Injury in Competitive Adolescent Alpine Skiers. Orthop. J. Sport. Med. 6, (2018).
11. Anderson, M. J., Browning, W. M., Urband, C. E., Kluczynski, M. A. & Bisson, L. J. A Systematic Summary of Systematic Reviews on the Topic of the Anterior Cruciate Ligament. Orthop. J. Sport. Med. 4, 1–23 (2016).
12. Okoroha, K. R. et al. Amount of minutes played does not contribute to anterior cruciate ligament injury in national basketball association athletes. Orthopedics 40, e658–e662 (2017).
13. Bisciotti, G. N. et al. Anterior cruciate ligament injury risk factors in football. Journal of Sports Medicine and Physical Fitness vol. 59 1724–1738 (2019).
14. Koga, H. et al. Mechanisms for noncontact anterior cruciate ligament injuries: Knee joint kinematics in 10 injury situations from female team handball and basketball. Am. J. Sports Med. 38, 2218–2225 (2010).
15. Niederer, D., Engeroff, T., Wilke, J., Vogt, L. & Banzer, W. Return to play, performance, and career duration after anterior cruciate ligament rupture: A case–control study in the five biggest football nations in Europe. Scand. J. Med. Sci. Sport. 28, 2226–2233 (2018).
16. Garin, D. R. E. A. Lesión de ligamneto cruzado anterior. Medigraphic 88,89,90,91,92,93,94,95 (2016).
17. Waldén, M., Hägglund, M., Magnusson, H. & Ekstrand, J. Anterior cruciate ligament injury in elite football: A prospective three-cohort study. Knee Surgery, Sport. Traumatol. Arthrosc. 19, 11–19 (2011).
18. Tood, Benjamí; Nacleiro, Emily;Seth, S. Management of Anterior Cruciate Ligament Injury. Oliver J Edited by Araujo K 1,2,3 (2017).
19. Padua, D. A. et al. National athletic trainers' association position statement: Prevention of anterior cruciate ligament injury. J. Athl. Train. 53, 5–19 (2018).
20. Czamara, A. & Królikowska, A. Two-plane assessment of knee muscles isometric and isokinetic torques after anterior cruciate ligament reconstruction. Med. Sci. Monit. 24, 4882–4893 (2018).
21. Huang, W., Zhang, Y., Yao, Z. & Ma, L. Clinical examination of anterior cruciate ligament rupture: A systematic review and meta-analysis. Acta Orthop. Traumatol. Turc. 50, 22–31 (2016).
22. Hughes, J. D., Rauer, T., Gibbs, C. M. & Musahl, V. Diagnosis and treatment of rotatory knee instability. Journal of Experimental Orthopaedics vol. 6 (2019).
23. Zicaro, J. P., Garcia, I., Yacuzzi, C. & Costa, M. Reparación del Ligamento Cruzado Anterior con Utilización de Tutor Interno : Técnica Quirúrgica y Revisión de la Literatura. vol. 26 56–62 (2019).
24. Seco, J. Fisioterapia en especialidades clínicas. in Panamericana 247,248 (2016).
25. Cristiani, R., Engström, B., Edman, G., Forssblad, M. & Stålman, A. Revision anterior cruciate ligament reconstruction restores knee laxity but shows inferior functional knee outcome compared with primary reconstruction. Knee Surgery, Sport. Traumatol. Arthrosc. 27, 137–145 (2019).
26. Shumborski, S. et al. Allograft Donor Characteristics Significantly Influence Graft Rupture After Anterior Cruciate Ligament Reconstruction in a Young Active Population. Am. J. Sports Med. 48, 2401–2407 (2020).
27. Yang, X. gang et al. Network meta-analysis of knee outcomes following anterior cruciate ligament reconstruction with various types of tendon grafts. International Orthopaedics vol. 44 365–380 (2020).
28. Webster, K. E., Feller, J. A., Kimp, A. J. & Whitehead, T. S. Revision Anterior Cruciate Ligament Reconstruction Outcomes in Younger Patients: Medial Meniscal Pathology and High Rates of Return to Sport Are Associated With Third ACL Injuries. Am. J. Sports Med. 46, 1137–1142 (2018).
29. Shelbourne, K. D., Benner, R. W. & Gray, T. Results of Anterior Cruciate Ligament Reconstruction with Patellar Tendon Autografts: Objective Factors Associated with the Development of Osteoarthritis at 20 to 33 Years after Surgery. Am. J. Sports Med. 45, 2730–2738 (2017).
30. Piussi, R. et al. Recovery of preoperative absolute knee extension and flexion strength after ACL reconstruction. BMC Sports Sci. Med. Rehabil. 12, (2020).
31. Cristiani, R. et al. Increased knee laxity with hamstring tendon autograft compared to patellar tendon autograft: a cohort study of 5462 patients with primary anterior cruciate ligament reconstruction. Knee Surgery, Sport. Traumatol. Arthrosc. 27, 381–388 (2019).

32. Andrzej Czamara, Def, W. T. & Cde, T. B. The effect of physiotherapy on knee joint extensor and flexor muscle strength after anterior cruciate ligament reconstruction using hamstring tendon. 17, 33–41 (2011).
33. Wilk, K. E. & Arrigo, C. A. Rehabilitation Principles of the Anterior Cruciate Ligament Reconstructed Knee: Twelve Steps for Successful Progression and Return to Play. Clinics in Sports Medicine vol. 36 189–232 (2017).
34. Gonzales, Ana;Ramos, Adriana;Rojas, E. Correlación entre las escalas unidimensionales utilizadas en la medición del dolor postoperatoriole. Revista Mexicana de Anestesiología 8 (2018).
35. Felson, D. T. et al. Synovitis and the risk of knee osteoarthritis: The MOST Study. Osteoarthr. Cartil. 24, 458–464 (2016).
36. Zhao, L. et al. Outcome of bone-patellar tendon-bone vs hamstring tendon autograft for anterior cruciate ligament reconstruction: A meta-analysis of randomized controlled trials with a 5-year minimum follow-up. Medicine (Baltimore). 99, e23476 (2020).
37. Buckthorpe, M., La Rosa, G. & Villa, F. Della. RESTORING KNEE EXTENSOR STRENGTH AFTER ANTERIOR CRUCIATE LIGAMENT RECONSTRUCTION: A CLINICAL COMMENTARY. Int. J. Sports Phys. Ther. 14, 159–172 (2019).
38. Fukuda, T. Y. et al. Open kinetic chain exercises in a restricted range of motion after anterior cruciate ligament reconstruction: A randomized controlled clinical trial. Am. J. Sports Med. 41, 788–794 (2013).
39. Capin, J. J. & Snyder-Mackler, L. The current management of patients with patellofemoral pain from the physical therapist's perspective. Ann. Jt. 3, 40–40 (2018).
40. Zampeli, F. et al. Restoring tibiofemoral alignment during ACL reconstruction results in better knee biomechanics. Knee Surgery, Sport. Traumatol. Arthrosc. 26, 1367–1374 (2018).
41. Fu, F. H., van Eck, C. F., Tashman, S., Irrgang, J. J. & Moreland, M. S. Anatomic anterior cruciate ligament reconstruction: a changing paradigm. Knee Surgery, Sport. Traumatol. Arthrosc. 23, 640–648 (2015).
42. Lim, J. M., Cho, J. J., Kim, T. Y. & Yoon, B. C. Isokinetic knee strength and proprioception before and after anterior cruciate ligament reconstruction: A comparison between home-based and supervised rehabilitation. J. Back Musculoskelet. Rehabil. 32, 421–429 (2019).
43. Brewer, B. W., Cornelius, A. E., Van Raalte, J. L., Tennen, H. & Armeli, S. Predictors of adherence to home rehabilitation exercises following anterior cruciate ligament reconstruction. Rehabil. Psychol. 58, 64–72 (2013).
44. Kruse, L. M., Gray, B. & Wright, R. W. Rehabilitation after anterior cruciate ligament reconstruction: A systematic review. Journal of Bone and Joint Surgery - Series A vol. 94 1737–1748 (2012).
45. van Grinsven, S., van Cingel, R. E. H., Holla, C. J. M. & van Loon, C. J. M. Evidence-based rehabilitation following anterior cruciate ligament reconstruction. Knee Surgery, Sport. Traumatol. Arthrosc. 18, 1128–1144 (2010).
46. Nabıyev, V. N. et al. Cryo-compression therapy after elective spinal surgery for pain management: A cross-sectional study with historical control. Neurospine 15, 348–352 (2018).
47. Czamaraabcdefg, A., Tomaszewskidef, W., Bobercde, T. & Lubarskib, B. The effect of physiotherapy on knee joint extensor and flexor muscle strength after anterior cruciate ligament reconstruction using hamstring tendon.
48. Forogh, B., Aslanpour, H., Fallah, E., Babaei-Ghazani, A. & Ebadi, S. Adding high-frequency transcutaneous electrical nerve stimulation to the first phase of post anterior cruciate ligament reconstruction rehabilitation does not improve pain and function in young male athletes more than exercise alone: a randomized single-b. Disabil. Rehabil. 41, 514–522 (2019).
49. Moran, U., Gottlieb, U., Gam, A. & Springer, S. Functional electrical stimulation following anterior cruciate ligament reconstruction: A randomized controlled pilot study. J. Neuroeng. Rehabil. 16, (2019).
50. Bischoff, L. et al. Effects on proprioception by Kinesio taping of the knee after anterior cruciate ligament rupture. Eur. J. Orthop. Surg. Traumatol. 28, 1157–1164 (2018).
51. Liu, K., Qian, J., Gao, Q. & Ruan, B. Effects of Kinesio taping of the knee on proprioception, balance, and functional performance in patients with anterior cruciate ligament rupture: A retrospective case series. Med. (United States) 98, (2019).
52. Adams, D., Logerstedt, D., Hunter-Giordano, A., Axe, M. J. & Snyder-Mackler, L. Current concepts for anterior cruciate ligament reconstruction: A criterion-based rehabilitation progression. J. Orthop. Sports Phys. Ther. 42, 601–614 (2012).
53. Zebis, M. K. et al. Electromyography Evaluation of Bodyweight Exercise Progression in a Validated Anterior Cruciate Ligament Injury Rehabilitation Program: A Cross-Sectional Study. Am. J. Phys. Med. Rehabil. 98, 998–1004 (2019).
54. Başar, B., Başar, G., Aybar, A., Kurtan, A. & Başar, H. The effects of partial meniscectomy and meniscal repair on the knee proprioception and function. J. Orthop. Surg. 28, (2020).
55. Gokeler, A., Neuhaus, D., Benjaminse, A., Grooms, D. R. & Baumeister, J. Principles of Motor Learning to Support Neuroplasticity After ACL Injury: Implications for Optimizing Performance and Reducing Risk of Second ACL Injury. Sports Medicine vol. 49 853–865 (2019).
56. Yang, X. gang, Feng, J. tao, He, X., Wang, F. & Hu, Y. cheng. The effect of knee bracing on the knee function and stability following anterior cruciate ligament reconstruction: A systematic review and meta-analysis of randomized controlled trials. Orthopaedics and Traumatology: Surgery and Research vol. 105 1107–1114 (2019).

Received: 20 Febrero 2021
Accepted: 20 Mayo 2021

REVIEW / ARTÍCULO DE REVISIÓN

Experiencias en el uso de energía renovable en la República del Ecuador

Experiencies in the use of renewable energies in the Republic of Ecuador

Julio Gómez-Assan, Rosa Ajila-Freire
DOI. 10.21931/RB/2021.06.03.29

Resumen: La tendencia a nivel mundial es utilizar energía renovable para depender menos de los combustibles fósiles y a su vez minimizar la contaminación ambiental, el Ecuador y sus gobiernos han realizado esfuerzos para generar este tipo de energía para contribuir a la matriz productiva del mismo. El objetivo de este estudio es determinar los proyectos y cambios que ha tenido la producción tanto de energía primaria como de energía renovable durante los años 2008 y 2018. El estudio se lo realizó a nivel mundial y de país; en lo que respecta al país se identificó experiencias del uso de energías renovables, se recopilaron datos para su respectivo análisis a nivel internacional y nacional, nos centramos en las principales obras de energía renovable funcionando y en proyectos dentro del proceso transformador de la matriz productiva energética del Ecuador. Para la elaboración de esta revisión bibliográfica se recopilaron artículos, folletos, libros pertinentes y relevantes publicados en los últimos 10 años. Se eligieron fuentes con datos originales y se descartó las que dependían de éstas. En el ámbito ecuatoriano, se determinó el valor del kilovatio instalado según la fuente de energía, su capacidad instalada y la energía producida. No hemos avanzado en proyectos de energía maremotriz y geotérmica.

Palabras clave: Centrales, energía, eólica, fotovoltaica, geotérmica, renovable.

Abstract: The global trend is to use renewable energy to rely less on fossil fuels and minimize environmental pollution; Ecuador and its governments have made efforts to generate this energy to contribute to its productive matrix. This study aims to determine the projects and changes that production of both primary energy and renewable energy has had during 2008 and 2018. The study was conducted globally and as a country; regarding the country, experiences of the use of renewable energies were identified, data were collected for their respective analysis at the international and national levels, we focused on the leading renewable energy works in operation and on projects within the transformative process of Ecuador's energy production matrix. Articles, brochures, relevant and relevant books published over the past 10 years. Sources with unique information were picked, and those that relied upon them were wrecked. In the Ecuadorian ambit, the estimation of the kilowatt introduced by the source and fuel, its introduced limit, and the energy created is resolved. We have not progressed on geothermal flowing energy projects.

Key words: Power plants, energy, wind, photovoltaic, geothermal, renewable.

Introducción

A nivel mundial, el consumo de energía provenientes de combustibles fósiles en el 2005 era del 80,7%, en el 2015 hubo un ligero descenso llegando a 79,6%. El uso de combustibles renovables y residuos combustibles en el 2005 estaba en el 8,1% de la demanda total de energía y ha experimentado un descenso, llegando al 3,9% en el 2015[1]. En el Ecuador, la explotación petrolera empezó en el año 1970 lo que provocó la modernización de su economía y un mayor crecimiento económico, por lo tanto, una creciente demanda de energía. En el año 2008, se produjeron 185000 kBEP mientras que en el 2018 fue de 189000 kBEP[2]. Según un informe del 2015 de la Fundación Empresa & Clima ubicada en España, se indica que las emisiones totales en el mundo en el año 2014 fueron de 32.000 millones de toneladas de CO_2, con un aumento del 0.8% respecto al año anterior. La principal actividad emisora es la generación de electricidad y calor, con el 42%, seguida de industrias manufactureras y de construcción con el 19% y del transporte por carretera con el 17%[3]. El objetivo de esta investigación es dar a conocer la producción de energía renovable a nivel mundial y a nivel local en los últimos años, así como los principales proyectos, su capacidad instalada. A nivel país, los principales proyectos ejecutados, sus costos de ejecución y una comparación del valor de la inversión por kW instalado tomando como ejemplos cuatro proyectos de diferente energía. Adicionalmente determinar proyectos de energía hidráulica que están en fase de estudio o construcción.

Panorama Mundial

La producción de energía primaria entre el 2008 y 2018 ha aumentado, salvo el caso de la energía nuclear. Ver tabla 1, cuyas unidades están en mega toneladas de petróleo (Mtoe)[4]. Siendo la energía eléctrica un elemento de suma importancia en la sociedad actual, puesto que es una de las variables necesarias para el desarrollo industrial de los países, así como para el bienestar de los pueblos, por lo que se hace conveniente mantener la continuidad en la prestación del servicio eléctrico.

Fuente	2008	2018
Petróleo	4085	4496
Gas	2589	3265
Carbón	3383	3838
Biocombustible	1154	1327
Eólica-Solar	89	286
Hidráulica	275	362
Nuclear	712	706
Total Mtoe	12287	14276

Tabla 1. Producción de energía primaria mundial de los años 2008 y 2018. Fuente: tomado de la página web de International Energy Agency, Datos y Estadísticas (4)

La producción de energía eléctrica a partir de las diferentes fuentes de energía ha aumentado del 2008 al 2018, a excepción de la producida por energía nuclear y petróleo. Ver tabla 2[4].

La energía renovable se ha establecido como la fuente

Carrera de Tecnología Superior en Ensamblaje y Mantenimiento de Equipos de Cómputo, Instituto Técnico Superior Vicente Rocafuerte-Guayaquil, Ecuador.

Corresponding author: jgomez@istvr.edu.ec

Generación electricidad por fuente	2008	2018
Carbón	8249	10159
Gas	4375	6150
Petróleo	1036	783
Núclear	2733	2710
Hidráulica	3286	4325
Eólica	170	1273
Biocombustible	218	518
Fotovoltaica	11	554
Residuos	67	118
Geotermica	64	88
Otras fuentes	25	34
Solar térmica	0,6	11
Maremotríz	0,4	1
Total TWh	20235	26724

Tabla 2. Generación mundial de electricidad por fuente. Fuente: tomado de la página web de International Energy Agency, Datos y Estadísticas (4)

principal de generación de electricidad y entre ellas, la que predomina es la hidroeléctrica, se ha mantenido estable su participación, siendo del 16% en el 2008 como en el 2018, del total de producción de electricidad[4]. Sí de esta información, sólo analizamos la producción de energía eléctrica, sin incluir a las centrales hidroeléctricas, entre esos mismos años, obtenemos un incremento del 433%[1] en unidades de TWh, siendo las de mayor crecimiento las energía eólica y fotovoltaica. Esta producción de energía va de la mano con la capacidad instalada que en el 2008 fue de 280 GW y en el 2018 de 1246 GW, lo que representa un aumento del 345%[5,6]. Del total de la capacidad de la energía renovable, la hidráulica representó en el 2018 el 47,6%.

Los países con mayor potencia instalada son China, Brasil y Canadá[7]. China cuenta con una capacidad de 322 GW y posee tres centrales hidroeléctricas entre las diez más grandes del mundo por potencia instalada, en primer lugar, está la de Tres Gargantas que posee 22,5 GW[8]. Le sigue Brasil.

La energía eólica terrestre (proyectos ubicados en el continente) ha crecido a pasos agigantados en los últimos 20 años, convirtiéndose en una fuente principal de energía limpia y competitiva en todo el mundo, la capacidad total de energía eólica a nivel mundial ahora supera los 651 GW en el 2019. En términos de capacidad instalada, los tres principales mercados a finales de 2019 son: China, Estados Unidos y Alemania[9]. El parque eólico de Gansu, es el más grande del mundo, ubicado en China con una capacidad de 8 GW[9].

La eólica marina (proyectos ubicados en la superficie del mar), está desempeñando un papel cada vez más importante en la conducción de instalaciones eólicas mundiales[9], al momento cuenta con una capacidad instalada de 29,1 GW[10]. El parque Walney Extension tiene una capacidad de 659 MW, está situado en el mar de Irlanda, a unos 19 kilómetros de la costa de la isla de Walney (Reino Unido), posee 189 turbinas[11].

En el 2017, la electricidad generada a partir de la biomasa, es la tercera después de la hidráulica y eólica[12]. Los mayores productores a partir de los biocombustibles y residuos en el 2017 fueron: China con 92923 GWh, Estados Unidos con 70656 GWh y Brasil con 52255 GWh sin embargo; por capacidad instalada, en primer lugar, está Brasil con 14,5 GW, Estados Unidos con 12,86 GW y tercero está China con 11,2 GW[13].

La tecnología solar fotovoltaica es una de las principales alternativas para afrontar decididamente la problemática energética global[14]. En el 2018, la capacidad instalada en el mundo fue de 485 GW y los países que tienen la mayor capacidad instalada son: China con 175 GW, le sigue Japón con 55 GW y en tercer lugar aparece Estados Unidos con 51 GW. En la India se ubica el más grande parque solar llamado Bhadla con 2,2 GW, le sigue el proyecto Pavagada Solar Park de 2 GW, también ubicado en la India y en tercer lugar está el parque solar en el desierto de Tengger en China, con una capacidad de 1,5 GW[15].

Por último, nombraremos a la electricidad cuyo origen sea del tipo geotérmica, la capacidad instalada en el mundo, en el 2019 fue de 13,9 GW, donde los principales países con capacidad instalada son: Estados Unidos con 2,5 GW, Indonesia con 2,1 GW y Filipinas con 1,9 GW. Llama la atención que estén estos dos países, Indonesia año a año, ha venido incrementando su capacidad, considerando que poseen el 40% del potencial geotérmico del mundo, pero no se ha desarrollado del todo bien, alcanzando sólo el 6%[16].

Energía en Ecuador

En el 2010, las centrales termoeléctricas representaban (generan energía a base de combustibles fósiles) el 54% de la potencia efectiva en MW, mientras que las centrales hidráulicas/renovables era del 46%[17], ver figura 1.

Este panorama cambia y en el 2019, las termoeléctricas caen al 35.01% y las hidráulicas/renovables suben al 64.99%.

Ecuador tiene como recurso energético primario principal los combustibles fósiles, el petróleo con sus derivados y gas natural llegando al 83,8% y sólo el 16,2% proviene de energías renovables. A continuación, se indica el de participación de centrales eléctricas de acuerdo a su tipo en el 2010[18].

Proyectos de energía eólica

En el año 2007, se inauguró el primer parque eólico en la isla San Cristóbal del Archipiélago de Galápagos, con una potencia instalada de 2.4 MW[19]. En el 2019, la producción total de energía fue de 86 GWh. En la provincia de Loja se encuentra el parque eólico más alto del mundo, Villonaco, que abastece el 25% de la energía que demanda la provincia[20]. En la tabla 3, se puede apreciar los principales parques eólicos que se encuentran operando y en construcción, dando como resultado una capacidad instalada de 21.15 MW. Dos parques están ubicados en las Islas Galápagos y uno en la provincia de Loja.

Parques eólicos	Potencia (MW)	Estado
Isla san cristóbal	2,40	Operativo
Isla Santa Cruz-Baltra	2,25	Operativo
Villonaco-Loja	16,50	Operativo
Minas Huascachaca-Loja	51,70	En construcción

Tabla 3. Principales parques Eólicos del Ecuador.

Proyectos de energía solar

Ecuador debido a su ubicación geográfica puede utilizar la energía solar durante todo el año. La energía solar se utiliza principalmente para usos térmicos como calentamiento de agua y climatización de edificios y para la generación de electricidad a base de paneles fotovoltaicos.

La radiación solar global promedio en su territorio fluctúa entre 4.1 y 4.9 kWh/m2/día[21]. La energía fotovoltaica dio sus primeros aportes en el año 2005 fluctuando entre 10 y 30 MWh hasta el año 2006, luego hubo un aumento a 60 MWh en el año 2011, llegando a 38 GWh en el 2019. En el año 2011, el Conelec por medio de la regulación 004/11, determinó el tratamiento para la energía producida con recursos energéticos renovables no convencionales para centrales menores a

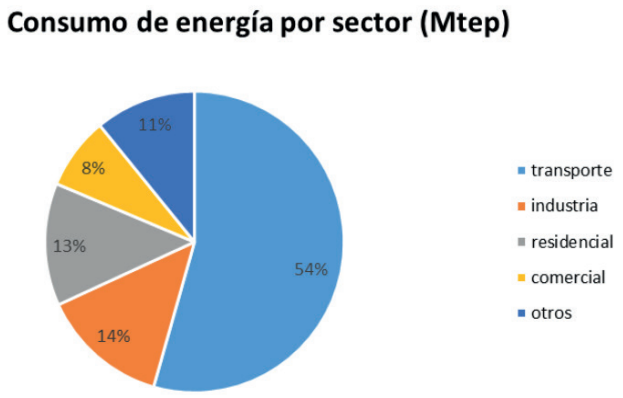

Figura 1. Consumo de energía por sector en el 2010 en Ecuador.

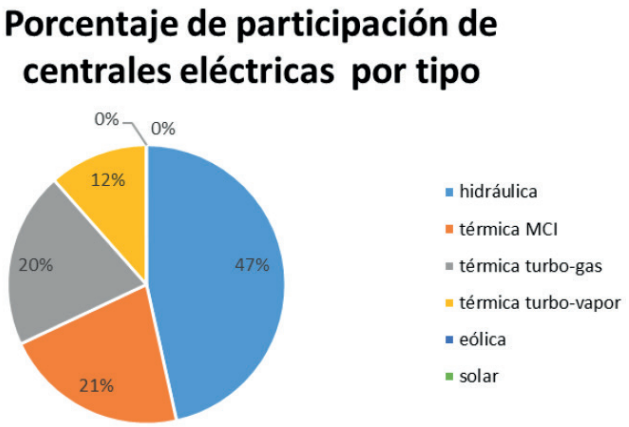

Figura 2. Porcentaje de participación de centrales eléctricas de acuerdo a su tipo en el 2010.

Figura 3. Parque eólico de Villonaco ubicado en la provincia de Loja, foto tomada de la página web de Celec Gensur, galería.

50 MW. Bajo esta regulación, a las generadoras fotovoltaicas se les cancelará 40.03 c USD/KWh en el territorio nacional y 44.03 c USD/KWh en la región insular[22]. Actualmente, este tipo de energía tiene una potencia efectiva de 26.74 MW. Los principales proyectos de energía solar a base de paneles fotovoltaicos se indican en la tabla 4.

Planta	MW
Galápagos-Pto Ayora	1,5
Galápagos Baltra	0,2
Pimampiro	1
Imbabura-Tren Salinas	2
Imbabura Salinas	1
Total	5,7

Tabla 4. Principales proyectos fotovoltaicos en el Ecuador.

Proyectos de energía de la biomasa-biogás

El proyecto San Carlos de cogeneración entró en funcionamiento en el 2005, se convirtió en el primer proyecto de este tipo del país, en lograr un registro internacional, en la Organización de las Naciones Unidad, como proyecto de mecanismo de desarrollo limpio[23]. En el año 2019, la potencia efectiva de este tipo de energía fue de 142.90 MW y la producción de energía llega a 455 GWh. Los principales proyectos de este tipo de energía se muestran en la tabla 5.

Proyectos de energía hidráulica

Ecuador es el país con la más alta concentración de ríos por kilómetro cuadrado en el hidroeléctrica, que es la base del cambio de matriz energética iniciado en el gobierno anterior. La cordillera andina es la línea divisoria de aguas entre la cuenca hidrográfica del río Amazonas, que discurre hacia el este, y del océano Pacífico, que incluye los ríos Mataje, Santiago, Coca, Esmeraldas, Chone, Guayas y Jubones, entre otros[20]. Este tipo de energía primaria incrementó su participación, pasando del 1% en 1970 a casi el 4% en la actualidad. En el 2006, la capacidad instalada era de 3300 MW, alcanzando los 5073 MW en el 2018. La producción de este tipo de energía es 24.665 GWh. En la tabla 6 se observa la potencia nominal de cada fuente renovable.

Las principales centrales hidroeléctricas que están funcionando se muestran en la siguiente tabla (Tabla 7) con su respectiva potencia en MW.

Entre los principales proyectos que se encuentran en construcción están el Zamora-Santiago que aprovechará las aguas del río Zamora, se estima una potencia superior a los 3000 MW; el Paute-Cardenillo que constituye el peldaño final del desarrollo integral de la cuenca del río Paute, tendrá una capacidad instalada de 595 MW; el Mazar-Dudas que captará las aguas del río Mazar, se espera obtener una potencia instalada del 20,82 MW, se encuentra en la provincia de Cañar y Quijos que tendrá una potencia instalada de 50 MW, aprovechará las agua del mismo nombre en la provincia de Napo,

Planta	Potencia MW	GWh	Fuente
Ecolectric Valdez	36,5	76,64	Bagazo de caña
San Carlos	35	133,86	Bagazo de caña
IANCEM-Ibarra	3		Bagazo de caña

Tabla 5. Principales plantas de energía de biomasa-biogás en Ecuador

Energía	Potencia MW	Participación
Hidráulica	5073	96,20%
Eólica	21	0,40%
Fotovoltaica	27	0,52%
Biomasa	144	2,74%
Biogas	7	0,14%

Tabla 6. Potencia nominal instalada según tipo de energía en Ecuador.

Central	Potencia MW
Coca Codo Sinclai	1500
Paute	2600
San Francisco	270
Pucará	219
Agoyan	156
Delsitanisagua	180
Manduriaco	65
Total	4990

Tabla 7. Centrales hidroeléctricas en funcionamiento en Ecuador.

la obra tiene un 46% de avance[24]. En la tabla 8 se muestran algunos de los proyectos que todavía no entran en operación, con la potencia y energía estimada.

Proyectos de energía geotérmica

La exploración geotérmica se inició en el Ecuador hace más de 30 años con el Instituto Ecuatoriano de Electrificación (INECEL), sin embargo, fue cerrada en 1993, debido principalmente a los bajos precios del petróleo, a la falta de un marco regulatorio y a la no disponibilidad de un capital inicial de riesgo[25]. El Ecuador al estar ubicado en el cinturón de fuego del Pacífico posee un potencial térmico estimado de 1700 MW, es decir, un poco más que la potencia de la central hidroeléctrica Coca Codo Sinclair. En la práctica, la utilización del recurso geotérmico se limita a balnearios y piscinas termales. Se han realizado estudios de prefactibilidad en cinco proyectos. Los análisis definieron un potencial en cuatro zonas específicas: Tufiño-Chiles (frontera Ecuador-Colombia), Chalupas (Cotopaxi), Cachimbiro (Imbabura) y Chacana (Pichincha). En la siguiente tabla se indica la potencia estimada de cada proyecto.

Proyecto	Potencia MW	GWh/año
Zamora Santiago	3000	15000
Paute Cardenillo	595	
Mazar Dudas	20,82	125,3
Quinjos	50	355

Tabla 8. Proyectos hidroeléctricos (no terminados) del Ecuador.

Proyecto	Mwe
Tufiño-Chiles	138
Cachimbiro	113
Chalupas	283
Chacana	418
Total	952

Tabla 9. Principales proyectos geotérmicos del Ecuador.

El valor promedio de los estudios, perforación y entrada de operaciones oscila entre 15 millones y 25 millones USD. También se necesitan tres años para que la perforación de prueba proporcione los suficientes datos que permitan proseguir con el desarrollo del proyecto[26].

Proyectos de energía del mar

En el Ecuador aún no se ha aplicado a gran escala la generación de electricidad a través de este tipo de energía debido a la falta de interés de las entidades públicas[27]. El perfil costanero de Ecuador por su extensión de 640 km motiva la búsqueda de un recurso energético en el Océano Pacífico. Según una investigación realizada por Juan S. Guamán, donde se indica que por la existencia de la corriente Sub-Superficial Ecuatorial del Pacífico se puede aprovechar la energía existente en esta corriente marina debido a su velocidad de 1.5 m/s, que es mayor al requerimiento mínimo de 1.0 m/s. Luego indica que, para reemplazar a una central termoeléctrica, se necesita una inversión de 85 millones USD[28].

Se ha realizado un sencillo cálculo, considerando valores de la inversión por proyecto terminado y la potencia instalada, se obtuvo la siguiente tabla, en donde se indica el costo de la inversión para obtener un kilovatio (kW) de potencia. Se tomaron como ejemplo cuatro proyectos.

Conclusiones

Para la producción de energía dependemos indiscutiblemente del petróleo y ese panorama no ha cambiado desde el auge petrolero del año 2000. El objetivo del gobierno anterior de cambiar la matriz energética del Ecuador, dio paso a la inauguración de más centrales hidroeléctricas, como la Coca Codo Sinclair de 1500 MW. Debido al subsidio al gas y a la gasolina no se avizora cambio para utilizar fuentes de energía renova-

Proyecto	Inversión ($)	Inversión/Kw
Villanaco (eólico)	48,3 M	2930
Pimampiro (solar)	3,5 M	3500
San Carlos (biomasa)	No obtuvimos respuesta	
San Francisco (Hidraulico	550 M	2030

Tabla 10. Inversión en dólares por kW instalado según el tipo de energía.

bles, especialmente en el sector del transporte y residencial. El aumento de la potencia nominal de la energía renovable se debe al financiamiento del Estado.

Estamos viviendo una época en que las empresas eléctricas garantizan la entrega de la energía debido a que no tenemos problemas de estiaje o sequía en las zonas donde se ubican las centrales, por lo tanto, la población urbana no siente la necesidad de adquirir otras fuentes de energía eléctrica. Finalmente, los esfuerzos estatales deben apuntar a aprovechar la energía geotérmica debido a su gran potencial térmico, así tendríamos otra fuente de energía sin depender de las hidroeléctricas.

Después de la energía hidráulica, sigue la producida por biomasa, luego la eólica. La primera y la tercera son inversiones y proyectos estatales, mientras que la segunda proviene de inversiones privadas. Parecería que la inversión estatal no apunta a los proyectos de celdas fotovoltaicas.

En la comparación de la inversión necesaria para instalar un kilovatio de potencia, no se obtuvo el valor del proyecto del Ingenio San Carlos, después de realizar las respectivas consultas en su página web.

Agradecimientos

Los autores agradecen a la docente investigadora Lissenia Sornoza Quijije por sus valiosos aportes y ayuda incondicional para la culminar con éxito de este trabajo de revisión bibliográfica.

Referencias bibliográficas

1. World Bank Group [online]. Disponible en: https://data.worldbank.org/topic/energy-and- mining.
2. IIGE, "Balance Energético Nacional 2018", [on line]. Disponible en: https://www.recursosyenergia.gob.ec/5900-2
3. A. de la Heras Abás, Informe de situación de las emisiones de CO2 en el mundo. Año 2014, Cataluña, Fundación Universitaria Iberoamericana, 2016, pp. 35.
4. International Energy Agency, Datos y Estadísticas, [on line]. Disponible en: https://www.iea.org/data-and-statistics
5. REN21, "Renewables Global Status Report: 2009" [on line]. Disponible en: https://www.ren21.net/wp-content/uploads/2019/05/GSR2009_Full-Report_English.pdf
6. REN21, "Renewables 2019 Global Status Report" [on line]. Disponible en: https://www.ren21.net/wp-content/uploads/2019/05/gsr_2019_full_report_en.pdf , ISBN 978-3-9818911-7-1
7. Sevilla, B. "Ranking mundial de los países con mayor potencia hidráulica instalada en 2018" [on line]. Disponible en: https://es.statista.com/estadisticas/641232/potencia-hidraulica-instalada-por-paises/#statisticContainer
8. El Periódico de la Energía, "Las 10 hidroeléctricas más grandes del mundo" [on line]. Disponible en: https://elperiodicodelaenergia.com/las-10-centrales-hidroelectricas-mas-grandes-del-mundo/
9. Global Wind Energy Council [on line]. Disponible en: https://gwec.net/global-wind-report-2019/
10. Global Wind Energy Council, "Global Wind Report 2019", Rue Belliard 51-53 1000 Brussels, Belgium, 2020, pp. 41
11. Revista Muy Interesante, [on line]. Disponible en: https://www.muyinteresante.es/tecnologia/video/ ¿Cuál es el mayor parque eólico marino del mundo? (muyinteresante.es)
12. World Bioenergy Association, "Global Bioenergy Statistics 2019" [on line], pp. 15. Disponible en: https://worldbioenergy.org/uploads/191129%20WBA%20GBS%202019_HQ.pdf
13. International Renewable Energy Agency IRENA [on line]. Disponible en: https://www.irena.org/bioenergy
14. Power Technology, "Las plantas de energía solar más grandes del mundo", [on line]. Disponible en: https://www.power-technology.com/features/the-worlds-biggest-solar-power-plants/
15. Our World In Data, "Capacidad instalada de energía solar, 2018", [on line]. Disponible en: https://ourworldindata.org/renewable-energy
16. Piensa en Geotermia, "Inversión geotérmica en Indonesia para llegar a $1,7 billones en 2018" [on line]. Disponible en: https://www.piensageotermia.com/inversion-geotermica-en-indonesia-para-llegar-a-1-7-billones-en-2018/
17. Olade, "Panorama energético de América Latina y el Caribe 2020", 1ra. ed. Ecuador, 2020, pp. 137
18. Conelec, "Boletín estadístico sector eléctrico ecuatoriano 2010" [on line]. Disponible en: https://www.regulacionelectrica.gob.ec/wp-content/uploads/downloads/2015/12/Estadística-Sector-Eléctrico-Ecuatoriano-2010.pdf
19. Reve, "La energía eólica en Ecuador" [online]. Disponible en: https://www.evwind.com/2010/08/11/la-energia-eólica-en-ecuador/
20. eltelégrafo, "el parque eólico más alto del mundo en Ecuador" [online]. Disponible en: https://www.eltelegrafo.com.ec/noticias/economia/4/parque-eolico-mas-alto-del-mundo-en-ecuador
21. Corporación para la investigación energética, "Atlas solar solar del Ecuador con fines de generación eléctrica", Quito, 2008, pp. 10-46.
22. Conelec, "Regulación No. Conelec-004-11" [online]. Disponible en: https://regulacionelectrica.gob.ec/wp-content/uploads/downloads/2015/10/conelec_004_11_ernc.pdf
23. San Carlos, página Web, http://www.sancarlos.com.ec/modelo-de-produccion-sostenible/cogeneracion-de-energia-electrica/
24. Celec, [online]. Disponible en:https://www.celec.gob.ec
25. Reve, "La energía geotérmica en Ecuador" [online]. Disponible en: https://www.evwind.com/2012/06/26/la-energia-geotermica-en-ecuador/
26. A. García, "El uso de energía geotérmica se extiende por todo el planeta" [online]. Disponible en: https://www.elcomercio.com/tendencias/ener giageotermica-planeta-cop20-lima.html.
27. R. Rodríguez, M. Chimbo. "Aprovechamiento de la energía undimotriz en el Ecuador". Ingenius No.17, (Enero- Junio), pp. 24.
28. J. Guamán, J. Espinoza, E. Ribeiro. "Energía del mar para su integración en la matriz energética del Ecuador". Revista Maskana, pp. 314-317.

Received: 25 marzo 2021
Accepted: 10 julio 2021

REVIEW / ARTÍCULO DE REVISIÓN

Tecnología IgY: Estrategia en el tratamiento de enfermedades infecciosas humanas

IgY Technology: Strategy in the treatment of human infectious diseases

Nathaly Cruz Tipantiza[1] and Marbel Torres Arias[2]

DOI. 10.21931/RB/2021.06.03.30

Resumen: La aparición de microorganismos resistentes a antibióticos, el descubrimiento de nuevos agentes patógenos con potencial pandémico y el aumento de una población inmunocomprometida han dejado casi obsoleta la terapia antimicrobiana, terapia comúnmente usada para tratar enfermedades infecciosas. Por otro lado, las investigaciones acerca del uso del anticuerpo IgY para desarrollar inmunidad pasiva han demostrado el potencial que tiene la tecnología IgY para tratar enfermedades infecciosas víricas y bacterianas. Donde los anticuerpos IgY de aves se destacan por su alta especificidad, rendimiento y escalabilidad de producción a menor costo, con relación a los anticuerpos IgG de mamíferos. El objetivo de esta revisión es determinar la importancia del uso de los anticuerpos IgY como tratamiento terapéutico y profiláctico frente a los patógenos causantes de infecciones virales y bacterianas en humanos, mediante la recopilación de ensayos clínicos, productos comerciales y patentes registradas en el período de 2010-2021. Finalmente, con este estudio se estableció que la tecnología IgY es una herramienta biotecnológica versátil y eficaz para tratar y prevenir enfermedades infecciosas, al reducir los síntomas y la carga del patógeno.

Palabras clave: Anticuerpo IgY, bacteria, terapia pasiva, virus.

Abstract: The emergence of antibiotic-resistant microorganisms, the discovery of new pathogens with pandemic potential, and the rise of an immunocompromised population have rendered antimicrobial therapy, a commonly used therapy to treat infectious diseases, almost obsolete. On the other hand, research into the use of IgY antibodies to develop passive immunity has demonstrated the potential of IgY technology to treat viral and bacterial infectious diseases. Avian IgY antibodies stand out for their high specificity, performance, and scalability at a lower cost relative to mammalian IgG antibodies. This review aims to compile information on the use of IgY antibodies as therapeutic and prophylactic treatment against pathogens causing viral and bacterial infections in humans by collecting clinical trials, commercial products, and patents registered in 2010-2021. Finally, this study established that IgY technology is a versatile and effective biotechnological tool to treat and prevent infectious diseases by reducing symptoms and pathogen burden.

Key words: IgY antibody, bacteria, passive therapy, virus.

Introducción

Cuando un hospedero se encuentra en desequilibrio disminuye la capacidad de protección del sistema inmunológico permitiendo la entrada de microorganismos. Estos patógenos desencadenan una infección, que se define como "la presencia y multiplicación de un microorganismo en los tejidos, fluidos o cavidades de un huésped"[1]. La colonización de los patógenos en conjunto con otros factores ambientales permiten la invasión del huésped generando daños a nivel local o sistémico, causando un infeccion[2].

Durante el siglo XIX era común el uso de sueros de origen animal (sueros heterólogos) para tratar enfermedades infecciosas, sin embargo la idea fue abandonada por la toxicidad asociada a su administración y la introducción de la quimioterapia antimicrobiana en 1909[3]. A pesar de todo, las infecciones virales y bacterianas siguen siendo las principales causas de mortalidad y morbilidad en el mundo, representando aún un desafío en la salud humana[4]. La pérdida de eficacia de la quimioterapia antimicrobiana se atribuye al aumento de individuos inmunodeprimidos, la reaparición de enfermedades que se consideraban ya erradicadas (sarampión, viruela), nuevos agentes infecciosos (SARS COV-2) y el desarrollo de resistencia a los antimicrobianos (RAM)[5,6]. Por esta razón, se busca un tratamiento capaz de reconocer epítopos específicos, y así evitar la entrada, propagación, y neutralización de factores de virulencia sin dañar las células huésped. Permitiendo que el sistema inmunológico elimine los patógenos y evite desarrollar una infección crónica.

Por otro lado surge el interés por el uso de sueros de origen animal, generado por el sistema inmune de aves, dada su capacidad para generar anticuerpos que brindan inmunidad pasiva a su descendencia[7,8]. Existen tres isotipos de inmunoglobulinas aviares: IgA e IgM presentes en la clara, e IgY presente en la yema; siendo este, el de principal interés terapeútico por su alta especificidad contra antígenos de mamíferos altamente conservados[9]. Fue así que desde 1995 se asigna el término "tecnología IgY" al proceso de producción y aplicación de anticuerpos IgY aviares[10], reportandose aplicaciones en el área veterinaria, inmuno-diagnóstica y de investigación[11].

En el año 2010 empieza el apogeo de esta tecnología en la medicina humana como alternativa al uso de antibióticos y por su bajo costo de producción[12]. Se ha documentado la eficacia del uso de IgY para tratar y prevenir infecciones bacterianas y víricas causantes de patologías como caries dental, periodontitis, gastritis, diarrea, entre otras[13]. De forma general se ha visto

[1] Departamento de Ciencias de la Vida y la Agricultura, Carrera de Ingeniería en Biotecnología, Universidad de las Fuerzas Armadas ESPE, Ecuador.
[2] Departamento de Ciencias de la Vida y la Agricultura, Carrera de Ingeniería en Biotecnología, Universidad de las Fuerzas Armadas ESPE, Ecuador y Laboratorio de Inmunología y Virología, CENCINAT, GISAH, Universidad de las Fuerzas Armadas, ESPE, Ecuador.

Corresponding author: mmtorres@espe.edu.ec

que IgY facilita la eliminación del patógeno a través del intestino, evitando la replicación y propagación del mismo[9]. Se ha evaluado la administración sistémica del anticuerpo IgY aviar en comparación con IgG de mamiferos, evidenciándose una acción más rápida y local[14]. Asimismo, la inmunoterapia oral con IgY demostró su versatilidad y seguridad de uso al poder ser aplicada como fármaco y nutracéutico en un rango amplio de pacientes, desde recién nacidos, adultos, embarazadas hasta pacientes con inmunodeficientes e infecciones activas[15].

Tras una breve descripción de la tecnología IgY, sus ventajas y aplicaciones, esta revisión resume el uso potencial de IgY aviar como inmunoterapia contra infecciones bacterianas y virales en humanos. Para ello se recopiló mediante páginas web oficiales y bases de datos científicas los principales ensayos clínicos, patentes y productos comerciales disponibles en el período de 2010-2021.

Tecnología IgY

En 1893 el científico Felix Klemperer reporta el primer uso de IgY aviar (IgY antitoxina tetánica) para generar inmunidad pasiva en ratones, permitiendo que estos sobrevivan a dosis consideradas letales de esta toxina[16]. Sin embargo, fue hasta el año 1959 donde el bienestar animal se convierte en una preocupación ética para la comunidad científica, lo que atrae nuevamente el interés por el experimento de Klemperer[17]. Fue entonces, que desde la década de 1980 se empieza a desarrollar una amplia gama de aplicaciones para IgY, principalmente en investigación, diagnóstico e inmunoterapia en medicina veterinaria[12,18].

En 1995, el Doctor Claus Staak, asigna el término "tecnología IgY" al proceso de producción y aplicación de anticuerpos IgY aviares[10]. De forma paralela en 1996, el Centro Europeo para la Validación de Métodos Alternativos (CEVMA) recomienda el uso de IgY como alternativa al uso de IgG de mamífero, convirtiendo la tecnología IgY en una práctica internacionalmente aceptada[19]. Por último, a partir del año 2010 y hasta la actualidad se ha evidenciado un incremento del uso de IgY en la medicina humana como herramienta de diagnóstico e inmunoterapia[11,15].

Inmunoglobulina IgY vs Inmunoglobulina IgG

IgY es un isotipo de inmunoglobulina secretada por aves, anfibios, reptiles y peces pulmonados[20], es considerado el precursor evolutivo de IgG e IgE de mamíferos por su similitud funcional con ambos anticuerpos y a nivel estructural con IgE[21]. A nivel inmunológico IgY es el equivalente de IgG de mamíferos, sin embargo, difieren en aspectos funcionales y estructurales. Por ejemplo, IgY posee una masa molecular (~180 kDa) en comparación a IgG (~160 kDa)[22] ya que posee cuatro dominios constantes en la cadena pesada (CH1-CH4) mientras que IgG solo posee tres (CH1-CH3). Asimismo, IgY carece de la región bisagra entre el dominio CH1 y CH2 al igual que IgE de mamífero[10]. Esta ausencia otorga a IgY una flexibilidad restringida en comparación a IgG afectando su capacidad de precipitar antígenos multivalentes[23,24]. No obstante, su limitada flexibilidad le ha permitido reconocer mejor los antígenos, es decir tener una alta especificidad, y además le ha otorgado una mayor resistencia a la degradación y fragmentación proteolítica, manteniéndose estable a temperaturas de entre 30-70°C y un pH de 3,5-11[25].

Estas diferencias estructurales y funcionales entre los anticuerpos IgY aviar y su homólogo IgG de mamífero le han concedido ciertas ventajas, como (1) generar una mayor respuesta inmune contra epítopos de proteínas conservadas y proteínas que evaden el sistema inmune de mamíferos[26], (2) disminuir la reactividad cruzada[27], (3) no activa el sistema complemento humano, y por último, (4) IgY reduce los falsos positivos en pruebas clínicas al carecer de los sitios de unión en la región Fc, por ejemplo, no reacciona con el factor reumatoide (RF)[28], tampoco con los receptores Fc bacterianos (proteína A y G)[29] ni con los aglutinógenos eritrocitarios A y B[30].

Modo de acción de IgY

En la actualidad, aún se desconocen los mecanismos específicos que emplea la inmunoglobulina IgY para proteger al huésped contra los patógenos[31], pero se sabe de forma general que combina las funciones de IgG: opsonizar y fijar antígenos e IgE: mediar reacciones anafilácticas, específicamente las de hipersensibilidad de tipo I o inmediato[32]; por lo que se han propuesto mecanismos de acción generales para explicar las funciones efectoras que permiten la protección al huésped (Figura 1), como:

Aglutinación

IgY actúa como un "pegamento biológico", al aglutinar e inmovilizar los patógenos y facilitar su eliminación por el intestino[11]. Esto se afirma con el estudio de Tsubokura *et al.*[33] al desarrollar IgY-anti *Campylobacter jejuni* y registrar una disminución del 99% de bacterias en el intestino, y un aumento del 80-95% de bacterias en los recuentos bacterianos fecales.

Bloqueo de adherencia

Mecanismo principal de IgY, aprovecha su alta especificidad y permite unirse a epítopos particulares del patógeno, inhibiendo la adherencia de este a la superficie celular y previniendo la propagación intercelular (mecanismo común en virus)[34]. Por ejemplo, Xu *et al.*[9] propone que si IgY se une a un antígeno de superficie (proteínas de la membrana, fimbrias o flagelos) que sea crucial para la colonización bacteriana, se lograría afectar las funciones normales de crecimiento, producción y liberación de toxinas.

Neutralización de toxinas

IgY puede evitar el desarrollo de una infección sin inhibir directamente al patógeno, al neutralizar las toxinas secretadas por los mismos y evitar el desarrollo de efectos fisiopatológicos que estos podrían desencadenar[35]. Por ejemplo, la patente WO2013009843 describe las composiciones de IgY anti-LPS contra bacterias gastrointestinales en animales, demostrando ser eficaces en la disminución de toxinas y patógenos del tracto digestivo, además de registrar actividad antiinflamatoria[36].

Opsonización

La unión IgY-patógeno, genera alteraciones estructurales en el patógeno tornándolo más suceptible a fagocitarse. Por ejemplo, en el estudio in vitro de Lee *et al.*[37] se encontró que IgY- anti *Salmonella typhimurium* se unía a un antígeno de superficie de la membrana celular, generando alteraciones estructurales en la superficie bacteriana. Por otro lado se propone que IgY puede mejorar la capacidad fagócitica de las células inmunes del hospedero, pese a carecer del sitio de unión de la región Fc. Esto se evidencio en el estudio de Zhen *et al.*[38] donde la IgY- anti *Escherichia coli* mejoró la actividad fagocitica de macrófagos y neutrófilos.

Productividad de IgY de la yema del huevo

IgY es el único anticuerpo aviar capaz de transferirse de la sangre de su progenitora a los oocitos maduros, otorgando

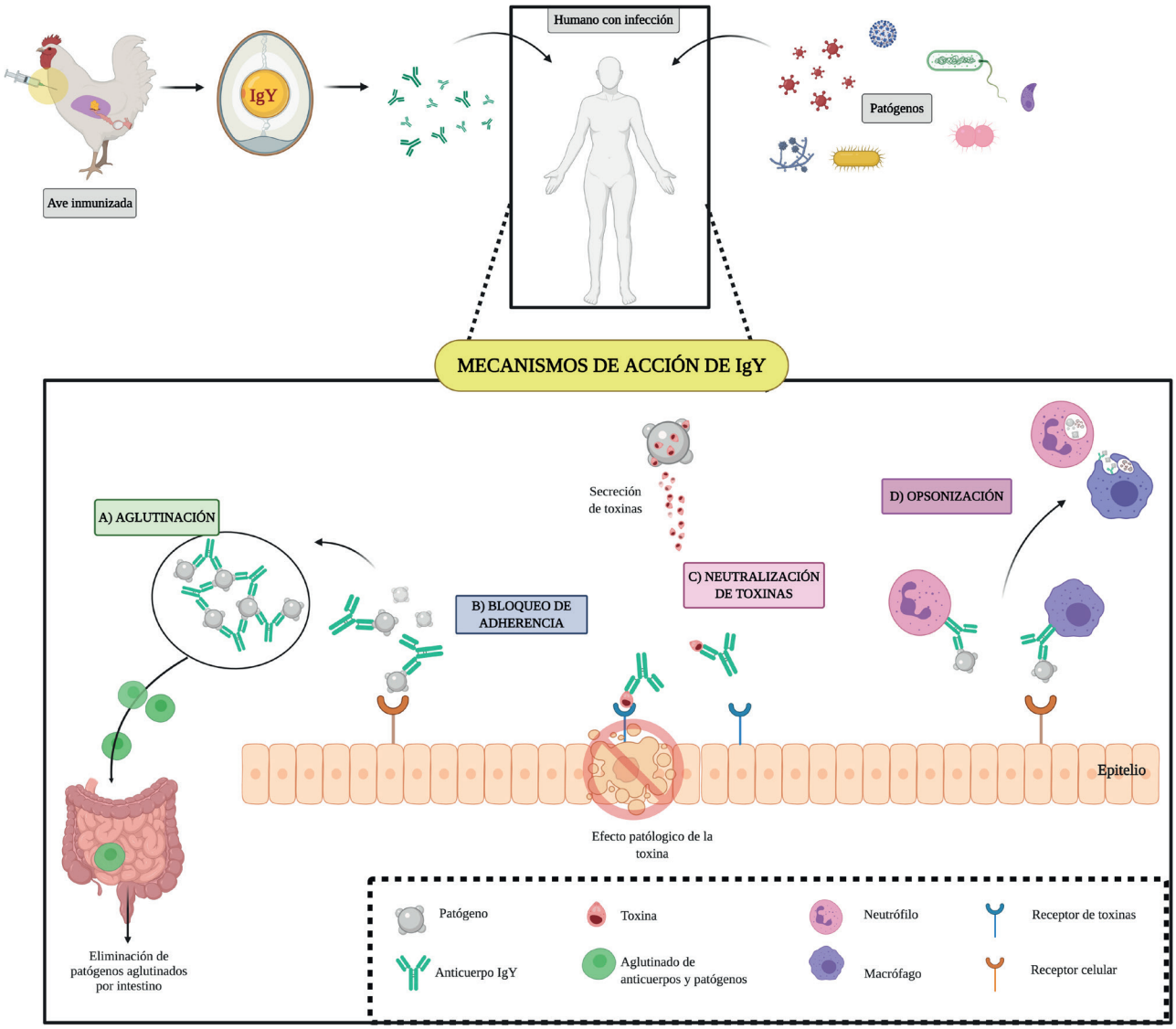

Figura 1. Mecanismos de acción de anticuerpos IgY.

protección al embrión de posibles infecciones patogénicas[39]. En base a este principio inmunológico y considerando que la yema de huevo es una fuente económica y accesible para obtener anticuerpos, la tecnología IgY desarrolla una metodología práctica, repetible, segura y de bajo costo para la producción de IgY[30]. Se comienza por inmunizar a las gallinas (por vía subcutánea, intramuscular o intradérmica), con el fin de desarrollar una respuesta inmunológica adaptativa humoral[40]. Para ello se pueden utilizar diferentes tipos de antígenos como patógenos inactivados, proteínas recombinantes o proteínas obtenidas de ADN plasmídico[41]. Una vez inmunizada el ave, el antígeno se procesa y genera los anticuerpos IgY que por inmunidad pasiva se transfieren del plasma sanguíneo a la yema del huevo, este traspaso se da a partir del quinto o sexto día post inoculación[42]. Tras obtener el huevo, se separa la yema de la clara y se procede a remover la fracción lipídica por delipidación[43]. Se recupera la fracción acuosa y se precipita con polietilenglicol o sales de amonio o sodio, obteniendo un pellet de proteínas totales en donde se encuentran las IgY[44]. Por último se realiza una purificación por técnicas cromatográficas o de ultrafiltración, y se cuantifica la concentración de anticuerpo IgY obtenido[45].

La eficiencia de producción de la tecnología IgY para obtener un anticuerpo con alto rendimiento, pureza y actividad depende de varios aspectos como (1) la raza y dieta de las aves, siendo las mejores razas de gallinas ponedoras ISA Brown y Lohmann Selected Leghorn. Por otro lado Villaguala *et al.*[46] propone evaluar la relación yema:albúmina, independientemente de la raza al considerar una relación directa para obtener una concentración mayor de IgY. (2)La modulación de la respuesta humoral donde se vio que la vía intramuscular produce niveles más altos que la subcutánea[47]. (3) El uso o no de inmunoestimulantes o adyuvantes, donde los adyuvantes a base de aceite, como el adyuvante completo de Freund (FCA) y el incompleto (FIA) siguen siendo los adyuvantes de elección en producción[48], sin embargo, se sabe que estos desencadenan efectos secundarios en el ave. Lévesque *et al.*[49] ha propuesto la adición de inmunoestimulantes CpG ODN en conjunto con el adyuvante FIA, al conseguir aumentar la producción de IgY específica hasta en un 480%. (4) El tiempo y refuerzo del antígeno, considerando que la concentración en la yema es directamente proporcional al tiempo de exposición del antígeno en el ave[50]. Y por último, (5) el método de purificación aplicado, las técnicas de cromatografía y UF son útiles a nivel de laboratorio, sin embargo, la aplicación de estos métodos para la producción de IgY a gran escala se limita por problemas relacionados con la seguridad alimentaria y los altos costos[51]. A ni-

vel industrial se emplean coagulantes polisacáridos naturales como pectina, alginato de sodio, goma xantana, carboximetilcelulosa y carragenina, obteniéndose una precipitación de más del 90% de las lipoproteínas de la yema[48]. De esta forma, la Tecnología IgY ha reportado altos rendimientos de producción, obteniendo 300-325 huevos al año por gallina inmunizada de los que se extraen de 100-150 mg de IgY por yema con una especificidad del 5 al 10% contra el antígeno inoculado[31,52].

Por otro lado, IgY se puede conservar por hasta 6 meses a temperatura ambiente, por hasta 3 meses a temperaturas de hasta 50°C, y de 5-10 años a 4°C[11]. A largo plazo se recomienda conservarlas a un máximo de -20°C[53] o liofilizadas[44]. En la industria farmacéutica y alimenticia es común almacenar las IgY en forma pulverizada, tras aplicar un secado por atomización[54]; además, se suelen adicionar estabilizadores como carbohidratos, azúcares, polioles y otros complejos, para aumentar la estabilidad térmica y de pH de IgY[55].

Aplicaciones de IgY

La tecnología IgY ha evolucionado drásticamente en los últimos años, y es gracias a su estructura, propiedades y características lo que la han convertido en uno de los principales anticuerpos terapéuticos y profilácticos contra enfermedades en animales y humanos[24]. Ha logrado abarcar una gran variedad de campos, desde el área de diagnóstico e investigación, hasta la de producción alimenticia y farmacológica[13]. A continuación, se abordará de forma rápida algunas aplicaciones potenciales del anticuerpo IgY (Figura 2), para una revisión más detallada, véanse las ref. 10, 13 y 48.

IgY para inmunoensayos

La alta sensibilidad, especificidad y avidez de IgY la han convertido en un componente esencial para inmunoensayos cuantitativos y cualitativos[18]. Se ha utilizado IgY como biomarcador de calidad ambiental y seguridad alimentaria[56], permitiendo detectar sustancias como: fármacos residuales, alérgenos, hormonas, toxinas, antígenos (de origen viral, bacteriano, parasitario, vegetal o animal)[57–59], entre otros. También se ha utilizado como reactivo inmunodiagnóstico, donde la avidez de IgY con proteínas conservadas de mamíferos la han convertido en el sustituto de IgG en pruebas clínicas al eliminar falsos positivos y disminuir interferencias[10], incluso se ha usado en la detección y cuantificación de biomarcadores de cáncer gástrico[60], cáncer de mama y ovario[61]. Además, Zhang *et al.*[62] demostró que IgY se puede utilizar como un anticuerpo secundario, al ser capaz de conjugarse con las enzimas (peroxidasa e isotiocianato), reaccionar con el anticuerpo primario (IgG de ratón) y amplificar las señales antígeno-anticuerpo.

En consecuencia, IgY ya se aplica a varios formatos de inmunoensayos, tales como: ELISA[63], Western blot[45], cromatografía[64], ensayos inmunoenzimáticos[65], ensayos de fluorescencia[66], entre otros.

IgY como suplemento

El interés del consumidor por llevar un estilo de vida más sano, ha permitido que durante los últimos 20 años se produzca y utilice de forma masiva anticuerpos IgY en forma de suplemento funcional[13]. Se han desarrollado suplementos nutricionales, cosméticos y farmacéuticos que se pueden ingerir de forma segura, mejoran la calidad de vida de humanos y animales domésticos[67].

IgY como agente antitoxinas

La administración sistemática de IgY ha reportado una nula inflamación inespecífica y un bajo índice de efectos secundarios[68], que en combinación con su función efectora de neutralización de toxinas la han convertido en una estrategia perfecta para el desarrollo de antídotos[69]. Por ejemplo, en países tropicales y subtropicales la mordedura de serpientes venenosas, escorpiones y arañas representan aún un peligro para la salud pública[70], comúnmente se utilizan inyecciones con sueros producidos en caballos, cabras y ovejas, pero estos inducen efectos secundarios como la enfermedad del suero o shock anafiláctico[71]. Thalley *et al.*[72] demostró a nivel *in vivo* el uso de IgY como antitoxina contra serpientes cascabel y escorpiones, siendo esta capaz de neutralizar los efectos letales y actuar como antídoto de amplio espectro. De igual forma, LeClaire *et al.*[73] reportó el desarrollo y uso de IgY anti-enterotoxina B estafilocócica (SEB), un agente microbiano letal utilizado en guerras biológicas, donde IgY actuó como agente anti bioterrorista al reducir la cantidad de citotoxinas inflamatorias y proteger a ratones y simios de dosis letales de SEB administradas en forma de aerosol.

IgY como agente antitumoral

La supresión de la respuesta del sistema apoptótico en conjunto con la auto-renovación y supervivencia de las células tumorales, generan resistencia a la quimioterapia, tratamiento común para tumores[74]. Es aquí donde IgY se muestra como un potencial agente antitumoral al inducir la apoptosis en células cancerosas. Por ejemplo, Xiao *et al.*[75] demostró que IgY anti- HER2 conjugadas con nanotubos de carbono permiten la destrucción selectiva de células de cáncer de mama. Por otro lado, Chávez *et al.*[76] evidenció que IgY-anti-abrina ejercia actividad citotóxica contra el biomarcador de células (CD133) en glioblastoma.

IgY como agente antiobesidad

La obesidad es una enfermedad grave de la sociedad actual, considerada como un trastorno metabólico de lípidos y enzimas; por ello se han propuesto desarrollar fármacos con inhibidores de lipasa pancreática, tanto naturales como sintéticos[77]. Hace poco Hirose *et al.*[78] desarrolló una IgY anti-lipasa, que tras probarse a nivel *in vivo* e *in vitro*, redujó el tejido adiposo y el nivel de grasa hepática en sangre. IgY actuó como agente antiobesidad, al inhibir y reducir la absorción intestinal de lipasa, y aumentar la excreción fecal de triglicéridos.

IgY como agente antiinfeccioso

La prevención y tratamiento temprano de enfermedades infecciosas es indispensable para combatir la morbilidad y la mortalidad asociada a patógenos como: virus, bacterias, parásitos y hongos[3]. La capacidad de IgY para neutralizar y eliminar patógenos a través del intestino lo han convertido en un potencial agente antiinfeccioso. Por ejemplo, la inmunoterapia antimicótica con IgY se ha vuelto atractiva como complemento a los fármacos antimicóticos existentes, asociada a micosis invasiva[79]. Se han desarrollado preparaciones a base de IgY que inhiben la adhesión y disminuyen la colonización del hongo *Candida albicans*[80], un gel de uso oral desarrollado por Takeuchi *et al.*[81]. Asimismo se ha reportado el uso de IgY en parasitología, como método de diagnóstico temprano[82,83]. Thirumalai *et al.*[31] demostró que las preparaciones de IgY policlonal son la forma más experimentada y adecuada de inmunoterapia, puesto que se pueden aislar grandes cantidades con una alta especificidad. Por ejemplo, Sampaio *et al.*[82] y Grando *et al.*[84] evaluaron el potencial terapéutico de IgY- anti *Trypanosoma*, a nivel *in vitro* e *in vivo*, reportando un aumento en la viabilidad de las células y la supervivencia de los animales infectados. Asimismo Espín *et al.*[85] desarrolló una IgY anti- Leishmania

mexicana, que permite detectar concentraciones mínimas (5-50 µg/mL) del parásito.

IgY para contrarrestar respuestas autoinmunes

IgY ha demostrado un potencial para disminuir las respuestas autoinmunes asociadas a enfermedades y alérgenos. Husby *et al.*[86] desarrolló una IgY anti-gliadina (glicoproteína presente en cereales) para tratar la enfermedad celíaca, enfermedad generada por la intolerancia al glúten, consiguiendo inhibir la absorción de gliadina y evitar la respuesta inflamatoria. Worledge *et al.*[87] reportó el uso de IgY anti- TNFα (factor de necrosis tumoral) para tratar la enfermedad de Crohn y la colitis ulcerosa, consiguiendo un efecto preventivo y más eficaz que los fármacos antiinflamatorios. Incluso se ha desarrollado una IgY (IgY- anti αGal) que evita el rechazo de xenotrasplantes en primates, al impedir que los anticuerpos naturales xenoreactivos interactúan con el tejido porcino trasplantado[88]. Por último, se ha empleado IgY como agente anti-alergénico (Figura 2), Weixu *et al.*[89] evaluó el efecto de IgY- anti IL-β1/TNF-α en cobayas con rinitis alérgica, donde observó una reducción del número de eosinófilos, neutrófilos y linfocitos en los pulmones.

IgY como terapia de infecciones humanas

En la actualidad se exige una constante demanda de terapias que desarrollen inmunidad inmediata y a largo plazo, con una producción continua y escalable, que garantice pureza y suministro constante[90]. Los anticuerpos IgY se muestran como una inmunoterapia pasiva prometedora y eficaz en el tratamiento de muchas infecciones[91], principalmente del sistema respiratorio, digestivo y oral[92]. A continuación, se abordará el uso de IgY para la prevención y terapia de infecciones bacterianas y virales, mediante la recopilación de ensayos clínicos registrados (Tabla 1), patentes (Tabla 2) y productos comerciales (Tabla 3) desarrolladas en el periodo de 2010-2021.

Infecciones bacterianas

Los patógenos bacterianos se caracterizan por su capacidad de replicarse de forma autónoma y por secretar factores de virulencia fácilmente propagables como: toxinas, pigmentos, proteínas y moléculas de señalización[93]. Que en conjunto con la aparición de bacterias multirresistentes, por el uso indiscriminado de antibióticos, ha convertido las infecciones bacterianas en una amenaza para la salud pública en todo el mundo[94]. Como alternativa al uso de antibióticos se propone utilizar anticuerpos IgY, puesto que su capacidad de adhesión disminuye y previene la colonización bacteriana, sobre todo en la etapa inicial, impidiendo que se transformen en infecciones crónicas[10].

Se ha evaluado el uso de IgY contra patógenos de la cavidad oral, tales como *Prevotella intermedia*[95], *Fusobacterium nucleatum*[42], *Streptococcus mutans*[96], *Porphyromonas gingivalis*[97], entre otras. Tras la administración oral de IgY en pastillas, sprays y enjuagues bucales (Tabla 1) se evitó desarrollar caries, acumular placa dental y posibles reinfecciones, incluso trataron la periodontitis y gingivitis[98]. También, se ha administrado IgY de forma intranasal contra patógenos del tracto respiratorio, tales como *Mycobacterium tuberculosis*[99], *Staphylococcus aureus*[100] y *Pseudomona aeruginosa*[101]. Donde IgY neutralizó los patógenos en el tracto respiratorio y pulmones,

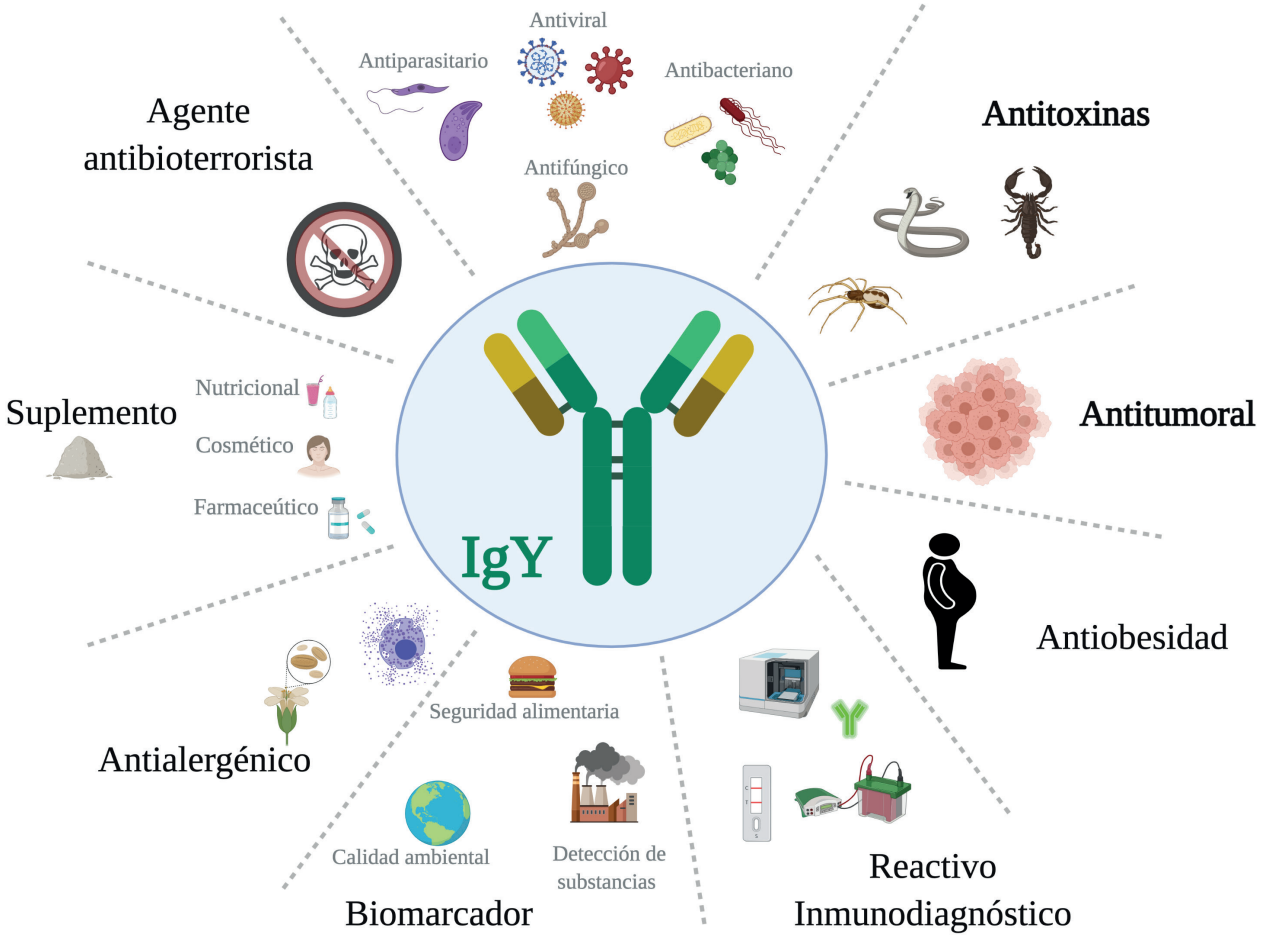

Figura 2. Aplicaciones del anticuerpo IgY.

además se vio que al utilizar IgY como adyuvante de antibióticos este permite reducir la colonización en los pulmones[102].

Por otro lado, los principales patógenos asociados a intoxicaciones alimentarias y gastritis son las bacterias gastrointestinales *Escherichia coli*, *Salmonella spp.*[103], *Clostridium difficile*[104], *Helicobacter pylori*[105,106], *Vibrio cholerae*[107], entre otras. Es necesario eliminar patógenos del estómago para evitar que se desarrollen afecciones más severas como úlceras y cáncer de estómago[108]. Se han realizado ensayos clínicos para investigar el efecto de IgY por administración oral, en fármacos (GastimunHP y GastimunHp Plus) y suplementos dietéticos (IM-01) (Tabla1), donde se evidencia de forma general que estos brindan protección contra enterobacterias y mejoran los síntomas clínicos como la diarrea[109]. Asimismo, se ha evaluado el uso de IgY contra bacterias asociadas al desarrollo de acné (*Propionibacterium acnes*) y dermatitis atópica (*Staphylococcus aureus*)[110], donde IgY ha permitido controlar la secreción de enterotoxinas y mejorar la barrera cutánea[100].

Finalmente, se ha evaluado el uso de IgY contra bacterias resistentes a antibióticos betalactámicos como *Acinetobacter baumannii*[111], *Klebsiella pneumoniae* y *Escherichia coli* (Tabla 1), logrando erradicar el transporte intestinal de las enzimas BLEE (betalactamasas de expectro extendido) responsables de generar resistencia a este tipo de antibióticos[12].

Infecciones Virales

Los virus son organismos contagiosos con una alta capacidad de adaptabilidad y potencial pandémico, que se caracterizan por utilizar las vías del propio huésped para replicarse y propagarse[112]. Pese a que ya se disponen de vacunas para algunas enfermedades virales, estas generan incertidumbre acerca de su eficacia, capacidad de producción y entrega masiva[113]. Es así, que en 1990 el desarrollo de IgY anti-rotavirus[114] válida el uso de la tecnología IgY como tratamiento de infecciones virales, puesto que, responde a la necesidad urgente de producir anticuerpos contra componentes virales específicos en un corto tiempo, un bajo costo y sin dañar las células huésped[92].

Se ha propuesto el uso de IgY para tratar infecciones causadas por virus altamente contagiosos y mortales como el ébola[115], hepatitis[116], dengue[117,118], zika[119], entre otros; donde la IgY ha permitido neutralizar la replicación viral, atenuar la infección y disminuir la letalidad en infecciones leves y asintomáticas.

Ademas la administración oral de IgY para tratar infecciones gastrointestinales asociadas a rotavirus y norovirus. En el ensayo clínico del producto PTM202 con IgY- anti rotavirus que se probó en niños con diarrea, tras su aplicación se mejoraron los síntomas asociados como la diarrea y fiebre (Tabla 1)[120]. Por otro lado, Dai *et al.*[114] evalúo la producción a gran escala de IgY anti-norovirus, obteniéndose en tan solo 3 meses concentraciones de 4,7-9,2 mg/mL de yema de huevo, demostrando el potencial antiviral y diagnóstico de IgY.

En infecciones respiratorias virales los primeros informes de utilización de la tecnología IgY fue hace 20 años, al aplicar IgY por administración intranasal en modelos animales y tener éxito en virus como: virus sincitial respiratorio, virus de la gripe, virus de Sendai, entre otros[9]. Posteriormente se logró llegar a ensayos clínicos en humanos para los virus de la influenza A (H1N1[121] y H5N1[122]), influenza B[123], Hantavirus[124,125], SARS[54], entre otros. Donde IgY consiguió neutralizar la infectividad y reducir la replicación de estos virus en los pulmones, previniendo síndromes respiratorios agudos y graves.

IgY como potencial inmunoterapia para el COVID-19

En diciembre de 2019 en Wuhan-China se reportó un grupo de pacientes con neumonía asociada al coronavirus del síndrome respiratorio agudo severo 2 (SARS-CoV-2)[126], virus que ha mostrado una alta letalidad infecciosa y significativa mortalidad. Esta infección respiratoria se caracteriza por su alto grado de propagación y adaptabilidad, que en conjunto con las malas prácticas de bioseguridad ejecutadas por la población han permitido que se desarrolle la actual pandemia del COVID-19[92]. En consecuencia ha sido de suma urgencia el desarrollo de terapias y profilácticos efectivos[127]. En base a la experiencia con el tratamiento del SARS, Fu *et al.*[54] propone una combinación de vacuna, inmunización pasiva y fármacos, para controlar de forma eficaz este tipo de infecciones.

La proteína pico (S) del SARS está compuesta por dos subunidades, la subunidad S1 que contiene el dominio de unión al receptor (RBD) y la subunidad S2 que media la fusión entre el virus y la célula huésped[128]. Por esta razón la proteína S se ha convertido en el principal epítopo para desarrollar medicamentos antivirales, vacunas y anticuerpos[129]. Tomando en cuenta esta noción, la tecnología IgY se muestra como un potencial material clínico antiinfeccioso. Lu *et al.*[130] desarrolló IgY-S específica para el epítopo SIIAYTMSL de la proteína S, epítopo que se superpone a la región de escisión de las subunidades S1 y S2. IgY-S exhibió una alta inmunorreactividad en ensayos ELISA y su uso permitiría prevenir la infección de las células mediante un bloqueo físico. Es decir, IgY- S evita el acceso de las enzimas proteolíticas al sitio de escisión S1/S2 y se evade la fusión de la membrana de las células y el virus. Somasundaram *et al.*[131] propone desarrollar un anticuerpo recombinante de fragmento variable de cadena única (scFv) contra la subunidad S1, puesto que, IgY monoclonal ha demostrado ser más específica en comparación con IgY policlonal al reconocer un único epítopo. Se propone obtener esta IgY monoclonal anti S1 mediante tecnología de presentación de fagos ya que esta tecnología es más estandarizada, reproducible y adecuada para la producción a gran escala. Asimismo, a nivel preclínico se ha desarrollado el aerosol nasal IGY-110 que busca neutralizar el SARS-CoV-2 en la cavidad nasal, área primaria de infección[132]. Por otro lado, se ha empezado a reclutar pacientes para probar la seguridad y tolerabilidad de IgY anti-SARS-CoV-2 (Tabla 1) administrada por vía intranasal en participantes sanos, con el fin de prevenir la infección.

Patentes de IgY

IgY ha demostrado a lo largo de la historia tener un amplio potencial para desarrollar aplicaciones a base de inmunización pasiva, a partir del año 2000 el aumento de investigaciones y publicaciones[12]. Leiva *et al.*[143] menciona que a partir del 2010 se empiezan a generar patentes de IgY asociadas al diagnóstico, terapia y profilaxis en medicina humana, principalmente en patologías como periodontitis, gingivitis, úlceras gástricas, infecciones asociadas al virus del papiloma humano, disbiosis, problemas nutricionales y metabólicos.

Hay que considerar que la estructura de la inmunoglobulina IgY no es patentable, no obstante, es posible patentar el método de preparación de IgY (obtención, purificación y conservación), su forma de producción y el producto a base de IgY[18]. Por ejemplo, la solicitud de patente WO2016191389 establece un nuevo método para preparar IgY contra las bacterias causantes de periodontitis (*Porphyromonas gingivalis* / *Streptococcus mutans*/ *Aggregatibacter actinomycetemcomitans*) mediante la inmunización de gallinas con polipéptidos sintéticos[144]. Asimismo, la solicitud de patente WO2014011853 describe el método para la producción a gran escala de IgY-anti-NoV P (proteína de la cápside de norovirus) mediante la inmuniza-

Producto / Antígeno	Función	Fase / Estatus	Efecto	Identificador / Referencia
Gotero IgY-anti-*SARS-CoV-2*	Prevenir el síndrome respiratorio agudo y grave	Fase I / Reclutamiento	No disponible	NCT04567810 / [117]
PTM202 IgY- anti -rotavirus /*Escherichia coli* /*Salmonella* / *Shigella*	Mejorar la diarrea infantil aguda y el peso de los niños	No aplicable/ Completado	Reducción en la duración de la diarrea aguda no sanguinolenta.	NCT02385773 / [118]
IM-01 IgY-anti- toxinas A y B / esporas de *Clostridium difficile*	Mejorar síntomas clínicos de diarrea	Fase II /Reclutamiento	No disponible	NCT04121169 / [119]
Pastilla IgY-anti- gingipaína *Porphyromona gingivalis*	Tratar la periodontitis	No aplicable / Completado	Reducción de carga bacteriana e índice de sangrado gingival.	NCT02705885 / [120]
Aoliding spray IgY- anti-*Streptococcus mutans*	Prevenir caries en niños en edad preescolar	Fase III / Activo	No disponible	NCT02341352 / [121]
GastimunHP IgY-anti-ureasa *Helicobacter pylori*	Tratar la gastritis crónica	No aplicable/ Completado	No disponible	NCT02721355 / [122]
GastimunHp Plus IgY-anti-*Helicobacter pylori*	Apoyar el tratamiento de úlcera péptica	No aplica / Reclutamiento	No disponible	NCT04025983 / [123]
Enjuague bucal IgY-anti- *Pseudomona aeruginosa*	Evitar infecciones bucales en pacientes con fibrosis quística	Fase II / Completado	Disminución del tiempo para contraer una nueva infección por bacterias u hongos oportunistas.	NCT00633191 / [124]
Enjuague bucal IgY- anti- *Pseudomona aeruginosa*	Prolongar tiempo de reinfección tras infección aguda o intermitente	Fase III / Completado	Buen perfil de tolerancia; pero no demostró beneficio en pacientes con fibrosis quística.	NCT01455675 / [125]
Solución oral IgY- anti- ESBL-*Klebsiella pneumoniae* y *Escherichia coli*	Erradicar el transporte intestinal con BLEE	Fase II / Completado	No disponible	EudraCT : 2009-011446-26 / [126]

Tabla 1. Principales ensayos clínicos de anticuerpos IgY como tratamiento terapéutico y profiláctico de infecciosas víricas y bacterianas en humanos. Se incluyó únicamente ensayos clínicos registrados en las bases de datos gubernamentales de Clinical Trials de EEUU, Europa y Japón durante el periódo de 2010-2021. Esta lista incluye ensayos clínicos registrados en bases de datos de organizaciones gubernamentales de EEUU (https://clinicaltrials.gov/), Japón (https://www.umin.ac.jp/ctr/) y Europa (https://www.clinicaltrialsregister.eu/), las bases de datos se accedieron por última vez el 15 de enero de 2021.

ción de las gallinas con partículas recombinantes de norovirus, además estandariza las condiciones en las que IgY se logra mantener estable (70 °C durante 30 minutos o a un pH de 4-9 por 3 h[145]). En el caso de productos patentados a base de IgY tenemos la solicitud de patente CN104739719, una fórmula de una pasta de dientes a base de IgY anti-*S. mutans* con compuestos como lisozima y extractos de plantas.

En la tabla 2 se presentan más patentes de IgY como inmunoterapia de infecciones virales y bacterianas en humanos, para ello, se revisaron las patentes registradas entre 2010-2021 en la base de datos Patentscope.

Productos comerciales de IgY

Desde hace más de 20 años se ha registrado un incremento en la comercialización de IgY a nivel mundial buscando promover la salud de los seres humanos y animales[155], donde se ha visto que los fundadores, líderes y expertos en tecnología IgY son los países asiáticos tales como Corea del Sur, Japón, China y Vietnam. Este incremento en la comercialización de IgY se refleja con la variedad de ensayos clínicos con resultados alentadores que se han logrado patentar y llevar al mercado como fármacos y suplementos nutracéuticos, basados en formulaciones monoespecíficas o mixtas de IgY (Tabla 3)[67,68]. La administración parenteral de IgY mediante formulaciones orales e intranasales son las más comunes, ya que permiten mantener estable IgY a temperatura ambiente por más tiempo. Además, cuentan con un registro de perfil de seguridad al usar IgY en forma de huevo entero en polvo, la yema entera en polvo o únicamente la IgY purificada[13].

En el ámbito veterinario se ha utilizado IgY en animales domésticos para mejorar la eficiencia de su alimentación, la tasa de crecimiento y de forma general la salud del animal[156]. Aquí

Producto / Antígeno	Compañía	Efecto	Uso	Ref.
Ovopron ® IgY- anti- ureasa *Helicobacter pylori*	Pharma Foods International Co., Ltd.	Erradica y previene infección, úlceras gástricas y duodenales.	Yogurt, tabletas	135
i26 ® IgY- contra 26 patógenos entéricos humanos	Arkion Life Sciences	Mejora la función digestiva, equilibra la flora intestinal y regula el estrés inflamatorio intestinal.	Tabletas, cápsulas	130
Ovalgen® HP IgY-anti- *Helicobacter pylori*	EW Nutrition & Corporación Ghen	Fortalece sistema inmune intestinal, evitando la gastritis	Yogurt, comprimidos, cápsulas	136
Ovalgen® DC IgY-anti- *Streptococcus mutans*		Cuidado bucal y salud dental, evitando caries	Yogurt, tabletas, dulces, enjuague bucal, pasta de dientes	
Ovalgen® PG IgY-anti- *Porphyromonas gingivalis*		Cuidado bucal, salud de las encías, evitando periodontitis y gingivitis.	Cosméticos, tabletas, goma de mascar, enjuagues bucales, pasta de dientes	
Ovalgen® FL IgY-anti-Influenza		Prevención y mitigación de infecciones del tracto respiratorio, principalmente gripe estacional	Tabletas, goma de mascar, filtros de aire, mascarillas	
Ovalgen® CA IgY-anti-Candida albicans		Cuidado bucal y de la piel	Gel dental, cosméticos	
Ovalgen® RV IgY-anti- rotavirus humano		Fortalecimiento intestinal de niños	Leche de fórmula para bebé	
Ovalgen® CS IgY-anti-Cronobacter sakazakii		Fortalecimiento intestinal de niños	Leche de fórmula para bebé	
Muno-IgY ™ --	Life Sciences	Suplemento dietético de recuperación inmunológica	Tabletas	137
Ulcer lock® IgY-anti- ureasa- *Helicobacter pylori*/ *a*nti - *O157: H7- Escherichia coli* /anti- *Salmonella*	DAN Biotech Inc.	Erradica y previene infecciones, mejorando las úlceras gástricas e intoxicación alimentaria	Aditivo alimentario en polvo y líquido	138
Gasto lock® IgY-anti-*rotavirus*/ anti- *Escherichia coli* /anti-*Salmonella*		Fortalecimiento intestinal de neonatos y niños, mejorando la diarrea aguda	Leche de fórmula para bebé, aditivo alimentario en productos lácteos y postres.	139
Cleanato® IgY-anti- *Staphylococcus aureus*		Mejora la barrera cutánea y controla las enterotoxinas estafilocócicas en dermatitis atópica.	Spray, cremas, jabones, cosméticos	140

Tabla 2. Patentes de IgY como inmunoterapia de infecciones bacterianas y víricas en humanos. Abreviaturas NoV P: proteína de la cápside de norovirus; VPH: virus del papiloma humano ; L1: proteína de la cápside del virus del papiloma humano ; E6/E7: oncoproteínas del virus del papiloma humano.

encontramos empresas como Aova Technologies que ofrece la línea de productos BIG™ para ganado y peces utilizados en acuicultura[157]. PRN Pharmacal con el suplemento alimenticio GastroMate® que apoya la salud digestiva de perros y cachorros[158]. BIOINNOVO con el polvo IgY DNT que se incorpora a la dieta láctea de terneros para controlar agentes como rotavirus A, coronavirus, *Escherichia coli* y *Salmonella*[159]. Trouw Nutrition con la línea Protimax® para ganado con productos como: Protimax®-T Forte para aumentar el peso y prevenir infecciones por patógenos entéricos como *Escherichia coli*, *Salmonella*, *Clostridium perfringens*, rotavirus, coronavirus y *Cryptosporidium*; y EggMotion como suplemento alimenticio para la salud intestinal de mascotas[160].

Igualmente, en el ámbito de la salud humana se han desarrollado una variedad de productos de consumo diario que van desde lácteos y pastillas hasta cremas, jabones y mascarillas (Tabla 3). Básicamente estos productos fortalecen el sistema inmune y previenen la adhesión de patógenos en la boca, tracto gastrointestinal y rostro[67,161]. Existen empresas que han desarrollado productos para uso humano y animal. Pharma Foods International Co. Ltd con el ingrediente funcional Ovopron IgY para el tratamiento y prevención de infecciones asociadas a *Helicobacter pylori* en humanos (Tabla 3). Arkion Life Sciences con su la línea i26® Companion para mascotas que ayuda en la salud bucal y sensibilidad digestiva, mejorando la salud de articulaciones, piel y pelaje. Suplementos para humanos como i26® un suplemento probiótico y Muno-IgY ™ como suplemento dietético[162] (Tabla 3). También tenemos a EW Nutrition con la línea Globigen® para mejorar la nutrición y el estado de salud intestinal de rumiantes y porcinos jóvenes durante el período de destete. Dentro de esta línea encontramos productos como: Globigen Jump Start , Globigen Sow y Globigen Life Start. Por otro lado, desarrolló el suplemento alimenticio y cosmético Ovalgen® para el cuidado de la salud humana. Se ha utilizado Ovalgen® como ingrediente funcional de la serie de productos IgYGate®: GastimunHP y GastimunHP Plus para el tratamiento de gastritis y úlceras gástricas, IgYGate®-F contra gripes estacionales ,y como herramienta de apoyo al tratamiento de caries y gingivitis IgYGate® DC-PG[163] (Tabla 3). Por último, Dan Biotech Inc. con su línea Ig-Lock® permite prevenir y controlar infecciones intestinales asociadas a *Escherichia coli*, parvovirus, coronavirus y adenovirus en animales domésticos como perros, aves de corral, ganado vacuno y porcino. Por otro lado, para humanos desarrollo la línea Cleanato® para el cuidado de la piel y Ulcer lock® / Gasto lock® para el fortalecimiento gastrointestinal[164] (Tabla 3).

Ventajas de la Tecnología IgY

Como se ha visto el uso de tecnología IgY en relación a anticuerpos convencionales traen un serie de ventajas como: (1) reemplaza el sangrado de los animales por la recolección de huevos, promoviendo el bienestar animal y disminuyendo el sufrimiento asociado a manipulaciones dolorosas[155], (2) se necesita una baja carga de antígeno para inducir una respuesta inmune específica[156], (3) tiene una alta escalabilidad de producción a un menor costo y tiempo, aproximadamente cinco semanas desde el período de inmunización[44], (4) gracias a su especificidad y acción in situ, no inducen resistencia bacteriana o alteraciones en la flora microbiana normal[67], (5) no genera efectos secundarios tóxicos ya que al estar purificada no contiene albúmina, por lo que, puede incluso utilizarse en pacientes con alergia al huevo[34], (6) al ser una tecnología de inmunización pasiva es aplicable en un rango de edad amplio de pacientes, desde recién nacidos hasta adultos incluidos pacientes inmunodeficientes y embarazadas[92], (7) posee una mayor estabilidad en comparación a anticuerpos mamíferos, esto gracias a su composición genética más sencilla[171], (8) tiene una amplia versatilidad permitiendo utilizarse como anticuerpo policlonal, monoclonal, fragmentado o quimérico[172], y por último (9) ejerce un efecto antimicrobiano e inmunoestimulante adicional gracias a la presencia de proteínas bioactivas encontradas en las preparaciones de IgY en forma de huevo entero en polvo o yema entera en polvo, tales como fosfoproteína fosvitina[173] y derivados del ácido siálico (propiedades antivirales)[174].

Conclusiones

Como se ha visto desde los años 80 hasta la actualidad la tecnología IgY se ha empleado como una herramienta diagnóstica, terapéutica y profiláctica, logrando posicionarse a nivel industrial y comercial en todo el mundo. El uso de huevos como fuente de anticuerpos IgY ha permitido desarrollar una metodología de producción práctica, escalable y de bajo costo. Estos anticuerpos IgY aviar han atraído cada vez más la atención de la comunidad científica para reemplazar a los anticuerpos IgG de mamíferos, puesto que, sus particularidades estructurales y funcionales le han otorgado una mayor especificidad, baja reactividad cruzada y alta vida media circulante. En cuanto a su modo de acción se han descubierto los mecanismos de acción general, donde si bien IgY no ejerce una erradicación microbiana total permite reducir significativamente la carga de patógenos hasta el punto en el que la propia inmunidad del paciente puede erradicarlos. Se han propuesto que las funciones efectoras de IgY son: el bloqueo de adherencia del patógeno, neutralización de epítopos específicos incluidos toxinas, opsonización del patógeno y formación de aglutinados de antígenos-anticuerpos para eliminarlos a través del intestino.

Desde 2010 se registra una mayor acogida de la tecnología IgY en la medicina humana gracias a sus propiedades antiinfecciosas, antitumorales, antitoxinas, antiinflamatorias y antiobesidad. Afirmando que el uso de anticuerpos IgY permite tratar y prevenir infecciones víricas y bacterianas. Este hecho se evidencia con el incremento de ensayos clínicos, patentes y productos a base de IgY, por ejemplo, ya se comercializan una gran variedad de productos de consumo diario, tales como: fármacos, cosméticos, filtros de mascarilla, suplementos y nutracéuticos. Además el uso de IgY en lugar de antibióticos para tratar este tipo de infecciones responde a la grave problemática de salud que representa el desarrollo de patógenos resistentes a antimicrobianos.

Por último, como hemos visto el mundo se enfrenta a uno de los mayores desafíos sanitarios con la actual pandemia del COVID-19, evidenciando la necesidad urgente de nuevas o mejoradas terapias. Y como alternativa del uso de la tecnología IgY como herramienta biotecnológica segura, eficaz, económica y versátil para disminuir la incidencia, prevalencia y severidad de varias enfermedades infecciosas.

Referencias bibliográficas

1. García Palomo JD, Agüero Balbín J, Parra Blanco JA, Santos Benito MF. Enfermedades infecciosas. Concepto. Clasificación. Aspectos generales y específicos de las infecciones. Criterios de sospecha de enfermedad infecciosa. Pruebas diagnósticas complementarias. Criterios de indicación. Medicine (Baltimore) 2010; 10: 3251–3264.

Antígeno	Título	Patente	Ref
IgY- anti- *Staphylococcus aureus/ Citrobacter/ Corynebacteria / Klebsiella*	Composición de productos farmacéuticos y cosméticos	WO2002002642	143
IgY- anti-toxina-*Clostridium tetani*	Antitoxina tetánica (de origen de yema de huevo de gallina)	IN1907/MUM/2006	144
IgY-anti-*Helicobacter pylori*	Composición farmacéutica que comprende anticuerpos IgY anti-*H. pylori* ureasa y un inhibidor de la secreción de ácido gástrico	EP1172116	145
IgY-anti-*Bacillus cereus*	Generación de anticuerpos de pollo contra patógenos microbianos *Bacillus cereus* de uñas humanas	IN201941048986	146
IgY- anti - *Vibrio parahaemolyticus*	Anticuerpo anti-vibrio parahaemolyticus de yema de pollo, método de preparación y aplicación del mismo	CN101343320	147
IgY-anti-*Mycobacterium tuberculosis*	Preparación inmune de anticuerpos específicos IgY y su aplicación en la prevención y el tratamiento de la infección por *Mycobacterium tuberculosis*	CN1569231	148
IgY.-anti-*Streptococcus mutans*	Combinación de IgY contra la caries dental	US20040126384	149
IgY - anti-*Porphyromonas gingivalis* / *Fusobacterium nucleatum*	Enjuague bucal para prevenir la gingivitis y el mal aliento preparado con anticuerpo IgY específico anti-*Porphyromonas gingivalis y Fusobacterium nucleatum*	CN102860932	150
IgY- anti- toxinas A y B *Clostridium difficile*	Composiciones contra toxinas bacterianas	WO2013009843	151
IgY-anti-*Rotavirus A*	IgY contra el rotavirus	KR1020010016599	152
IgY anti-*SARS-CoV*	Anticuerpo contra SARS-CoV IgY y su método de preparación	CN1621417	153
IgY-anti-partícula P-*Norovirus*	IgY de partículas de norovirus P y sus derivados	US20140017257	154
IgY-anti-VPH	Nuevo preparado anti-virus del papiloma humano (VPH) y endometritis	CN104056268	155
IgY-anti-VPH-L1-E6-E7 (proteínas del Virus del Papiloma Humano)	Anti-HPV-L1 y E6 / E7- IgY de amplio espectro , anticuerpo de molécula pequeña y aplicación del mismo	CN110054686	156

Tabla 3. Productos suplementados con IgY para uso humano. Datos tomados de la base de datos Patentscope.

2. Dobson AP, Carper ER. Infectious Diseases and Human Population History: Throughout history the establishment of disease has been a side effect of the growth of civilization. BioScience 1996; 46: 115–126.
3. Casadevall A. Antibody-based therapies for emerging infectious diseases. Emerg Infect Dis 1996; 2: 200–208.
4. Kaufmann SHE, Dorhoi A, Hotchkiss RS, Bartenschlager R. Host-directed therapies for bacterial and viral infections. Nat Rev Drug Discov 2018; 17: 35–56.
5. Nii-Trebi NI. Emerging and Neglected Infectious Diseases: Insights, Advances, and Challenges. BioMed Res Int 2017; 2017: 5245021.
6. Oral HB, Ozakin C, Akdiş CA. Back to the future: antibody-based strategies for the treatment of infectious diseases. Mol Biotechnol 2002; 21: 225–239.
7. Patterson R, Youngner JS, Weigle WO, Dixon FJ. Antibody Production and Transfer to Egg Yolk in Chickens. J Immunol 1962; 89: 272–278.
8. Thomsen K, Christophersen L, Bjarnsholt T, Jensen PØ, Moser C, Høiby N. Anti-Pseudomonas aeruginosa IgY antibodies augment bacterial clearance in a murine pneumonia model. J Cyst Fibros Off J Eur Cyst Fibros Soc 2016; 15: 171–178.
9. Xu Y, Li X, Jin L, Zhen Y, Lu Y, Li S et al. Application of chicken egg yolk immunoglobulins in the control of terrestrial and aquatic animal diseases: a review. Biotechnol Adv 2011; 29: 860–868.
10. Schade R, Calzado EG, Sarmiento R, Chacana PA, Porankiewicz-Asplund J, Terzolo HR. Chicken egg yolk antibodies (IgY-technology): a review of progress in production and use in research and human and veterinary medicine. Altern Lab Anim ATLA 2005; 33: 129–154.
11. Thu HM, Myat TW, Win MM, Thant KZ, Rahman S, Umeda K et al. Chicken Egg Yolk Antibodies (IgY) for Prophylaxis and Treatment of Rotavirus Diarrhea in Human and Animal Neonates: A Concise Review. Korean J Food Sci Anim Resour 2017; 37: 1–9.
12. Leiva CL, Gallardo MJ, Casanova N, Terzolo H, Chacana P. IgY-technology (egg yolk antibodies) in human medicine: A review of patents and clinical trials. Int Immunopharmacol 2020; 81: 106269.
13. Hatta H, Horimoto Y. Chapter 16: Applications of Egg Yolk Antibody (IgY) in Diagnosis Reagents and in Prevention of Diseases. In: Eggs as Functional Foods and Nutraceuticals for Human Health. 2019, pp 305–328.
14. Rahman S, Van Nguyen S, Icatlo Jr. FC, Umeda K, Kodama Y. Oral passive IgY-based immunotherapeutics. Hum Vaccines Immunother 2013; 9: 1039–1048.
15. Muller S, Schubert A, Dyck T, Oelkrug C. IgY antibodies in human nutrition for disease prevention. Nutr J 2015; 14: 109.
16. Klemperer F. Ueber natürliche Immunität und ihre Verwerthung für die Immunisirungstherapie. Arch Für Exp Pathol Pharmakol 1893; 31: 356–382.
17. Schade R, Hlinak A. Egg Yolk Antibodies, State of the Art and Future Prospects. ALTEX 1996; 13: 5–9.
18. Schade R, Terzolo H. IgY-technology: application and trends. [Internet]. 2006. Available from: https://www.researchgate.net/publication/267702265_IgY-technology_application_and_trends
19. Schade R, Staak C, Hendriksen C, Erhard M, Hugl H, Koch G et al. La producción de anticuerpos aviares (yema de huevo): IgY: Informe y recomendaciones del taller ECVAM 21 1,2. Altern Lab Anim 1996; 24: 925–934.
20. Warr G, Magor K, Higgins D. IgY: clues to the origins of modern antibodies. Immunol Today 1995; 16: 392–398.
21. Pereira EPV, Van Tilburg MF, Florean EOPT, Guedes MIF. Egg yolk antibodies (IgY) and their applications in human and veterinary health: A review. Int Immunopharmacol 2019; 73: 293–303.
22. Sun S, Mo W, Ji Y, Liu S. Preparation and mass spectrometric study of egg yolk antibody (IgY) against rabies virus. Rapid Commun Mass Spectrom RCM 2001; 15: 708–712.
23. Faith RE, Clem LW. Passive cutaneous anaphylaxis in the chicken. Immunology 1973; 25: 151–164.
24. Spillner E, Braren I, Greunke K, Seismann H, Blank S, du Plessis D. Avian IgY antibodies and their recombinant equivalents in research, diagnostics and therapy. Biologicals 2012; 40: 313–322.
25. Hernández Castillo LM, Duque Restrepo AM, Martínez Delgado CM. Tecnología IgY para el control de enfermedades infecciosas como la caries dental. Tesis [Internet]. Universidad CES. 2015. Available from: https://repository.ces.edu.co/handle/10946/390
26. Sesarman A, Mihai S, Chiriac MT, Olaru F, Sitaru AG, Thurman JM et al. Binding of avian IgY to type VII collagen does not activate complement and leucocytes and fails to induce subepidermal blistering in mice. Br J Dermatol 2008; 158: 463–471.
27. Chacana P, Terzolo H, Gutierrez E. Tecnología IgY o aplicaciones de los anticuerpos de yema de huevo de gallina. Rev Med Vet 2004; 85: 179–189.
28. Nguyen HH, Tumpey TM, Park H-J, Byun Y-H, Tran LD, Nguyen VD et al. Prophylactic and Therapeutic Efficacy of Avian Antibodies Against Influenza Virus H5N1 and H1N1 in Mice. PLoS ONE 2010; 5. doi:10.1371/journal.pone.0010152.
29. Carlander D, Stålberg J, Larsson A. Chicken Antibodies: A Clinical Chemistry Perspective. Ups J Med Sci 1999; 104: 179–189.
30. Contreras VT, Lima ARD, Navarro MC, Arteaga RY, Graterol D, Cabello L et al. Producción y purificación de anticuerpos (IgY) a partir de huevos de gallinas inmunizadas con epimastigotas de Trypanosoma cruzi. Salus 2005; 9: 21–27.
31. Thirumalai D, Visaga Ambi S, Vieira-Pires RS, Xiaoying Z, Sekaran S, Krishnan U. Chicken egg yolk antibody (IgY) as diagnostics and therapeutics in parasitic infections - A review. Int J Biol Macromol 2019; 136: 755–763.
32. Lundqvist ML, Middleton DL, Radford C, Warr GW, Magor KE. Immunoglobulins of the non-galliform birds: Antibody expression and repertoire in the duck. Dev Comp Immunol 2006; 30: 93–100.
33. Tsubokura K, Berndtson E, Bodgstedt A, Kaijser B, Kim M, Ozeki M et al. Oral administration of antibodies as prophylaxis and therapy in Campylobacter jejuni-infected chickens. Clin Exp Immunol 1997; 108: 451–455.
34. Abbas AT, El-Kafrawy SA, Sohrab SS, Azhar EIA. IgY antibodies for the immunoprophylaxis and therapy of respiratory infections. Hum Vaccines Immunother 2018; 15: 264–275.
35. Arimitsu H, Sasaki K, Kohda T, Shimizu T, Tsuji T. Evaluation of Shiga toxin 2e-specific chicken egg yolk immunoglobulin: Production and neutralization activity. Microbiol Immunol 2014; 58: 643–648.
36. Mitteness BM, Phillips C., Inventors; Camas Incorporated, assignee: Compositions Against Bacterial Toxins. World Intellectual Property Organization patent WO 2013009843. 2013 Jan 7.
37. Lee EN, Sunwoo HH, Menninen K, Sim JS. In vitro studies of chicken egg yolk antibody (IgY) against Salmonella enteritidis and Salmonella typhimurium. Poult Sci 2002; 81: 632–641.
38. Zhen Y-H, Jin L-J, Guo J, Li X-Y, Lu Y-N, Chen J et al. Characterization of specific egg yolk immunoglobulin (IgY) against mastitis-causing Escherichia coli. Vet Microbiol 2008; 130: 126–133.
39. Murai A. Maternal Transfer of Immunoglobulins into Egg Yolks of Birds. J Poult Sci 2013; 50: 185–193.
40. Ferreira Á, Santos JP, Sousa L de O, Martin I, Alves EGL, Rosado IR. Gallus gallus domesticus: immune system and its potential for generation of immunobiologics. Ciênc Rural 2018; 48. doi:10.1590/0103-8478cr20180250.
41. Nakamura R, Pedrosa-Gerasmio IR, Alenton RRR, Nozaki R, Kondo H, Hirono I. Anti-PirA-like toxin immunoglobulin (IgY) in feeds passively immunizes shrimp against acute hepatopancreatic necrosis disease. J Fish Dis 2019; 42: 1125–1132.
42. Xu FX, Xu YP, Jin LJ, Liu H, Wang LH, You JS et al. Effectiveness of egg yolk immunoglobulin (IgY) against periodontal disease-causing Fusobacterium nucleatum. J Appl Microbiol 2012; 113: 983–991.
43. Barroso P, Murcia H, Vega N, Pérez G. Purification of IgY against Salvia bogotensis lectin. Biomédica 2005; 25: 496–510.
44. Pauly D, Chacana PA, Calzado EG, Brembs B, Schade R. IgY Technology: Extraction of Chicken Antibodies from Egg Yolk by Polyethylene Glycol (PEG) Precipitation. J Vis Exp JoVE 2011. doi:10.3791/3084.

45. Tong C, Geng F, He Z, Cai Z, Ma M. A simple method for isolating chicken egg yolk immunoglobulin using effective delipidation solution and ammonium sulfate. Poult Sci 2015; 94: 104–110.
46. Villaguala C, González C, Pastene E, Farías C, Sáez K, Retamal-Díaz A et al. Obtención de inmunoglobulinas de yema de huevo contra Helicobacter pylori producidos en gallinas araucanas. Arch Med Vet 2016; 48: 79–88.
47. Chang HM, Ou-Yang RF, Chen YT, Chen CC. Productivity and some properties of immunoglobulin specific against Streptococcus mutans serotype c in chicken egg yolk (IgY). J Agric Food Chem 1999; 47: 61–66.
48. Kovacs-Nolan J, Mine Y. 17 - Using egg IgY antibodies for health, diagnostic and other industrial applications. In: Van Immerseel F, Nys Y, Bain M (eds). Improving the Safety and Quality of Eggs and Egg Products. Woodhead Publishing, 2011, pp 346–373.
49. Lévesque S, Martinez G, Fairbrother JM. Improvement of adjuvant systems to obtain a cost-effective production of high levels of specific IgY. Poult Sci 2007; 86: 630–635.
50. Agrawal R, Hirpurkar SD, Sannat C, Gupta AK. Comparative study on immunoglobulin Y transfer from breeding hens to egg yolk and progeny chicks in different breeds of poultry. Vet World 2016; 9: 425–431.
51. Hatta H, Kapoor MP, Juneja LR. Bioactive Components in Egg Yolk. In: Egg Bioscience and Biotechnology. John Wiley & Sons, Ltd, 2008, pp 185–237.
52. Amro WA, Al-Qaisi W, Al-Razem F. Production and purification of IgY antibodies from chicken egg yolk. J Genet Eng Biotechnol 2018; 16: 99–103.
53. Rose ME, Orlans E, Buttress N. Immunoglobulin classes in the hen's egg: Their segregation in yolk and white. Eur J Immunol 1974; 4: 521–523.
54. Fu C-Y, Huang H, Wang X-M, Liu Y-G, Wang Z-G, Cui S-J et al. Preparation and evaluation of anti-SARS coronavirus IgY from yolks of immunized SPF chickens. J Virol Methods 2006; 133: 112–115.
55. Yokoyama H, Peralta RC, Diaz R, Sendo S, Ikemori Y, Kodama Y. Passive protective effect of chicken egg yolk immunoglobulins against experimental enterotoxigenic Escherichia coli infection in neonatal piglets. Infect Immun 1992; 60: 998–1007.
56. Mudili V, Makam SS, Sundararaj N, Siddaiah C, Gupta VK, Rao PVL. A novel IgY-Aptamer hybrid system for cost-effective detection of SEB and its evaluation on food and clinical samples. Sci Rep 2015; 5: 15151.
57. Caza J, Fernandez R, Torres M, Muñoz D, Ortiz Tirado J, Bangeppagari M et al. The development, purification and characterization of anti- vitellogenin antibodies raised in hens (gallus gallus domesticus) against tilapia (oreochromis niloticus) vitellogenin protein. J Microbiol Biotechnol Food Sci 2018. doi:10.15414/jmbfs.2019.8.5.1165-1168.
58. He J, Hu J, Thirumalai D, Schade R, Du E, Zhang X. Development of indirect competitive ELISA using egg yolk-derived immunoglobulin (IgY) for the detection of Gentamicin residues. J Environ Sci Health B 2016; 51: 8–13.
59. Li C, Zhang Y, Eremin SA, Yakup O, Yao G, Zhang X. Detection of kanamycin and gentamicin residues in animal-derived food using IgY antibody based ic-ELISA and FPIA. Food Chem 2017; 227: 48–54.
60. Noack F, Helmecke D, Rosenberg R, Thorban S, Nekarda H, Fink U et al. CD87-positive tumor cells in bone marrow aspirates identified by confocal laser scanning fluorescence microscopy. Int J Oncol 1999; 15: 617–623.
61. Pan Z-L, Ji X-Y, Shi Y-M, Zhou J, He E, Skog S. Serum thymidine kinase 1 concentration as a prognostic factor of chemotherapy-treated non-Hodgkin's lymphoma patients. J Cancer Res Clin Oncol 2010; 136: 1193–1199.
62. Zhang Q, He D, Xu L, Ge S, Wang J, Zhang X. Generation and evaluation of anti-mouse IgG IgY as secondary antibody. Prep Biochem Biotechnol 2020; 50: 788–793.
63. Ferreira Júnior A, Santos JP, Bassi PB, F.F.Bittar J, Bittar ER. IgY-Technology Applied to Studies of Toxoplasma gondii Infection. Toxoplasmosis 2017. doi:10.5772/67997.
64. Nagaraj S, Ramlal S, Kingston J, Batra HV. Development of IgY based sandwich ELISA for the detection of staphylococcal enterotoxin G (SEG), an egc toxin. Int J Food Microbiol 2016; 237: 136–141.
65. He J, Wang Y, Sun S, Zhang X. Evaluation of Chicken IgY Generated Against Canine Parvovirus Viral-Like Particles and Development of Enzyme-Linked Immunosorbent Assay and Immunochromatographic Assay for Canine Parvovirus Detection. Viral Immunol 2015; 28: 489–494.
66. Silva A dos S da, Vasconcelos GALBM de, Kappel LA, Pinto MA, Paula VS de. An immunoenzymatic assay for the diagnosis of hepatitis A utilising immunoglobulin Y. Mem Inst Oswaldo Cruz 2012; 107: 960–963.
67. Rahman S, Nguyen S, Icatlo F, Umeda K, Kodama Y. Oral passive IgY-based immunotherapeutics. Hum Vaccines Immunother 2013; 9. doi:10.4161/hv.23383.
68. Kovacs-Nolan J, Phillips M, Mine Y. Advances in the value of eggs and egg components for human health. J Agric Food Chem 2005; 53: 8421–8431.
69. Araújo AS, Lobato ZIP, Chávez-Olórtegui C, Velarde DT. Brazilian IgY-Bothrops antivenom: Studies on the development of a process in chicken egg yolk. Toxicon Off J Int Soc Toxinology 2010; 55: 739–744.
70. Gutiérrez JM, Theakston RDG, Warrell DA. Confronting the neglected problem of snake bite envenoming: the need for a global partnership. PLoS Med 2006; 3: e150.
71. Alvarez A, Montero Y, Jimenez E, Zerpa N, Parrilla P, Malavé C. IgY antibodies anti-Tityus caripitensis venom: purification and neutralization efficacy. Toxicon Off J Int Soc Toxinology 2013; 74: 208–214.
72. Thalley BS, Carroll SB. Rattlesnake and scorpion antivenoms from the egg yolks of immunized hens. Biotechnol Nat Publ Co 1990; 8: 934–938.
73. LeClaire RD, Hunt RE, Bavari S. Protection against Bacterial Superantigen Staphylococcal Enterotoxin B by Passive Vaccination. Infect Immun 2002; 70: 2278–2281.
74. Yang J, Jin Z, Yu Q, Yang T, Wang H, Liu L. The selective recognition of antibody IgY for digestive system cancers. Chin J Biotechnol 1997; 13: 85–90.
75. Xiao Y, Gao X, Taratula O, Treado S, Urbas A, Holbrook RD et al. Anti-HER2 IgY antibody-functionalized single-walled carbon nanotubes for detection and selective destruction of breast cancer cells. BMC Cancer 2009; 9: 351.
76. Chavez Cortez E-G, Vargas Felix G, Rangel López E, Sotelo J, Martínez-Canseco C, Pérez-de la Cruz V et al. Production and Evaluation of an Avian IgY Immunotoxin against CD133+ for Treatment of Carcinogenic Stem Cells in Malignant Glioma: IgY Immunotoxin for the Treatment of Glioblastoma. J Oncol 2019. doi:10.1155/2019/2563092.
77. Rb B, Kk B. Pancreatic lipase inhibitors from natural sources: unexplored potential. Drug Discov Today 2007; 12: 879–889.
78. Hirose M, Ando T, Shofiqur R, Umeda K, Kodama Y, Nguyen SV et al. Anti-obesity activity of hen egg anti-lipase immunoglobulin yolk, a novel pancreatic lipase inhibitor. Nutr Metab 2013; 10: 70.
79. Datta K, Hamad M. Immunotherapy of Fungal Infections. Immunol Invest 2015; 44: 738–776.
80. Kamikawa Y, Fujisaki J, Nagayama T, Kawasaki K, Hirabayashi D, Hamada T et al. Use of Candida-specific chicken egg yolk antibodies to inhibit the adhering of Candida to denture base materials: prevention of denture stomatitis. Gerodontology 2016; 33: 342–347.
81. Takeuchi S, Motohashi J, Kimori H, Nakagawa Y, Tsurumoto A. Effects of oral moisturising gel containing egg yolk antibodies against Candida albicans in older people. Gerodontology 2016; 33: 128–134.
82. Sampaio LCL, Baldissera MD, Grando TH, Gressler LT, Capeleto D de M, de Sa MF et al. Production, purification and therapeutic potential of egg yolk antibodies for treating Trypanosoma evansi infection. Vet Parasitol 2014; 204: 96–103.
83. Wolf Nassif P, DE Mello TFP, Navasconi TR, Mota CA, Demarchi IG, Aristides SMA et al. Safety and efficacy of current alternatives in the topical treatment of cutaneous leishmaniasis: a systematic review. Parasitology 2017; 144: 995–1004.
84. Grando TH, Baldissera MD, de Sá MF, do Carmo GM, Porto BCZ, Aguirre GSV et al. Avian antibodies (IgY) against Trypanosoma cruzi: Purification and characterization studies. J Immunol Methods 2017; 449: 56–61.

85. Espín Arroba S, Ayala L, Ortíz M, Seqqat R, Torres Arias M. Characterization and Immunologic Response of IgY Against Leishmania Mexicana. Appl Med Res 2021; 8: 86–89.
86. Husby S, Koletzko S, Korponay-Szabó IR, Mearin ML, Phillips A, Shamir R et al. European Society for Pediatric Gastroenterology, Hepatology, and Nutrition guidelines for the diagnosis of coeliac disease. J Pediatr Gastroenterol Nutr 2012; 54: 136–160.
87. Worledge KL, Godiska R, Barrett TA, Kink JA. Oral administration of avian tumor necrosis factor antibodies effectively treats experimental colitis in rats. Dig Dis Sci 2000; 45: 2298–2305.
88. Fryer J, Firca J, Leventhal J, Blondie B, Malcolm A, Ivancic D et al. IgY antiporcine endothelial cell antibodies effectively block human antiporcine xenoantibody binding. Xenotransplantation 1999; 6: 98–109.
89. Wei-xu H, Wen-yun Z, Xi-ling Z, Zhu W, Li-hua W, Xiao-mu W et al. Anti-Interleukin-1 Beta/Tumor Necrosis Factor-Alpha IgY Antibodies Reduce Pathological Allergic Responses in Guinea Pigs with Allergic Rhinitis. Mediators Inflamm 2016. doi:10.1155/2016/3128182.
90. Bentes GA, Lanzarini NM, Lima LRP, Manso PP de A, da Silva A dos S, Mouta S da S e et al. Using immunoglobulin Y as an alternative antibody for the detection of hepatitis A virus in frozen liver sections. Mem Inst Oswaldo Cruz 2015; 110: 577–579.
91. Casadevall A, Scharff MD. Return to the past: the case for antibody-based therapies in infectious diseases. Clin Infect Dis Off Publ Infect Dis Soc Am 1995; 21: 150–161.
92. Constantin C, Neagu M, Diana Supeanu T, Chiurciu V, A. Spandidos D. IgY - turning the page toward passive immunization in COVID-19 infection (Review). Exp Ther Med 2020; 20: 151–158.
93. Bebbington C, Yarranton G. Antibodies for the treatment of bacterial infections: current experience and future prospects. Curr Opin Biotechnol 2008; 19: 613–619.
94. Munita JM, Arias CA. Mechanisms of Antibiotic Resistance. Microbiol Spectr 2016; 4. doi:10.1128/microbiolspec.VMBF-0016-2015.
95. Hou Y-Y, Zhen Y-H, Wang D, Zhu J, Sun D-X, Liu X-T et al. Protective effect of an egg yolk-derived immunoglobulin (IgY) against Prevotella intermedia-mediated gingivitis. J Appl Microbiol 2014; 116: 1020–1027.
96. Bachtiar EW, Bachtiar BM, Soejoedono RD, Wibawan IW, Afdhal A. Biological and Immunogenicity Property of IgY Anti S. mutans ComD. Open Dent J 2016; 10: 308–314.
97. Sandoval R. Inmunoterapia sintética para infecciones por bacterias gram-positivas y gram-negativas. Ecuad ES Calid Rev Científica Ecuat 2020; 7. doi:10.36331/revista.v7i1.93.
98. Schade R, Zhang X-Y, Terzolo HR. Use of IgY Antibodies in Human and Veterinary Medicine. In: Huopalahti R, López-Fandiño R, Anton M, Schade R (eds). Bioactive Egg Compounds. Springer: Berlin, Heidelberg, 2007, pp 213–222.
99. Sudjarwo SA, Eraiko K, Sudjarwo GW, Koerniasari. The Activity of Immunoglobulin Y Anti-Mycobacterium tuberculosis on Proliferation and Cytokine Expression of Rat Peripheral Blood Mononuclear Cells. Pharmacogn Res 2017; 9: S5–S8.
100. Guimarães MCC, Amaral LG, Rangel LBA, Silva IV, Matta CGF, Matta MF de R. Growth inhibition of Staphylococcus aureus by chicken egg yolk antibodies. Arch Immunol Ther Exp (Warsz) 2009; 57: 377–382.
101. Norouzi F, Behrouz B, Ranjbar M, Mousavi Gargari SL. Immunotherapy with IgY Antibodies toward Outer Membrane Protein F Protects Burned Mice against Pseudomonas aeruginosa Infection. J Immunol Res 2020; 2020: 7840631.
102. Sugita-Konishi Y, Shibata K, Yun SS, Hara-Kudo Y, Yamaguchi K, Kumagai S. Immune Functions of Immunoglobulin Y Isolated from Egg Yolk of Hens Immunized with Various Infectious Bacteria. Biosci Biotechnol Biochem 1996; 60: 886–888.
103. Esmailnejad A, Abdi-Hachesoo B, Hosseini Nasab E, Shakoori M. Production, purification, and evaluation of quail immunoglobulin Y against Salmonella typhimurium and Salmonella enteritidis. Mol Immunol 2019; 107: 79–83.
104. Marjorie Pizarro-Guajardo, Díaz-González F, Álvarez-Lobos M, Paredes-Sabja D. Characterization of Chicken IgY Specific to Clostridium difficile R20291 Spores and the Effect of Oral Administration in Mouse Models of Initiation and Recurrent Disease. Front Cell Infect Microbiol 2017; 7. doi:10.3389/fcimb.2017.00365.
105. Hong KS, Ki M-R, Ullah HMA, Lee E-J, Kim YD, Chung M-J et al. Preventive effect of anti-VacA egg yolk immunoglobulin (IgY) on Helicobacter pylori-infected mice. Vaccine 2018; 36: 371–380.
106. Malekshahi ZV, Gargari SLM, Rasooli I, Ebrahimizadeh W. Treatment of Helicobacter pylori infection in mice with oral administration of egg yolk-driven anti-UreC immunoglobulin. Microb Pathog 2011; 51: 366–372.
107. Pu M. Generation and Characterization of specific Chicken Egg Yolk Antibodies (IgY) against Microbial Bio-terroristic Agent (Vibrio cholerae). Res J Anim Vet Fish Sci 2014; 2: 2320–6535.
108. Uemura N, Okamoto S, Yamamoto S, Matsumura N, Yamaguchi S, Yamakido M et al. Helicobacter pylori infection and the development of gastric cancer. N Engl J Med 2001; 345: 784–789.
109. Gordon G, Morán G, Ayala L, Seqqat R, Fernández R, Torres M. Generation and Characterization of IgY antibodies from Lohmann Brown Hens Immunized with Salmonella spp. for their Subsequent Application in Nanotherapy. Biol Med 2016; 80. doi:10.4172/0974-8369.1000284.
110. Revathy J, Karthika S, Sentila R, Michael A. In vitro evaluation of the efficacy of chicken egg yolk antibodies (IgY) generated against Propionibacterium acnes. Int J Cosmet Sci 2014; 36: 68–73.
111. Shi H, Zhu J, Zou B, Shi L, Du L, Long Y et al. Effects of specific egg yolk immunoglobulin on pan-drug-resistant Acinetobacter baumannii. Biomed Pharmacother 2017; 95: 1734–1742.
112. Shahani L, Heredia EJ, Chemaly RF. Antiviral therapy for respiratory viral infections in immunocompromised patients. Expert Rev Anti Infect Ther 2017; 15: 401–415.
113. Dubé E, Laberge C, Guay M, Bramadat P, Roy R, Bettinger J. Vaccine hesitancy: an overview. Hum Vaccines Immunother 2013; 9: 1763–1773.
114. Dai Y-C, Zhang X-F, Tan M, Huang P, Lei W, Fang H et al. A Dual Chicken IgY Against Rotavirus and Norovirus. Antiviral Res 2013; 97: 293–300.
115. Zhang Y, Wei Y, Li Y, Wang X, Liu Y, Tian D et al. IgY antibodies against Ebola virus possess post-exposure protection and excellent thermostability. bioRxiv 2020. doi:10.1101/2020.05.21.108159.
116. Chen DCP., Inventor; Asia Hepato Gene Co., assignee: Compositions and Methods for Treating Hepatitis Virus Infection. World Intellectual Property Organization patent WO 2012016429. 2012 Feb 9.
117. Fink AL, Williams KL, Harris E, Alvine TD, Henderson T, Schiltz J et al. Dengue virus specific IgY provides protection following lethal dengue virus challenge and is neutralizing in the absence of inducing antibody dependent enhancement. PLoS Negl Trop Dis 2017; 11. doi:10.1371/journal.pntd.0005721.
118. O'Donnell KL, Fink A, Nilles ML, Bradley DS. Dengue NS1-specific IgY antibodies neutralizes dengue infection without inducing antibody dependent enhancement. J Immunol 2017; 198: 225.3-225.3.
119. O'Donnell KL, Meberg B, Schiltz J, Nilles ML, Bradley DS. Zika Virus-Specific IgY Results Are Therapeutic Following a Lethal Zika Virus Challenge without Inducing Antibody-Dependent Enhancement. Viruses 2019; 11. doi:10.3390/v11030301.
120. Wang X, Song L, Tan W, Zhao W. Clinical efficacy of oral immunoglobulin Y in infant rotavirus enteritis. Medicine (Baltimore) 2019; 98. doi:10.1097/MD.0000000000016100.
121. Yang Y, Wen J, Zhao S, Zhang K, Zhou Y. Prophylaxis and therapy of pandemic H1N1 virus infection using egg yolk antibody. J Virol Methods 2014; 206: 19–26.
122. Wallach MG, Webby RJ, Islam F, Walkden-Brown S, Emmoth E, Feinstein R et al. Cross-Protection of Chicken Immunoglobulin Y Antibodies against H5N1 and H1N1 Viruses Passively Administered in Miceα . Clin Vaccine Immunol CVI 2011; 18: 1083–1090.
123. Wen J, Zhao S, He D, Yang Y, Li Y, Zhu S. Preparation and characterization of egg yolk immunoglobulin Y specific to influenza B virus. Antiviral Res 2012; 93: 154–159.
124. Brocato R, Josleyn M, Ballantyne J, Vial P, Hooper JW. DNA Vaccine-Generated Duck Polyclonal Antibodies as a Postexposure Prophylactic to Prevent Hantavirus Pulmonary Syndrome (HPS). PLoS ONE 2012; 7. doi:10.1371/journal.pone.0035996.

125. Haese N, Brocato RL, Henderson T, Nilles ML, Kwilas SA, Josleyn MD et al. Antiviral Biologic Produced in DNA Vaccine/Goose Platform Protects Hamsters Against Hantavirus Pulmonary Syndrome When Administered Post-exposure. PLoS Negl Trop Dis 2015; 9. doi:10.1371/journal.pntd.0003803.
126. Zhu N, Zhang D, Wang W, Li X, Yang B, Song J et al. A Novel Coronavirus from Patients with Pneumonia in China, 2019. N Engl J Med 2020; 382: 727–733.
127. Forni G, Mantovani A. COVID-19 vaccines: where we stand and challenges ahead. Cell Death Differ 2021; : 1–14.
128. Du L, He Y, Zhou Y, Liu S, Zheng B-J, Jiang S. The spike protein of SARS-CoV--a target for vaccine and therapeutic development. Nat Rev Microbiol 2009; 7: 226–236.
129. Sternberg A, Naujokat C. Structural features of coronavirus SARS-CoV-2 spike protein: Targets for vaccination. Life Sci 2020; 257: 118056.
130. Lu Y, Wang Y, Zhang Z, Huang J, Yao M, Huang G et al. Generation of Chicken IgY against SARS-COV-2 Spike Protein and Epitope Mapping. J Immunol Res 2020. doi:10.1155/2020/9465398.
131. Somasundaram R, Choraria A, Antonysamy M. An approach towards development of monoclonal IgY antibodies against SARS CoV-2 spike protein (S) using phage display method: A review. Int Immunopharmacol 2020. doi: 85: 106654.
132. IgY Antibody Against Covid-19. Protheragen Inc. [Internet]. 2020. Available from: https://www.protheragen.com/pdf-down/igy-antibody-against-covid-19/
133. ClinicalTrials.gov [Internet]. Stanford University. 2020 Sep 28. Identifier NCT04567810, A Phase 1 Study in Healthy Participants to Evaluate the Safety, Tolerability, and Pharmacokinetics of Single -Ascending and Multiple Doses of an Anti-Severe Acute Respiratory Syndrome Coronavirus 2 (SARS-CoV-2) Chicken Egg Antibody (IgY)(cited 2 Dec2020). Available from:https://clinicaltrials.gov/ct2/show/study/NCT04567810
134. ClinicalTrials.gov [Internet]. University of Colorado, Denver. 2017 Jan 4. Identifier NCT02385773, A Double Blind, Randomized, Placebo-Controlled Trial to Assess the Impact of the Nutritional Product PTM202 on Acute and Long-Term Recovery From Childhood Diarrheal Disease (cited 16 Dec2020). Available from:https://clinicaltrials.gov/ct2/show/NCT02385773
135. ClinicalTrials.gov [Internet]. ImmuniMed Inc. 2019 Oct 8. Identifier NCT04121169, Clinical Effectiveness of Egg-derived Polyclonal Antibodies (IM-01) for the Treatment of Mild-moderate Clostridium Difficile Infection (CDI) (cited 16 Dec2020). Available from: https://clinicaltrials.gov/ct2/show/NCT04121169
136. ClinicalTrials.gov [Internet]. Immunology Research Institute in Gifu. 2016 Mar 7. Identifier NCT02705885, Evaluation of IgY Antibody Effectiveness in Supportive Therapy of Periodontitis Patients (cited 13 May2021). Available from: https://clinicaltrials.gov/ct2/show/NCT02705885
137. ClinicalTrials.gov [Internet]. Chen X.. 2015 Jan 13. Identifier NCT02341352, Study on Children's Dental Caries Prevention and Mechanism (cited 16 Dec2020). Available from: https://clinicaltrials.gov/ct2/show/NCT02341352
138. ClinicalTrials.gov [Internet]. Immunology Research Institute in Gifu. 2016 Aug 29. Identifier NCT02721355, Evaluation of a Health Food Supplement Containing Anti-Helicobacter Pylori Urease IgY Antibody on Patients With Chronic Gastritis in Hanoi, Vietnam (cited 16 Dec2020). Available from:https://clinicaltrials.gov/ct2/show/NCT02721355
139. ClinicalTrials.gov [Internet]. Institute of Gastroenterology and Hepatology, Vietnam. 2020 Jul 27. Identifier NCT04025983, Effectiveness of GastimunHp Plus in Supporting the Treatment of Peptic Ulcer Disease With Helicobacter Pylori Infection (cited 16 Dec2020). Available from: https://clinicaltrials.gov/ct2/show/NCT04025983
140. ClinicalTrials.gov [Internet]. Immunsystem AB. 2016 Aug 31. Identifier NCT00633191, Post Marketing Study of Anti-pseudomonas IgY in Prevention of Recurrence of Pseudomonas Aeruginosa Infections Infections in Cystic Fibrosis (CF) Patients (cited 2 Dec2020). Available from: https://clinicaltrials.gov/ct2/show/study/NCT00633191
141. ClinicalTrials.gov [Internet]. Mukoviszidose Institut gGmbH. 2017 Jul 3. Identifier NCT01455675, Phase III Study to Evaluate Clinical Efficacy and Safety of Avian Polyclonal Anti-Pseudomonas Antibodies (IgY) in Prevention of Recurrence of Pseudomonas Aeruginosa Infection in Cystic Fibrosis Patients (cited 2 Dec2020). Available from: https://clinicaltrials.gov/ct2/show/study/NCT01455675
142. ClinicalTrials.gov [Internet]. Uppsala University. 2011 Jul 4. Identifier EUCTR2009-011446-26-SE, Chicken antibodies (IgY) for the eradication of ESBL-Klebsiella pneumoniae and E coli in carriers (cited 18 Dec2020). Available from: https://www.cochranelibrary.com/central/doi/10.1002/central/CN-01802509/full?highlightAbstract=igy%7Cigi
143. Leiva CL, Gallardo MJ, Casanova N, Terzolo H, Chacana P. Data for: IgY-technology (egg yolk antibodies) in human medicine: a review of patents and clinical trials. 2020; 2. doi:10.17632/9ryvhgm3d2.2.
144. Nordgren R, Dias Figueiredo M., Inventors; Merial, Inc., assignee:Compositions Containing Antimicrobial Igy Antibodies, for Treatment and Prevention of Disorders and Diseases Caused by Oral Health Compromising (ohc) Microorganisms. World Intellectual Property Organization patent WO 2016191389. 2016 Dec 1.
145. Dai Y-C, Jiang X., Inventors; Children's Hospital Medical Center Dai, assignee: Igy from Norovirus P Particles and Their Derivatives. World Intellectual Property Organization patent WO 2014011853. 2014 Jan 16.
146. Pradip K M., Inventor; Immunimed Inc., assignee: Polyclonal antibodies against Clostridium difficile and uses thereof. United States patent US 154008029. 2015 Dec 24.
147. Wei S, Yiqiang A, Qing G., Inventors; Xuzhou Biotechnology Co., Ltd., assignee: Preparation method of egg yolk antibody containing helicobacter pylori resisting IgY and application. Chinese patent CN 198343666. 2017 May 10.
148. Levin M, Vani E., Inventors; Karunya Institute Of Technology And Sciences, assignee: Chicken antibody generation against microbial pathogen bacillus cereus from human nail. Indian patent IN 283165535. 2019 Nov 28.
149. Zhong Q, Wang B, Pu J, Fang X, Liao Z., Inventors; South China Agricultural University, assignee: Anti-vibrio parahaemolyticus chicken yolk antibody, preparation method and application thereof. Chinese patent CN 83537470. 2012 Jun 27.
150. Hui Z, Bai Z, Bao H, Ming H., Inventors; Jilin Modern Traditional Chinese Medicine Engineering Research Center Co., Ltd, assignee: Toothpaste capable of quickly relieving pain, diminishing inflammation, inhibiting bacteria, preventing dental caries and freshening breath. Chinese patent CN 145093694. 2015 Jul 1.
151. Jianfen C., Inventor; Shanghai Maxam Daily Chemical Co.,Ltd., assignee: Gingivitis and gingivitis ozostomia preventing mouthwash prepared by anti-porphyromonas gingivalis and IgY antibody with fusobacterium nucleatum specificity. Chinese patent CN 85796831. 2014 May 2014.
152. Aiguo B, Tongsen L, Cheng L., Inventors; Hangzhou Yasheng Biotechnology co., Ltd., assignee: Preparation method of composite IgY against periodontal disease pathogenic bacteria. Chinese patent CN 124076022. 2015 Oct 29.
153. Xiong Y., Inventor; Guangzhou Annel Biotechnology Co., Ltd. , Ltd, assignee: New anti-human papilloma virus (HPV) and endometritis preparation. Chinese patent CN 123483343. 2014 Sep 24.
154. Bao S, Yang R, Wang C, Cao T, Gong Q., Inventors; Shenzhen Yachen Intelligent Biological Engineering Co. , assignee: Broad spectrum anti-HPV-L1 and E6/E7-IgY, small molecule antibody and application thereof. Chinese patent CN 250122865. 2019 Jul 26.
155. Terzolo H. Aplicaciones de tecnología de las inmunoglobulinas de yema de huevo (IgY) de gallina. ResearchGate 2010; : 173–183.
156. Li X, Wang L, Zhen Y, Li S, Xu Y. Chicken egg yolk antibodies (IgY) as non-antibiotic production enhancers for use in swine production: a review. J Anim Sci Biotechnol 2015; 6: 40.
157. Kovacs-Nolan J, Mine Y. Egg Yolk Antibodies for Passive Immunity. Annu Rev Food Sci Technol 2012; 3: 163–182.

158. GastroMate. PRN Pharmacal. [Internet]. 2021. Available from: https://www.prnpharmacal.com/products/critical-care/gastromate/
159. Bioinnovo IgY DNT Terneros. Vetanco[Internet]. 2017. Available from: https://www.vetanco.com/es/produto/bioinnovo-igy-dnt/
160. Products & Services as Pet Food. Trouw Nutrition [Internet]. Available from: 2020.https://www.trouwnutritionusa.com/en/products/
161. Horie K, Horie N, Abdou AM, Yang J-O, Yun S-S, Chun H-N et al. Suppressive effect of functional drinking yogurt containing specific egg yolk immunoglobulin on Helicobacter pylori in humans. J Dairy Sci 2004; 87: 4073–4079.
162. About i26. I26--Health. Arkion Life Sciences [Internet]. 2016. Available from: https://www.i26forhealth.com/i26-companion
163. Health Food Products.EW Nutrition [Internet]. 2020. Available from: https://ew-nutrition.com/healthfood/health-food-products/
164. Dan Biotech [Internet]. 2016. Available from: http://www.danbio.com/en/sub.php?menucode=0401
165. Ovopron ®. Pharma Foods International Co., Ltd. [Internet]. 2019. Available from: https://www.pharmafoods.co.jp/en/products/ovopron
166. Muno-IgYTM .IGY Life Sciences [Internet]. 2021. Available from: https://www.ulprospector.com/es/na/Food/Detail/18617/524018/Muno-IgY
167. Ovalgen Products. EW Nutrition [Internet]. 2020. Available from: https://ew-nutrition.com/healthfood/health-food-products/ovalgen/
168. Ulcer-Lock Product. Dan Biotech [Internet]. 2016. Available from: http://www.danbio.com/en/sub.php?menucode=0402&-category=0201&idx=17
169. Gasto-Lock Product. Dan Biotech [Internet]. 2016. Available from: http://www.danbio.com/en/sub.php?menucode=0402&-category=0201&idx=20
170. AtoIB (Cosmetic effective for atopic dermatitis). Dan Biotech [Internet]. 2016. Available from: http://www.danbio.com/en/sub.php?menucode=0402&category=0201&idx=19
171. Jensenius JC, Andersen I, Hau J, Crone M, Koch C. Eggs: conveniently packaged antibodies. Methods for purification of yolk IgG. J Immunol Methods 1981; 46: 63–68.
172. Harley C, Vieira-Pires RS. Antibody fragment technology and avian IgY antibodies: a powerful combination. 2016; 3: 62–66.
173. Brady D, Gaines S, Fenelon L, Mcpartlin J, O'Farrelly C. A Lipoprotein-derived Antimicrobial Factor from Hen-egg Yolk is Active Against Streptococcus Species. J Food Sci 2002; 67: 3096–3103.
174. Zhang H, Mine Y. CHAPTER 11:Antiviral Properties of Egg Components. In: Eggs as Functional Foods and Nutraceuticals for Human Health. Royal Society of Chemistry: Reino Unido, 2019, pp 198–210.

Received: 23 Febrero 2021
Accepted: 15 Junio 2021

REVIEW / ARTÍCULO DE REVISIÓN

Lab on a Chip: Bioreactors miniaturization for rapid optimization of biomedical processes and its impact on SARS-CoV-2 diagnosis

C.P.Ortega[1], D.A Corredor[1], M.E Santillán[1], W.S Ger[1], J.M Noceda[1,2], J.M Pais-Chanfrau[2,3], L.E Trujillo[1,2] DOI. 10.21931/RB/2021.06.03.31

Abstract: Lab on a Chip (LoC) as part of Microbioreactors (MBRs) constitute an emergent technology to carry out microbioprocesses based on microfluidics research. In this review, the usefulness of LoCs is exposed since its inception, demonstrating that it is a multidisciplinary research field, gathering different science branches to develop this technology. As a result, a beneficial point of advancement is reached, producing useful consumables for humanity. Some of the described LoCs throughout this work are also used to detect infectious diseases caused by bacteria or viruses, allowing accelerated studies on emerging or high-impact diseases, such as COVID-19. Here are also displayed with an updated panorama, different strategies to improve the use, applications in the biomedical field, and spread of these devices aimed at their availability to solve social problems.

Key words: Bioprocesses, COVID-19, micro bioreactors, Organ on a Chip, plasmonic, Point of Care.

Introduction

The emergence of micro-bioreactors (MBRs) comes from two main fields: microfluidic technology and molecular biology. In the early 1950s, photolithography development gave rise to microfabrication, which allowed scientists to develop the first microdevices, known as micro-size transistors. Over the years, microtechnology began to gain new approaches and applications, so chemical tests start to miniaturize. The appearance of these techniques allowed to get high precision data with a high-resolution level using small sample amounts[1].

A growing interest in MBRs development, which typically works at the milliliter (mL) and microliter (µl) scale, is thought to be more convenient to collect chemical and biological information related to bioprocesses or diagnosis tests[2,3]. Apart from working on a micrometric scale[4], the MBRs operation mode includes conventional bioreactors, discontinuous (batch), fed-batch, or continuous systems[2]. However, differently from conventional reactors, MRBs mainly use two modalities: those that consist of microwells and those based on microfluids[1].

MBRs development was carried out to parallelize an integrative high-performance and quickly experimental design in several studies. The acceleration of quantitative microbial phenotyping stands out over conventional cultivation techniques and turns out to be economical, competitive, and effective for bioprocesses in the pharmaceutical and industrial sectors[5]. It seeks to miniaturize conventional cultivation to achieve MBRs that provide rapid data output, as they can be adapted by fabricating different types, sizes, and shapes. They also allow a reduction in experimentation expenses, require fewer installations and less time, and give the possibility of automation[6].

Bioreactors miniaturization leads to obtaining bioprocesses or diagnosis tests just reduced to chips so-called Lab on a chip (LoC), which integrate and miniaturize some laboratory functions in a single device[7]. Its development is interdisciplinary since it involves biology, chemistry, physics, software sciences, and material engineering. LoCs main characteristics consist in the arrangement of multiple components integrated into a single artifact. Additionally, they can be automated; each bioprocess can be independently treated as an individual experiment in multiple microsystems[8], thus increasing sensitivity, decreasing reagent consumption, and having efficient sterilization, sample detection, and product separation[9].

Portable LoC platforms are used in Severe Acute Respiratory Syndrome coronavirus studies detected in 2019 (SARS-CoV-2), constituting an emerging research area with significant potential for diagnosis. SARS-CoV-2 is responsible for the COVID-19 disease, which was classified as a pandemic on March 11 2020. The countries with the highest number of infections are United States, India, Brazil, Russia, and the United Kingdom, but worldwide gathered data reveals that there are a total of ninety-three million infections and more than two million confirmed deaths until January 17, 2021[10].

This work aims to provide an updated panorama to national researchers on the use and powerful potential applications of miniaturized systems based on Lab on a Chip, its applications in the biomedical field, and the advances that this technology offers in the study of SARS-CoV-2.

MICRO BIOREACTORS

Table 1 summarizes some of the most used MBRs models to date. The diversity of MBR designs gives the possibility to adapt the purposes of the equipment according to the user's needs and requirements. Currently, MBRs have been used in high-throughput screening techniques to evaluate the biological activity of different molecules of interest[11].

Additionally, in industry, MBRs are widely used to manufacture pharmaceuticals, chemicals, enzymes, and food from cell factories[6,12].

An indispensable requirement in developing a bioprocess is selecting ideal conditions, such as optimal growth of microorganisms and adequate growth medium, and a strategy that guarantees the final product with the required quality. However, the productive parameters and the operational characteristics of a bioprocess can change and affect the environment's physiological and molecular cell response. Therefore, it is essential to know and study the main biochemical, microbiological, and physical factors that influence obtaining high concentrations of biotechnological products and guarantee the control of the culture and its conditions throughout the bioprocess[13,14].

[1] Departamento de Ciencias de la Vida y la Agricultura, Laboratorio Multidisciplinario, Universidad de las Fuerzas Armadas – ESPE, Sangolquí, Ecuador.
[2] Grupo de Investigación de Biotecnología Industrial y Bioproductos Centro de Nanociencia y Nanotecnología – CENCINAT, Universidad de las Fuerzas Armadas ESPE, Sangolquí, Ecuador.
[3] FICAYA, Universidad Técnica del Norte (UTN), Ibarra, Imbabura, Ecuador.

Corresponding author: letrujillo3@espe.edu.ec

An appropriate MBR will retain the functionality of conventional bioreactors in a miniaturized form and allow the integration of additional sensors. Therefore, the following criteria should be met in an MBR: i) biocompatibility of the chosen material, ii) adequate aeration, iii) temperature control, iv) biomass measurement, v) dissolved oxygen detection, and vi) pH measurement[15]. These characteristics allow bioprocess experiments to be carried out under dynamic and flexible conditions[1].

LAB ON A CHIP (LoCs)

As an exciting branch of MBRs, LoCs can integrate optic (for luminescence or absorbance measurements), magnetic, electrical, and micro-resonator sensors. They allow the application of fast and effective biomarker detection protocols without being physically linked to a specialized laboratory or hospital. Thus, micro bioreactors are compacted-size devices that confer versatility to control and monitor chronic or epidemic outbreak-related diseases since they facilitate the collection, transport, extraction, and sample analysis, thus increasing the population coverage[16].

The production and manufacture of LoCs follow a logical and orderly process that improves their development, which is detailed in Figure 1. The primary materials for their manufacture are silica and polymers like poly dimethyl siloxane (PDMS) and polytetrafluoroethylene (PTFE)[7]. Its main manufacturing methods are engraving and lithography[17,18].

The transition from large laboratories to simple chips has been due to microfabrication techniques, facilitating the use of LoCs such as Point of Care (POC) tests, which are laboratory tests that are applied near the patient's location and can be applied even by the same patient because no prior training is needed with these tests[19].

LoCs has predominantly become a valuable tool for the future of medicine. For example, LoCs such as Point of Care (POC) tests constitute laboratory tests applied near the patient's location and can be applied even by the same patient since prior training is needed[19]. However, due to several limitations, a transition from LoCs was made to a device with a few square centimeters capable of emulating conditions of experimentation, screening, and *in vitro* personalized medicine of biopsies or derived cells for a multiplatform system of a tissue, which was called Organ-on-a-Chip (OoC)[20].

OoC systems are instruments whose main objective is to imitate the tissue-tissue interface of living organisms of the animal kingdom, focusing mainly on the most relevant processes of the organism, which include: adsorption, distribution, metabolism, and elimination[21].

OoCs are microfluidic-based devices designed for the cultivation of live cells in continuously perfused micrometer-sized chambers. Generally, these micrometric chambers are composed of 3D polymeric microchannels, which are transparent and lined by living cells, which are responsible for replicating three critical aspects of intact organs: the 3D microarchitecture defined by the spatial distribution of multiple types of tissues; tissue-tissue functional interfaces; and complex organ-specific biochemical and mechanical microenvironments[22].

OoC systems can be used as specialized *in vitro* models

Model	Definition	Advantages	Usage example
Stirred Microbioreactors	The miniaturization of stirred tanks in a conventional way using alternatives such as electromagnetic stirring or magnetic microbeads[47].	Uniform process conditions, high oxygen transfer rate, and homogeneity. Helps with experimental parallelization and obtaining robust data[47].	The stirred MBR with resonance achieves a homogenate through capillary waves; this was evidenced after obtaining a 4 times more significant biomass growth with this system in the bacterium *Escherichia coli*[5].
Perfusion Microbioreactors	Membrane-based systems that simulate fluid flow in tissues or organs[48].	Allow culture cells to have homogeneous microenvironments and better mass transfer conditions[48].	Semi-permeable membrane perfusion MBRs between microchannels for unrestricted growth and bacterial screening that do not limit the availability of essential nutrients to bacterial cells and restrict chemotaxis[49].
Arrays Microbioreactors	Hybrids between a bioreactor and a microfluidic device. Represented by each culture well and a system that provides independent media flow to each well[50].	Smaller volume, high throughput, independent culture wells, steady-state conditions, enhanced mass transport, application of physical signals[50].	Induction of cardiomyocyte proliferation and highlight the importance of *in vitro* screening in regenerative heart therapies without the use of animal models in high-density micro bioreactors[51].

Table 1. Microbioreactor models and examples of their uses.

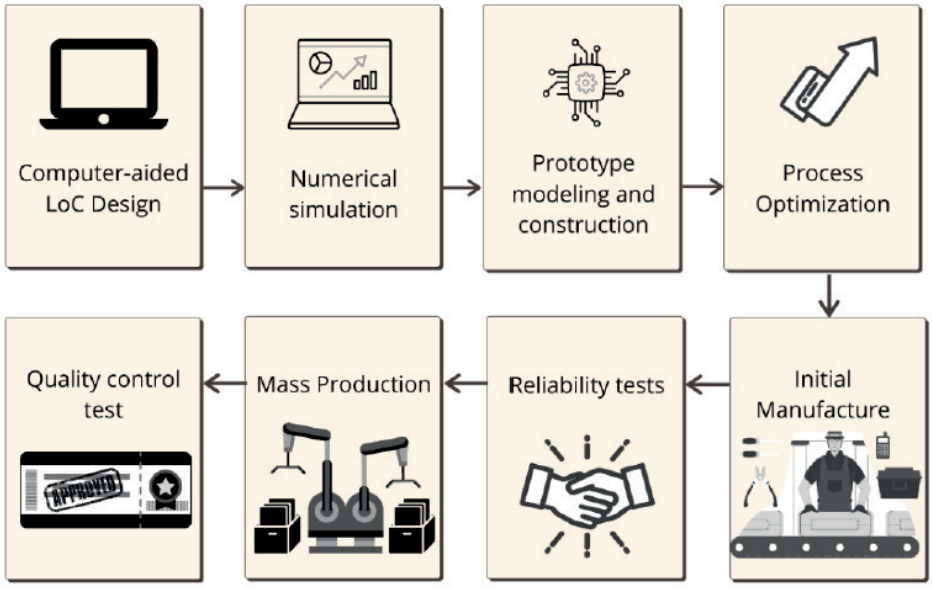

Figure 1. The process to develop a Lab on a Chip (LoC). In the case of inconveniences at any stage, the process must be repeated. Adapted from: Shanti, Teo, and Stefanini (2018)[41]. Created with Canva.com.

that allow the simulation of microenvironments, investigation of physical stimuli, and pharmacological modulation of complex biological processes[22]. Several systems can be designed, such as i) Simple systems, which have a single perfused microfluidic chamber containing a type of cultured cells that exhibit tissue functions, for example, hepatocyte systems or kidney epithelial cells. ii) Complex systems, which have two or more microchannels connected by porous membranes, lined on opposite sides by different types of cells, recreate interfaces between tissues, such as a pulmonary alveolar-capillary interface or even a blood-brain barrier[23].

LOCS APPLICATIONS IN BIOMEDICAL RESEARCH

MBRs development in the health sector focuses on studying the new drugs' effects[24], the development of culture systems[25], production, and manufacturing of diagnostic equipment[26]. The main advantages in the medical sector are the cultivation of cells in three dimensions, the use of OoC, high yield, and the production of biomass and personalized medicine applications[27].

Cytotoxicity studies

OoCs are instruments that provide a variety of applications in the field of pharmacology, they stand out for their ability to imitate different environments of the animal organism to evaluate toxicity. In the study by Coppeta *et al.*(2017), a cross-platform design based on reconfigurable human cells that supports the function of individual organs is presented[18].

Heart on a Chip (HoC) has shown the potential to facilitate and shorten drug development. In the study by Mandenius (2018), a prototype of HoC is designed based on cardiomyocytes obtained from the development of induced pluripotent stem cells (iPSC)[11,28]. This and other OoC studies can be seen in Figure 2.

Disease's study and diagnosis

OoCs can simulate intracellular environments and broad screening for drugs and cell responses, whereas LoCs allow rapid diagnosis of diseases that can be detected using human fluid samples[7,29]. This section will provide examples of the advancement of this technology and the integration of miniaturized conventional tests.

LoC-based platforms have been increasingly developed for the analysis and detection of biomarkers. They allow better sample preparation, handling, high throughput, and portability. Also, provide attractive features such as marker-free detection, higher sensitivity, and the integration of novel detection techniques that reduce testing time and simplify processes[30]. The comparison between LoC-based platforms and conventional tests is shown in Figure 3.

Malaria is a disease that requires quick and easy ways of diagnosis, so LoCs have been beneficial for developing rapid tests[31]. The main LoC diagnostic techniques to detect malaria are based on real-time capillary PCR (q-PCR), which has a sensitivity of 97.4% and a specificity of 93.8% compared to conventional q-PCR[32]. Other LoC-based diagnostic techniques for malaria include microfluidic chips that perform Enzyme-Linked ImmunoSorbent Assay (ELISA) to detect histidine-rich protein 2 (HRP-2). Besides, chips were developed for studies of individual cells, in which cells infected with malaria are identified for their properties in microfluidics[31].

The study has extensively developed in LoC for its diagnosis and OoC for its culture in viruses. In a dual microchannel design with human liver cells separated by a porous membrane (liver-sinusoid-on-a-chip), an optimal replication rate of the Hepatitis B Virus (HBV) was achieved, measured by the presence of viral DNA secreted by the cells and the expression of the central antigen of hepatitis B (HBcAg) was determined. Differentiation and functions of the hepatocytes were maintained during the trial; approximately 73.3% of the hepatocytes expressed HBcAg[33].

Research on SARS-COV-2

The Severe Acute Respiratory Syndrome (SARS-CoV) caused an epidemic between 2002-2004; this misfortune allowed the development of a microfluidic system manufactured using the photolithography technique. The chip had been tested to detect the coronavirus SARS-CoV; this system had a laser fluorescence detection, capable of giving a positive rate of SARS clinical samples up to 94.44%. The research had shown a higher positive rate than a conventional PCR, with shorter test times and lower costs[34].

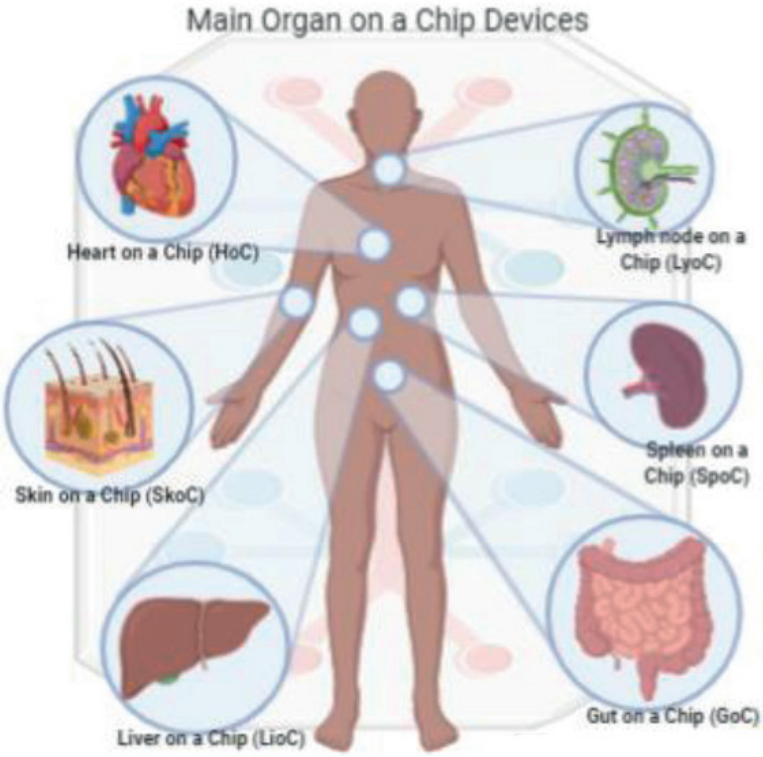

Figure 2. Main Organ on a Chip (OoC) devices, based on impermeable and microfluidic membranes to mimic the tissue-tissue interface of living organisms, Heart on a chip: a three-dimensional cell microstructure is generally used for toxicology tests in cardiomyocytes. Lymph node on a chip: used in research simulating microstructures of the paracortical region of the lymph node to examine the dynamics of interaction between dendritic cells and T cells. Skin on a chip: they are preferentially based on mimicking the active immune cells of the skin and physiological research adding vascularization in skin models with endothelial cells. Spleen on a chip: system consisting of two channels, the first one with a fast liquid flow and the other with a slow liquid flow to balance hydrodynamic forces and imitate the filter function in the spleen. Liver on a Chip: for its therapeutic research on functions, metabolism, detoxification, and response to drugs, an OoC of interest developed from hepatocytes and endothelial cells. Gut on a chip: usually used for phase I drug development and is helpful to examine the small intestine functions. Based on Shanti *et al.*(2018).

In the COVID-19 pandemic, LoCs were developed as diagnostic tools based on qRT-PCR; these provide significant advantages such as using a small sample volume, rapid detection, and the incorporation of the Gold Standard test to diagnose SARS-CoV-2 in a miniature portable form[35,36].

Another application of LoC is to detect the RNA transduction of SARS-CoV-2 without the need for qRT-PCR. Instead, the genetic material is detected by hybridization with probes; a diode laser allows quantifying the viral RNA by excitation of the probe hybrid with the RdRp-COVID, ORF1ab-COVID SARS-CoV-2 and E protein genes. This technique significantly improved the stability, sensitivity, and reliability of the chip[37].

A novel method for detecting SARS-CoV-2 is plasmonic, which is the excitation of a metal-dielectric target molecule that generates a signal when catching an RNA target. It has shown high sensitivity and detects samples with low concentrations of nucleic acids. These advantages allow the use of LoCs in versatile ways to detect viruses[38].

SARS-CoV-2 diagnosis by qRT-PCR test didn't cover the presented demands, so some LoCs had an emergency use authorization to solve this trouble. These authorizations were given by the Food and Drug Administration (FDA) in the United States[39]. The SARS-CoV-2 detection LoCs on the market can be seen in Table 2.

Complementing the use of LoCs for diagnosis, the Applikon® company has researched the use of MBR Micro-matrix for possible vaccines against COVID-19 by the Virology Laboratory and the Bioprocess Engineering group of Wageningen University. The MBR is being applied to optimize cell growth parameters for the production of the Spike protein in Sf9 cells[40].

FUTURE PERSPECTIVES

There are many possibilities for future exploration and technical issues that need to be addressed to turn MBRs emerging technologies into valuable tools. The innovation of detection methods and the miniaturization of instruments need to be improved, which requires collaboration between scientists with experience in different fields. Among the improvements that must be made, the material used to manufacture the microfluidic device must not influence the cellular response behavior. Currently, PDMS is the standard material used for manufacturing; however, it is highly lipophilic to bind to molecules in the perfusion medium or bind to introduced drugs[41].

An essential requirement for commercialization and a challenge for complex microfluidic structures is scalability. As a result, scalability considerations must drive the materials, the design, and the fabrication methods used for such devices. Advances in 3D printing technology will likely start to bridge that gap shortly to build plastic-based MBRs[42].

Based on the variety of diagnostic chips capable of detecting COVID-19, portability, sensitivity, and performance are the ruling guideline to implement a virus-specific diagnostic strategy. The SARS-CoV-2 biomarkers enable plasmonic and colorimetry for developing chip tests that ensure correct diagnosis, opening the possibility of an integrated POC system[38,43]. Given this potential for rapid results, plasmonic-based sensors can reduce the total analytical time from hours or days to minutes, which would allow patients to receive their diagnosis in less time, reducing nosocomial transmission and minimizing the burden on clinical laboratories[38].

Although rapid diagnostic LoCs can bring benefits for those affected, in the future, these devices should have an integrated internet communication system with real-time data transmission capacity and updated monitoring (integrated transmitting antenna), which allows data acquisition to enter into a health network, this would have a significant impact on the management of current or future pandemics[44].

A new method of detection and analysis of samples is through the use of smartphones (SP), thanks to their sophisticated technological characteristics, such as high-quality cameras, great computational power, and easy connectivity; these have facilitated its integration as an analytical detection tool. SP-based tests measure optical variables such as bright field, colorimetry, luminescence, and fluorescence[42].

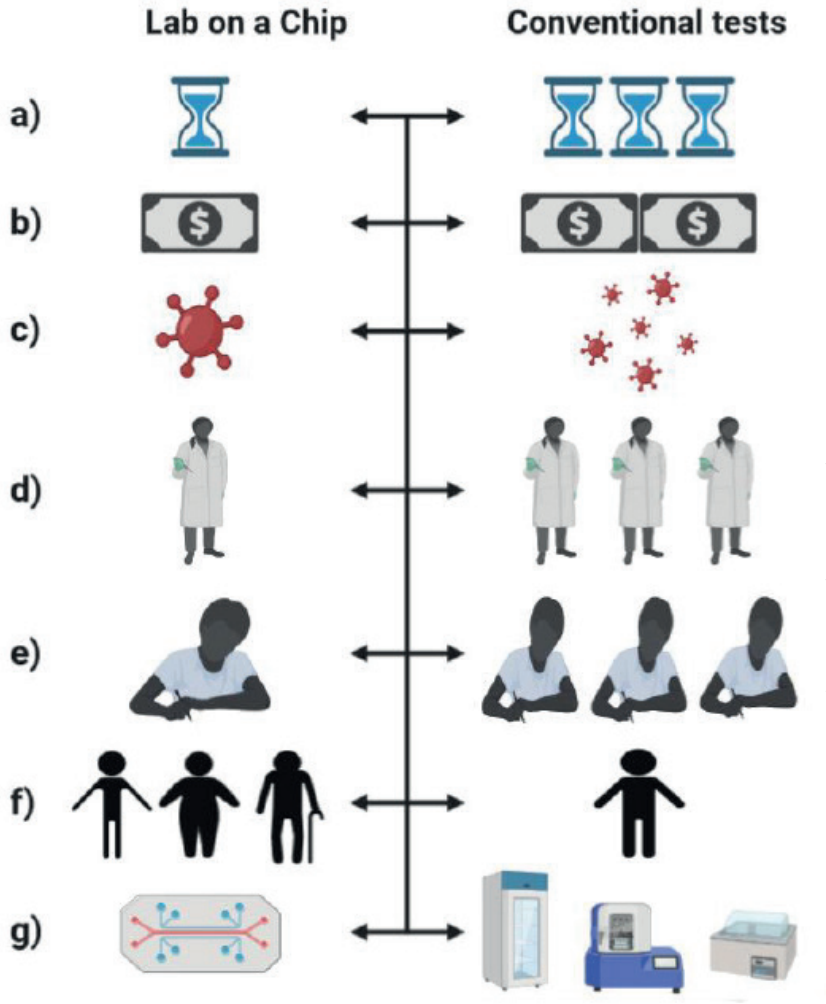

Figure 3. Comparison of Lab on a Chip (LoC) versus conventional tests. a) The time required for diagnoses in LoC is more minor than conventional tests. b) Your usage costs decrease due to lower reagent consumption. c)The risk of possible infections or nosocomial transmission decreases because patients obtain their results in a shorter time. d) A smaller laboratory staff is needed. e) Required training is simpler. f) The reach or coverage of the population is greater. g) Due to their portability, they facilitate handling and mobilization.

The identification of viruses using SP has been proved on different systems such as detection of Ebola virus-specific antibodies, RT-LAMP tests for detecting the human immunodeficiency virus (HIV) and Zika virus, and diagnosing influenza with gold nanoparticles test[39]. Sun *et al.*(2020) study the detection from LAMP of 5 bacterial and viral pathogens that cause respiratory infections in equines, using the SP Motorola Nexus 6 to measure fluorescence. The system managed to differentiate positive and negative controls and detect one or more pathogens simultaneously in an hour (ideal for co-infection diagnosis). Furthermore, the large capacity of SPs to be used as analytical equipment makes them an excellent option for designing rapid tests for SARS-CoV-2 without the need to invest in expensive equipment[45].

Microfluidic chips provide favorable support for OoC development that capture the attention of global research due to the breakthroughs that have been made in this field. The ultimate goal of OoC is to integrate numerous organs on a single chip and build a more complex multi-organ chip model, ultimately achieving a "Human on a chip"[46].

Conclusions

This work gave an overview of the applications of LoCs devices, highlighting their value in cytotoxicity studies and their importance as diagnostic tools, their advances in disease studies make great successes in biomedicine concerning health care. Besides, LoCs and OoCs have demonstrated the fantastic performance of this technology, with the most avant-garde research on LoCs focused on SARS-CoV-2, plasmonic-based chips, integration of communication systems between the tests with medical data-network and the use of SmartPhones as analytical devices. The LoCs were positioned as POC tests, which would open the door to a faster diagnosis without the need for biomedical or hospital equipment and better manage different diseases thanks to Lab on a Chips.

Acknowledgements

The authors thank the Universidad de las Fuerzas Armadas, ESPE and the Industrial Biotechnology and Bioproducts Research Group, CENCINAT, due to the opportunity provided to us as their invaluable help and guidance during the development of this work.

Competing interests

The authors declare that they have no conflicting interests.

Bibliographic references

1. Prado, R. C. & Borges, E. R. Microbioreactors as engineering tools for bioprocess development. Brazilian J. Chem. Eng. 35, 1163–1182 (2018).
2. Pasirayi, G. et al. Microfluidic Bioreactors for Cell Culturing: A Review. 3, (2011).

Product	Developer	Performance
ID NOW®	Abbott™	RT-PCR. Can detect positive samples in 5 minutes and negative samples in 13 minutes.
Filmarray®2.0	BioFire™	The instrument integrates nucleic acid extraction, purification, PCR amplification, and sequential detection using microfluidic technology.
GeneXpert ®	Cepheid™	A small kit that integrates sample preparation, nucleic acid amplification, and molecular detection analysis.
RTisochip®	CapitalBio™	RT-PCR, not only detects SARS-CoV-2 but also detects 6 common respiratory viruses such as influenza.
Point of Care (POC) instrument	Cannon™	Amplify DNA samples and detect SARS-CoV-2 in 35 minutes (10 minutes if uses respiratory samples).

Table 2. Products based on Lab on a Chip (LoC) are in the market for the diagnosis of SARS-CoV-2. Adapted from Zhuang *et al.*(2020).

3. Marques, M. P. C. & Szita, N. Bioprocess microfluidics: applying microfluidic devices for bioprocessing. Curr. Opin. Chem. Eng. 18, 61–68 (2017).
4. Lattermann, C. & Büchs, J. 2 Design and Operation of Microbioreactor Systems for Screening and Process Development. (2016).
5. Hemmerich, J., Noack, S., Wiechert, W. & Oldiges, M. Microbioreactor Systems for Accelerated Bioprocess Development. Biotechnology Journal 13, (2018).
6. Nagraik, T., Salcedo, A. G., Solle, D. & Scheper, T. Process Optimization using High Throughput Automated Micro-Bioreactors in Chinese Hamster Ovary Cell Cultivation. JoVE (Journal Vis. Exp. e60577 (2020).
7. Herold, K. E. & Rasooly, A. Lab-on-a-Chip Technology (Vol. 1) Fabrication and Microfluidics. (2009).
8. Mohammed, M. I., Haswell, S. & Gibson, I. Lab-on-a-chip or Chip-in-a-lab: Challenges of Commercialization Lost in Translation. Procedia Technol. 20, 54–59 (2015).
9. Giannitsis, A. T. Biomeditsiiniliste kiiplaborite valmistamine. Est. J. Eng. 17, 109–139 (2011).
10. WHO. WHO Coronavirus Disease (COVID-19) Dashboard. https://covid19.who.int/table (2020). Available at: https://covid19.who.int/table. (Accessed: December 16 2020)
11. Mandenius, C. F. Conceptual design of micro-bioreactors and organ-on-chips for studies of cell cultures. Bioengineering 5, (2018).
12. Ravindran, S. et al. Microbioreactors and Perfusion Bioreactors for Microbial and Mammalian Cell Culture. in Biotechnology and Bioengineering (IntechOpen, 2019). doi:10.5772/intechopen.83825
13. Zepeda, A. B., Pessoa Jr, A. & Farías, J. G. Carbon metabolism influenced for promoters and temperature used in the heterologous protein production using Pichia pastoris yeast. brazilian J. Microbiol. 49, 119–127 (2018).
14. Parekh, M. et al. Microbioreactor for lower cost and faster optimisation of protein production. Analyst 145, 6148–6161 (2020).
15. Zanzotto, A. Integrated Microbioreactors for Rapid Screening and Analysis of Bioprocesses. (2005).
16. Romao, V. C. et al. Lab-on-Chip Devices: Gaining Ground Losing Size. ACS Nano 11, 10659–10664 (2017).
17. Stoytcheva, M. & Zlatev, R. Lab-on-a-chip fabrication and application. (BoD–Books on Demand, 2016).
18. Coppeta, J. R. et al. A portable and reconfigurable multi-organ platform for drug development with onboard microfluidic flow control. Lab Chip 17, 134–144 (2017).
19. Goble, J. A. & Rocafort, P. T. Point-of-care testing: Future of chronic disease state management? Journal of Pharmacy Practice 30, 229–237 (2017).
20. Azizipour, N., Avazpour, R., Rosenzweig, D. H., Sawan, M. & Ajji, A. Evolution of biochip technology: A review from lab-on-a-chip to organ-on-a-chip. Micromachines 11, 1–15 (2020).
21. Khalid, N., Kobayashi, I. & Nakajima, M. Recent lab-on-chip developments for novel drug discovery. Wiley Interdiscip. Rev. Syst. Biol. Med. 9, 1–17 (2017).
22. Esch, E. W., Bahinski, A. & Huh, D. Organs-on-chips at the frontiers of drug discovery. Nature Reviews Drug Discovery 14, 248–260 (2015).
23. Bhatia, S. N. & Ingber, D. E. Microfluidic organs-on-chips. Nature Biotechnology 32, 760–772 (2014).
24. Christoffersson, J. & Mandenius, C. F. Using a microfluidic device for culture and drug toxicity testing of 3D cells. in Methods in Molecular Biology 1994, 235–241 (Humana Press Inc., 2019).
25. Velugula-Yellela, S. R. et al. Use of high-throughput automated microbioreactor system for production of model igG1 in CHO cells. J. Vis. Exp. 2018, 58231 (2018).
26. Barisam, M., Saidi, M. S., Kashaninejad, N. & Nguyen, N. T. Prediction of necrotic core and hypoxic zone of multicellular spheroids in a microbioreactor with a U-shaped barrier. Micromachines 9, (2018).

27. Gottwald, E. & Altmann, B. Advanced 3D-Cell Culture Techniques in Micro-Bioreactors. (2020).
28. Marsano, A. et al. Beating heart on a chip: A novel microfluidic platform to generate functional 3D cardiac microtissues. Lab Chip 16, 599–610 (2016).
29. Hemmerich, J. et al. Less Sacrifice, More Insight: Repeated Low-Volume Sampling of Microbioreactor Cultivations Enables Accelerated Deep Phenotyping of Microbial Strain Libraries. Biotechnol. J. 14, 1–26 (2019).
30. Wu, J. et al. Lab-on-a-chip platforms for detection of cardiovascular disease and cancer biomarkers. Sensors (Switzerland) 17, (2017).
31. Kolluri, N., Klapperich, C. M. & Cabodi, M. Towards lab-on-a-chip diagnostics for malaria elimination. Lab Chip 18, 75–94 (2018).
32. Taylor, S. C. & Mrkusich, E. M. The state of RT-quantitative PCR: firsthand observations of implementation of minimum information for the publication of quantitative real-time PCR experiments (MIQE). J. Mol. Microbiol. Biotechnol. 24, 46–52 (2014).
33. Kang, Y. B., Rawat, S., Duchemin, N., Bouchard, M. & Noh, M. Human liver sinusoid on a chip for hepatitis B virus replication study. Micromachines 8, 1–13 (2017).
34. Zhou, X. et al. Determination of SARS-coronavirus by a microfluidic chip system. Electrophoresis 25, 3032–3039 (2004).
35. Sharma, S., Kumar, V., Chawla, A. & Logani, A. Rapid detection of SARS-CoV-2 in saliva: can an endodontist take the lead in point-of-care COVID-19 testing? International Endodontic Journal 53, 1017–1019 (2020).
36. Udugama, B. et al. Diagnosing COVID-19: The Disease and Tools for Detection. ACS Nano 14, 3822–38Udugama, B., Kadhiresan, P., Kozlowski, H. (2020).
37. Qiu, G. et al. Dual-Functional Plasmonic Photothermal Biosensors for Highly Accurate Severe Acute Respiratory Syndrome Coronavirus 2 Detection. ACS Nano 14, 5268–5277 (2020).
38. Tymm, C., Zhou, J., Tadimety, A., Burklund, A. & Zhang, J. X. J. Scalable COVID-19 Detection Enabled by Lab-on-Chip Biosensors. Cell. Mol. Bioeng. 13, 313–329 (2020).
39. Zhuang, J., Yin, J., Lv, S., Wang, B. & Mu, Y. Advanced "lab-on-a-chip" to detect viruses – Current challenges and future perspectives. Biosensors and Bioelectronics 163, (2020).
40. Applikon. Applikon bioreactors used in search for COVID-19 vaccine. (2020). Available at: https://www.applikon-biotechnology.com/en/about-applikon/news-events/applikon-bioreactors-used-in-search-for-covid-19-vaccine/. (Accessed: December 16 2020)
41. Shanti, A., Teo, J. & Stefanini, C. In vitro immune organs-on-chip for drug development: A review. Pharmaceutics 10, (2018).
42. Arshavsky-Graham, S. & Segal, E. Lab-on-a-Chip Devices for Point-of-Care Medical Diagnostics. in (2020). doi:10.1007/10_2020_127
43. Zhu, H., Fohlerová, Z., Pekárek, J., Basova, E. & Neužil, P. Recent advances in lab-on-a-chip technologies for viral diagnosis. Biosens. Bioelectron. 153, 112041 (2020).
44. Zhu, H., Fohlerová, Z., Pekárek, J., Basova, E. & Neužil, P. Recent advances in lab-on-a-chip technologies for viral diagnosis. Biosens. Bioelectron. 153, 112041 (2020).
45. Sun, F. et al. Smartphone-based multiplex 30-minute nucleic acid test of live virus from nasal swab extract. Lab Chip 20, 1621–1627 (2020).
46. Wu, Q. et al. Organ-on-a-chip: Recent breakthroughs and future prospects. BioMedical Engineering Online 19, (2020).
47. Tan, C. K. et al. Electromagnetic stirring in a microbioreactor with non-conventional chamber morphology and implementation of multiplexed mixing. J. Chem. Technol. Biotechnol. 90, 1927–1936 (2015).
48. Jonczyk, R. et al. Living Cell Microarrays: An Overview of Concepts. Microarrays 5, 11 (2016).
49. Vit, F. F. et al. Perfusion microbioreactor system with permeable membranes to monitor bacterial growth. J. Chem. Technol. Biotechnol. 94, 712–720 (2019).
50. Figallo, E. et al. Micro-bioreactor array for controlling cellular microenvironments. Lab Chip 7, 710–719 (2007).
51. Titmarsh, D. M. et al. Induction of human iPSC-derived cardiomyocyte proliferation revealed by combinatorial screening in high density microbioreactor arrays. Sci. Rep. 6, 1–15 (2016).

Received: 2 March 2021
Accepted: 12 July 2021

REVIEW / ARTÍCULO DE REVISIÓN

Metachromatic Leukodystrophy: Diagnosis and Treatment Challenges

Nayibe Tatiana Sanchez-Alvarez[1,2,3], Paula Katherine Bautista-Niño[2], Juanita Trejos-Suárez[3], Norma Cecilia Serrano-Diaz[2]

DOI. 10.21931/RB/2021.06.03.32

Abstract: Metachromatic leukodystrophy is a neurological disease of the lysosomal deposit that has a significant impact given the implications for the neurodegenerative deterioration of the patient. Currently, there is no treatment available that reverses the development of characteristic neurological and systemic symptoms. Objective. Carry out an updated bibliographic search on the most critical advances in the treatment and diagnosis for LDM. A retrospective topic review published in English and Spanish in the Orphanet and Pubmed databases. Current treatment options, such as enzyme replacement therapy and hematopoietic stem cell transplantation aimed at decreasing the rapid progression of the disease, improving patient survival; however, these are costly. The pathophysiological events of intracellular signaling related to the deficiency of the enzyme Arylsulfatase A and subsequent accumulation of sulphatides and glycosylated ceramides have not yet been established. Recently, the accumulation of C16 sulphatides has been shown to inhibit glycolysis and insulin secretion in pancreatic cells. The significant advance in technology has allowed timely diagnosis in patients suffering from LDM; however, they still do not have an effective treatment.

Key words: Metachromatic leukodystrophy, treatment, diagnosis, prevalence.

Introduction

Metachromatic leukodystrophy (LDM) is a neurodegenerative lysosomal deposition disease caused by a deficiency in the enzyme Arylsulfatase A (ARSA), which leads to an accumulation of sulfates in lysosomes, lipids of great importance in the structure of myelin. The lysosomal deposition of sulphatides in neurons and myelinating cells produces severe demyelination and neurodegeneration of central (CNS) and peripheral nervous systems (PNS)[1,2].

According to the progress of the disease and the onset of symptoms, it is classified into three stages: late infantile, juvenile, and adult[3]. Although there is still no effective treatment to reverse the symptoms, different therapeutic strategies are in the research and deepening phase[3].

There are no pathological mechanisms by which the accumulation of sulfates leads to lamyelination in CNS and PNS cells. However, in in vitro and in vivo models of pancreatic B cells, the accumulation of sulphatides can inhibit insulin secretion and therefore disable the glycolytic function of the cells[4–6]. The main objective of this review is to carry out an updated bibliographic search on the most critical advances in the treatment and diagnosis of LDM.

Methods

Retrospective review article consisted of searching for articles published in English and Spanish in the Orphanet and Pubmed databases with the keywords, Medical Subject Headings (MeSH): Metachromatic leukodystrophy, treatment, diagnosis, prevalence.

Review articles, meta-analyses, systematic reviews, and studies that preferably had descriptions of cellular mechanisms in LDM were included; 80 relevant references are included due to their historical antecedents considered valuable to complement the information and have LDM criteria. Other references support the descriptions of essential mechanisms in this pathology.

Results

3086 articles containing MeSH were found: When specifying "Metachromatic leukodystrophy", 1,650 articles were found, 410 with the words "Metachromatic leukodystrophy, treatment," 932 with "Metachromatic leukodystrophy, diagnosis" and 94 "Metachromatic leukodystrophy, prevalence". Of all the articles, 80 references were located considering that metachromatic leukodystrophy is the infantile stage and studies in which new diagnostic technologies and treatments were mentioned, Figure 1.

LEUKODYSTROPHIES

According to the National Institute of Health of the United States (NIH) and the Neurological Disorders Unit, leukodystrophies or leukoencephalopathies[7] are a group of rare diseases caused by genetic defects, leading to the presence of chemical deposits within cells of both the CNS and the PNS, resulting in the deterioration of the myelin sheath[8,9].

This pathology is characterized by demyelinating processes that primarily affect the CNS and later the PNS[10,11]. Leukodystrophies have an incidence of 1 in 7,500 live births; however, only half of the patients receive a specific diagnosis[7,12].

The European Association of Leukodystrophies (ELA) classification includes those caused by peroxisomal content, lysosome, vacuolation, undetermined atypical hypomyelination. All of these leukodystrophies target myelin; in some cases, its degradation occurs, and in others, there is no formation of it[13,14].

Specific leukodystrophies include metachromatic leukodystrophy, Krabbé disease, adrenoleukodystrophy, Pelizaeus-Merzbacher disease, Canavan disease, and childhood ataxia hypomyelination of the central nervous system (also known as substance disappearance disease or white matter), Alexander's disease, Refsum's disease, and cerebrotendinous xanthomatosis[15].

The progress of the disease is rapid and devastating. It can occur at any age, both in childhood and in adults[12]. Currently,

[1] Universidad del Valle, Faculty of Health, Biomedical Sciences Doctorate Program, Colombia.
[2] Universidad del Valle, Faculty of Health, Biomedical Sciences Doctorate Program,Colombia.
[3] Universidad de Santander, Faculty of Health Sciences, CliniUDES Research Group, Bucaramanga, Santander, Colombia.

Corresponding author: tatianasanchezalvarez@hotmail.com

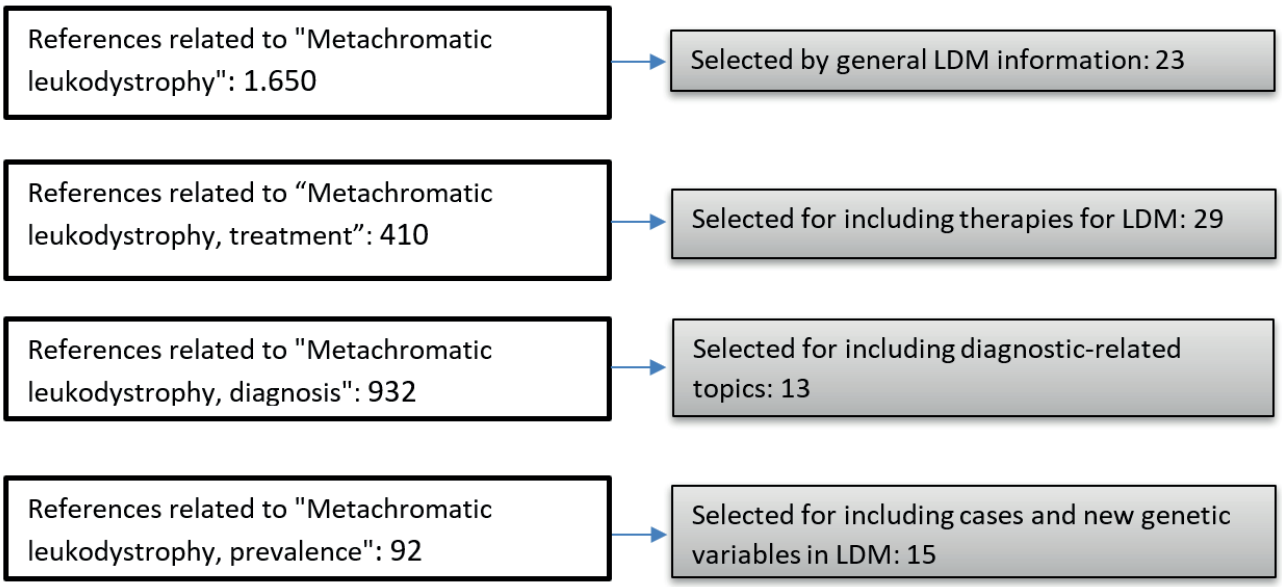

Figure 1. List of findings and selection of references for this review article.

few reports are generated on diagnostic tests, treatment, and the course of this disease. The current diagnosis is based on clinical history, examinations, radiological and laboratory findings, including genetic tests[12,15]. This review summarizes the knowledge about the epidemiology, pathophysiology, diagnosis, and treatment of Metachromatic Leukodystrophy.

Metachromatic Leukodystrophy (MLD)

MLD was first described in 1910 by Perisini and Alzheimer's in adult patients[3,16]. In 1925, Scholz published a pathological clinical study of juvenile MLD, and 34 years later, Peiffer showed that the neural tissues in Scholz's study had metachromatically stained sections. In 1958, independently, Jatzkewitz discovered that the metachromatic sections resulted from the accumulation of sulphatides. On the other hand, Austin and his colleagues were the ones who discovered the defect in the activity of the enzyme arylsulfatase A. Greenfield made the first report of infantile MLD in 1933, and the term "metachromatic leukodystrophy" (metachromatischen Leukodystrophien) was first used by Peiffer in 1959 to describe what was previously known as "diffuse cerebral sclerosis"[16,17].

MLD (OMIM # 250100) is a lysosomal storage disorder with an autosomal recessive pattern of inheritance, so carriers of one copy of the abnormal gene are not affected by the disease[18,19]. MLD is caused by mutations in the ARSA gene, located on chromosome 22q13.33[20], that encodes the lysosomal enzyme Arylsulfatase A (ARSA) (ARSA; OMIM 607574, GenBank accession number, NG_009260)[21,22].

Among the types of mutations that have been reported in ARSA are amino acid substitutions, nonsense mutations, deletions, and sense-change mutation. ARSA is a crucial enzyme in the catabolism of sphingolipids, an abundant component of myelin, Figure 2. The progressive accumulation of sulphatides in the lysosomes of neurons and myelinating cells (Schwann cells in the PNS, oligodendrocytes in the CNS) causes severe demyelination and neurodegeneration progressive neurological deficits, and premature death in childhood form[23].

MLD has three clinical subtypes: late-infantile, juvenile, and adult[17]. Each of the subtypes has characteristics that make them different from each other.

Late childhood MLD

The start occurs before 30 months. Typical findings are weakness, hypotonia, clumsiness, frequent falls, difficulty walking, and dysarthria. As the disease progresses, motor, cognitive, and language skills deteriorate. Later signs include spasticity, pain, seizures, impaired vision, and hearing. Of the cases of MLD, 50 to 60% are of late childhood presentation[24]. In the final stages, children have tonic spasms, mindless posture, and general ignorance of their environment[17].

Juvenile MLD

The clinical signs of this pathology appear between 30 months and 16 years of age. This clinical form of the disease represents 20 to 30% of MLD cases[25]. Initial manifestations include decreased school performance and the appearance of behavioral problems, followed by gait disturbances. Progression is similar but slower than in the late-infant form[17].

Adult MLD

Symptom presentation occurs after 16, sometimes up to the fourth or fifth decade, and represents 10 - 20% of the MLD cases[25]. Initial signs include problems with school or work performance, personality changes, emotional lability, or psychosis; in other patients, neurological symptoms (weakness and loss of coordination that progresses to spasticity and incontinence) or seizures predominate. Peripheral neuropathy is common. The course of the disease is variable, with periods of stability interspersed with periods of decline. The final stage is similar to the juvenile and infantile forms[17].

Epidemiology - Prevalence

Currently, there are no relevant reports of prevalence worldwide, since there is talk of a set of orphan llama diseases, considered in the countries of the European Union as one that affects one in 2,000 people; less than 200,000 people affect the United States, less than 50,000 people in Japan, less than one in 10,000 in Taiwan and one in 5,000 in Colombia[26].

However, in the Orphanet database that describes the MLD, an estimated prevalence of 1 case in 625,000, with an incidence of 0.5 and 1 in 50,000[25,27–30].

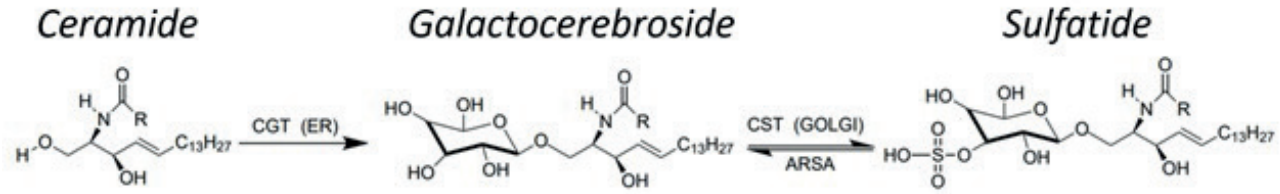

Figure 2. Synthetic sulfatide route.

In Latin America, the reports generated so far are focused on describing cases and mutations in the ARSA gene[31–37].

PATHOPHYSIOLOGICAL MECHANISMS OF THE DISEASE

MLD is a neurodegenerative disease characterized by the accumulation of sulfates (sulfated glycosphingolipids, especially sulfogalactocerebrosides or sulfogalactosylceramides) in the central nervous system, kidneys, and in other organs such as the retina, liver, testes, pancreas, sweat glands, adrenal cortex, and tissue. rectal[38]. The PNS is systematically affected, causing a decrease in nerve conduction velocities. This disorder progresses to a state of decerebration after a few years, resulting in death within 5 years after the onset of symptoms[39].

Galactosylceramide (GalC) and its sulfated form, the sulphatides, are two glycosphingolipids found in high concentrations in the CNS and PNS cell membranes. GalC and sulphatides comprise 23% and 4% of the total mass of myelin lipids, respectively, and together account for about a third of the content of the myelin sheath[40,41]. Among the primary myelinating cells, oligodendrocytes and sulfate-producing Schwann cells[42]. In the nervous system, sulphatides are related to intercellular recognition, cell differentiation, the interaction of the myelinating cell with the axon, the maintenance of the axonal structure, and nerve conduction[39-42].

The myelin sheath is an extended membrane, which spirally wraps around a portion of the axon. Each myelin sheath is extended by modifying the cell membrane of oligodendrocytes and Schwann cells, forming a structure with several myelin segments surrounding the axon (Figure 3)[40].

Each oligodendrocyte can contribute to the protection of around 50 different axons. In addition to its importance in driving the nerve impulse, myelin may have a symbiotic relationship with the axon[45]. Other publications suggest that the develop-

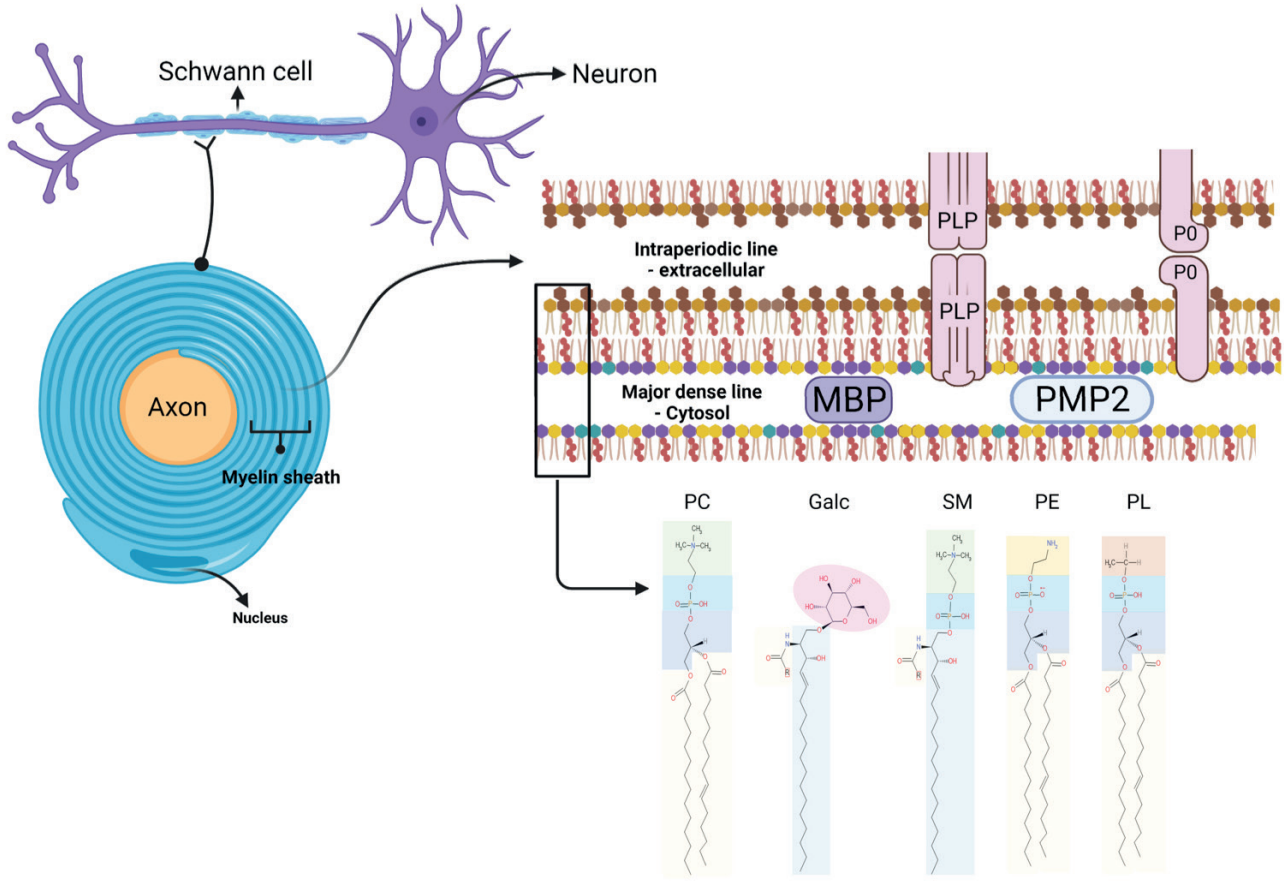

Figure 3. Structure of the myelin sheath. Source: Figure adapted from Poitelon Y. *et al.*, 2020[26]. Diagram of the structure of the myelin sheath, (I) myelinated axon, (II) myelin sheath, (III) Bilayer membrane, and (IV) Lipid classes. Myelin is formed by the opposition of the external surfaces and the internal surfaces of the myelin bilayer that constitute the intraperiodic line and the dense main line, respectively (II, III). The myelin bilayer has an asymmetric lipid composition (III, IV). The myelin protein is also distributed asymmetrically, such as PLP (Proteolipid Protein) and P0 in the intraperiodic line and the dense mainline, the PMP2 protein in the dense main line (III), as well as the composition of cholesterol, phospholipids (e.g., Plasmogen, lecithin, sphingomyelin), glycolipids (eg, Galactosylceramide) and other phospholipids. Proteins P0, PMP2, and enrichment of sphingomyelin in myelin are specific for myelin PNS.

ment of myelin occurs synergistically with the axon and that the axonal cytoskeleton does not form correctly in the absence of myelin[46]. Myelin is usually synthesized in MLD. However, the progressive accumulation of sulfatides induces instability of the myelin membrane, leading to final demyelination.

Myelin formation occurs in two ways. In the CNS, widely branched oligodendrocytes form myelin around multiple axons at the same time, allowing for higher neuronal density in the brain. On the other hand, in the PNS, Schwann cells circularize an axon with several layers of myelin, forming a multilayer structure. Although the primary function of myelin is the same in the CNS and PNS, the molecular requirements for myelin formation differ. In general terms, myelination is a complex process during which a set of proteins and lipids are synthesized in a coordinated way by glial cells (Schwann cells and Oligodendrocytes). i) the pluripotent precursors of Schwann and Oligodendrocyte cells must differentiate; for this, a set of transcription factors is involved in the cell's potential development and its myelinating function. ii) the precursor cells must migrate to the myelination site; this step is believed to require communication between the migrant cells and the axons. iii) when the cell contacts the axon, transcriptional and post-transcriptional changes force the exit of the cell cycle and the differentiation of the cell into a mature Oligodendrocyte or Schwann cell. iv) Myelin synthesis is carried out around the axon to form a compact and functional structure to finally v) ensure that the structure and function of myelin are preserved through the continuous expression and synthesis of each of the components of myelin[46].

Although many of the myelin components have been related to the assembly and maintenance of the structure of this[47], Galactolipids and sulfatides, the main components of myelin, have received significant attention. The synthesis and maturation of most of these compounds begin in the endoplasmic reticulum and rapidly spreads to the extracellular space through the early secretion system[48,49].

As already mentioned, this myelination process is continuous, establishing a balance in the amount of each of its compounds.

Diverse studies[50–52] have shown that mitochondria and lysosomes are critical organelles for the maintenance of homeostasis in myelinating cells; likewise, there is a close relationship between these two and the interaction directly with cellular stress[50], In this way, communication between mitochondria and lysosomes can lead to mitophagy, processes in which damaged mitochondria target autophagosomes for lysis. Autophagosomes subsequently fuse with lysosomes / late endosomes to generate autolysosomes that mediate the degradation of mitochondria, or in contrast, mitochondria and lysosomes can also interact directly through nondegradable processes through the dynamic formation of sites of Membrane contact between organelles in healthy mammalian cells, leading to transfer of lipid, calcium, and iron metabolites, regulation of organelle dynamics, such as mitochondrial division and endosomal division[50].

However, the misregulation of mitochondria or contacts with lysosomes can simultaneously lead to the dysfunction of both organelles in various lysosomal storage disorders (LSD) such as MLD, which has been genetically and functionally related to mitochondrial and lysosomal defects[53].

DIAGNOSIS

Diagnosis of MLD requires a high level of complexity; however, Technological development is allowing the evolution of new diagnostic strategies aimed not only at identifying ARSA enzyme deficiency but also at the presence of findings such as progressive neurological dysfunction or evidence of typical lesions on magnetic resonance imaging, characteristic of the disease.

For the diagnosis of MLD, one of the following events must be present:

- Identification of biallelic ARSA pathogenic variants in molecular genetic tests (see Table 1).
- Identification of increased urinary excretion of sulfatides.
- Identification of metachromatic lipid deposits in a nerve or brain biopsy.

THERAPIES - TREATMENT

Due to the lack of information on this disease, few treatments aimed at safeguarding the lives of patients, mainly because the barrier between the blood and the brain limits the access of the recombinant product to the nervous tissues[54,55].

Currently, there is no treatment available to reverse the fatal outcome of this devastating disease; therapy is only supportive, disease severity and lack of effective therapies describe the need for innovative therapeutic approaches[54], however, according to the database of clinicaltrials.gov, To date, 36 clinical trials have been registered, of which 6 are in an active state, focused on determining the natural history of the disease, efficacy, and safety of HGT-1110 (recombinant human arylsulfatase A), gene therapy based on lentiviral vectors, biomarker search, Human placental-derived stem cell transplantation in participants with MLD.

Symptom treatment and support

At the beginning of the disease, the patient is treated with remedies for epilepsy, muscle relaxants for contractures, physical therapy to improve nerve and muscle function, stimulation to maximize the intellect, and finally support to the families of those affected so that the parents and/or caregivers can anticipate decisions about wheelchairs, feeding tubes, and other care[9,36,56].

Enzyme replacement therapy

Enzyme replacement therapy has become the most promising therapeutic option for various lysosomal diseases due to its potential to compensate for the deficiency; it is currently available as a treatment for some disorders such as Fabry, Gaucher, Pompe, mucopolysaccharidosis I, II, VI and it's under development for others like MLD[54]. However, this type of therapy remains challenging because the blood-brain barrier is impervious to lysosomal enzymes[57,58].

Currently, there are three-phase I and II studies reporting the safety, efficacy, and pharmacodynamics of this type of therapy in patients with MLD[59–61]. In this therapy, recombinant human arylsulfatase A (rhASA) has been used, which has generated changes in the concentrations of sulfates in CSF and urine of the patients from the beginning to the end of the study, demonstrating an excellent therapeutic start[61,62].

Gene therapy

Therapy based on the overexpression of wild-type ARSA in different cell types. This type of therapy has been successful when autologous hematopoietic stem cells obtained from patients with MLD are used, in which the ARSA gene is overexpressed by gene transfer using retroviral or lentiviral vectors[63]. The wild-type synthesized ARSA secreted by these genetically engineered autologous hematopoietic stem cells are

Test	Function	Methods	Basis	Reference
Biochemical test	Evaluate ARSA activity.	Bladder Stimulation, Urine Analysis.	Dose of the sulfatides in urine and the molecular analysis of the same.	37,52
Molecular genetic testing	Three classes of ARSA alleles are distinguished that produce low enzymatic ARSA activity.	Tests single gene	ARSA sequence analysis is performed first and then an analysis of deletion / duplication targeting a gene if only one or none are found pathogenic variant.	15
		Multigene panel.	Includes ARSA and other genes of interest	15
		More comprehensive genomic testing: exome sequencing and the genome sequencing.	Provide or suggest a diagnosis not previously considered (eg, the mutation of agenor different genes that results in a similar clinical presentation).	15
Urinary sulfatides	Determine the concentration of abnormally high sulfatides in the urine.	High performance liquid chromatography (HPLC), mass spectrometry and thin layer chromatography (TLC).	Sulfatide excretion is measured in a 24-hour urine sample or normalized to urinary creatinine excretion. Heterozygous ARSA-PD / ARSA-MLD compounds can excrete higher than normal amounts of sulfatides, but the excretion of sulfatides in urine is not as high as in individuals with MLD (usually> 10 times normal).	15
Metachromatic lipid deposits in a nerve or brain biopsy	Sulfatides interact strongly with certain positively charged dyes used to stain tissues, resulting in a change in the color of the stained tissue called metachromasia.	Hirsch-Peiffer stain	When sections of frozen tissue are treated with acidified cresyl violet (Hirsch-Peiffer stain), the sulfatide-rich storage deposits stain golden brown.	15
Radiological, histopathological and neurophysiological examinations	Assess brain status and involvement.	Resonance Magnetic	MRI of the brain shows typical lesions of MLD, as a relevant compromise of the cerebral white matter.	37

Table 1. Diagnostic methods for the identification of MLD.

absorbed by adjacent ARSA-deficient cells through the mannose-6-phosphate receptor system[64].

Today, there are complete and ongoing clinical trials in which gene therapy has been used as an adjunct in patients with MLD[65].

Hematopoietic stem cell therapy

With this type of therapy, it is possible to reach the blood-brain barrier by using hematopoietic stem cells that differentiate into microglial cells[66]. In principle, once the donor's microglial cells cross the blood-brain barrier, they can secrete the wild-type ARSA enzyme, taken up by ARSA-deficient receptor neuronal cells. This uptake is performed by the mannose-6-phosphate receptor system, which carries the enzyme directly to the lysosomes, where the sulfatides accumulate in the ARSA receptor-deficient neural cells[63,67].

Despite being a promising therapy in clinical trials, it has been shown that the main complication that can occur in treated patients is the presence of graft-versus-host disease. The drugs used for this type of therapy have been busulfan, cyclophosphamide, anti-thymocyte globulin (ATG), tested on both children and adults[67,68].

Brain gene therapy with adeno-associated virus (AAV) vectors

This type of therapy is ideal for treating MLD patients since the genetic message for the ARSA gene could be sent directly to the SNC. This therapy has the use of AAV vectors that have low immunogenicity, low oncogenic potential through insertion mutagenesis, and in addition to this, three main characteristics that make it unique:

- Because it is safe, it can be administered directly in the CNS to Through the intraparenchymal, intracerebroventricular, and intracisternal routes where the ARSA protein is expressed persistently and permanently in a single dose.
- Once this therapy is administered at the site of action, it has the ability to prevent the symptoms of the disease[69–71].
- The ARSA protein when expressed in healthy cells is capable of cross-correcting neighboring cells, therefore cells that are corrected will secrete the protein that is endocitated through the mannose-6-phosphate receptor (M6P) pathway[72].

AAVs that have been used so far for the treatment of MLD have been AAV5, and then with the discovery of serotypes derived from non-human primates, studies with AAVrh were conducted[71,73–75].

CRISPR Cas9

This technique has become a novel and widely used research tool with which rapid, easy and efficient genetic modification is achieved[76], with which alleles that cause disease are repaired by changing the DNA sequence at the exact location of the chromosome[10]. The acronym CRISPR Cas9 comes from Clustered Regularly Interspaced Short Palindromic Repeats, in Spanish "Short Palindromic Repeats Grouped and Regularly interspaced".

This technology has enabled two-stage genome editing. In the first, guide RNA, which is specific to a DNA sequence, is associated with the enzyme Cas9 endonuclease, which works by cutting DNA. In the second stage, natural repair mechanisms of the cut DNA are activated. In which indel (insertion-deletion) can be generated or, moreover, a specific sequence is incorporated exactly at the original cut site. For this, the sequence of interest is supplied to the cell in such a way that it is integrated into the DNA[77].

This technology brings hope of a cure not only for MLD but for many other genetic diseases such as Alzheimer's, Cancer, AIDS, Cystic Fibrosis, etc., for many genetic diseases. It should be noted that to date it has not been used as a treatment for patients with this type of disease[78].

Conclusions

Despite great research efforts to find an effective treatment for MLD, these approaches have not been effective not only because of the low efficiency of gene editing but because gene therapies must cross the blood-brain barrier. which becomes a challenge. Therefore, patients with MLD continue without any treatment and, above all, there are still gaps in knowledge about the management of this disease.

Given the limitations presented by existing therapies in the treatment of MLD, it is necessary to investigate new therapies to increase the effectiveness of the treatment.

Considering the panorama in MLD, it is essential to continue in the constant search that points to the understanding of epidemiology and diagnostic tools for the disease.

Financial support

This project was funded by the project entitled "Metabolism of sulfatides, glycolysis and mitochondrial function in metachromatic leukodystrophy" in the call for research projects in basic sciences 712-2015, of Minciencias. Whose principal investigator is Dr. Norma C. Serrano.

Conflict of interests

None

Abbreviations

MLD: Metachromatic Leukodystrophy

CNS: Central Nervous System

PNS: Peripheral Nervous System

CRISPR Cas9: Short Palindromic Repetitions Grouped and Regularly Spaced

ATP: Adenosine triphosphate

GalC: Galactosylceramide

rhASA: Recombinant Human Arylsulfatase A

ATG: Anti-thymocyte Globulin

Bibliographic references

1. Takahashi T, Suzuki T. Role of sulfatide in normal and pathological cells and tissues. J Lipid Res. 2012;53(8):1437-50.
2. Tan M, Fuller M, Zabidi-Hussin Z, Hopwood JJ, Meikle PJ. Biochemical profiling to predict disease severity in metachromatic leukodystrophy. Mol Genet Metab. 2010;99(2):142-8.
3. OMIM - Herencia mendeliana en línea en el hombre [Internet]. [Updated April 16, 2021, cited 13 of July de 2019]. available in: https://www.omim.org/
4. Blomqvist M, Carrier M, Andrews T, Pettersson K, Mansson JE, Rynmark BM, et al. In vivo administration of the C16:0 fatty acid isoform of sulfatide increases pancreatic sulfatide and enhances glucose-stimulated insulin secretion in Zucker fatty (fa/fa) rats. Diabetes Metab Res Rev. 2005;21(2):158-66.
5. Boslem E, Meikle PJ, Biden TJ. Roles of ceramide and sphingolipids in pancreatic α -cell function and dysfunction. Islets. 2012;4(3):177-87.
6. Buschard K, Blomqvist M, Månsson J-E, Fredman P, Juhl K, Gromada J. C16:0 Sulfatide Inhibits Insulin Secretion in Rat α -Cells by Reducing the Sensitivity of KATP Channels to ATP Inhibition. Diabetes. 2006;55(10):2826.
7. Gulati S, Jain P, Chakrabarty B, Kumar A, Gupta N, Kabra M. The spectrum of leukodystrophies in children: Experience at a tertiary care centre from North India. Ann Indian Acad Neurol. 2016;19(3):332-8.
8. Leucodistrofia : National Institute of Neurological Disorders and Stroke (NINDS) [Internet]. [Updated December 21, 2016, cited 12 de November of 2019]. available in: https://espanol.ninds.nih.gov/trastornos/leucodistrofia.htm
9. Leucodistrofia metacromática | Genetic and Rare Diseases Information Center (GARD) – an NCATS Program [Internet]. [updated 10/6/2015, cited 31 de December of 2018]. available in: https://rarediseases.info.nih.gov/espanol/12627/leucodistrofia-metacromatica

10. Van der Knaap MS, Wolf NI, Heine VM. Leukodystrophies: Five new things. Neurol Clin Pract. 2016;6(6):506-14.
11. Beerepoot S, Nierkens S, Boelens JJ, Lindemans C, Bugiani M, Wolf NI. Peripheral neuropathy in metachromatic leukodystrophy: current status and future perspective. Orphanet J Rare Dis. 2019
12. Gordon H, Letsou A, Bonkowsky J. The Leukodystrophies. Semin Neurol. 2014;34(03):312-20.
13. Association Européenne Contre les Leucodystrophies. Accueil - [Internet]. [cited 15 of November of 2019]. available in: https://ela-asso.com/
14. Brignone MS, Lanciotti A, Camerini S, De Nuccio C, Petrucci TC, Visentin S, et al. MLC1 protein: a likely link between leukodystrophies and brain channelopathies. Front Cell Neurosci. 2015;9:66-66.
15. Gordon-Lipkin E, Fatemi A. Current Therapeutic Approaches in Leukodystrophies: A Review. J Child Neurol. 2018;33(13):861-8.
16. Nyhan WL, Barshop BA, Ozand PT. Atlas of Metabolic Diseases Second edition. CRC Press; 2005.
17. Gomez-Ospina N. Arylsulfatase A Deficiency. En: Adam MP, Ardinger HH, Pagon RA, Wallace SE, Bean LJH, Stephens K, et al., editores. GeneReviews((R)). Seattle WA: University of Washington, Seattle. GeneReviews is a registered trademark of the University of Washington, Seattle; 1993.
18. Almarzooqi S, Quadri A, Albawardi A. Gallbladder Polyps in Metachromatic Leukodystrophy. Fetal Pediatr Pathol. 2018;37(2):102-8.
19. Van den Broek BTA, Page K, Paviglianiti A, Hol J, Allewelt H, Volt F, et al. Early and late outcomes after cord blood transplantation for pediatric patients with inherited leukodystrophies. Blood Adv. 2018;2(1):49-60.
20. Golchin N, Hajjari M, Malamiri RA, Aminzadeh M, Mohammadi-asl J, Golchin N, et al. Identification of a novel mutation in ARSA gene in three patients of an Iranian family with metachromatic leukodystrophy disorder. Genet Mol Biol. 2017;40(4):759-62.
21. Belli G, Bartolini E, Bianchi A, Mascalchi M, Stagi S. Central Precocious Puberty in a Child With Metachromatic Leukodystrophy. Front Endocrinol. 2018;9.
22. Bindu P, Mahadevan A, Taly A, Christopher R, Gayathri N, Shankar S. Peripheral neuropathy in metachromatic leucodystrophy. A study of 40 cases from south India. J Neurol Neurosurg Psychiatry. 2005;76(12):1698-701.
23. Calbi V, Fumagalli F, Consiglieri G, Penati R, Acquati S, Redaelli D, et al. Use of Defibrotide to help prevent post-transplant endothelial injury in a genetically predisposed infant with metachromatic leukodystrophy undergoing hematopoietic stem cell gene therapy. Bone Marrow Transpl. 2018.
24. Wang RY, Bodamer OA, Watson MS, Wilcox WR. Lysosomal storage diseases: Diagnostic confirmation and management of presymptomatic individuals. Genet Med. 2011;13(5):457-84.
25. Dehghan Manshadi M, Kamalidehghan B, Aryani O, Khalili E, Dadgar S, Tondar M, et al. Four novel ARSA gene mutations with pathogenic impacts on metachromatic leukodystrophy: a bioinformatics approach to predict pathogenic mutations. Ther Clin Risk Manag. 2017;13:725-31.
26. Ministerio de Salud y Protección Social, Consuelo Pinzón Gutiérrez, Fredy Orlando Mendivelso Duarte, Sandra Patricia Misnaza Castrillón. HUÉRFANAS-RARAS code: 342 [Internet]. p. 19. available in: https://www.ins.gov.co/buscador-eventos/Lineamientos/PRO%20Enfermedades%20hu%C3%A9rfanas%20y%20raras.pdf#search=enfermedades%20raras
27. Prevalence of rare diseases: Bibliographic data [Internet]. [cited 28 of November of 2018]. available in: http://online.fliphtml5.com/trmf/ktss/#p=10
28. Kehrer C, Groeschel S, Kustermann-Kuhn B, Burger F, Kohler W, Kohlschutter A, et al. Language and cognition in children with metachromatic leukodystrophy: onset and natural course in a nationwide cohort. Orphanet J Rare Dis. 2014;9(18):1750-1172.
29. Krägeloh-Mann I, Groeschel S, Kehrer C, Opherk K, Nägele T, Handgretinger R, et al. Juvenile metachromatic leukodystrophy 10 years post transplant compared with a non-transplanted cohort. Bone Marrow Transplant. 2012;48:369.
30. Doherty K, Frazier SB, Clark M, Childers A, Pruthi S, Wenger DA, et al. A closer look at ARSA activity in a patient with metachromatic leukodystrophy. Mol Genet Metab Rep. 2019;19.
31. Artigalás O, Lagranha VL, Saraiva-Pereira ML, Burin MG, Lourenço CM, van der Linden H, et al. Clinical and biochemical study of 29 Brazilian patients with metachromatic leukodystrophy. J Inherit Metab Dis. 2010;33(S3):257-62.
32. Virgens MYF, Siebert M, Bock H, Burin M, Giugliani R, Saraiva-Pereira ML. Genotypic characterization of Brazilian patients with infantile and juvenile forms of metachromatic leukodystrophy. Gene. 2015;568(1):69-75.
33. Saute JAM, Souza CFM de, Poswar F de O, Donis KC, Campos LG, Deyl AVS, et al. Neurological outcomes after hematopoietic stem cell transplantation for cerebral X-linked adrenoleukodystrophy, late onset metachromatic leukodystrophy and Hurler syndrome. Arq Neuropsiquiatr. 2016;74(12):953-66.
34. Alvarez-Leal M, Contreras-Hernández D, Chávez A, Diaz-Contreras JA, Careaga-Olivares J, Zúñiga-Charles MA, et al. Leukocyte arylsulfatase A activity in patients with alcohol-related cirrhosis: Arylsulfatase A in Chronic Alcoholic Cirrhosis. Am J Hum Biol. 2001;13(3):297-300.
35. Echeverri Olga Y, Salazar Diego A, Rodriguez-Lopez A, Janneth G, Almeciga-Diaz Carlos J, Barrera Luis A. Understanding the Metabolic Consequences of Human Arylsulfatase A Deficiency through a Computational Systems Biology Study. Cent Nerv Syst Agents Med Chem. 2016.
36. Espejo LM, de la Espriella R, Hernández JF. Leucodistrofia metacromática. Presentación de caso. Rev Colomb Psiquiatr. 2017;46(1):44-9.
37. Álvarez-Pabón Yelitza. Leucodistrofia metacromática infantil tardía: Presentación de un caso. Arch Argent Pediatr. 2019;117(1).
38. Fumagalli DF, Fumagalli AI, Biffi A, Cesani M, Corea F, Sessa M, et al. Leucodistrofia metacromática: del diagnóstico a la terapia génica como perspectiva terapéutica. 1982;6.
39. https://www.orpha.net/consor/cgi-bin/OC_Exp.php?Lng=ES&Expert=512. Orphanet: Leucodistrofia metacromática [Internet]. [cited 31 of December de 2018]. available in: https://www.orpha.net/consor/cgi-bin/OC_Exp.php?Lng=ES&Expert=512
40. Ozgen H, Baron W, Hoekstra D, Kahya N. Oligodendroglial membrane dynamics in relation to myelin biogenesis. Cell Mol Life Sci. 2016;73:3291-310.
41. Vos JP, Lopes-Cardozo M, Gadella BM. Metabolic and functional aspects of sulfogalactolipids. Biochim Biophys Acta BBA - Lipids Lipid Metab. 1994;1211(2):125-49.
42. Sherman DL, Brophy PJ. Mechanisms of axon ensheathment and myelin growth. Nat Rev Neurosci. 2005;6(9):683-90.
43. Berntson Z, Hansson E, Ronnback L, Fredman P. Intracellular sulfatide expression in a subpopulation of astrocytes in primary cultures. J Neurosci Res. 1998;52(5):559-68.
44. Fullerton PM. Peripheral nerve conduction in metachromatic leucodystrophy (sulphatide lipidosis). J Neurol Neurosurg Psychiatry. 1964;27(2):100-5.
45. Popovich PG, Jakeman LB, McTigue DM. Glial Responses to Injury. En: Encyclopedia of Neuroscience [Internet]. Elsevier; 2009 [cited 26 July 2020]. p. 853-9. Available at: https://linkinghub.elsevier.com/retrieve/pii/B9780080450469000188
46. Brady ST, Witt AS, Kirkpatrick LL, de Waegh SM, Readhead C, Tu P-H, et al. Formation of Compact Myelin Is Required for Maturation of the Axonal Cytoskeleton. J Neurosci. 1999;19(17):7278-88.
47. Mikoshiba K, Okano H, Tamura TA, Ikenaka K. Structure and Function of Myelin Protein Genes. Annu Rev Neurosci. 1991;14(1):201-17.
48. Krämer E-M, Koch T, Niehaus A, Trotter J. Oligodendrocytes Direct Glycosyl Phosphatidylinositol-anchored Proteins to the Myelin Sheath in Glycosphingolipid-rich Complexes. J Biol Chem. 1997;272(14):8937-45.
49. Taylor CM, Coetzee T, Pfeiffer SE. Detergentα insoluble glycosphingolipid/cholesterol microdomains of the myelin membrane. J Neurochem. 2002;81(5):993-1004.
50. Wong YC, Kim S, Peng W, Krainc D. Regulation and Function of Mitochondria–Lysosome Membrane Contact Sites in Cellular Homeostasis. Trends Cell Biol. 2019;29(6):500-13.
51. Plotegher N, Duchen MR. Crosstalk between Lysosomes and Mitochondria in Parkinson's Disease. Front Cell Dev Biol. 2017 [cited 11 April 2020];5. Available at: https://www.ncbi.nlm.nih.gov/pmc/articles/PMC5732996/

52. Deus CM, Yambire KF, Oliveira PJ, Raimundo N. Mitochondria–Lysosome Crosstalk: From Physiology to Neurodegeneration. Trends Mol Med. enero de 2020;26(1):71-88.
53. Platt FM, d'Azzo A, Davidson BL, Neufeld EF, Tifft CJ. Lysosomal storage diseases. Nat Rev Dis Primer. 2018;4(1):27.
54. Biffi A, Lucchini G, Rovelli A, Sessa M. Metachromatic leukodystrophy: an overview of current and prospective treatments. Bone Marrow Transpl. 2008;42(2):275.
55. Lagranha VL, Baldo G, de Carvalho TG, Burin M, Saraiva-Pereira ML, Matte U, et al. In vitro correction of ARSA deficiency in human skin fibroblasts from metachromatic leukodystrophy patients after treatment with microencapsulated recombinant cells. Metab Brain Dis. 2008;23(4):469-84.
56. Eichler FS, Cox TM, Crombez E, Dali CÍ, Kohlschütter A. Metachromatic Leukodystrophy: An Assessment of Disease Burden. J Child Neurol. 2016;31(13):1457-63.
57. Bockenhoff A, Cramer S, Wolte P, Knieling S, Wohlenberg C, Gieselmann V, et al. Comparison of Five Peptide Vectors for Improved Brain Delivery of the Lysosomal Enzyme Arylsulfatase A. J Neurosci. 2014;34(9):3122-9.
58. Desnick RJ, Schuchman EH. Enzyme Replacement Therapy for Lysosomal Diseases: Lessons from 20 Years of Experience and Remaining Challenges. Annu Rev Genomics Hum Genet. 2012;13(1):307-35.
59. Biffi A, Montini E, Lorioli L, Cesani M, Fumagalli F, Plati T, et al. Lentiviral Hematopoietic Stem Cell Gene Therapy Benefits Metachromatic Leukodystrophy. Science. 2013;341(6148). Available at: http://science.sciencemag.org/content/341/6148/1233158.abstract
60. Kehrer C, Blumenstock G, Gieselmann V, Krägeloh-Mann I, GERMAN LEUKONET. The natural course of gross motor deterioration in metachromatic leukodystrophy. Dev Med Child Neurol. 2011;53(9):850-5.
61. Efficacy METAZYM for the Treatment Metachromatic Leukodystrophy Treated With Hematopoietic Stem Cell Transplantation - No Study Results Posted - ClinicalTrials.gov [Internet]. [cited 10 April 2020]. Available in: https://clinicaltrials.gov/ct2/show/results/NCT01303146
62. Shire. A Single Center, Open-label, Non-randomized, Uncontrolled, Multiple-dose, Dose Escalation Study of the Safety, Pharmacokinetics and Efficacy of Metazym for the Treatment of Patients With Late Infantile Metachromatic Leukodystrophy (MLD) [Internet]. clinicaltrials.gov; 2018 dic [citado 24 de julio de 2020]. Report No.: results/NCT00418561. Disponible en: https://clinicaltrials.gov/ct2/show/results/NCT00418561
63. Patil SA, Maegawa GH. Developing therapeutic approaches for metachromatic leukodystrophy. Drug Des Devel Ther. 2013;7:729-45.
64. Saftig P, Klumperman J. Lysosome biogenesis and lysosomal membrane proteins: trafficking meets function. Nat Rev Mol Cell Biol. 2009;10:623.
65. Intracerebral Gene Therapy for Children With Early Onset Forms of Metachromatic Leukodystrophy - Full Text View - ClinicalTrials.gov [Internet]. [cited 27 January 2019]. Available at: https://clinicaltrials.gov/ct2/show/NCT01801709
66. Asheuer M, Pflumio F, Benhamida S, Dubart-Kupperschmitt A, Fouquet F, Imai Y, et al. Human CD34+ cells differentiate into microglia and express recombinant therapeutic protein. Proc Natl Acad Sci U S A. 2004;101(10):3557-62.
67. Stem Cell Transplant for Inborn Errors of Metabolism - Full Text View - ClinicalTrials.gov [Internet]. [cited 27 January 2019]. Available at: https://clinicaltrials.gov/ct2/show/NCT00176904
68. Masonic Cancer Center, University of Minnesota. Treatment of Lysosomal and Peroxisomal Inborn Errors of Metabolism by Bone Marrow Transplantation [Internet]. clinicaltrials.gov; 2017 dic [cited 24 July 2020]. Report No.: study/NCT00176904. Available at: https://clinicaltrials.gov/ct2/show/study/NCT00176904
69. Rauschka H, Colsch B, Baumann N, Wevers R, Schmidbauer M, Krammer M, et al. Late-onset metachromatic leukodystrophy: Genotype strongly influences phenotype. Neurology. 2006;67(5):859-63.
70. Golebiowski D, Bradbury AM, Kwon C-S, van der Bom IMJ, Stoica L, Johnson AK, et al. AAV Gene Therapy Strategies for Lysosomal Storage Disorders with Central Nervous System Involvement. En: Bo X, Verhaagen J, editores. Gene Delivery and Therapy for Neurological Disorders [Internet]. New York, NY: Springer New York; 2015 [cited 27 January 2019]. p. 265-95. (Neuromethods). Available at: https://doi.org/10.1007/978-1-4939-2306-9_11
71. Rosenberg JB, Sondhi D, Rubin DG, Monette S, Chen A, Cram S, et al. Comparative Efficacy and Safety of Multiple Routes of Direct CNS Administration of Adeno-Associated Virus Gene Transfer Vector Serotype rh.10 Expressing the Human Arylsulfatase A cDNA to Nonhuman Primates. Hum Gene Ther Clin Dev. 1 de septiembre de 2014;25(3):164-77.
72. Rosenberg JB, Kaminsky SM, Aubourg P, Crystal RG, Sondhi D. Gene Therapy for Metachromatic Leukodystrophy. J Neurosci Res. 2016;94(11):1169-79.
73. Piguet F, Sondhi D, Piraud M, Fouquet F, Hackett NR, Ahouansou O, et al. Correction of Brain Oligodendrocytes by AAVrh.10 Intracerebral Gene Therapy in Metachromatic Leukodystrophy Mice. Hum Gene Ther. 2012;23(8):903-14.
74. Sondhi D, Hackett NR, Peterson DA, Stratton J, Baad M, Travis KM, et al. Enhanced Survival of the LINCL Mouse Following CLN2 Gene Transfer Using the rh.10 Rhesus Macaque-derived Adeno-associated Virus Vector. Mol Ther. 2007;15(3):481-91.
75. Sondhi D, Johnson L, Purpura K, Monette S, Souweidane MM, Kaplitt MG, et al. Long-Term Expression and Safety of Administration of AAVrh.10hCLN2 to the Brain of Rats and Nonhuman Primates for the Treatment of Late Infantile Neuronal Ceroid Lipofuscinosis. Hum Gene Ther Methods. 2012;23(5):324-35.
76. Ormond KE, Mortlock DP, Scholes DT, Bombard Y, Brody LC, Faucett WA, et al. Human Germline Genome Editing. Am J Hum Genet. 2017;101(2):167-76.
77. Thurtleα Schmidt DM, Lo T. Molecular biology at the cutting edge: A review on CRISPR/CAS9 gene editing for undergraduates. Biochem Mol Biol Educ. 2018;46(2):195-205.
78. Ashrafi MR, Amanat M, Garshasbi M, Kameli R, Nilipour Y, Heidari M, et al. An update on clinical, pathological, diagnostic, and therapeutic perspectives of childhood leukodystrophies. Expert Rev Neurother. 2020;20(1):65-84.
79. Manual de Pruebas Diagnosticas de Laboratorio Clinico. Alejandro Almarza; 130 p.
80. Winzeler AM, Mandemakers WJ, Sun MZ, Stafford M, Phillips CT, Barres BA. The Lipid Sulfatide Is a Novel Myelin-Associated Inhibitor of CNS Axon Outgrowth. J Neurosci. 2011;31(17):6481-92.

Received: 15 march 2021
Accepted: 10 July 2021

REVIEW / ARTÍCULO DE REVISIÓN

Tecnología IgY: Estrategia en el tratamiento de enfermedades infecciosas humanas

Biotechnological tools in the diagnosis, prevention, and treatment of pandemics

Pamela Molina[1] and Marbel Torres Arias[2]

DOI. 10.21931/RB/2021.06.03.33

Resumen: Las pandemias son consideradas como un problema emergente de salud pública a nivel mundial, las cuales además de caracterizarse por tasas altas de morbilidad y mortalidad, ocasionan conflictos en los aspectos sociales, económicos y políticos. Las herramientas biotecnológicas, por su parte, han ido evolucionando conforme al avance tecnológico-científico, lo que ha permitido optimizar métodos de diagnóstico con alta sensibilidad y especificidad, además de mejorar el desarrollo de productos biológicos para la prevención y terapia de enfermedades. El objetivo de esta revisión es identificar la actualización de las herramientas biotecnológicas en el diagnóstico, tratamiento terapéutico y profiláctico frente a los patógenos causantes de las enfermedades pandémicas a lo largo de la historia, mediante la recopilación de información científica. Con este estudio se logró establecer que las herramientas y productos de origen biotecnológico han constituido un papel fundamental en el control de pandemias a través de la innovación constante que ha permitido alcanzar resultados eficientes tanto en diagnóstico como en el tratamiento.

Palabras clave: Diagnóstico, herramientas biotecnológicas, pandemias, productos biológicos, vacunas.

Abstract: Pandemics are considered as an emerging public health problem worldwide, which in addition to being characterized by high rates of morbidity and mortality cause conflicts in social, economic and political aspects. Biotechnological tools, for their part, have evolved according to technological-scientific advance, which has allowed optimizing diagnostic methods with high sensitivity and specificity; in addition to improving the development of biological products for the prevention and therapy of diseases. The objective of this review is to identify the performance of biotechnological tools in the diagnosis, therapeutic and prophylactic treatment against pathogens that cause pandemic diseases throughout history, through the collection of scientific information. Finally, with this study it was possible to establish that tools and products of biotechnological origin have constituted an fundamental role in the control of pandemics through constant innovation that has allowed achieving efficient results in both diagnosis and treatment.

Key words: Diagnostics, biotechnological tools, pandemics, biological products, vaccines.

Introducción

La manifestación de enfermedades infecciosas a lo largo de la historia de la humanidad además de ser una de las principales causas de mortalidad y morbilidad[1,2], han dejado secuelas letales y duraderas en el ámbito social, económico y político, siendo las de mayor proporción las enfermedades que han sido capaces de provocar pandemias[3–5]. Es así que una de las catástrofes más devastadoras que ha golpeado al mundo es la peste negra, en el siglo XIV, ocasionando el fallecimiento del 30-50% de la población europea de la época, en un corto periodo de tiempo (1347-1351)[6].

El desarrollo de enfermedades infecciosas emergentes puede ocurrir por tres eventos claves: 1) el cruce de barreras geográficas debido a la invasión de espacios silvestres, 2) el cruce de barreras por compatibilidad gracias a la evolución y 3) el levantamiento de barreras por el cambio de condiciones ambientales que favorecen la formación del nicho ecológico adecuado, siendo la primera la que define la situación[7]. Jones *et al.*[8] concluyeron en su investigación que el 60,3% de enfermedades infecciosas son originadas por patógenos zoonóticos y el 71.8% de estas son de origen silvestre, lo que indica que estos microorganismos figuran una amenaza potencial para la salud mundial, con perspectiva a la manifestación de epidemias y posibles pandemias, en caso de no tomar las medidas precautelares.

Durante el origen de una epidemia y/o pandemia, el diagnóstico temprano, el tratamiento, el seguimiento epidemiológico y la prevención de futuras infecciones han sido procesos fundamentales para el manejo clínico, control y mitigación de la enfermedad[9,10]. Aquí la biotecnología juega un papel fundamental, por lo que en este estudio se consideran las herramientas biotecnológicas modernas empleadas en el desarrollo de pruebas de diagnóstico, producción de moléculas biotecnológicas para el tratamiento y en el diseño de vacunas. Con el objetivo de identificar la evolución y optimización a través del tiempo de las herramientas biotecnológicas cuando nos enfrentamos a infecciones a nivel pandémico, mediante la comparación de sensibilidad y especificidad de los diferentes enfoques establecidos para el diagnóstico, y la recopilación de los resultados de los principales productos biotecnológicos llevados a ensayos clínicos en cada enfermedad.

Para la redacción del artículo se llevó a cabo una revisión bibliográfica exhaustiva en revistas de alto impacto, en las que se tomó en cuenta: artículos originales, revisiones, resúmenes de conferencias y demás. Obteniéndose datos actualizados de

[1] Departamento de Ciencias de la Vida y la Agricultura, Carrera de Ingeniería en Biotecnología, Universidad de las Fuerzas Armadas ESPE, Ecuador.
[2] Departamento de Ciencias de la Vida y la Agricultura, Carrera de Ingeniería en Biotecnología, Universidad de las Fuerzas Armadas ESPE, Ecuador y Laboratorio de Inmunología y Virología, CENCINAT, GISAH, Universidad de las Fuerzas Armadas, ESPE, Ecuador.

Corresponding author: mmtorres@espe.edu.ec

nueva tecnología desarrollada para diagnóstico, tratamientos biológicos, desarrollo de vacunas y su influencia en el manejo de epidemias y pandemias para apoyar al control de la Salud Publica.

Epidemias y pandemias importantes a partir de 1950

El término epidemia se refiere a "un brote de una enfermedad (especialmente una enfermedad infecciosa) que afecta a un gran número de personas dentro de una población al mismo tiempo"[11]. Por otro lado, pandemia se define como "una epidemia que ocurre en un área muy amplia, cruzas fronteras internacionales y generalmente afecta a un gran número de personas"[12].

Existen condiciones imprescindibles para la aparición de una epidemia, entre las características se hallan: transmisión eficiente entre humanos, un índice significativo de letalidad, falta de un tratamiento médico efectivo, una población inmunológicamente deprimida y una forma de diseminación rápida[13].

Es asi que, una pandemia se entiende como una enfermedad que ha alcanzado los cinco continentes, mientras que una epidemia es una enfermedad se esparce localmente[11,12].

A continuación, se abordarán el diagnóstico (Tabla 1), tratamientos biológicos (Tabla 2) y vacunas (Tabla 3) de las pandemias y epidemias más importantes en época cronológica, a partir del inicio de la biotecnología moderna (Figura 1).

H1N1 (1918-1919)

La pandemia de influenza más grave de la historia fue la gripe española H1N1 en 1918[14], cubrió el mundo en cuatro meses cobrando aproximadamente de 50 a 100 millones de vidas[15]. La falta de recursos limitó la identificación del origen de la gripe con lo que se hizo imposible el hallazgo de vacunas, además, no se logró controlar las infecciones secundarias con neumonía bacteriana debido a que la penicilina no se descubrió hasta 1928. A pesar del esfuerzo de las compañías farmacéuticas el virus desapareció antes de conseguir aislarlo[14].

H2N2 (1957-1960)

Segunda gran pandemia de influenza registrada, la gripe asiática surgió en Singapur a finales de febrero de 1957 y duró hasta 1960, fue provocada por un subtipo de virus de la influenza A, denominado H2N2[16,17]. A nivel mundial se registraron 1,1 millones de fallecimientos[18].

El diagnóstico de la enfermedad se ejecutó mediante pruebas serológicas de laboratorio. La identificación de anticuerpos contra el antígeno viral del subtipo H2N2 a partir de suero de personas afectadas se realizó con la técnica de fijación del complemento (FC) y la prueba de inhibición de la hemaglutinación (HAI) con el uso de tripsina y periodato de potasio para la inactivación de inhibidores específicos[19,20]. Los estudios y la experiencia de campo demostraron que la FC presentó mayor sensibilidad, sin embargo, existieron casos en los que se requirieron de las dos técnicas para un diagnóstico confirmatorio[20].

Tratamiento terapéutico y profiláctico

La mortalidad de la pandemia de gripe asiática se redujo aproximadamente un 97% en comparación con la pandemia de gripe española[15]. Una de las aportaciones fundamentales en el control de la propagación de la influenza asiática fue el rápido proceso de preparación y distribución de la vacuna frente

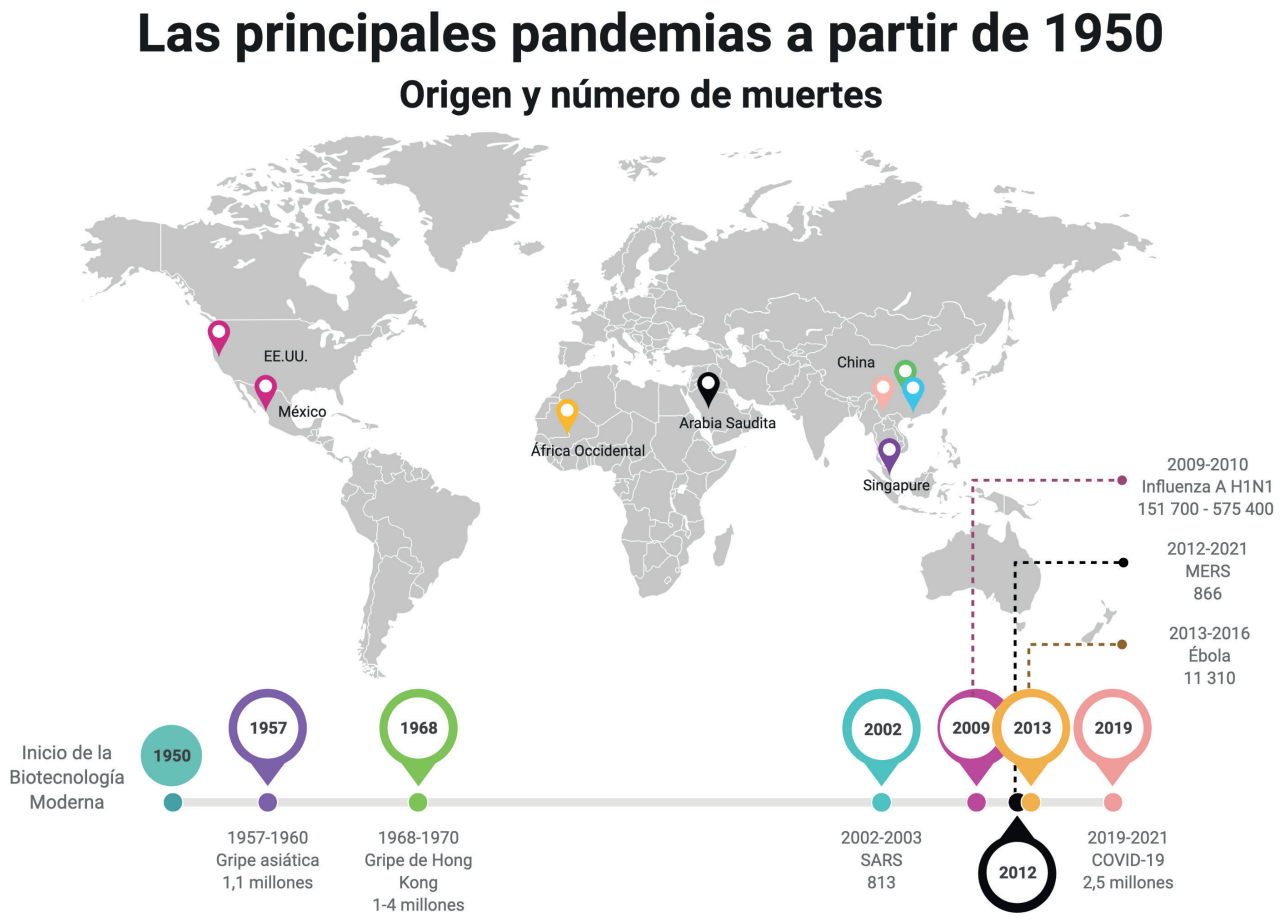

Figura 1. Las principales pandemias a partir de 1950. Origen y número de muertes a nivel mundial.

Pandemia	Año	Ensayo biotecnológico	Tipos	Sensibilidad / Especificidad	Referencias
H2N2 (Gripe asiática)	1957-1960	Inmunoensayos	Fijación del complemento	Sensibilidad: 76.4%	20
			HAI	Sensibilidad: 61.8%	
H3N2 (Gripe de Hong Kong)	1968-1970	Inmunoensayos	Fijación del complemento	Sensibilidad: 78%	29
			HAI	Sensibilidad: 92%	
SARS-CoV-1 (SARS)	2002-2003	Cultivo viral	Virus detectado por la aparición de efecto citopático e IFD	Sensibilidad: 15,4% Especificidad: 98%	39,41,42,44
		Inmunoensayos	ELISA	Sensibilidad: 68.4-98.4% Especificidad: 99.89%	
			IFI	Sensibilidad: 92% Especificidad: 92%	
		Técnicas moleculares	RT-PCR	Sensibilidad: 44-60% Especificidad: 96%	
			qRT-PCR	Sensibilidad: 80% Especificidad: 100%	
H1N1 (Influenza H1N1)	2009-2010	Cultivo viral	Virus detectado por la aparición de efecto citopático, ensayo de HA o tinción por IFD	Especificidad: >95%	62
		Inmunoensayos	Prueba rápida de antígenos	Sensibilidad: 10-70% Especificidad: >95%	
			IFD para la detección de antígenos	Sensibilidad: 47-93% Especificidad :>96%	
		Técnicas moleculares	-RT-PCR	Sensibilidad: 86-100%	
			-qRT-PCR	Especificidad: >99%	
MERS-CoV (MERS)	2012-2021	Técnicas moleculares	qRT-PCR	Sensibilidad: 92-100% Especificidad: 100%	80,81,219
EBOV (EVE)	2013-2016	Inmunoensayos	Pruebas rápidas de detección de antígenos	Sensibilidad: 84-97% Especificidad: 98- 100%	103,105
		Técnicas moleculares	Basadas en qRT-PCR	Sensibilidad: 82-100% Especificidad: 89- 100%	
SARS-CoV-2 (COVID-19)	2019-2021	Técnicas moleculares	qRT-PCR estándar	Sensibilidad: 85-97% Especificidad: 90-100%	141,220
			Pruebas moleculares rápidas	Sensibilidad: 68 - 100% Especificidad: 86.7- 98.3%	
		Inmunoensayos	Pruebas rápidas de detección de antígenos	Sensibilidad: 0- 94% Especificidad: 98.1- 99.9%	

Tabla 1. Especificidad y sensibilidad de las herramientas biotecnológicas frente al diagnóstico de pandemias.

al virus H2N2, se estima que en julio de 1957 inició el primer estudio clínico[21,22].

Existieron varias vacunas inactivadas de influenza en ensayos en humanos, desarrolladas a partir de líquido alantoideo de embriones de pollo infectados con diferentes cepas de influenza[23,24]. Entre las que se encontraron vacunas monovalentes[21–23,25] y polivalentes, en el caso de las polivalentes en algunas se incluyó el virus H2N2[25]. Para la inactivación del virus se manejaron técnicas como irradiación ultravioleta[21] y el empleo de formalina[22,23,25].

Las vacunas fueron probadas con diversas concentraciones de unidades de aglutinación de células de pollo (CCA) por mililitro, oscilando entre 200 CCA a 750 CCA[24], los resultados evidenciaron un porcentaje de eficacia estimado de 42% a 77%[24]. Asimismo, se observó que la protección inducida era directamente proporcional a la dosis administrada de vacuna ante la presencia de una cepa de H2N2, estos datos se evaluaron mediante FC e HAI, en los que se determinaron el aumento de los niveles de anticuerpos contra el virus de la influenza asiática posterior a la vacunación en pacientes participantes[21,23,25].

Debido a que Centro América y Sudamérica no contaban con los recursos ni la tecnología para el desarrollo de una vacuna, y sumando los problemas serios en la salud pública, los sistemas de control no fueron efectivos como en Norteamérica. Por lo que, solo grupos selectos de personas en Chile, Brasil y Argentina accedieron al medicamento[26].

H3N2 (1968-1970)

La siguiente pandemia provocada por un virus de la influenza A surgió en julio de 1968 al sureste de China, con el subtipo H3N2, extendiéndose hasta 1970. La enfermedad se denominó gripe de Hong Kong, la cual provocó entre 1 y 4 millones de muertes a nivel mundial[27,28]. El diagnóstico se basó en la identificación de síntomas combinado con ensayos serológicos. Para la detección de anticuerpos contra el virus H3N2 se empleó HAI y FC, con el uso de antígenos obtenidos del líquido alantoideo de huevo de las variantes aisladas de las diferentes propagaciones. Dando mejores resultados la HAI, sin embargo, fue recomendable realizar los dos métodos para obtener una máxima eficiencia en el serodiagnóstico[29].

Tratamiento terapéutico y profiláctico

Posterior al aislamiento viral y la confirmación de la aparición de H3N2, una variante antigénica del virus de la influenza con potencial epidémico, la cepa aislada fue distribuida a los laboratorios para la investigación y producción de vacunas[27,30]. En EE. UU., en noviembre del mismo año estuvo disponible el primer lote de producción con 110 000 dosis, se trató de una vacuna inactivada monovalente de 400 CCA, desarrollada en huevos fértiles de gallina con la cepa Aichi de la influenza H3N2. A diferencia de la anterior pandemia, en esta ocasión existió un mayor número de vacunados, principalmente personas pertenecientes al grupo prioritario. Las semanas siguientes al lanzamiento del primer lote se produjeron y comerciali-

Pandemia	Tratamiento	Descripción	Fase de desarrollo/ Identificación	Referencias
SARS-CoV-1 (SARS)	Plasma convaleciente	Administración de 200-400 ml (4-5 ml / kg) de plasma convaleciente compatible para supresión de la viremia	No existe	46
	Pentaglobulina	Inmunoglobulina intravenosa comercial enriquecida con IgM. Una dosis de 5 ml / kg / día durante 6 h por 3 días consecutivos	No existe	47
H1N1 (Influenza H1N1)	Inmunoglobulina intravenosa	H-IVIG obtenida de plasma convaleciente	No aplicable NCT01617317	65
	Plasma convaleciente	Plasma de convalecencia con un título de anticuerpos neutralizantes de ≥ 1: 160	No existe	66
MERS-CoV (MERS)	Plasma convaleciente	Actividad neutralizante eficaz con PRNT ≥1: 80	Fase 2 NCT02190799	90
	REGN3048B-REGN3051	mAb neutralizantes completamente humanos contra MERS-CoV dirigido al RBD de la proteína S	Fase 1 NCT03301090	91
	SAB-301	Anticuerpo IgG policlonal completamente humano dirigido a la proteína S	Fase 1 NCT02788188	93
	Interferón β-1b recombinante más lopinavir-ritonavir	Interferón presenta efectos inhibidores sobre el MERS-COV y lopinavir-ritonavir son antirretrovirales inhibidores de la proteasa	Fase 2/3 NCT02845843	87
	ZMapp	Cóctel de tres mAb anti-EBOV-GP	Fase 1/2 NCT02363322	109
	Plasma convaleciente	Intervención terapéutica contra la EVE	Fase 2/3 NCT02342171	108
	TKM-100802	ARNip que inhiben la expresión de VP35 y L-polimerasa.	Fase 2 PACTR201501000997429	111
EVE EBOV (EVE)	Interferón (IFN β-1a)	IFN-β1a posee actividad antiviral de amplio espectro	Fase 1/2 ISRCTN17414946	110
	Inmazeb (REGN-EB3)	Cóctel de tres anticuerpos dirigidos a la GP del EBOV. Aprobado con una dosis intravenosa de 150mg/kg.	Aprobado PALM: NCT03719586	112–114
	Ebanga (mAb114)	mAb anti-EBOV-GP, derivado de un sobreviviente del brote de Kikwit de 1995. Con una única dosis intravenosa de 50 mg/kg	Aprobado PALM: NCT03719586	112,115,116
SARS-CoV-2 (COVID-19)	Bamlanivimab (LY-CoV555 o LY3819253)	mAb neutralizante, dirigido al RBD de la proteína S del SARS-CoV-2. Aprobado con dosis única de 700 mg	Fase 2 NCT04427501 EUA por la FDA	150–152

Tabla 2. Principales ensayos clínicos de herramientas biotecnológicas usadas como tratamiento terapéutico y profiláctico de pandemias.

	Bamlanivimab (LY3819253 o LY-CoV555) y etesevimab (LY3832479 o LY-CoV016)	mAb IgG1 neutralizantes que se unen a epítopos distintos pero superpuestos del RBD de la proteína S del SARS-CoV-2. Aprobado con dosis única intravenosa de 700mg (bamlanivimab 350mg e etesevimab 350 mg)	Fase 2/3 NCT04427501 EUA la FDA	150,153
	REGN-COV2 (casirivimab y imdevimab)	Cóctel de mAb humanos recombinantes que se unen a epítopos no superpuestos de la proteína del RBD de la proteína S del SARS-CoV-2. Aprobado con dosis única intravenosa de 2400 mg (casirivimab 1200 mg e imdevimab 1200 mg)	Fase 2/3 NCT04425629 EUA por la FDA	150,154
	Plasma convaleciente	Plasma humano extraído de individuos recuperados con anticuerpos contra el SARS-CoV-2. Se emplean 1 o más transfusiones según la respuesta del paciente	Varias etapas y estados ChiCTR2000029757 NCT04547660 NCT04338360 NCT04479163 NCT04712344 EUA por la FDA	155,157–159,221

Tabla 2. Principales ensayos clínicos de herramientas biotecnológicas usadas como tratamiento terapéutico y profiláctico de pandemias.

zaron alrededor de 123 millones de dosis[30].

Maassab *et al.*[31] diseñaron y probaron una vacuna de influenza viva atenuada desarrollada en huevos de gallina. La atenuación de una línea del virus de Hong Kong se llevó a cabo mediante cambios abruptos en la temperatura de incubación de la cepa viral, esta técnica acortó el proceso a 3 meses, en comparación con métodos anteriores que empleaban cambios decrecientes de temperatura de forma gradual, las cuales duraban de 6 a 8 meses. Los ensayos clínicos de esta vacuna demostraron aceptabilidad e inmunogenicidad de la cepa atenuada, por lo que este proceso se consideró prometedor para el desarrollo futuro de vacunas contra la influenza. Por otro lado, se aprobó la aplicación de vacunas de virus fraccionados, mediante éter[32] o desoxicolato de sodio[33], que se conformaron de fragmentos específicos del virus capaces activar la inmunidad de forma más segura. Las respuestas inmunológicas inducidas por dichas vacunas fueron tan eficientes como las desarrolladas por las vacunas convencionales, constituidas por el virus completo, además se observó menos efectos secundarios después de la vacunación[32,33].

Otra de las investigaciones que marcó el control de futuras epidemias y pandemias, fue el uso de recombinación genética para la facricación de una vacuna[34,35]. Este avance mostró que la producción de variantes genéticas adecuadas para la construcción de una vacuna, fue posible desarrollarlas de forma deliberada[34], sustituyendo a métodos de selección tradicionales[30]. La construcción del virus recombinante de alto rendimiento (X-31) se realizó mediante el reordenamiento genético de una cepa estándar de laboratorio de alto rendimiento (A0 / PR / 8), la cual proporcionó los genes de adaptación y crecimiento; con la cepa Aichi del virus de Hong Kong, considerada como una cepa de bajo rendimiento, la cual aportó los genes que codificarían el nuevo antígeno de interés[34]. Los ensayos clínicos de una vacuna inactivada recombinante con el virus X-31 mostraron ausencia de toxicidad, alta antigenicidad y protección frente a la influenza[35].

SARS-CoV-1 (epidemia 2002-2003)

El síndrome respiratorio agudo severo (SARS), provocado por el coronavirus del SARS (SARS-CoV) fue la primera gran epidemia del siglo XXI, apareció en Guangdong-China en noviembre de 2002 y finalizó en julio de 2003, hasta donde se registraron 8437 infectados y 813 muertes a nivel mundial[36,37].

Para el diagnóstico de la infección por SARS-CoV la Organización Mundial de la Salud (OMS) estableció tres ensayos de laboratorio, entre los que se encontraron: pruebas moleculares, pruebas de anticuerpos y cultivo celular[38], a partir de diferentes muestras clínicas como esputo, aspirado o lavado nasofaríngeo, hisopos nasofaríngeos y orofaríngeos, lavado bronquio alveolar, heces, orina y suero o plasma[39–41].

Una de las técnicas modernas fue la detección de ARN del coronavirus mediante RT-PCR dirigida al gen de la nucleocápside (N) o al marco abierto de lectura (ORF) 1b, con la que se consiguió alta especificidad; sin embargo, la sensibilidad fue inferior a la necesaria en los primeros días del desarrollo de la infección. Esta prueba se optimizó con el análisis de más de una muestra originaria del mismo paciente, o con la doble ejecución del ensayo, logrando el aumento de la sensibilidad del diagnóstico[39,40]. Otra forma de mejorar la sensibilidad y precisión del examen molecular fue el perfeccionamiento de los métodos de extracción de ARN previo a la qRT-PCR, facilitando la cuantificación de la carga viral y el reconocimiento precoz del SARS, por lo que se convirtió en el ensayo pilar para el diagnóstico prematuro de la enfermedad[41].

En el aislamiento viral a partir de cultivo celular se emplearon muestras clínicas para infectar células cómo células de riñón fetal de mono rhesus (FRhK-4) o células Vero E6, en las que se analizó el efecto citopático y se realizó tinción por

Pandemia	Tipo de vacuna	Vacuna candidata	Desarrollada por	Fase/Identificación	Dosis	Resultados Previos o Eficacia	Referencias
H2N2 (Gripe asiática)	Virus inactivado	Vacuna monovalente	-	Ensayos clínicos	1 o 2	42% - 77%	24
		Vacuna polivalente	-	Ensayos clínicos	1	21% -46%	21
H3N2 (Gripe de Hong Kong)	Virus inactivado	Vacunas desarrolladas por varios productores	Varios fabricantes en EE.UU.	Aprobado	1	Vacuna segura y altamente antigénica	30
		Vacuna recombinante	Evans Medical, Ltd.; Eli Lilly and Company	Ensayos clínicos	1 o 2 Al día 0 y 30	No presentó toxicidad. Se observó aumento de anticuerpos neutralizantes en suero y fue mayor a partir de la segunda vacunación	34,35
	Viva atenuada	Vacuna de influenza viva atenuada	Michigan State Department of Health Laboratories	Ensayos clínicos	1	Se demostró aceptabilidad e inmunogenicidad	31
	Virus fraccionado	Vacuna antigénica de subunidad dividida	Fluogen, Parke, Davis & Company	Ensayos clínicos	1	Vacuna segura con menos efectos secundarios en comparación con la vacuna tradicional de virus completo	32,33
SARS-CoV-1 (SARS)	Virus inactivado	Vacuna inactivada contra el SARS-CoV	Sinovac	Fase 1	2	Vacuna segura y bien tolerada. Seroconversión del 100% en todos los participantes al día 42 mientras que al día 56 disminuye (100-91.1%)	232
	Vacuna de ADN	VRC-SRSDNA015-00-VP	National Institute of Allergy and Infectious Diseases (NIAID)	Fase 1/ NCT00099463	3 A los días 0, 28 y 56	Segura y bien tolerada. Produjo anticuerpos neutralizantes en el 80% de los participantes, respuesta de células T CD4 en el 100% y respuestas de T CD8 en el 20%	224
H1N1 (Influenza H1N1)	Virus inactivado dividido sin adyuvante	Vacuna inactivada contra la influenza pandémica H1N1	CSL Limited	Aprobado por la FDA	1	-	71
		Vacuna inactivada contra la influenza pandémica H1N1	Sanofi Pasteur	Aprobado por la FDA	1 o 2 *	-	70
		Vacuna inactivada contra la influenza pandémica H1N1	Novartis Vaccines and Diagnostics Limited	Aprobado por la FDA	1 o 2 *	-	68
	Viva atenuada	Vacuna atenuada contra la influenza pandémica H1N1	MedImmune LLC	Aprobado por la FDA	1 o 2*	-	72
	Virus inactivado dividido con adyuvante AS03	Vacuna inactivada con adyuvante contra la influenza pandémica H1N1	GlaxoSmithKline (GSK) Biologicals	Aprobado por la EMA	1	Eficacia del 72%	74
	Subunidad proteica con adyuvante MF59	Vacuna inactivada con adyuvante contra la influenza pandémica H1N1	Novartis Vaccines	Aprobado por la EMA	1	-	73
MERS-CoV (MERS)	Vacuna de ADN	GLS-5300 (INO-4700)	GeneOne Life Science, Inc.; Inovio Pharmaceuticals; International Vaccine Institute	Fase 1/2 NCT03721718 NCT02670187	2 o 3 A las 0 y 8 semanas; o a las 0, 4 y 12 semanas	En un ensayo de fase 1 se determinó que la vacuna fue bien tolerada sin efectos adversos con inmunogenicidad sólida	94
	Vector viral de replicación incompetente	MVA-MERS-S	CTC North GmbH & Co. KG; Universitätskliniku m Hamburg-Eppendorf	Fase 1 NCT04119440 NCT03615911	2 A los 0 y 28 días	Perfil de seguridad tolerable sin efectos adversos	86
		ChAdOx1 MERS	King Abdullah International Medical Research Center; University of Oxford	Fase 1 NCT03399578 NCT04170829	1	La vacuna fue segura y activó eficazmente las respuestas humoral y celular	95
		BVRS-GamVac	Gamaleya Research Institute of Epidemiology and Microbiology; Health Ministry of the Russian Federation	Fase 1/2 NCT04130594	1	-	233

Tabla 3. Desarrollo de vacunas frente a pandemias.

		BVRS-GamVac-Combi	Gamaleya Research Institute of Epidemiology and Microbiology; Health Ministry of the Russian Federation	Fase 1/2 NCT04128059	2 A los 0 y 21 días	-	233
EBOV (EVE)	Vector viral recombinante de replicación competente	Ervebo (rVSV-ZEBOV)	Merck Inc	Aprobado por la EMA y FDA	1	Eficacia del 95,7%	121–123
		GamEvac-Combi (VSV-EBOV + Ad5-EBOV)	CREMS	Fase 4 NCT03072030 EUA: Federación de Rusia	2 Primera: VSV-EBOV Segunda, 21 días después: Ad5-EBOV	La vacuna fue segura. Indujo una fuerte respuesta inmunitaria humoral y celular en el 100% de los voluntarios adultos sanos	118,234
	Vector viral de replicación incompetente	Zabeno (Ad26.ZEBOV) Mvabea (MVA-BN®-Filo)	Johnson & Johnson	Fase 3 NCT02661464, NCT03820739 Autorizada para su comercialización en circunstancias excepcionales por la EMA	2 Primera: Zabeno Segunda, ocho semanas después: Mvabea	Los datos de eficacia en humanos se han extrapolado de estudios con primates no humanos	99,124–126
		Ad5-EBOV	Instituto de Biotecnología de Beijing y Tianjin Cansino Biotechnology Inc	Fase 3 NCT02575456 EUA: China	1	Vacuna segura y altamente inmunogénica en adultos con una dosis óptima de $8 \cdot 0 \times 10^{10}$ partículas virales	118,235
		ChAd3-EBO-Z	GlaxoSmithKline	Fase 2 NCT02548078 NCT02485301	1	ChAd3-EBO-Z fue inmunogénica y bien tolerada en adultos y niños, con respuestas humorales y específicas de la GP del EBOV, 30 días después de la vacunación	236,237
		QazCovid-in®-vaccine	Research Institute for Biological Safety Problems; Rep of Kazakhstan	Fase 3 NCT04691908	2 A los 0 y 21 días	-	150
	Vector viral de replicación incompetente	ChAdOx1 nCoV-19 (AZD1222)	AstraZeneca y Universidad de Oxford	Fase 4 NCT04760132 EUA: Reino Unido, México, Unión Europea, Ecuador, India y México.	1-2 A los 0 y 28 días	70,4% de eficacia	150,171
		Spunik V (Gam-COVID-Vac)	Gamaleya Research Institute; Health Ministry of the Russian Federation	Fase 3 NCT04530396 EUA: Rusia, Argentina, Bolivia, Serbia, Belarus, Algeria, Emiratos Árabes Unidos, Palestina y Egipto	2 A los 0 y 21 días	91,1% de eficacia	150,243
		Ad5-nCoV	CanSino Biological Icn.; Beijing Institute of Biotechnology	Fase 3 NCT04526990 EUA: China, México y Pakistan	1	65,7% de eficacia	150,244
		Ad26.COV2.S	Janssen Pharmaceutical	Fase 3 NCT04505722 EUA: EE.UU. y Bahrein	1 o 2 A los 0 y 56 días	72% de eficacia en EE.UU., 66% en América Latina y 57% en Sudáfrica	150,164,165
	Subunidades proteicas	NVX-CoV2373	Novavax	Fase 3 NCT04611802	2 A los 0 y 21 días	89,3% de eficiencia en Reino Unido y 60% en Sudáfrica	150,221,245
		Comirnaty (BNT162b2)	Pfizer-BioNTech	Fase 4 NCT04760132 EUA: EE.UU., Unión Europea, Reino Unido, Brasil, Nueva Zelanda Argentina, Colombia y Ecuador	2 A los 0 y 21 días	94.6% de eficacia	150,169

Tabla 3. Desarrollo de vacunas frente a pandemias.

Vacuna de ARN	mRNA-1273	Moderna y National Institute of Allergy and Infectious Diseases (NIAID)	Fase 4 NCT04760132 EUA: EE.UU., Unión Europea, Reino Unido y Suiza	2 A los 0 y 28 días	94.1% de eficacia	150,163
	CVnCoV Vaccine	CureVac AG	Fase 3 NCT04674189	2 A los 0 y 28 días	Los resultados de un estudio fase 1 se destacaron es segura y bien tolerada	150,246
Vacuna de ADN	nCov Vaccine	Zydus Cadila	Fase 3 CTRI/2020/07/026352	3 A los 0, 28 y 56 días	-	150

Nota: *Se recomiendan dos dosis administradas con aproximadamente 4 semanas de diferencia (≥21 días aceptables) para niños de 6 meses a 9 años.

†FDA: Administración de Medicamentos y Alimentos; EMA: Agencia Europea de Medicamentos; EUA: Autorización de Uso de Emergencia

Tabla 3. Desarrollo de vacunas frente a pandemias.

inmunofluorescencia. Los resultados indicaron un rendimiento menor en comparación con los ensayos moleculares, debido a que únicamente muestran la presencia del virus vivo[39,42]. Finalmente, la detección de seroconversión fue la prueba estándar para la confirmación virológica retrospectiva de la infección por SARS-CoV, se manejó ELISA e IFI para la identificación de anticuerpos IgG, los cuales se reconocieron después de la primera semana de infección[39,43,44].

Tratamiento terapéutico y profiláctico

Debido a que no existió un tratamiento específico para el SARS, se probaron varios agentes inmunomoduladores y compuestos con potencial antivírico[45,46]. La terapia con plasma convaleciente fue una de las alternativas de tratamiento y prevención. La administración antes de los 14 días desde el inicio de la infección o durante la fase virémica y seronegativa, presentó una tasa de alta médica más temprana y una tasa de mortalidad menor en comparación con los pacientes que recibieron el plasma posterior a los 14 días. Además, no se evidenció efectos secundarios inmediatos después de la aplicación del plasma[46]. Por otro lado, la pentaglobulina se administró como una solución enriquecida en IgM a 12 pacientes en etapa grave de SARS. Diez personas tuvieron una recuperación favorable sin eventos adversos, posterior al tratamiento. Como evidencia se estableció el progreso relevante en las puntuaciones radiográficas y en el requerimiento de oxígeno[47].

En el caso del tratamiento profiláctico, se produjeron varias vacunas candidatas contra el SARS-CoV. Zhou *et al.*[48] llevaron a cabo estudios preclínicos de una vacuna inactivada con formaldehído, en monos Rhesus. Los resultados expusieron que a una dosis de 50 µg, la vacuna fue capaz de inducir inmunidad humoral específica 7 días después de la primera inmunización y el título de anticuerpos IgG se elevó posterior a la segunda inmunización; mientras que con la administración de dosis de 0.5 y 5 µg se observó inmunidad parcial. Además, no se presenció efectos adversos significativos en los animales inmunizados hasta con una dosis de 5000 µg y en el 41.7% de los monos que recibieron la vacuna se determinó anticuerpos IgA anti-SARS-V en las mucosas nasofaríngeas.

Yang *et al.*[49] experimentaron una vacuna de ADN que tradujo la glicoproteína Spike (S) del SARS-CoV, en modelos animales, la cual estimuló respuestas de células T, producción de anticuerpos neutralizantes e inmunidad protectora. La replicación viral se redujo seis veces en los pulmones de los ratones inmunizados después de la infección por el coronavirus. Las vacunas de vectores virales fueron otra opción, Gao *et al.*[50], desarrollaron tres vectores basados en adenovirus, los que expresaron proteínas antigénicas de estructura del SARS-CoV con codones optimizados, entre las que se encontraron el fragmento S1 de la proteína S, la proteína de membrana (M) y la proteína N. La inmunización se realizó con una combinación de los tres vectores en macacos Rhesus al día 0, y una vacuna de refuerzo con el mismo régimen a los 28 días. En todos los animales tratados se encontró anticuerpos neutralizantes específicos contra el fragmento S1 y respuesta de células T contra la proteína N, al mismo tiempo, todas las muestras de suero de los animales vacunados mostraron una gran capacidad neutralizante contra el virus SARS-CoV.

A pesar de que no se logró llegar a ensayos clínicos durante esta pandemia, en años posteriores dos vacunas lograron desarrollar estudios clínicos fase 1 (Tabla 3).

H1N1 (2009-2010)

El virus de la influenza A H1N1 de origen porcino apareció por primera vez en abril de 2009 en los Estados Unidos y en México[51], la pandemia finalizó en agosto de 2010, sin embargo, el virus continúa circulando y provocando la gripe estacional[52]. Se estima que la pandemia dejó 151 700 - 575 500 muertes a nivel mundial[53].

La OMS[54] estableció varias pruebas de laboratorio para la confirmación de la infección causada por el virus de influenza de origen porcino (S-OIV) H1N1. Entre las que se encontraron: diagnóstico molecular con ensayos de RT-PCR y qRT-PCR; aislamiento y la tipificación viral, detección de antígenos para lo que se recomendaron pruebas rápidas de flujo lateral e IFD, y finalmente ensayos serológicos como HAI y micro-neutralización para la evaluación de títulos de anticuerpos contra S-OIV. Las muestras de vías respiratorias superiores fueron las más recomendadas, como aspirados e hisopos nasofaríngeos, hisopos nasales o de garganta; además se empleó muestras de suero en pacientes convalecientes para el reconocimiento de títulos de anticuerpos[55].

La qRT-PCR fue la prueba de referencia para el diagnóstico de la influenza A (H1N1), la identificación de diferentes genes diana fue apropiado para el diagnóstico preciso[54,56]. La primera prueba de este tipo aprobada por la Administración de Alimentos y Medicamentos (FDA) con una autorización de uso de emergencia (EAU), fue realizada por los Centros para el Control y Prevención de Enfermedades (CDC) y fue dirigida al gen de la proteína M, la cual mostró una sensibilidad 99.3% y una especificidad del 92.3%, se trató de un ensayo singleplex para la tipificación y subtipificación viral[57–59]. Para el diagnóstico mediante cultivo viral, la OMS recomendó aislar el virus en células de riñón canino Madin-Darby (MDCK) en presencia de tripsina o en huevos embrionados[54]. Entre las desventajas de esta técnica se establecieron el tiempo tardío para la obtención de resultados (3-14 días) y la baja sensibilidad58.

Las pruebas rápidas de diagnóstico de influenza (RIDTS)

mostraron una sensibilidad variable y menor que las pruebas moleculares y el cultivo viral, por lo que un resultado negativo no descartó la infección por el virus de la influenza A (H1N1)[57,60]. Vasoo *et al.*[61] evaluaron tres RIDTS para el virus de la influenza pandémica A/H1N1 en muestras positivas confirmadas con RT-PCR. Las sensibilidades halladas estuvieron en un nivel de bajo a moderado (46.7%, 38.3% y 53.3%) y presentaron una excelente especificidad, sin reactividad cruzada con otros virus estacionales. El ensayo de IFD, otra de las pruebas para la detección de antígenos mostró amplia disponibilidad y un tiempo de procesamiento promedio de 2-4 horas, sin embargo, al igual que las RIDTS no fueron capaces de distinguir la influenza H1N1 2009 de otros virus de la influenza A[62].

Tratamiento terapéutico y profiláctico

Un porcentaje de la población mayor a los 65 años poseían anticuerpos contra el nuevo virus de esta influenza pandémica, esto pudo ser posible por la exposición anterior al virus H1N1 en 1918[52]. Debido a la aparición del S-OIV H1N1 en humanos con una composición genética previamente no conocida, diferente al virus de la influenza A estacional[63]; además de la fácil transmisibilidad entre humanos[64], el sistema de salud mundial inició rápidamente el desarrollo de antivirales y de una nueva vacuna para el tratamiento y prevención de la infección.

La terapia con inmunoglobulina intravenosa hiperinmune (H-IVIG) obtenida a partir de plasma convaleciente de personas recuperadas fue probado como una alternativa antiviral en pacientes con infección por la influenza pandémica, los resultados mostraron que la administración de H-IVIG dentro de los 5 días posteriores al inicio de los síntomas se asoció a una disminución de la carga viral y reducción de mortalidad[65]. De igual manera, la administración de plasma convaleciente con un título de anticuerpos neutralizantes ≥ 1:160 en pacientes afectados, disminuyó la carga viral, las respuestas de citocinas séricas y la mortalidad[66].

Para el control de esta pandemia se autorizaron dos tipos de vacunas monovalentes, un grupo de vacunas inactivadas divididas de administración intramuscular y otro grupo de vacunas atenuadas en aerosol de administración intranasal[67].

En septiembre de 2009, la FDA aprobó las primeras vacunas para el tratamiento contra la gripe porcina con la cepa A / California / 7/2009 (H1N1)[68,69], entre las que se encontraron tres vacunas monovalentes, inactivadas y sin adyuvante, fabricadas por Sanofi Pasteur[70], Novartis Vaccines and Diagnostics Limited[68] y CSL Limited[71], con 15 µg de hemaglutinina (HA), y la cuarta fue una vacuna, monovalente, viva atenuada y sin adyuvante elaborada por MedImmune LLC[72]. En Europa la Agencia Europea de Medicamentos (EMA) aprobó vacunas con adyuvantes en una emulsión aceite-agua, una de ellas con MF59 y 7.5 µg de HA desarrollada por Novartis Vaccines[73], y otra con AS03 y 3.75 µg de HA fabricada por GlaxoSmithKline (GSK) Biologicals[74]. Una revisión sistemática identificó que las vacunas inactivadas monovalentes A (H1N1) pdm09 fueron efectivas para prevenir la influenza pandémica. En los niños, las vacunas con adyuvante fueron más efectivas en comparación con las vacunas sin adyuvante 75. Por otro lado, otro estudio que analizó la efectividad de una vacuna inactivada con adyuvante y una atenuada, mostró que las vacunas fueron eficaces para prevenir la infección confirmada por la influenza pandémica A (H1N1) 2009 a a partir de una semana después de la vacunación[74].

MERS-CoV (epidemia 2012-2021)

La epidemia Síndrome Respiratorio de Medio Oriente (MERS) fue causada por el coronavirus del MERS (MERS-CoV), descrito por primera vez en Arabia Saudita en junio de 2012[76], continúa vigente hasta la fecha. La mayoría de casos aparecen en el Medio Oriente debido a la exposición directa de sus habitantes a fuentes zoonóticas. Hasta la actualidad se han notificado 2566 casos confirmados y 882 muertes[77].

Entre las pruebas de laboratorio empleadas para la detección de MERS se encuentran las moleculares y las serológicas. Los ensayos moleculares se utilizan para el diagnóstico de la infección viral activa en personas con síntomas clínicos o que han estado en contacto con casos confirmados con MERS-CoV. Por otra parte, los estudios serológicos llevados a cabo por la detección de anticuerpos, se aplican con fines de vigilancia e investigación, y no de diagnóstico[78].

El ensayo de qRT-PCR a partir de muestras respiratorias inferiores, superiores, suero y heces, ha sido la técnica tradicional en el diagnóstico de MERS-CoV. Para la confirmación de la infección se requiere un resultado positivo de qRT-PCR para dos regiones genómicas únicas y específicas del virus, o un resultado positivo para una sola diana y la secuenciación de otra[78,79]. Entre las dianas genéticas recomendadas para la detección primaria del MERS se encuentran las regiones aguas arriba del gen de la proteína E (UpE) y el gen N[79,80], mientras que las pruebas confirmatorias se orientaron al ORF1a, ORF1b o al gen N[79,81].

Se han investigado otras posibles técnicas moleculares apropiadas para el diagnóstico. Por ejemplo, la RT-RPA mostró una especificidad comparable a la de la RT-PCR, con beneficios adicionales como el corto tiempo de determinación (3-7 minutos) y la facilidad de movilidad[82]. La RT-LAMP fue posible llevarla a cabo en menos de una hora, con una alta especificidad y sin reacciones cruzadas[83]. Huang *et al.*[84] optimizaron dicha técnica, y establecieron un ensayo de visualización de ácidos nucleicos con la combinación del ensayo RT-LAMP y una tira de visualización de flujo vertical (RT-LAMP-VF), con el fin de detectar el gen N del MERS-CoV, con alta especificidad, en un tiempo estimado de 35 minutos y sin el empleo de equipos de alto costo.

Tratamiento terapéutico y profiláctico

La atención de apoyo y la prevención de complicaciones, como el síndrome de dificultad respiratoria y las infecciones nosocomiales son las principales estrategias para prevenir la epidemia del MERS. Hasta el momento, se han registrado vacunas y antivirales en fase de desarrollo[85-87].

Varias de las opciones de tratamiento, se han basado en anticuerpos neutralizantes[88,89]. En el brote de Corea en el 2015, se evaluó la infusión de plasma convaleciente en 3 de 13 pacientes con insuficiencia respiratoria producto del MERS. El empleo de plasma con un título en la prueba de neutralización por reducción de placa (PRNT) de 1:80 reveló una respuesta serológica significativa en comparación con el de un título PRNT de 1:40. Los autores recomendaron el uso de plasma convaleciente de donantes con una actividad neutralizante PRNT ≥1: 80 para conseguir resultados eficaces[90]. Por otro lado, de Wit *et al.*[91] evaluaron la eficacia terapéutica y profiláctica de dos anticuerpos monoclonales (mAb) neutralizantes completamente humanos (REGN3048 y REGN3051) que se dirigen al dominio de unión al receptor (RBD) de la proteína S del MERS-CoV en primates no humano, los resultados mostraron niveles altos de actividad neutralizante y reducción de la carga viral en los pulmones de los animales, sin embargo, se observó una mejor respuesta como régimen profiláctico. Además, se llevó a cabo un ensayo de seguridad, tolerabilidad, farmaco-

cinética e inmunogenicidad de la combinación de REGN3048 y REGN3051, administrado por vía intravenosa en voluntarios sanos, este estudio ha completado su fase 1 (NCT03301090).

Los anticuerpos policlonales son otra opción terapéutica, Luke *et al.*[92] produjeron inmunoglobulina G (IgG) policlonal completamente humana contra la proteína de pico del MERS-CoV, a partir de la inmunización de ganado transcromosómico. En modelos murinos, estos anticuerpos (SAB-301) tuvieron la capacidad de reducir los títulos virales con la aplicación de una única dosis a las 24 o 48 horas, después de la exposición del coronavirus. Un estudio clínico de fase 1, en el que se evaluó la seguridad, tolerabilidad y farmacocinética de SAB-301 en adultos sanos, interpretó que las infusiones únicas de SAB-301 con una concentración de hasta 50 mg / kg parecen ser seguras y bien toleradas[93].

La combinación de antivirales e interferones ha sido la base de varios tratamientos ensayados. Un estudio clínico fase 2/3 en el que se probó la combinación de interferón β-1b recombinante más lopinavir-ritonavir, durante 14 días, concluyó que el tratamiento produjo menor mortalidad en comparación con el placebo en pacientes confirmados con MERS y produjo efectos adversos graves en el 9% de la población. Existieron mejores resultados cuando este se aplicó entre los 7 días posteriores a la aparición de síntomas[87].

Desde el inicio de la epidemia provocada por el MERS-CoV, se planteó el objetivo de desarrollar una vacuna contra el virus, por lo que diferentes grupos de investigadores alrededor del mundo se han unido al proceso. La vacuna GLS-5300 basada en plásmido de ADN que expresa la proteína S del MERS-CoV[94], en el ensayo fase 1 reveló que las respuestas inmunitarias fueron independientes de la concentración de la dosis, además se observó seroconversión en 86% de los participantes y respuestas de células T en el 71% después de dos dosis, mientras que en el grupo que se administró tres dosis se presenció seroconversión en el 94% de los participantes y respuestas de células T en el 76%, asimismo se observaron anticuerpos neutralizantes en el 50% de la población estudiada[94]. Además, se están llevando a cabo dos ensayos clínicos fase 1/2 en los que se está evaluando la inmunogenicidad y la seguridad de las vacunas de vectores virales BVRS-GamVac-Combi (NCT04128059) y BVRS-GamVac (NCT04130594).

Las otras dos vacunas que publicaron sus ensayos fase 1 se basaron en vectores virales de replicación incompetente, en las que se evaluó la seguridad, tolerabilidad e inmunogenicidad. La vacuna MVA-MERS-S, basada en la Vacuna Modificada de Ankara (MVA) que expresa la glicoproteína S[86]; y la vacuna ChAdOx1 MERS vectorizada de adenovirus de chimpancé (ChAdOx1) que de igual forma expresa la proteína S de longitud completa[95]. En los resultados, los dos ensayos mostraron seguridad con ausencia de efectos secundarios graves, además de respuestas humorales y celulares contra el MERS-CoV[86,95]. En el caso de la vacuna MVA-MERS-S en el 75% de los participantes se observó seroconversión después de la segunda inmunización con dosis baja y en el 100% con la dosis alta. Se detectaron respuestas de células T en el 83% y en el 91% de la población dependiendo del tipo de dosis administrada[86].

ÉBOV (epidemia 2013-2016)

La enfermedad del virus del ébola (EVE), es una infección grave y letal provocada por el virus del ébola de Zaire (EBOV), que apareció por primera vez en República Democrática del Congo en 1976[96]. Sin embargo, el brote más grande reportado en la historia surgió en diciembre de 2013 en África Occidental y duró hasta 2016, periodo en el que se registraron 18 616 casos y 11 310 muertes[97]. Los brotes de EBOV del 2013-2016 y los últimos brotes registrados en República Democrática del Congo[98], han permitido mejorar la comprensión de la enfermedad y optimizar las estrategias para la prevención, el diagnóstico, la atención clínica y el tratamiento de EVE, debido a la aplicación de técnicas moleculares modernas en la caracterización del virus[99,100].

Las pruebas de diagnóstico para el EVE recomendadas por la OMS son las pruebas de ácido nucleico automatizadas o semiautomatizadas para la detección de ARN viral y las pruebas rápidas de detección de antígenos como test de vigilancia[101]. En general, la sangre es la muestra de preferencia para el diagnóstico en pacientes y los hisopos orofaríngeos son de utilidad para el diagnóstico post mortem[101,102].

La qRT-PCR es la prueba estándar para el diagnóstico, capaz de detectar el virus de 3-6 días después del inicio de los síntomas[102,103]. Uno de los ensayos importantes desarrollados y con EUA por la FDA y la OMS, en el brote del 2013-2016, fue la prueba molecular automatizada Gene Xpert Ebola (Cepheid) basada en qRT-PCR con señal fluorescente de sondas para control de calidad, que amplifica dos genes del EBOV, el gen N y el de la glicoproteína (GP), el doble objetivo de esta prueba permitió disminuir falsos negativos cuando se analizaron muestras con nuevas variantes de virus, los resultados mostraron una alta sensibilidad analítica (100%) y especificidad (99.5-100%), con un tiempo corto de respuestas, en comparación con la RT-PCR común[104]; este ensayo fue empleado en su mayoría en el último brote de República del Congo (2018-2020)[99].

Además, se han diseñado varias pruebas portátiles de flujo lateral para la detección rápida de antígenos[105]. La primera prueba de este tipo aprobada por la FDA en el 2019 fue OraQuick Ebola Rapid Antigen Test de OraSure Technologies, un ensayo inmunocromatográfico dirigido a la proteína viral 40 (VP40) o de la matriz proteica con una sensibilidad de 97.1-100% y una especificidad del 98-100%[106,107].

Tratamiento terapéutico y profiláctico

Durante el gran brote de EVE del 2013-2016 varios fármacos biotecnológicos con actividad antiviral o como inmunoterapia contra EBOV fueron llevados a ensayos clínicos, entre los que estuvieron: administración de plasma convaleciente[108]; un cóctel de tres anticuerpos monoclonales neutralizantes (ZMapp) dirigidos hacia la GP de superficie del EBOV[109]; interferón IFNβ-1a[110]; y un producto de nanopartículas lipídicas de ARNip que inhibe la producción de dos proteínas virales fundamentales, la L-polimerasa, la cual interviene en la transcripción y replicación del EVE, y la proteína viral 35 (VP35), comprometida con la destrucción de la respuesta inmune del huésped[111]. Sin embargo, estas terapias no cumplieron con los criterios establecidos para ser aprobadas para su uso masivo[99,103].

Durante el brote de República del Congo de 2018 inició el ensayo Pamoja Tulinde Maisha (PALM) que significa "Juntos salvamos vidas", un ensayo controlado, aleatorio, abierto y multicéntrico, en el que se estudió las terapias experimentales más prometedoras. Esta investigación comparó a Zmapp contra tres nuevos agentes: remdesivir, mAb114 y REGN-EB3 (NCT03719586)[112]. Inmazeb (REGN-EB3) fue el primer fármaco aprobado por la FDA para tratar el EVE (14 de octubre de 2020) con una única perfusión intravenosa de 150 mg por kg[113]. Se trata de un cóctel de tres anticuerpos IgG1 humanizados en una proporción 1:1:1 dirigidos a la tres epítopes no superpuestos de la GP del EBOV, los tres anticuerpos pueden unirse simultáneamente bloqueando la unión y entrada del virus a

la célula huésped[114]. El segundo tratamiento aprobado por la FDA, en diciembre de 2020, fue Ebanga (mAb114), un único anticuerpo monoclonal IgG1 dirigido a un epítope altamente conservado del dominio de unión al receptor de la GP del EBOV, este es administrado por vía intravenosa con una sola dosis de 50 mg/kg[115]. Ebanga previene la interacción de GP del EBOV con el receptor NPC1, bloqueando la infección del virus a la célula huésped[116].

Debido a que la GP del EBOV es el inmunógeno más importante detectado[117], la mayoría de las vacunas en desarrollo durante el brote de ébola 2013-2016 fueron diseñadas para activar la respuesta inmune del huésped frente a este antígeno[118]. Entre las vacunas candidatas llevadas a ensayos clínicos se encontró rVSV-ZEBOV, una vacuna de vector viral competente para la replicación basada en el virus de estomatitis vesicular recombinante que expresa la GP de superficie del EBOV del Zaire[119]. El ensayo *Ebola ça Suffit* ("Ébola esto es suficiente") de fase 3 llevado a cabo en Guinea en el 2015, evaluó la eficacia y efectividad de una sola dosis intramuscular de la vacuna rVSV-ZEBOV con una estrategia de vacunación en anillo abierta y aleatorizada por grupos, mediante la cual se administra la vacuna a individuos con conexión social o geográfica a un caso confirmado[119]. La eficacia de la vacuna fue del 100%, con alta tolerancia en los seres humanos, una activación rápida de la respuesta inmune después de una única dosis y sin casos confirmados entre las personas vacunadas después de los 10 días de inmunización[120]. En 2019 esta vacuna denominada Ervebo desarrollada por Merck Inc., fue la primera vacuna aprobada por la EMA y por la FDA para su uso médico[121,122], con una eficacia estimada de 95.7% evaluada por la OMS en 90 000 personas asociadas al brote del 2018 de República Democrática del Congo[123].

Otra de las vacunas empleadas para la prevención del EVE es la vacuna fabricada por Johnson & Johnson, autorizada para su comercialización en circunstancias excepcionales por la EMA en julio de 2020[124]. Esta vacuna fue desarrollada en el brote de 2013- 2016 y ha alcanzado ensayos clínicos de fase 1, los que demostraron seguridad, tolerabilidad e inmunogenicidad[125]. El régimen de vacunación consta de dos dosis conformado por vacunas diferentes: Zabeno (Ad26.ZEBOV), una vacuna de adenovirus humano serotipo 26 no replicante que codifica la GP del EBOV de Zaire, y una vacuna de refuerzo administrada ocho semanas después, denominada Mvabea ® (MVA-BN-Filo), constituida por MVA de replicación incompetente que expresa tres GP y una nucleoproteína de diferentes variantes del virus del Ébola[125,126].

SARS-CoV-2 (2019-2021)

La pandemia en curso de la enfermedad por coronavirus 2019 (COVID-19), provocada por el Coronavirus del Síndrome Respiratorio Agudo Severo 2 (SARS-CoV-2), inició en diciembre de 2019 en un mercado de animales en Wuhan, provincia de Hubei, China[127]. Hasta inicios de marzo de 2021, la OMS ha reportado 113.6 millones de casos confirmados, 2.5 millones de muertes en todo el mundo y 223 países afectados[128].

En el caso de esta pandemia, la FDA recomendó tres tipos de pruebas: las pruebas de diagnóstico que identifican una infección activa por presencia del virus, las pruebas serológicas o de anticuerpos y las pruebas de manejo de pacientes con COVID-19 para detectar biomarcadores relacionados con la inflamación[129,130].

La prueba estándar para el diagnóstico de COVID-19 es la qRT-PCR[131], esta técnica molecular va dirigida a regiones altamente conservados o que se expresan con abundancia como el gen E, N, S y el gen de la ARN polimerasa dependiente de ARN (RdRp) del ORF1ab[132,133]. Sin embargo, a pesar de la alta especificidad de la prueba ha demostrado sensibilidad inestable, comparada con otras técnicas como la tomografía computarizada (TC) de tórax, esto puede depender varios factores como: la carga viral del paciente, la forma de muestreo, el procesamiento y el transporte de la muestra, la tasa de detección de los diferentes fabricantes, entre otras[133,134].

Con los antecedentes antes mencionados el objetivo de varios grupos de investigación se han centrado en diseñar pruebas de diagnóstico alternativas, entre ellas se halla la RT-LAMP, una tecnología de amplificación de ADN, que se emplea para detectar ARN del SARS-CoV-2, los resultados se logran obtener en aproximadamente 45 minutos en muestras con una baja concentración viral, sin el empleo de equipamiento costoso debido a que la reacción final se puede observar a simple vista por un cambio colorimétrico; además el diseño de los cebadores ha sido dirigido a regiones conservadas con baja frecuencia de mutación como el gen S, gen ORF1ab y el gen N, lo que garantiza la especificidad[135,136]. Huang *et al.*[137] probaron el ensayo RT-LAMP en un solo paso, es decir sin la extracción de ARN, el resultado fue la amplificación de ARN directamente de una muestra; por lo que aseguraron que la meta final es desarrollar un dispositivo capaz de extraer, purificar, retro transcribir ARN, y llevar a cabo la amplificación isotérmica mediada por bucle (LAMP) para la detección de SARS-CoV-2.

La tecnología Crispr-Cas es una nueva herramienta biotecnológica que ha revolucionado el diagnóstico molecular de rápida detección, alta precisión y sensibilidad, gran versatilidad y portabilidad sin la intervención de equipos sofisticados de laboratorio[138]. En mayo de 2020 la FDA otorgó una EUA a la primera prueba de CRISPR combinada con RT-LAMP para el diagnóstico de la infección activa por SARS-CoV-2 en el punto de atención, denominada SHERLOCK, desarrollada por Sherlock BioSciences[139]. Este protocolo se basa en la enzima Cas13a guiada por el ARN Crispr (ARNcr) para reconocer un ARN de cadena simple o un ARN mensajero viral, cuando el complejo Crispr -Cas se une a su diana, la actividad nucleasa colateral de la enzima conduce a la escisión inespecífica de una molécula marcada con fluorescencia, tras este proceso la señal será detectada mediante fluorescencia o tiras de flujo lateral[140]. Según Joung *et al.*[141] SHERLOCK proporciona una sensibilidad comparable con la qRT-PCR y posee un límite de detección de 100 copias del genoma viral; en muestras de hisopados de nariz, boca o garganta, además de fluido pulmonar[141].

Otro de los kits de diagnóstico frente a COVID-19 disponible comercialmente y basado en los mismos principios es DETECTR, diseñado por Mammoth Biosciences[138]. Este sistema por su parte usa la enzima Cas12a para dirigirse a una secuencia de ADN de doble cadena (dsADN) del SARS-CoV-2, una vez hallada la diana genética la enzima escinde indiscriminadamente moléculas indicadoras de ADN de cadena simple (ssADN) marcadas con el flouróforo y ocurre el mismo proceso antes mencionado[140,142]. DETECTR muestra una alternativa visual y más rápida que la técnica estándar para la tipificación de secuencias moleculares del SARS-CoV-2, con una sensibilidad del 95% y una especificidad del 100%[142].

Las pruebas rápidas de detección de antígenos son otra opción para el diagnóstico de COVID-19, estos inmunoensayos están esquematizados para localizar partículas virales en muestras nasofaríngeas o de frotis nasal. Las ventajas de las pruebas de antígenos es la rapidez de detección, aproximadamente 15 minutos, a un bajo costo y alta especificidad[143,144]. Hasta la fecha la FDA ha otorgado la EUA a quince test comerciales con este principio[129].

La pandemia por COVID-19 sigue vigente y cada día que pasa continúa la I + D en pruebas de diagnóstico más rápidas, simples, baratas, escalables y precisas en comparación con las existentes[145]. Como el desarrollo de biosensores fototérmicos plasmónicos de doble función con una alta precisión[146], o un ensayo de CRISPR potencializado y ultrasensible con la posibilidad de ser integrado en un chip de microfluidos que pueda ser leído por un teléfono celular inteligente[147,148].

Tratamiento terapéutico y profiláctico

Existe una gran variedad de tratamientos en investigación para el COVID-19 por ejemplo antivirales, terapias celulares y genéticas, inmunomoduladores, anticuerpos neutralizantes y tratamientos combinadas; de los cuales, varios se encuentran en ensayos en etapa temprana donde se evalúan la seguridad y dosificación, mientras que otros se hallan en etapa tardía en los que se prueba la seguridad y la efectividad[149]. Por otro lado, se han empleado múltiples plataformas biotecnológicas tanto tradicionales como modernas para el desarrollo de vacunas contra el COVID-19[150,151] (Figura 3).

Las terapias basadas en anticuerpos neutralizantes se han mostrado efectivas en las primeras etapas de la infección por SARS-CoV-2, cuando el virus empieza su proceso de replicación y el huésped aún no reacciona con una respuesta inmune eficaz[152]. La FDA ha concedido la EUA a ciertos anticuerpos monoclonales neutralizantes anti-SARS-COV-2 dirigidos al RBD de la proteína S como tratamiento para pacientes ambulatorios con COVID-19 de leve a moderado, la función de estos anticuerpos es bloquear la unión del RBD a la célula huésped y neutralizar el virus[153,154].

Bamlanivimab, ha alcanzado estudios clínicos fase 2, los resultados obtenidos en un análisis intermedio sugirieron que una única infusión intravenosa de este mAb con una dosis de 2800 mg aceleró la disminución de la carga viral, además los pacientes no hospitalizados que recibieron el tratamiento mostraron síntomas más leves y una tasa de hospitalización menor que el grupo placebo. Sin embargo, no es posible sacar conclusiones finales, por lo que se necesitan datos de ensayos clínicos más amplios[155]. Al mismo tiempo se está llevando a cabo un ensayo fase 2/3 para determinar el efecto de la monoterapia de bamlanivimab y la terapia combinada de bamlanivimab con etesevimab. El estudio concluyó que el tratamiento combinado se asoció con una reducción de la carga viral estadísticamente significativa al día 11, en contraste con la monoterapia y el grupo placebo[156].

Finalmente, el análisis intermedio del estudio clínico fase 1/3 del cóctel de anticuerpos humanos neutralizantes REGN-COV2 (casirivimab y imdevimab), informó que una sola dosis de REGN-COV2 de 2,4 g o 8,0 g fue capaz de reducir la carga viral al día 7 con un efecto mayor en pacientes con anticuerpos séricos negativos (anticuerpos endógenos) contra el SARS-CoV-2. Asimismo, el porcentaje de participantes con visitas médicas fue menor en el grupo que recibió el cóctel de anticuerpos que en el grupo placebo[157].

Una tecnología tradicional, el plasma convaleciente de título alto, es decir con la relación señal/corte (s/c) de ≥12.0 a ≥9.5 en la prueba Ortho VITROS Anti-SARS-CoV-2 IgG, es otro de los productos biológicos aprobados como EUA por la FDA[153]. Los resultados de los diferentes estudios varían, en pacientes con COVID-19 grave o potencialmente mortal no presenta una mejora clínica estadísticamente significativa[158,159], mientras que otros proporcionan datos sólidos de que la transfusión de plasma convaleciente en pacientes hospitalizados es segura con una administración temprana dentro del curso clínico[160–162].

Actualmente, existen 182 vacunas en desarrollo preclínico y 74 en desarrollo clínico de las cuales 3 han obtenido la EUA por parte de la FDA, pertenecientes a Moderna Therapeutics, Pfizer-BioNTech y Johnson & Johnson[150].

Moderna Therapeutics junto con Instituto Nacional de Alergias y Enfermedades Infecciosas (NIAID) produjeron la primera vacuna en ser llevada a ensayos clínicos, se trata de mRNA-1273, una vacuna de ARN encapsulada en nanopartículas lipídicas que contiene la información de la proteína de S de longitud completa estabilizada previa a la fusión, un ensayo fase 3 determinó una eficacia del 94.1% con dos dosis de 100 µg de esta vacuna[163]. La vacuna producida por Johnson & Johnson, Ad26.COV2.S, es una vacuna de dosis única (5×10^{10} partículas virales) basada en un adenovirus serotipo 26 incompetente para la replicación que expresa la proteína S del SARS-CoV-2, los ensayos clínicos muestran diferentes eficacias de la vacuna frente al virus; 72% en EE.UU., 66% en Latino América y 57% en Sudáfrica[150,164,165].

Por otro lado, la primera vacuna para la prevención de COVID-19 que recibió un EUA fue BNT162b2 de Pfizer-BioNTech, el 2 de diciembre por la Agencia Reguladora de Medicamentos y Productos Sanitarios (MHRA) del Reino Unido[166] y el 11 de diciembre de 2020 por la FDA[167].

En Ecuador esta vacuna desarrollada por Pfizer-BioNTech, fue la primera en ser aprobada para uso de emergencia por la Agencia Nacional de Regulación, Control y Vigilancia Sanitaria (ARCSA)[168]. BNT162b2 es una vacuna de ARNm modificado con nucleósidos y formulada con partículas lipídicas que codifica la proteína S transmembrana de longitud completa. Un ensayo global fase 2/3 manifestó que la administración de dos dosis (30 µg de vacuna por dosis) de BNT162b2 con 21 días de diferencia alcanza 95% de eficacia en la prevención de COVID-19 y un perfil de seguridad caracterizado por dolor leve en el lugar de la inyección, dolor de cabeza y fatiga, con una baja incidencia de efectos secundarios graves[169].

La segunda vacuna aprobada por el ARCSA es ChAdOx1 nCoV-19 (AZD1222)[170], una vacuna de vector no replicante ChAdOx1 que contiene el gen de la proteína S del virus, diseñada por AstraZeneca y la Universidad de Oxford. Un análisis de cuatro ensayos con una administración de dos dosis (dosis estándar 5×10^{10} partículas virales) demostró que en aquellos participantes que recibieron dos dosis estándar la eficacia de la vacuna fue del 62%, mientras que en el grupo que adoptó media dosis estándar seguida de una dosis completa la eficacia fue de 90%, obteniendo una eficacia global de la vacuna del 70,4% contra el COVID-19 sintomático con un perfil de seguridad aceptable[171].

A continuación se describirán las herramientas de la biotecnología y sus múltiples aplicaciones, además se mencionarán sus características más importantes empleadas en el control, manejo y prevención de las diferentes pandemias.

Herramientas biotecnológicas

En 1919, el ministro de alimentos húngaro, Kark Ereky, mencionó por primera vez la palabra biotecnología refiriéndose a todas las áreas de trabajo en las cuales los productos son obtenidos a partir de materia prima orgánica mediante la intervención de organismos vivos[172]. Sobre esta base la biotecnología ha ido evolucionando y ha sido dividida en tres periodos en función del tiempo: la biotecnología antigua, la biotecnología clásica y la biotecnología moderna[173,174]. El último periodo inició con la revelación del modelo de doble hélice del ácido desoxirribonucleico (ADN) en 1953, desde este evento, la bio-

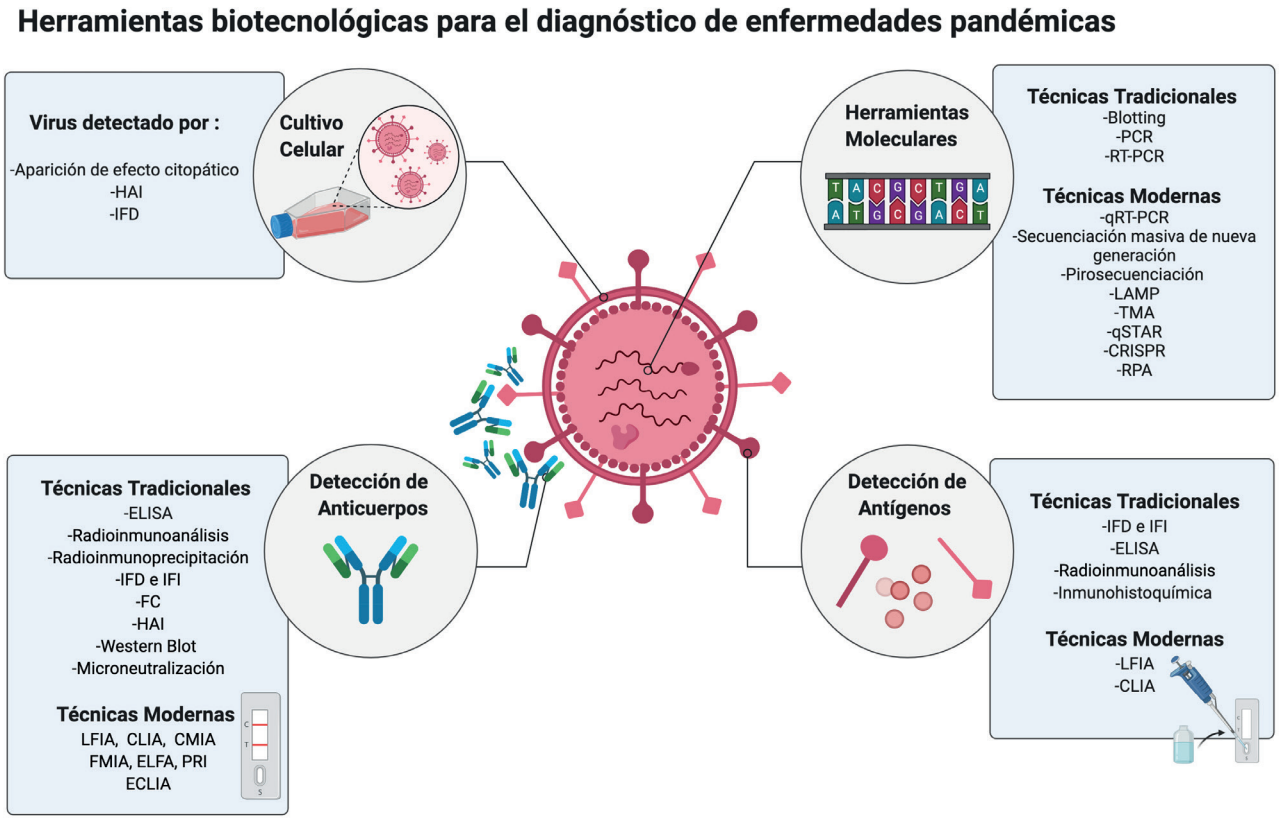

Figura 2. Herramientas biotecnológicas para el diagnóstico de enfermedades pandémicas - Ventajas y desventajas.

tecnología fue considerada como una ciencia moderna capaz de desarrollar sus propias aplicaciones[175], basadas en técnicas modernas como las técnicas de ADN recombinante[176] o la técnica de la hibridoma[177].

En la actualidad se puede definir a la biotecnología como una ciencia multidisciplinaria e interdisciplinaria que emplea organismos vivos, células o sus derivados para el desarrollo de productos y procesos orientados al bienestar humano empleando diversos tipos de herramientas y tecnologías[173,178]. Otra de las clasificaciones de esta ciencia se basa en un código de colores que diferencia las principales áreas[179]. Un área de la biotecnología de interés en esta revisión es la biotecnología roja, médica o farmacéutica, que se relaciona con la producción y desarrollo de métodos de diagnóstico y productos biofarmaceúticos como biofármacos recombinantes, productos de ingeniería de tejidos, productos de ingeniería de proteínas, anticuerpos monoclonales, vacunas, medicamentos regenerativos (terapia de células madre y génica), nanopartículas y biosensores[173,178,179]. Las herramientas biotecnológicas han permitido la obtención de estos productos a escala industrial, incluyendo agentes novedosos y tradicionales los cuales eran producidos en minoría, para lo que se emplean bioprocesamientos conocidos como biotecnología blanca o industrial[178,179].

Era de las "OMICAS" para el desarrollo de herramientas biotecnológicas

Las tecnologías "omicas" inspiradas en el proceso natural de producción de biomoléculas en las células, han aportado significativamente en el avance del diagnóstico, manejo y pronóstico de varias enfermedades, siendo elementales para el perfeccionamiento de la medicina personalizada de próxima generación[180,181], debido a que permiten una mejor comprensión de los mecanismos moleculares y celulares que interfieren en la progresión de una enfermedad en humanos[180]. Entre las "ómicas" con mayor avance están la genómica, transcriptómica, proteómica y metabolómica[181], siendo la genómica y proteómica las "omicas", con un protagonismo superior en la investigación de diagnóstico y tratamiento en enfermedades infecciosas[182]. La genómica trata de la estructura, función, evolución y mapeo de genomas, con el objetivo de cuantificar y caracterizar genes[180]. La obtención y análisis de secuencias completas de los genomas de patógenos causantes de enfermedades emergentes ha sido valioso para el análisis filogenético de estos microorganismos, conocer su origen, caracterizar los patrones de transmisión, el desarrollo acelerado de pruebas de diagnóstico eficientes, además, ha sido la base para el diseño de nuevas tecnologías terapéuticas, incluidos biotecnológicos y ha permitido la identificación de epítopes claves para la construcción de vacunas. Asimismo, ha influido en el seguimiento epidemiológico de las pandemias y en la detección de nuevas variantes virales[76,183–186].

La proteómica, por otro lado, estudia todas las proteínas presentes en una célula, tejido u organismo, centrándose en las propiedades bioquímicas, roles funcionales y sus cambios frente al crecimiento o a estímulos internos y externos[182,187,188]. La proteómica a través de espectrometría de masas facilita los análisis de precisión, sensibles y de alto rendimiento de proteínas a gran escala[187]. Además, es posible comprender y descubrir interacciones claves proteína-proteína, redes de señalización, interacciones complejas huésped-patógeno, respuestas del huésped al invasor y los mecanismos de aprovechamiento del microorganismo, lo que ha proporcionado información sobre la patogénesis de una enfermedad, caracterización de biomarcadores para métodos de diagnóstico y fármacos antivirales durante una epidemia[182,188]. Al mismo tiempo el prototipado por espectrometría de masas puede ser un método de diagnóstico alternativo[188].

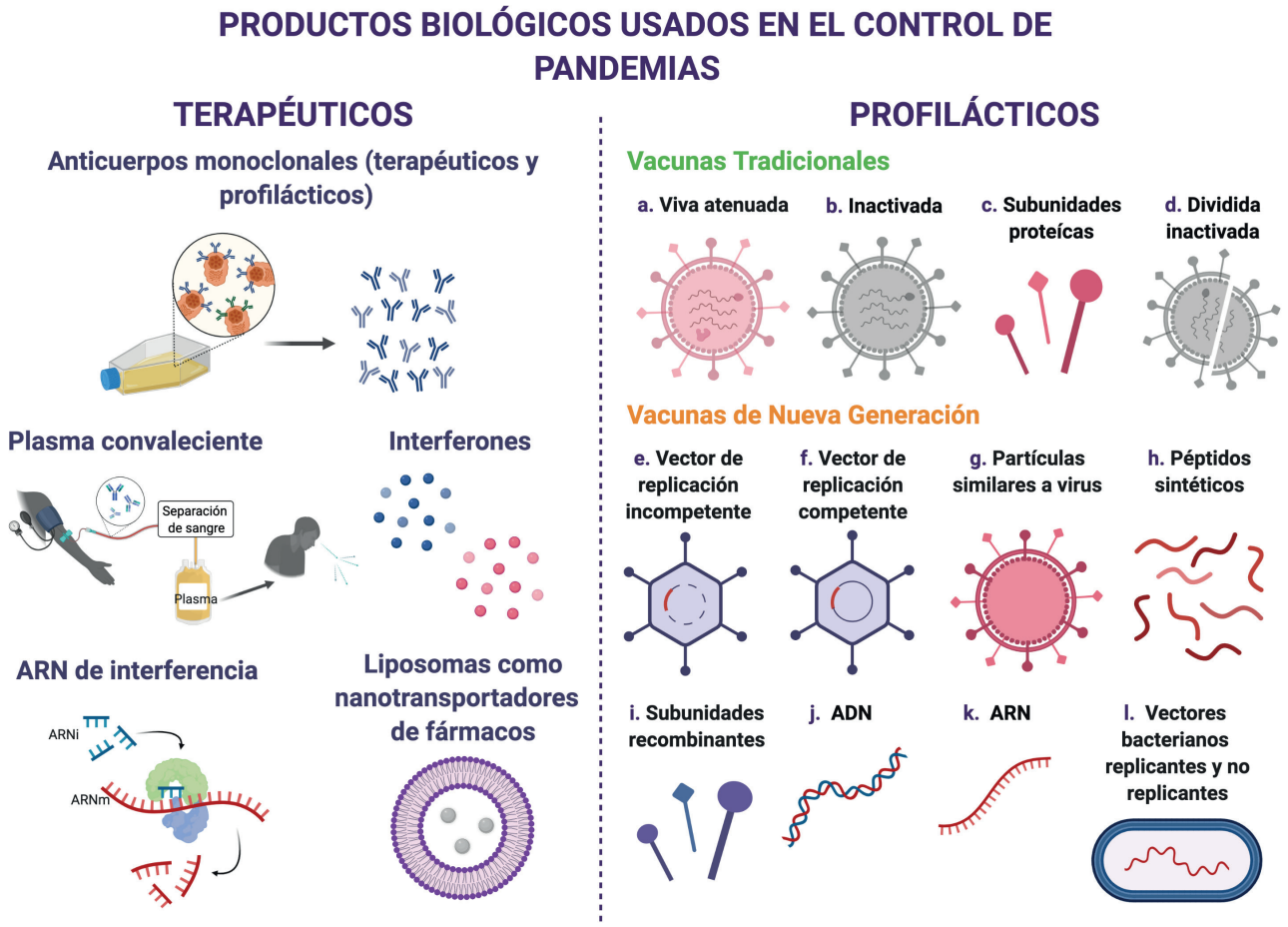

Figura 3. Productos biológicos usados en el control de pandemias (Creado en BioRender).

Herramientas biotecnológicas en el diagnóstico

Las herramientas biotecnológicas modernas aplicadas para el diagnóstico se han optimizado a lo largo de la aparición de las diferentes pandemias, gracias a la investigación y el avance tecnológico, con el fin de producir pruebas sencillas, de bajo costo, que requieran menor tiempo de detección, con sensibilidad y especificidad alta[58,148,189]. Los métodos para la identificación de patógenos se han basado principalmente en cultivo viral[58], detección de antígenos[61,105], identificación indirecta de anticuerpos[20,29] y detección de ácidos nucleicos[42,130,132] (Figura 2). Debido a la necesidad de pruebas de diagnóstico en el punto de atención (POCT) se están efectuando estudios trascendentales para convertir las técnicas conocidas en herramientas POCT rápidas, eficientes y ultrasensibles, sin la necesidad de mano de obra experimentada y laboratorios sofisticados[84,130,189,190].

Técnicas de diagnóstico molecular

Los test moleculares son las pruebas de diagnóstico con mayor demanda en los últimos años, debido a su elevada sensibilidad y precisión[133,189]. Estas tecnologías mecanizadas detectan y amplifican secuencias específicas y conservadas del genoma del patógeno en muestras de pacientes infectados[41,133]. Las cuales se describen a continuación:

Reacción en cadena de la polimerasa (PCR)

Es una técnica que se emplea para amplificar exponencialmente pequeños fragmentos de ADN diana. El principio de la PCR se fundamenta en el ciclo repetitivo de tres reacciones: desnaturalización, alineación y extensión, el proceso se repite de 30 a 40 veces, con el doble de la cantidad de material genético objetivo en cada ciclo. Al final se producen millones de fragmentos de la secuencia de ADN diana, en un período corto de tiempo[191].

Existen algunas variaciones de la PCR. PCR de transcripción inversa (RT-PCR) inicia con la obtención de ADNc a partir de ARN mediante transcripción inversa, seguido por la amplificación del ADNc. Esta técnica se usa para la detección de virus de ARN[80]. PCR cuantitativa en tiempo real (qPCR) se basa en el empleo de sondas marcadas con fluorescencia que permiten cuantificar los productos de PCR a medida que se generan, en esta técnica el ciclo de temperatura ocurre más rápido que en los ensayos de PCR estándar, la hibridación de sondas se produce continuamente durante la reacción de amplificación y el tinte fluorescente acoplado a la sonda emite una señal solo cuando tiene lugar la hibridación[192]. Por otro lado, PCR múltiple es utilizada para la identificación simultánea de varias secuencias de genes que pertenecen al mismo patógeno o a una mezcla de diferentes patógenos. Esta técnica permite ahorrar tiempo y reactivos al dirigirse a múltiples dianas a la vez[193]. Otro tipo de PCR es la PCR anidada, este ensayo implica dos reacciones de amplificación secuenciales con un par de cebadores diferentes en cada una, el segundo conjunto de cebadores amplifica un objetivo secundario dentro del producto de la primera reacción. Esto proporciona ejecutar un mayor número de ciclos mientras se reducen los productos no específicos, aumentando la especificidad y sensibilidad de detección[194,195].

Técnicas de diagnóstico molecular en desarrollo

A lo largo del tiempo se han ido desarrollando técnicas moleculares modernas para el diagnóstico (Figura 2).

La amplificación isotérmica mediada por LOOP (LAMP) amplifica secuencias específicas de ADN empleando un conjunto de cuatro o seis cebadores únicos, la mezcla de reacción se incuba en una sola temperatura y el producto de amplificación puede detectarse por la presencia de precipitado de pirofosfato de magnesio como subproducto del proceso de amplificación o por fluorescencia bajo luz UV, además es posible monitorear la reacción en tiempo real midiendo la turbidez del pirofostato. Este ensayo se caracteriza por su simplicidad y alta sensibilidad[83,135,196]. La técnica LAMP se combina con una transcripción inversa para la identificación de ARN (RT-LAMP)[83,137].

Por otro lado, las Repeticiones Palindrómicas Cortas agrupadas y Regularmente Espaciadas (CRISPR), secuencias asociadas con las nucleasas Cas son la base de la tecnología CRISPR/Cas. CRISPR son una familia de secuencias de ADN propias de organismos procariota y Cas son un grupo de endonucleasas que precisan de un ARN guía para reconocer y cortar una secuencia complementaria de ADN. Estas enzimas pueden ser programadas para ser dirigidas a ARN viral[142,197]. La amplificación mediada por transcripción (TMA) es un ensayo de amplificación isotérmica de un único tubo que emplea una transcriptasa inversa y una polimerasa de ARN para amplificar segmentos específicos de ADN o ARN con mayor eficiencia que la RT-PCR[198]. Mientras que una alternativa isotérmica de la PCR, es la amplificación isotérmica de recombinasa y polimerasa (RPA), un ensayo rápido, portátil y de detección múltiple[189].

Inmunoensayos en el diagnóstico

Las pruebas de anticuerpos identifican el aumento de estas proteínas en el suero de pacientes, los anticuerpos son producto de la activación de una respuesta inmune humoral pos infección de microorganismos patógenos[44]. Estos ensayos suelen estar diseñados para detectar anticuerpos humanos IgA, IgM o/y IgG, usualmente, los anticuerpos IgM son hallados pocos días después de la infección, y los anticuerpos IgG aparecen más tarde[199]. Los estudios de cuantificación de anticuerpos permiten determinar infecciones recientes o pasadas[200,201], sin embargo, estas pruebas no se las utiliza para diagnosticar pacientes infectados debido a problemas de mutaciones de células B[202] y deficiencia en la producción de anticuerpos[203], por lo que son aprovechadas como una herramienta de estudios serológicos para conocer el estado de la respuesta inmune[204] y para evaluar la dinámica de las respuestas humorales activadas por vacunas[70,95,125] (Figura 2).

Otro tipo de inmunoensayo son las pruebas de detección de antígenos (Figura 2), que se encargan de identificar directamente partículas de patógenos en muestras biológicas, es decir son capaces de detectar la infección activa en personas afectadas. Las más comunes son las pruebas rápidas de detección de antígenos (RAP) que se basan en inmunoensayos de flujo lateral (LFIA)[61], estas realizan una determinación cualitativa del antígeno mediante un anticuerpo específico inmovilizado en el dispositivo[205]. Las RAP son ideales en pacientes que se encuentran en la etapa inicial de la enfermedad, cuando la carga viral es comúnmente elevada; además en sujetos con exposición a casos confirmados. La sensibilidad de las RAP es menor en comparación con las pruebas moleculares y el cultivo viral[206,207]. En consecuencia, los resultados negativos de las pruebas basadas en este método no son capaces de descartar infecciones.

Productos biotecnológicos

Los productos de origen biológico son moléculas grandes y complejas, compuestos de azúcares, proteínas o ácidos nucleicos o combinaciones de estas sustancias, también pueden ser entidades vivas como células y tejidos que se emplean para diagnosticar, prevenir, tratar o curar enfermedades. Estos productos se obtienen de fuentes naturales (humanos, animales, microorganismos, células animales o vegetales), y se producen mediante métodos biotecnológicos y otras tecnologías de vanguardia como la nanotecnología[208,209].

Los productos biológicos constituyen un producto creciente en el mercado farmacéutico, a nivel mundial los gastos en productos biológicos sumaron $277 mil millones durante el 2017 y se predice que en el 2022 aumenten a $452 mil millones[210]. Estos biofármacos se encuentran protegidos por una mayor cantidad de patentes que los fármacos de origen químico puesto que la fabricación biológica posee mayor complejidad, por lo que es necesario conservar la propiedad intelectual no sólo sobre las composiciones de materia, sino también sobre los procesos de fabricación[211,212]. El gran número de patentes existentes representan un desafío al momento de identificar los procesos que deben ser eludidos para evitar litigios, por lo que el proyecto de Ley de Transparencia de Patentes Biológicas propuesto en el Congreso de los EE. UU. en 2019, busca solucionar este conflicto estableciendo una lista de búsqueda imperativa de patentes que resguarda los productos biológicos, la cual se incorporará en el Libro Púrpura de la FDA[211,213].

Por otro lado, a diferencia de los fármacos de molécula pequeña la mayoría de biológicos son composiciones complejas y heterogéneas que requieren principios asépticos en todo el proceso de fabricación[208]. Es así que la licencia de comercialización de un producto biológico es otorgada por organismos reguladores como la FDA y la EMA, que cumplen con los requisitos que garantizan seguridad, pureza y potencia continua del producto[214].

Los principales productos biotecnológicos dirigidos a enfermedades causantes de pandemias se observan en la Figura 3.

Los anticuerpos monoclonales (mAb) neutralizantes se aíslan de personas recuperadas de la infección o de modelos animales inmunizados y se pueden administrar en pacientes antes o después de una infección viral para aplicaciones terapéuticas o profilácticas, los cuales van dirigidos a una diana específica del patógeno evitando la infección de este a la célula huésped[93,114,155]. Por otro lado, los interferones (IFN) son proteínas señalizadoras de origen natural producidas por células del sistema inmunológico, que poseen propiedades antivirales e inmunomoduladoras no específicas[87,110]. Son estimulados por infecciones virales, estos se secretan y se unen a la célula afectada o a sus células vecinas y activa la expresión de genes con función antiviral[215]. Existen tres clases principales de interferones empleados en farmacoterapia los alfa (IFN-α), los beta (IFN-β) y los gamma (INF-γ)[216]. Comúnmente los interferones son estudiados en combinación con otros agentes antivirales, ribavirina o lopinavir / ritonavir[87,217]. Otro de los tratamientos valorados en la aparición de pandemias es el empleo de ARN de interferencia, como ARN de interferencia pequeños (siRNA) y micro ARN (miARN), la función de estas moléculas es la supresión de la expresión de genes claves de los patógenos mediante interferencia por ARN[111,218,219].

Vacunas

Las plataformas empleadas para el diseño de vacunas han evolucionado conforme las necesidades de la humanidad y la disponibilidad de tecnología (Figura 3).

Vacunas de virus (inactivadas y atenuadas)

En las vacunas inactivadas se aplican enfoques químicos

o físicos para eliminar las propiedades infecciosas del patógeno[21,23]. Las ventajas de estas vacunas son la facilidad de producción, además de su seguridad y eficacia en el reconocimiento inmunológico, sin embargo, el rendimiento podría ser limitado debido a la baja producción del virus y la necesidad de instalaciones de altos niveles de bioseguridad[48,71].

Las vacunas vivas atenuadas constan de una versión debilitada del patógeno que se replica limitadamente con el fin de no causar la enfermedad y al mismo tiempo activar las respuestas inmunes de manera similar a una infección natural. Algunas de las desventajas son los problemas de seguridad y el desafío en el proceso de atenuación[31,72].

Vacunas basadas en proteínas (subunidad proteica y partículas similares a virus)

En el caso de las vacunas de subunidades se administran proteínas altamente antigénicas del patógeno en el individuo, debido a su baja complejidad antigénica su eficacia protectora puede ser limitada, además de provocar respuestas inmunes no regulares[220,221]. Las vacunas de partículas similares al virus constan de proteínas de la cápside viral, que generan una alta activación del sistema inmune debido a la repetición de sus estructuras, además confieren seguridad debido a la ausencia de material genético del patógeno, sin embargo, existen complicaciones en el proceso diseño de la plataforma[222].

Vacunas de vectores virales (replicantes y no replicantes)

Las vacunas de vectores virales se basan en un virus modificado con un gen que exprese una proteína de interés del patógeno en cuestión. Los vectores virales de replicación incompetente son virus inhabilitados para la replicación mediante la eliminación de partes de su genoma, entre las ventajas de esta plataforma es que no es necesario manipular el patógeno *in vivo*, estos vectores son capaces de activar respuestas inmunitarias celulares y humorales, y existe gran experiencia en la producción de este tipo de vacunas[95,125]. Por otro lado, para el empleo de vectores de replicación competente se considera a virus que no se replican de manera eficiente o virus de animales que no causan enfermedades en humanos, la ventaja de esta plataforma es que tiene la capacidad de promover una inmunidad robusta debido a que existe una infección real[119].

Vacunas génicas (ADN o ARN)

En este tipo de vacunas la información genética del patógeno, ADN o ARN, es administrada para luego dirigirse a las células del individuo vacunado y expresar una proteína de interés capaz de activar efectivamente el sistema inmunitario y lograr defender al huésped en caso en una futura infección. La tecnología de ADN se puede producir a gran escala, sin embargo, muestran baja inmunogenicidad y necesitan de dispositivos eficientes para su administración[94,223,224]. Mientras que, las vacunas de ARNm poseen capacidad de desarrollo breve, elevada potencia y fabricación rentable, pero requiere almacenamiento a bajas temperaturas para su estabilidad, sin embargo, con los últimos desarrollos referentes a ARNm encapsulado en nanopartículas se podría almacenar este tipo de vacunas a temperaturas de 4°C[169,225].

Discusión y conclusiones

En cuanto a las herramientas de diagnóstico, se debe tener en cuenta que ninguna prueba biológica puede alcanzar una especificidad del 100% y una sensibilidad del 100%[130]. Por su parte, la sensibilidad se define como la capacidad de una prueba de arrojar un resultado positivo en una persona enferma, mientras que la especificidad es la capacidad de la prueba de obtener un resultado negativo en un sujeto libre de la enfermedad[226,227]. Como se muestra en la comparación de resultados de la Tabla 1, la sensibilidad y especificidad de cada una de las técnicas no son 100%, sin embargo, las herramientas moleculares presentan la mejor alternativa para el diagnóstico de enfermedades pandémicas, reduciendo en gran medida los falsos positivos y falsos negativos, elevando así la eficiencia de las pruebas. Según Yuan *et al.*[148] los resultados del diagnóstico dependen de varias condiciones como las características del kit de detección, sus controles, su especificidad, sensibilidad y calidad de la muestra, como se demuestra en la Figura 2, nuevamente las técnicas moleculares alcanzan un porcentaje superior en comparación con el cultivo celular que presenta dificultades en el tiempo de ejecución, baja sensibilidad; y los inmunoensayos para la detección de antígenos, los cuales no se recomiendan como un diagnóstico confirmatorio debido al alto índice de falsos negativos. No obstante, las pruebas de antígenos debido a que permiten la obtención resultados acelerados a un menor costo, se pueden aplicar masivamente teniendo un mayor impacto en la salud pública.

La qRT-PCR ha sido la técnica más empleada como estándar de oro para el diagnóstico de pandemias, sin embargo, a pesar de los altos índices de especificidad y sensibilidad, han surgido algunos problemas como costos elevados, tiempo de procesamiento, requerimiento de personal capacitado y altos estándares de bioseguridad, por lo que se están desarrollando varias alternativas con resultados prometedores como LAMP, CRISPR-Cas y biosensores con el fin de minimizar las desventajas y optimizar el diagnóstico de enfermedades pandémicas[148,189].

Por otro lado, el gran avance en el desarrollo de los productos biotecnológicos se debe a varias ventajas como su alta eficiencia, efectos secundarios más seguros y reducidos en contraste con los fármacos de moléculas pequeñas, además de los costos relativamente bajos que presentan en comparación con sus beneficios y terapias completamente innovadoras. En el caso de la fabricación de vacunas fue posible observar una diferencia significativa en esta pandemia del SARS-CoV-2 en contraposición con brotes anteriores, gracias al nivel científico actual, debido que a pesar de la capacidad de investigación, de los avances biomédicos y biotecnológicos, y del desarrollo de la tecnología, las vacunas podrían tardar años, hasta décadas en ser llevadas al mercado para el beneficio de la humanidad, como es el caso de la primera vacuna contra el EBOV aprobada en el 2019 por la FDA y la EMA[122]. En la actualidad, la situación ha sido diferente frente a la pandemia de COVID-19, a un año y tres meses del inicio del brote del SARS-CoV-2 existen 3 vacunas aprobadas por la FDA, 4 vacunas candidatas en fase 4 y 12 vacunas en estudios clínicos fase 3[150], los expertos afirman que todo el proceso de fabricación y experimentación se han dado en un tiempo récord gracias a la gran inversión tanto pública como privada que se ha llevado a cabo y al sobrelapamiento de las fases preclínicas y clínicas en los diferentes estudios.

Las perspectivas futuras sobre las herramientas y productos biotecnológicos son prometedoras, con técnicas de diagnóstico eficientes con características ultrasensibles con requerimientos de concentraciones a escala nano y tecnología basadas en inteligencia artificial o biología sintética[148,228], las cuales permitirán brindar un apoyo intensivo en el diagnostico y seguimiento en la propagación de la enfermedad y transmisión del patógeno. Los biofármacos, por su parte, constitu-

yen la vanguardia de la investigación biomédica, por lo que se aspira que en el futuro representen una opción más eficiente en el control de enfermedades infecciosas que en la actualidad carecen de tratamiento o poseen muy pocas alternativas[208], además de terapias personalizadas optimizando drásticamente la seguridad y eficacia de los medicamentos[178].

Finalmente, podemos concluir que el desarrollo y uso de las herramientas biotecnológicas actuales han revolucionado el campo de la medicina en este caso el control de enfermedades emergentes con potencial pandémico. Con todos los conocimientos y lecciones adquiridas a lo largo de las diferentes pandemias y epidemias ocurridas a través de la historia, en posteriores brotes se poseerá la capacidad de un mejor manejo y contención de las enfermedades.

Referencias bibliográficas

1. Dobson AP, Carper ER. Infectious diseases and human population history. Bioscience 1996; 46: 115–126.
2. World Health Organization. Disease burden and mortality estimates: Cause-specific mortality, 2000–2016. 2017.http://www.who.int/healthinfo/global_burden_disease/estimates/en/ (accessed 27 Feb2021).
3. Smith KM, Machalaba CC, Seifman R, Feferholtz Y, Karesh WB. Infectious disease and economics: The case for considering multi-sectoral impacts. One Heal 2019; 7: 100080.
4. Nicola M, Alsafi Z, Sohrabi C, Kerwan A, Al-Jabir A, Iosifidis C et al. The socio-economic implications of the coronavirus pandemic (COVID-19): A review. Int J Surg 2020; 78: 185–193.
5. Koplan JP, McPheeters M. Plagues, public health, and politics. Emerg Infect Dis 2004; 10: 2039–2043.
6. DeWitte SN. Mortality risk and survival in the aftermath of the medieval Black Death. PLoS One 2014; 9: e96513.
7. Ogden NH, Wilson JRU, Richardson M, Hui C, Davies SJ, Kumschick S et al. Emerging infectious diseases and biological invasions : a call for a One Health collaboration in science and management. R Soc Open Sci 2019; 6. doi:https://doi.org/10.1098/rsos.181577.
8. Jones KE, Patel NG, Levy MA, Storeygard A, Balk D, Gittleman JL et al. Global trends in emerging infectious diseases. Nature 2008; 451: 990–994.
9. Sun Q, Qiu H, Huang M, Yang Y. Lower mortality of COVID-19 by early recognition and intervention: experience from Jiangsu Province. Ann Intensive Care 2020; 10. doi:10.1186/s13613-020-00650-2.
10. Rauch S, Jasny E, Schmidt KE, Petsch B. New vaccine technologies to combat outbreak situations. Front Immunol 2018; 9. doi:10.3389/fimmu.2018.01963.
11. Hine R. A Dictionary of Biology. 2019 doi:10.1093/acref/9780198821489.001.0001.
12. Porta M. A Dictionary of Epidemiology. 2016 doi:10.1093/acref/9780199976720.001.0001.
13. Adalja AA, Watson M, Toner ES, Cicero A, Inglesby T V. The characteristics of pandemic pathogens. 2018https://www.centerforhealthsecurity.org/our-work/pubs_archive/pubs-pdfs/2018/180510-pandemic-pathogens-report.pdf.
14. Taubenberger JK, Morens DM. 1918 Influenza: The mother of all pandemics. Emerg. Infect. Dis. 2006; 12: 15–22.
15. Johnson N, Muelle J. Updating the accounts: global mortality of the 1918 – 1920 'spanish' influenza pandemic. Bull Hist Med 2002; 76: 105–115.
16. Dunn FL. Pandemic influenza in 1957: Review of international spread of new asian strain. J Am Med Assoc 1958; 166: 1140–1148.
17. Glezen WP. Emerging infections: pandemic influenza. Epidemiol Rev 1996; 18: 64–76.
18. Viboud C, Simonsen L, Fuentes R, Flores J, Miller MA, Chowell G. Global mortality impact of the 1957 – 1959 influenza pandemic. J Infect Dis 2016; 213: 738–745.
19. Blumenfeld H, Kilbourne E, Louria D, Rogers D. Studies on influenza in the pandemic of 1957-1958. I. An epidemiologic, clinical and serologic investigation of an intrahospital epidemic, with a note on vaccination efficacy. J Clin Invest 1958; 38: 199–212.
20. Jensen KE, Hogan RB. Laboratory diagnosis of asian influenza. Public Health Rep 1958; 73: 140–144.
21. Gundelfinger BF, Stille WT, Bell JA. Effectiveness of influenza vaccines during an epidemic of asian influenza. N Engl J Med 1958; 259: 1005–1009.
22. Culver JO, Nitz RE, Lennette EH. The protective effect of monovalent asian-strain vaccine against asian influenza. J Am Med Assoc 1957; 165: 2174–2177.
23. Dull BH, Jensen KE, Rakich JH, Cohen A, Henderson DA, Pirkle CI. Monovalent asian influenza vaccine: evaluation of its use during two waves of epidemic asian influenza in partly immunized penitentiary population. J Am Med Assoc 1960; 172: 87–93.
24. Davenport FM. Role of the commission on influenza. Public Health Rep 1958; 73: 133–139.
25. Meiklejohn G, Morris AJ. Influenza vaccination. Ann Intern Med 1958; 49: 529–535.
26. Langmuir A. Epidemiology of Asian influenza. With special emphasis on the United States. Am Rev Respir Dis 1961; 83: 2–14.
27. Cockburn WC, Delon PJ, Ferreira W. Origin and progress of the 1968-69 Hong Kong influenza epidemic. Bull World Health Organ 1969; 41: 345–348.
28. Rogers K. 1968 Flu pandemic. Encycl. Br. 2020.https://www.britannica.com/event/1968-flu-pandemic (accessed 21 Sep2020).
29. Coleman MT, Dowdle WR. Properties of the Hong Kong influenza virus. I. General characteristics of the Hong Kong virus. Bull World Health Organ 1969; 41: 415–418.
30. Murray R. Production and testing in the USA of influenza virus vaccine made from the Hong Kong variant in 1968-69. Bull World Health Organ 1969; 41: 495–496.
31. Maassab HF, Francis T, Davenport FM, Hennessy A V, Minuse E, Anderson G. Laboratory and clinical characteristics of attenuated strains of influenza virus. Bull World Health Organ 1969; 41: 589–594.
32. Brandon FB, Cox F, Quinn E, Timm EA, Mclean IW. Influenza immunization: clinical studies with ether-split subunit vaccines. Bull World Health Organ 1969; 41: 629–637.
33. Warburton MF. Desoxycholate-split influenza vaccines. Bull World Health Organ 1969; 41: 639–641.
34. Kilbourne ED. Future influenza vaccines and the use of genetic recombinants. Bull World Health Organ 1969; 41: 643–645.
35. Couch RB, Douglas RG, Fedson DS, Kasel JA. Correlated studies of a recombinant influenza-virus vaccine. III. Protection against experimental influenza in man. J Infect Dis 1971; 124: 473–480.
36. Ksiazek TG, Erdman D, Goldsmith CS, Zaki SR, Peret T, Emery S et al. A novel coronavirus associated with severe acute respiratory syndrome. N Engl J Med 2003; 348: 1953–1966.
37. World Health Organization. Cumulative number of reported probable cases of SARS. 2015.https://www.who.int/csr/sars/country/2003_07_11/en/ (accessed 25 Jan2021).
38. World Health Organization. Alert, verification and public health management of SARS in the post-outbreak period. 2003.https://www.who.int/csr/sars/postoutbreak/en/ (accessed 30 Dec2020).
39. Chan KH, Poon LLLM, Cheng VCC, Guan Y, Hung IFN, Kong J et al. Detection of SARS coronavirus in patients with suspected SARS. Emerg Infect Dis 2004; 10: 294–299.
40. Yam WC, Chan KH, Poon LLM, Guan Y, Yuen KY, Seto WH et al. Evaluation of reverse transcription-PCR assays for rapid diagnosis of severe acute respiratory syndrome associated with a novel coronavirus. J Clin Microbiol 2003; 41: 4521–4524.
41. Poon LLM, Chan KH, Wong OK, Yam WC, Yuen KY, Guan Y et al. Early diagnosis of SARS Coronavirus infection by real time RT-PCR. J Clin Virol 2003; 28: 233–238.
42. Chan PKS, To WK, Ng KC, Lam RKY, Ng TK, Chan RCW et al. Laboratory diagnosis of SARS. Emerg Infect Dis 2004; 10: 825–831.
43. Peiris JSM, Lai ST, Poon LLM, Guan Y, Yam LYC, Lim W et al. Coronavirus as a possible cause of severe acute respiratory syndrome. Lancet 2003; 361: 1319–1325.

44. Shi Y, Yi Y, Li P, Kuang T, Li L, Dong M et al. Diagnosis of Severe Acute Respiratory Syndrome (SARS) by Detection of SARS coronavirus nucleocapsid antibodies in an antigen-capturing enzyme-linked immunosorbent assay. J Clin Microbiol 2003; 41: 5781–5782.
45. Lu A, Zhang H, Zhang X, Wang H, Hu Q, Shen L et al. Attenuation of SARS coronavirus by a short hairpin RNA expression plasmid targeting RNA-dependent RNA polymerase. Virology 2004; 324: 84–89.
46. Cheng Y, Wong R, Soo YOY, Wong WS, Lee CK, Ng MHL et al. Use of convalescent plasma therapy in SARS patients in Hong Kong. Eur J Clin Microbiol Infect Dis 2005; 24: 44–46.
47. Ho JC, Wu AY, Lam B, Ooi GC, Khong P-L, Ho PL et al. Pentaglobin in steroid-resistant severe acute respiratory syndrome. Int J Tuberc Lung Dis 2004; 8: 1173–1179.
48. Zhou J, Wang W, Zhong Q, Hou W, Yang Z, Xiao SY et al. Immunogenicity, safety, and protective efficacy of an inactivated SARS-associated coronavirus vaccine in rhesus monkeys. Vaccine 2005; 23: 3202–3209.
49. Yang ZY, Kong WP, Huang Y, Roberts A, Murphy BR, Subbarao K et al. A DNA vaccine induces SARS coronavirus neutralization and protective immunity in mice. Nature 2004; 428: 561–564.
50. Gao W, Tamin A, Soloff A, D'Aiuto L, Nwanegbo E, Robbins PD et al. Effects of a SARS-associated coronavirus vaccine in monkeys. Lancet 2003; 362: 1895–1896.
51. Centers for Disease Control and Prevention. Update: novel influenza A (H1N1) virus infections - worldwide, May 6, 2009. MMWR Morb Mortal Wkly Rep 2009; 58: 453–458.
52. Centers for Disease Control and Prevention. 2009 H1N1 Pandemic (H1N1pdm09 virus). 2019.https://www.cdc.gov/flu/pandemic-resources/2009-h1n1-pandemic.html (accessed 25 Jan2021).
53. Dawood FS, Iuliano AD, Reed C, Meltzer MI, Shay DK, Cheng PY et al. Estimated global mortality associated with the first 12 months of 2009 pandemic influenza A H1N1 virus circulation: a modelling study. Lancet Infect Dis 2012; 12: 687–695.
54. World Health Organization. WHO information for laboratory diagnosis of pandemic (H1N1) 2009 virus in humans α revised. 2009https://www.who.int/csr/resources/publications/swineflu/WHO_Diagnostic_RecommendationsH1N1_20090521.pdf.
55. Peiris JM, Poon LLM, Guan Y. Emergence of a novel swine-origin influenza A virus (S-OIV) H1N1 virus in humans. J Clin Virol 2009; 45: 169–173.
56. Centers for Disease Control and Prevention. Interim guidance on specimen collection, processing, and testing for patients with suspected novel influenza A (H1N1) virus infection. 2009.https://www.cdc.gov/h1n1flu/specimencollection.htm (accessed 20 Jan2021).
57. Balish A, Warnes C, Wu K, Barnes N, Emery S, Berman L et al. Evaluation of rapid influenza diagnostic tests for detection of novel influenza A (H1N1) virus - United States, 2009. Morb Mortal Wkly Rep 2009; 58: 826–829.
58. Kumar S, Henrickson KJ. Update on influenza diagnostics: lessons from the novel H1N1 influenza A pandemic. Clin Microbiol Rev 2012; 25: 344–361.
59. World Health Organization. CDC protocol of realtime RTPCR for influenza A (H1N1). Atlanta, 2009.
60. Kim D, Poudel B. Tools to Detect Influenza Virus. Yosei Med J 2013; 54: 560–566.
61. Vasoo S, Stevens J, Singh K. Rapid antigen tests for diagnosis of pandemic (Swine) influenza A/H1N1. Clin Infect Dis 2009; 49: 1090–1093.
62. Centers for Disease Control and Prevention. Interim Recommendations for Clinical Use of Influenza Diagnostic Tests During the 2009-10 Influenza Season. 2009.https://www.cdc.gov/h1n1flu/guidance/diagnostic_tests.htm#_ftn1 (accessed 4 Feb2021).
63. Garten RJ, Davis CT, Russell CA, Shu B, Lindstrom S, Balish A et al. Antigenic and Genetic Characteristics of the Early Isolates of Swine-Origin 2009 A(H1N1) Influenza Viruses Circulating in Humans. Science 2009; 325: 197–201.
64. Yang Y, Sugimoto JD, Halloran ME, Basta NE, Chao DL, Matrajt L et al. The transmissibility and control of pandemic influenza A (H1N1) virus. Science 2009; 326: 729–733.
65. Hung IFN, To KKW, Lee CK, Lee KL, Yan WW, Chan K et al. Hyperimmune IV immunoglobulin treatment: A multicenter double-blind randomized controlled trial for patients with severe 2009 influenza A(H1N1) infection. Chest 2013; 144: 464–473.
66. Hung IFN, To KKW, Lee CK, Lee KL, Chan K, Yan WW et al. Convalescent plasma treatment reduced mortality in patients with severe pandemic influenza A (H1N1) 2009 virus infection. Clin Infect Dis 2011; 52: 447–456.
67. Prevention C for DC and. Key Facts About 2009 H1N1 Flu Vaccine. 2010.https://www.cdc.gov/h1n1flu/vaccination/vaccine_keyfacts.htm (accessed 5 Feb2021).
68. Centers for Disease Control and Prevention. Update on Influenza A (H1N1) 2009 Monovalent Vaccines. MMWR Morb Mortal Wkly Rep 2009; 58: 1100–1101.
69. Neumann G, Kawaoka Y. The first influenza pandemic of the new millennium. Influenza Other Respi Viruses 2011; 5: 157–166.
70. Plennevaux E, Sheldon E, Blatter M, Reeves-Hoché MK, Denis M. Immune response after a single vaccination against 2009 influenza A H1N1 in USA: a preliminary report of two randomised controlled phase 2 trials. Lancet 2010; 375: 41–48.
71. Greenberg ME, Lai MH, Hartel GF, Wichems CH, Gittleson C, Bennet J et al. Response to a monovalent 2009 influenza A (H1N1) vaccine. New Engl J Med 2009; 361: 2405–2413.
72. Mallory RM, Malkin E, Ambrose CS, Bellamy T, Shi L, Yi T et al. Safety and immunogenicity following administration of a live, attenuated monovalent 2009 H1N1 influenza vaccine to children and adults in two randomized controlled trials. PLoS One 2010; 5: e13755.
73. Clark TW, Pareek M, Hoschler K, Dillon H, Nicholson KG, Groth N et al. Trial of 2009 influenza A (H1N1) monovalent MF59-adjuvanted vaccine. N Engl J Med 2009; 361: 2424–2435.
74. Hardelid P, Fleming DM, Mcmenamin J, Andrews N, Robertson C, SebastianPillai P et al. Effectiveness of pandemic and seasonal influenza vaccine in preventing pandemic influenza A(H1N1)2009 infection in England and Scotland 2009-2010. Eurosurveillance 2011; 16: 19763.
75. Lansbury LE, Smith S, Beyer W, Karamehic E, Pasic-Juhas E, Sikira H et al. Effectiveness of 2009 pandemic influenza A(H1N1) vaccines: A systematic review and meta-analysis. Vaccine 2017; 35: 1996–2006.
76. Zaki AM, Van Boheemen S, Bestebroer TM, Osterhaus ADME, Fouchier RAM. Isolation of a novel coronavirus from a man with pneumonia in Saudi Arabia. N Engl J Med 2012; 367: 1814–1820.
77. World Health Organization. Middle East respiratory syndrome coronavirus (MERS-CoV) – The Kingdom of Saudi Arabia. 2021. http://www.who.int/csr/don/01-february-2021-mers-saudi-arabia/en/ (accessed 16 Feb2021).
78. Centers for Disease Control and Prevention. Laboratory Testing for MERS-CoV. 2019.https://www.cdc.gov/coronavirus/mers/lab/lab-testing.html#molecular (accessed 21 Dec2020).
79. World Health Organization. Laboratory testing for Middle East Respiratory Syndrome Coronavirus- Interim guidance (revised). 2018https://www.who.int/csr/disease/coronavirus_infections/mers-laboratory-testing/en/ (accessed 18 Dec2020).
80. Corman VM, Eckerle I, Bleicker T, Zaki A, Landt O, Eschbach-Bludau M et al. Detection of a novel human coronavirus by real-time reverse-transcription polymerase chain reaction. Eurosurveillance 2012; 17. doi:10.2807/ese.17.39.20285-en.
81. Corman VM, Müller MA, Costabel U, Timm J, Binger T, Meyer B et al. Assays for laboratory confirmation of novel human coronavirus (hCoV-EMC) infections. Eurosurveillance 2012; 17: 20334.
82. Abd El Wahed A, Patel P, Heidenreich D, Hufert FT, Weidmann M. Reverse transcription recombinase polymerase amplification assay for the detection of middle east respiratory syndrome coronavirus. PLoS Curr 2013; 5. doi:10.1371/currents.outbreaks.62df1c7c75ffc96cd59034531e2e8364.
83. Shirato K, Yano T, Senba S, Akachi S, Kobayashi T, Nishinaka T et al. Detection of Middle East respiratory syndrome coronavirus using reverse transcription loop-mediated isothermal amplification (RT-LAMP). Virol J 2014; 11. doi:https://doi.org/10.1186/1743-422X-11-139.

84. Huang P, Wang H, Cao Z, Jin H, Chi H, Zhao J et al. A rapid and specific assay for the detection of MERS-CoV. Front Microbiol 2018; 9. doi:10.3389/fmicb.2018.01101.
85. Memish ZA, Perlman S, Van Kerkhove MD, Zumla A. Middle East respiratory syndrome. Lancet 2020; 395: 1063–1077.
86. Koch T, Dahlke C, Fathi A, Kupke A, Krähling V, Okba NMA et al. Safety and immunogenicity of a modified vaccinia virus Ankara vector vaccine candidate for Middle East respiratory syndrome: an open-label, phase 1 trial. Lancet Infect Dis 2020; 20: 827–838.
87. Arabi YM, Asiri AY, Assiri AM, Balkhy HH, Al Bshabshe A, Al Jeraisy M et al. Interferon beta-1b and lopinavir–ritonavir for middle east respiratory syndrome. N Engl J Med 2020; 383: 1645–1656.
88. Widjaja I, Wang C, van Haperen R, Gutiérrez-Álvarez J, van Dieren B, Okba NMA et al. Towards a solution to MERS: protective human monoclonal antibodies targeting different domains and functions of the MERS-coronavirus spike glycoprotein. Emerg Microbes Infect 2019; 8: 516–530.
89. Raj VS, Okba NMA, Gutierrez-Alvarez J, Drabek D, van Dieren B, Widagdo W et al. Chimeric camel / human heavy-chain antibodies protect against MERS-CoV infection. Sci Adv 2018; 4: eaas9667.
90. Ko JH, Seok H, Cho SY, Ha YE, Baek JY, Kim SH et al. Challenges of convalescent plasma infusion therapy in Middle East respiratory coronavirus infection: A single centre experience|. Antivir Ther 2018; 23: 617–622.
91. de Wit E, Feldmann F, Okumura A, Horne E, Haddock E, Saturday G et al. Prophylactic and therapeutic efficacy of mAb treatment against MERS-CoV in common marmosets. Antiviral Res 2018; 156: 64–71.
92. Luke T, Wu H, Zhao J, Channappanavar R, Coleman CM, Jiao J-A et al. Human polyclonal immunoglobulin G from transchromosomic bovines inhibits MERS-CoV in vivo. Sci Transl Med 2016; 8: 326ra21.
93. Beigel JH, Voell J, Kumar P, Raviprakash K, Wu H, Jiao JA et al. Safety and tolerability of a novel, polyclonal human anti-MERS coronavirus antibody produced from transchromosomic cattle: a phase 1 randomised, double-blind, single-dose-escalation study. Lancet Infect Dis 2018; 18: 410–418.
94. Modjarrad K, Roberts CC, Mills KT, Castellano AR, Paolino K, Muthumani K et al. Safety and immunogenicity of an anti-Middle East respiratory syndrome coronavirus DNA vaccine: a phase 1, open-label, single-arm, dose-escalation trial. Lancet 2019; 19: 1013–1022.
95. Folegatti PM, Bittaye M, Flaxman A, Lopez FR, Bellamy D, Kupke A et al. Safety and immunogenicity of a candidate Middle East respiratory syndrome coronavirus viral-vectored vaccine: a dose-escalation, open-label, non-randomised, uncontrolled, phase 1 trial. Lancet Infect Dis 2020; 20: 816–826.
96. Pattyn S, van der Groen G, Jacob W, Piot P, Courteille G. Isolation of Marburg-like virus from a case of hæmorrhagic fever in Zaire. Lancet 1977; 309: 573–574.
97. World Health Organization. Ebola outbreak 2014-2016. 2016. http://www.who.int/csr/disease/ebola/en/ (accessed 23 Oct2020).
98. Centers for Disease Control and Prevention. 2020 Democratic Republic of the Congo, Equateur Province. 2020.https://www.cdc.gov/vhf/ebola/outbreaks/drc/2020-june.html (accessed 6 Feb2021).
99. Jacob ST, Crozier I, Fischer WA, Hewlett A, Kraft CS, Vega MA de La et al. Ebola virus disease. Nat Rev Dis Prim 2020; 6. doi:https://doi.org/10.1038/s41572-020-0147-3.
100. Dudas G, Carvalho LM, Bedford T, Tatem AJ, Baele G, Faria NR et al. Virus genomes reveal factors that spread and sustained the Ebola epidemic. Nature 2017; 544: 309–315.
101. World Health Organization. Ebola virus disease. 2020. https://www.who.int/news-room/fact-sheets/detail/ebola-virus-disease (accessed 6 Feb2021).
102. Erickson BR, Sealy TK, Flietstra T, Morgan L, Kargbo B, Matt-Lebby VE et al. Ebola virus disease diagnostics, Sierra Leone: analysis of real time RT-PCR values in clinical blood and oral swab specimens. J Infect Dis 2016; 214: S258–S262.
103. Malvy D, McElroy AK, de Clerck H, Günther S, van Griensven J. Ebola virus disease. Lancet 2019; 393: 936–948.
104. Pinsky BA, Sahoo MK, Sandlund J, Kleman M, Kulkarni M, Grufman P et al. Analytical performance characteristics of the cepheid GeneXpert Ebola Assay for the detection of Ebola virus. PLoS One 2015; 10: e0142216.
105. Cnops L, De Smet B, Mbala-Kingebeni P, van Griensven J, Ahuka-Mundeke S, Ariën KK. Where are the Ebola diagnostics from last time? Nature 2019; 565: 419–421.
106. OraSure Technologies I. OraQuick ® Ebola rapid antigen test customer letter. Bethlehem, 2019https://www.orasure.com/documents/products/ebola/Ebola_Instruction_PI-ENG.pdf (accessed 6 Feb2021).
107. U.S. Food and Drug Administration. FDA allows marketing of first rapid diagnostic test for detecting Ebola virus antigens. 2019.https://www.fda.gov/news-events/press-announcements/fda-allows-marketing-first-rapid-diagnostic-test-detecting-ebola-virus-antigens (accessed 6 Feb2021).
108. van Griensven J, De Weiggheleire A, Delamou A, Smith PG, Edwards T, Vandekerckhove P et al. The use of ebola convalescent plasma to treat ebola virus disease in resource-constrained settings: a perspective from the field. Clin Infect Dis 2016; 62: 69–74.
109. The PREVAIL II Writing Group for the Multi-National PREVAIL II Study Team. A randomized, controlled trial of ZMapp for ebola virus infection. N Engl J Med 2016; 375: 1448–1456.
110. Konde MK, Baker DP, Traore FA, Sow MS, Camara A, Barry AA et al. Interferon α -1a for the treatment of Ebola virus disease: A historically controlled, single-arm proof-of-concept trial. PLoS One 2017; 12: e0169255.
111. Dunning J, Sahr F, Rojek A, Gannon F, Carson G, Idriss B et al. Experimental treatment of Ebola virus disease with TKM-130803: A single-arm phase 2 clinical trial. PLoS Med 2016; 13: e1001997.
112. Mulangu S, Dodd LE, Davey RT, Tshiani Mbaya O, Proschan M, Mukadi D et al. A randomized, controlled trial of ebola virus disease therapeutics. N Engl J Med 2019; 381: 2293–2303.
113. U.S. Food and Drug Administration. FDA Approves First Treatment for Ebola Virus. 2020.https://www.fda.gov/news-events/press-announcements/fda-approves-first-treatment-ebola-virus (accessed 9 Feb2021).
114. Sivapalasingam S, Kamal M, Slim R, Hosain R, Shao W, Stoltz R et al. Safety, pharmacokinetics, and immunogenicity of a co-formulated cocktail of three human monoclonal antibodies targeting Ebola virus glycoprotein in healthy adults: a randomised, first-in-human phase 1 study. Lancet Infect Dis 2018; 18: 884–893.
115. U.S. Food and Drug Administration. FDA Approves Treatment for Ebola Virus. 2020.https://www.fda.gov/drugs/drug-safety-and-availability/fda-approves-treatment-ebola-virus (accessed 9 Feb2021).
116. Gaudinski MR, Coates EE, Novik L, Widge A, Houser K V., Burch E et al. Safety, tolerability, pharmacokinetics, and immunogenicity of the therapeutic monoclonal antibody mAb114 targeting Ebola virus glycoprotein (VRC 608): an open-label phase 1 study. Lancet 2019; 393: 889–898.
117. Park DJ, Dudas G, Wohl S, Goba A, Whitmer SLM, Andersen KG et al. Ebola virus epidemiology, transmission, and evolution during seven months in Sierra Leone. Cell 2015; 161: 1516–1526.
118. Henao Restrepo AM. Update on candidate Ebola vaccines: available data on immunogenicity, efficacy and safety. 2018https://www.who.int/immunization/sage/meetings/2018/october/SAGE_october_2018_ebola_Henaorestrepo.pdf (accessed 9 Feb2021).
119. Henao-Restrepo AM, Longini IM, Egger M, Dean NE, Edmunds WJ, Camacho A et al. Efficacy and effectiveness of an rVSV-vectored vaccine expressing Ebola surface glycoprotein: interim results from the Guinea ring vaccination cluster-randomised trial. Lancet 2015; 386: 857–866.
120. Henao-Restrepo AM, Camacho A, Longini IM, Watson CH, Edmunds WJ, Egger M et al. Efficacy and effectiveness of an rVSV-vectored vaccine in preventing Ebola virus disease: final results from the Guinea ring vaccination, open-label, cluster-randomised trial (Ebola Ça Suffit!). Lancet 2017; 389: 505–518.

121. European Commission. Vaccine against Ebola: Commission grants market authorisation. 2019.https://ec.europa.eu/commission/presscorner/detail/en/IP_19_6246 (accessed 21 Dec2020).
122. US Food and Drug Administration. First FDA-approved vaccine for the prevention of Ebola virus disease, marking a critical milestone in public health preparedness and response. 2019.https://www.fda.gov/news-events/press-announcements/first-fda-approved-vaccine-prevention-ebola-virus-disease-marking-critical-milestone-public-health (accessed 21 Aug2020).
123. World Health Organization. Preliminary results on the efficacy of rVSV-ZEBOV-GP Ebola vaccine using the ring vaccination strategy in the control of an Ebola outbreak in the Democratic Republic of the Congo: an example of integration of research into epidemic response. 2019https://www.who.int/csr/resources/publications/ebola/ebola-ring-vaccination-results-12-april-2019.pdf (accessed 10 Feb2021).
124. Johnson & Johnson. Johnson & Johnson Announces European Commission Approval for Janssen's Preventive Ebola Vaccine . 2020.https://www.jnj.com/johnson-johnson-announces-european-commission-approval-for-janssens-preventive-ebola-vaccine#_ednref6 (accessed 10 Feb2021).
125. Milligan ID, Gibani MM, Sewell R, Clutterbuck EA, Campbell D, Plested E et al. Safety and immunogenicity of novel adenovirus type 26-and modified vaccinia Ankara-vectored Ebola vaccines: A randomized clinical trial. JAMA 2016; 315: 1610–1623.
126. Winslow RL, Milligan ID, Voysey M, Luhn K, Shukarev G, Douoguih M et al. Immune responses to novel adenovirus type 26 and modified vaccinia virus Ankara-vectored ebola vaccines at 1 year. JAMA 2017; 317: 1075–1077.
127. Zhu N, Zhang D, Wang W, Li X, Yang B, Song J et al. A novel coronavirus from patients with pneumonia in China, 2019. N Engl J Med 2020; 382: 727–733.
128. World Health Organization. WHO Coronavirus Disease (COVID-19) Dashboard. 2021.https://covid19.who.int/ (accessed 1 Mar2021).
129. U.S. Food & Drug Administration. In vitro diagnostics EUAs. 2021.https://n9.cl/wxx8 (accessed 1 Mar2021).
130. Vandenberg O, Martiny D, Rochas O, van Belkum A, Kozlakidis Z. Considerations for diagnostic COVID-19 tests. Nat Rev Microbiol 2020; 19: 171–183.
131. Liu R, Han H, Liu F, Lv Z, Wu K, Liu Y et al. Positive rate of RT-PCR detection of SARS-CoV-2 infection in 4880 cases from one hospital in Wuhan, China, from Jan to Feb 2020. Clin Chim Acta 2020; 505: 172–175.
132. Chu DKW, Pan Y, Cheng SMS, Hui KPY, Krishnan P, Liu Y et al. Molecular diagnosis of a novel coronavirus (2019-nCoV) causing an outbreak of pneumonia. Clin Chem 2020; 66: 549–555.
133. Touma M. COVID-19: molecular diagnostics overview. J Mol Med 2020; 98: 947–954.
134. Fang Y, Zhang H, Xie J, Lin M, Ying L, Pang P et al. Sensitivity of Chest CT for COVID-19: Comparison to RT-PCR. Radiology 2020; 296: E115–E117.
135. Yan C, Cui J, Huang L, Du B, Chen L, Xue G et al. Rapid and visual detection of 2019 novel coronavirus (SARS-CoV-2) by a reverse transcription loop-mediated isothermal amplification assay. Clin Microbiol Infect 2020; 26: 773–779.
136. Park G, Ku K, Baek S, Kim S, Kim S Il, Kim B et al. Development of reverse transcription loop-mediated isothermal amplification assays targeting Severe Acute Respiratory Syndrome Coronavirus 2 (SARS-CoV-2). J Mol Diagnostics 2020; 22: 729–735.
137. Huang WE, Lim B, Hsu C-C, Xiong D, Wu W, Yu Y et al. RT-LAMP for rapid diagnosis of coronavirus SARS-CoV-2. Microb Biotechnol 2020; 13: 950–961.
138. Rahimi H, Salehiabar M, Barsbay M, Ghaffarlou M, Kavetskyy T, Sharafi A et al. CRISPR Systems for COVID-19 Diagnosis. ACS Sensors 2021; 6: 1430–1445.
139. U.S. Food and Drug Administration. Sherlock CRISPR SARS-CoV-2 Kit. Cambridge, 2020https://www.fda.gov/media/137747/download.
140. Jolany Vangah S, Katalani C, Booneh HA, Hajizade A, Sijercic A, Ahmadian G. CRISPR-Based Diagnosis of Infectious and Noninfectious Diseases. Biol Proced Online 2020; 22. doi:10.1186/s12575-020-00135-3.
141. Joung J, Ladha A, Saito M, Segel M, Bruneau R, Huang MLW et al. Point-of-care testing for COVID-19 using SHERLOCK diagnostics. medRxiv 2020. doi:10.1101/2020.05.04.20091231.
142. Broughton JP, Deng X, Yu G, Fasching CL, Servellita V, Singh J et al. CRISPR – Cas12-based detection of SARS-CoV-2. Nat Biotechnol 2020; 38: 870–874.
143. Centers for Disease Control and Prevention. Interim Guidance for Antigen Testing for SARS-CoV-2. 2020.https://www.cdc.gov/coronavirus/2019-ncov/lab/resources/antigen-tests-guidelines.html (accessed 1 Mar2021).
144. Dinnes J, Deeks JJ, Adriano A, Berhane S, Davenport C, Dittrich S et al. Rapid, point-of-care antigen and molecular-based tests for diagnosis of SARS-CoV-2 infection. Cochrane Database Syst Rev 2020; 8: CD013705.
145. Sheridan C. COVID-19 spurs wave of innovative diagnostics. Nat Biotechnol 2020; 38: 769–772.
146. Qiu G, Gai Z, Tao Y, Schmitt J, Kullak-Ublick GA, Wang J. Dual-Functional Plasmonic Photothermal Biosensors for Highly Accurate Severe Acute Respiratory Syndrome Coronavirus 2 Detection. ACS Nano 2020; 14: 5268–5277.
147. Huang Z, Tian D, Liu Y, Lin Z, Lyon CJ, Lai W et al. Ultra-sensitive and high-throughput CRISPR-p owered COVID-19 diagnosis. Biosens Bioelectron 2020; 164: 112316.
148. Yuan X, Yang C, He Q, Chen J, Yu D, Li J et al. Current and perspective diagnostic techniques for COVID-19. ACS Infect Dis 2020; 6: 1998–2016.
149. U.S Food & Drug Administration. Coronavirus Treatment Acceleration Program (CTAP). 2021.https://www.fda.gov/drugs/coronavirus-covid-19-drugs/coronavirus-treatment-acceleration-program-ctap (accessed 26 Feb2020).
150. World Health Organization. Draft landscape and tracker of COVID-19 candidate vaccines. 2021.https://www.who.int/publications/m/item/draft-landscape-of-covid-19-candidate-vaccines (accessed 1 Mar2021).
151. Kyriakidis NC, López-Cortés A, González EV, Grimaldos AB, Prado EO. SARS-CoV-2 vaccines strategies: a comprehensive review of phase 3 candidates. NPJ Vaccines 2021; 6. doi:10.1038/s41541-021-00292-w.
152. Jiang S, Zhang X, Yang Y, Hotez PJ, Du L. Neutralizing antibodies for the treatment of COVID-19. Nat Biomed Eng 2020; 4: 1134–1139.
153. U.S. Food and Drug Administration. Emergency Use Authorization. 2021.https://www.fda.gov/emergency-preparedness-and-response/mcm-legal-regulatory-and-policy-framework/emergency-use-authorization#coviddrugs (accessed 13 Feb2021).
154. National Institutes of Health. Anti-SARS-CoV-2 monoclonal antibodies. 2021.https://www.covid19treatmentguidelines.nih.gov/anti-sars-cov-2-antibody-products/anti-sars-cov-2-monoclonal-antibodies/ (accessed 13 Feb2021).
155. Chen P, Nirula A, Heller B, Gottlieb RL, Boscia J, Morris J et al. SARS-CoV-2 neutralizing antibody LY-CoV555 in outpatients with Covid-19. N Engl J Med 2021; 384: 229–237.
156. Gottlieb RL, Nirula A, Chen P, Boscia J, Heller B, Morris J et al. Effect of bamlanivimab as monotherapy or in combination with etesevimab on viral load in patients with mild to moderate COVID-19. JAMA 2021; 325: 632–644.
157. Weinreich DM, Sivapalasingam S, Norton T, Ali S, Gao H, Bhore R et al. REGN-COV2, a neutralizing antibody cocktail, in outpatients with Covid-19. N Engl J Med 2021; 384: 238–251.
158. Li L, Zhang W, Hu Y, Tong X, Zheng S, Yang J et al. Effect of convalescent plasma therapy on time to clinical improvement in patients with severe and Life-threatening COVID-19: a randomized clinical trial. JAMA 2020; 324: 460–470.
159. Agarwal A, Mukherjee A, Kumar G, Chatterjee P, Bhatnagar T, Malhotra P. Convalescent plasma in the management of moderate covid-19 in adults in India: Open label phase II multicentre randomised controlled trial (PLACID Trial). BMJ 2020; 371: m3939.

160. Joyner MJ, Bruno KA, Klassen SA, Kunze KL, Johnson PW, Lesser ER et al. Safety update: COVID-19 convalescent plasma in 20,000 hospitalized patients. Mayo Clin Proc 2020; 95: 1888–1897.
161. Libster R, Pérez Marc G, Wappner D, Coviello S, Bianchi A, Braem V et al. Early high-titer plasma therapy to prevent severe Covid-19 in older adults. N Engl J Med 2021; 384: 610–618.
162. Liu STH, Lin HM, Baine I, Wajnberg A, Gumprecht JP, Rahman F et al. Convalescent plasma treatment of severe COVID-19: a propensity score–matched control study. Nat Med 2020; 26: 1708–1713.
163. Baden LR, El Sahly HM, Essink B, Kotloff K, Frey S, Novak R et al. Efficacy and safety of the mRNA-1273 SARS-CoV-2 vaccine. N Engl J Med 2021; 384: 403–416.
164. Sadoff J, Le Gars M, Shukarev G, Heerwegh D, Truyers C, de Groot AM et al. Interim results of a phase 1–2a trial of Ad26. COV2.S Covid-19 vaccine. N Engl J Med 2021. doi:10.1056/NEJMoa2034201.
165. Johnson & Johnson. Johnson & Johnson announces single-shot Janssen COVID-19 vaccines candidate met primary endpoints in interim analysis of its phase 3 ENSEMBLE trial . 2021. https://www.jnj.com/johnson-johnson-announces-single-shot-janssen-covid-19-vaccine-candidate-met-primary-endpoints-in-interim-analysis-of-its-phase-3-ensemble-trial (accessed 15 Feb2021).
166. Ledford H, Cyranoski D, Van Noorden R. The UK has approved a COVID vaccine - here's what scientists now want to know. Nature 2020; 588: 205–206.
167. U.S. Food & Drug Administration. Pfizer-BioNTech COVID-19 Vaccine. 2020.https://www.fda.gov/emergency-preparedness-and-response/coronavirus-disease-2019-covid-19/pfizer-biontech-covid-19-vaccine (accessed 1 Mar2021).
168. Ministerio de Salud Pública. Inició la vacunación contra la COVID-19 en Ecuador. 2021.https://www.salud.gob.ec/en-ecuador-inicio-la-vacunacion-contra-la-covid-19/ (accessed 14 Feb2021).
169. Polack FP, Thomas SJ, Kitchin N, Absalon J, Gurtman A, Lockhart S et al. Safety and efficacy of the BNT162b2 mRNA Covid-19 vaccine. N Engl J Med 2020; 383: 2603–2615.
170. Ministerio de Salud Pública. Vacuna de AstraZeneca contra la COVID-19 se aplicará en Ecuador. 2021.https://www.salud.gob.ec/vacuna-de-astrazeneca-contra-la-covid-19-se-aplicara-en-ecuador/ (accessed 14 Feb2021).
171. Voysey M, Clemens SAC, Madhi SA, Weckx LY, Folegatti PM, Aley PK et al. Safety and efficacy of the ChAdOx1 nCoV-19 vaccine (AZD1222) against SARS-CoV-2: an interim analysis of four randomised controlled trials in Brazil, South Africa, and the UK. Lancet 2021; 397: 99–111.
172. Bud R. History of ' biotechnology '. Nature 1989; 337: 10.
173. Amarakoon II, Hamilton C, Mitchell SA, Tennant PF, Roye ME. Biotechnology. In: Pharmacognosy: Fundamentals, Applications and Strategies. Elsevier Inc., 2017, pp 549–563.
174. Verma A, Agrahari S, Rastogi S, Singh A. Biotechnology in the realm of history. J Pharm Bioallied Sci 2011; 3: 321–324.
175. Bud R. Biotechnology in the twentieth century. Soc Stud Sci 1991; 21: 415–457.
176. Wright S. Recombinant DNA technology and its social transformation, 1972-1982. Osiris 1986; 2: 303–360.
177. Köhler G, Milstein C. Continuous cultures of fused cells secreting antibody of predefined specificity. Nature 1975; 256: 495–497.
178. Gupta V, Sengupta M, Prakash J, Tripathy BC. An Introduction to Biotechnology. In: Basic and Applied Aspects of Biotechnology. Springer Singapore: Singapore, 2017, pp 1–21.
179. DaSilva EJ. The colours of biotechnology: science, development and humankind. Electron J Biotechnol 2004; 7.http://www.ejbiotechnology.info/index.php/ejbiotechnology/article/view/1114 (accessed 15 Dec2020).
180. Olivier M, Asmis R, Hawkins GA, Howard TD, Cox LA. The need for multi-omics biomarker signatures in precision medicine. Int J Mol Sci 2019; 20: 4781.
181. Eckhardt M, Hultquist JF, Kaake RM, Hüttenhain R, Krogan NJ. A systems approach to infectious disease. Nat Rev Genet 2020; 21: 339–354.
182. Sperk M, Van Domselaar R, Rodriguez JE, Mikaeloff F, Sá Vinhas B, Saccon E et al. Utility of proteomics in emerging and re-emerging infectious diseases caused by RNA viruses. J Proteome Res 2020; 19: 4259–4274.
183. Cherry JD, Krogstad P. SARS: The first pandemic of the 21st century. Pediatr Res 2004; 56. doi:10.1203/01.PDR.0000129184.87042.FC.
184. Zumla A, Chan JFW, Azhar EI, Hui DSC, Yuen KY. Coronaviruses-drug discovery and therapeutic options. Nat Rev Drug Discov 2016; 15: 327–347.
185. Gire SK, Goba A, Andersen KG, Sealfon RSG, Park DJ, Kanneh L et al. Genomic surveillance elucidates Ebola virus origin and transmission during the 2014 outbreak. Science (80-) 2014; 345: 1369–1372.
186. Rahimi A, Mirzazadeh A, Tavakolpour S. Genetics and genomics of SARS-CoV-2: A review of the literature with the special focus on genetic diversity and SARS-CoV-2 genome detection. Genomics 2021; 113: 1221–1232.
187. Schubert OT, Röst HL, Collins BC, Rosenberger G, Aebersold R. Quantitative proteomics: challenges and opportunities in basic and applied research. Nat Protoc 2017; 12: 1289–1294.
188. Grenga L, Armengaud J. Proteomics in the COVID-19 battlefield: first semester check-up. Proteomics 2020; 21: e2000198.
189. Srivastava S, Upadhyay DJ, Srivastava A. Next-Generation molecular diagnostics development by CRISPR/Cas tool: rapid detection and surveillance of viral disease outbreaks. Front Mol Biosci 2020; 7. doi:10.3389/fmolb.2020.582499.
190. World Health Organization. Urgently needed: rapid, sensitive, safe and simple Ebola diagnostic tests. 2014.https://www.who.int/mediacentre/news/ebola/18-november-2014-diagnostics/en/ (accessed 19 Nov2020).
191. National Human Genome Research Institute. Polymerase Chain Reaction (PCR) fact sheet. 2020.https://www.genome.gov/about-genomics/fact-sheets/Polymerase-Chain-Reaction-Fact-Sheet (accessed 27 Jan2021).
192. VanGuilder HD, Vrana KE, Freeman WM. Twenty-five years of quantitative PCR for gene expression analysis. Biotechniques 2008; 44: 619–626.
193. Poritz MA, Lingenfelter B. Multiplex PCR for detection and identification of microbial pathogens. In: Springer C (ed). Advanced Techniques in Diagnostic Microbiology. Springer, Cham, 2018, pp 475–493.
194. Zhang Y, Dai C, Wang H, Gao Y, Li T, Fang Y et al. Analysis and validation of a highly sensitive one-step nested quantitative real-time polymerase chain reaction assay for specific detection of severe acute respiratory syndrome coronavirus 2. Virol J 2020; 17. doi:10.1186/s12985-020-01467-y.
195. Green MR, Sambrook J. Nested polymerase chain reaction (PCR). Cold Spring Harb Protoc 2019; 2019. doi:10.1101/pdb.prot095182.
196. Mori Y, Nagamine K, Tomita N, Notomi T. Detection of loop-mediated isothermal amplification reaction by turbidity derived from magnesium pyrophosphate formation. Biochem Biophys Res Commun 2001; 289: 150–154.
197. The McGovern Institute for Brain Research. What is CRISPR? Ask the Brain. Massachusetts Inst. Technol. 2019.https://mcgovern.mit.edu/2019/01/01/crispr-in-a-nutshell/ (accessed 27 Jan2021).
198. Carter LJ, Garner L V., Smoot JW, Li Y, Zhou Q, Saveson CJ et al. Assay techniques and test development for COVID-19 diagnosis. ACS Cent Sci 2020; 6: 591–605.
199. Racine R, Winslow GM. IgM in microbial infections: Taken for granted? Immunol Lett 2009; 125: 79–85.
200. Wang H, Li X, Li T, Zhang S, Wang L, Wu X et al. The genetic sequence, origin, and diagnosis of SARS-CoV-2. Eur J Clin Microbiol Infect Dis 2020; 39: 1629–1635.
201. Li Z, Yi Y, Luo X, Xiong N, Liu Y, Li S et al. Development and clinical application of a rapid IgM-IgG combined antibody test for SARS-CoV-2 infection diagnosis. J Med Virol 2020; 92: 1518–1524.

202. Davis CW, Jackson KJL, McElroy AK, Halfmann P, Huang J, Chennareddy C et al. Longitudinal analysis of the human B cell response to ebola virus infection. Cell 2019; 177: 1566-1582.e17.
203. Okba NMA, Stalin Raj V, Widjaja I, GeurtsvanKessel CH, De Bruin E, Chandler FD et al. Sensitive and specific detection of low-level antibody responses in mild Middle East respiratory syndrome coronavirus infections. Emerg Infect Dis 2019; 25: 1868–1877.
204. Augustine R, Das S, Hasan A, S A, Abdul Salam S, Augustine P et al. Rapid antibody-based COVID-19 mass surveillance: relevance, challenges, and prospects in a pandemic and post-pandemic world. J Clin Med 2020; 9: 3372.
205. Broadhurst MJ, Kelly JD, Miller A, Semper A, Bailey D, Groppelli E et al. ReEBOV Antigen Rapid Test kit for point-of-care and laboratory-based testing for Ebola virus disease: a field validation study. Lancet 2015; 386: 867–874.
206. Centers for Disease Control and Prevention. Interim Guidance for Rapid Antigen Testing for SARS-CoV-2. 2020.https://www.cdc.gov/coronavirus/2019-ncov/lab/resources/antigen-tests-guidelines.html#table2 (accessed 24 Nov2020).
207. Chen Y, Chan KH, Kang Y, Chen H, Luk HKH, Poon RWS et al. A sensitive and specific antigen detection assay for Middle East respiratory syndrome coronavirus. Emerg Microbes Infect 2015; 4: e26.
208. U.S. Food & Drug Administration. What Are 'Biologics' Questions and Answers. 2018.https://www.fda.gov/about-fda/center-biologics-evaluation-and-research-cber/what-are-biologics-questions-and-answers (accessed 28 Jan2021).
209. U.S. Food & Drug Administration. Licensed Biological Products with Supporting Documents. 2021.https://www.fda.gov/vaccines-blood-biologics/licensed-biological-products-supporting-documents (accessed 1 Mar2021).
210. Instituto IQVIA. Advancing Biosimilar Sustainability in Europe. 2018.https://www.iqvia.com/insights/the-iqvia-institute/reports/advancing-biosimilar-sustainability-in-europe (accessed 25 Apr2021).
211. Druedahl LC, Almarsdóttir AB, Kälvemark Sporrong S, De Bruin ML, Hoogland H, Minssen T et al. A qualitative study of biosimilar manufacturer and regulator perceptions on intellectual property and abbreviated approval pathways. Nat Biotechnol 2020; 38: 1253–1256.
212. Price WN, Rai AK. How logically impossible patents block biosimilars. Nat Biotechnol 2019; 37: 862–863.
213. Collins S. Biologic Patent Transparency Act (S. 659). In: 116th Congress (2019-2020). 2019https://www.congress.gov/bill/116th-congress/senate-bill/659/text (accessed 25 Apr2021).
214. U.S. Food and Drug Administration. Frequently Asked Questions About Therapeutic Biological Products. 2015.https://www.fda.gov/drugs/therapeutic-biologics-applications-bla/frequently-asked-questions-about-therapeutic-biological-products (accessed 25 Apr2021).
215. Steel J, Staeheli P, Mubareka S, García-sastre A, Palese P, Lowen AC. Transmission of pandemic H1N1 influenza virus and impact of prior exposure to seasonal strains or interferon treatment. J Virol 2010; 84: 21–26.
216. Samuel CE. Antiviral actions of interferons. Clin Microbiol Rev 2001; 14: 778–809.
217. Falzarano D, de Wit E, Rasmussen AL, Feldmann F, Okumura A, Scott DP et al. Treatment with interferon-α 2b and ribavirin improves outcome in MERS-CoV-infected rhesus macaques. Nat Med 2013; 19: 1313–1317.
218. Li BJ, Tang Q, Cheng D, Qin C, Xie FY, Wei Q et al. Using siRNA in prophylactic and therapeutic regimens against SARS coronavirus in Rhesus macaque. Nat Med 2005; 11: 944–951.
219. Gallicano GI, Casey JL, Fu J, Mahapatra S. Molecular targeting of vulnerable RNA sequences in SARS CoV-2: identifying clinical feasibility. Gene Ther 2020. doi:10.1038/s41434-020-00210-0.
220. Tang J, Zhang N, Tao X, Zhao G, Guo Y, Tseng C-TK et al. Optimization of antigen dose for a receptor-binding domain-based subunit vaccine against MERS coronavirus. Hum Vaccin Immunother 2015; 11: 1244–1250.
221. Keech C, Albert G, Cho I, Robertson A, Reed P, Neal S et al. Phase 1–2 trial of a SARS-CoV-2 recombinant spike protein nanoparticle vaccine. N Engl J Med 2020; 383: 2320–2332.
222. Fuenmayor J, Gòdia F, Cervera L. Production of virus-like particles for vaccines. N Biotechnol 2017; 39: 174–180.
223. Tebas P, Kraynyak KA, Patel A, Maslow JN, Morrow MP, Sylvester AJ et al. Intradermal SynCon® Ebola GP DNA vaccine is temperature stable and safely demonstrates cellular and humoral immunogenicity advantages in healthy volunteers. J Infect Dis 2019; 220: 400–410.
224. Martin JE, Louder MK, Holman LSA, Gordon IJ, Enama ME, Larkin BD et al. A SARS DNA vaccine induces neutralizing antibody and cellular immune responses in healthy adults in a Phase I clinical trial. Vaccine 2008; 26: 6338–6343.
225. Pardi N, Hogan MJ, Porter FW, Weissman D. mRNA vaccines — a new era in vaccinology. Nat Rev Drug Discov 2018; 17: 261–279.
226. Glaros AG, Kline RB. Understanding the accuracy of tests with cutting scores: The sensitivity, specificity, and predictive value model. J Clin Psychol 1988; 44: 1013–1023.
227. Shreffler J, Huecker MR. Diagnostic Testing Accuracy: Sensitivity, Specificity, Predictive Values and Likelihood Ratios. StatPearls. 2021.http://www.ncbi.nlm.nih.gov/pubmed/32491423 (accessed 25 Apr2021).
228. Pereira R, Oliveira J, Sousa M. Bioinformatics and computational tools for next-generation sequencing analysis in clinical genetics. J Clin Med 2020; 9: 132.
229. Pas SD, Patel P, Reusken C, Domingo C, Corman VM, Drosten C et al. First international external quality assessment of molecular diagnostics for Mers-CoV. J Clin Virol 2015; 69: 81–85.
230. Böger B, Fachi MM, Vilhena RO, Cobre AF, Tonin FS, Pontarolo R. Systematic review with meta-analysis of the accuracy of diagnostic tests for COVID-19. Am J Infect Control 2021; 49: 21–29.
231. Joyner MJ, Senefeld JW, Klassen SA, Mills JR, Johnson PW, Theel ES et al. Effect of convalescent plasma on mortality among hospitalized patients with COVID-19: Initial three-month experience. medRxiv 2020. doi:10.1101/2020.08.12.20169359.
232. Lin JT, Zhang JS, Su N, Xu JG, Wang N, Chen JT et al. Safety and immunogenicity from a Phase I trial of inactivated severe acute respiratory syndrome coronavirus vaccine. Antivir Ther 2007; 12: 1107–1113.
233. Li Y Der, Chi WY, Su JH, Ferrall L, Hung CF, Wu TC. Coronavirus vaccine development: from SARS and MERS to COVID-19. J. Biomed. Sci. 2020; 27. doi:10.1186/s12929-020-00695-2.
234. Dolzhikova I V., Zubkova O V., Tukhvatulin AI, Dzharullaeva AS, Tukhvatulina NM, Shcheblyakov D V. et al. Safety and immunogenicity of GamEvac-Combi, a heterologous VSV- and Ad5-vectored Ebola vaccine: An open phase I/II trial in healthy adults in Russia. Hum Vaccines Immunother 2017; 13: 613–620.
235. Zhu FC, Wurie AH, Hou LH, Liang Q, Li YH, Russell JBW et al. Safety and immunogenicity of a recombinant adenovirus type-5 vector-based Ebola vaccine in healthy adults in Sierra Leone: a single-centre, randomised, double-blind, placebo-controlled, phase 2 trial. Lancet 2017; 389: 621–628.
236. Tapia MD, Sow SO, Mbaye KD, Thiongane A, Ndiaye BP, Ndour CT et al. Safety, reactogenicity, and immunogenicity of a chimpanzee adenovirus vectored Ebola vaccine in children in Africa: a randomised, observer-blind, placebo-controlled, phase 2 trial. Lancet Infect Dis 2020; 20: 719–730.
237. Tapia MD, Sow SO, Ndiaye BP, Mbaye KD, Thiongane A, Ndour CT et al. Safety, reactogenicity, and immunogenicity of a chimpanzee adenovirus vectored Ebola vaccine in adults in Africa: a randomised, observer-blind, placebo-controlled, phase 2 trial. Lancet Infect Dis 2020; 20: 707–718.
238. Mallapaty S. China COVID vaccine reports mixed results — what does that mean for the pandemic? Nature 2021. doi:10.1038/d41586-021-00094-z.
239. Xia S, Duan K, Zhang Y, Zhao D, Zhang H, Xie Z et al. Effect of an inactivated vaccine against SARS-CoV-2 on safety and immunogenicity outcomes: interim analysis of 2 randomized clinical trials. JAMA 2020; 324: 951–960.

240. Xia S, Zhang Y, Wang Y, Wang H, Yang Y, Gao GF et al. Safety and immunogenicity of an inactivated SARS-CoV-2 vaccine, BBIBP-CorV: a randomised, double-blind, placebo-controlled, phase 1/2 trial. Lancet Infect Dis 2021; 21: 39–51.
241. Ella R, Vadrevu KM, Jogdand H, Prasad S, Reddy S, Sarangi V et al. Safety and immunogenicity of an inactivated SARS-CoV-2 vaccine, BBV152: a double-blind, randomised, phase 1 trial. Lancet Infect Dis 2021. doi:10.1016/s1473-3099(20)30942-7.
242. Pu J, Yu Q, Yin Z, Zhang Y, Li X, Li D et al. An in-depth investigation of the safety and immunogenicity of an inactivated SARS-CoV-2 vaccine. medRxiv 2020. doi:10.1101/2020.09.27.20189548.
243. Logunov DY, Dolzhikova I V, Shcheblyakov D V, Tukhvatulin AI, Zubkova O V, Dzharullaeva AS et al. Safety and efficacy of an rAd26 and rAd5 vector-based heterologous prime-boost COVID-19 vaccine: an interim analysis of a randomised controlled phase 3 trial in Russia. Lancet 2021. doi:10.1016/s0140-6736(21)00234-8.
244. Zhu FC, Guan XH, Li YH, Huang JY, Jiang T, Hou LH et al. Immunogenicity and safety of a recombinant adenovirus type-5-vectored COVID-19 vaccine in healthy adults aged 18 years or older: a randomised, double-blind, placebo-controlled, phase 2 trial. Lancet 2020; 396: 479–488.
245. Novavax. Novavax COVID-19 vaccine demonstrates 89.3% efficacy in UK phase 3 trial . 2021.https://ir.novavax.com/news-releases/news-release-details/novavax-covid-19-vaccine-demonstrates-893-efficacy-uk-phase-3 (accessed 15 Feb2021).
246. Kremsner P, Mann P, Bosch J, Fendel R, Gabor JJ, Kreidenweiss A et al. Phase 1 assessment of the safety and immunogenicity of an mRNA- lipid nanoparticle vaccine candidate against SARS-CoV-2 in human volunteers. medRxiv 2020. doi:10.1101/2020.11.09.20228551.

Received: 10 Marzo 2021
Accepted: 20 Julio 2021

REVIEW / ARTÍCULO DE REVISIÓN

Relationship of SARS-CoV-2 and chronic diseases of nutritional origin

Johanna Pilay Bajaña[1], Evelyn Ramírez Carguacundo[1], María José Vizcaino Tumbaco[2], Daniel Silva-Ochoa[1,2], Davide Di Grumo[3], Luis Dorado-Sanchez[4], Silvia Orellana-Manzano[3], Patricia Manzano[1,5], Andrea Orellana-Manzano[1,2,3*]

DOI. 10.21931/RB/2021.06.03.34

Abstract: The worldwide spread of the virus has claimed multiple lives, especially in vulnerable groups. Therefore, an investigation was carried out to present a viable solution for health personnel using the "JES" algorithm. The present study used the research to determine the possible complications presented by the sick individual, providing a viable and accessible healthcare personnel solution through the proposed "JES" algorithm. A non-experimental, descriptive, correlational, and explanatory research is presented. According to pathologies of interest, the articles were taken virtually from scientific journals present in Google Scholar and PubMed. The excluded publications were: articles that do not detail the established protocol for detecting SARS-CoV-2, studies that do not present a significant number of people with Covid-19 disease, articles that the person has the covid-19 disease but no underlying diseases of nutritional origin. It focused on the vulnerable or higher risk population group, including scientific information from children (over five years old), adults (over 18 years old), and older adults (over 65 years old) found in countries of the Asian and American continents. The R program analyzed the scientific articles using the ggplot2 package with a pie and bar diagram. A higher prevalence in men than women (56% vs. 44%) stood out. Likewise, arterial hypertension was presented in the first place with 40.82%, followed by diabetes with 30.61%, obesity with 12.24%, overweight and dyslipidemia with 6.12%, malnutrition with 4.08%. There was a higher prevalence of stable individuals (29%) within the health facility than those admitted to the ICU (20%). Adults with 69.39%, followed by older adults with 16.33%, and mixed ages with 14.29%. Comorbidities stand out as risk factors in people infected with SARS-CoV-2, regardless of age. A more significant contagion was observed in the male versus female population; since men do not develop a rapid immune response and have a high content of cytokines that at the time of infection are released more quickly and can cause more significant damage

Key words: Chronic diseases, vulnerable population, SARS-CoV-2, nutrition.

Introduction

The World Health Organization defines chronic diseases as long-term chronic diseases and progressively slower[1]. Among them are heart diseases, high blood pressure (40.82%), diabetes mellitus 2 (30.61%), severe obesity (BMI> 40) (12.24%), and dyslipidaemias(6.12%)[2].

The virus is known as SARS-CoV-2[3], whose disease is caused by COVID-19[4]. It is considered a new type of infectious and highly contagious coronavirus in a latency state[5]. Its mechanism of action consists of the host organism's infection through the ACE2 receptor[6], distributed to various organs and tissues such as lungs, heart, kidneys, intestine, and endothelial cells[7]. Clinical practice has determined that a population is considered vulnerable or at higher risk of contagion[8], such as the elderly and people at any stage of life with chronic diseases[9,10]. Those people who have at least one of these chronic conditions mentioned above and are not under medical supervision should pay more attention and health care against SARS-CoV-2[8]. The Pan American Health Organization emphasizes more outstanding care in vulnerable groups since 1 in 4 people show a greater risk of obtaining unfavorable results due to underlying diseases[11]. Therefore, a search for information was carried out to relate the diseases of nutritional origin mentioned above with those who present the SARS-CoV-2 condition allowing us to know the relationship between them and the severity of complications[12].

Methods

Exhaustive bibliographic research was carried out, compiling 40 articles at the international level, adding nine more publications found within the previously selected articles, excluding those not indexed, for subsequent analysis focused on health professionals. These articles, "original articles," were carried out in China, the United States, Italy, Mexico, France, and at a multicenter level from January 2020 to July 2020. It is considered non-experimental, descriptive, and explanatory research by searching bibliographic materials published from 2018 to 2020, taken virtually through search engines such as PubMed[A9] [A10] and Google Scholar. Pathologies of nutritional origin of interest categorized these scientific articles, as shown in figures 1 and 2. The excluded publications were selected as follows: articles that do not detail an established protocol for detecting SARS-CoV-2. These studies do not present a significant number of people with Covid-19 disease (less than 50 people), articles that the person has the covid-19 disease but not underlying diseases of nutritional origin. The information found with limited access, prepaid, and documents in development stands out regarding the restrictions. The keywords used for this search are SARS-CoV-2, Coronavirus, arterial hypertension, type 2 diabetes, dyslipidemia, and malnutrition, the latter being divided into malnutrition, overweight, and obesity. It was compiled through scientific studies carried out in China (26), United States (10), Italy (8), France (3), and

[1] ESPOL Polytechnic University, Facultad de Ciencias de la Vida (FCV), Campus Gustavo Galindo, Km. 30.5 vía Perimetral, Guayaquil, Ecuador.
[2] ESPOL Polytechnic University, Laboratory for Biomedical Research, Facultad de Ciencias de la Vida (FCV), Guayaquil, Ecuador.
[3] Escuela de Odontología, Universidad Espíritu Santo, Ecuador
[4] Hospital General Monte Sinatí, Guayaquil, Ecuador.
[5] ESPOL Polytechnic University, Centro de Investigaciones Biotecnológicas del Ecuador (CIBE), Guayaquil, Ecuador.

Corresponding author: akorella@espol.edu.ec

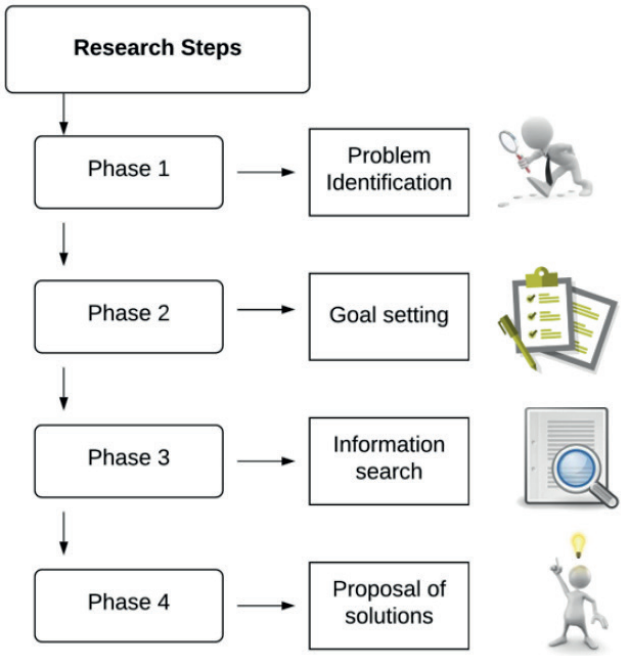

Figure 1. Productos biológicos usados en el control de pandemias (Creado en BioRender).

Mexico (1). The choice of these countries was made according to the number of relevant articles found up to the moment of the analysis, which provided outstanding information on the relationship between SARS-CoV-2 and the pathologies of interest, a protocol established for obtaining results, as well as variables of interest, highlighting the different age groups, sex, country of study, detection method of the SARS-CoV-2, sample size, nutritional parameters, and the results obtained in said scientific studies.

The algorithm was carried out using the web-based diagramming tool called Lucidchart in its entirety due to the ease of implementation it presents and the different options it offers the user. It was based on the ten practical recommendations published by the European Society for Clinical Nutrition and Metabolism (ESPEN) in 2020, which presents an indicated guide for the nutritional management of patients with COVID-19. It contains relevant information about adequate nutritional management to treat patients with chronic diseases and SARS-CoV-2 simultaneously, highlighting the use of screening. Likewise, it indicates essential nutritional parameters to consider in the sick patient, such as BMI, ascites, folds, and brachial circumference.

For those patients with unfavorable results and a higher probability of mortality after contracting the SARS-COV-2 infection (older adults and people with multiple comorbidities), it is recommended to control the presence of malnutrition through screening tests for later timely evaluation using the NRS criteria. 2002 was established for hospitalized patients.

Likewise, it is recommended to maintain a good nutritional status for the prevention or treatment of malnutrition since it reduces complications and subsequent negative results in patients with nutritional risk due to the presence of nausea, vomiting, and diarrhea (typical of SARS-CoV-2), affecting the average intake and absorption of food in the body.

Optimal maintenance of nutritional status is prioritized through dietary advice from experienced professionals (Registered Dietitians, Experienced Nutrition Scientists, Clinical Nutritionists, and Specialty Physicians).

A daily intake of 27 kcal per kg of body weight is suggested in patients with multiple comorbidities over 65 years and 30 kcal per kg of body weight/day in patients with a much lower average weight and multiple comorbidities. However, these values are indicative and must be adjusted according to the energy intake in older people, nutritional status, physical activity, disease status, and food tolerance.

In patients with severe underweight, the goal of 30 kcal/kg of body weight should be gradually due to the refeeding syndrome.

It is estimated using already established formulas (1 g of protein per kg of body weight in older people) regarding protein needs. However, it must be adjusted according to nutritional status, physical activity, disease status, and food tolerance. The fat and carbohydrate needs are adapted according to the patient's energy needs in a ratio of 30:70 (people without respiratory deficiency) and 50:50 (ventilated patients).

The use of oral nutritional supplements is recommended to achieve optimal nutritional goals through individualized dietary advice with at least 400 kcal/day, including 30 g or more

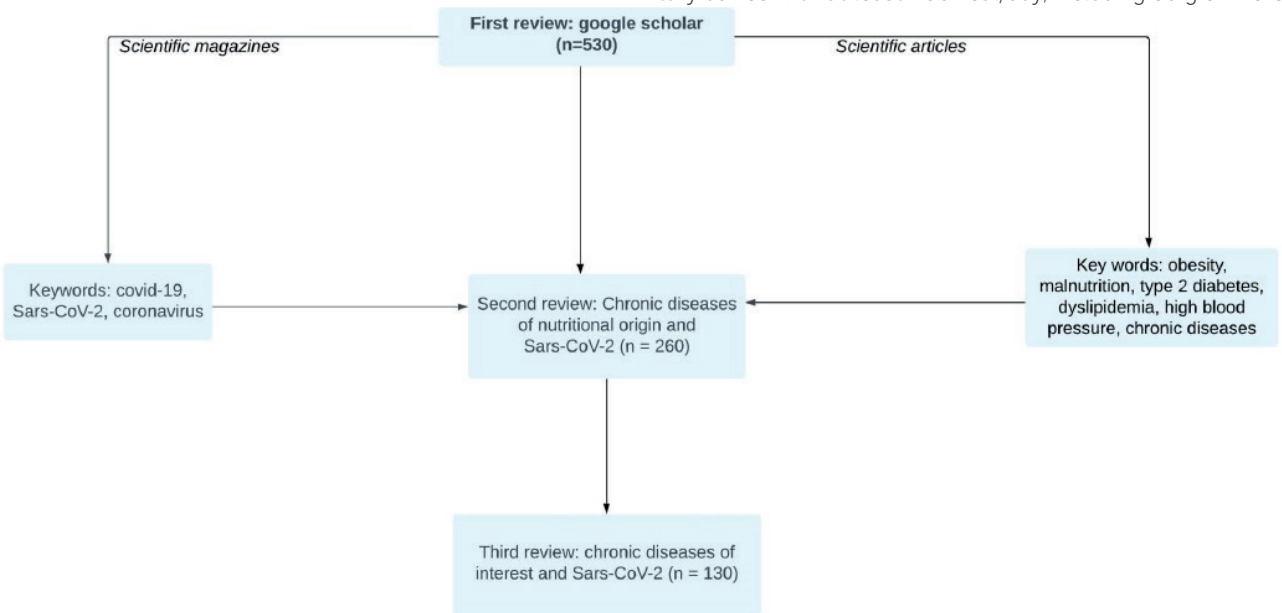

Figure 2. General steps for obtaining information from this document.

protein per day and its continuation for at least one month.

Patients with type II diabetes mellitus, arterial hypertension, and malnutrition should be treated according to nutritional guidelines already established for each pathology, taking into account glucose levels, blood pressure, and caloric intake, respectively.

Results

Chronic diseases of nutritional origin such as diabetes mellitus, hypertension, dyslipidemia, undernourishment, and obesity were observed in patients with SARS-CoV-2. These comorbidities help a better accommodation and progression of this virus in organs such as lungs, intestine, heart, and even brain conditions. Therefore, a general distribution was made with all previously selected articles, obtaining the following percentages (Figure 3): arterial hypertension (40.82%), diabetes mellitus (30.61%), obesity (12.24%), overweight (6.12%), dyslipidemia (6.12%) and undernourishment (4.08%), considering the risk factors in this vulnerable population, as we can see in table 1.

Additionally, information was obtained according to the country of origin (Figure 4), obtaining the following results ordered from highest to lowest respectively: China 26 articles (53.06%), followed by the United States with 10 (20.41%), Italy with 8 (16.33%), France with 3 (6.12%) and articles on par between Mexico and multicenter level with 1 (2.04%) respectively. Likewise, the presence of a higher prevalence in men with SARS-CoV-2 compared to the women analyzed (56% vs. 44%) stands out. The presence of deceased people was not given in all the scientific articles reviewed. However, it can range from two to more than five thousand people (up to 23%). It should be noted that the variable number of deceased persons was later discarded from this analysis due to the little information presented following all the documents chosen.

According to Table II, presented in the supplementary material section, a higher prevalence of individuals who remained stable within the health facility was observed than those admitted to the ICU (29 vs. 20). In the age ranges, the presence of adults stood out, obtaining a total of 34 articles (69.39%), followed by older adults with 8 (16.33%) and finally mixed ages with 7 (14.29%). For its part, the average age was a minimum of 21 years and a maximum of 79 years.

The algorithm presented in Figure 5 is composed of nutritional parameters and nutritional monitoring for the pathology of interest according to the presence of SARS-CoV-2 in the individual. Likewise, it presents a general approach by the nutritionist through the Score according to NRS2002, dividing it into a score less than three and a score greater than 3, highlighting the intake of proteins and carbohydrates in the first case and a rapid nutritional intervention through supplementation for the second. In general, specific monitoring is suggested every 48 to 72 hours maximum, adjusting your energy requirements if necessary.

Discussion

This article was developed with Open Access research that had no economic cost at the time of its preparation since all the information was obtained free of charge through high-impact scientific journals.

However, in public health, the generation of additional costs due to the stay in the ICU of public hospitals is estimated, with values ranging between $ 1,000 to $ 3,000 per day, depending on the complications that the patient's health status presents[13]. While in hospitals and private clinics, the prices vary between $ 1,000 to $ 5,000 per day, depending on the establishment, health status, and the care required for their improvement during the first wave in Ecuador[14]. For this reason, the consolidated information present in this document is

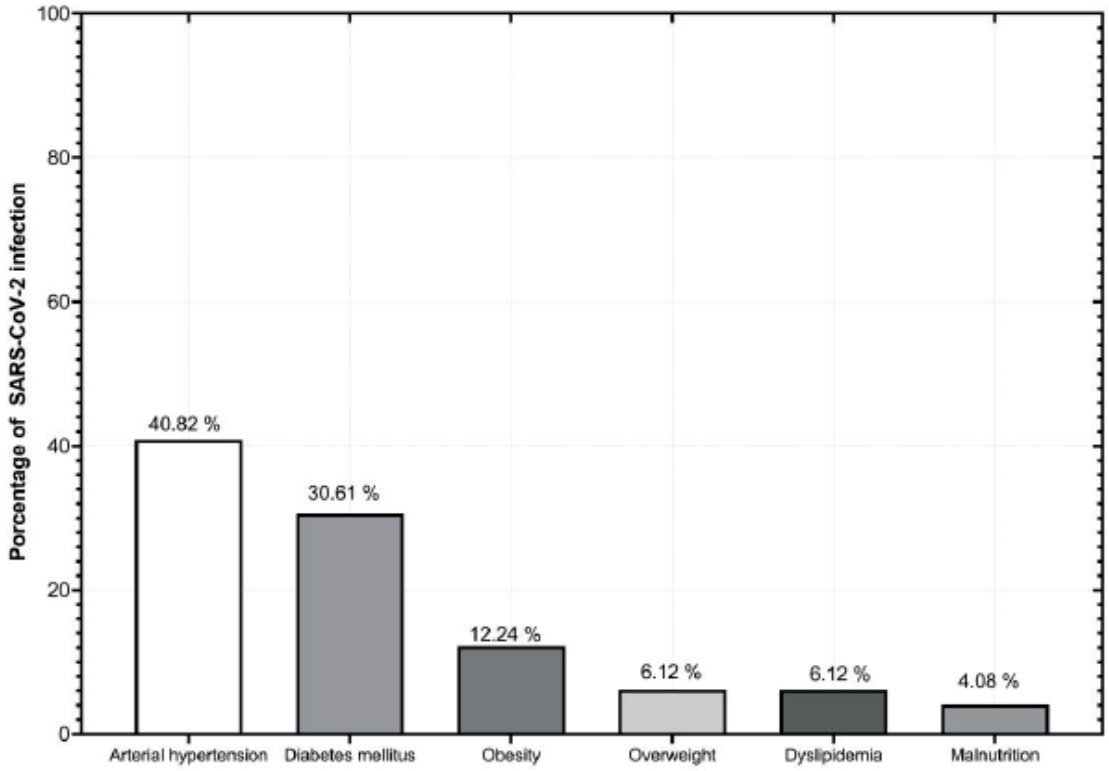

Figure 3. Chronic diseases identified in patients infected by SARS-CoV-2.

N (Study population)	Male (%)	Female (%)	Average age in yo	ICU	Pathology	Dead (%)	Country	Patients Infected with SARS-CoV-2	Infection according the country (June 2020)	References
5700	3437 (60)	2263 (40)	63	Yes	Diabetes mellitus	553 (21)	United States	5700	2'423.490	[20]
52	35 (67)	17 (33)	59	Yes	Diabetes mellitus	32 (62)	China	52	83.483	[21]
140	71 (51)	69 (49)	57	No	Dyslipidaemia	N/D	China	140	83.483	[22]
191	119 (62)	72 (38)	56	No	Arterial hypertension	54 (29)	China	191	83.483	[23]
7337	136 (48)	146 (52)	62	No	Arterial hypertension	N/D	China	7337	83.483	[23]
33	30 (91)	3 (9)	64	Yes	Diabetes mellitus	1 (3)	Italy	33	239.961	[18]
3802	1612 (41)	2190 (58)	58	No	Overweight	N/D	France	3802	162.936	[24]
2209	N/D	N/D	N/D	No	Diabetes mellitus	N/D	China	2209	83.483	[25]
3403	N/D	N/D	N/D	No	Arterial hypertension	N/D	China	3403	83.483	[26]
50	27 (54)	23 (46)	52	Yes	Arterial hypertension	2 (7)	China	50	83.483	[27]
180	N/D	N/D	50	No	Overweight	N/D	United States	180	2'423.490	[28]
609	410 (68)	199 (32)	68	No	Diabetes mellitus	179 (29)	Italy	609	239.961	[29]
108	43	65	52	No	Diabetes mellitus	12	China	108	83.483	[30]
1576	890	686	49	No	Arterial hypertension	N/D	China	1576	83.483	[31]
291	N/D	N/D	N/D	Yes	Overweight	N/D	France	291	162.936	[32]
50	27	23	21	No	Obesity	N/D	United States	50	2'423.490	[33]
1527	883	644	N/D	No	Diabetes mellitus	N/D	China	1527	83.483	[34]
463	204	259	57.5	Yes	Overweight	93	United States	463	2'423.490	[35]
201	128	73	51	No	Arterial hypertension	N/D	China	201	83.483	[36]
142	38	104	N/D	No	Obesity	N/D	United States	142	2'423.490	[37]
214	N/D	N/D	N/D	No	Dislipidemia	N/D	China	214	83.483	[38]
597	295	302	67	No	Diabetes mellitus	N/D	China	597	83.483	[39]
1591	1304	287	63	Yes	Arterial hypertension	405	Italy	1591	239.961	[40]
123	45	78	76.6	Yes	Undernourishment	10	Italy	123	239.961	[41]
124	90	34	60	Yes	Obesity	18	France	124	162.936	[42]
177133	29803	21830	46.65	Yes	Arterial hypertension	5332	México	177133	208.392	[43]
100	62	48	70	No	Arterial hypertension	N/D	Italy	100	239.961	[44]
81	42	39	49	No	Arterial hypertension	N/D	China	81	83.483	[45]
1482	806	676	50	No	Diabetes mellitus	N/D	United States	1482	2'423.490	[46]
112	53	59	62	Yes	Arterial hypertension	17	China	112	83.483	[47]
3615	N/D	N/D	60	Yes	Obesity	N/D	United States	3615	2'423.490	[47]
182	65	117	68.5	No	Undernourishment	N/D	China	182	83.483	[48]
41	30	11	49	Yes	Diabetes mellitus	6	China	41	83.483	[49]
191	131	60	63	Yes	Arterial hypertension	42	Italy	191	239.961	[50]
179	97	82	65	No	Arterial hypertension	21	China	179	83.483	[51]
416	205	211	64	Yes	Arterial hypertension	N/D	China	416	83.483	[51]
355	249	106	79.5	No	Diabetes mellitus	355	Italy	355	239.961	[52]
103	63	40	60	Yes	Obesity	N/D	United States	103	2'423.490	[53]

Table 1. Classification of articles according to variables of interest.

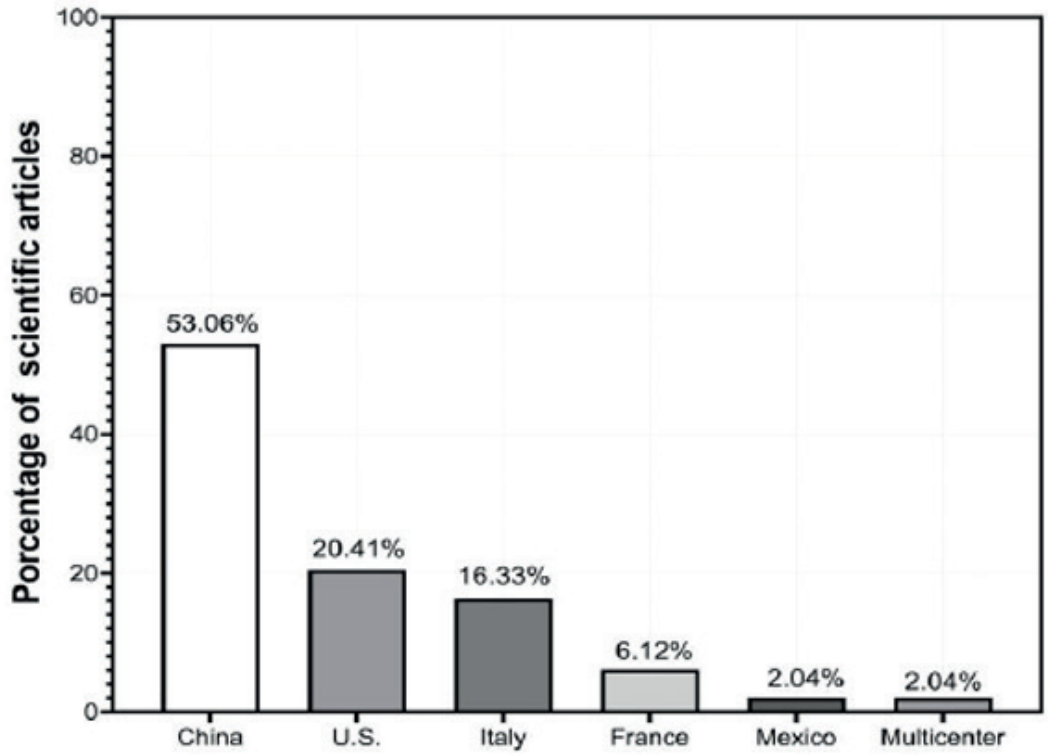

Figure 4. Scientific articles by country of origin.

Analysis	Sex				Deaths		Middle Ages	NUMBER OF VIRUS INFECTIONS
	Male (N)	%	Female (N)	%	Results (N)	%		
Minimum	27	26.76	3	9	1	0.80	21	33
Maximum	29803	91.00	21830	73.24	5332	100	79.50	177.13
Median	131	56.50	104	45.60	42	17.59	58	274
Mean	1364	56.90	1081	44.15	330	23.02	57.78	5053

Table 2. Deaths according to sex and age.

essential, since it is expected to reduce costs in these areas, as well as a greater understanding about the pathologies of nutritional origin present in cases with the SARS-Cov-2 virus, preventing conditions critical health measures in the sick individual and turn, generating an economically viable solution for society.

Table I highlights the strengths and weaknesses found in the previous systematic review obtained from reliable scientific articles such as gender, current information from countries that reported more extensive clinical trials on confirmed coronavirus cases, pathology, number of infected, among others.

Among the weaknesses is the small variety of countries analyzed due to clinical trials not found until the end of this document's research period and a null contribution by the selected documents about the treatment given to each patient diagnosed with comorbidities SARS-CoV-2.

The indications and guidelines for future research lie in expanding the sample size of scientific articles analyzed, the addition of other comorbidities of nutritional origin as the object of study, and a more generous selection of documents that present the number of people who died SARS-CoV-2 and comorbidities. The percentage of countries analyzed was obtained using the R program version 1.3.1056 using the ggplot2 package with a sector and bar diagram, highlighting China, followed by the United States and Italy. Regarding the age range, the presence of adults (69.39%) and older adults (16.33%) stood out, which were obtained through the previously described program.

According to reviews and subsequent updates in the high-impact literature, it is known that suffering from chronic non-communicable diseases and COVID-19 disease is still high risk, as the CDC mentions the number of times of risk that the person has when suffering one or more NCDs varying between 3 and 5 times the risk of severity[15].

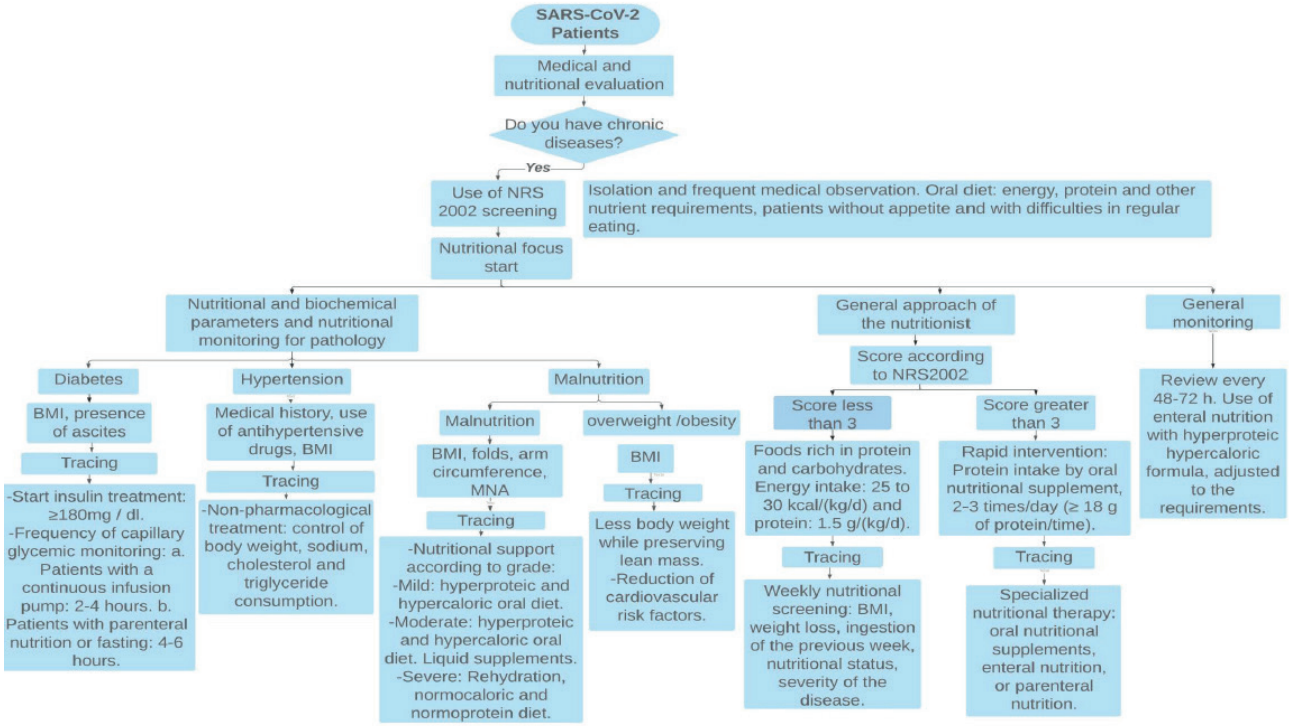

Figure 5. Nutritional Algorithm.

Conclusions

Comorbidities are considered risk factors in sick individuals with SARS-CoV-2, highlighting hypertension with 40.82%, diabetes with 30.61%, and obesity with 12.24% concerning the total articles analyzed. SARS-CoV-2 affects any age group, highlighting the presence of adults with 69.39%, followed by older adults with 16.33%, according to studies carried out in health centers internationally. Men's presence was 56% compared to women with 44%, denoting more significant contagion in the male population. The individuals found in the ICU department were 40.82% compared to 59.19% who did not require it due to the timely intervention. Comorbidities can be significantly aggravated if not controlled and under timely medical supervision. Among the weaknesses, incorporating nutritional treatments for each comorbidity and/or specific pathology and the majority incorporation of individuals in the childhood stage stands out for a more significant expansion of the study field. It is recommended to carry out nutritional treatments with other pathologies and with more significant expansion in age ranges, as well as the incorporation of information that it deems appropriate for a better analysis of the situation.

Acknowledgments

The authors wish to acknowledge the support of ESPOL, FCV-60-2020, for letting the study be part of the COVID-19 research.

Bibliographic references

1. Organizacion Mundial de la Salud O. OMS | Enfermedades crónicas. World Health Organization; 2017.
2. OPS. Las ENT de un vistazo: Mortalidad por enfermedades no transmisibles y prevalencia de sus factores de riesgo en la Región de las Américas. Organización Panamericana de la salud, Washington, D.C. OPS; 2019 Dec.
3. Remuzzi A, Remuzzi G. COVID-19 and Italy: what next? Vol. 395, The Lancet. Lancet Publishing Group; 2020. p. 1225–8.
4. Schwartz DA. An Analysis of 38 Pregnant Women with COVID-19, Their Newborn Infants, and Maternal-Fetal Transmission of SARS-CoV-2: Maternal Coronavirus Infections and Pregnancy Outcomes. Arch Pathol Lab Med. 2020 Mar;
5. Fifield K. Cómo la enfermedad COVID-19 afecta los órganos del cuerpo. 2020.
6. South AM, Diz DI, Chappell MC. COVID-19, ACE2, and the cardiovascular consequences. Am J Physiol Circ Physiol. 2020 May;318(5):H1084–90.
7. Varga Z, Flammer AJ, Steiger P, Haberecker M, Andermatt R, Zinkernagel AS, et al. Endothelial cell infection and endotheliitis in COVID-19. Vol. 395, The Lancet. Lancet Publishing Group; 2020. p. 1417–8.
8. Acosta G, Escobar G, Bernaola G, Alfaro J, Taype W, Marcos C, et al. Original Breve Caracterización De Pacientes Con Covid-19 Grave Atendidos En Un Hospital Treated in a National Referral Hospital in Peru. Rev Peru Med Exp Salud Publica. 2020;2019(2):253–8.
9. Enviroment D of H and. Enfermedades crónicas y COVID-19: lo que necesita saber. 2020.
10. Gandhi RT, Lynch JB, del Rio C. Mild or Moderate Covid-19. N Engl J Med. 2020 Apr.
11. OPS/OMS. Directora de la OPS dice que la lucha contra la pandemia COVID-19 debe incluir atención de enfermedades crónicas - OPS/OMS | Organización Panamericana de la Salud. Organización Panamericana de la la Salud. 2020.
12. Thais M, -Urizarri P, Raúl, Aguilera-Rodríguez, Luis E, Mederos A-. hipertensión, diabetes y enfermedad renal crónica como factores de riesgo para covid-19 grave. I Congreso Virtual de Ciencias Básicas Biomédicas de Granma. 2020.
13. Rodriguez A. El Telégrafo - Noticias del Ecuador y del mundo - Un día en cuidados intensivos cuesta más de $ 1.500. El Telégrafo. 2020.
14. Heredia V, Rosero M. IESS no está derivando a pacientes con covid-19 a clínicas privadas. 2020.
15. Morejón A. Enfermedades Crónicas No Transmisibles Y Covid-19: La Convergencia De Dos Crisis Globales. Scielo. 2020;
16. Wang D, Hu B, Hu C, Zhu F, Liu X, Zhang J, et al. Clinical Characteristics of 138 Hospitalized Patients with 2019 Novel Coronavirus-Infected Pneumonia in Wuhan, China. JAMA - J Am Med Assoc. 2020 Mar;323(11):1061–9.

17. Cappuccio FP, Siani A. Covid-19 and cardiovascular risk: Susceptibility to infection to SARS-CoV-2, severity and prognosis of Covid-19 and blockade of the renin-angiotensin-aldosterone system. An evidence-based viewpoint. Nutr Metab Cardiovasc Dis. 2020;30:1227–35.
18. Piva S, Filippini M, Turla F, Cattaneo S, Margola A, De Fulviis S, et al. Clinical presentation and initial management critically ill patients with severe acute respiratory syndrome coronavirus 2 (SARS-CoV-2) infection in Brescia, Italy. J Crit Care. 2020;58:29–33.
19. Li J, Wang X, Chen J, Zhang H, Deng A. Association of Renin-Angiotensin System Inhibitors with Severity or Risk of Death in Patients with Hypertension Hospitalized for Coronavirus Disease 2019 (COVID-19) Infection in Wuhan, China. JAMA Cardiol. 2020;
20. Mehra MR, Desai SS, Kuy S, Henry TD, Patel AN. Cardiovascular Disease, Drug Therapy, and Mortality in Covid-19. N Engl J Med. 2020 Jun;382(25):e102.
21. Yang X, Yu Y, Xu J, Shu H, Xia J, Liu H, et al. Clinical course and outcomes of critically ill patients with SARS-CoV-2 pneumonia in Wuhan, China: a single-centered, retrospective, observational study. Lancet Respir Med. 2020 May;8(5):475–81.
22. Zhang J, Dong X, Cao Y, Yuan Y, Yang Y, Yan Y, et al. Clinical characteristics of 140 patients infected with SARSα CoVα 2 in Wuhan, China. Allergy. 2020 Jul;75(7):1730–41.
23. Zhou F, Yu T, Du R, Fan G, Liu Y, Liu Z, et al. Clinical course and risk factors for mortality of adult inpatients with COVID-19 in Wuhan, China: a retrospective cohort study. Lancet. 2020 Mar;395(10229):1054–62.
24. de Lusignan S, Dorward J, Correa A, Jones N, Akinyemi O, Amirthalingam G, et al. Risk factors for SARS-CoV-2 among patients in the Oxford Royal College of General Practitioners Research and Surveillance Centre primary care network: a cross-sectional study. Lancet Infect Dis. 2020 Sep;20(9):1034–42.
25. Singh AK, Gupta R, Misra A. Comorbidities in COVID-19: Outcomes in hypertensive cohort and controversies with renin angiotensin system blockers. Diabetes Metab Syndr Clin Res Rev. 2020 Jul;14(4):283–7.
26. Bajgain KT, Badal S, Bajgain BB, Santana MJ. Prevalence of comorbidities among individuals with COVID-19: A rapid review of current literature. American Journal of Infection Control. Mosby Inc.; 2020.
27. Zachariah P, Johnson CL, Halabi KC, Ahn D, Sen AI, Fischer A, et al. Epidemiology, Clinical Features, and Disease Severity in Patients with Coronavirus Disease 2019 (COVID-19) in a Children's Hospital in New York City, New York. JAMA Pediatr. 2020 Oct;174(10):202430.
28. Garg S, Kim L, Whitaker M, O'Halloran A, Cummings C, Holstein R, et al. Hospitalization rates and characteristics of patients hospitalized with laboratory-confirmed coronavirus disease 2019 — Covid-net, 14 states, March 1–30, 2020. Vol. 69, Morbidity and Mortality Weekly Report. Department of Health and Human Services; 2020. p. 458–64.
29. Tedeschi S, Giannella M, Bartoletti M, Trapani F, Tadolini M, Borghi C, et al. Clinical Impact of Renin-angiotensin System Inhibitors on In-hospital Mortality of Patients With Hypertension Hospitalized for Coronavirus Disease 2019. Clin Infect Dis. 2020 Jul;71(15):899–901.
30. Yao Q, Wang P, Wang X, Qie G, Meng M, Tong X, et al. A retrospective study of risk factors for severe acute respiratory syndrome coronavirus 2 infections in hospitalized adult patients. Polish Arch Intern Med. 2020 May;130(5):390–9.
31. Yang J, Zheng Y, Gou X, Pu K, Chen Z, Guo Q, et al. prevalence of comorbidities and its effects in coronavirus disease 2019 patients: A systematic review and meta-analysis. Int J Infect Dis. 2020 May;94:91–5.
32. Petrova D, Salamanca-Fernández E, Barranco MR, Pérez PN, Juan Jiménez Moleón J, Sánchez M-J. La obesidad como factor de riesgo en personas con COVID-19: Posibles mecanismos e implicaciones. Atención Primaria. 2020 May;
33. Huang Z, Cao J, Yao Y, Jin X, Luo Z, Xue Y, et al. The effect of RAS blockers on the clinical characteristics of COVID-19 patients with hypertension. Ann Transl Med. 2020 Apr;8(7):430–430.
34. Li B, Yang J, Zhao F, Zhi L, Wang X, Liu L, et al. prevalence and impact of cardiovascular metabolic diseases on COVID-19 in China. Vol. 109, Clinical Research in Cardiology. Springer; 2020. p. 531–8.
35. Suleyman G, Fadel RA, Malette KM, Hammond C, Abdulla H, Entz A, et al. Clinical Characteristics and Morbidity Associated With Coronavirus Disease 2019 in a Series of Patients in Metropolitan Detroit. Vol. 3, JAMA network open. NLM (Medline); 2020. p. e2012270.
36. Wu C, Chen X, Cai Y, Xia J, Zhou X, Xu S, et al. Risk Factors Associated With Acute Respiratory Distress Syndrome and Death in Patients With Coronavirus Disease 2019 Pneumonia in Wuhan, China. JAMA Intern Med. 2020 Jul;180(7):934.
37. Roxby AC, Greninger AL, Hatfield KM, Lynch JB, Dellit TH, James A, et al. Outbreak investigation of COVID-19 among residents and staff of an independent and assisted living community for older adults in Seattle, Washington. JAMA Intern Med. 2020 Aug;180(8):1101–5.
38. Zheng KI, Gao F, Wang XB, Sun QF, Pan KH, Wang TY, et al. Letter to the Editor: Obesity as a risk factor for greater severity of COVID-19 in patients with metabolic associated fatty liver disease. Metabolism. 2020 Jul;108:154244.
39. Wei X, Zeng W, Su J, Wan H, Yu X, Cao X, et al. Hypolipidemia is associated with the severity of COVID-19. J Clin Lipidol. 2020 May;14(3):297–304.
40. Grasselli G, Zangrillo A, Zanella A, Antonelli M, Cabrini L, Castelli A, et al. Baseline Characteristics and Outcomes of 1591 Patients Infected with SARS-CoV-2 Admitted to ICUs of the Lombardy Region, Italy. JAMA - J Am Med Assoc. 2020 Apr;323(16):1574–81.
41. Doglietto F, Vezzoli M, Gheza F, Lussardi GL, Domenicucci M, Vecchiarelli L, et al. Factors Associated with Surgical Mortality and Complications among Patients with and without Coronavirus Disease 2019 (COVID-19) in Italy. JAMA Surg. 2020 Aug;155(8):691–702.
42. Simonnet A, Chetboun M, Poissy J, Raverdy V, Noulette J, Duhamel A, et al. High Prevalence of Obesity in Severe Acute Respiratory Syndrome Coronavirusα 2 (SARSα CoVα 2) Requiring Invasive Mechanical Ventilation. Obesity. 2020 Jul;28(7):1195–9.
43. Bello-Chavolla OY, Bahena-López JP, Antonio-Villa NE, Vargas-Vázquez A, González-Díaz A, Márquez-Salinas A, et al. Predicting Mortality Due to SARS-CoV-2: A Mechanistic Score Relating Obesity and Diabetes to COVID-19 Outcomes in Mexico. J Clin Endocrinol Metab. 2020 Aug;105(8):2752–61.
44. Moriconi D, Masi S, Rebelos E, Virdis A, Manca ML, De Marco S, et al. obesity prolongs the hospital stay in patients affected by COVID-19, and may impact on SARS-COV-2 shedding. Obes Res Clin Pract. 2020 May;14(3):205–9.
45. Engin AB, Engin ED, Engin A. Two important controversial risk factors in SARS-CoV-2 infection: Obesity and smoking. Vol. 78, Environmental Toxicology and Pharmacology. Elsevier B.V.; 2020. p. 103411.
46. Finer N, Garnett SP, Bruun JM. COVIDα 19 and obesity. Clin Obes. 2020 Jun;10(3):e12365.
47. Watanabe M, Risi R, Tuccinardi D, Baquero CJ, Manfrini S, Gnessi L. Obesity and SARS-CoV-2: a population to safeguard. Diabetes/Metabolism Research and Reviews. John Wiley and Sons Ltd; 2020.
48. Li T, Zhang Y, Gong C, Wang J, Liu B, Shi L, et al. prevalence of malnutrition and analysis of related factors in elderly patients with COVID-19 in Wuhan, China. Eur J Clin Nutr. 2020 Jun;74(6):871–5.
49. Devaux CA, Rolain JM, Raoult D. ACE2 receptor polymorphism: Susceptibility to SARS-CoV-2, hypertension, multi-organ failure, and COVID-19 disease outcome. Vol. 53, Journal of Microbiology, Immunology and Infection. Elsevier Ltd; 2020. p. 425–35.
50. Tsioufis C, Dimitriadis K, Tousoulis D. The interplay of hypertension, ACE-2 and SARS-CoV-2: Emerging data as the "Ariadne's thread" for the "labyrinth" of COVID-19. Vol. 61, Hellenic Journal of Cardiology. Hellenic Cardiological Society; 2020. p. 31–3.
51. Brojakowska A, Narula J, Shimony R, Bander J. Clinical Implications of SARS-CoV-2 Interaction With Renin Angiotensin System. J Am Coll Cardiol. 2020 Jun;75(24):3085–95.

52. Iaccarino G, Borghi C, Cicero AFG, Ferri C, Minuz P, Muiesan ML, et al. Renin-Angiotensin System Inhibition in Cardiovascular Patients at the Time of COVID19: Much Ado for Nothing? A Statement of Activity from the Directors of the Board and the Scientific Directors of the Italian Society of Hypertension. High Blood Press Cardiovasc Prev. 2020 Apr;27(2):105–8.
53. Kalligeros M, Shehadeh F, Mylona EK, Benitez G, Beckwith CG, Chan PA, et al. Association of Obesity with Disease Severity Among Patients with Coronavirus Disease 2019. Obesity. 2020 Jul;28(7):1200–4.

Received: 16 April 2021
Accepted: 10 July 2021

REVIEW / ARTÍCULO DE REVISIÓN

Hormonal and neuroendocrine control of reproductive function in teleost fish

Adrian Rodríguez Gabilondo, Liz Hernández Pérez, Rebeca Martínez Rodríguez*
DOI. 10.21931/RB/2021.06.03.35

Abstract: The worldwide spread of the virus has claimed multiple lives, especially in vulnerable groups. Therefore, an investigation was carried out to present a viable solution for health personnel using the "JES" algorithm. The present study used the research to determine the possible complications presented by the sick individual, providing a viable and accessible healthcare personnel solution through the proposed "JES" algorithm. A non-experimental, descriptive, correlational, and explanatory research is presented. According to pathologies of interest, the articles were taken virtually from scientific journals present in Google Scholar and PubMed. The excluded publications were: articles that do not detail the established protocol for detecting SARS-CoV-2, studies that do not present a significant number of people with Covid-19 disease, articles that the person has the covid-19 disease but no underlying diseases of nutritional origin. It focused on the vulnerable or higher risk population group, including scientific information from children (over five years old), adults (over 18 years old), and older adults (over 65 years old) found in countries of the Asian and American continents. The R program analyzed the scientific articles using the ggplot2 package with a pie and bar diagram. A higher prevalence in men than women (56% vs. 44%) stood out. Likewise, arterial hypertension was presented in the first place with 40.82%, followed by diabetes with 30.61%, obesity with 12.24%, overweight and dyslipidemia with 6.12%, malnutrition with 4.08%. There was a higher prevalence of stable individuals (29%) within the health facility than those admitted to the ICU (20%). Adults with 69.39%, followed by older adults with 16.33%, and mixed ages with 14.29%. Comorbidities stand out as risk factors in people infected with SARS-CoV-2, regardless of age. A more significant contagion was observed in the male versus female population; since men do not develop a rapid immune response and have a high content of cytokines that at the time of infection are released more quickly and can cause more significant damage

Key words: Hormonal control, neuroendocrine, reproductive function, teleost fish, aquaculture.

Introduction

Aquaculture is the fastest-growing food production sector globally and plays an essential role in meeting the food demand of populations. In this stage, incorporating new technologies that allow increasing the number of cultivable species is crucial[1,2]. For several years, the aquaculture sector has focused mainly on establishing the minimum requirements for the development, growth, and reproductive success of the different species[3,4]. The study of endocrinology in teleost fish has been fundamental for understanding the functional roles of hormones in biological systems. In recent years, the existence of a complex and infinite number of interactions between hormones and nerve structures has been demonstrated[5-9]. Reproduction is one of the most important biological processes of organisms since the survival and perpetuation of the species depend on it[1,10]. The control of reproductive events allows the application of selection programs to improve the growth rate, the survival of the species, reduce the problems associated with sexual maturation and generate monosex populations[11,12]. The quality of spawning depends on environmental factors such as photoperiod, temperature, salinity, tank volume, substrate vegetation, etc[1,13]. The initiation of reproduction is affected by the number of energy reserves in the body and is sensitive to various metabolic factors.

The neuroendocrine mechanisms responsible for the association between energy balance and fertility are represented by metabolic hormones and neuropeptides that affect the hypothalamic center. In teleosts, as in other vertebrates, reproduction is coordinated by the hypothalamic-pituitary-gonad (HPG) axis[14-16]. However, there is very little research on reproductive biology and these species' molecular and cellular mechanisms[12,17,18]. This review presents a general bibliographic compilation of the main hormonal and neuroendocrine aspects of the control of reproductive function in teleost fish. Therefore, it will try to provide an overview of the most significant findings in recent years.

Hormonal control of reproduction in teleost fish

The control of reproduction in fish is a multifactorial process involving environmental, social, neuronal, endocrine, and metabolic agents. a cascade of hormones regulates[19,20] reproduction. The mechanisms involved in this process depend on the HPG axis (Figure 1)[15,16]. Hormones and neuropeptides are produced in specific neuronal regions of the brain, mainly in the hypothalamus. These can directly inhibit or stimulate gonadotropins (GtH) release into the bloodstream or indirectly through their functions on gonadotropin-releasing hormone (GnRH)[21,19]. The beginning of sexual maturation in fish presents two simultaneous events: the release of gonadotropin-releasing hormone (GnRH)[22-25] and the activation of GtH receptors in the gonads[26]. The activation of these receptors stimulates the production of germ cells, the synthesis of sex steroids and growth factors, and the effectors of gonadal development[12,27,19]. At the level of the pituitary gland, different molecules are secreted, such as: luteinizing hormone (LH), follicle-stimulating hormone (FSH), growth hormone (GH), prolactin (PRL), thyroid-stimulating hormone (TSH), among others[21]. These hormones participate in osmoregulation processes, growth, gonadal steroid production, the onset of pu-

Metabolic Modifiers for Aquaculture, Agricultural Biotechnology Department, Center for Genetic Engineering and Biotechnology, Havana, Cuba.

Corresponding author: rebeca.martinez@cigb.edu.cu

berty, and reproductive behavior of fish[7,12,28-30]. In addition, a series of neuroendocrine factors and hypothalamic neuropeptides have been identified that regulate behavior, eating, and energy balance. Their physiological and metabolic functions guarantee survival and growth during the reproductive stage[16]. Within these neuropeptides, we can mention the GH releasing hormone (GHRH), pituitary adenylate cyclase-activating polypeptide (PACAP), Somatostatin (SS), the thyrotropin-releasing hormone (TRH), Dopamine, Neuropeptide-Y (NPY), gamma-aminobutyric acid (GABA), neurokinin B (NKB) and gonadotropin inhibiting hormone (GnIH)[18,31-36]. In addition, among these neuropeptides is also included Kisspeptin (Kiss)[37], which constitutes an important regulator of the synthesis and release of GnRH[38,39,40,41]. Another very novel neuropeptide is Phoenixin (PNX), which regulates physiological processes such as food consumption, proliferation, and cell differentiation[42,43]. Moreover, it has been reported to be involved in reproductive function; due to its role in gene expression regulation in the hypothalamus and pituitary[44,45]. High concentrations of phoenixin in the central and peripheral nervous systems suggest that the peptide may serve as a multi site-directed signaling molecule[44,46,47]. In general, these brain factors, in addition to being involved in the secretion of pituitary hormones, regulate other physiological systems, but they greatly influence reproduction[12,30,36,48]. At each level of the axis, a limited number of target cells are under the influence of many factors. The final cellular response is the overall effects of these mediators on the components of intracellular signal transduction[49]. Mature gonads secrete sex steroids (estrogens and androgens), which negatively regulate hormonal secretions in the hypothalamus and pituitary gland. This closed-loop system maintains the homeostasis of the reproductive system[12]. In general, according to their functions on the reproductive cycle, FSH has a vitellogenin function and LH a maturational function[50-53].

Gonadotropin-releasing hormone (GnRH)

In fish, as in all vertebrates, reproduction is regulated by the hypothalamus through gonadotropin-releasing hormone (GnRH)[16,54]. This hormone constitutes the critical element of the neuroendocrine control of reproduction[16,55-58]. The (GnRHs) constitute a family of peptide molecules whose nature and diversity have been evidenced in teleost fish[59]. Three structural variants of GnRH have been identified in various vertebrate species: GnRH1, GnRH2, and GnRH3[56,57,58,60,61]. However, the molecular mechanisms that link the 3 isoforms of GnRH with reproduction in fish are not well clarified[62].Mammals only possess GnRH1 and GnRH2, while teleost fish have two or all three types of GnRH[41]. Most teleost fish, including Perciformes and Pleuronectiformes, present all three GnRH isoforms[36,55,57,63]. Other fish species such as salmon (*Salmoninae*), zebrafish (*Danio rerio*) and goldfish (*Carassius auratus*) possess only two forms of GnRH (GnRH2 and GnRH3)[14,36,64,65] GnRH1 is expressed mainly in the olfactory bulb, ventral telencephalon, and the pre-optic zone. GnRH2, a conserved form from fish to mammals, is expressed mainly in the midbrain[36].

GnRH3 constitutes the specific form of GnRH in fish[66,67] and has a similar distribution to GnRH1. The three structural variants of GnRH have different physiological functions.

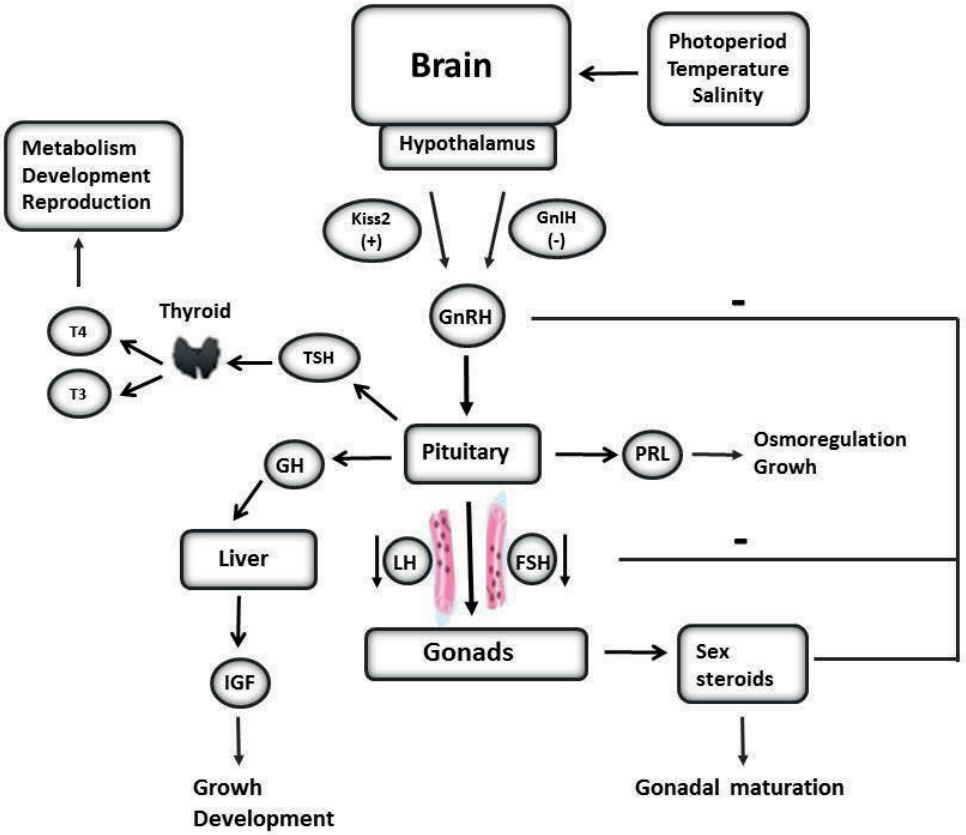

Figure 1. Hypothalamic-Pituitary-Gonads (HPG) axis. Gonadotropin-Releasing Hormone (GnRH); follicle-stimulating hormone (FSH); luteinizing hormone (LH); prolactin (PRL); growth hormone (GH); Kisspeptin (Kiss2); Gonadotropin inhibitory hormone (GnIH); Growth factors (IGF); Thyroid-stimulating hormone (TSH); Triiodothyronine (T3); Tetraiodothyronine (T4). GnRH secretion acts on a population of gonadotropic cells of the pituitary, which release LH and FSH. In addition, the pituitary is the site of synthesis, storage, and release of GH, TSH, and PRL; it is considered a transducer that, through its secretions, regulates endocrine functions, such as reproduction, osmoregulation, growth, and metabolism.

GnRH1 is considered the hypothalamic variant capable of stimulating gonadotropin secretion and constitutes the fundamental regulator of the pituitary in mammals[56,58]. In teleost fish, GnRH1 has its physiological importance in the regulation of gonadotropin secretion and gametogenesis[14]. GnRH2 is involved in regulating eating behavior[58,68,69,70,71] and probably has an intermediary role between food intake and reproduction[72,73]. It is highly probable that both GnRH2 and other GnRH isoforms expressed in the olfactory region play a role in the perception of social and pheromonal signals[36,74]. GnRH3 participates in the control of reproductive behaviors in several fish species[14] .For example, this isoform stimulates the nesting behavior of male dwarf Gourami (*Trichogaster lalius*)[14]. In adult zebrafish lacking GnRH3 neurons, there was evidence of an arrest in oocyte development and also a reduction in the mean diameter of the oocytes. These findings suggest that hypophysiotropic GnRH3 neurons are critical for normal oocyte development and reproduction[75]. Both this study and those carried out by Palevitch *et al.* 2007[76], suggest that GnRH3 is the hypophysiotropic GnRH capable of regulating the HPG axis in species lacking GnRH1, such as zebrafish. The action of GnRHs on target cells is mediated by specific binding to their membrane receptors (GnRHR)[36]. Corresponding to the primary role of GnRH in controlling reproduction, GnRHRs are mainly localized in the brain to mediate the neuromodulatory actions of GnRH in other neuronal systems and in gonadotropic cells of the pituitary to regulate gonadotropin secretion. Furthermore, GnRHRs, like GnRHs, are found in the gonads and other peripheral tissues, exerting multiple physiological actions[36,77]. In general, the primary function attributed to GnRH is the stimulation of the synthesis and release of GtH in teleost fish[36,55,77-81] Besides, it can regulate the gonadal maturation, the development of germ cells (oogenesis and spermatogenesis), gonadal steroid production, ovulation, spermiation, and spawning[36,57] In addition, it is involved in the control of the release and expression of growth hormone, somatolactin, and prolactin[82,83]. Considering the published results in the literature, the effects of GnRHs on the control of reproductive function depend on the species, sex, and reproductive status, as well as the complex endocrine interactions along the HPG axis[57,83].

Kisspeptin

Kisspeptin regulates the HPG axis[34,84,85,86], and in the initiation of sexual maturation[84,87]. Kisspeptin expression is more abundant in the brain, particularly in the hypothalamus[84,88]. It originates from neuronal populations in the hypothalamus and projects into the median eminence (EM) and preoptic area (POA) regions, where GnRH neurons are also found[89,90,91]. However, its expression has been evidenced in peripheral tissues such as the intestine, kidney, liver, pancreas, adipose tissue, and gonads[92]. In mammals, only (*kiss1*) coding for kisspeptin and (kiss1r) coding for the receptor have been identified[93]. However, in some teleost species due to a third duplication of the genome, two genes coding for kisspeptin (*kiss1* and *kiss2*) have been identified[86,93] Some of these species are medaka (*Oryzias latipes*)[84], zebrafish[84,94], sea bass (*Lateolabrax japonicus*), and redfish (*Sciaenops ocellatus*)[95]. Other species, such as the puffer fish (*Takifugu niphobles*)[87] and Senegalese sole (*Solea senegalensis*) contain only the kiss2 gene[96]. The kisspeptin receptor (kiss-R) in fish is expressed in tissues such as the brain, pituitary, gonads, heart, kidney, liver, and muscle[84,87,97-99]. Different teleosts species have two or even three genes encoding for kisspeptin receptors (*kiss1r, kiss2r, kiss3r*)[93,100]. For example, kiss1r and kiss2r have been identified in medaka, zebrafish, goldfish, striped bass (*Morone saxatilis*), and European bass (*Dicentrarchus labrax*). However, kiss2r has only been identified in Nile tilapia (*Oreochromis niloticus*), cobia (*Rachycentron canadum*), gray mullet (*Mullus barbatus*), spotted grouper (*Epinephelus fuscoguttatus*), Senegalese sole, among others[101]. Kiss3r, the expression demonstrated in zebrafish[97], goldfish[102], medaka[103], striped bass (Zmora *et al.*, 2012), and European eel (*Anguilla anguilla*)[104]. There is evidence in fish of the participation of kisspeptins and their receptors in the feedback mechanisms of sex steroids[40]. The role of kisspeptin in reproduction is based mainly on the stimulation of GnRH release, indirectly modulating the release of LH and FSH[93,105]. In mammalian models, kisspeptin regulates the release of LH through projections on GnRH neurons. However, in the case of teleosts, these functions are not clear[62]. Zhao *et al.* 2014[106] provided interesting data on the modulatory effects of kiss1 and kiss2 on neuronal GnRH subpopulations. First, they reported that treatment with kiss1 or kiss2 during the first day after fertilization stimulated the proliferation of GnRH3 neurons in the peripheral nervous system. However, only kiss1 stimulated the proliferation of terminal and hypothalamic nerve populations of GnRH3 neurons[106]. In zebrafish (GnRH3) and striped bass (GnRH1), few preoptic GnRH neurons appear to be innervated by kisspeptin[94,107,108]. However, European seabass (*Dicentrarchus labrax*) and medaka hypothalamic GnRH3 neurons are not associated with kisspeptin fibers[88,109]. Zmora *et al.* 2015[110], found kiss1 immunoreactive nerve endings that reach LH cells, suggesting the existence of a direct pituitary site of action of kisspeptin These results are similar to those published by Shahjahan *et al.* in 2014[14] where the expression of kisspeptin is evidenced in the pituitary gland of goldfish and puffer fish (*Takifugu rubripes*). Studies in goldfish[37,99] and sea bass[111] have confirmed a direct stimulation in the secretion of LH and FSH in pituitary cells in response to kisspeptin administration. On the other hand, in goldfish, kiss1 significantly increased LH-β, GH and PRL mRNA levels through *in vitro* studies[99]. Interestingly, both kiss1 and kiss2 regulate FSH-β expression levels in pituitary cell cultures in striped bass (*Morone saxatilis*). However, only Kiss1 can regulate LH-β mRNA levels in seabass negatively[110]. In sexually mature female zebrafish, administration of Kiss2 by intraperitoneal injection significantly increased FSH and LH mRNA levels. On the other hand, the administration of kiss1 by the same route did not have significant differences in GtH gene expression levels[84,112]. The stronger effect of kiss2 compared to kiss1 was also observed in the release of FSH and LH in sea bass[95,112]. A similar trend was observed for the effects of kisspeptins on the stimulating effect on gonadal maturation in seabass and striped bass[113]. In contrast, intraperitoneal injections of kiss2 stimulated mRNA expression of FSH rather than LH in female spotted grouper[114]. Furthermore, in goldfish, intraperitoneal injections of kiss1, but not kiss2, stimulated the release of LH in sexually mature females[102]. Also, it has been reported that kiss2 may have effects on food intake and growth function[88,96,115]. Furthermore, it can act as a link between food intake, energy homeostasis, and reproduction[116-118]. In general, these findings indicate the role of kiss1 and kiss2 in gonadotropin regulation is species-specific. Collectively, the differences between the species derive from their reproductive behavior and the stages of reproduction.

Gonadotropin inhibitory hormone (GnIH)

Multifactorial control of reproduction also involves other neurohormones such as gonadotropin inhibitory hormone (GnIH)[20]. In fish, GnIH is expressed mainly in the brain and pi-

tuitary, although its expression has also been evidenced in the spleen, gonads, muscle, eyes, and kidney[119-122]. GnIH acts by binding to GnIH receptors (GnIH-R) that belong to the family of G protein-coupled receptors. Two GnIH-Rs (GPR147 and GPR74) have been identified in vertebrates, but only GPR147 appears to be present in fish[122-124]. GPR147 have been identified in fish's central and peripheral tissues, including the brain, pituitary, eyes, heart, intestine, kidney, liver, spleen, muscle, and gonads[125-127]. As its name suggests, the main function of GnIH is the inhibition of gonadotropin release through the inhibition of GnRH and kisspeptin[128,129], an action that has been described in many vertebrates. However, the physiological functions of GnIH in fish are not precise yet. Contradictory effects have been observed in fish, both *in vivo*[130] and *in vitro*[131] For example, administration of GnIH to pituitary cell cultures of mature female Nile tilapia increased LH and FSH mRNA levels[18,130]. It has been shown that in goldfish, GnIH inhibits both the synthesis and the release of gonadotropins in the early stages of gonadal maturation but not in spawning[132]. Administration of GnIH to zebrafish by intraperitoneal injection decreases plasma LH levels in adult goldfish[125,132]. However, the inhibitory effect of GnIH injections was not observed in juvenile stages[132]. *In vitro* studies showed that the administration of GnIH from goldfish stimulates the expression of gonadotropins in pufferfish with apparent seasonal differences in reproduction[132,133]. These findings indicate that, in teleosts, the physiological effect of GnIH on the HPG axis differs between gonadotropin synthesis and release and depends on the reproductive stage. Even though researchers have shown that GnIH exerts both stimulatory and inhibitory actions, depending on the season and species, both GnRH and GnIH are considered essential components of the multifactorial control of reproduction[20].

Gonadotropins (GtHs)

In teleosts, as in all vertebrates, the functions of the gonads are maintained thanks to the actions of the gonadotropins. They have a central role in the regulation of gametogenesis[134] and the steroidogenesis necessary for the development of sexual behavior and secondary sexual characteristics[1,78,80,135]. Gonadotrops are cells specialized in producing gonadotropins such as follicle-stimulating hormone (FSH) and luteinizing hormone (LH). Both are glycoproteins made up of two non-covalently associated subunits (α and β). The α subunit has 92 amino acids (aa) and is common in both gonadotropins. The β subunit has 121 aa for LH and 118 aa for FSH. This subunit is specific for recognition by their cellular receptor and also confers biological activity[15,53,134,136]. These hormones exert their effects by binding to G protein-coupled surface receptors, called the LH receptor (LH-R) and the FSH receptor (FSH-R)[134,137,138]. Both receptors are mainly expressed in the gonads[139]. In the ovary, LH-R is expressed in theca cells, luteal cells, and interstitial cells, regulating actions such as the synthesis of steroid hormones, ovulation, and the formation of the corpus luteum[139]. In the testicle, LH-R is expressed in Leydig cells, where it stimulates the synthesis of testosterone (T), a precursor hormone of testicular maturation via spermatogenesis.139 LH is related to the manifestation of secondary sexual characteristics in males, and its highest plasma levels are in the spermiation stage. In addition, it intervenes in the capture and incorporation of blood vitellogenin to the oocyte. In the final phase of oocyte maturation, LH levels increase, leading to the production of dihydroxyprogesterone (17α-20β). The 17α-20β is involved in the haploid processes before ovulation and in sodium and potassium transport control[139]. For its part, FSH-R is expressed in the ovary, exclusively in granulosa cells. Its activation by the action of FSH contributes to follicular development and stimulates the synthesis of 17β estradiol. The 17β estradiol acts on the liver to initiate and maintain vitellogenin synthesis in oocytes and is involved in gonadal maturation processes.

Furthermore, FSH induces aromatase expression and thus modulates ovarian estrogen synthesis. On the other hand, in the testis, FSH-R is expressed in Sertoli cells[139]. In trout, plasma FSH increased at the beginning of oogenesis and in the initial phases of spermatogenesis[140]. Also, in Pacific salmon (*Oncorhynchus tshawytscha*), the levels of FSH remained high and declined immediately before ovulation and spermiation. In physiological studies carried out in this same species, FSH-β expression levels increased during the initiation of gonadal growth and decreased in spawning[141]. These results coincide with Schulz *et al.* in 2001[142], where they state that FSH is involved in the initial phases of gametogenesis, and LH mainly regulated the last stages of gonadal maturation. Previous studies have reported that FSH mRNA levels increased while LH mRNA decreased during the transition from female to male in Epinephelus merra. This was associated with testicular development and suggests that FSH could trigger sex change in this species[143]. In recent studies, the expression of LH-β mRNA in the pituitary of carp (*Cyprinus carpio*) increased significantly during the maturation of the male; however, FSH-β mRNA expression did not change significantly during development[136]. As published by Yaron *et al.* in 2003[29], LH-<UNK> and FSH-<UNK> gene expression levels of LH-β and FSH-β were very low in the juvenile stage of carp, while they increased during the ovulation period. In general terms, FSH mainly controls the first stages of spermatogenesis, and LH regulates testicular maturation, ovulation, and spermiation[16,50-52].

Growth hormone (GH)

The growth hormone of teleost fish is a 21-23 kDa protein made up of a single polypeptide chain. Similar to what happens in mammals, GH in fish is produced by somatotropic cells in the anterior region of the pituitary gland[144]. Furthermore, its expression has been confirmed in other fish tissues, including the brain, liver, spleen, and gonads[145,146]. GH is an essential endocrine regulator in many physiological processes in vertebrates. In fish, it is involved in events such as somatic growth, energy metabolism, reproduction, appetite, the function of the immune system, and the regulation of ionic and osmotic balance[147,148]. In addition, it influences aspects of behavior such as aggressiveness and the ability to avoid predators[149]. This hormone is released from the pituitary in response to hypothalamic signals and exerts its effects on target tissues[148,150] binding to the GHR-I and GHRII receptors (hormone receptor growth I and II, respectively)[148,149]. Growth hormone receptors (GHRs) are members of the type I cytokine receptor family[151]. They have been identified in several fish species, such as turbot (*Scopthalmus maximus*)[146], salmon (*Oncorhynchus masou*)[152], and Mozambique tilapia (*Oreochromis mossambicus*)[153]. These receptors are expressed in a wide variety of tissues, including the brain, pituitary, skin, heart, liver, gallbladder, intestine, adipose tissue, kidney, spleen, gonads, and muscle[152-154]. However, the primary expression is in the liver (or hepatopancreas), where GHRs have a significant role in regulating somatic growth[148]. GH binds to its specific receptors in the liver and promotes the release of insulin-like growth factor-I and II (IGF-I and IGF-II), whose primary function is to mediate and increase the growth-promoting function of GH[155]. IGF-I is involved in reproduc-

tion and particularly in mediating the effects of GH on somatic growth[154]. Furthermore, it has been associated with fish metabolism, development, reproduction and osmoregulation[148,150]. In the case of IGF-II, its mRNA has been detected in the liver and the brain, heart, kidney, gills, gastrointestinal tract, pancreatic islets, skeletal muscle, and gonads of fish[150]. This transcript is expressed in juvenile and adult fish, contrary to what has been reported for mammals where its expression occurs only during the early stages of development[156]. GH exerts a lipolytic and anabolic function. The lipolytic action is independent of IGFs and facilitates fats as an energy source in catabolic and malnutrition states[157]. The anabolic action of GH is related to protein metabolism and is mediated by IGFs[157]. The biological functions of IGFs are mediated by binding to specific transmembrane receptors, present in both fish and mammals.

In sexually mature ovaries of Nile tilapia, high levels of mRNA of both GHRs were detected. While in testes of this same species, the highest levels were observed after the stage of sexual maturation[148]. Changes in the expression of IGFs in the gonads and the neuroendocrine regulation of GnRH, GnIH, FSH, LH, GH and the GH / IGF system have been associated with promoting testicular steroidogenesis. They also have a significant influence on the oocyte maturation processes in several species[154,156,158,160]. Taken together, these observations suggest that GH, IGFs, and gonads are closely related and involved in controlling reproductive function.

Prolactin (PRL)

PRL is synthesized mainly by the lactotrophic or PRL-secreting cells found in the pituitary[160,161]. It has a variable length (between 170 and 205 amino acids (aa) depending on the species, with signal peptides of 23-24 aa. Two isoforms have been found in teleosts (PRL188 and PRL177), with different biological activities[83]. Prolactin is generally produced at high levels in pituitary tissues; however, its expression has been evidenced in other tissues such as the liver, intestine, gonads, gills, kidney, spleen, brain, and muscle[162,163]. Plasma PRL levels in Nile tilapia are increased during maternal behavior, suggesting hormonal control[164]. Other studies indicate that PRL mRNA levels and mature protein have been found in the gonads of different fish species, including Mozambique tilapia[167], Nile tilapia[165], goldfish[162,166], and rainbow trout (*Oncorhynchus mykiss*)[166]. This suggests that PRL may be involved in spermatogenesis, vitellogenesis, and ovulation. However, no significant differences were found in PRL mRNA levels during sexual maturation of Japanese eels through *in vitro* studies by Ozaki *et al.* in 2007[168]. According to Onuma *et al.* in 2010[169], in salmon, the levels of PRL mRNA and gonadotropins significantly were increased in the stage of maturation and gonadal development, which suggests that these hormones may be associated with the development of the reproductive system. In addition, PRL levels seem to be involved in many more functions such as developing reproductive cycles, incubation behavior, or feeding the fry[170,171]. It has also been shown to stimulate steroidogenesis in the ovaries and testes and increase their mRNA and plasma levels during sexual maturation in salmonids and tilapia[153,166]. The regulation of PRL synthesis and release into the pituitary is known to be influenced by hypothalamic neurohormones, sex steroids, and plasma factors from other tissues[171]. It is proposed that this hormone can act in an autocrine or paracrine manner and represents an exciting area for future research[171,172].

Thyroid hormones (HTs)

Thyroid hormones (HTs) are involved in various biological events in fish, such as regulating metabolism, growth, development, and reproduction, among others[173-177]. HTs (T3 and T4) are found in two forms in the blood: free and bound to transporter proteins. Less than 1% is in the free form and therefore easily accessible to target cells[178]. The secretion of HTs is under the control of the hypothalamic-pituitary-thyroid axis (Figure 2)[175,177-179]. In the hypothalamus, some neurons synthesize, transport, and release various factors that stimulate or inhibit the release of HTs to the neurohypophysis. Among the stimulatory factors are thyrotropin-releasing hormone (TRH) and the inhibitors Somatostatin and TSH inhibitory factors. Thyroid-stimulating hormone (TSH) is released to the bloodstream, where it reaches the thyroid gland and stimulates the synthesis and release of the two HTs (T3 and T4) into the blood[178,179]. These hormones are lipidic, so they can cross the plasma membrane and reach the cytoplasm. T4 is secreted under normal conditions, while T3, known as the active hormone, is produced mainly from the conversion of T4 to T3. Two enzymes catalyze this process with deiodase activity (DIO1 and DIO2)[180]. T3 crosses the nuclear membrane to interact with its THR α and THR β receptors in the nucleus.

Once the hormone-receptor complex is formed, there is a self-regulation of the expression of the genes (THRα and THR β) that code for the THR α and THR β receptors[177,179]. Some of the first studies in fish was carried out in Pacific salmon, Atlantic salmon (*Salmo salar*), and striped bass (*Morone saxalitis*), where it was evidenced that the thyroid hormones T3 and T4 are transferred from the mother to the egg and are used during the absorption of the yolk sac in the larval period, to later be synthesized by the larva in the exogenous feeding period[181]. In salmon, the increase in plasma T4 levels has been seen in the early stages of gonadal maturation but decreases as vitellogenesis and testicular maturation occur[182]. In stellate sturgeon (*Acipenser stellatus*), high thyroid activity occurs in conjunction with gonadal maturation during preponderance migration and at spawning. In salmonids, the increase in T3 was related to vitellogenesis or the last stages of oocyte development[12,179]. *In vitro* and *in vivo* studies have shown that T3 treatments caused a decrease in LH mRNA levels in goldfish[183,184]. In other trials, T3 administrations in carp increased vitellogenin mRNA (Vtg) levels in the liver, a critical factor in gonadal maturation[185]. However, T3 treatment decreased the expression of estrogen receptors in golden carp testes[176]. In zebrafish, the administration of T3 stimulated the proliferation of Sertoli cells and spermatogonia in the testes[186]. In general, the effects of HTs on reproductive function are species dependent[187,188].

Gonadal development in females and males

Reproductive processes in teleost fish include puberty, spermatogenesis, spawning, and cellular processes such as steroidogenesis[16]. The gonads have the enzymes necessary for the synthesis of steroids and their transformation into a whole series of intermediaries involved in the different phases of reproduction. They produce three types of steroids necessary for reproduction: estrogens or C18 steroids, androgens or C19 steroids, and progestogens or C21 steroids[189]. Gonadal steroids exert their actions on target tissues by binding to specific intracellular receptors since, thanks to their lipophilic nature, they easily penetrate and diffuse within the cell[190,191]. In teleost testes, the synthesis of steroid (androgenic) hormones takes place in Leydig cells. Testosterone (T) is mainly synthesized and, to a lesser extent, 17α-hydroxy-4-pregnen-3-one (DHT), Androstenedione, and 11-ketotestosterone (11-KT)[192]. T is es-

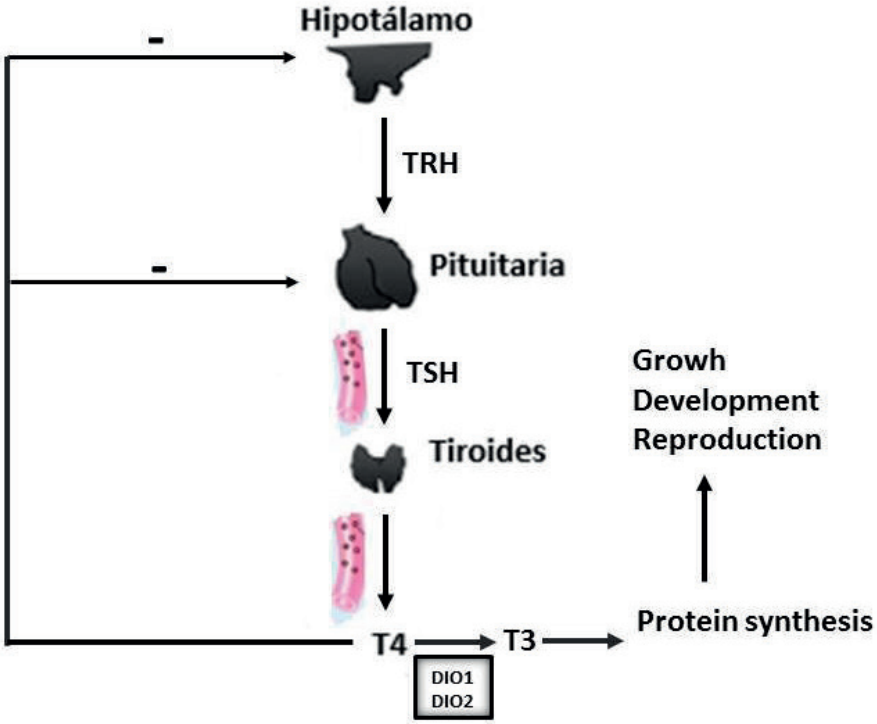

Figure 2. Hypothalamic-Pituitary-Thyroid Axis (HPT). Thyrotropin Releasing Hormone (TRH); Thyroid-stimulating hormone (TSH); Triiodothyronine (T3); Tetraiodothyronine (T4); Enzymes with deiodinase activity (DIO1 and DIO2).

sential in the spermatogenic process and has great importance in female reproductive processes since it acts as a precursor of estrogen biosynthesis. 11-KT is a critical factor in the maturation of gametes, the development of secondary sexual characteristics, and reproductive behavior[193-196]. Spermatogenesis depends on the action of gonadotropins, and their binding mediates this function to their receptors in the gonads. Once this union occurs, the synthesis and secretion route of different sex steroids is activated[197].

In oogenesis, hormones of a steroid and peptide nature are synthesized, which are essential for regulating the reproductive axis in females[53]. The oocyte maturation process occurs within the ovarian follicles and is produced mainly 17β-estradiol (E_2). According to Nagahama and Yamashita in 2008[198], in teleost fish, there are three essential regulators of oocyte maturation: Gonadotropins, maturation inducing hormone (MIH), and maturation promoting factor (MPF). Before oocyte maturation, a change in the steroidogenic pathway from E_2 to DHP occurs in ovarian follicles[199]. This change during ovarian development is regulated mainly by changes in the availability of steroidogenic enzymes[198]. MIH activates MPF and triggers a series of changes associated with oocyte maturation.

One of the most critical processes for the maturation of the oocyte is vitellogenesis. Its principal function is the sequestration and packaging of vitellogenin (Vtg) and the absorption of very-low-density lipoproteins[200,201]. Vtg is synthesized in the liver and is specific to maturing females (Devlin and Nagahama, 2002). The growing ovarian follicles selectively sequester this through specific receptors (VtgRs) that give rise to the formation of Vtg-coated vesicles[202]. Vesicles fuse with lysosomes leads to the formation of multivesicular bodies (MVB). During vitellogenesis, gonadotropins stimulate the production of Testosterone (T) by theca cells, and subsequently, it is aromatized to 17-β estradiol (E_2) in the granulosa cells of the ovarian follicle. In response to this stimulation, plasma E_2 levels increase, which stimulates the production of Vtg in the liver, which is recognized by VtgR and incorporated by the oocyte through micropinocytosis (Figure 3)[1,27]. At the end of vitellogenesis, plasma LH levels increase, and in turn, E2 levels decrease. This results in a transient increase in plasma levels of T and maturation-inducing steroids (MIS), which act at the follicular layers' level to induce the oocyte's final maturation[1]. After the rupture of the follicle, the oocyte is released, in a process called ovulation[196]. Once ovulation occurs, follicular cells undergo morphological changes that lead to the secretion of progesterone (P) and E_2[190,203]. In general, both vitellogenesis and the final maturation of the oocyte are crucial events in the reproductive physiology of females.

Another group of steroid hormones such as corticosteroids, which are usually related to stress, play an essential regulatory role in other physiological processes[196]. In teleost fish, corticosteroids are mainly synthesized in the inter-renal tissue, specifically the head kidney. Plasma corticosteroid concentrations in fish depend on species, sex, and reproductive status[204]. Plasma levels of corticosteroids vary significantly throughout the reproductive cycle. For both females and males, some species contain high cortisol levels in plasma during the pre-spawning period, such as the rainbow trout[205], perch (*Perca fluviatilis*)[206], and masu salmon[207]. In general, steroid hormones play a fundamental role in controlling the reproductive function of teleost fish. These present direct or feedback effects through different hormonal cascades on reproductive functions in fish and constitute critical factors in the regulation of the HPG axis[196]. The gonadal maturation process in fish is highly complex since it includes the production, maturation, release of gametes, synthesis of hormones, and sexual behavior, which requires a large amount of available energy[208]. Although the role of energy in sexual maturation and reproduction has been evidenced. There are still gaps in the knowledge about the influence of metabolic and nutritional status on the regulation of gonadal function in fish[16].

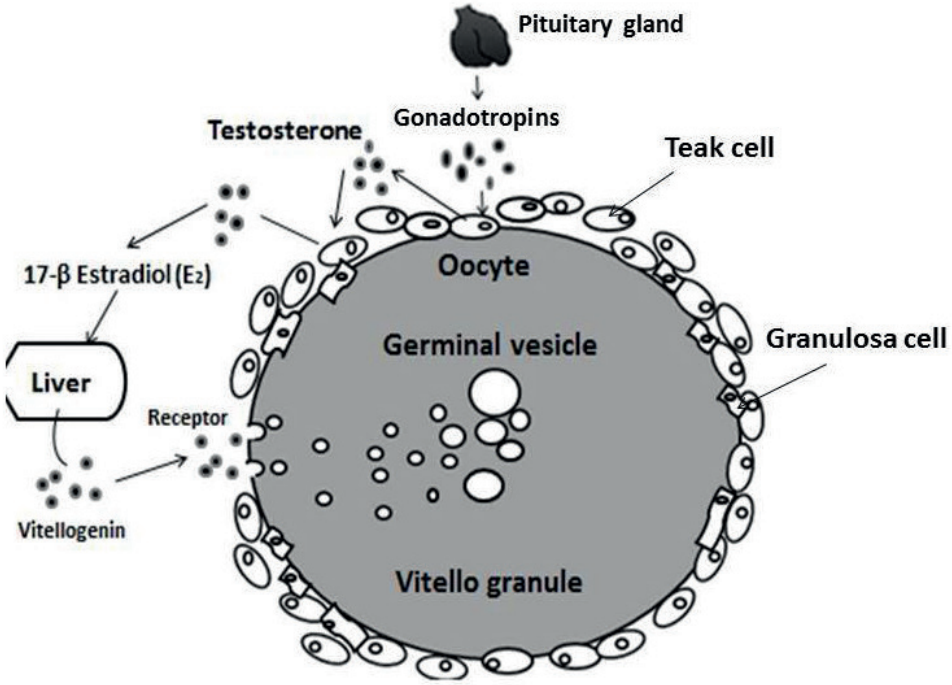

Figure 3. Hormonal regulation of vitellogenesis in teleost fish.

Conclusions

In this review, the fundamental aspects involved in controlling the reproductive function of teleost fish were addressed. The role of hormonal and neuroendocrine regulation of these species is described, which guarantees the proper functioning of the physiological machinery in reproductive events. The hypothalamic and pituitary hormones involved in reproduction in fish point to the immense complexity of endocrine regulation of reproductive processes. A brief overview of the integrative role of some neuropeptides in the regulation of feeding, metabolism, growth, and reproduction was also shown. However, especially in fish, knowledge about these integrative functions of regulatory peptides is not well studied.

Bibliographic references

1. Zohar Y and Mylonas CC. Endocrine manipulations of spawning in cultured fish: from hormones to genes. Aquaculture 2001; 197:99-136.
2. Reid GK, Helen J, Gurney-Smith, Flaherty M, Garber AF, Forster I, et al. Climate change and aquaculture: considering adaptation potential. Aquaculture Environ Interact 2019; 11: 603-624.
3. NRC. Nutrient requirements of fish and shrimp. The National Academies Press, Washington, D.C. 2011; 228.
4. Pohlenz C, Delbert M, Gatlin III. Interrelationships between fish nutrition and health. Aquaculture 2014; 431:111-117.
5. Bruce A. Stress in Fishes: A Diversity of Responses with Particular Reference to Changes in Circulating Corticosteroids. Integrative and Comparative Biology 2002; 42(3):517–525.
6. McCornick S, O'Dea M, Moeckel A, Thrandur B. Endocrine and physiological changes in Atlantic salmon smolts following hatchery release. Aquaculture 2003; 222:45-57.
7. Mancera JM and Cormick S. Role of Prolactin, Growth Hormone, Insulin-like Growth Factor I and Cortisol in Teleost Osmoregulation In: Fish Osmoregulation. Ed. B.G. Kapoor, Science Publishers 2007; p 497-515.
8. Subhash M. The role of thyroid hormones in stress response of fish. Gen Comp Endocrinol 2011; 172:198-210.
9. Fregeneda-Grandes J, Hernandez-Navarro S, Fernandez-Coppe I, Correa-Guimaraes A, Ruíz-Potosme N, Navas-Gracia L, et al. Seasonal and sex related variations in serum steroid hormone level in wild and farmed Brown trout Salmo trutta L.in the north-west of Spain. J Water and health 2013; 11:720-728
10. Manlik O. The importance of Reproduction for Conservation of Slow-Growing animal populations. Reproductive Sciences in Animal Conservation 2019; 13-39.
11. Solar I. Biotecnología aplicada a la acuicultura. Aquanoticias Internacional N° 66, 2002; Pp 6-10.
12. Mylonas C, Fostier Al, Zanuy S. Broodstock management and hormonal manipulations of fish reproduction. Gen Comp Endocrinol. 2010; 165:516-534.
13. Valdebenito. Hormone therapy for the artificial control of sexual maturity in fish culture: a review. Arch Med 2008; Vol 40:115-123.
14. Shahjahan M, Kitahashi T, Parhar IS, Davenport AP and Bonner T. Central Pathways Integrating Metabolism and Reproduction in Teleosts. Frontiers in Endocrinology 2014; DOI: 10.3389/fendo.2014.00036.
15. Levavi-Sivan B, Bogerd J, Mañanós EL, Gómez A, Lareyre JJ. Perspectives on fish gonadotropins and their receptors. Gen Comp Endocrinol 2010; 165:412-437.

16. Hatef A and Unniappan S. Metabolic hormones and the regulation of spermatogenesis in fishes. Theriogenology 2019; 134:121-128.
17. Unniappan S. Ghrelin: an emerging player in the regulation of reproduction in non-mammalian vertebrates. General and comparative endocrinology 2010; 167(3):340-343.
18. London S and Volkoff H. Effects of fasting on the central expression of appetite-regulating and reproductive hormones in wild-type and Casper zebrafish (Danio rerio). General and Comparative Endocrinology 2019; 282:113-207.
19. Biran J, Levavi-Sivan B. Endocrine Control of Reproduction. Fish 2018; 6:362-368.
20. Ma Y, Ladisaa C, Changa JP, Habibi HR. Multifactorial control of reproductive and growth axis in male goldfish: Influences of GnRH, GnIH and thyroid hormone. Molecular and Cellular Endocrinology 2020; 500:110-629.
21. Weltzien FA, Andersson E, Andersen Ø, Shalchian-Tabrizi K, Norberg B. The brain-pituitary-gonad axis in male teleosts, with emphasis on the flatfish (Pleuronectiformes). Comp Biochem Physiol 2004; 137:447-477.
22. Peter RE, Yu KL. Neuroendocrine regulation of ovulation in fishes: basic and applied aspects. Rev Fish Biol Fisher 1997; 7:173-197.
23. Okuzawa K. Puberty in teleosts. Fish Physiol Biochem 2002; 26(1):31-41.
24. Jalabert B. Particularities of reproduction and oogenesis in teleost fish compared to mammals. Reprod Nutr 2005; 45:261-279.
25. Taranger GL, Carrillo M, Schulz RW, Fontaine P, Zanuy S, Felip A, et al. control of puberty in farmed fish. Gen Comp Endocrinol. 2010; 165(3):483-515.
26. Cueto JM. Control Hormonal de la Reproducción en Peces. Universidad de Cádiz, Departamento de Biología (Facultad de Ciencias del Mar y Ambientales) 2016.
27. Schulz RW, De Franca, Lareyre LR, LeGac JJ, Garcia CF, Nobrega H, et al. Spermatogenesis in fish. Gen. Comp. Endocrinol 2010; 165:390-411.
28. Riley LG, Hirano T, Grau EG. Rat Ghrelin Stimulates Growth Hormone and Prolactin Release in the Tilapia, Oreochromis mossambicus. Zoological science 2002; 19:797-800.
29. Yaron Z, Gur G, Melamed P, Rosenfeld H, Elizur A, Levavi-Sivan B. Regulation of fish gonadotropins. International Review of Cytology 2003; 225:131-185.
30. Aizen J, Harel J, Levavi-Sivan B. Development of specific enzyme-linked immunosorbent assay for determining LH and FSH levels in tilapia, using recombinant gonadotropins. Gen Comp Endocrinol 2007; 153:323-332.
31. Gahete MD, Durán-Prado M, Luque RM, Martínez-Fuentes AJ, Quintero A, Gutiérrez-Pascual E, et al. Understanding the multifactorial control of growth hormone release by somatotropes: lessons from comparative endocrinology. Ann. N. Y. Acad. Sci 2009; 1163:137-153.
32. Li W, Lin H. The endocrine regulation network of growth hormone synthesis and secretion in fish: Emphasis on the signal integration in somatotropes. Sci. China Life Sci 2010; 53:462-470.
33. Dai X, Zhang W, Zhuo Z, He J, Yin Z. Neuroendocrine regulation of somatic growth in fishes. Sci. China Life Sci 2015; 58:137-147.
34. Parhar IS, Ogawa S, Ubuka T. Reproductive neuroendocrine pathways of social behavior. Front Endocrinol 2016; 7:28
35. Albaa G, Michele N, Mouradb N, Paredesa JF, Vázqueza SFJ, Olmedaa JFL. Daily rhythms in the reproductive axis of Nile tilapia (Oreochromis niloticus): Plasma steroids and gene expression in brain, pituitary, gonad and egg. Aquaculture 2019; 507:313-321.
36. Muñoz-Cueto, JA., Zmora N, Paullada-Salmerón JA, Marvel M, Mañanos E, & Zohar Y. The gonadotropin-releasing hormones: lessons from fish. General and comparative endocrinology 2020; 291: 113-422.
37. Chang JP, Mar A, Wlasichuk M, Wong AOL. Kisspeptin-1 directly stimulates LH and GH secretion from goldfish pituitary cells in a Ca (2+) dependent manner. Gen Comp Endocrinol 2012; 179:38-46.
38. Topaloglu AK, Kotan LD. Molecular causes of hypogonadotropic hypogonadism. Curr Opin Obstet Gynecol 2010; 22:264-70.
39. Pinilla L, Aguilar E, Dieguez C, Millar RP, Tena-Sempere M. Kisspeptins and reproduction: physiological roles and regulatory mechanisms. Physiol Rev 2012; 92:1235-316.
40. Parhar I, Ogawa S, Kitahashi T. RF-amide peptides as mediators in environmental control of GnRH neurons. Prog Neurobiol 2012; 98:176-96.
41. Mizrahi N, Gilon C, Atre I, Ogawa S, Ishwar S, Parhar et al. Deciphering Direct and Indirect Effects of Neurokinin B and GnRH in the Brain-Pituitary Axis of Tilapia. Frontiers in Endocrinology 2019; Vol 10 Article 469. doi: 10.3389/fendo.2019.00469.
42. Rajeswari JJ, Blanco A M, & Unniappan S. Phoenixin-20 suppresses food intake, modulates glucoregulatory enzymes, and enhances glycolysis in zebrafish. American Journal of Physiology-Regulatory, Integrative and Comparative Physiology 2020; 318(5):917-928.
43. Schalla MA, & Stengel, A. Phoenixin A pleiotropic gut-Brain peptide. International journal of molecular sciences 2018; 19(6):1726.
44. Yosten GL, Lyu RM., Hsueh AJ, Avsianα Kretchmer O, Chang JK, Tullock CW& Samson, WK. A novel reproductive peptide, phoenixin. Journal of neuroendocrinology 2013; 25(2):206-215.
45. Wang M, Chen HP, Zhai Y, Jiang DN, Liu JY, Tian CX, & Li GL. Phoenixin: Expression at different ovarian development stages and effects on genes ralated to reproduction in spotted scat, Scatophagus argus. Comparative Biochemistry and Physiology Part B: Biochemistry and Molecular Biology 2019; 228:17-25.
46. Prinz P, Scharner S, Friedrich T, Schalla M, Goebel-Stengel M, Rose M, et al. Central and peripheral expression sites of phoenixin-14 immunoreactivity in rats. Biochem Biophysical Res Comm 2017; 493: 195-201.
47. Yuan T, Sun Z, Zhao W, Wang T, Zhang J, Niu D. Phoenixin: a newly discovered peptide with multi-functions. Protein Pept Lett 2017; 24: 472-5.
48. Yaron Z, Gur G, Melamed P, Rosenfeld H, Elizur A, Levavi-Sivan B. Regulation of fish gonadotropins. Int Rev Cytol 2003; 225:131-185.
49. Kim DK, Cho EB, Luna MJ, Parque S, Hwang JI, Kah O, et al. Revisiting the evolution of gonadotropin-releasing hormones and their receptors in vertebrates: Secrets hidden in genomes. Gen Comp Endocrinol 2011; 170:68-78.
50. Zanuy S, Carrillo M. La reproducción de los peces teleósteos y su aplicación en acuicultura. En: Espinosa de los Monteros J, Labarta U (eds). Reproducción en acuicultura. CAICYT. Madrid, España, 1987, Pp 1-131.
51. Luckenbach JA, Iliev DB, Goetz FW, Swanson P. Identification of differentially expressed ovarian genes during primary and early secondary oocyte growth in coho salmon, Oncorhynchus kisutch. Reprod Biol Endocrinol 2008; 6-2.
52. Zanuy S, Carrillo M, Rocha A, Molés G. II Regulación y control hormonal del proceso reproductor de los teleósteos. En: Carrillo M, Espinosa de los Monteros J (eds). La reproducción de los peces: aspectos básicos y sus aplicaciones en acuicultura. OESA, CSIC, MMAMRN, Madrid, España 2009; 97-172.
53. Falcone TH. Ovarian Hormones: Structure, Biosynthesis, Function, Mechanism of Action, and Laboratory Diagnosis in Clinical reproductive medicine and surgery. Springer 2013; 15-44.
54. Feng K, Luo HR, Hou MG, Li YM, Chen J, Zh, ZY, et al. Alternative splicing of GnRH2, and GnRH2-associated peptide plays roles in gonadal differentiation of the rice field eel, Monopterus albus. Gen. Comp. Endocrine 2018.
55. Kah O, Lethimonier C, Somoza G, Guilgur LG, Vaillant C, and Lareyre JJ. GnRH and GnRH receptors in metazoa: a historical, comparative and evolutive perspective. Gen. Comp. Endocrinol 2007; 153:346-364.
56. Okubo K, Nagahama Y. Structural and functional evolution of gonadotropin releasing hormone in vertebrates. Acta Physiol 2008; 193:3-15.
57. Zohar Y, Muñoz-Cueto JA, Elizur A, Kah O. Neuroendocrinology of reproduction in teleost fish. Gen Comp Endocrinol 2010; 165:438-455.
58. Ma Y, Ladisaa C, Changa JP, Habibia HR. Multifactorial control of reproductive and growth axis in male goldfish: Influences of GnRH, GnIH and thyroid hormone. Molecular and Cellular Endocrinology 2020; 110-629.

59. Burgus R, Butcher M, Amoss M, Ling N, Monahan M, Rivier J et al. Primary structure of the ovine hypothalamic luteinizing hormone releasing factor (LRF) (LH-hypothalamus-LRF-gas chromatography-mass spectrometry decapeptide-Edman degradation). Proc Natl Acad Sci USA 1972; 69:278-282.
60. Klausen C, Chang JP, Habibi HR. Time- and dose-related effects of gonadotropin- releasing hormone on growth hormone and gonadotropin subunit gene expression in the goldfish pituitary. Can J Physiol Pharmacol 2003; 80:915-924.
61. Chang JP, Pemberton JG. Comparative aspects of GnRH-Stimulated signal transduction in the vertebrate pituitary-contributions from teleost model systems. Mol Cell Endocrinol 2018; 463:142-167.
62. Somoza GM, Mechaly AS, Trudeau VL. Kisspeptin and GnRH interactions in the reproductive brain of teleosts, General and Comparative Endocrinology 2020.
63. Choi D. Evolutionary viewpoint on GnRH (gonadotropin-releasing hormone) in chordata amino acid and nucleic acid sequences. Dev. Reprod 2018; 22:119-132.
64. Parhar IS, Tosaki H, Sakuma Y, Kobayashi M. Sex differences in the brain of goldfish: gonadotropin-releasing hormone and vasotocinergic neurons. Neuroscience 2001; 104(4):1099-110.
65. Whitlock KE, Postlethwait J and Ewer J. Neuroendocrinology of reproduction: Is gonadotropin-releasing hormone (GnRH) dispensable? Frontiers in Neuroendocrinology 2019; 53, Article 100738.
66. Sherwood N, Eiden L, Brownstein M, Spiess J, Rivier J, Vale W. Characterization of a teleost gonadotropin-releasing hormone. Proc Natl Acad Sci. USA. 1983; 80(9):2794-2798.
67. Hildahl J, Sandvik GK, Edvardsen RB, Fagernes C, Norberg B, Haug TM et al. Identification and gene expression analysis of three GnRH genes in female Atlantic cod during puberty provides insight into GnRH variant gene loss in fish. Gen Comp Endocrinol 2011; 172:458-467.
68. Schneider JS, Rissman EF. Gonadotropin-releasing hormone II: a multi-purpose neuropeptide. Integr Comp Biol 2008; 48:588-595.
69. Matsuda K, Nakamura K, Shimakura S, Miura T, Kageyama H, Uchiyama M, et al. Inhibitory effect of chicken gonadotropin-releasing hormone II on food intake in the goldfish, Carassius auratus. Horm. Behav 2008; 54:83-89.
70. Nishiguchi R, Azuma M, Yokobori E, Uchiyama M, Matsuda K. Gonadotropin-releasing hormone 2 suppresses food intake in the zebrafish, Danio rerio. Front. Endocrinology 2012; 3-122.
71. Xia W, Smith O, Zmora N, Xu S, Zohar Y. Comprehensive analysis of GnRH2 neuronal projections in zebrafish. Sci Rep 2014; 4:36-76.
72. Marvel MM, Spicer OS, Wong TT, Zmora N, Zohar Y. Knockout of Gnrh2 in zebrafish (Danio rerio) reveals its roles in regulating feeding behavior and oocyte quality. Gen. Comp Endocrinol 2019; 280:15-23.
73. Blanco AM. Hypothalamic and pituitary-derived growth and reproductive hormones and the control of energy balance in fish. General and Comparative Endocrinology 2020; doi: https://doi.org/ 10.1016/j.ygcen.2019.113322.
74. Forlano PM, Bass AH. Neural and hormonal mechanisms of reproductive-related arousal in fishes. Horm. Behav 2011. 59:616-629.
75. Abraham E, Palevitch O, Gothilf Y, Zohar Y. Targeted gonadotropin-releasing hormone-3 neuron ablation in zebrafish: effects on neurogenesis, neuronal migration, and reproduction. Endocrinology 2010; 151(1):332-340.
76. Palevitch O, Kight K, Abraham E, Wray S, Zohar Y, Gothilf Y. Ontogeny of the GnRH systems in zebrafish brain: in situ hybridization and promoter-reporter expression analyses in intact animals. Cell Tissue Res 2007; 327(2):313-322.
77. Lethimonier C, Madigou T, Munoz-Cueto JA, Lareyre JJ, Kah O. Evolutionary aspects of GnRHs, GnRH neuronal systems and GnRH receptors in teleost fish. Gen Comp Endocrinol 2004; 135(1):1-16.
78. Clarke IJ, Cummins JT. The temporal relationship between gonadotropin releasing hormone (GnRH) and luteinizing hormone (LH) secretion in ovariectomized ewes. Endocrinology 1982; 111(5):1737-1739.
79. Millar RP. GnRHs and GnRH receptors. Animal Reproduction Science 2005; 88(1), 5-28.
80. Bedecarrats GY. Control of the reproductive axis: Balancing act between stimulatory and inhibitory inputs. Poult Sci 2015; 94 (4):810-815.
81. Kanda S. Evolution of the regulatory mechanisms for the hypothalamic-pituitary-gonadal axis in vertebrates–hypothesis from a comparative view. General and comparative endocrinology 2019; 194:300-310.
82. Weber GM, Powell JF, Park M, Fischer WH, Craig AG., Rivier, et al. evidence that gonadotropin-releasing hormone (GnRH) functions as a prolactin-releasing factor in a teleost fish (Oreochromis mossambicus) and primary structures for three native GnRH molecules. J. Endocrinol 1997; 155:121-132.
83. Seale P. Endocrine regulation of prolactin cell function and modulation of osmoreception in the Mozambique tilapia. Gen. Comp. Endocrinol 2013; 192: 191-203.
84. Kitahashi T, Ogawa S, Parhar IS. Cloning and expression of kiss2 in the zebrafish and medaka. Endocrinology 2009; 150(2):821-831.
85. Ogawa S, Ramadasan PN, Goschorska M, Anantharajah A, Parhar IS. Cloning and expression of tachykinins and their association with kisspeptins in the brains of zebrafish. J Comp Neurol 2012; 520(13):2991–3012.
86. London S and Volkoff H. Effects of fasting on the central expression of appetite-regulating and reproductive hormones in wild-type and Casper zebrafish (Danio rerio). General and Comparative Endocrinology 2019; 282:113-207.
87. Shahjahan M, Motohashi E, Doi H, Ando H. Elevation of Kiss2 and its receptor gene expression in the brain and pituitary of grass puffer during the spawning season. Gen. Comp Endocrinol 2010; 169:48–57.
88. Escobar S, Felip A, Gueguen MM, Zanuy S, Carrillo M, Kah O, et al. expression of kisspeptins in the brain and pituitary of the European sea bass (Dicentrarchus labrax). J Comp Neurol 2013; 521:933-948.
89. Franceschini I, Lomet D, Cateau M, Delsol G, Tillet Y, Caraty A. Kisspeptin immunoreactive cells of the ovine preoptic area and arcuate nucleus co-express estrogen receptor alpha. Neurosci. Lett 2006; 401:225-230.
90. Pompolo S, Pereira A, Estrada KM, Clarke IJ. Colocalization of kisspeptin and gonadotropin-releasing hormone in the ovine brain. Endocrinology 2006; 147:804-810.
91. Ohga H, Adachi H, Matsumori K, Kodama R, Nyuji M, Selvaraj S, et al. mRNA levels of kisspeptins, kisspeptin receptors, and GnRH1 in the brain of chub mackerel during puberty. Comparative Biochemistry and Physiology 2015; Part A 179:104–112.
92. Selvaraj S, Kitano H, Fujinaga Y, Ohga H, Yoneda M, Yamaguchi, et al. Molecular characterization, tissue distribution, and mRNA expression profiles of two kiss genes in the adult male and female chub mackerel (Scomber japonicus) during different gonadal stages. Gen Comp Endocrinol 2010: 169:28 38.
93. Ohga H, Selvaraj S, Matsuyama M. The roles of kisspeptin system in the reproductive physiology of fish with special reference to chub mackerel studies as main axis. Front. Endocrinol 2018; 9:147.
94. Servili A, Le Page, Leprince Y, Caraty J, Escobar A, Parhar S, et al. Organization of two independent kisspeptin systems derived from evolutionary-ancient kiss genes in the brain of zebrafish. Endocrinology 2011; 152:1527-1540.
95. Felip A, Zanuy S, Pineda R, Pinilla L, Carrillo M, Tena-Sempere M, et al. evidence for two distinct Kiss genes in non-placental vertebrates that encode kisspeptins with different gonadotropin-releasing activities in fish and mammals. Mol Cell Endocrinol 2009; 312:61-71.
96. Mechaly AS, Viñas J, Piferrer F. Gene structure analysis of kisspeptin-2 (Kiss2) in the Senegalese sole (Solea senegalensis): characterization of two splice variants of Kiss2, and novel evidence for metabolic regulation of kisspeptin signaling in non-mammalian species. Mol Cell Endocrinol 2011; 339:14-24.
97. Biran J, Ben-Dor S, Levavi-Sivan B. Molecular identification and functional characterization of the kisspeptin/kisspeptin receptor system in lower vertebrates. Biol Reprod 2008; 79:776-786.

98. Van Aerle R, Kille P, Lange A, Tyler CR. Evidence for the existence of a functional Kiss1/Kiss1 receptor pathway in fish. Peptides 2008; 29:57-64.
99. ang B, Jiang Q, Chan T, Ko WK, Wong AO. Goldfish kisspeptin: molecular cloning, tissue distribution of transcript expression, and stimulatory effects on prolactin, growth hormone and luteinizing hormone secretion and gene expression via direct actions at the pituitary level. Gen Comp Endocrinol 2010; 165:60-71.
100. Pasquier, J., Kamech, N., Lafont, A. G., Vaudry, H., Rousseau, K., & Dufour, S. Kisspeptin/kisspeptin receptors. J Mol Endocrinol 2014; 52:101-117.
101. Mechaly AS, Vinas J, Piferrer F. The kisspeptin system genes in teleost fish, their structure and regulation, with particular attention to the situation in Pleuronectiformes. Gen Comp Endocrinol 2013; 188:258-268.
102. Li S, Zhang Y, Liu Y, Huang X, Huang W, Lu D, Zhu P et al. Structural and functional multiplicity of the kisspeptin/GPR54 system in goldfish (Carassius auratus). Journal of Endocrinology 2009; 201:407-418.
103. Lee YR, Tsunekawa K, Moon MJ, Um HN, Hwang JI, Osugi T, Otaki N, et al. Molecular evolution of multiple forms of kisspeptins and GPR54 receptors in vertebrates. Endocrinology 2009, 150:2837-2846.
104. Pasquier J, Lafont AG, Jeng SR, Morini M, Dirks R, Van den Thillart G, Tomkiewicz et al. Multiple kisspeptin receptors in early osteichthyans provide new insights into the evolution of this receptor family. PLoS ONE 2012; 7 e48931.
105. Elizur A. The KiSS1/GPR54 system in fish. Peptides 2009; 30:164-170.
106. Zhao Y, Lin MC, Mock A, Yang M, Wayne NL. Kisspeptins modulate the biology of multiple populations of gonadotropin-releasing hormone neurons during embryogenesis and adulthood in zebrafish (Danio rerio). PLoS One 9 2014; e104330
107. Zmora N, Stubblefield J, Zulperi Z, Biran J, Levavi-Sivan B, Muñoz-Cueto JA, et al. Differential and gonad stage-dependent roles of kisspeptin1 and kisspeptin2 in reproduction in the modern teleosts, morone species. Biol. Reprod 2012; 86:1-12.
108. Ogawa S, Sivalingam M, Anthonysamy R, Parhar IS. Distribution of Kiss2 receptor in the brain and its localization in neuroendocrine cells in the zebrafish. Cell Tiss. Res 2020; 379:349-372.
109. Kanda S, Akazome Y, Mitani Y, Okubo K, Oka Y. Neuroanatomical evidence that kisspeptin directly regulates isotocin and vasotocin neurons. PLoS ONE 8 2013; e62776. https://doi.org/10.1371/journal.pone.0062776
110. Zmora N, Stubblefield JD, Wong TT, Levavi-Sivan B, Millar RP, Zohar Y. Kisspeptin 504 Antagonists Reveal Kisspeptin 1 and Kisspeptin 2 Differential Regulation of Reproduction in the 505 Teleost, Morone saxatilis. Biol Reprod 2015; 93:76.
111. Espigares F, Zanuy S, Gómez A. Kiss2 as a regulator of LH and FSH secretion via paracrine/autocrine signaling in the teleost fish European Sea Bass (Dicentrarchus labrax). Biol of Reprod 2015; 114:1-12.
112. Kitahashi, T. and Parhar, I. S. Comparative aspects of kisspeptin gene regulation. Gen. Comp. Endocrinol 2013; 181:197-202.
113. Beck BH, Fuller SA, Peatman E, McEntire, ME, Darwish A, Freeman DW. Chronic exogenous kisspeptin administration accelerates gonadal development in basses of the genus Morone. Comp Biochem Physiol 2012; 162:265-273.
114. Shi Y, Zhang Y, Li S, Liu Q, Lu D, Liu M, et al. Molecular identification of the Kiss2/Kiss1ra system and its potential function during 17 -methyltestosterone-induced sex reversal in the orange-spotted grouper, Epinephelus coioides. Biol Reprod 2010; 83:63-74.
115. Mechaly AS, Tovar-Bohórquez MO, Mechaly AE, Suku E, Pérez MR, Giorgetti A, et al. evidence of alternative splicing as a regulatory mechanism for Kissr2 in pejerrey fish. Front. Endocrinol 2018; 9-604.
116. Tsatsanis C, Dermitzaki E, Avgoustinaki P, Malliaraki N, Mytaras V, Margioris AN. The impact of adipose tissue-derived factors on the hypothalamic-pituitary-gonadal (HPG) axis. Hormones 2015; 14(4):549-562.
117. Castellano JM, Bentsen AH, Mikkelsen JD, Tena-Sempere M.Kisspeptins: bridging energy homeostasis and reproduction. Brain Res 2015; 1364:129-138.
118. De Bond JA, Smith JT. Kisspeptin and energy balance in reproduction. Reproduction 2015; 147:53-63.
119. Sawada K, Ukena K, Satake H, Iwakoshi E, Minakata H, Tsutsui K. Novel fish hypothalamic neuropeptide. Eur J Biochem 2002; 269:6000-6008.
120. Biswas S, Jadhao AG, Pinelli C, Palande NV, Tsutsui K. GnIH and GnRH expressions in the central nervous system and pituitary of Indian major carp, Labeo rohita during ontogeny: An immunocytochemical study. Gen Comp Endocrinol 2015; 220:88-92.
121. Di Yorio MP, Sirkin P, Delgadin TH, Shimizu A, Tsutsui K, Somoza GM, et al. Gonadotrophin Inhibitory hormone in the cichlid fish Cichlasoma dimerus: structure, brain distribution and differential effects on the secretion of gonadotrophins and growth hormone. J Neuroendocrinol 2016; 28. https://doi.org/10.1111/jne.12377.
122. Paullada-Salmerón JA, Cowan M, Aliaga-Guerrero M, Gómez A, Zanuy S, Mañanos, E, et al. LPXRFa peptide system in the European sea bass: A molecular and immunohistochemical approach. J Comp Neurol 2016; 524:176-198.
123. Ogawa S, Parhar IS. Structural and functional divergence of gonadotropininhibitory hormone from jawless fish to mammals. Front Endocrinol 2014; 5:177.
124. Wang Q, Qi X, Guo Y, Li S, Zhang Y, Liu X, et al. Molecular identification of GnIH/GnIHR signal and its reproductive function in protogynous hermaphroditic orange-spotted grouper (Epinephelus coioides). Gen Comp Endocrinol 2015; 216:9-23.
125. Zhang Y, Li S, Liu Y, Lu D, Chen H, Huang X, et al. Structural diversity of the gnih/gnih receptor system in teleost: Its involvement in early development and the negative control of LH release. Peptides 2010; 31:1034-1043.
126. Ogawa S, Sivalingam M, Biran J, Golan M, Anthonysamy RS, Levavi-Sivan B, et al. Distribution of LPXRFa, a gonadotropin-inhibitory hormone ortholog peptide, and LPXRFa receptor in the brain and pituitary of the tilapia. J Comp Neurol 2016; 524:2753-2775.
127. Wang B, Yang G, Liu Q, Qin J, Xu Y, Li W, et al. Characterization of LPXRFa receptor in the half-smooth tongue sole (Cynoglossus semilaevis): Molecular cloning, expression profiles, and differential activation of signaling pathways by LPXRFa peptides. Comp. Biochem. Physiol. A Mol Integr Physiol 2018; 223:23-32.
128. Kriegsfeld LJ, Feng Mei D, Bentley GE, Ubuka T, Mason AO, Inoue K, et al. Identification and characterization of a gonadotropin inhibitory system in the brains of mammals. PNAS 2006; 103(7):2410-2415.
129. Ubuka T, Son YL, Tsutsui K. Molecular, cellular, morphological, physiological and behavioral aspects of gonadotropin-inhibitory hormone. Gen Comp Endocrinol 2016; 227:27-50.
130. Biran J, Golan M, Mizrahi N, Ogawa S, Parhar IS, Levavi-Sivan B. LPXRFa, the piscine ortholog of GnIH, and LPXRF receptor positively regulate gonadotropinsecretion in tilapia (Oreochromis niloticus). Endocrinology 2014; 155 (11):4391- 4401.
131. Amano M, Moriyama S, Iigo M, Kitamura S, Amiya, N, Yamamori K, et al. Novel fish hypothalamic neuropeptides stimulate the release of gonadotrophins and growth hormone from the pituitary of sockeye salmon. J Endocrinol 2006; 188: 417-423.
132. Moussavi M, Wlasichuk M, Chang JP, Habibi HR. Seasonal effect of GnIH on gonadotrope functions in the pituitary of goldfish. Mol Cell Endocrinol 2012; 350:53-60.
133. Shahjahan M, Ikegami T, Osugi T, Ukena K, Doi, H, Hattori A, et al. Synchronised expressions of LPXRFamide peptide and its receptor genes: seasonal, diurnal and circadian changes during spawning period in grass puffer. J. Neuroendocrinol 2011; 23, 39-51.
134. Yan H, Ijiri S, Wu Q, Kobayashi T, Li ST, Adachi S, Nagahama Y. Expression Patterns of Gonadotropin Hormones and Their Receptors During Early Sexual Differentiation in Nile Tilapia Oreochromis niloticus. Biology of Reproduction 2012; 116:1-11.

135. Shupnik MA. Gonadotropin gene modulation by steroids and gonadotropin-releasing hormone. Biol. Reprod 1996; 54(2):279-286.
136. Burow S, Fontainea R, Von Krogha K, Mayerb I, Nourizadeh-Lillabadia R, Hollander-Cohenc L, et al. Medaka follicle-stimulating hormone (Fsh) and luteinizing hormone (Lh): Developmental profiles of pituitary protein and gene expression levels. General and Comparative Endocrinology 2018; 272:93-108.
137. Simoni M, Gromoll J, Nieschlag E. The follicle-stimulating hormone receptor: biochemistry, molecular biology, physiology, and pathophysiology. Endocr Rev 1997; 18:739-773.
138. Kumar RS, Trant JM. Piscine glycoprotein hormone gonadotropin and thyrotropin receptors: a review of recent developments. Comp Biochem Physiol 2001; 129:347-355.
139. Falcone T, Hurd WW. Clinical Reproductive Medicine and Surgery: A Practical Guide, DOI 10.1007/978-1-4614-6837-0_2, © Springer Science Business Media New York 2013.
140. Santos M, Rand-Weaver, Tyler CR. Follicle stimulating hormone and its alpha and beta subunits in rainbow trout (Oncorhynchus mykiss): Purification, characterization, development of radioimmunoassays, and their seasonal plasma and pituitary concentrations in females. Biol Reprod 2001; 65:288-294.
141. Vischer, Tevez, Ackermans, Van Dijk, Schulz y Bogerd J. Cloning and spatiotemporal expression of follicle-stimulating hormone α subunit complementary DNA in the African catfi sh (Clarius gariepinus). Biol. Reprod 2003; 68:1324-1332.
142. Schulz RW, Vischer HF, Cavaco JE, Santos EM, Tyler CR, Goos HJ, et al. Gonadotropins, their receptors, and the regulation of testicular functions in fish. Comp Biochem Physiol B Biochem Mol Biol 2001; 129:407-417.
143. Kobayashi Y, Alam MA, Horiguchi R, Shimizu A, Nakamura M. Expresión Sexualmente dimórfico de subunidades de gonadotropina en la pituitaria de pro-mero panal togynous (Epinephelus merra): evidencia de que el folículo-estimulante hormone (FSH) induce el cambio de sexo gonadal. Biol Reprod 2010; 82:1030-1036.
144. Chang JP, Wong AOL. Growth hormone regulation in fish: a multifactorial model with hypothalamic, peripheral and local autocrine/paracrine signals. In: Fish Neuroendocrinology. Fish Physiology 28. Farrell AP, Brauner CJ (Eds). Academic Press, UK. 2009;151-195.
145. Dong H, Zeng L, Duan D, Zhang H, Wang Y, Li W, et al. Growth hormone and two forms of insulin-like growth factors I in the giant grouper (Epinephelus lanceolatus): molecular cloning and characterization of tissue distribution. Fish Physiol. Biochem 2010; 36:201-212.
146. Blanco AM. Hypothalamic and pituitary-derived growth and reproductive hormones and the control of energy balance in fish. General and Comparative Endocrinology 2020; doi: https://doi.org/ 10.1016/j.ygcen.2019.113322.
147. Canosa LF, Chang JP, Peter RE. Neuroendocrine control of growth hormone in fish. Gen Comp Endocrinology 2011; 151:1-26.
148. Bertucci JI, Blanco AM, Sundarrajan L, Rajeswari JJ, Velasco C, Unniappan S. Nutrient Regulation of Endocrine Factors Influencing Feeding and Growth in Fish. Frontiers in Endocrinology 2019; 10, Article 83.
149. Pérez-Sánchez J, Calduch-Giner JA, Mingarro M, de Celis SVR, Gomez-Requeni P, Saera-Vila A, et al. Overview of fish growth hormone family. New insights in genomic organization and heterogeneity of growth hormone receptors. Fish Physiol Biochem 2002; 27:243–58.
150. Reinecke M, Björnsson BT, Dickhoff WW, McCormick SD, Navarro I, Power DM, et al. Growth hormone and insulin-like growth factors in fish: where we are and where to go. Gen Comp Endocrinol 2005; 142:20-4
151. Brooks AJ, Waters MJ. The growth hormone receptor: mechanism of activation and clinical implications. Nat Rev Endocrinol 2010; 6:515-525.
152. Fukada H, Ozaki Y, Pierce AL, Adachi S, Yamauchi K, Hara A, et al. Salmon growth hormone receptor: molecular cloning, ligand specificity, and response to fasting. Gen Comp Endocrinol 2004; 139:61-71.
153. Pierce AL, Fox BK, Davis LK, Visitacion N, Kitahashi T, Hirano T et al. Prolactin receptor, growth hormone receptor, and putative somatolactin receptor in Mozambique tilapia: Tissue specific expression and differential regulation by salinity and fasting. Gen Comp. Endocrinol 2007; 154:31-40.
154. Reinecke M. Insulin-like growth factors and fish reproduction. Biol. Reprod 2010; 82: 656-661.
155. Daughaday WH. Growth hormone axis overview-somatomedin hypothesis. Pediatr Nephrol 2010; 14:537-540.
156. Reinecke M, Collet C. The phylogeny of the insulin-like growth factors. Int Rev Cytol 1998; 183:1-94.
157. Norbeck LA, Kittilson JD, Sheridan MA. Resolving the growth-promoting and metabolic effects of growth hormone: Differential regulation of GH-IGF-I system components. Gen Comp Endocrinol 2007; 151:332-341.
158. Zhou R, Yu SMY, Ge W. Expression and functional characterization of intrafollicular GH–IGF system in the zebrafish ovary. Gen Comp Endocrinol 2016; 232:32-42.
159. Pérez L, Ortiz-Delgado B, Manchado JM. Molecular characterization and transcriptional regulation by GH and GnRH of insulin-like growth factors I and II in White seabream (Diplodus sargus). Gene 2016; 578:251-262.
160. Breves JP, McCormick SD, Karlstrom RO. Prolactin and teleost ionocytes: New insights into cellular and molecular targets of prolactin in vertebrate epithelia. Gen. Comp Endocrinol 2014; 203:21-28.
161. Dobolyi A, Oláh S, Keller D, Kumari R, Fazekas E, Csikós V, Cservenák M. Secretion and function of pituitary prolactin in evolutionary perspective. Frontiers in Neuroscience 2020; 14, 621.
162. Imaoka T, Matsuda M, and Mori T. Extrapituitary expression of the prolactin gene in the goldfish, African clawed frog and mouse. Zool. Sci 2000; 17:791-796.
163. Boutet I, Lorin-Nebel C, De Lorgeril J, Guinand B. Molecular characterisation of prolactin and analysis of extrapituitary expression in the European sea bass Dicentrarchus labrax under various salinity conditions. Comp. Biochem. Physiol. D Genomics Proteomics 2007; 2:74-83.
164. Summers K, Zhu Y. Positive selection on a prolactin paralog following gene duplication in cichlids: adaptive evolution in the context of parental. Copeia 2008; 4: 872-876.
165. Sandra O, Le Rouzic P, Cauty C, Edery M, Prunet P. Expression of the prolactin receptor (tiPRL-R) gene in tilapia Oreochromis niloticus: Tissue distribution and cellular localization in osmoregulatory organs. J Mol Endocrinol 2000; 24:215-224.
166. Kawauchi H, Sower SA, Moriyama S. The Neuroendocrine Regulation of Prolactin and Somatolactin secretion in fish. Fish Physiology 2009; 28:197-234.
167. Edery M, Young G, Bern HA, Steiny S. Prolactin receptors in tilapia (Sarotherodon mossambicus) tissues: binding studies using I-125 labeled ovine prolactin. Gen Comp Endocrinol 1984; 56:19-23.
168. Ozaki Y, Ishida K, Saito K, Ura K, Adachi S, Yamauchi K. Immunohistochemical changes in production of pituitary hormones during artificial maturation of female Japanese eel Anguilla japonica. Fish Sci 2007; 73:574-584.
169. Onuma TA, Ban M, Makino K, Katsumata H, Hu WW, Ando H, et al. Changes in gene expression for GH/PRL/SL family hormones in the pituitaries of homing chum salmon during ocean migration through upstream migration. Gen Comp Endocrinol 2010; 166:537-548.
170. Power DM. Developmental ontogeny of prolactin and its receptor in fish. Gen. Comp. Endocrinol 2005; 142:25-33.
171. Whittington CM, Wilson AB. The role of prolactin in fish reproduction. Gen Comp Endocrinol 2013; 191:123-136.
172. Harvey S, Martínez-Moreno G, Luna M, Arámburo C. Autocrine/paracrine roles of extrapituitary growth hormone and prolactin in health and disease: An overview. Gen Comp Endocrinology 2014; 154:31-40.
173. Cyr DG, Eales JGG. Interrelation ships between thyroidal and reproductive endocrine systems in fish. Rev Fish Biol Fish 1996; 6:165–200.

174. Cyr DG, Eales JGG. In vitro effects of TH on gonadotropin-induced estradiol-17α secretion by ovarian follicles of rainbow trout, Salmo gairdneri. Gen Comp Endocrinol 1988; 69:80-87.
175. Blanton, ML, Specker JL. The Hypothalamic-Pituitary-Thyroid (HPT) axis in fish and its role in fish development and reproduction. Crit Rev Toxicol 2007; 37:97-115.
176. Nelson ER, Allan ERO, Pang FY, Habibi HR. Thyroid hormone and reproduction: Regulation of estrogen receptors in goldfish gonads. Mol. Reprod. Dev 2010; 77:784-794.
177. Tovo-Neto A, Da Silva Rodríguez M, Habibi HR, Nóbrega RH. Thyroid hormone actions on male reproductive system of teleost fish., General and Comparative Endocrinology 2018; doi: https://doi.org/10.1016/j.ygcen.2018.04.023
178. Yu L, Han Z, Liu C. A review on the effects of PBDEs on thyroid and reproduction systems in fish. Gen Comp Endocrinol 2015; http://dx.doi.org/10.1016/j.ygcen.2014.12.010
179. Mylonas, Sullivan, Hinshaw. Thyroid hormones in brown trout (Salmo trutta) reproduction and early development. Fish Physiol. Biochem 1994; 13:485-493.
180. Basset JHD, Harvey CB, Williams GR. Mechanisms of thyroid hormone receptor-specific nuclear and extra nuclear actions. Mol Cell Endocrinol 2003; 213:1-11.
181. Brown L, Sullivan CV, Bern HA, Dickhoff WW. Occurrence of thyroid hormones in early developmental stages of teleost fish. Am. Fish Soc Symp 1987; 2:144-150.
182. Parhar IS, Soga T, Sakuma Y. Thyroid hormone and estrogen regulate brain region-specific messenger ribonucleic acids encoding three gonadotropin-releasing hormone genes in sexually immature male fish, Oreochromis niloticus. Endocrinology 2000; 141:1618-1626.
183. Allan ER, Habibi, HR. Direct effects of triiodothyronine on production of anterior pituitary hormones and gonadal steroids in goldfish. Mol Reprod Dev 2012; 79:592–602.
184. Nelson ER, Habibi HR. Functional significance of nuclear estrogen receptor subtypes in the liver of goldfish. Endocrinology 2010; 151:1668-1676.
185. Nelson ER, Habibi HR. Thyroid hormone regulates vitellogenin by inducing estrogen receptor alpha in the goldfish liver. Mol Cell Endocrinol 2016; 436:259-267.
186. Morais RD, Nóbrega RH, Gómez-González NE, Schmidt R, Bogerd, J, França, LR, et al. Thyroid hormone stimulates the proliferation of sertoli cells and single type A spermatogonia in adult zebrafish (Danio rerio) testis. Endocrinology 2013; 154:4365-4376.
187. Eales JG, Plate EM, Adams BA, Allison WT, Martens G, Hawryshyn CW. The effects of thyroxine or a GnRH analogue on thyroid hormone deiodination in the olfactory epithelium and retina of rainbow trout, Oncorhynchus mykiss, and sockeye salmon, Oncorhynchus nerka. Gen Comp Endocrinol 2006; 127:59-65.
188. Habibi, HR, Nelson E.R, Allan ERO. New insights into thyroid hormone function and modulation of reproduction in goldfish. Gen Comp Endocrinol 2012; 175:19-26.
189. Tokarz J, Möller G, de Angelis MH and Adamski J. Steroids in teleost fishes: a functional point of view. Steroids 2015; 103:123-144.
190. Guyton JE. Elsevier AC. Tratado de Fisiología Médica (ed. Décimotercera edición, 2016).
191. Filby AL and Tyler CR. Molecular characterization of estrogen receptors 1, 2a, and 2b and their tissue and ontogenic expression profiles in fathead minnow (Pimephales promelas). Biology of reproduction 2005; 73(4):648-662.
192. Borg B. Androgens in teleost fishes. Comp Biochem Physiol 1994; 109C (3):219-245.
193. Matty AJ. Gonadal Hormones. Fish endocrinology 1985; pp138-173. Croom Helm Ltd., London.
194. Lubzens E, Young G, Bobe J, Cerda, J. Oogenesis in teleosts: how fish eggs are formed. Gen Comp Endocrinol 2010; 165:367-389.
195. Segner H, Van Kemenade BL, Chadzinska M. The immunomodulatory role of the hypothalamus-pituitary-gonad axis: Proximate mechanism for reproduction-immune tradeoffs? Developmental & Comparative Immunology 2017; 66:43-60.
196. Soranganba N, Singh IJ. Role of Some Steroidogenic Hormones in Fish Reproduction., Chemical Science Review and Letters 2019, 8(29):64-69.
197. Canazas NR. Evolución Gonadal de Las Hembras de Trucha Arco iris (Oncorhynchus Mykiss) de la Piscigranja Pumahuanca-Urubamba, Tesis de Grado UNSAC, 119; 2015.
198. Nagahama Y, Yamashita M. Regulation of oocyte maturation in fish. Development, growth & differentiation 2008; 50(s1).
199. Devlin R.H, Nagahama Y. Sex determination and sex differentiation in fish: an overview of genetic, physiological, and environmental influences. Review article. Aquaculture 2002; 208:191-364.
200. Nagahama Y, Yoshikuni M, Yamashita M, Tanaka M. Regulation of oocyte maturation in fish. In: Sherwood, N.M., Hew, C.L. (Eds.), Fish Physiology. Academic Press, San Diego, CA, pp. 393–439. Neurol 1994; 524:176-198.
201. Babin PJ, Carnevali O, Lubzens E, Schneider WJ. Molecular aspects of oocyte vitellogenesis in fish. Springer 2007:39–76.
202. Hiramatsu N, Matsubara T, Fujita T, Sullivan CV, Hara A. Multiple piscine vitellogenins: biomarkers of fish exposure to estrogenic endocrine disruptors in aquatic environments. Mar Biol 2006; 149:35-47.
203. Stocco C, Telleria G, Gibori. The molecular control of corpus luteum formation, rolfunction, and regression. Endocr Rev 2007; 28:117-149.
204. Milla S, Wang N, Mandiki SN, Kestemont P. Corticosteroids: Friends or foes of teleost fish reproduction? Comparative Biochemistry and Physiology Part A: Molecular & Integrative Physiology 2009; 153(3):242-251.
205. Kusakabe M, Nakamura I, Young G. 11beta-hydroxysteroid dehydrogenase complementary deoxyribonucleic acid in rainbow trout: cloning, sites of expression, and seasonal changes in gonads. Endocrinology 2003; 144:2534-2545.
206. Noaksson E, Linderoth M, Gustavsson B, Zebühr Y, Balk L. Reproductive status in female perch (Perca fluviatilis) outside a sewage treatment plant processing leachate from a refuse dump. Sci. Total Environ 2005; 340: 97-112.
207. Westring CG, Ando H, Kitahashi T, Bhandari RK, Ueda H, Urano A, et al. Seasonal changes in CRF-I and urotensin I transcript levels in masu salmon: correlation with cortisol secretion during spawning. Gen Comp Endocrinol 2008; 155:126-140.
208. Leibowitz, Wortley. Hypothalamic control of energy balance: different peptides, different functions. Peptides 2004; 25:473-504.

Received: 7 May 2021
Accepted: 4 August 2021


UNIVERSIDAD
YACHAY
TECH
DE LA CURIOSIDAD ACADÉMICA
A LA INNOVACIÓN TECNOLÓGICA
ESCUELA DE
CIENCIAS MATEMÁTICAS
Y COMPUTACIONALES
ESCUELA DE
CIENCIAS FÍSICAS
Y NANOTECNOLOGÍA
ESCUELA DE
CIENCIAS QUÍMICAS
E INGENIERÍA
ESCUELA DE
CIENCIAS DE LA TIERRA,
ENERGÍA Y AMBIENTE
ESCUELA DE
CIENCIAS BIOLÓGICAS
E INGENIERÍA

Docencia, investigación, extensión y proyección social al servicio del territorio

UCO
Universidad Católica de Oriente
Vigilada Mineducación

Fortalezas **institucionales**

- Biotecnología
- Limnología
- Derechos Humanos – Posconflicto
- Internacionalización
- Inclusión Social
  - SER Servicio Educativo Rural
  - Educación de Alfabetización
- MIS – Instituto de formación para el trabajo y el desarrollo humano
- Formación humanística "Ruta Humanística en el currículo - Cátedra abierta Madre de la Sabiduría"
- Investigación y desarrollo tecnológico
- Comprometida con la calidad
- Centro de Estudios Territoriales
- Biodiversidad
  - Herbario
  - Ictiología
  - Litoteca

Áreas del **conocimiento**

- Ciencias Agropecuarias
- Ciencias de la Educación
- Ciencias de la Salud
- Ciencias Económicas y Administrativas
- Ciencias Sociales
- Derecho
- Ingenierías
- Teología y Humanidades

- 26 programas de pregrado
- 16 programas de posgrado
  - 1 doctorado
  - 8 maestrías
  - 7 especializaciones

www.uco.edu.co Universidad catolicadeoriente @uconia

Contacto institucional Universidad Católica de Oriente
Sector 3, Cra. 46 No. 40B 50 - **PBX:** (57)(4) 569 90 90. Ext. 694
Fax: (57)(4) 531 09 72 - **Email:** uco@uco.edu.co